Forced Symmetry Breaking of Euclidean Equivariant Partial Differential Equations, Pattern Formation and Turing Instabilities.

by

Martyn Parker

A Thesis submitted in partial fulfilment of the requirements for the degree of Doctor of Philosophy in Mathematics

Mathematics Institute
University of Warwick

January, 2003

Contents

Acknowledgements x

Declaration xi

Summary xii

I Forced Symmetry Breaking 1

1 Symmetry-Breaking Bifurcations 2
- 1.1 Group Theory . . . 3
- 1.2 Invariant Theory . . . 4
- 1.3 Steady-State Symmetry-Breaking . . . 6
- 1.4 Stability of Solution Branches . . . 8
- 1.5 Heteroclinic Cycles and Networks . . . 8
- 1.6 PDEs with Euclidean Symmetry . . . 10
  - 1.6.1 Problem Formulation . . . 10
  - 1.6.2 Actions of the Euclidean Group . . . 11
  - 1.6.3 Symmetry-Breaking Bifurcations . . . 11
  - 1.6.4 Fourier Series . . . 12

2 Forced Symmetry Breaking 14
- 2.1 Invariant Manifolds . . . 16
  - 2.1.1 Normally Hyperbolic Manifolds . . . 16
  - 2.1.2 Equivariant Flows on Invariant Manifolds . . . 17
- 2.2 Group Actions . . . 18
- 2.3 One-Dimensional Flows on Homogeneous Spaces . . . 19
  - 2.3.1 Decomposition of the Orbit Space . . . 19
  - 2.3.2 Symmetry Properties of the Skeleton . . . 20
  - 2.3.3 Projection of the Skeleton into the Orbit Space . . . 21
  - 2.3.4 Flows on the Skeleton . . . 23
- 2.4 Classification of the Skeleton . . . 24
- 2.5 Behaviour of the Perturbed Manifold . . . 25
  - 2.5.1 Parametrisation of the Skeletons . . . 26
  - 2.5.2 Flows on the Perturbed Skeleton . . . 27
- 2.6 Forced Symmetry Breaking of Euclidean Equivariant Systems . . . 31
  - 2.6.1 Fredholm Operators . . . 31
  - 2.6.2 Liapunov–Schmidt Reduction . . . 32

II Forced Symmetry Breaking of 2D Planforms 35

3 Steady-State Bifurcation with 2D Euclidean Symmetry 36

4 Forced Symmetry Breaking on the Square Lattice **39**
4.1 Introduction . . . 39
4.2 Four-Dimensional Representation . . . 40
4.2.1 Existence of the Translation Free Axial Solution . . . 41
4.2.2 Forced Symmetry Breaking to $\mathbf{D}_4$ . . . 41
4.2.3 Forced Symmetry Breaking to $\mathbf{D}_2[\rho^2, \kappa\rho]$ . . . 53
4.2.4 Forced Symmetry Breaking to $\mathbf{D}_2[\rho^2, \kappa]$ . . . 54
4.2.5 Conclusion and Perturbed Planforms . . . 64
4.3 Eight-Dimensional Representation . . . 66
4.3.1 Existence of Translation Free Axial Solutions . . . 67
4.3.2 Forced Symmetry Breaking of Square and Anti-Square Solutions . . . 68
4.3.3 Conclusion . . . 70
4.4 Review . . . 71

5 Forced Symmetry Breaking on the Hexagonal Lattice **73**
5.1 Introduction . . . 73
5.2 Six-Dimensional Representation . . . 74
5.2.1 Existence of Translation Free Axial Solution . . . 75
5.2.2 Forced Symmetry Breaking to $\mathbf{D}_6$ . . . 75
5.2.3 Forced Symmetry Breaking to $\mathbf{D}_3[\rho^2, \kappa]$ . . . 84
5.2.4 Forced Symmetry Breaking to $\mathbf{D}_3[\rho^2, \kappa\rho]$ . . . 86
5.2.5 Forced Symmetry Breaking to $\mathbf{D}_2[\rho^3, \kappa]$ . . . 94
5.2.6 Forced Symmetry Breaking to $\mathbf{D}_2[\rho^3, \kappa\rho]$ . . . 96
5.2.7 Forced Symmetry Breaking to $\mathbf{D}_2[\rho^3, \kappa\rho^2]$ . . . 99
5.2.8 Conclusion and Planforms . . . 102
5.3 Twelve-Dimensional Representation . . . 102
5.3.1 Existence of Translation Free Axial Solution . . . 103
5.3.2 Forced Symmetry Breaking of Super Hexagons . . . 104
5.3.3 Examples . . . 105
5.4 Review . . . 107

III Forced Symmetry Breaking of 3D Planforms **109**

6 Steady-State Bifurcations with 3D Symmetry **110**

7 Forced Symmetry Breaking on the SC Lattice **114**
7.1 Introduction . . . 114
7.2 Six-Dimensional Representation . . . 115
7.2.1 Existence of Translation Free Axial Solution . . . 115
7.2.2 Forced Symmetry Breaking to $\mathbb{O}$ . . . 116
7.2.3 Forced Symmetry Breaking to $\mathbf{D}_4[\rho_x, \kappa_6]$ . . . 131
7.2.4 Forced Symmetry Breaking to $\mathbb{T}$ . . . 136
7.2.5 Forced Symmetry Breaking to $\mathbf{D}_3[\tau_1, \kappa_5]$ . . . 140
7.2.6 Forced Symmetry Breaking to $\mathbf{D}_2[\rho_x^2, \kappa_6]$ . . . 143
7.2.7 Forced Symmetry Breaking to $\mathbf{D}_2[\rho_x^2, \rho_y^2]$ . . . 146
7.2.8 Example . . . 148
7.3 High Dimensional Representations . . . 149
7.3.1 Existence of Translation Free Axial Solutions . . . 150
7.3.2 Examples . . . 151
7.4 Conclusion . . . 152

8 Forced Symmetry Breaking on the FCC Lattice **154**
8.1 Introduction . . . 154
8.2 Eight-Dimensional Representation . . . 155
8.2.1 Existence of Translation Free Axial Solution . . . 156
8.2.2 Forced Symmetry Breaking to $\mathbb{O}$ . . . 156
8.2.3 Forced Symmetry Breaking to $\mathbf{D}_4[\rho_x, \kappa_6]$ . . . 168
8.2.4 Forced Symmetry Breaking to $\mathbb{T}$ . . . 171
8.2.5 Forced Symmetry Breaking to $\mathbf{D}_3[\tau_1, \kappa_5]$ . . . 174
8.2.6 Forced Symmetry Breaking to $\mathbf{D}_2[\rho_x^2, \kappa_6]$ . . . 177
8.2.7 Forced Symmetry Breaking to $\mathbf{D}_2[\rho_x^2, \rho_y^2]$ . . . 179
8.2.8 Example . . . 181
8.3 High Dimensional Representations . . . 182
8.3.1 Existence of Translation Free Axial Solutions . . . 182
8.3.2 Examples . . . 183
8.4 Conclusion . . . 184

9 Forced Symmetry Breaking on the BCC Lattice **185**
9.1 Introduction . . . 185
9.2 Twelve-Dimensional Representation . . . 186
9.2.1 Existence of Translation Free Axial Solutions . . . 186
9.2.2 Forced Symmetry Breaking to $\mathbb{O}$ . . . 187
9.2.3 Forced Symmetry Breaking to $\mathbf{D}_4[\rho_x, \kappa_6]$ . . . 201
9.2.4 Forced Symmetry Breaking to $\mathbb{T}$ . . . 204
9.2.5 Forced Symmetry Breaking to $\mathbf{D}_3[\tau_3, \kappa_3]$ . . . 207
9.2.6 Forced Symmetry Breaking to $\mathbf{D}_2[\rho_x^2, \kappa_6]$ . . . 209
9.2.7 Forced Symmetry Breaking to $\mathbf{D}_2[\rho_x^2, \rho_y^2]$ . . . 211
9.2.8 Example . . . 213
9.3 High Dimensional Representations . . . 215
9.3.1 Existence of Translation Free Axial Solutions . . . 215
9.3.2 Examples . . . 217
9.4 Conclusion . . . 218

IV Pattern Formation and Turing Instabilities **220**

10 Pattern Formation and Turing Instabilities **221**
10.1 Pattern Formation . . . 221
10.2 Turing Instabilities in the CIMA reaction . . . 223
10.2.1 Introduction . . . 223
10.2.2 Experimental Apparatus . . . 225
10.2.3 Bifurcation with Approximate BCC Symmetry . . . 226
10.2.4 Discussion . . . 227
10.3 Nonlinear Optical Systems . . . 231
10.3.1 Introduction . . . 231
10.3.2 Discussion . . . 234
10.4 Polyacrylamide-Methylene Blue-Oxygen Reaction . . . 235
10.4.1 Introduction . . . 235
10.4.2 Experimental Apparatus and Results . . . 235
10.4.3 Discussion . . . 236
10.5 General Discussion and Conclusion . . . 236

11 Concluding Remarks **238**
11.1 Summary of Results . . . 238
11.2 Future Work . . . 238

A **239**
A.1 The Symmetry Package . . . 239
A.2 Invariants for Subgroups of $\mathbf{D}_4$ . . . 240
A.2.1 Four-Dimensional Representation . . . 240
A.3 Invariants for Subgroups of $\mathbf{D}_6$ . . . 241
A.3.1 Invariants and Equivariants for $\mathbf{D}_3[\rho^2, \kappa\rho]$ . . . 242

B **244**
B.1 Notation and Preliminaries . . . 244
B.2 Proof of the Main Result . . . 245
B.3 Subgroups of $\mathbb{O} \oplus \mathbf{Z}_2^c$ . . . 247

C **249**

Bibliography **252**

List of Figures

3.1 Translation free axial planforms found on the square lattice 37
3.2 Translation free axial planforms found on the hexagonal lattice 37

4.1 The skeleton $\mathbb{X}_{\mathbf{D}_4}$ for forced symmetry breaking on the square lattice 44
4.2 The projected skeleton $\mathbb{X}^p_{\mathbf{D}_4}$ for forced symmetry breaking on the square lattice . 47
4.3 The skeleton $\mathbb{X}_{\mathbf{D}_2[\rho^2,\kappa]}$ for forced symmetry breaking on the square lattice 55
4.4 Projected skeleton $\mathbb{X}^p_{\mathbf{D}_2[\rho^2,\kappa]}$ with two possible flows. 57
4.5 Example degenerate flow on $\mathbb{X}_{\mathbf{D}_2[\rho^2,\kappa]}$ 65
4.6 Example nondegenerate flow on $\mathbb{X}_{\mathbf{D}_2[\rho^2,\kappa]}$ 65
4.7 Effects of breaking symmetry on the square planform 66
4.8 Example flows on $\mathbb{X}_{\mathbf{D}_4}$ in the eight-dimensional representation 71

5.1 The skeleton $\mathbb{X}_{\mathbf{D}_6}$ for forced symmetry breaking on the hexagonal lattice 80
5.2 Two flows on $\mathbb{X}^p_{\mathbf{D}_6}$ for forced symmetry breaking on the hexagonal lattice 84
5.3 The skeleton $\mathbb{X}_{\mathbf{D}_3[\rho^2,\kappa]}$ for forced symmetry breaking on the hexagonal lattice . . 85
5.4 Two flows on $\mathbb{X}^p_{\mathbf{D}_3[\rho^2,\kappa]}$ for forced symmetry breaking on the hexagonal lattice. . 87
5.5 The skeleton $\mathbb{X}_{\mathbf{D}_3[\rho^2,\kappa\rho]}$ for forced symmetry breaking on the hexagonal lattice . . 88
5.6 A heteroclinic cycle on $\mathbb{X}^p_{\mathbf{D}_3[\rho^2,\kappa\rho]}$ for forced symmetry breaking on the hexagonal lattice 89
5.7 The skeleton $\mathbb{X}_{\mathbf{D}_2[\rho^3,\kappa]}$ for forced symmetry breaking on the hexagonal lattice . . 94
5.8 Two flows on $\mathbb{X}^p_{\mathbf{D}_2[\rho^3,\kappa]}$ for forced symmetry breaking on the hexagonal lattice. . 96
5.9 The skeleton $\mathbb{X}_{\mathbf{D}_2[\rho^2,\kappa\rho]}$ for forced symmetry breaking on the hexagonal lattice . . 97
5.10 Two flows on the projected skeleton $\mathbb{X}^p_{\mathbf{D}_2[\rho^3,\kappa\rho]}$ for forced symmetry breaking on the hexagonal lattice. 99
5.11 The skeleton $\mathbb{X}_{\mathbf{D}_2[\rho^2,\kappa\rho^2]}$ for forced symmetry breaking on the hexagonal lattice . 100
5.12 Two flows on the projected skeleton $\mathbb{X}^p_{\mathbf{D}_2[\rho^3,\kappa\rho^2]}$ for forced symmetry breaking on the hexagonal lattice 101
5.13 Effects of symmetry breaking on the hexagonal planform 103
5.14 Example flow on $\mathbb{X}_{\mathbf{D}_3[\rho^2,\kappa\rho]}$ for the twelve-dimensional representation 106
5.15 Effect of symmetry breaking on super hexagons 107
5.16 More accurate rendering of super hexagons under forced symmetry breaking . . . 108

6.1 Translation free axial solution on the SC lattice 111
6.2 Translation free axial solutions on the FCC lattice 111
6.3 Translation free axial solutions on the BCC lattice 112

7.1 The projected skeleton $\mathbb{X}^p_{\mathbf{O}}$ on the SC lattice 130
7.2 Example flows on $\mathbb{X}^p_{\mathbf{O}}$ on the SC lattice 131
7.3 The projected skeleton $\mathbb{X}^p_{\mathbf{D}_4[\rho_z,\kappa_6]}$ on the SC lattice 135
7.4 The projected skeleton $\mathbb{X}^p_{\mathbf{T}}$ on the SC lattice 140
7.5 The projected skeleton $\mathbb{X}^p_{\mathbf{D}_3[\tau_1,\kappa_8]}$ on the SC lattice 142
7.6 The projected skeleton $\mathbb{X}^p_{\mathbf{D}_2[\rho_z^2,\kappa_6]}$ on the SC lattice 145

7.7 The projected skeleton $\mathbb{X}^p_{\mathbf{D}_2[\rho_x^2,\rho_y^2]}$ on the SC lattice . . . 148
7.8 Example SC planform for forced symmetry breaking to $\mathbb{O}$ . . . 149
7.9 Example planform for forced symmetry breaking to $\mathbb{O}$ in the 24-dimensional type 1 representation . . . 152
7.10 Example planform for forced symmetry breaking to $\mathbb{O}$ in the 24-dimensional type 2 representation . . . 153
7.11 Example planform for forced symmetry breaking to $\mathbb{O}$ in the 48-dimensional representation . . . 153

8.1 The projected skeleton $\mathbb{X}^p_{\mathbb{O}}$ on the FCC lattice . . . 167
8.2 The projected skeleton $\mathbb{X}^p_{\mathbf{D}_4[\rho_x,\kappa_6]}$ on the FCC lattice . . . 171
8.3 The projected skeleton $\mathbb{X}^p_{\mathbb{O}'}$ on the FCC lattice . . . 174
8.4 The projected skeleton $\mathbb{X}^p_{\mathbf{D}_3[\tau_1,\kappa_5]}$ on the FCC lattice . . . 177
8.5 The projected skeleton $\mathbb{X}^p_{\mathbf{D}_2[\rho_x^2,\kappa_6]}$ on the FCC lattice . . . 179
8.6 The projected skeleton $\mathbb{X}^p_{\mathbf{D}_2[\rho_x^2,\rho_y^2]}$ on the FCC lattice . . . 181
8.7 Example planform for forced symmetry breaking to $\mathbb{O}$ on the FCC lattice . . . 182
8.8 Example planform for forced symmetry breaking to $\mathbb{O}$ on the FCC lattice in the 24-dimensional representation . . . 184

9.1 The projected skeleton $\mathbb{X}^p_{\mathbb{O}}$ for the BCC lattice . . . 200
9.2 The projected skeleton $\mathbb{X}^p_{\mathbf{D}_4[\rho_x,\kappa_6]}$ for the BCC lattice . . . 203
9.3 The projected skeleton $\mathbb{X}^p_{\mathbb{O}}$ for the BCC lattice . . . 206
9.4 The projected skeleton $\mathbb{X}^p_{\mathbf{D}_3[\tau_3,\kappa_3]}$ for the BCC lattice . . . 209
9.5 The projected skeleton $\mathbb{X}^p_{\mathbf{D}_2[\rho_x^2,\kappa_6]}$ for the BCC lattice . . . 211
9.6 The projected skeleton $\mathbb{X}^p_{\mathbf{D}_2[\rho_x^2,\rho_y^2]}$ . . . 213
9.7 Perturbation of the cube along the body diagonal. . . . 214
9.8 Example planform for forced symmetry breaking on the BCC lattice . . . 215
9.9 Example planform for forced symmetry breaking on the BCC lattice in the 24-dimensional type 1 representation . . . 218
9.10 Example planform for forced symmetry breaking on the BCC lattice in the 24-dimensional type 2 representation . . . 218
9.11 Example planform for forced symmetry breaking on the BCC lattice in the 48-dimensional . . . 219

10.1 The experimental apparatus of Ouyang and Swinney. . . . 225
10.2 Experimental black-eyes . . . 226
10.3 Black-eyes in the BCC Planform . . . 226
10.4 Perturbed black-eyes in the BCC planform . . . 227
10.5 Perturbed black-eyes in the BCC planform . . . 228
10.6 Perturbed black-eyes in the BCC planform along a heteroclinic connection . . . 228
10.7 The experimental apparatus of Zhou and co-workers. . . . 229
10.8 Stripes, hexagons and black-eyes in a slice of the BCC planform . . . 230
10.9 Kerr-slice feedback mirror experimental apparatus . . . 232
10.10The liquid-crystal light-valve experimental apparatus of Vorontsov and Samson. . 233
10.11BCC pattern produced using the twenty-four-dimensional type 2 representation . 235

B.1 Cube centred at the origin . . . 244
B.2 Containment relations for conjugacy classes of subgroups of $\mathbb{O}$. . . . 246

List of Tables

4.1 Fixed-point submanifolds for nontrivial subgroups of $\mathbf{D}_4$ . . . 43
4.2 Induced action of $\mathbf{D}_4$ on $\mathscr{C}_{\mathbf{D}_4}$ . . . 46
4.3 Isotropy data for $\mathscr{C}_{\mathbf{D}_4}$ . . . 46
4.4 Knots relative to $C \in \mathscr{C}_{\mathbf{D}_4}$, for C a topological circle . . . 47
4.5 Eigenvalues at the equilibria on $\mathbb{X}_{\mathbf{D}_2[\rho^2,\kappa\rho]}$ . . . 53
4.6 Induced action of $\mathbf{D}_2[\rho^2,\kappa]$ on $\mathscr{C}_{\mathbf{D}_2[\rho^2,\kappa]}$ . . . 56
4.7 Isotropy data for $C \in \mathscr{C}_{\mathbf{D}_2[\rho^2,\kappa]}$ . . . 56
4.8 Eigenvalues of the translation free axial solution in the eight-dimensional representation . . . 68

5.1 Action of $\mathbf{D}_6$ induced on $\mathscr{C}_{\mathbf{D}_6}$ . . . 82
5.2 Isotropy data for $C \in \mathscr{C}_{\mathbf{D}_6}$ . . . 82
5.3 Knots relative to $C \in \mathscr{C}_{\mathbf{D}_6}$ when C is a topological circle . . . 83
5.4 Action of $\mathbf{D}_3[\rho^2,\kappa]$ induced on $\mathscr{C}_{\mathbf{D}_3[\rho^2,\kappa]}$ . . . 86
5.5 Isotropy data for $C \in \mathscr{C}_{\mathbf{D}_3[\rho^2,\kappa]}$ . . . 86
5.6 Action of $\mathbf{D}_3[\rho^2,\kappa\rho]$ induced on $\mathscr{C}_{\mathbf{D}_3[\rho^2,\kappa\rho]}$ . . . 88
5.7 Isotropy data for $C \in \mathscr{C}_{\mathbf{D}_3[\rho^2,\kappa\rho]}$ . . . 89
5.8 Action of $\mathbf{D}_2[\rho^3,\kappa]$ induced on $\mathscr{C}_{\mathbf{D}_2[\rho^3,\kappa]}$ . . . 95
5.9 Isotropy data for $C \in \mathscr{C}_{\mathbf{D}_2[\rho^3,\kappa]}$ . . . 95
5.10 Action of $\mathbf{D}_2[\rho^3,\kappa\rho]$ induced on $\mathscr{C}_{\mathbf{D}_2[\rho^3,\kappa\rho]}$ . . . 98
5.11 Isotropy data for $C \in \mathscr{C}_{\mathbf{D}_2[\rho^3,\kappa\rho]}$ . . . 98
5.12 Action of $\mathbf{D}_2[\rho^3,\kappa\rho^2]$ induced on $\mathscr{C}_{\mathbf{D}_2[\rho^3,\kappa\rho^2]}$ . . . 100
5.13 Isotropy data for $C \in \mathscr{C}_{\mathbf{D}_2[\rho^3,\kappa\rho^2]}$ . . . 101

7.1 Action of the elements of $\mathbb{O}$ on $\mathbb{C}^3$ for the SC lattice . . . 117
7.2 Action of $\mathbb{O}$ induced on X_0 for the SC lattice . . . 124
7.3 Action of $\mathbb{O}$ induced on $\mathscr{C}_{\mathbb{O}}$ for the SC lattice . . . 124
7.4 Table 7.3 continued . . . 125
7.5 Table 7.3 continued . . . 126
7.6 Table 7.3 continued . . . 127
7.7 Isotropy data for $C \in \mathscr{C}_{\mathbb{O}}$ on the SC lattice . . . 129
7.8 The knots relative to the orbit representatives of the $C \in \mathscr{C}_{\mathbb{O}}$ on the SC lattice . . . 129
7.9 Action of $\mathbf{D}_4[\rho_x,\kappa_6]$ on $\mathbb{C}^3$ for the SC lattice . . . 131
7.10 Action of $\mathbf{D}_4[\rho_x,\kappa_6]$ induced on X_0 for the SC lattice . . . 132
7.11 Action of $\mathbf{D}_4[\rho_x,\kappa_6]$ induced on $\mathscr{C}_{\mathbf{D}_4[\rho_x,\kappa_6]}$ for the SC lattice . . . 133
7.12 Isotropy data for $C \in \mathscr{C}_{\mathbf{D}_4[\rho_x,\kappa_6]}$ for the SC lattice . . . 134
7.13 Knots relative to orbit representatives of each $C \in \mathscr{C}_{\mathbf{D}_4[\rho_x,\kappa_6]}$ for the SC lattice . . . 135
7.14 Action of $\mathbb{T}$ on $\mathbb{C}^3$ for the SC lattice . . . 136
7.15 Action of $\mathbb{T}$ induced on X_0 for the SC lattice . . . 137
7.16 Action of $\mathbb{T}$ induced on $\mathscr{C}_{\mathbb{T}}$ for the SC lattice . . . 137
7.17 Table 7.16 continued . . . 138
7.18 Isotropy data for $C \in \mathscr{C}_{\mathbb{T}}$ on the SC lattice . . . 139
7.19 Knots relative to orbit representatives of $C \in \mathscr{C}_{\mathbb{T}}$ . . . 139

7.20 Action of $\mathbf{D}_3[\tau_1, \kappa_5]$ on $\mathbb{C}^3$ for the SC lattice. . . . 140
7.21 Action of $\mathbf{D}_3[\tau_1, \kappa_5]$ induced on X_0 for the SC lattice. . . . 141
7.22 Action of $\mathbf{D}_3[\tau_1, \kappa_5]$ induced on $\mathscr{C}_{\mathbf{D}_3[\tau_1,\kappa_5]}$ for the SC lattice. . . . 141
7.23 Isotropy data for $C \in \mathscr{C}_{\mathbf{D}_3[\tau_1,\kappa_5]}$ on the SC lattice. . . . 142
7.24 Action of $\mathbf{D}_2[\rho_x^2, \kappa_6]$ on $\mathbb{C}^3$ for the SC lattice. . . . 143
7.25 Action of $\mathbf{D}_2[\rho_x^2, \kappa_6]$ induced on X_0 for the SC lattice. . . . 144
7.26 Action of $\mathbf{D}_2[\rho_x^2, \kappa_6]$ induced on $\mathscr{C}_{\mathbf{D}_2[\rho_x^2,\kappa_6]}$ for the SC lattice. . . . 144
7.27 Isotropy data for $C \in \mathscr{C}_{\mathbf{D}_2[\rho_x^2,\kappa_6]}$ on the SC lattice. . . . 144
7.28 Knots relative to orbit representatives of $C \in \mathscr{C}_{\mathbf{D}_2[\rho_x^2,\kappa_6^2]}$ for the SC lattice. . . . 145
7.29 Action of $\mathbf{D}_2[\rho_x^2, \rho_y^2]$ on $\mathbb{C}^3$ for the SC lattice. . . . 146
7.30 Action of $\mathbf{D}_2[\rho_x^2, \rho_y^2]$ induced on X_0 on the SC lattice. . . . 147
7.31 Isotropy data for $C \in \mathscr{C}_{\mathbf{D}_2[\rho_x^2,\rho_y^2]}$ on the SC lattice. . . . 147
7.32 Knots relative to the orbit representatives of the $C \in \mathscr{C}_{\mathbf{D}_2[\rho_x^2,\rho_y^2]}$ for the SC lattice. 148
7.33 The axial subgroups of the 24 and 48-dimensional representations of the SC lattice 150

8.1 Action of $\mathbb{O}$ on $\mathbb{C}^4$ for the FCC lattice. . . . 157
8.2 Action of $\mathbb{O}$ induced on X_0 for the FCC lattice. . . . 162
8.3 Action of $\mathbb{O}$ induced on $\mathscr{C}_{\mathbb{O}}$ for the FCC lattice. . . . 163
8.4 Table 8.3 continued 164
8.5 Table 8.3 continued 165
8.6 Table 8.3 continued 166
8.7 Isotropy data for $C \in \mathscr{C}_{\mathbb{O}}$ on the FCC lattice. . . . 166
8.8 Knots relative to orbit representatives of $C \in \mathscr{C}_{\mathbb{O}}$ for the FCC lattice. . . . 167
8.9 Action of $\mathbf{D}_4[\rho_x, \kappa_6]$ on $\mathbb{C}^4$ for the FCC lattice. . . . 168
8.10 Action of $\mathbf{D}_4[\rho_x, \kappa_6]$ induced on X_0 for the FCC lattice. . . . 169
8.11 Action of $\mathbf{D}_4[\rho_x, \kappa_6]$ induced on $\mathscr{C}_{\mathbf{D}_4[\rho_x,\kappa_6]}$ for the FCC lattice. . . . 169
8.12 Isotropy data for $C \in \mathscr{C}_{\mathbf{D}_4[\rho_x,\kappa_6]}$ on the FCC lattice. . . . 170
8.13 Knots relative to orbit representatives of $C \in \mathscr{C}_{\mathbf{D}_4[\rho_x,\kappa_6]}$ for the FCC lattice. . . . 170
8.14 Action of $\mathbb{T}$ on $\mathbb{C}^4$ for the FCC lattice. . . . 171
8.15 Action of $\mathbb{T}$ induced on X_0 for the FCC lattice. . . . 172
8.16 Action of $\mathbb{T}$ induced on $\mathscr{C}_{\mathbb{T}}$ for the FCC lattice. . . . 173
8.17 Isotropy data for $C \in \mathscr{C}_{\mathbb{T}}$ on the FCC lattice. . . . 173
8.18 Knots relative to orbit representatives of $C \in \mathscr{C}_{\mathbb{T}}$ for the FCC lattice. . . . 174
8.19 Action of $\mathbf{D}_3[\tau_1, \kappa_5]$ on $\mathbb{C}^4$ for the FCC lattice. . . . 175
8.20 Action of $\mathbf{D}_3[\tau_1, \kappa_5]$ induced on X_0 for the FCC lattice. . . . 175
8.21 Action of $\mathbf{D}_3[\tau_1, \kappa_5]$ induced on $\mathscr{C}_{\mathbf{D}_3[\tau_1,\kappa_5]}$ for the FCC lattice. . . . 176
8.22 Isotropy data for $C \in \mathscr{C}_{\mathbf{D}_3[\tau_1,\kappa_5]}$ on the FCC lattice. . . . 176
8.23 Action of $\mathbf{D}_2[\rho_x^2, \kappa_6]$ on $\mathbb{C}^4$ for the FCC lattice. . . . 177
8.24 Action of $\mathbf{D}_2[\rho_x^2, \kappa_6]$ induced on X_0 for the FCC lattice. . . . 178
8.25 Isotropy data for $C \in \mathscr{C}_{\mathbf{D}_2[\rho_x^2,\kappa_6]}$ on the FCC lattice. . . . 178
8.26 Knots relative to orbit representatives of $C \in \mathscr{C}_{\mathbf{D}_2[\rho_x^2,\kappa_6^2]}$ for the FCC lattice. . . . 179
8.27 Action of $\mathbf{D}_2[\rho_x^2, \rho_y^2]$ on $\mathbb{C}^4$ for the FCC lattice. . . . 179
8.28 Action of $\mathbf{D}_2[\rho_x^2, \rho_y^2]$ induced on X_0. . . . 180
8.29 Isotropy data for $C \in \mathscr{C}_{\mathbf{D}_2[\rho_x^2,\rho_y^2]}$ on the FCC lattice. . . . 180
8.30 Knots relative to orbit representatives of $C \in \mathscr{C}_{\mathbf{D}_2[\rho_x^2,\rho_y^2]}$ for the FCC lattice. . . . 181
8.31 The axial subgroups of the 24 and 48-Dimensional Representations of the FCC lattice 183

9.1 Action of $\mathbb{O}$ on $\mathbb{C}^6$ for the BCC lattice. . . . 188
9.2 Action of $\mathbb{O}$ induced on X_0 for the BCC lattice. . . . 195
9.3 Action of $\mathbb{O}$ induced on $\mathscr{C}_{\mathbb{O}}$ for the BCC lattice. . . . 195
9.4 Table 9.3 continued 196
9.5 Table 9.3 continued 197
9.6 Table 9.3 continued 198

9.7 Isotropy data for $C \in \mathscr{C}_{\mathbb{O}}$ for the BCC lattice. 199
9.8 Knots relative to orbit representatives of $C \in \mathscr{C}_{\mathbb{O}}$ for the BCC lattice. 200
9.9 Action of $\mathbf{D}_4[\rho_x, \kappa_6]$ on $\mathbb{C}^6$ for the BCC lattice. 201
9.10 Action of $\mathbf{D}_4[\rho_x, \kappa_6]$ induced on X_0 for the BCC lattice. 202
9.11 Action of $\mathbf{D}_4[\rho_x, \kappa_6]$ induced on $\mathscr{C}_{\mathbf{D}_4[\rho_x, \kappa_6]}$ for the BCC lattice. 202
9.12 Isotropy data for $C \in \mathscr{C}_{\mathbf{D}_4[\rho_x, \kappa_6]}$ for the BCC lattice. 202
9.13 Knots relative to orbit representatives of $C \in \mathscr{C}_{\mathbf{D}_4[\rho_x, \kappa_6]}$ for the BCC lattice. . . . 203
9.14 Action of $\mathbb{T}$ on $\mathbb{C}^6$ for the BCC lattice. 204
9.15 Action of $\mathbb{T}$ induced on X_0 for the BCC lattice. 205
9.16 Action of $\mathbb{T}$ induced on $\mathscr{C}_{\mathbb{T}}$ for the BCC lattice. 205
9.17 Isotropy data for $C \in \mathscr{C}_{\mathbb{T}}$ for the BCC lattice. 206
9.18 Action of the elements of $\mathbf{D}_3[\tau_3, \kappa_3]$ on $\mathbb{C}^6$ for the BCC lattice. 207
9.19 Action of $\mathbf{D}_3[\tau_3, \kappa_3]$ induced on X_0 for the BCC lattice. 208
9.20 Action of $\mathbf{D}_3[\tau_3, \kappa_3]$ induced on $\mathscr{C}_{\mathbf{D}_3[\tau_3, \kappa_3]}$ for the BCC lattice. 208
9.21 Isotropy data for $C \in \mathscr{C}_{\mathbf{D}_3[\tau_3, \kappa_3]}$ for the BCC lattice. 208
9.22 Action of the elements of $\mathbf{D}_2[\rho_x^2, \kappa_6]$ on $\mathbb{C}^6$ for the BCC lattice. 209
9.23 Action of $\mathbf{D}_2[\rho_x^2, \kappa_6]$ induced on X_0 for the BCC lattice. 210
9.24 Isotropy data for $C \in \mathscr{C}_{\mathbf{D}_2[\rho_x^2, \kappa_6]}$ for the BCC lattice. 210
9.25 Knots relative to orbit representatives of $C \in \mathscr{C}_{\mathbf{D}_2[\rho_x^2, \kappa_6^2]}$ for the BCC lattice. . . . 211
9.26 Action of $\mathbf{D}_2[\rho_x^2, \rho_y^2]$ on $\mathbb{C}^6$ for the BCC lattice. 211
9.27 Action of $\mathbf{D}_2[\rho_x^2, \rho_y^2]$ induced on X_0 for the BCC lattice. 212
9.28 Isotropy data for $C \in \mathscr{C}_{\mathbf{D}_2[\rho_x^2, \rho_y^2]}$ for the BCC lattice. 213
9.29 Knots relative to orbit representatives of $C \in \mathscr{C}_{\mathbf{D}_2[\rho_x^2, \rho_y^2]}$ for the BCC lattice. . . . 213
9.30 The axial subgroups of the 24- and 48-dimensional representations of the BCC lattice 216

B.1 The action of $\mathbb{O}$ on $\mathbb{R}^3$. 245

Acknowledgements

During the gestation period of this thesis I have come to know so many people, all of whom deserve thanks, or at least five minutes of fame(!) between these pages. You can never thank all the people you want to, so if any one is missing, then sorry, it was not a deliberate omission, rather a brain failure on my part.

- Well how else could I have enjoyed myself so much over the past three years if it was not for the members of Acorn House. So a big thanks for so many brilliant, memorable and not so re-memorable times to: Toby, Caroline (Caz), Matt, Charlotte (Lotster), Andy (Tong), Yuzura, Chris, Asli, Javier, Ken, Sav and last, but by no means least, Marcus.
- Special thanks to Richard, Susie, Stu, Jo, Dave, Sue and Nigel for all the fun and entertainment well beyond our undergraduate days.
- Where would I be without all the people around the department, just to name a few: the football gang, including Ade, Mike, Ingi, Richard, Jan and all the rest.
- Thanks are also due to some people that don't fit into one of the categories, so yes you are now in these hallowed pages. So thanks to Caroline Poos, Tim Honeywell, Jit Mistry, Sav (the surname slips my mind), Stu Price and just about anyone else I know.
- All the people I have had the pleasure of teaching, for making the times between research such a joy.
- Of course my parents and my brother who have been eternally supportive through my now almost eternal education.
- I would like to thank my supervisors Prof. Ian Stewart and Dr. Gabriela Gomes for their patience when my research looked like it was going in random and uncertain directions; their encouragement, support and for introducing me, (in my opinion), to one of the most fascinating and enthralling areas of mathematics. Before I began research the last thing I would have seen myself using was algebra. So a big thanks for opening my eyes.
- Finally, (and they will never read this) the creators of South Park and The Simpsons, the only two programs on television that can guarantee a laugh no matter how many times you watch them.

This research was supported by EPSRC studentship number 99802336.

Declaration

Unless stated otherwise all material presented in this thesis is original work of the author under the supervision of Prof. Ian Stewart and Dr. Gabriela Gomes. Some portions of Chapter 1 have appeared in a different form in the authors MSc. dissertation [74]. Part IV of this thesis was formulated during discussions with Gabriela Gomes.

Summary

Many natural phenomena may be modelled using systems of differential equations that possess symmetry. Often the modelling process introduces additional symmetries that are only approximately present in the real physical system. This thesis investigates how the inclusion of small symmetry breaking effects changes the behaviour of the original solutions, such a process is called *forced symmetry breaking.*

Part I introduces the general equivariant bifurcation theory required for the rest of this work. In particular, we generalise previous techniques used to study forced symmetry breaking to a certain class of Euclidean invariant problems. This allows the study of the effects of forced symmetry breaking on spatially periodic solutions to differential equations.

Part II considers spatially periodic solutions in two dimensions that are supported by the square or hexagonal lattices. The methods of Part I are applied to investigate how the translation free solutions, supported by these lattices, are altered when the perturbation term possesses certain symmetries. This leads to a partial classification theorem, describing the behaviour of these solutions.

This classification is extended in Part III to three-dimensional solutions. In particular, the cubic lattices: simple, face centred, and body centred cubic, are considered. The analysis follows the same lines as Part II, but is necessarily more complex. This complexity is also present in the results, there are much richer dynamical possibilities.

Parts II and III lead to a partial classification of the behaviour of spatially periodic solutions to differential equations in two and three dimensions.

Finally in Part IV the results of Part III, concerning the body centred cubic lattice, are applied to the black-eye Turing instability. In particular, the model of Gomes [39] is cast in a new light where forced symmetry breaking is present, leading to several qualitative predictions. Nonlinear optical systems and the Polyacrylamide-Methylene Blue-Oxygen reaction are also discussed.

Part I

Forced Symmetry Breaking of Equivariant Differential Equations

Chapter 1

Symmetry-Breaking Bifurcations

One of the most powerful mathematical tools for investigating pattern forming phenomena is equivariant bifurcation theory, see Golubitsky *et al.* [35]. This powerful theoretical tool distinguishes those aspects of the problem which are a consequence of the underlying symmetry, and those which depend on the specifics of the mathematical model. This gives advantages over other methods, allowing the study of entire classes of systems, related only by their symmetry, in a generic framework. In the symmetric context it is not surprising that certain disparate—but symmetrically related—physical systems, can exhibit remarkably similar behaviour, this is often called *model independence* [33].

The study of systems of differential equations with symmetry requires the language of groups, in particular Lie groups. In this chapter we present the abstract theory required when studying the symmetry-breaking bifurcations of such systems. We present many elementary, but nonetheless important and powerful ideas from the theory of Lie groups. Firstly in Section 1.1 we formulate the group representation theory that is required in the sequel. Of central importance to all the remaining material are the irreducible representations of a group. The two results that we present are: the existence of a decomposition of a group action into irreducible representations, then how the nonuniqueness of such decompositions may be rectified. To overcome the problem of nonuniqueness we need an idea of isomorphic representations.

Once we have found solutions to a system of symmetric equations, we wish to study their stability so that we may find those solutions that are physically relevant. To achieve this aim in Section 1.2 we introduce a suitable theory of group invariant functions and mappings which commute with a group action. With this theory in place, given a symmetry group we may describe the most general vector field that commutes with this group. In Section 1.3 we consider steady-state symmetry-breaking, discussing the important methods employed to classify the symmetry of bifurcating solutions, and the issue of their existence and uniqueness. The solutions that are guaranteed to exist have symmetries that correspond to certain "special" subgroups of the symmetry group of the system. We show in Section 1.4 how the symmetry of a system of equations may be exploited to simplify the calculations of the stability of bifurcating solutions. This vital tool enormously simplifies some otherwise lengthy and tedious calculations. Section 1.5 contains a brief review of heteroclinic cycles and networks.

Certain systems of PDEs such as the Kuramoto–Sivashinsky, Navier–Stokes, the Boussinesq and reaction-diffusion equations have Euclidean symmetry when posed on unbounded domains. These equations represent something of a problem; the Euclidean group is not compact and the previous theoretical framework is no longer applicable. To get around this problem we show how to "compactify" the problem by restricting to solutions with a prescribed spatial periodicity. Of course this is only one approach, but it is the one we study in the remainder of this work. This compactification allows us to reduce our PDEs to an abstract set of finite dimensional ODEs[1], which commute with a compact group. From this point the process follows the general theory outlined above for compact groups. A certain class of (translation free axial) solutions

[1] These equations are often referred to as Landau equations.

have been classified for PDEs in one, two and three dimensions, see Dionne and Golubitsky [20] and Dionne [19]. This classification was performed using only group theory. In Section 1.6 we present the methods which are used to reduce bifurcation problems with Euclidean symmetry to ones with a compact symmetry group.

The material in this chapter is based on that in Golubitsky *et al.* [35], Chapters XII, XIII and the other references cited in the text.

1.1 Group Theory

Let Γ be a Lie group acting linearly on a vector space $\mathbf{V}$. A subspace $\mathbf{W} \subset \mathbf{V}$ is called Γ-invariant if $\gamma\mathbf{w} \in \mathbf{W}$ for all $\mathbf{w} \in \mathbf{W}$ and $\gamma \in \Gamma$. A representation or action of Γ on $\mathbf{V}$ is irreducible if the only Γ-invariant subspaces are $\{0\}$ and $\mathbf{V}$. A subspace $\mathbf{W} \subset \mathbf{V}$ is said to be Γ-irreducible if $\mathbf{W}$ is Γ-invariant and the action of Γ on $\mathbf{W}$ is irreducible.

The Lie groups that we are concerned with, or at least will apply the theory in this chapter to, are compact. Of major importance to the theory of compact Lie groups is the existence of a left (right) invariant integral, the *Haar integral* on the group Γ. The existence of such an integral leads to the following fundamental decomposition theory for compact Lie groups.

Theorem 1.1
Let Γ be a compact Lie group acting on a vector space $\mathbf{V}$. Then there exist Γ-irreducible subspaces $\mathbf{V}_1, \ldots, \mathbf{V}_s$ of $\mathbf{V}$ such that

$$\mathbf{V} = \mathbf{V}_1 \oplus \ldots \oplus \mathbf{V}_s.$$

Proof. See Golubitsky *et al.* [35], Chapter XII, p. 33. □

This theorem has a deficiency, in that the decomposition need not be unique. To tackle this problem we introduce the idea of isomorphic actions of a Lie group. Let Γ act on vector spaces $\mathbf{V}$ and $\mathbf{W}$. Then $\mathbf{V}$ and $\mathbf{W}$ are Γ-isomorphic if there exists a linear isomorphism $A : \mathbf{V} \to \mathbf{W}$ such that $A(\gamma \cdot \mathbf{v}) = \gamma * A(\mathbf{v})$, where $\cdot$ denotes the action of the group Γ on $\mathbf{V}$ and $*$ the action on $\mathbf{W}$. This allows us to achieve a far more useful statement than Theorem 1.1.

Remark 1.2
We will drop the $\cdot$ to denote action, and write $\gamma\mathbf{x}$ for $\gamma \cdot \mathbf{x}$.

Theorem 1.3
Let Γ be a compact Lie group acting on $\mathbf{V}$. Then

1. *Up to Γ-isomorphism there exist a finite number of distinct Γ-irreducible subspace of $\mathbf{V}$. Denote these subspaces by $\mathbf{U}_1, \ldots, \mathbf{U}_t$.*
2. *Define $\mathbf{W}_k$ to be the sum of all Γ-irreducible subspaces $\mathbf{W}$ of $\mathbf{V}$ such that $\mathbf{W}$ is Γ-isomorphic to $\mathbf{U}_k$.*

Then

$$\mathbf{V} = \mathbf{W}_1 \oplus \ldots \oplus \mathbf{W}_t. \tag{1.1}$$

The subspaces $\mathbf{W}_k$ are called *isotypic components* of $\mathbf{V}$ of type $\mathbf{U}_k$ for the action of Γ. The decomposition (1.1) is called the *isotypic decomposition.*

Proof. See Golubitsky *et al.* [35], Chapter XII, pages 36–38. □

There is a stronger notion of irreducible actions and representations of Lie groups which is more suited to our needs. A representation of a group Γ on $\mathbf{V}$ is *absolutely irreducible* if the only

linear map commuting with the action of Γ is a real scalar multiple of the identity. If a representation of a group is absolutely irreducible then it is irreducible in the sense introduced above. In general the converse is not true except for complex (rather than real) representations. In this case Schur's lemma provides the required correspondence between the two representations.

1.2 Invariant Theory

Let Γ be a Lie group acting on a vector space $\mathbf{V}$. A real-valued function $f : \mathbf{V} \to \mathbb{R}$ is invariant under Γ, or Γ-invariant if

$$f(\gamma \mathbf{x}) = f(\mathbf{x}) \tag{1.2}$$

for all $\mathbf{x} \in \mathbf{V}$ and $\gamma \in \Gamma$. An invariant polynomial is a real-valued polynomial satisfying (1.2). Let $\mathcal{P}_\Gamma$ denote the set of invariant polynomials. If Γ is compact, then the Hilbert-Weyl theorem guarantees a finite set of generating invariant polynomials, called a *Hilbert basis* for the ring $\mathcal{P}_\Gamma$ (see Golubitsky *et al.* [35], p. 46.) Let $\mathcal{E}_\Gamma$ denote the ring of Γ-invariant germs $\mathbf{V} \to \mathbb{R}$. Then we have the following.

Theorem 1.4 (Schwarz)
Let Γ be a compact Lie group acting on a vector space $\mathbf{V}$. Let $u_1, \ldots, u_s$ be a Hilbert basis for $\mathcal{P}_\Gamma$. Let $f \in \mathcal{E}_\Gamma$. Then there exists a smooth germ $h : \mathbb{R}^s \to \mathbb{R}$ such that

$$f(\mathbf{x}) = h\left(u_1(\mathbf{x}), \ldots, u_s(\mathbf{x})\right).$$

Proof. See Golubitsky *et al.* [35], Chapter XII, p. 46. □

A mapping $\mathbf{g} : \mathbf{V} \to \mathbf{V}$ is Γ-equivariant if

$$\mathbf{g}(\gamma \mathbf{x}) = \gamma \mathbf{g}(\mathbf{x})$$

for all $\gamma \in \Gamma$ and $\mathbf{x} \in \mathbf{V}$. Let $\vec{\mathcal{P}}_\Gamma$ and $\vec{\mathcal{E}}_\Gamma$ denote the set of equivariant polynomials and smooth germs respectively. Then $\vec{\mathcal{P}}_\Gamma$ is a module over the ring $\mathcal{P}_\Gamma$ and similarly $\vec{\mathcal{E}}_\Gamma$ is a module over the ring $\mathcal{E}_\Gamma$. The equivariant polynomials $\mathbf{g}_1, \ldots, \mathbf{g}_r$ generate $\vec{\mathcal{P}}_\Gamma$ over $\mathcal{P}_\Gamma$ if every Γ-equivariant polynomial $\mathbf{g}$ may be written

$$\mathbf{g} = f_1 \mathbf{g}_1 + \ldots + f_r \mathbf{g}_r$$

for invariant polynomials $f_1, \ldots, f_r$. The definition for generating equivariants of $\vec{\mathcal{E}}_\Gamma$ over $\mathcal{E}_\Gamma$ is analogous. If Γ is a compact Lie group then there exists a finite set of Γ-equivariant polynomials $\mathbf{g}_1, \ldots, \mathbf{g}_r$, which generate the module $\vec{\mathcal{P}}_\Gamma$, (Theorem 5.2 of Golubitsky *et al.* [35]). The following theorem due to Poénaru gives a critical relation between the generators of $\vec{\mathcal{P}}_\Gamma$ over $\mathcal{P}_\Gamma$, and those for the module $\vec{\mathcal{E}}_\Gamma$ over the ring $\mathcal{E}_\Gamma$.

Theorem 1.5 (Poénaru)
Let Γ be a compact Lie group and let $\mathbf{g}_1, \ldots, \mathbf{g}_r$ generate $\vec{\mathcal{P}}_\Gamma$ over $\mathcal{P}_\Gamma$, then $\mathbf{g}_1, \ldots, \mathbf{g}_r$ generate $\vec{\mathcal{E}}_\Gamma$ over $\mathcal{E}_\Gamma$.

Proof. See Golubitsky *et al.* [35], Chapter XII, p. 51. □

Poincaré Series

The computation of the invariants and equivariants for an arbitrary action of a compact Lie group Γ on a vector space $\mathbf{V}$ is, at best, complex. However, there is a computational tool, which provides us with help in this direction. Here we introduce Poincaré series (or Hilbert series), these series are generating functions for the invariants and equivariants, providing us with the

number of invariants or equivariants of a chosen degree. The material presented here can be found in Chossat and Lauterbach [12].

Let Γ be a compact Lie group acting linearly on a vector space $\mathbf{V}$ which we identify with $\mathbb{R}^n$. Choose coordinates $x_1, \ldots, x_n$ on $\mathbb{R}^n$ relative to the basis on $\mathbf{V}$. Given any $\gamma \in \Gamma$ the action of γ is given by a matrix M with real entries. It is convenient to view the matrix M as acting on $\mathbb{C}^n$, this action is given by using the matrix M but regarding the entries as complex. There is a natural inclusion of the ring of polynomials $\mathbb{R}[x_1, \ldots, x_n]$ in the ring of complex polynomials $\mathbb{C}[x_1, \ldots, x_n]$. A basis over $\mathbb{R}$ for the vector space of Γ-invariant polynomials of degree d is also a basis over $\mathbb{C}$ for the complex vector space of Γ-invariant polynomials of degree d. The polynomial ring $\mathbb{C}[x_1, \ldots, x_n]$ is graded,

$$\mathbb{C}[x_1, \ldots, x_n] = R_0 \oplus R_1 \oplus R_2 \oplus \ldots,$$

where R_i is the vector space of all homogeneous polynomials of degree i. Therefore the ring of Γ-invariant polynomials $\mathcal{P}_\Gamma$ over $\mathbf{V}$ is also graded,

$$\mathcal{P}_\Gamma = \mathcal{P}_\Gamma^0 \oplus \mathcal{P}_\Gamma^1 \oplus \mathcal{P}_\Gamma^2 \oplus \ldots,$$

where $\mathcal{P}_\Gamma^i = \mathcal{P}_\Gamma \cap R_i$.

Definition 1.6
The *Poincaré series* of the graded algebra $\mathcal{P}_\Gamma$ is the generating function for $\dim \mathcal{P}_\Gamma^d$ for $d = 0, 1, \ldots$. This generating function is

$$\Upsilon_\Gamma(t) = \sum_{d=0}^{\infty} \dim\ (\mathcal{P}_\Gamma^d)\, t^d.$$

There is an explicit formula for this generating function due to Molien, see Chossat and Lauterbach [12].

Theorem 1.7
Let Γ be a compact Lie group acting on a vector space $\mathbf{V}$. Then the Poincaré series of $\mathcal{P}_\Gamma$ is

$$\Upsilon_\Gamma(t) = \int_\Gamma \frac{1}{det(1_\Gamma - \gamma t)},$$

where the integral is with respect to the Haar measure on Γ and 1_Γ is the identity in Γ.

In general such an integral can be difficult to compute, but such difficulties can be resolved with the use of the *Symmetry* package [28] for Maple [66]. The coefficents of the Poincaré series for the invariants provide the number of invariant polynomials of a particular degree; the coefficent of the t^j term gives the number of polynomial invariants of degree j. This provides an upper bound for the number of generators at a particular degree. However, it does not tell us how many generators there are, which can be less.

Next we consider the equivariants. The result is simple since equivariant can be regarded as invariants with respect to a different group action.

Definition 1.8
The *Poincaré series* of the graded module $\vec{\mathcal{P}}_\Gamma$ over the ring $\mathcal{P}_\Gamma$ is the generating function

$$\Xi_\Gamma(z) = \sum_{d=0}^{\infty} \dim\ \left(\vec{\mathcal{P}}_\Gamma^d\right) z^d.$$

There is an explicit formula, see Chossat and Lauterbach [12].

Theorem 1.9
Let Γ be a compact Lie group acting on a vector space $\mathbf{V}$. Then the Poincaré series of the module $\vec{\mathcal{P}}_\Gamma$ over the ring $\mathcal{P}_\Gamma$ is

$$\Xi_\Gamma(z) = \int_\Gamma \frac{tr(\gamma^{-1})}{det(1_\Gamma - \gamma z)},$$

where the integral is with respect to the Haar measure on Γ.

For orthogonal representations, that is when $\Gamma \subseteq \mathbf{O}(n)$, we have $\mathrm{tr}(\gamma^{-1}) = \mathrm{tr}(\gamma)$. As for the invariants we can use the Symmetry package to aid the computation of the Poincaré series for the equivariants. The Poincaré series for the equivariants tells us the number of polynomial equivariants at a choosen degree. So, the coefficent of the t^j term in the series provides us with the number of equivariants of degree j. This information is very useful when computing equivariant vector fields to a particular degree; it provides a check that ensures all equivariant terms are present.

1.3 Steady-State Symmetry-Breaking

To study the steady-state symmetry-breaking bifurcations of systems of ODEs

$$\frac{\mathrm{d}\mathbf{x}}{\mathrm{d}t} + \mathbf{g}(\mathbf{x}, \lambda) = 0, \tag{1.3}$$

where $\mathbf{g} : \mathbb{R}^n \times \mathbb{R} \to \mathbb{R}^n$ is Γ-equivariant, $\mathbf{x} \in \mathbb{R}^n$ and $\lambda \in \mathbb{R}$ is a bifurcation parameter, we develop the essential ideas, which are required to state the fundamental existence and uniqueness result for solutions to (1.3). We assume that $\mathbf{g}(\mathbf{0}, 0) = \mathbf{0}$ and that (1.3) has undergone the Liapunov–Schmidt reduction (see Golubitsky and Schaeffer [31],) so we may assume that $(\mathrm{d}\mathbf{g})_{0,0} = \mathbf{0}$. It is (one of) the aims of equivariant bifurcation theory to classify a class of solutions to generic equations of the form (1.3). The next proposition together with the Liapunov–Schmidt reduction provides us with the assumption that the action of Γ on $\mathbb{R}^n$ in (1.3) is absolutely irreducible.

Proposition 1.10
Let $\mathbf{g} : \mathbb{R}^N \times \mathbb{R} \to \mathbb{R}^N$ be a one-parameter family of Γ-equivariant mappings with $\mathbf{g}(\mathbf{0}, 0) = \mathbf{0}$. Let $V = \ker(\mathrm{d}\mathbf{g})_{0,0}$. Then generically the action of Γ on V is absolutely irreducible.

Proof. This is Golubitsky *et al.* [35], Chapter XIII, p. 82. □

The *orbit* of a Lie group Γ acting on a vector space $\mathbf{V}$ at $\mathbf{x} \in \mathbf{V}$ is the set

$$\Gamma\mathbf{x} = \{\gamma\mathbf{x} | \gamma \in \Gamma\}.$$

Note that if $\mathbf{g}$ is Γ-equivariant and $\mathbf{g}(\mathbf{x}) = \mathbf{0}$ then $\mathbf{g}(\gamma\mathbf{x}) = \mathbf{0}$ for all $\gamma \in \Gamma$. So $\mathbf{g}$ vanishes on the whole orbit of $\mathbf{x}$. As far as the map $\mathbf{g}$ is concerned, we cannot distinguish between points which lie in the same orbit. The *isotropy subgroup* of $\mathbf{x} \in \mathbf{V}$ is

$$\Sigma_\mathbf{x} = \{\gamma \in \Gamma | \gamma\mathbf{x} = \mathbf{x}\}.$$

The isotropy subgroup provides a measure of how much symmetry a solution $\mathbf{x} \in \mathbf{V}$ has. Often we will use the more compact terminology "isotropy" rather than "isotropy subgroup" of a solution. The calculation of isotropy subgroups is greatly simplified by the simple observation that points on the same group orbit have conjugate isotropy subgroups, that is

$$\Sigma_{\gamma\mathbf{x}} = \gamma\Sigma_\mathbf{x}\gamma^{-1}$$

for all $\gamma \in \Gamma$. To all isotropy subgroups $\Sigma_{\mathbf{x}} \subset \Gamma$ there is an associated vector subspace of $\mathbf{V}$

$$\mathrm{Fix}_{\mathbf{V}}(\Sigma) = \{\mathbf{v} \in \mathbf{V} \big| \sigma\mathbf{v} = \mathbf{v}\}$$

called the fixed-point subspace of Σ. It is usual to drop the $\mathbf{V}$ and just write $\mathrm{Fix}(\Sigma)$. Importantly, the fixed-point subspace is invariant under all Γ-equivariant mappings, even though they may be nonlinear.

A bifurcation problem with symmetry group Γ is a germ $\mathbf{g}$ satisfying $\mathbf{g}(\mathbf{0}, 0) = \mathbf{0}$, $(\mathrm{d}\mathbf{g})_{0,0} = \mathbf{0}$ and $\mathbf{g}$ is Γ-equivariant, that is $\mathbf{g}(\gamma\mathbf{x}, \lambda) = \gamma\mathbf{g}(\mathbf{x}, \lambda)$. Now assume that the action of Γ on $\mathbf{V}$ is absolutely irreducible, as we may by Proposition 1.10. Since $\mathbf{g}(\gamma\mathbf{x}, \lambda) = \gamma\mathbf{g}(\mathbf{x}, \lambda)$ we have

$$(\mathrm{d}\mathbf{g})_{0,\lambda}\gamma = \gamma(\mathrm{d}\mathbf{g})_{0,\lambda}.$$

Hence $(\mathrm{d}\mathbf{g})_{0,\lambda} = c(\lambda)\mathrm{I}$ by absolute irreducibility, where I denotes the identity matrix. Since $(\mathrm{d}\mathbf{g})_{0,0} = \mathbf{0}$ it follows that $c(0) = 0$. Assuming generically that

$$c'(0) \neq 0, \tag{1.4}$$

we may now state the fundamental existence and uniqueness result for steady-state bifurcation problems with symmetry.

Theorem 1.11 (Equivariant Branching Lemma)
Let Γ be a Lie group acting absolutely irreducibly on a vector space $\mathbf{V}$, and let $\mathbf{g}$ be a Γ-equivariant bifurcation problem satisfying (1.4). Let Σ be an isotropy subgroup satisfying

$$\dim \mathrm{Fix}(\Sigma) = 1.$$

Then there exists a unique smooth branch of solutions to $\mathbf{g} = \mathbf{0}$ such that the isotropy subgroup of each solution is Σ.

In fact there is a slightly different formulation of this result given by Golubitsky *et al.* [35], which can be useful in certain applications. We use the non-standard name "alternative equivariant branching lemma".

Theorem 1.12 (Alternative Equivariant Branching Lemma)
Let Γ be a Lie group acting on a vector space $\mathbf{V}$. Assume

1. $\mathrm{Fix}(\Gamma) = \{0\}$.
2. *$\Sigma \subset \Gamma$ is an isotropy subgroup satisfying* $\dim \mathrm{Fix}(\Sigma) = 1$.
3. *$\mathbf{g} : \mathbf{V} \times \mathbb{R} \to \mathbf{V}$ is a Γ-equivariant bifurcation problem satisfying*

$$(\mathrm{d}\mathbf{g}_\lambda)_{0,0}(\mathbf{v}_0) \neq \mathbf{0}$$

where $\mathbf{v}_0 \in \mathrm{Fix}(\Sigma)$ is nonzero.

Then there exist a smooth branch of solutions $(t\mathbf{v}_0, \lambda(t))$ to $\mathbf{g}(t, \lambda) = \mathbf{0}$.

Proof. See Golubitsky *et al.* [35], Chapter XIII, p. 83. □

Following Golubitsky *et al.* [34] we call isotropy subgroups which satisfy the condition $\dim \mathrm{Fix}(\Sigma) = 1$, *axial subgroups*. The equivariant branching lemma gives a recipe for finding branches of solutions to steady-state bifurcation problems with symmetry. Given an isotropy subgroup $\Sigma \subset \Gamma$, compute $\dim \mathrm{Fix}(\Sigma)$. If $\dim \mathrm{Fix}(\Sigma) = 1$ there is a guaranteed solution branch. However, we have no idea if any of the solution branches we find using the equivariant branching lemma are stable or unstable.

1.4 Stability of Solution Branches

We consider the stability of solutions to systems of ODEs, which are equivariant under the action of a Lie group Γ. The presence of symmetry both simplifies and complicates the analysis by forcing some of the eigenvalues of the Jacobian matrix $(\mathrm{d}\mathbf{g})$ at a solution to zero.

An equilibrium solution branch $\mathbf{x}_0$, of the bifurcation problem is *orbitally stable* if it is neutrally stable and whenever $\mathbf{x}(t)$ is near to $\mathbf{x}_0$ then $\lim_{t\to\infty}\mathbf{x}(t)$ exists and lies in $\Gamma\mathbf{x}_0$. There is an associated linear criterion for stability. An equilibrium $\mathbf{x}_0$ is *linearly orbitally stable* if the eigenvalues of $(\mathrm{d}\mathbf{g})$ at a solution branch $\mathbf{x}_0$, other than those forced to zero by symmetry have positive real part[2]. Indeed we have the following relation

Theorem 1.13
Linear orbital stability implies orbital stability.

Proof. This is Golubitsky *et al.* [35], Chapter XIII, p. 88. □

Before we discuss the restrictions symmetry places on the Jacobian matrix $(\mathrm{d}\mathbf{g})$ at an equilibrium, we mention the following. If the Γ-equivariant bifurcation problem contains a quadratic term, then all solutions guaranteed to exist by the equivariant branching lemma are unstable, see Golubitsky *et al.* [35], p. 89, or Ihrig and Golubitsky [54] for the original result. In this case it is necessary to consider the degenerate bifurcation problem.

Since $\mathbf{g}(\mathbf{z})$ commutes the with action of Γ, large restrictions are imposed on the eigenvalues of $(\mathrm{d}\mathbf{g})$. Let $\gamma \in \Gamma$, then $\gamma\mathbf{g}(\mathbf{z}) = \mathbf{g}(\gamma\mathbf{z})$ this implies $(\mathrm{d}\mathbf{g})_{\gamma\mathbf{z}}\gamma = \gamma(\mathrm{d}\mathbf{g})_{\mathbf{z}}$. Now if $\gamma \in \Sigma_{\mathbf{z}}$—the isotropy subgroup corresponding to the solution $\mathbf{z}$, then $(\mathrm{d}\mathbf{g})_{\mathbf{z}}$ commutes with the action of γ. We may also restrict the form of $(\mathrm{d}\mathbf{g})$ by finding null eigenvectors. Let γ_t be a smooth curve in Γ with $\gamma_0 = \mathrm{I}$, the identity in Γ, and $\mathbf{z} \in \mathbf{V}$ a solution. Then $\mathbf{g}(\mathbf{z}) = 0$ and $\mathbf{g}$ vanishes on the whole orbit of $\mathbf{z}$, that is $\mathbf{g}(\gamma_t\mathbf{z}) = \mathbf{0}$, so $(\mathrm{d}\mathbf{g})_{\mathbf{z}}\mathbf{v} = 0$ where $\mathbf{v} = \mathrm{d}(\gamma_t\mathbf{z})\big|_{t=0}$. So if γ_t is a curve in Γ that crosses $\Sigma_{\mathbf{z}}$ with nonzero speed then $(\mathrm{d}\mathbf{g})_{\mathbf{z}}$ has $\mathbf{v}$, which is nonzero, as a null eigenvector. The number of null eigenvectors is given by $\dim(\Gamma) - \dim(\Sigma_{\mathbf{z}})$.

Although the method just illustrated is very useful for calculating the eigenvalues of the Jacobian matrix at a solution, when studying more complicated bifurcation problems a second method provides a better approach. This method is more representation theoretic and uses the isotypic decomposition considered in Theorem 1.3. A theorem of Golubitsky *et al.* [35] (Chapter XII, Theorem 3.5) states that since the Jacobian is a linear map which commutes with the action of a isotropy subgroup $\Sigma \subset \Gamma$, it leaves the isotypic components of the action of Σ invariant. Therefore, if we form the isotypic decomposition of an isotropy subgroup Σ, then this gives a set of coordinates on which $(\mathrm{d}\mathbf{g})$ is in block diagonal form. The calculation of the eigenvalues can be simplified further by noting that the action of Γ will force null eigenvectors and that $(\mathrm{d}\mathbf{g})$ restricted to an isotypic component $\mathbf{W}_i$ commutes with the action of Σ on $\mathbf{W}_i$.

1.5 Heteroclinic Cycles and Networks

In this section we are interested in dynamics which manifest themselves as recurrent behaviour, where recurrent in this sense means long periods of "static" behaviour, followed by sudden changes and eventual relaxation into a new (but possibly identical up to symmetry) static state. Such behaviour is often best explained by heteroclinic cycles (or more generally networks). The material in this section is based on that contained in Chossat and Lauterbach [12] and Kirk and Silber [55].

A nonlinear dynamical system possessing a heteroclinic cycle is characterised by the following; a collection of equilibria $\{e_1, \ldots, e_n\}$ and a set of heteroclinic connections $\{h_1(t), \ldots, h_n(t)\}$, where $h_j(t) \to e_j$ as $t \to -\infty$ and $h_j(t) \to e_{j+1}$ as $t \to \infty$ and $e_{n+1} = e_1$. Such cycles are very

[2]It is a rather arbitrary choice as to whether positive or negative eigenvalues represent stable solutions. It depends if the ODE is $\dot{\mathbf{x}} = \mathbf{g}(\mathbf{x})$ or $\dot{\mathbf{x}} + \mathbf{g}(\mathbf{x}) = \mathbf{0}$ $(\dot{\mathbf{x}} = -\mathbf{g}(\mathbf{x}))$. The important point is the choice must be used consistently.

common in symmetric systems, where symmetry forces invariant subspaces, in fact they can be structurally stable, in that they persist under perturbations which respect the symmetry. One example of a structurally stable heteroclinic cycle is that of Guckenheimer and Holmes [44], which has $\mathbf{Z}_2^3 + \mathbf{Z}_3$ symmetry and is a simplified model of rotating convection considered by Busse and Heikes [5]. The definition of heteroclinic cycles has been generalised and the following is that of Krupa and Melbourne [58].

Definition 1.14
Suppose $e_1, \ldots, e_n$ are hyperbolic equilibria of (1.3) with stable and unstable manifolds $W^s(e_j)$ and $W^u(e_j)$ for $j = 1, \ldots, n$. Then the set of group orbits of the unstable manifolds

$$X = \{W^u(\gamma e_j) \big| j = 1, \ldots, n, \ \gamma \in \Gamma\}$$

forms a *heteroclinic cycle* provided dim $W^u(e_j) \geq 1$ and

$$W^u(e_j) - \{e_j\} \subseteq \bigcup_{\gamma \in \Gamma} W^s(\gamma e_{j+1}).$$

Here $e_{n+1} = e_1$.

If $n = 1$ in the above definition then the cycle X is called a *homoclinic cycle.*

Definition 1.15

1. A heteroclinic cycle X is said to be *stable* if for any neighbourhood U of X there exists a neighbourhood $V \subseteq U$ of X such that all trajectories starting in V remain in U for all forward time.

2. A heteroclinic cycle X is said to be *asymptotically stable* if X is stable and there exists a neighbourhood V of X such that all trajectories starting in V converge to X in forward time.

3. If the cycle is not stable, then it is *unstable.*

Several authors have address the stability of heteroclinic cycles. Dos Reis [22] provided a simple sufficient condition for cycles in $\mathbb{R}^2$ and this was generalised by Krupa and Melbourne [58], who give a necessary and sufficient conditions. More recently the results of Krupa and Melbourne were improved and generalised further [57]. Here a complete classification theory for (simple) heteroclinic cycles in $\mathbb{R}^4$ is achieved[3] (an increase in dimension of one over the results in Krupa and Melbourne [58]). The generalities introduced above do not serve to cover all situations we shall consider. It is possible for more general arrangements to occur where there are coexisting heteroclinic cycles, not related by symmetry. The following definition is from Kirk and Silber [55]:

Definition 1.16
Let $\mathcal{H}_1, \ldots, \mathcal{H}_n$, where $n \geq 2$ be a collection of heteroclinic cycles. We say that $\mathcal{H} = \cup_{j=1}^n \mathcal{H}_j$ forms a *heteroclinic network* if there do not exist networks (or cycles) $\mathcal{H}_1$ and $\mathcal{H}_2$ such that $\mathcal{H} = \mathcal{H}_1 \cup \mathcal{H}_2$ where $\mathcal{H}_1 \cap \mathcal{H}_2 = \emptyset$.

An alternative and more general definition can be found in [2], but Kirk and Silber's definition is sufficient for all our work. Heteroclinic networks have been found in a number of situations, of which the work of Lauterbach and Roberts [63] is of most interest to us. Although the work of Dos Reis [22] and Krupa and Melbourne [58, 57] provides stability conditions for heteroclinic cycles, they are not applicable to heteroclinic networks. The unstable manifold of an equilibrium e_j does not lie in the stable manifold of an equilibrium e_{j+1}, so the necessity condition of Krupa and Melbourne fails. In this case the cycles are not asymptotically stable.

[3]We do not state the stability results of these authors since they are not applicable to the situations we shall study.

However, Melbourne [68] has shown that nonasymptotically stable cycles can still be physically relevant. In particular Melbourne introduces "essential asymptotically stability", that is, the cycle attracts almost all trajectories which start nearby. The work of Kirk and Silber [55] studies an example heteroclinic network and derive some interesting dynamical properties, we shall comment on this later in our work.

1.6 Partial Differential Equations with Euclidean Symmetry

In this section we consider systems of PDEs which possess two-dimensional Euclidean symmetry. Since the Euclidean group is not compact, the methods of the previous sections cannot be applied. The resolution to this problem is a really an answer to the question, "What type of solutions do we seek to the PDEs?" In general we seek spatially periodic solutions, that is planforms, or patterns in everyday language. However, Euclidean invariant PDEs display more elaborate behaviour than just planforms, for example target patterns, spirals and meandering spirals, see Chossat and Lauterbach [12] and the references there in. These planforms (when we are considering the two-dimensional problem) often have rectangular, rhombic, square or hexagonal symmetry. Consequently, rather than considering the full Euclidean invariant problem, we can restrict attention to the solutions we can expect to have these discrete symmetries. For this reason we introduce the valuable ideas of lattice symmetry and Fourier series. This allow us to reduce the system of PDEs to ODEs which are equivariant under a suitable compact group. This compact group is the symmetry group of some two or three-dimensional lattice. When this reduction is complete the bifurcation problem may be studied using the standard techniques introduced previously. The material in the section is based on that contained in Dionne *et al.* [21] and Melbourne [69].

1.6.1 Problem Formulation

Consider a parametrised family of PDEs, which have the form

$$\frac{\partial}{\partial t}\mathbf{u}(\mathbf{x},t) = \mathbf{F}\left(\mathbf{u}(\mathbf{x},t),\lambda\right) \tag{1.5}$$

where $\mathbf{F} : \mathcal{X} \times \mathbb{R} \to \mathcal{Y}$ is a nonlinear operator between suitable function spaces $\mathcal{X}$ and $\mathcal{Y}$, and $\lambda \in \mathbb{R}$ is a bifurcation parameter. The function $\mathbf{u} : \mathbb{R}^m \times \mathbb{R} \to \mathbb{R}^n$ is a function in $\mathcal{X}$ of a spatial variable $\mathbf{x} \in \mathbb{R}^m$ and time t.

We assume that (1.5) has Euclidean symmetry. The Euclidean group $\mathbf{E}(m)$ is the group of motions of $\mathbb{R}^m$ that preserve distance. This group consists of rotations, reflections and translations. It can be written as the semidirect sum of the orthogonal group $\mathbf{O}(m)$, which consists of rotations and reflection of $\mathbb{R}^m$ and the translation group of $\mathbb{R}^m$, which is the group $\mathbf{R}^m$ itself and is a normal subgroup of $\mathbf{E}(m)$, that is

$$\mathbf{E}(m) = \mathbf{O}(m) \dot{+} \mathbf{R}^m.$$

We denote an element of $\mathbf{E}(m)$ by $(\mathbf{A},\mathbf{b})$, where $\mathbf{A} \in \mathbf{O}(m)$ and $\mathbf{b} \in \mathbf{R}^m$. The action of $(\mathbf{A},\mathbf{b})$ on $\mathbb{R}^m$ is defined by

$$(\mathbf{A},\mathbf{b})\mathbf{x} = \mathbf{A}\mathbf{x} + \mathbf{b}.$$

This action means that the product of two elements $(\mathbf{A},\mathbf{b})$ and $(\mathbf{C},\mathbf{d}) \in \mathbf{E}(m)$ is given by

$$(\mathbf{A},\mathbf{b})(\mathbf{C},\mathbf{d}) = (\mathbf{AC},\mathbf{b}+\mathbf{Ad}).$$

Now there are various ways that the Euclidean group can act on functions $\mathbf{u} : \mathbb{R}^m \times \mathbb{R} \to \mathbb{R}^n$, depending on the value of n. Bosch Vivancos *et al.* [3] consider two-dimensional Euclidean systems and demonstrates that the nature of this action is crucial to the bifurcation problem and the expected planforms. Melbourne [69] extends this work to the general setting.

1.6.2 Actions of the Euclidean Group

We consider how different actions of the Euclidean group $\mathbf{E}(m)$ on the functions $\mathbf{u} : \mathbb{R}^m \times \mathbb{R} \to \mathbb{R}^n$ affect the nature of the bifurcation problem. We follow the work of Melbourne [69]. Let $h : \mathbf{O}(m) \to GL(\mathbb{R}^n)$ be a representation of $\mathbf{O}(m)$ on $\mathbb{R}^n$ and let $h_\mathbf{A}$ be the image of $\mathbf{A} \in \mathbf{O}(m)$ under h.

Definition 1.17
A *physical action* of $\mathbf{E}(m)$ on $\mathbf{u} : \mathbb{R}^m \times \mathbb{R} \to \mathbb{R}^n$ is an action which takes the form

$$(\gamma\mathbf{u})(\mathbf{x}, t) = h_\mathbf{A}\mathbf{u}(\gamma^{-1}\mathbf{x}, t)$$

for all $\gamma = (\mathbf{A}, \mathbf{b}) \in \mathbf{E}(m)$ and $(\mathbf{x}, t) \in \mathbb{R}^m \times \mathbb{R}$.

For the case $n = 1$, the only physical actions of $\mathbf{E}(2)$ are *scalar* and *pseudoscalar* actions. These correspond to $h_\mathbf{A} = \mathrm{I}$ and $h_\mathbf{A} = \det(\mathbf{A})$. We say that a PDE is scalar or pseudoscalar if the action of the Euclidean group is scalar or pseudoscalar respectively. Reaction-diffusion systems provide examples of scalar PDEs, and the Navier–Stokes equations provide an example of a pseudoscalar set of PDEs. Bosch Vivancos *et al.* [3] show that the expected planforms in pseudoscalar systems are different from those in a scalar systems. This distinction between planforms is due to the different group action and interpretations of the symmetries in the physical space of the system. Golubitsky and Stewart [33] discuss many examples including fluid flow, liquid crystals and the primary visual cortex, where the correct interpretation of the symmetry group (and in particular the eigenfunctions) is critical. Melbourne [69] shows that in three dimensions the situation is more complicated. In addition to scalar and pseudoscalar actions, there exists a countable infinity of physical actions of $\mathbf{E}(3)$. These actions are in correspondence with the two-dimensional representations of $\mathbf{O}(2)$. In fact more is proved: the steady-state bifurcation of an $\mathbf{E}(n)$-equivariant system is in a sense determined by the irreducible representations of $\mathbf{O}(n-1)$.

1.6.3 Symmetry-Breaking Bifurcations

We assume that there is an Euclidean-invariant time-independent solution of (1.5) for all values of λ. Without loss of generality we assume that this spatially uniform solution corresponds to $\mathbf{u} = \mathbf{0}$, that is

$$\mathbf{F}(\mathbf{0}, \lambda) = \mathbf{0}.$$

Furthermore, we assume that this solution is stable for $\lambda < 0$, unstable for $\lambda > 0$ and that $\lambda = 0$ corresponds to a steady-state symmetry-breaking bifurcation point. The critical problem when considering symmetry-breaking bifurcations with $\mathbf{E}(m)$ symmetry is that this group is not compact. This causes great difficulties when attempting to apply either the Liapunov–Schmidt reduction [31] or centre manifold theorem [87] to the PDEs, due to the presence of infinite dimensional representations. The standard method for overcoming this difficulty is to seek spatially periodic, time-independent solutions $\mathbf{u}(\mathbf{x}, t)$ to (1.5).

Lattices and Dual Lattices

First some terminology:

Definition 1.18
An *m-dimensional lattice* is generated by m linearly independent vectors $\boldsymbol{\ell_1} \ldots \boldsymbol{\ell_m} \in \mathbb{R}^m$

$$\mathcal{L} = \{n_1\boldsymbol{\ell_1} + \ldots + n_m\boldsymbol{\ell_m} | n_1, \ldots n_m \in \mathbb{Z}\}.$$

We say that a function $\mathbf{u}$ is $\mathcal{L}$-periodic if $\mathbf{u}(\mathbf{x} + \boldsymbol{\ell}) = \mathbf{u}(\mathbf{x})$ for all $\boldsymbol{\ell} \in \mathcal{L}$. The subspace $\mathcal{X}_\mathcal{L} \subset \mathcal{X}$ of periodic functions is $\mathcal{X}_\mathcal{L} = \{f \in \mathcal{X} | f(\mathbf{x} + \boldsymbol{\ell}) = f(\mathbf{x}) \text{ for all } \boldsymbol{\ell} \in \mathcal{L}\}$.

Definition 1.19
The *dual lattice* $\mathcal{L}^*$ of $\mathcal{L}$ is the set

$$\mathcal{L}^* = \left\{ \mathbf{k} \in \mathbb{R}^m \,\middle|\, \mathbf{x} \mapsto e^{2\pi i \mathbf{k}\cdot\mathbf{x}} \text{ is } \mathcal{L}\text{-periodic} \right\}.$$

The functions $e^{2\pi i \mathbf{k}\cdot\mathbf{x}}$ are called *plane waves*. When restricting the solutions of (1.5) to the subspace $\mathcal{X}_\mathcal{L}$ of $\mathcal{L}$-periodic functions, the group of symmetries Γ is a compact group. Specifically, Γ is the largest group constructed from $\mathbf{E}(m)$ that preserves $\mathcal{X}_\mathcal{L}$ and $\mathcal{Y}_\mathcal{L}$, that is $\gamma\mathcal{X}_\mathcal{L} \subset \mathcal{X}_\mathcal{L}$ for all $\gamma \in \Gamma$. Now Γ has a semidirect product form

$$\Gamma = \mathbf{H}_\mathcal{L} \dot{+} \mathbf{T}^m$$

where $\mathbf{H}_\mathcal{L} \subset \mathbf{O}(m)$ is the finite subgroup of rotations and reflections that preserves the lattice and $\mathbf{T}^m = \mathbb{R}^m/\mathcal{L}$ is the m-torus of translations modulo the lattice. The discrete group $\mathbf{H}_\mathcal{L}$ is called the *holohedry* of the lattice.

Since (1.5) is assumed to undergo a steady-state bifurcation at $\lambda = 0$, we demand that

$$\mathbf{V} = \ker(\mathrm{d}\mathbf{F})_{\mathbf{0},0} \neq \{0\}.$$

We are considering $\mathcal{L}$-periodic solutions, so $\mathbf{V}$ is finite dimensional and generically by Proposition 1.10, the action of Γ on $\mathbf{V}$ is absolutely irreducible. Hence by applying the Liapunov–Schmidt reduction (or Centre Manifold Theorem) we achieve a finite dimensional bifurcation problem.

1.6.4 Fourier Series

We assume that a general $\mathbf{u} \in \mathcal{X}_\mathcal{L}$ can be expanded in a convergent Fourier series

$$u_j(\mathbf{x},t) = \sum_{\mathbf{k}\in\mathcal{L}^*} (a_{j,\mathbf{k}}(t) e^{2\pi i \mathbf{k}\cdot\mathbf{x}} + c.c.) \quad j = 1,\ldots,n$$

where $a_{j,\mathbf{k}} \in \mathbb{C}$ is the time-independent amplitude of the $\mathbf{k}^{\text{th}}$ Fourier mode and *c.c.* denotes complex conjugate. The set of equilibrium solutions

$$\left\{ A_\mathbf{k} e^{2\pi i \mathbf{k}\cdot\mathbf{x}} \right\}$$

where $|\mathbf{k}| = k_c$, of the linearized problem at $\lambda = 0$ are called *critical* or *neutral* modes. The sphere $|\mathbf{k}| = k_c$ in the m-dimensional $\mathbf{k}$-space is called the *critical sphere*. The $A_\mathbf{k}$'s are constant n-dimensional vectors, unique up to scalar multiple. The dimension of the bifurcation problem depends on the number of vectors $\mathbf{k} \in \mathcal{L}^*$ which lie on the critical sphere. Now we may identify the kernel of the linear operator $(\mathrm{d}\mathbf{F})_{(\mathbf{0},0)}$

$$\ker((\mathrm{d}\mathbf{F})_{(\mathbf{0},0)}) = \left\{ \mathbf{u} = \sum_{j=1}^{s} z_j e^{2\pi i \mathbf{K}_j\cdot\mathbf{x}} \mathbf{u}_j + c.c. \,\middle|\, z_j \in \mathbb{C},\ |\mathbf{K}_j| = k_c \right\}$$

with the vector space

$$\begin{aligned} \mathbf{V} &= \left\{ \mathbf{v} = \sum_{j=1}^{s} z_j e^{2\pi i \mathbf{K}_j\cdot\mathbf{x}} + c.c. \,\middle|\, z_j \in \mathbb{C},\ |\mathbf{K}_j| = k_c \right\} \\ &\cong \mathbb{C}^s \end{aligned} \tag{1.6}$$

where the isomorphism between $\mathbf{V}$ and $\mathbb{C}^s$ is naturally defined as $\mathbf{v} \mapsto \mathbf{z} = (z_1,\ldots,z_s)$. As a real vector space $\dim(\mathbf{V}) = 2s$. The PDEs, by a Liapunov–Schmidt reduction or restriction to the centre manifold, give a system of ODEs

$$\dot{\mathbf{z}} = \mathbf{g}(\mathbf{z},\lambda) \quad \text{where } \mathbf{g} : \mathbb{C}^s \times \mathbb{R} \to \mathbb{C}^s. \tag{1.7}$$

Here $\mathbf{g}(\mathbf{0}, \lambda) = \mathbf{0}$ and the Jacobian matrix at the bifurcation point $(\mathrm{d}\mathbf{g})_{\mathbf{0},0}$, is the zero matrix. Note in particular that if Γ is the symmetry group of (1.7) then $\mathbf{g}(\mathbf{z}, \lambda)$ satisfies the equivariance condition

$$\gamma\mathbf{g}(\mathbf{z}, \lambda) = \mathbf{g}(\gamma\mathbf{z}, \lambda) \quad \text{for all } \gamma \in \Gamma.$$

The action of the group Γ can be computed explicitly on $\mathbb{C}^s$ by considering its action on the critical Fourier modes in (1.6). Once this action is calculated, the isotropy subgroups and their dimensions maybe found and so the equivariant branching lemma guarantees the existence of solutions for those subgroups, which are axial. Following Golubitsky *et al.* [34] we call the planforms associated to the axial subgroups, *axial planforms.*

Chapter 2

Forced Symmetry Breaking

In this chapter we study general equivariant systems as "first order" approximations to physical systems, and show how the solutions of such models can behave when "second order" effects are considered. These rather cryptic remarks will be made precise below. For the moment it suffices to understand them in the following sense. A mathematical model of a physical system may, by reasonable modelling hypothesis, have more symmetry than the real system. Provided the symmetry is "close" enough to the real system, the solutions of this model should capture the key properties of the physical system. This is a first order approximation. Suppose we now add some additional information to the model, which slightly perturbs the model to one with less symmetry. This new model should illuminate additional features not present in the original system, giving a second order approximation to the physical system. An example should make the ideas clear. Suppose we wish to model convection in the Sun (or any star for that matter). A reasonable modelling hypothesis is to assume the Sun is a sphere and so the modelling equations have full spherical symmetry—this is the first order model. However, the Sun is rotating, so a natural improvement is to perturb the system slightly to include (small) terms, which respect only the rotation of the Sun—this gives a second order approximation. Naturally, this process can be continued until we have a system with no symmetry, but then the question must be asked, what properties of the physical system are significant? There are an infinite number of ways to break the symmetry of a first order system so that it has no symmetry!

In this chapter we study the "forced symmetry breaking" of steady-state solutions to systems of equivariant differential equations. The meaning of forced symmetry breaking[1] is the addition of explicit terms to the system of equations which break the symmetry to some smaller group. The aim of this chapter is to give a treatment of the ideas required to study this topic in a systematic, rather than an *ad hoc*, way.

Let Γ be a (compact) Lie group. Suppose that we have a system of ODEs

$$\dot{\mathbf{z}} = \mathbf{f}(\mathbf{z}, \lambda), \tag{2.1}$$

where $\mathbf{f} : \mathbf{V} \times \mathbb{R} \to \mathbf{V}$ is Γ-equivariant and $\lambda \in \mathbb{R}$ is a bifurcation parameter. There are two distinct problems that arise through forced symmetry breaking of (2.1). The first and most difficult is to consider the effect of adding terms to equation (2.1) on all points in $\mathbf{V}$. The difficulty with this approach (as discussed by Lauterbach [61]) is the occurrence of multiple eigenvalues and bifurcation points, yielding highly complex calculations and bifurcation diagrams. Such complexities render such a direct, and general approach, inapplicable to many problems. The second approach asked a more specific question. We consider a single (steady-state) solution $\mathbf{x} \in \mathbf{V}$ to (2.1). As we know (from Chapter 1) the solution $\mathbf{x} \in \mathbf{V}$ forms a group orbit $\widetilde{X} = \Gamma\mathbf{x}$ of solutions. The group orbit $\widetilde{X}$ is (under generic conditions) a (normally hyperbolic) submanifold of $\mathbf{V}$ (see Field [25] for the conditions for normally hyperbolicity). Thus a more tractable

[1] There are many other names in the literature for what we call forced symmetry breaking, for example, system symmetry breaking, explicit symmetry breaking.

object to study is $\widetilde{X}$ rather than the entire space $\mathbf{V}$. The question we ask is, how does the group orbit $\widetilde{X}$ behave when we add symmetry breaking terms to (2.1)? Of course by asking a more specific question, and focusing on a single geometric object representing a single solution, the general behaviour of (2.1) will be lost. However, from a computational point of view, we find this second method the only sensible approach to take and so focus on this process.

Many authors have studied forced symmetry breaking of various equivariant systems, both steady-state [30] and Hopf [14, 16, 48, 60]. The techniques of these authors have, in general, used the first method considered above. These works are interested in the persistence (or not) of equilibria, although the behaviour of homoclinic cycles has been considered [11]. Golubitsky and Schaeffer [30] discuss forced symmetry breaking via singularity theory, making a distinction between the problem when the symmetry group of (2.1) is finite, and when it is continuous. When the group Γ is finite the codimension of the bifurcation problem is finite and is still finite when the symmetry is ignored. Thus it is possible to formulate a singularity theory approach to forced symmetry breaking in this case. However, when the symmetry group Γ has a continuous component the bifurcation problem has infinite codimension (the example in the paper being $\Gamma = \mathbf{O}(2)$). It is shown that by considering a larger class of equivalences a finite codimension problem can be formulated, so it is possible to use singularity theory to study forced symmetry breaking. Although this approach could be interesting, this is really only theoretical. One only has to view the paper of Buzano and Golubitsky [6] to see that the singularity theory of forced symmetry breaking would be very messy to say the least. Indeed, since the original formulation of this idea (in 1983) there has been little work in this direction, although the papers of Furter *et al.* [27, 26] are notable. More recently, Dangelmayr and Knobloch [16] and Crawford and Knobloch [14] studied the forced symmetry breaking of an $\mathbf{O}(2)$ symmetric Hopf bifurcation. Two different cases are considered: (1) degenerate bifurcations when the reflection symmetry is broken [14] and (2) nondegenerate bifurcation when the circular symmetry is broken [16]. An interesting example was considered by Chossat [11]. Here the reflection symmetry of an $\mathbf{O}(2)$-symmetric homoclinic cycle was broken. It was shown that there exists a dense open set of $\mathbf{SO}(2)$-equivariant perturbations which give quasiperiodic flow on a 2-torus.

Even though interesting results have been derived using the first approach, the methods employed are not universal and in the $\mathbf{O}(2)$ cases often exploit the fact the equations can be decoupled. We will focus on a systematic approach to the second problem—what happens to the group orbit of a solution? Crucially a formulation has recently been given to this problem [62, 63]. This approach has focused mainly on $\mathbf{O}(3)$ forced symmetry breaking from steady-state solutions, although a recent result on Hopf bifurcation has appeared [47]. In this chapter we present a formulation of the steady-state theory of forced symmetry breaking and make an extension to the Euclidean equivariant context.

Let Γ be a (compact) Lie group acting on a manifold X. Let Σ be the isotropy subgroup of $\mathbf{x} \in X$ and Δ a (closed) subgroup of Γ. This chapter is organised as follows. In Section 2.1 we study invariant (sub)manifolds of X, in particular Subsection 2.1.1 introduces normally hyperbolic manifolds. Normal hyperbolicity is fundamental to the persistence of certain types of manifolds and their structure under perturbations. In Subsection 2.1.2 we consider equivariant flows and show that a Δ-equivariant flow on a submanifold $\widetilde{X} \subset X$ can be realised as the restriction of a Δ-equivariant flow on X. Next in Section 2.2 we consider group actions on the homogeneous space Γ/Σ, which is diffeomorphic to the group orbit. We begin a systematic approach to the problem of forced symmetry breaking in Section 2.3, where flow invariant decompositions $\mathscr{C}_\Delta$ and $\mathbb{X}_\Delta$ of Γ/Σ are introduced. In Subsection 2.3.2 we illustrate how the group action of Δ on Γ/Σ can be exploited to help determine the form of $\mathbb{X}_\Delta$. Next in Subsection 2.3.3 we project $\mathbb{X}_\Delta$ into the orbit space. This projection "forgets" the group structure and allows us in Subsection 2.3.4 to prove the existence of equilibria, heteroclinic connections and periodic orbits on $\mathbb{X}_\Delta$ (depending on the structure of $\mathbb{X}_\Delta$). In Section 2.4 we provide a classification of $\mathbb{X}_\Delta$ which can be performed using only group theory. Until this point all the theory has focused on the "model" space $\widetilde{X}$ for the true (and unknown) perturbed invariant manifold $\widetilde{X}_\varepsilon$. In Section 2.5 we formulate a collection of results which allow us to relate the behaviour of Δ-equivariant vector fields on $\widetilde{X}$ to their behaviour on $\widetilde{X}_\varepsilon$. Finally, in

Section 2.6 we discuss forced symmetry breaking of Euclidean invariant PDEs.

All material in the chapter is based on Lauterbach and Roberts [63], Lauterbach *et al.* [62] and Maier-Paape and Lauterbach [65] and the other references cited in the text.

2.1 Invariant Manifolds

In this section we address the following issue. Given a manifold X which is invariant under a vector field f, what happens to X if this vector field is perturbed? In particular our intended application is when the invariant manifold is the group orbit of steady-state solutions to a Γ-equivariant system of equations. We begin with the definition of normal hyperbolicity. Normal hyperbolicity is of extreme importance to the persistence of manifolds under perturbations.

2.1.1 Normally Hyperbolic Manifolds

The work of Hirsh *et al.* [49] gives a very comprehensive treatment of normally hyperbolic manifolds and their importance to persistence of manifolds under perturbations. Let us begin by defining what is meant by a normally hyperbolic manifold.

Definition 2.1 (Chossat and Lauterbach [12])
Let X be a finite dimensional smooth manifold. Let TX be the tangent bundle of X. Let $\tilde{X} \subset X$. Denote by $TX|_{\tilde{X}}$ the restriction of TX to $\tilde{X}$ and $T\tilde{X}$ the tangent bundle of $\tilde{X}$. Let $f : X \to TX$ be a vector field and Φ the flow on X corresponding to f. Let $\tilde{X}$ be a flow invariant submanifold of X. Then $\tilde{X}$ is called *r-normally hyperbolic*, if there exists a $t > 0$ such that the map $\Psi = \Phi(t, \cdot)$ has the following properties:

1. The tangent bundle $TX|_{\tilde{X}}$ has the splitting
$$TX|_{\tilde{X}} = T\tilde{X} \oplus N^u \oplus N^s.$$
2. Each of these bundles is Ψ-invariant.
3. For $k = 1, \ldots, r$
$$\begin{aligned} \inf\{\|D\Psi_{N^u} v\| \,|\, \|v\| = 1\} &> \|D\Psi_{T\tilde{X}}\|^k, \\ \inf\{\|D\Psi_{T\tilde{X}} v\| \,|\, \|v\| = 1\} &> \|D\Psi_{N^s} v\|. \end{aligned}$$

This rather interesting definition allowed Hirsh *et al.* [49] to derive the following fundamental persistence result. This result represents the starting point for all the work that shall follow.

Theorem 2.2
Let X be a compact finite dimensional smooth manifold. Let $f : X \to TX$ be a vector field on X. Suppose that $\tilde{X}$ is a flow (corresponding to f) invariant normally hyperbolic submanifold of X. Then, there exists a neighbourhood W of f in the space of C^r-vector fields on X, such that for each vector field $\tilde{f} \in W$, there exists a unique manifold $\tilde{X}_\varepsilon$ near to $\tilde{X}$ and C^r diffeomorphic to $\tilde{X}$.

Proof. This is Hirsh *et al.* [49], Theorem 4.1. The existence of the diffeomorphism follows from the discussion of Lauterbach and Roberts [63], p. 26. □

Although this theorem is stated only for compact manifolds, it holds for any manifold that may be smoothly compactified, see Lauterbach and Roberts [63]. This will be the case for all situations that we shall be considering. Now we may generalise Theorem 2.2 to equivariant systems.

Let X be a smooth finite dimensional manifold. Let Γ be a compact Lie group acting smoothly on X. Then Lauterbach and Roberts [63] give the following generalisation of Theorem 2.2. We use the non-standard name "equivariant persistence theorem".

Theorem 2.3 (Equivariant Persistence Theorem)
Let Γ be a compact Lie group acting smoothly on a finite dimensional smooth manifold X. Let $f \in \vec{\mathcal{E}}_\Gamma$ be a Γ-equivariant vector field on X and suppose that Φ_f is the flow on X corresponding to f. Let $\tilde{X} \subset X$ be a compact submanifold, invariant under the flow Φ_f and the action of Γ. Suppose that $\tilde{X}$ is normally hyperbolic. Let $\Delta \subset \Gamma$ be a subgroup of Γ. Let $g \in \vec{\mathcal{E}}_\Delta$ be a Δ-equivariant vector field on X. Let Φ_g be the flow on X corresponding to g. Suppose that $\|f - g\| < \varepsilon$. Then, if ε is sufficiently small, there exists a unique manifold $\tilde{X}_\varepsilon$ near to $\tilde{X}$, invariant under the flow Φ_g. Moreover, there exist a Δ-equivariant diffeomorphism $\Theta : \tilde{X} \to \tilde{X}_\varepsilon$.

Proof. This is Lauterbach and Roberts [63] Proposition 1.1. □

We shall not require the full generality of this result. In fact the invariant manifold $\tilde{X}$ in our applications will have trivial flow. The invariant manifolds we shall consider will be groups orbits of steady-state solutions to Γ-equivariant bifurcation problems. Indeed, if $\tilde{X}$ is a manifold of solutions to an equivariant bifurcation problem (with compact symmetry group), then we have the following generic hypothesis, see Field [25], Theorem A.20.

1. Let $\tilde{x} \in \tilde{X}$. Then $(df_{\tilde{x}})$ has 0 as an eigenvalue of multiplicity dim $\tilde{X}$ and no other eigenvalues of the imaginary axis.

Under this hypothesis (which is necessary and sufficient for normal hyperbolicity) we have the following result derived from Theorem 2.3.

Theorem 2.4
Let $\tilde{X} \subset X$ be a smooth Γ-equivariant manifold of steady states for a smooth vector field $f \in \vec{\mathcal{E}}_\Gamma$ such that hypothesis 1 above is satisfied. Let $\Delta \subset \Gamma$ be a subgroup of Γ. Let $g \in \vec{\mathcal{E}}_\Delta$ be sufficiently close to f. Then there exists a smooth, Δ-invariant and flow invariant manifold $\tilde{X}_\varepsilon$ close to $\tilde{X}$. Moreover, there exists a Δ-equivariant diffeomorphism $\Theta : \tilde{X}_\varepsilon \to \tilde{X}$.

Proof. This is Lauterbach and Roberts [63], Proposition 1.2. □

The conclusion of the above theorems is rather simple, but still very useful. Under a Δ-equivariant perturbation, the behaviour of the perturbed invariant manifold $\tilde{X}_\varepsilon$ can be studied via the original manifold $\tilde{X}$. However, a natural question is how the vector field on the manifold X is related to the that on $\tilde{X}$.

2.1.2 Equivariant Flows on Invariant Manifolds

Here we show that given a Γ-equivariant flow Φ on a smooth manifold X and a flow invariant submanifold $\tilde{X}$, we can realise a Δ-equivariant flow on $\tilde{X}$ as the restriction of a Δ-equivariant flow on X. Indeed, this is the content of the next proposition.

Proposition 2.5
Let $g \in \vec{\mathcal{E}}_\Delta$ be a Δ-equivariant vector field on a finite dimensional smooth manifold X. Let Φ be the flow on X corresponding to g. Let $\tilde{X}$ be a submanifold of X and $\Phi|_{\tilde{X}}$ the restriction of Φ to $\tilde{X}$. Then for each compact neighbourhood W of $\tilde{X}$ and for all $\varepsilon > 0$, there exists a $\delta > 0$ such that for any flow $\Psi_{\tilde{X}}$ on $\tilde{X}$ with $\|\Psi_{\tilde{X}} - \Phi_{\tilde{X}}\|_{C^1} < \delta$ there exists a Δ-equivariant flow Ψ on X such that $\Psi_{\tilde{X}} = \Psi_{\tilde{X}}$ and $\|\Phi - \Psi\|_{C^1(W)} < \varepsilon$.

Proof. This is Lauterbach and Roberts [63] Proposition 1.3. □

In our applications the flow Φ on $\tilde{X}$ is trivial, however this is not (necessarily) true of Ψ on $\tilde{X}$. We shall see that this property leads to interesting dynamics.

2.2 Group Actions

In Section 2.1 we saw how normal hyperbolicity can be exploited to give very useful persistence results for invariant manifolds. We now wish to use these results in the framework of steady-state bifurcation theory.

Let Γ be a (compact) Lie group acting on a smooth finite dimensional manifold X. Let f be a smooth Γ-equivariant vector field on X and let Φ be the flow corresponding to f. Let $x \in X$ and suppose the isotropy of x is $\Sigma \subset \Gamma$. Then the group orbit $\tilde{X} = \Gamma x$ of x, is invariant under the flow Φ. In fact more is true; the orbit Γx is diffeomorphic to the homogenous space Γ/Σ. If we suppose that $\tilde{X}$ is normally hyperbolic, a hypothesis which is valid generically by Field [25], then we may apply the results of Section 2.1. Let $\Delta \subseteq \Gamma$ be a closed subgroup. Define an action of Δ on the space Γ/Σ by

$$\begin{aligned} \Delta \times (\Gamma/\Sigma) &\to (\Gamma/\Sigma), \\ (\delta, [\gamma]_\Sigma) &\to [\delta\gamma]_\Sigma. \end{aligned} \tag{2.2}$$

Then we have the following result.

Theorem 2.6
Suppose that $\tilde{X} = \Gamma x$ is normally hyperbolic. Let g be a Δ-equivariant vector field satisfying the hypothesis of Theorem 2.3. Let $\tilde{X}_\varepsilon$ be the manifold given by Theorem 2.3. Then there exists a Δ-equivariant diffeomorphism

$$\Theta : \Gamma/\Sigma \to \tilde{X}_\varepsilon.$$

Proof. This is Lauterbach and Roberts [63], Proposition 1.4. □

This theorem allows us to study forced symmetry breaking of a group orbit of steady-state solutions using the space Γ/Σ as a "model" space equipped with the action in (2.2). It can be shown that the result in Theorem 2.6 is independent of the conjugacy class of Σ and Δ, see Lauterbach and Roberts [63], Proposition 1.5.

At this point we have a group action of Δ on the space Γ/Σ and it is natural to ask what the isotropy subgroups of this action are. From this it is then natural to ask what the fixed-point submanifolds are. Let Δ' be a subgroup of Δ. Then the fixed-point submanifold of Δ' is defined by

$$\mathrm{Fix}_{\Gamma/\Sigma}(\Delta') = \{x \in \Gamma/\Sigma \,|\, \delta x = x, \text{ for all } \delta \in \Delta'\}.$$

Note that we have expressed explicitly the space Γ/Σ in which the fixed-point submanifold is contained. This is to avoid confusion with the fixed-point submanifold $\mathrm{Fix}(\Sigma)$ which is contained in X. The fixed-point submanifold $\mathrm{Fix}_{\Gamma/\Sigma}(\Delta')$ is invariant under Δ-equivariant flows.

We now turn to the computation of the fixed-point submanifold for an arbitrary subgroup Δ' of Δ. It transpires that we can compute these fixed-point submanifolds in a rather nice way. We begin by recalling a notion that was originally introduced by Ihrig and Golubitsky [54]. We define the *subnormaliser* of Δ' in Σ by,

$$\mathrm{N}_\Gamma(\Delta', \Sigma) = \{\gamma \in \Gamma \,|\, \Delta' \subseteq \gamma\Sigma\gamma^{-1}\}.$$

This allows us to compute the fixed-point submanifolds using only group theoretical methods.

Proposition 2.7
Let Δ act on Γ/Σ as in (2.2). Let Δ' be a subgroup of Δ. Then $\mathrm{Fix}(\Delta') = N_\Gamma(\Delta', \Sigma)/\Sigma$.

Proof. This is Lauterbach and Roberts [63], Proposition 1.7. □

We may use the following lemma to aid the calculation of the subnormaliser.

Lemma 2.8
Let Σ be an isotropy subgroup of Γ and Δ' a closed subgroup. Then $N_\Gamma(\Delta', \Sigma) = \{\gamma \in \Gamma | \gamma Fix(\Sigma) \subseteq Fix(\Delta)\}$.

Here the fixed-point submanifolds are contained in the manifold X, not the homogeneous space Γ/Σ. So the action of the group Δ' on X is given by the restriction of the action of Γ.

Proof. See Ihrig and Golubitsky [54], Lemma 5.4. In fact, Lemma 5.4 contains more than is stated here. $N_\Gamma(\Delta', \Sigma)$ is a real analytic variety and is compact in Γ. □

We now wish to measure the symmetry of an element $x \in \Gamma/\Sigma$. We define the isotropy subgroup of $x \in \Gamma/\Sigma$ by

$$\text{Stab}(x) = \{\delta \in \Delta | \delta x = x\}.$$

We have used the notation Stab to differentiate between the isotropy subgroups $\Sigma_x \subseteq \Gamma$ for the action of Γ on X and the isotropy subgroup, $\text{Stab}(x)$ of $x \in \Gamma/\Sigma$ for the action of Δ on Γ/Σ. This complete the basic theory of forced symmetry breaking of steady states.

2.3 One-Dimensional Flows on Homogeneous Spaces

We have completed the basic theory for forced symmetry breaking of group orbits. However, we require a systematic method for ordering the information. In this section we consider one-dimensional flows on the space Γ/Σ and show how using group theory it is possible to classify the types of flows that can be expected. More precisely we show that we can find a stratified manifold $\mathbb{X}_\Delta \subset \Gamma/\Sigma$ on which there may be equilibria, heteroclinic connections or periodic orbits. The structure of the flow and the position of equilibria on $\mathbb{X}_\Delta$ are strongly influenced by the subgroups of Δ.

2.3.1 Decomposition of the Orbit Space

In this section we define a "nice" decomposition of the space Γ/Σ into zero and one-dimensional pieces.

Let $x \in \Gamma/\Sigma$. Let $C = C(x)$ be the connected component of $\text{Fix}(\text{Stab}(x)) \subseteq \Gamma/\Sigma$ which contains x. In general a component C could be very complex, and thus it may have highly elaborate dynamics on it. For this reason we consider only a selection of all the possible connected components C. Let $\mathscr{C}_\Delta$ be the collection of those C's which are homeomorphic to $\{0\}$ or S^1-the standard circle. The set $\mathscr{C}_\Delta$ is invariant under the Δ-action.

Using the collection $\mathscr{C}_\Delta$ of subsets of Γ/Σ we may define a stratified submanifold of Γ/Σ.

Definition 2.9
Let

$$\mathbb{X}_\Delta = \bigcup_{C \in \mathscr{C}_\Delta} C \subset \Gamma/\Sigma.$$

The set $\mathbb{X}_\Delta$ is called the ***skeleton*** of Γ/Σ with respect to Δ.

To save repetition we shall normally just use the term "skeleton". A Δ-equivariant flow on Γ/Σ induces a Δ-equivariant flow on $\mathbb{X}_\Delta$. The crux of this work is to study these Δ-equivariant flows.

Since the space $\mathbb{X}_\Delta$ is a stratified manifold it naturally splits into strata. In fact, the strata are flow invariant.

Definition 2.10
Let $x \in \mathbb{X}_\Delta$. Let $S(x)$ be the connected component of the stratum containing x. Define $\mathscr{S}_\Delta = \{S(x) | x \in \mathbb{X}_\Delta\}$.

We may now define flow invariant subsets of $\mathbb{X}_\Delta$ as follows.

Definition 2.11
Given the set $\mathscr{S}_\Delta$ define:

- $E_{(\Delta,\Gamma/\Sigma)} = \{s \in \mathscr{S} | s \text{ is homeomorphic to } \{0\}\}$,
- $H_{(\Delta,\Gamma/\Sigma)} = \{s \in \mathscr{S} | s \text{ is homeomorphic to } \mathbb{R}\}$,
- $P_{(\Delta,\Gamma/\Sigma)} = \{s \in \mathscr{S} | s \text{ is homeomorphic to } S^1\}$.

The choice of letters above reflects the fact that the elements of $E_{(\Delta,\Gamma/\Sigma)}$ correspond to equilibria, $H_{(\Delta,\Gamma/\Sigma)}$ to heteroclinic connections and $P_{(\Delta,\Gamma/\Sigma)}$ to periodic orbits.

2.3.2 Symmetry Properties of the Skeleton

At this point we wish to determine the "isotropy", that is the symmetry, of elements in $\mathscr{C}_\Delta$ and $\mathscr{S}_\Delta$. Doing so allows us to restrict the form of the skeleton. We begin by defining a new "isotropy" subgroup, that of a set.

Definition 2.12
Let $C \in \mathscr{C}_\Delta$ or $\mathscr{S}_\Delta$. Define the *pointwise isotropy* of C as

$$\text{stab}(C) = \{\delta \in \Delta | \delta x = x \text{ for all } x \in C\}.$$

Actually, the above set is not an isotropy subgroup in the usual sense; however it does measure the symmetry of C with respect to the Δ action on Γ/Σ and that is why we use the term isotropy. In fact, the pointwise isotropy of C tells us which elements of Δ leave every point of C fixed. This is not the same (in general) as the elements of Δ which leave C setwise fixed. We would expect a strong relationship between $C \in \mathscr{C}_\Delta$ and stab(C). It is the aim of the rest of this section to explore this relationship. Intuitively we would expect an element of $E_{(\Delta,\Gamma/\Sigma)}$ which is contained in $C \in \mathscr{C}_\Delta$ to perhaps be fixed by more elements of Δ than those element which fix C itself. If we ignore such points then it is reasonable to think the elements which fix the whole set C are the same as those which fix any point $x \in C - E_{(\Delta,\Gamma/\Sigma)}$ (here $-$ denotes set-theoretic difference). Indeed we find:

Proposition 2.13
Given $C \in \mathscr{C}_\Delta$, which satisfies $C \not\subseteq E_{(\Delta,\Gamma/\Sigma)}$. Then stab$(C)$ = Stab(x) for all $x \in C - E_{(\Delta,\Gamma/\Sigma)}$.

Proof. See Lauterbach *et al.* [62], Lemma 3.7. □

Now suppose we are given $C_1, C_2 \in \mathscr{C}_\Delta$, both homeomorphic to $\mathbf{S^1}$. What can be said about the intersection $C_1 \cap C_2$. Importantly, the sets intersect at equilibria.

Proposition 2.14
Let $C_1, C_2 \in \mathscr{C}_\Delta$. Suppose $C_1 \neq C_2$ and that C_1 and C_2 are homeomorphic to S^1. Then $C_1 \cap C_2 \subseteq E_{(\Delta,\Gamma/\Sigma)}$.

Proof. See Lauterbach *et al.* [62], Lemma 3.9. □

Theorem 2.15
Given an Δ-equivariant vector field f with corresponding flow Φ on the skeleton $\mathbb{X}_\Delta$, then

1. *The elements of $E_{(\Delta,\Gamma/\Sigma)}$ are equilibria for f.*
2. *The flow $\Phi(x)$ has heteroclinic connections, joining elements of $E_{(\Delta,\Gamma/\Sigma)}$ if and only if $\Phi(x) \in H_{(\Delta,\Gamma/\Sigma)}$.*
3. *The flow $\Phi(x)$ is a periodic orbit if and only if $\Phi(x) \in P_{(\Delta,\Gamma/\Sigma)}$.*

This theorem is not a strong as it looks. We still need to show that *there are* Δ-equivariant vector fields on $\mathbb{X}_\Delta$ which satisfy the above.

2.3.3 Projection of the Skeleton into the Orbit Space

The permissible flows on the skeleton $\mathbb{X}_\Delta$ are restricted in several ways. The invariance under the Δ-action gives one restriction. Here we consider how the flows at different points are related. Define

$$\pi : \mathbb{X}_\Delta \to \Delta\backslash\mathbb{X}_\Delta \quad \text{by} \quad \pi(x) = {}_\Delta[x],$$

where ${}_\Delta[x]$ is the equivalence class of all points x which are members of the same group orbit. This is the projection of $x \in \mathbb{X}_\Delta$ into the orbit space. The flow at two points x and y is related if and only if $\pi(x) = \pi(y)$. We wish to know which points of $C \in \mathscr{C}_\Delta$ have this property, this is equivalent to finding which points lie on the same orbit.

Theorem 2.16
Given $C \in \mathscr{C}_\Delta$ and $x \in C$, the set $\Delta x \cap C$ is either finite or all of C.

Proof. See Lauterbach *et al.* [62]. Theorem 3.12. □

In view of this theorem we find two distinct types of periodic orbits. We categorise these in the next definition.

Definition 2.17
Let $p \in P_{(\Delta,\Gamma/\Sigma)}$. If $p \subset \Delta x$ for one (and hence all) $x \in P_{(\Delta,\Gamma/\Sigma)}$ then p is a relative equilibrium. The set of those set p is denoted by $P^e_{(\Delta,\Gamma/\Sigma)}$. Denote by $P^a_{(\Delta,\Gamma/\Sigma)}$ the set $P_{(\Delta,\Gamma/\Sigma)} - P^e_{(\Delta,\Gamma/\Sigma)}$.

This definition partitions the periodic orbits into two classes. Those, the relative equilibria, which project to one point in the orbit space, and those which do not have this property.

Although Theorem 2.16 gives us information concerning the set $\Delta x \cap C$, it would be nice to find some characterisation of this set. Given $C \in \mathscr{C}_\Delta$, the group Δ acts on the elements of C, but it also has an induced action on the set $\mathscr{C}_\Delta$ itself. More precisely, there is an induced action of the group Δ on set $\mathscr{C}_\Delta$ by permutation of its elements. For this action we may define a (setwise) isotropy. We can use this new isotropy to calculate $\Delta x \cap C$, as we see below.

Definition 2.18
Given the Δ action (2.2) on Γ/Σ, there is an induced action of Δ on $\mathscr{C}_\Delta$ by permutation. Given $C \in \mathscr{C}_\Delta$ the *setwise isotropy* of C is

$$\mathrm{Stab}(C) = \{\delta \in \Delta \big| \delta C = C\}.$$

Given $C \in \mathscr{C} \cup \mathscr{S}_\Delta$, the pointwise isotropy of $C \in \mathscr{C}_\Delta$ is normal in the setwise isotropy $\mathrm{Stab}(C)$. This allows us to form the group

$$\mathrm{S}(C) = \mathrm{Stab}(C)/\mathrm{stab}(C).$$

This group has a natural action on C.

Lemma 2.19
Suppose that $C \in \mathscr{C}_\Delta$ and $x \in C - E_{(\Delta,\Gamma/\Sigma)}$. Then

$$S(C)x = Stab(C)x = \Delta x \cap C.$$

Proof. See Lauterbach *et al.* [62], Lemma 3.15. □

Lemma 2.20
Suppose $C \in H \cup P^a$ and $x \in C$. Then there exists a connected open neighbourhood U_x of x in C such that $\pi|_{U_x}$ is injective.

Proof. See Lauterbach *et al.* [62] Lemma 3.18. □

This lemma need not hold for elements of $C \in \mathscr{C}_\Delta$. Now there are only three different types of behaviour for the neighbourhood found in Lemma 2.20.

Lemma 2.21
Given $C \in \mathscr{C}_\Delta - P^e_{(\Delta,\Gamma/\Sigma)}$. Let $x \in C - E_{(\Delta,\Gamma/\Sigma)}$. Define

$$A(x) = \{M \subset C - E | M \text{ is connected, open } x \in M \text{ and } \pi|_M \text{ is injective } \}.$$

Then $A(x)$ contains a maximal element M with respect to inclusion. It need not be unique, but there are three possibilities.

1. $M = C$.
2. $M \neq \emptyset$ *and* M *is simply connected, open and* $\partial M \subset E$ *is also non-empty.*
3. $M \neq \emptyset$ *and* M *is simply connected, open and* $\partial M = \{a, b\}$ *with* $a \neq b$ *and* $\pi(a) = \pi(b)$ *but* $a, b \notin E$.

Proof. See Lauterbach *et al.* [62] Lemma 3.19. □

Given $C \in \mathscr{C}_\Delta$ it is convenient to know whether there are any elements of H contained in C. For this reason we make the following definition.

Definition 2.22
Let $C \in \mathscr{C}_\Delta$. Then $K(C) = \{h \in H | h \subset C\}$.

The presence of symmetry on $\mathbb{X}_\Delta$ restricts the types of flows that can be expected. In particular on a chosen $C \in \mathscr{C}_\Delta$ we can expect points which are fixed under the group $\mathrm{Stab}(C)$, these points are axes of reflection symmetry and the presence of such symmetry restricts the possible flows. We make this precise.

Definition 2.23
Let $C \in \mathscr{C}_\Delta$ and $x \in C$. Suppose that x is a fixed-point of some element of $\mathrm{Stab}(C)$, then x is a *knot relative to* C.

Theorem 2.24
Let Δ act on the sets $P^a_{(\Delta,\Gamma/\Sigma)}$, $P^e_{(\Delta,\Gamma/\Sigma)}$, $H_{(\Delta,\Gamma/\Sigma)}$, $E_{(\Delta,\Gamma/\Sigma)}$ and $\mathscr{C}_\Delta$. Then we have

1. *Given $e \in E_{(\Delta,\Gamma/\Sigma)}$ or $h \in H_{(\Delta,\Gamma/\Sigma)}$. Then $S(e) = S(h) = \mathbf{1}$, the trivial group.*
2. *Given $p \in P^e_{(\Delta,\Gamma/\Sigma)}$ the group $S(p)$ is topologically isomorphic to $\mathbf{SO}(2)$.*
3. *Given $p \in P^a_{(\Delta,\Gamma/\Sigma)}$ then there are two alternatives:*
   (a) *If Alternative (1) holds in Lemma 2.21, then $S(p) = \mathbf{1}$.*
   (b) *If Alternative (3) holds in Lemma 2.21, then there exists some $g \in Stab(p)$ and some $m \in \mathbb{N}$ such that $S(p) = \mathbf{Z}_m$, where $\mathbf{Z}_m$ is generated by the element $[g]_{Stab(p)}$. The group $S(p)$ acts as rotation on p.*
4. *Given $C \in \mathscr{C}_\Delta$ with $K(C) \neq \emptyset$, then there are the following alternatives:*
   (a) *Suppose $Stab(C)$ contains $m \in \mathbb{N}$ orientation reversing elements; then $S(C) = \mathbf{D}_m$. We use the convention $\mathbf{D}_1 = \mathbf{Z}_2$. The group $S(p)$ acts as the group of m reflections about axes through opposite knots and $m - 1$ nontrivial rotations.*
   (b) *Suppose $Stab(C)$ contains no orientation reversing elements; then we have $S(C) = \mathbf{Z}_m$ for some $m \in \mathbb{N}$. We use the convention $\mathbf{Z}_1 = \mathbf{1}$. The group $S(C)$ acts as rotations on C.*

The rotations and reflections preserve $K(C)$.

This theorem is vitally important in two respects. Firstly it allows us to see the arrangement of the elements of $E_{(\Delta,\Gamma/\Sigma)}$ and $H_{(\Delta,\Gamma/\Sigma)}$ on the skeleton $\mathbb{X}_\Delta$. Secondly, it allows us to deduce that there *do* exist flows on $\mathbb{X}_\Delta$ such that elements of $E_{(\Delta,\Gamma/\Sigma)}$, $H_{(\Delta,\Gamma/\Sigma)}$ and $P_{(\Delta,\Gamma/\Sigma)}$ are equilibria, heteroclinic connections and periodic orbits, respectively.

Recall that we have an action of the group Δ on Γ/Σ. Let $\Delta\backslash\Gamma/\Sigma = \{{}_\Delta[x] \big| x \in \Gamma/\Sigma\}$ — the left quotient space. Given a subset $M \subset \Gamma/\Sigma$, define $\Delta\backslash M = \{{}_\Delta[x] \big| x \in M\}$. Then we have

Theorem 2.25
Let Δ act on Γ/Σ with the natural action. Define $\pi : \mathbb{X}_\Delta \to \Delta\backslash\mathbb{X}_\Delta$, by $\pi(x) = {}_\Delta[x]$. Then

1. *Let $m \in P^e_{(\Delta,\Gamma/\Sigma)} \cup E_{(\Delta,\Gamma/\Sigma)}$. Then $\Delta\backslash m$ is a one-point set.*
2. *Let $p \in P^a_{(\Delta,\Gamma/\Sigma)}$. Then the map $\pi|_p$ is a local homeomorphism, so there is an open and connected set $m \subset p$ and a homeomorphism*

$$f : \overline{m}/\sim \to \Delta\backslash p,$$

   $f(x) = {}_\Delta[x]$, where $\sim$ identifies the points in ∂m. Therefore $\Delta\backslash p$ is homeomorphic to $\mathbf{S}^1$.
3. *Given $h \in H_{(\Delta,\Gamma/\Sigma)}$, the mapping $\pi : h \to \Delta\backslash h$, defined by $\pi(x) = {}_\Delta[x]$ is a homeomorphism.*

We denote by $\mathbb{X}^p_\Delta$ the *projected skeleton* $\Delta\backslash\mathbb{X}_\Delta$.

2.3.4 Flows on the Skeleton

In this section we show that there exist flows on $\mathbb{X}_\Delta$ which have elements of $E_{(\Delta,\Gamma/\Sigma)}$, $H_{(\Delta,\Gamma/\Sigma)}$ and $P_{(\Delta,\Gamma/\Sigma)}$ as equilibria, heteroclinic connection and periodic orbits, respectively. To achieve this we must introduce some more theoretical machinery concerning the space $\Delta\backslash\Gamma/\Sigma$ and vector fields defined on this space. The material in this subsection is based on Lauterbach and Roberts [63] and Lauterbach *et al.* [62].

Let Γ be a compact Lie group acting (smoothly) on a smooth compact manifold X. It is well known that $\Gamma\backslash X$ is not in general a manifold. This space does have a smooth stratification: that is, it can be decomposed into a finite number of disjoint subsets each of which is a smooth manifold.

Let Σ be a subgroup of Γ and let $X^{(\Sigma)}$ denote the set of all points in X with isotropy conjugate to Σ. Then $X^{(\Sigma)}$ is a smooth Σ-invariant submanifold of X and $\Gamma\backslash X^{(\Sigma)}$ is a smooth manifold which can be identified with the subset of $\Gamma\backslash X$ which we denote by $(\Gamma\backslash X)^{(\Sigma)}$. Then $\Gamma\backslash X$ is the union of these orbit type strata.

We can give $\Gamma\backslash X$ a smooth structure. We say that a function of $\Gamma\backslash X$ is smooth if it is a real valued function, which pulls back to give a smooth Γ-invariant function on X. We define $C^\infty(\Gamma\backslash X) := C^\infty(X)^\Gamma$.

We now define a vector field on $\Gamma\backslash X$ as a $\mathbb{R}$-linear derivation of $C^\infty(\Gamma\backslash X)$. Let $V^\infty(\Gamma\backslash X)$ denote the space of all smooth vector fields on $\Gamma\backslash X$. A smooth vector field is said to be tangent to the orbit type stratum $(\Gamma\backslash X)^{(\Sigma)}$ if it maps the space of functions vanishing on $(\Gamma\backslash X)^{(\Sigma)}$ into itself. A smooth vector field is said to be stratum preserving if it is tangent to all the orbit type strata of $\Gamma\backslash X$. We denote the space of all strata preserving vector fields on $\Gamma\backslash X$ by $(SV)^\infty(\Gamma\backslash X)$.

The projection map $\pi : X \to \Gamma\backslash X$ induces a map

$$\pi_* : V^\infty(X) \to V^\infty(\Gamma\backslash X),$$

by $(\pi_* f) \circ \pi = \pi \circ f$. (This map may be extended to flows as well). Let $V^\infty_\Gamma(X)$ be the space of Γ-equivariant vector fields on X, then there is a map

$$\pi_* : V^\infty_\Gamma(X) \to (SV)^\infty(\Gamma\backslash X).$$

By the Smooth Lifting Theorem of Schwarz (see Lauterbach and Roberts [63]), this map is surjective. So every stratum preserving smooth vector field on $\Gamma\backslash X$ lifts to a smooth Γ-equivariant vector field on X. This property is essential. We may define similar ideas for the skeleton $\mathbb{X}_\Delta$ and $\mathbb{X}^p_\Delta$ since $\mathbb{X}_\Delta$ is invariant under the flows in $V^\infty_\Delta(\Gamma/\Sigma)$. Furthermore, $\mathbb{X}^p_\Delta$ is preserved by the strata preserving flows on $\Delta\backslash\Gamma/\Sigma$.

Let $m \in \mathscr{S}_{(\Delta,\Gamma/\Sigma)}$ then the map

$$\pi_* : V^\infty_\Delta(\pi^{-1}(\Delta\backslash m)) \to (SV)^\infty(\Delta\backslash m) = V^\infty(\Delta\backslash m), \tag{2.3}$$

is well defined and surjective. Again this map may be defined for flows. Using Theorems 2.24 and 2.25 we may deduce the following theorem.

Theorem 2.26
Let $m \in H_{(\Delta,\Gamma/\Sigma)} \cup P^a_{(\Delta,\Gamma/\Sigma)}$. Then the map in (2.3) is bijective. Furthermore, let $f \in (SV)^\infty(\Delta\backslash m)$ and let ϕ be the flow corresponding to f. Then the set $\Delta\backslash m$ is a periodic orbit of ϕ if and only if one and hence all orbits of $\pi_*^{-1}(\phi)$ are periodic. Suppose $S(m) = \mathbf{Z}_m$ and τ is the period of ϕ, then all orbits of $\pi_*^{-1}(\phi)$ have periods $m\tau$.

The next theorem considers the behaviour of relative equilibria.

Theorem 2.27
Let $p \in P^e_{(\Delta,\Gamma/\Sigma)}$. Then there is a topological isomorphism $\psi : \mathbf{S}^1 \to S(p)$. The mapping

$$\psi_* : \mathbb{R} \to V^\infty_\Delta(\pi^{-1}(\Delta\backslash p)) \tag{2.4}$$

defined by $\psi_*(r) = \phi^r$ where $\phi^r_t(x) = \psi([rt]_{\mathbf{Z}})x$ is bijective.

As a consequence of these theorems we have the following.

Theorem 2.28
Let $h \in H_{(\Delta,\Gamma/\Sigma)}$. Then there exist Δ-equivariant vector fields (and flows ϕ) on $\mathbb{X}_\Delta$ such that h is a heteroclinic connection of ϕ connecting equilibria in $E_{(\Delta,\Gamma/\Sigma)}$.

Let $p \in P_{(\Delta,\Gamma/\Sigma)}$. Then there are Δ-equivariant vector fields (and flows ϕ) on $\mathbb{X}_\Delta$ such that p is a periodic orbit of ϕ.

2.4 Classification of the Skeleton

In this section we show how group theory allows us to determine the structure of the skeleton. In particular, we show how we can determine the arrangement of the elements of $E_{(\Delta,\Gamma/\Sigma)}$ and $H_{(\Delta,\Gamma/\Sigma)}$ on $\mathbb{X}_\Delta$. For notational convenience, let $C \in \mathscr{C}_{(\Delta,\Gamma/\Sigma)}$. Then we shall refer to those elements of $E_{(\Delta,\Gamma/\Sigma)}$ which are contained in C as vertices, and those elements of $H_{(\Delta,\Gamma/\Sigma)}$ which are contained in C as edges.

Theorem 2.29
Let $C \in \mathscr{C}_{(\Delta,\Gamma/\Sigma)}$. Suppose $K(C) \neq \emptyset$. Then the knots relative to C always occur in pairs of vertices on $\mathbb{X}_\Delta$ dividing C into two connected components with the same number of edges in $K(C)$ on each component. There are two possible types of behaviour.

1. *Suppose there are no knots relative to C. Then $S(C)$ is isomorphic to some $\mathbf{Z}_m$ (with $\mathbf{Z}_1 = \mathbf{1}$) and acts on $K(C)$ by rotations on C.*

2. *Suppose that there are knots relative to C. Then $S(C)$ is isomorphic to some $\mathbf{D}_m$ (with $\mathbf{D}_1 = \mathbf{Z}_2$). This group acts as $m-1$ non-trivial rotations and m reflections on $K(C)$. The pairs of opposite knots give the axes of reflections. In particular m is the number of knots relative to C.*

This theorem gives a great number of symmetry restrictions on the form of $\mathbb{X}_\Delta$ and the flows that are permitted. It is obvious that the calculation of the knots relative to C is vitally important to classifying $\mathbb{X}_\Delta$. This calculation can be performed using the next lemma.

Lemma 2.30
Let $C \in \mathscr{C}_{(\Delta,\Gamma/\Sigma)}$ with $K(C) \neq \emptyset$. Then the knots relative to C are those elements $k \in C \cap E_{(\Delta,\Gamma/\Sigma)}$ for which

$$B(k) = (Stab(k) - stab(C)) \cap N_\Delta(stab(C)) \neq \emptyset$$

where $N_\Delta(stab(C))$ is the normalizer of $stab(C)$ in Δ. If $m \in \mathbb{N}$ is the number of knots relative to C then $S(C) = \mathbf{D}_{m/2}$.

Remark 2.31
We shall not normally require Lemma 2.30 to compute the knots on a particular C. Instead we can use Theorem 2.29 together with the fact that knots are always equilibria.

With these two results in place we are in a position to classify the form of $\mathbb{X}_\Delta$ for, in principle, any groups Γ, Σ and Δ. Then we can investigate the vector field on this skeleton. However, in some cases the skeleton can be very complex. For this reason we make another trip to the orbit space of $\mathbb{X}_\Delta$ and show that we may consider the projected skeleton to give information on the flows and vector fields on $\mathbb{X}_\Delta$.

We begin with some definitions. Given the sets $E_{(\Delta,\Gamma/\Sigma)}$, $H_{(\Delta,\Gamma/\Sigma)}$, $P^e_{(\Delta,\Gamma/\Sigma)}$ and $P^a_{(\Delta,\Gamma/\Sigma)}$, define $E^p_{(\Delta,\Gamma/\Sigma)} = \Delta\backslash E_{(\Delta,\Gamma/\Sigma)}$, $H^p_{(\Delta,\Gamma/\Sigma)} = \Delta\backslash H_{(\Delta,\Gamma/\Sigma)}$, $P^{ep}_{(\Delta,\Gamma/\Sigma)} = \Delta\backslash P^e_{(\Delta,\Gamma/\Sigma)}$ and $P^{ap}_{(\Delta,\Gamma/\Sigma)} = \Delta\backslash P^a_{(\Delta,\Gamma/\Sigma)}$. Then

$$\mathbb{X}^p_\Delta = E^p_{(\Delta,\Gamma/\Sigma)} \dot\cup H^p_{(\Delta,\Gamma/\Sigma)} \dot\cup P^{ep}_{(\Delta,\Gamma/\Sigma)} \dot\cup P^{ap}_{(\Delta,\Gamma/\Sigma)}.$$

By using Theorem 2.29 we can identify edges (elements of $H_{(\Delta,\Gamma/\Sigma)}$) which lie on the same group orbit, and for this reason we can construct $\mathbb{X}^p_\Delta$ without having to construct $\mathbb{X}_\Delta$ first. This idea is useful as the next theorem shows.

Theorem 2.32
Let Γ be a compact Lie group, Σ an isotropy subgroup and Δ a closed subgroup. Suppose $\mathbb{X}^p_\Delta$ is defined. Let $m \in H^p_{(\Delta,\Gamma/\Sigma)} \dot\cup E^p_{(\Delta,\Gamma/\Sigma)} \dot\cup P^{ep}_{(\Delta,\Gamma/\Sigma)} \dot\cup P^{ap}_{(\Delta,\Gamma/\Sigma)}$. Then a Δ-equivariant vector field on $\mathbb{X}_\Delta$ defines a Δ-equivariant vector field on $\pi^{-1}(m)$. Conversely, given $m \in H^p_{(\Delta,\Gamma/\Sigma)} \dot\cup E^p_{(\Delta,\Gamma/\Sigma)} \dot\cup P^{ep}_{(\Delta,\Gamma/\Sigma)} \dot\cup P^{ap}_{(\Delta,\Gamma/\Sigma)}$ any Δ-equivariant vector field on $\pi^{-1}(m)$ defines a Δ-equivariant vector field on $\mathbb{X}_\Delta$.

Therefore, it is sufficient to characterise the Δ-equivariant flows on $\pi^{-1}(m)$ for all $m \in H^p_{(\Delta,\Gamma/\Sigma)} \dot\cup E^p_{(\Delta,\Gamma/\Sigma)} \dot\cup P^{ep}_{(\Delta,\Gamma/\Sigma)} \dot\cup P^{ap}_{(\Delta,\Gamma/\Sigma)}$:

1. *If $m \in H^p_{(\Delta,\Gamma/\Sigma)} \dot\cup P^{ap}_{(\Delta,\Gamma/\Sigma)}$ then $V^\infty_\Delta(\pi^{-1}(m)) \cong V^\infty(m)$ using the map π_*, from (2.3).*
2. *If $m \in P^{ep}_{(\Delta,\Gamma/\Sigma)}$ then $V^\infty_\Delta(\pi^{-1}(m)) \cong \mathbb{R}$ using the map ψ_*, from (2.4).*
3. *Given $m \in E^p_{(\Delta,\Gamma/\Sigma)}$, the flow on $\pi^{-1}(m)$ is trivial, so $V^\infty_\Delta(\pi^{-1})(m)) \cong \{0\}$.*

This theorem shows that Δ-equivariant flows on the skeleton are uniquely related to the flows on the projected skeleton. In particular, if we find loops in the orbit space then it follows that there exist Δ-equivariant vector fields which realise heteroclinic cycles on the skeleton.

2.5 Behaviour of the Perturbed Manifold

In the previous sections we have illustrated how a systematic approach can be used to study forced symmetry breaking of equivariant differential equations. The material in those sections studied the behaviour of vector fields and flows on the "model" space $\widetilde{X}$ of the problem. More

precisely, suppose that Γ is a compact Lie group, with Σ an isotropy subgroup and Δ a closed subgroup. Then the results above tell us that we may study forced symmetry breaking of the group orbit $\widetilde{X}$ by considering Δ-equivariant vector fields on $\widetilde{X}$. However, the space $\widetilde{X}$ is only a model (a diffeomorphic one) of the true perturbed manifold $\widetilde{X}_\varepsilon$. A natural question is how the behaviour of a Δ-equivariant vector field on the model space is related to that on the manifold $\widetilde{X}_\varepsilon$. Of course one would hope that the behaviour is qualitatively the same, provided some kind of (as yet undetermined) nondegeneracy conditions hold. It is the aim of this section to give precise conditions for a correspondence between the behaviour of Δ-equivariant vector fields on the model space and that of the abstract (and unknown) manifold $\widetilde{X}_\varepsilon$.

Let $\Theta_\varepsilon : \widetilde{X} \to \widetilde{X}_\varepsilon$ be the Δ-equivariant diffeomorphism given in Theorem 2.6. Then Θ_0 is the identity map. Let $e_j \in E_{(\Delta,\widetilde{X})}$ and define $e_j^\varepsilon = \Theta_\varepsilon(e_j)$. Let $h_j \in H_{(\Delta,\widetilde{X})}$ and define $h_j^\varepsilon = \Theta_\varepsilon(h_j)$. Let $p_j \in P_{(\Delta,\widetilde{X})}$ and define $p_j^\varepsilon = \Theta_\varepsilon(p_j)$. Define $E^\varepsilon_{(\Delta,\widetilde{X}_\varepsilon)} = \{\Theta_\varepsilon(e) | e \in E_{(\Delta,\widetilde{X})}\}$, $H^\varepsilon_{(\Delta,\widetilde{X}_\varepsilon)} = \{\Theta_\varepsilon(h) | h \in H_{(\Delta,\widetilde{X})}\}$ and $P^\varepsilon_{(\Delta,\widetilde{X}_\varepsilon)} = \{\Theta_\varepsilon(p) | p \in P_{(\Delta,\widetilde{X})}\}$. Then we can define a skeleton on the perturbed invariant manifold $\widetilde{X}_\varepsilon$,

$$\mathbb{X}^\varepsilon_\Delta = E^\varepsilon_{(\Delta,\widetilde{X}_\varepsilon)} \cup H^\varepsilon_{(\Delta,\widetilde{X}_\varepsilon)} \cup P^\varepsilon_{(\Delta,\widetilde{X}_\varepsilon)} \subseteq \widetilde{X}_\varepsilon.$$

We call $\mathbb{X}^\varepsilon_\Delta$ the *perturbed skeleton*. We are interested in the behaviour of Δ-equivariant vector fields on $\mathbb{X}^\varepsilon_\Delta$. For this we need to make the additional assumption that the underlying manifold X has an inner product structure. This is not really an additional restriction, since this assumption holds for all applications that we shall consider.

2.5.1 Parametrisation of the Skeletons

In this section we address the problem of parametrising the various connections $h \in H_{(\Delta,\widetilde{X})}$ that occur in $\mathbb{X}_\Delta$. Using these parametrisations it is possible to calculate the direction of flow along an element $h \in H_{(\Delta,\widetilde{X})}$ for any Δ-equivariant perturbation $\mathbf{g}$[2].

Let $h \in H_{(\Delta,\widetilde{X})}$ and suppose that h connects two points e_i and $e_j \in E_{(\Delta,\widetilde{X})}$. By definition, there exists a subgroup Δ' of Δ such that h is contained in the fixed-point submanifold $\mathrm{Fix}_{\widetilde{X}}(\Delta')$, which is diffeomorphic to S^1. So we now consider $S^1 \subset \widetilde{X} = \Gamma x$ as a realisation of $\mathrm{Fix}_{\widetilde{X}}(\Delta')$. There exists a smooth function $\gamma^* : [0, 2\pi] \to \Gamma$ and an injective smooth function $\omega : [0, 2\pi] \to S^1$ such that $\omega(t) = \gamma^*(t)x$ is a nondegenerate parametrisation of the fixed-point submanifold $\mathrm{Fix}_{\widetilde{X}}(\Delta')$. In addition we have the property,

$$h = \{\omega(t) | t \in (0, t^*)\}, \quad 0 < t^* \leq 2\pi, \quad \omega(0) = e_i \text{ and } \omega(t^*) = e_j.$$

Let $\mathbf{g}$ be a Δ-equivariant vector field. Then the flow along a connection $h \in H_{(\Delta,\widetilde{X})}$, parametrised by ω_h is given by

$$\mathcal{F}^{\mathbf{g}}_h(t) = \langle \mathbf{g}(\omega_h(t)), \mathcal{T}_{\omega_h}(t) \rangle ,$$

where $\mathcal{T}_{\omega_h}(t) = (d/dt)\omega_h(t)$ is the tangent vector to $\omega_h(t)$ and $< ., . >$ is the inner product on X. We call the function $\mathcal{F}^{\mathbf{g}}_h$ the *flow formula*.

Definition 2.33
Let $h \in H_{(\Delta,\widetilde{X})}$ and suppose h connects the elements e_i and $e_j \in E_{(\Delta,\widetilde{X})}$. Let $\omega_h : [0, t^*] \to \widetilde{X}$ parametrise h, with $\omega_h(0) = e_i$ and $\omega_h(t^*) = e_j$. Let $\mathbf{g}$ be a Δ-equivariant vector field. Then $\mathbf{g}$ is an *admissible perturbation* for the connection h if $\mathcal{F}^{\mathbf{g}}_h(t) \neq 0$ for all $t \in (0, t^*)$. If $\mathbf{g}$ is an admissible perturbation for all connections $h \in H_{(\Delta,\widetilde{X})}$, then we call $\mathbf{g}$ an *admissible perturbation* and the corresponding flow an *admissible flow*.

We are particularly interested in those Δ-equivariant vector fields which give admissible perturbations. Why? Admissible perturbations are candidates for heteroclinic cycles on the skeleton. A remark is in order at this point.

[2]The same is possible for periodic orbits, but we shall not require this in the sequel.

Remark 2.34
It is possible for an admissible perturbation to be degenerate at the equilibria contained in $E_{(\Delta,\tilde{X})}$. *Such behaviour does not prevent the existence of heteroclinic cycles for any chosen example. However when an additional perturbation is added, the degeneracy will unfold giving (possible) additional equilibria close to the original equilibria, these additional equilibria form obstructions to heteroclinic cycles on the skeleton. We consider examples of this kind in Example 4.41.*

We use the parametrisation of the skeleton $\mathbb{X}_\Delta$ to provide a natural parametrisation for the perturbed skeleton $\mathbb{X}^\varepsilon_\Delta$.

Let $h^\varepsilon \in H^\varepsilon_{(\Delta,\tilde{X}_\varepsilon)}$ and suppose h^ε connects e^ε_i and $e^\varepsilon_j \in E^\varepsilon_{(\Delta,\tilde{X}_\varepsilon)}$. By definition there exist $h \in H_{(\Delta,\tilde{X})}$ and e_i, $e_j \in E_{(\Delta,\tilde{X})}$ such that $h^\varepsilon = \Theta_\varepsilon(h)$, $e^\varepsilon_i = \Theta_\varepsilon(e_i)$ and $e^\varepsilon_j = \Theta_\varepsilon(e_j)$. Let $\omega_h : [0,t^*] \to \tilde{X}$ be a parametrisation of h. Then the function $\omega^\varepsilon_h : [0,t^*] \to \tilde{X}_\varepsilon$ defined by $\omega^\varepsilon_h(t) = \Theta_\varepsilon(\omega_h(t))$ is a nondegenerate parametrisation of h^ε such that $\omega^\varepsilon_h(0) = e^\varepsilon_i$ and $\omega^\varepsilon_h(t^*) = e^\varepsilon_j$. Thus we now have a parametrisation for the connections in $H^\varepsilon_{(\Delta,\tilde{X}_\varepsilon)}$.

2.5.2 Flows on the Perturbed Skeleton

We now wish to determine for a given Δ-equivariant vector field $\mathbf{g}$, the direction of flow along a chosen connection $h^\varepsilon \in H^\varepsilon_{(\Delta,\tilde{X}_\varepsilon)}$. Define

$$\mathcal{F}^{\varepsilon,\mathbf{g}}_{h^\varepsilon}(t) = \left\langle \mathbf{g}(\omega^\varepsilon_{h^\varepsilon}(t)), \mathcal{T}_{\omega^\varepsilon_{h^\varepsilon}}(t) \right\rangle,$$

where $\mathcal{T}_{\omega_{h^\varepsilon}}(t) = (d/dt)\omega_{h^\varepsilon}(t)$. The next proposition allows us to determine the sign of $\mathcal{F}^{\varepsilon,\mathbf{g}}_{h^\varepsilon}(t)$ for any admissible perturbation $\mathbf{g}$.

Proposition 2.35
Let $\mathbf{g}$ *be a* Δ*-equivariant vector field and* $h^\varepsilon \in H^\varepsilon_{(\Delta,\tilde{X}_\varepsilon)}$. *Suppose* h^ε *connects* e^ε_i *and* $e^\varepsilon_j \in E^\varepsilon_{(\Delta,\tilde{X}_\varepsilon)}$. *Let* $\Theta_\varepsilon : \tilde{X} \to \tilde{X}_\varepsilon$ *be the* Δ*-equivariant diffeomorphism given in Theorem 2.6. Let* $h \in H_{(\Delta,\tilde{X})}$ *and* e_i, $e_j \in E_{(\Delta,\tilde{X})}$ *be chosen so that* $h^\varepsilon = \Theta_\varepsilon(h)$, $e^\varepsilon_i = \Theta_\varepsilon(e_i)$ *and* $e^\varepsilon_j = \Theta_\varepsilon(e_j)$. *Let* $\omega_h : [0,t^*] \to \tilde{X}$ *parametrise* h. *Suppose* $\mathcal{F}^{\mathbf{g}}_h(t) \neq 0$ *for all* $t \in (0,t^*)$. *Then for sufficiently small* ε *the sign of* $\mathcal{F}^{\varepsilon,\mathbf{g}}_h(t)$ *is given by that of* $\mathcal{F}^{\mathbf{g}}_h(t)$.

Proof. The connection h^ε is parametrised by the function $\omega_{h^\varepsilon}(t) = \Theta_\varepsilon(\omega_{h^\varepsilon}(t))$. Since Θ_0 is the identity map,

$$\omega_{h^\varepsilon}(t) = \omega_h(t) + \varepsilon\hat{\omega}_h(t) + O(\varepsilon^2),$$

for some function $\hat{\omega}_h(t)$. Hence $\mathcal{T}_{\omega_{h^\varepsilon}}(t) = \mathcal{T}_{\omega_h}(t) + \varepsilon\hat{\mathcal{T}}_{\omega_h}(t) + O(\varepsilon^2)$ and also

$$\begin{aligned} g(\omega_{h^\varepsilon}(t)) &= g(\omega_h(t) + \varepsilon\hat{\omega}_h(t)) \\ &= g(\omega_h(t)) + \varepsilon g'(\omega_h(t)) + O(\varepsilon^2). \end{aligned}$$

Therefore

$$\begin{aligned} \mathcal{F}^{\varepsilon,\mathbf{g}}_h(t) &= \left\langle g(\omega_h(t)) + \varepsilon g'(\omega_h(t)), \mathcal{T}_{\omega_h}(t) + \varepsilon\hat{\mathcal{T}}_{\omega_h}(t) \right\rangle \\ &= \langle g(\omega_h(t)), \mathcal{T}_{\omega_h}(t)\rangle + \varepsilon\left(\left\langle g(\omega_h(t)), \hat{\mathcal{T}}_{\omega_h}(t)\right\rangle + \langle g'(\omega_h(t)), \mathcal{T}_{\omega_h}(t)\rangle\right) + O(\varepsilon^2) \\ &= \mathcal{F}^{\mathbf{g}}_h(t) + \varepsilon\left(\left\langle g(\omega_h(t)), \hat{\mathcal{T}}_{\omega_h}(t)\right\rangle + \left\langle g'(\omega_h(t)), \mathcal{T}_{\omega_h}(t)\right\rangle\right) + O(\varepsilon^2). \end{aligned}$$

Since $\mathcal{F}^{\mathbf{g}}_h(t) \neq 0$ for all $t \in (0,t^*)$ we have that for sufficiently small ε,

$$\operatorname{sgn}(\mathcal{F}^{\varepsilon,\mathbf{g}}_h(t)) = \operatorname{sgn}(\mathcal{F}^{\mathbf{g}}_h(t)),$$

as required. □

This proposition covers the case of an admissible perturbation; that is, the case when there are no additional equilibria on the connection h. We now consider some very simple degenerate cases—when there are additional equilibria.

Definition 2.36
Let $h \in H_{(\Delta,\widetilde{X})}$ and suppose h connects the elements e_i and $e_j \in E_{(\Delta,\widetilde{X})}$. Let $\omega_h : [0,t^*] \to \widetilde{X}$ parametrise h, with $\omega_h(0) = e_i$ and $\omega_h(t^*) = e_j$. Let $\mathbf{g}$ be a Δ-equivariant vector field. Suppose there exist $t_1 \in (0,t^*)$ such that $\mathcal{F}_h^{\mathbf{g}}(t_1) = 0$ and $(d/dt)\mathcal{F}_h^{\mathbf{g}}(t_1) \neq 0$. Then $\mathbf{g}$ is called a *simple degenerate perturbation.* Any other perturbation $\mathbf{g}$ which is not admissible or a simple degenerate perturbation is called a *degenerate perturbation.*

The question now arises, what happens when we have a simple degenerate perturbation? We can no longer appeal to Proposition 2.35 to answer this question. The next proposition show that the behaviour is essentially the same.

Proposition 2.37
Let $\mathbf{g}$ be a Δ-equivariant vector field and $h^\varepsilon \in H^\varepsilon_{(\Delta,\widetilde{X}_\varepsilon)}$. Suppose h^ε connects e_i^ε and $e_j^\varepsilon \in E^\varepsilon_{(\Delta,\widetilde{X}_\varepsilon)}$. Let $\Theta_\varepsilon : \widetilde{X} \to \widetilde{X}_\varepsilon$ be the Δ-equivariant diffeomorphism given in Theorem 2.6. Let $h \in H_{(\Delta,\widetilde{X})}$, e_i and $e_j \in E_{(\Delta,\widetilde{X})}$ be chosen so that $h^\varepsilon = \Theta_\varepsilon(h)$, $e_i^\varepsilon = \Theta_\varepsilon(e_j)$ and $e_j^\varepsilon = \Theta_\varepsilon(e_j)$. Let $\omega_h : [0,t^*] \to \widetilde{X}$ parametrise h. Suppose there exists $t_0 \in (0,t^*)$ such that $\mathcal{F}_h^{\mathbf{g}}(t_0) = 0$ and $(d/dt)\mathcal{F}_h^{\mathbf{g}}(t_0) \neq 0$. Then for sufficiently small ε the sign of $\mathcal{F}_{h^\varepsilon}^{\varepsilon,\mathbf{g}}(t)$ is given by that of $\mathcal{F}_h^{\mathbf{g}}(t)$ for $t \neq t_0$. Moreover, there exist t_1 near t_0 such that $\mathcal{F}_{h^\varepsilon}^{\varepsilon,\mathbf{g}}(t_1) = 0$ and $(d/dt)\mathcal{F}_{h^\varepsilon}^{\varepsilon,\mathbf{g}}(t_1) \neq 0$.

Proof. By the proof of Proposition 2.35

$$\mathcal{F}_h^{\varepsilon,\mathbf{g}}(t) = \mathcal{F}_h^{\mathbf{g}}(t) + \varepsilon M(t),$$

where M is continuous on $[0,t^*]$ and so bounded. Since $\mathcal{F}_h^{\mathbf{g}}(t_0) = 0$, $(d/dt)\mathcal{F}_h^{\mathbf{g}}(t_0) \neq 0$, there exist $\delta > 0$ such that $\mathcal{F}_h^{\mathbf{g}}(t) \neq 0$ for all $t \in [t_0-\delta, t_0+\delta] - \{t_0\}$. Moreover, we may choose $\delta > 0$, smaller if necessary, so that $(d/dt)\mathcal{F}_h^{\mathbf{g}}(t) \neq 0$ for all $t \in [t_0-\delta, t_0+\delta]$. Now either $\mathcal{F}_h^{\mathbf{g}}(t) > 0$ for all $t \in (t_0, t_0+\delta]$ and $\mathcal{F}_h^{\mathbf{g}}(t) < 0$ for all $t \in [t_0-\delta, t_0)$, or vice versa. We suppose, without loss of generality, that $\mathcal{F}_h^{\mathbf{g}}(t) > 0$ for all $t \in (t_0, t_0+\delta]$ and $\mathcal{F}_h^{\mathbf{g}}(t) < 0$ for all $t \in [t_0-\delta, t_0)$.

Since $M(t)$ is bounded we may choose ε sufficiently small so that $\mathcal{F}_h^{\mathbf{g}}(t) + \varepsilon M(t) > 0$ for all $t \in (t_0, t_0+\delta]$ and $\mathcal{F}_h^{\mathbf{g}}(t) + \varepsilon M(t) < 0$ for all $t \in [t_0-\delta, t_0)$. By continuity there exists $t_1 \in [t_0-\delta, t_0+\delta]$ such that $\mathcal{F}_h^{\varepsilon,\mathbf{g}}(t_1) = 0$. Moreover, this zero is unique by the construction of the interval $[t_0-\delta, t_0+\delta]$.

Furthermore,

$$(d/dt)\mathcal{F}_h^{\varepsilon,\mathbf{g}}(t_1) = (d/dt)\mathcal{F}_h^{\mathbf{g}}(t_1) + \varepsilon M'(t_1).$$

Now $(d/dt)\mathcal{F}_h^{\mathbf{g}}(t_1) \neq 0$. If $(d/dt)\mathcal{F}_h^{\mathbf{g}}(t_1) + \varepsilon M'(t_1) = 0$ then we just need to choose ε small enough so that $(d/dt)\mathcal{F}_h^{\varepsilon,\mathbf{g}}(t_1) \neq 0$. □

This proposition shows that simple zeros on the skeleton correspond to simple zeros on the perturbed skeleton.

We now have a correspondence between the behaviour of the Δ-equivariant flows on the skeleton $\mathbb{X}_\Delta$ and the perturbed skeleton $\mathbb{X}_\Delta^p$ for admissible and simple degenerate perturbations. We summaries the results of Propositions 2.35 and 2.37 in the following Theorem:

Theorem 2.38
Let Γ be a compact Lie group acting on X. Let f be a Γ-equivariant bifurcation problem. Suppose there exists a bifurcating steady-state solution with isotropy $\Sigma \subset \Gamma$ and orbit $\widetilde{X} \subset X$. Let Δ be a closed subgroup of Γ and let g be Δ-equivariant and consider the perturbation $F : X \times \mathbb{R}^2 \to X$ defined by

$$F(x,\lambda,\varepsilon) = f(x,\lambda) + \varepsilon g(x).$$

Then there exist F and a Δ-invariant manifold $\widetilde{X}_\varepsilon$ which is Δ-equivariantly diffeomorphic to $\widetilde{X}$. Let $\mathbb{X}_\Delta$ be the skeleton of $\widetilde{X}$ and $\mathbb{X}^\varepsilon_\Delta$ the perturbed skeleton. Let $h \in H_{(\Delta,\widetilde{X})}$ connect e_i and $e_j \in E_{(\Delta,\widetilde{X})}$. Then for sufficiently small ε the simple zeros and signs of $\mathcal{F}^{\varepsilon,\mathbf{g}}_{h^\varepsilon}(t)$ are in direct correspondence with those of $\mathcal{F}^{\mathbf{g}}_h(t)$.

Proof. This is just Propositions 2.35 and 2.37. □

Higher Order Degeneracies

We have considered the simple behaviour that a perturbation $\mathbf{g}$ can exhibit. However, it is necessary to consider degenerate perturbations. Here we consider the types of behaviour that can occur on the perturbed skeleton when the perturbation $\mathbf{g}$ is degenerate, that is, the flow formula $\mathcal{F}^{\mathbf{g}}_h(t)$ has a degenerate zero. We are no longer able to give an exact correspondence between the behaviour on the skeleton and on the perturbed skeleton, but only a finite list of possible types of behaviour. We use singularity theory to investigate how the flow function behaves under small perturbations. The theory we present is actually well known. A comprehensive study is given in Golubitsky and Guillemin [29], a more specialised account in Guckenheimer and Holmes [45]. Golubitsky *et al.* [35] give a treatment in the context of bifurcation theory. Nevertheless we present these ideas in our framework of forced symmetry breaking to make the ideas more transparent in our context.

First Order Degeneracies. Suppose the function $\mathcal{F}^{\mathbf{g}}_h$ has the following property: there exists t_0 such that $\mathcal{F}^{\mathbf{g}}_h(t_0) = 0$, $\frac{d}{dt}\mathcal{F}^{\mathbf{g}}_h(t_0) = 0$ and $\frac{d^n}{dt^n}\mathcal{F}^{\mathbf{g}}_h(t_0) \neq 0$ for all $n \geq 2$. What type of behaviour can we expect from the function $\mathcal{F}^{\mathbf{g},\varepsilon}_{h^\varepsilon}(t)$ near t_0? In a neighbourhood of t_0 we may assume that $\mathcal{F}^{\mathbf{g}}_h(t) = at^2$, where $a \in \mathbb{R}$. The question we posed then becomes: what are the types of behaviour that can be expected from the universal unfolding of at^2? The universal unfolding of the function at^2 is the function $k(t) = at^2 + b$, where $b \in \mathbb{R}$. Hence, if $b \neq 0$ (a generic hypothesis) then the function k has either two real zeros or none. Therefore, by choosing ε sufficient small the function $\mathcal{F}^{\mathbf{g},\varepsilon}_{h^\varepsilon}$ has either two distinct real zeros or none in a neighbourhood on t_0. In summary we have:

Proposition 2.39
Let $\mathbf{g}$ be a Δ-equivariant vector field and $h^\varepsilon \in H^\varepsilon_{(\Delta,\widetilde{X}_\varepsilon)}$. Suppose h^ε connects e^ε_i and $e^\varepsilon_j \in E^\varepsilon_{(\Delta,\widetilde{X}_\varepsilon)}$. Let $\Theta_\varepsilon : \widetilde{X} \to \widetilde{X}_\varepsilon$ be the Δ-equivariant diffeomorphism given in Theorem 2.6. Let $h \in H_{(\Delta,\widetilde{X})}$, e_i and $e_j \in E_{(\Delta,\widetilde{X})}$ be chosen so that $h^\varepsilon = \Theta_\varepsilon(h)$, $e^\varepsilon_i = \Theta_\varepsilon(e_j)$ and $e^\varepsilon_j = \Theta_\varepsilon(e_j)$. Let $\omega_h : [0, t^*] \to \widetilde{X}$ parametrise h. Suppose there exists $t_0 \in (0, t^*)$ such that $\mathcal{F}^{\mathbf{g}}_h(t_0) = 0$, $(d/dt)\mathcal{F}^{\mathbf{g}}_h(t_0) = 0$ and $(d^n/dt^n)\mathcal{F}^{\mathbf{g}}_h(t_0) \neq 0$ for all $n \geq 2$. Then for sufficiently small ε the function $\mathcal{F}^{\varepsilon,\mathbf{g}}_{h^\varepsilon}(t)$ has one and only one of the following properties in a neighbourhood of t_0:

1. *The function $\mathcal{F}^{\varepsilon,\mathbf{g}}_{h^\varepsilon}(t)$ has no zeros in a neighbourhood of t_0. Thus there are no equilibria on the perturbed skeleton corresponding to the equilibria on the skeleton.*

2. *The function $\mathcal{F}^{\varepsilon,\mathbf{g}}_{h^\varepsilon}(t)$ has two distinct real zeros in a neighbourhood of t_0. So there are two perturbed equilibria corresponding to the single equilibrium on the skeleton.*

Furthermore, we cannot determine which type of behaviour will occur.

Proof. All follows from the discussion above. The fact that we cannot determine which type of behaviour occurs follows directly from the fact that we do not know the form of the diffeomorphism Θ_ε. □

It is this type of degeneracy that will often occur in our work.

Second Order Degeneracies. We now study the behaviour of the function $\mathcal{F}_h^{\mathbf{g}}$ when it satisfies the conditions: there exist t_0 such that $\mathcal{F}_h^{\mathbf{g}}(t_0) = \frac{d}{dt}\mathcal{F}_h^{\mathbf{g}}(t_0) = \frac{d^2}{dt^2}\mathcal{F}_h^{\mathbf{g}}(t_0) = 0$ and $\frac{d^n}{dt^n}\mathcal{F}_h^{\mathbf{g}}(t_0) \neq 0$ for all $n \geq 3$. In a neighbourhood of t_0 the function $\mathcal{F}_h^{\mathbf{g}}(t)$ has the form at^3. The universal unfolding of this function is given by $k(t) = at^3 + bt + c$. The bifurcation set for the function k is given by $4b^3 + 27ac^2 = 0$, see Guckenheimer and Holmes [45], p. 355. The bifurcation set has three regions. In the first the function k has three zeros, in the second k has one zero and in third k has two zeros. The third region is not generic, and k is actually degenerate in this region.

We summaries these results in the following proposition.

Proposition 2.40
Let $\mathbf{g}$ *be a* Δ*-equivariant vector field and* $h^\varepsilon \in H^\varepsilon_{(\Delta,\widetilde{X}_\varepsilon)}$. *Suppose* h^ε *connects* e_i^ε *and* $e_j^\varepsilon \in E^\varepsilon_{(\Delta,\widetilde{X}_\varepsilon)}$. *Let* $\Theta_\varepsilon : \widetilde{X} \to \widetilde{X}_\varepsilon$ *be the* Δ*-equivariant diffeomorphism given in Theorem 2.6. Let* $h \in H_{(\Delta,\widetilde{X})}$, e_i *and* $e_j \in E_{(\Delta,\widetilde{X})}$ *be chosen so that* $h^\varepsilon = \Theta_\varepsilon(h)$, $e_i^\varepsilon = \Theta_\varepsilon(e_j)$ *and* $e_j^\varepsilon = \Theta_\varepsilon(e_j)$. *Let* $\omega_h : [0, t^*] \to \widetilde{X}$ *parametrise* h. *Suppose there exists* $t_0 \in (0, t^*)$ *such that* $\mathcal{F}_h^{\mathbf{g}}(t_0) = 0$, $(d/dt)\mathcal{F}_h^{\mathbf{g}}(t_0) = (d^2/dt^2)\mathcal{F}_h^{\mathbf{g}}(t_0) = 0$ *and* $(d^n/dt^n)\mathcal{F}_h^{\mathbf{g}}(t_0) \neq 0$ *for all* $n \geq 3$. *Then for sufficiently small* ε *the function* $\mathcal{F}_{h^\varepsilon}^{\varepsilon,\mathbf{g}}(t)$ *has one and only one of the following properties in a neighbourhood of* t_0*:*

1. *The function* $\mathcal{F}_{h^\varepsilon}^{\varepsilon,\mathbf{g}}(t)$ *has one zero in a neighbourhood of* t_0. *Thus there is one equilibrium on the perturbed skeleton corresponding to the equilibrium on the skeleton.*
2. *The function* $\mathcal{F}_{h^\varepsilon}^{\varepsilon,\mathbf{g}}(t)$ *has two distinct real zeros in a neighbourhood of* t_0. *So there are two perturbed equilibria corresponding to the single equilibrium on the skeleton.*
3. *The function* $\mathcal{F}_{h^\varepsilon}^{\varepsilon,\mathbf{g}}(t)$ *has three distinct real zeros in a neighbourhood of* t_0. *So we have three equilibria on the perturbed skeleton corresponding to the equilibrium on the skeleton.*

Furthermore, we cannot determine which type of behaviour will occur, but generically at this type of degeneracy only 1 or 3 will occur.

Proof. The proof follows from the discussion above. □

It is possible to consider higher order degeneracies, and a complete theory is given in Golubitsky and Gulliemin [29]. However, we find no need to consider such degeneracies since they do not occur in our work. However, we do state the following theorem for completeness.

Theorem 2.41
Let $\mathbf{g}$ *be a* Δ*-equivariant vector field and* $h^\varepsilon \in H^\varepsilon_{(\Delta,\widetilde{X}_\varepsilon)}$. *Suppose* h^ε *connects* e_i^ε *and* $e_j^\varepsilon \in E^\varepsilon_{(\Delta,\widetilde{X}_\varepsilon)}$. *Let* $\Theta_\varepsilon : \widetilde{X} \to \widetilde{X}_\varepsilon$ *be the* Δ*-equivariant diffeomorphism given in Theorem 2.6. Let* $h \in H_{(\Delta,\widetilde{X})}$, e_i *and* $e_j \in E_{(\Delta,\widetilde{X})}$ *be chosen so that* $h^\varepsilon = \Theta_\varepsilon(h)$, $e_i^\varepsilon = \Theta_\varepsilon(e_j)$ *and* $e_j^\varepsilon = \Theta_\varepsilon(e_j)$. *Let* $\omega_h : [0, t^*] \to \widetilde{X}$ *parametrise* h. *Suppose there exists* $t_0 \in (0, t^*)$ *such that* $\mathcal{F}_h^{\mathbf{g}}(t_0) = \ldots = (d^{(n-1)}/dt^{(n-1)})\mathcal{F}_h^{\mathbf{g}}(t_0) = 0$ *and* $(d^{(m)}/dt^{(m)})\mathcal{F}_h^{\mathbf{g}}(t_0) \neq 0$ *for all* $m \geq n$. *Then for sufficiently small* ε *the behaviour of the function* $\mathcal{F}_{h^\varepsilon}^{\varepsilon,\mathbf{g}}(t)$ *in a neighbourhood of* t_0 *is given by the universal unfolding*

$$h(t) = a_0 + a_1 t + \ldots + a_{n-2}t^{n-2} + a_n t^n,$$

of $a_n t^n$, *where* $a_j \in \mathbb{R}$.

Proof. The conditions on the function $\mathcal{F}_h^{\mathbf{g}}(t)$ show that in a neighbourhood of t_0 the function has the form $a_n t^n$ where $a_n \in \mathbb{R}$. The behaviour of all perturbations of $a_n t^n$ are captured by the universal unfolding $a_0 + a_1 t + \ldots + a_{n-2}t^{n-2} + a_n t^n$, see Guckenheimer and Holmes [45]. □

This theorem states that there is only a finite number of possible types of behaviour on the perturbed skeleton when the perturbation term $\mathbf{g}$ is degenerate.

2.6 Forced Symmetry Breaking of Euclidean Equivariant Systems

In this section we describe how Liapunov–Schmidt reduction may be used to provide the formal machinery necessary for our study of forced symmetry breaking of planforms which occur in Euclidean equivariant systems. It is important to specify exactly what we mean by forced symmetry breaking of a planform. Planforms are functions that are periodic with respect to some lattice. When we introduce forced symmetry breaking effects, we do not allow an arbitrary perturbation; we must be more restrictive. We consider only those perturbations which are "supported" by the lattice. That is, perturbations, which are equivariant with respect to some subgroup of the symmetry group of the lattice and are periodic with respect to some "suitably nice" perturbation of the lattice. Obviously this implies that the class of perturbations we allow is much smaller than the general class of all Euclidean equivariant perturbations, but this approach is sensible. This situation may appear familiar, a common problem with the general methods of Section 1.6 is the stability of solutions can only be studied with respect to perturbations supported by the lattice. This problem is complex and has not yet been resolved. Thus our study of forced symmetry breaking is restricted to a certain class of perturbations.

This section is organised as follows. We begin in Subsection 2.6.1 by introducing some basic theory from functional analysis. In Subsection 2.6.2 we set up the forced symmetry breaking problem for Euclidean invariant systems, and apply Liapunov–Schmidt reduction to yield the reduced equations.

2.6.1 Fredholm Operators

Liapunov–Schmidt reduction in infinite dimensions requires additional theoretical tools so that we may sensibly take complements in infinite dimensional spaces. This subsection introduces the basic ideas we require; that is, Fredholm operators. The material here can be found in Golubitsky and Schaeffer [31].

Definition 2.42
Let $\mathcal{X}$ and $\mathcal{Y}$ be Banach spaces. A bounded linear operator $L : \mathcal{X} \to \mathcal{Y}$ is called Fredholm if the following two conditions hold:

1. $\ker L$ is a finite dimensional subspace of $\mathcal{X}$.
2. range L is a closed subspace of $\mathcal{Y}$ of finite codimension.

If L is Fredholm, the index of L is the integer $i(L) = \dim \ker L - \text{codim range } L$. The fundamental property of Fredholm operators is the existence of closed subspaces M and N such that

$$a)\ \mathcal{X} = \ker L \oplus M \quad b)\ \mathcal{Y} = N \oplus \text{range } L.$$

It is not in general true that M and N are orthogonal complements of $\ker L$ and range L, respectively[3]. We make the following assumptions,

1. Γ is a compact (Lie) group.
2. $\Phi : \mathcal{X} \times \mathbb{R}^{k+1} \to \mathcal{Y}$, $\Phi(0,0) = 0$ is a Γ-equivariant smooth map between Banach spaces.
3. Γ acts on $\mathcal{Y}$.
4. $L = (\mathrm{d}\Phi)_0$ is an elliptic differential operator.

[3]See Golubitsky and Schaeffer [31] p. 291 for an example.

The assumption that L is an elliptic differential operator rectifies the problem with taking complements, and we assume that L is a Fredholm operator of index zero[4]. The additional group structure implies that: 1) L commutes with Γ, 2) $\ker L$ is an invariant subspace of $\mathcal{X}$, and 3) range L is an invariant subspace of $\mathcal{Y}$. The generalities of Liapunov–Schmidt reduction now imply that the equations that result from the reduction are (or can be made) Γ-equivariant.

2.6.2 Liapunov–Schmidt Reduction

In this subsection we study Liapunov–Schmidt reduction of a system of PDEs to ODEs, when forced symmetry breaking terms are present. We adopt the hypotheses of the previous subsection, namely: Γ is a compact Lie group, Φ_1 is Γ-equivariant, Γ acts on $\mathcal{Y}$ and L_1 is an elliptic differential operator[5]. The methods of Section 1.6 show that

$$\ker L_1 = \{\mathbf{u} = \sum_{j=1}^{s} z_j e^{2\pi i \mathbf{K}_j \cdot \mathbf{x}} + c.c. \big| z_j \in \mathbb{C},\ |\mathbf{K}_j| = k_c\},$$

where the $\mathbf{K}_j$'s are the wave vectors of the dual lattice of length k_c. We begin with a definition.

Definition 2.43
Let $\mathcal{L}$ be a lattice with symmetry group Γ. A perturbation of $\mathcal{L}$ is a 1-parameter family of lattices $\mathcal{L}_\varepsilon$, with ε as parameter such that for each ε:

1. The symmetry group Δ of $\mathcal{L}_\varepsilon$ is a subgroup of Γ.
2. There exists a smooth function $\Psi_\varepsilon : \mathbb{R}^n \times \mathbb{R} \to \mathbb{R}^n$ such that $\Psi_\varepsilon(\mathcal{L}) = \mathcal{L}_\varepsilon$.

The conditions on a perturbed lattice are imposed so that it is a smooth distortion of the original lattice. In addition, to ensure that we can achieve the technical condition that the number of wave vectors are the same and may be expressed using the coordinates of the original lattice.

We now formulate our problem. Let $\Phi_1 : \mathcal{X} \times \mathbb{R} \to \mathcal{Y}$, $\Phi_1(0,0) = 0$, so Φ_1 is the original unperturbed system. Let $\Phi_2 : \mathcal{X} \to \mathcal{Y}$, $\Phi_2(0) = 0$ be a smooth map between $\mathcal{X}$ and $\mathcal{Y}$. Assume that Φ_2 is equivariant with respect to a subgroup Δ of Γ. As a bifurcation problem itself the Φ_2 has solutions that are supported by the perturbed lattice. Define $\Phi : \mathcal{X} \times \mathbb{R}^2 \to \mathcal{Y}$ by

$$\Phi(x, \lambda, \varepsilon) = \Phi_1(x, \lambda) + \varepsilon \Phi_2(x). \tag{2.5}$$

We want to solve $\Phi(x, \lambda, \varepsilon) = 0$ for x as a function of λ and ε near $(0,0,0)$. Importantly, the function in (2.5) is equivariant with respect to Γ when $\varepsilon = 0$ and only Δ when $\varepsilon \neq 0$. Let $L_2 = (\mathrm{d}\Phi_2)_0$. Then

$$L = (\mathrm{d}\Phi)_0 = (\mathrm{d}\Phi_1)_0 + \varepsilon(\mathrm{d}\Phi_2)_0 = L_1 + \varepsilon L_2.$$

If we assume that L_2 is an elliptic differential operator, then for sufficiently small ε, L is an elliptic differential operator. Recall that

$$\ker L_1 = \{\mathbf{u} = \sum_{j=1}^{s} z_j e^{2\pi i \mathbf{K}_j \cdot \mathbf{x}} + c.c. \big| z_j \in \mathbb{C},\ |\mathbf{K}_j| = k_c\}.$$

The are two methods to approach the kernel of L. The first method directly argues as follows. Let $\mathbf{u} \in \ker L$. When $\varepsilon = 0$, $\mathbf{u}_\varepsilon \in \ker L_1$. The definition of a perturbed lattice ensures that $\dim \ker L = \dim \ker L_1$. Thus we must have $\mathbf{u}_\varepsilon = \mathbf{u} + \varepsilon \hat{\mathbf{u}}$ for some vectors $\mathbf{u}_\varepsilon \in \ker L_1$ and $\hat{\mathbf{u}}$ must be a wave vector supported by the perturbed lattice. An alternative and direct calculation

[4] If we consider an example such as the Brusselator which gives a system of elliptic differential equations, then the operator defined by these equations is Fredholm of index zero, see Golubitsky and Schaeffer [31] p. 335.

[5] The use of subscripts will become clear shortly.

proceeds as follows: the kernel of L has the form (since we are seeking periodic functions with respect to the perturbed lattice),

$$\begin{aligned}\ker L &= \left\{ \mathbf{u}_\varepsilon = \sum_{j=1}^{s} z_j e^{2\pi \mathrm{i}\mathbf{K}_j^\varepsilon \cdot \mathbf{x}} + c.c. \right\} \\ &= \left\{ \mathbf{u}_\varepsilon = \sum_{j=1}^{s} z_j e^{2\pi \mathrm{i}\mathbf{K}_j \cdot \Psi_\varepsilon^{-1}(\mathbf{x})} + c.c. \right\}\end{aligned}$$

Now Ψ_ε^{-1} is assumed to be smooth and satisfies the condition $\Psi_\varepsilon^{-1} = \mathrm{id}$ when $\varepsilon = 0$, so

$$\begin{aligned}&= \left\{ \mathbf{u}_\varepsilon = \sum_{j=1}^{s} z_j e^{2\pi \mathrm{i}\mathbf{K}_j \cdot (\mathbf{x} + \hat{\Psi}_\varepsilon(\mathbf{x}))} + c.c. \right\} \\ &= \left\{ \mathbf{u}_\varepsilon = \sum_{j=1}^{s} z_j e^{2\pi \mathrm{i}\mathbf{K}_j \cdot \mathbf{x}} e^{2\pi \mathrm{i}\mathbf{K}_j \cdot \hat{\Psi}_\varepsilon(\mathbf{x}))} + c.c. \right\} \\ &= \left\{ \mathbf{u}_\varepsilon = \sum_{j=1}^{s} (z_j + \varepsilon \hat{z}_j) e^{2\pi \mathrm{i}\mathbf{K}_j \cdot \mathbf{x}} + c.c. \right\} \\ &= \left\{ \mathbf{u}_\varepsilon = \mathbf{u} + \varepsilon \hat{\mathbf{u}} \middle| \mathbf{u} \in \ker L \right\}.\end{aligned}$$

It follows that when $\varepsilon = 0$, $\ker L = \ker L_1$ is Γ-invariant. Whilst, when $\varepsilon \neq 0$, $\ker L$ is only Δ-invariant. Since L is an elliptic differential operator it follows from Golubitsky and Schaeffer [31] pages 333 and 334, that L is a Fredholm operator of index zero. So we may choose invariant complements M and N such that

$$\mathcal{X} = \ker L \oplus M, \quad \mathcal{Y} = N \oplus \text{range } L. \tag{2.6}$$

We are now in a position to perform the reduction.

Let $E_\varepsilon : \mathcal{Y} \to \text{range } L$ be projection with respect to the split of $\mathcal{X}$ in (2.6). Then the equation $\Phi(x, \lambda, \varepsilon) = 0$ is equivalent to,

$$\begin{aligned}E_\varepsilon \Phi(x, \lambda, \varepsilon) &= 0, \\ (I - E_\varepsilon)\Phi(x, \lambda, \varepsilon) &= 0.\end{aligned}$$

The map E_ε must satisfy the condition that $E_\varepsilon = E + \varepsilon \hat{E}$, where E is the corresponding projection map given by the reduction of the equation $\Phi_1 = 0$, that is the map in the unperturbed case. So E_ε must be Γ-equivariant when $\varepsilon = 0$, this follows directly from Proposition 3.3 of Golubitsky and Schaeffer [31], as does the Δ-equivariance when $\varepsilon \neq 0$. It then follows that the map $I - E_\varepsilon$ satisfies the same equivariance conditions. Define $F : \ker L \times M \times \mathbb{R}^2 \to \text{range } L$, by

$$F(v, w, \lambda, \varepsilon) = E_\varepsilon \Phi(v + w, \lambda, \varepsilon).$$

Since L is an invertible elliptic differential operator, the implicit function theorem states that there exists a function $W : \ker L \times \mathbb{R}^2 \to M$ such that

$$E_\varepsilon \Phi(v + W(v, \lambda, \varepsilon), \lambda, \varepsilon)) = 0.$$

The function $W(v, \lambda, \varepsilon)$ satisfies the same equivariance property as E_ε. Indeed, when $\varepsilon = 0$, $W(v, \lambda, \varepsilon) = W(v, \lambda)$, where $W(v, \lambda)$ is the function found in the unperturbed problem. So $W(v, \lambda, \varepsilon) = W(v, \lambda) + \varepsilon \hat{W}(v, \lambda, 0)$. The reduced function is now defined by

$$\phi(v, \lambda, \varepsilon) = (I - E_\varepsilon)\Phi(v + W(v, \lambda, \varepsilon), \lambda, \varepsilon).$$

We must now use the fact that this reduced function must be equal to ϕ_1—the reduced function in the unperturbed problem—when $\varepsilon = 0$, to simplify ϕ. We perform this simplification in a number of steps.

Step 1: The function $I - E_\varepsilon$ must have the form $I - E + \varepsilon F$, where E is the function which occurs in the Liapunov–Schmidt reduction of the unperturbed function Φ_1 and F is some function.

Step 2: Consider the expression

$$\begin{aligned}\phi(v,\lambda,\varepsilon) &= (I - E_\varepsilon)\Phi(v,\lambda,\varepsilon)\\ &= (I - E)\Phi(v,\lambda,\varepsilon) + \varepsilon F\Phi(v,\lambda,\varepsilon).\end{aligned}$$

We must simplify both parts of this expression.

Step 3: Consider the term $(I - E)\Phi$. Taylor expansion about $\lambda = 0$ and $\varepsilon = 0$ implies that

$$\begin{aligned}(I - E)\Phi(v,\lambda,\varepsilon) &= (I - E)\left(\Phi_1(v + W(v,\lambda,\varepsilon),\lambda) + \varepsilon\Phi_2(v + W(v,\lambda,\varepsilon))\right)\\ &= (I - E)\left(\Phi_1(v + W(v,\lambda),\lambda) + \varepsilon\hat{\Phi}_1(v,\lambda) + \varepsilon\Phi_2(v + W(v,\lambda)) + \varepsilon^2\hat{\Phi}_2(v,\lambda)\right)\\ &= \phi_1(v,\lambda) + (I - E)\left(\varepsilon\hat{\Phi}_1(v) + \varepsilon\lambda\widetilde{\Phi}_1(v) + \varepsilon\Phi_2(v + W(v,0)) + \varepsilon\lambda\widetilde{\Phi}_2(v)\right.\\ &\quad \left.+\varepsilon^2\hat{\Phi}_2(v,0) + \varepsilon^2\lambda\hat{\Phi}_2'(v)\right)\\ &= \phi_1(v,\lambda) + \varepsilon\phi_2(v) + \varepsilon\lambda\phi_3(v) + \varepsilon^2\phi_4(v) + \varepsilon^2\lambda\phi_5(v).\end{aligned}$$

This completes the simplification of the $(I - E)\Phi(v,\lambda,\varepsilon)$ term.

Step 4: Consider the term $F\Phi$. Again by Taylor expansion we have

$$\begin{aligned}F\Phi(v,\lambda,\varepsilon) &= \varepsilon F\left(\Phi_1(v + W(v,\lambda),\lambda) + \varepsilon\hat{\Phi}_1(v,\lambda) + \varepsilon\Phi_2(v + W(v,\lambda)) + \varepsilon^2\hat{\Phi}_2(v,\lambda)\right)\\ &= \varepsilon F\left(\Phi_1(v,0) + \varepsilon\hat{\Phi}_1(v) + \lambda\bar{\Phi}_1(v) + \varepsilon\lambda\widetilde{\Phi}_1(v) + \varepsilon\Phi_2(v + W(v,0)) + \varepsilon\lambda\widetilde{\Phi}_2(v)\right.\\ &\quad \left.+\varepsilon^2\hat{\Phi}_2(v,0) + \varepsilon^2\lambda\hat{\Phi}_2'(v)\right)\\ &= \varepsilon\phi_6(v) + \varepsilon\lambda\phi_7(v) + \varepsilon^2\phi_8(v) + \varepsilon^2\lambda\phi_9(v) + \varepsilon^3\phi_{10}(v) + \varepsilon^3\lambda\phi_{11}(v).\end{aligned}$$

This completes the simplification of $F\Phi$.

Step 5: Combining together Steps 3 and 4 we find that the Liapunov–Schmidt reduced function has the form

$$\phi(v,\lambda,\varepsilon) = \phi_1(v,\lambda) + \varepsilon\phi_2(v) + \varepsilon\lambda\phi_3(v) + \varepsilon^2\phi_4(v) + \varepsilon^2\lambda\phi_5(v) + \varepsilon^3\phi_6(v) + \varepsilon^3\lambda\phi_7(v),$$

where $\phi_1(v)$ is the reduced function of Φ_1 in the unperturbed case. This function commutes with Γ when $\varepsilon = 0$ and Δ when $\varepsilon \neq 0$. It is now possible to choose coordinates on $\ker L$ and $(\text{range } L)^\perp$ to achieve a set of reduced equations. We have not been able to find a method of "scaling away" the terms of quadratic order and higher in ε and λ. However, since we are local to the origin and free to vary ε close to zero, the following truncation would make sense,

$$\phi(v,\lambda,\varepsilon) \approx \phi_1(v,\lambda) + \varepsilon\phi_2(v),$$

or by choosing coordinates we may write the reduced system as equations in the form

$$\mathbf{F}(z,\lambda,\varepsilon) = \mathbf{f}(\mathbf{z},\lambda) + \varepsilon\mathbf{g}(\mathbf{z}). \tag{2.7}$$

The process given above allows us to reduce any system of PDEs (under suitable hypothesis) where forced symmetry breaking is present to a system of scalar equations. All our work from this point assume that the reduction has been performed and the reduced equations are of the form in (2.7).

Part II

Forced Symmetry Breaking of Planforms in Two Dimensions

Chapter 3

Steady-State Bifurcation with Two-Dimensional Euclidean Symmetry

Pattern formation in two-dimensional systems has been the focus of a great deal of research over recent years, applied to many diverse fields such as: Rayleigh–Bénard convection, solidification, and chemical reaction-diffusion systems in Turing instability. In particular, equivariant bifurcation theory has been the main theoretical tool—exploiting the symmetry of the situations. In this part we make a partial classification of the behaviour exhibited by two-dimensional patterns (planforms) when the symmetry of the modelling equations is broken.

The Euclidean group $\mathbf{E}(2)$ is not compact, but the techniques of Section 1.6 reduce a general $\mathbf{E}(2)$-equivariant bifurcation problem to finding solutions that are spatially doubly periodic. These solutions are periodic with respect to the square or hexagonal lattice. (The solutions can be periodic with respect to the rhombic lattice as well, but we shall not consider this situation.) On the square lattice the bifurcation problem is reduced to a $\Gamma_s = \mathbf{D}_4 \dot{+} \mathbf{T}^2$-equivariant bifurcation problem, whilst on the hexagonal lattice we get a $\Gamma_h = \mathbf{D}_6 \dot{+} \mathbf{T}^2$-equivariant bifurcation problem.

Bifurcation problems with $\mathbf{D}_4 \dot{+} \mathbf{T}^2$ symmetry have been studied by numerous authors. Dionne and Golubitsky [20] derive the symmetry of the axial solutions and a study of the stability of the primary bifurcations undertaken in [21]. Golubitsky and Stewart [33] give a highly comprehensive (but by no means exhaustive) collection of applications for steady-state bifurcation on the square lattice, in particular they study: reaction-diffusion systems, liquid crystals, hallucination patterns and fluid flows—giving emphasis to the difference in planforms for the scalar and pseudoscalar actions of the Euclidean group.

In experiments and the physical environment we see more hexagonal patterns than square ones. For this reason steady-state bifurcation on the hexagonal lattice has seen a considerable research effort. This work began with Sattinger [75]. Then Buzano and Golubitsky [6], motivated by Rayleigh–Bénard convection, used singularity theory (see Golubitsky and Schaeffer [31]) to study the degenerate $\mathbf{D}_6 \dot{+} \mathbf{T}^2$-equivariant bifurcation problem. The use of singularity theory is necessary in this case due to the presence of quadratic equivariants in the branching equations. Their work on the normal forms and universal unfoldings allowed a classification of the behaviour expected from the primary bifurcating branches—namely hexagons and rolls. The analysis of Buzano and Golubitsky represents, essentially, the limit of singularity theory, although modern computers have improved the situation. Further to this study, Golubitsky *et al.* [36] studied this problem with an additional $\mathbf{Z}_2$ symmetry, which removed all even order terms from the branching equations. This new problem exhibited two additional primary solutions—triangles and the patchwork quilt. The patchwork quilt solution is always unstable. A complete classification of the translation free axial planforms for the hexagonal lattice was

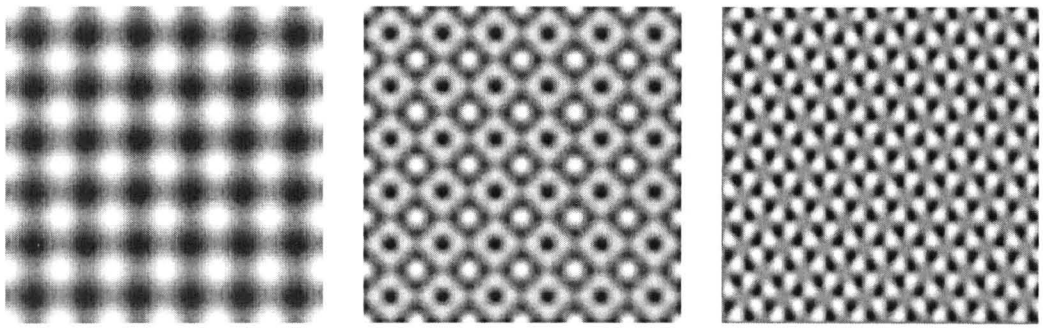

(a) Squares (b) Super squares (c) Anti-squares

Figure 3.1: Translation free axial planforms found on the square lattice. (a) Squares are the only translation free axial planform in the four-dimensional representation of Γ_s. (b) Super squares and anti-squares are the only translation free axial planforms in the eight-dimensional representation of Γ_s.

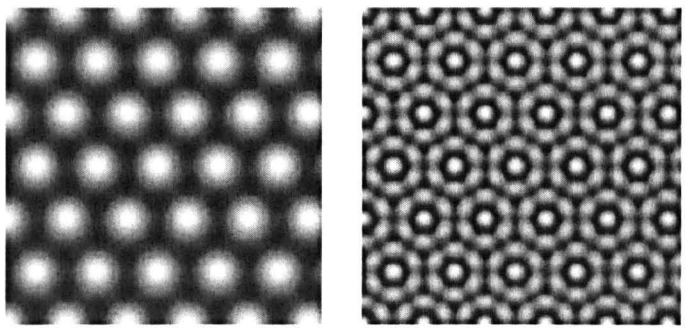

(a) Hexagons (b) Super hexagons

Figure 3.2: Translation free axial planforms found on the hexagonal lattices. (a) Hexagons are the only translation free axial planform in the six-dimensional representation of Γ_h. (b) Super hexagons are the only translation free axial planforms in the twelve-dimensional representation of Γ_h.

obtained by Dionne and Golubitsky [20]. Later a stability analysis of the twelve-dimensional problem was given by Dionne *et al.* [21].

In this part we study the forced symmetry breaking of group orbits of the translation free axial solutions which occur on the square and hexagonal lattices. The classification of Dionne and Golubitsky [20] shows there are a total of five different translation free axial solutions on the square and hexagonal lattices. On the square lattice these solutions are named: squares, super squares and anti-squares. Figure 3.1 present renderings of these planforms. On the hexagonal lattice the solutions are termed hexagons and super hexagons. In Figure 3.2 illustrates these two planforms.

The general set up we adopt is to restrict the space of solutions of the PDEs to those that are periodic with respect to the square or hexagonal lattices. The methods of Section 1.6 reduce our problem to a system of ODEs

$$\dot{\mathbf{z}} = \mathbf{f}(\mathbf{z}, \lambda),$$

where $\mathbf{f} : \mathbb{C}^s \times \mathbb{R} \to \mathbb{C}^s$ and $s = 2$ or 4 on the square lattice and $s = 3$ or 6 on the hexagonal lattice. The results of Dionne and Golubitsky [20] prove the existence of bifurcating group orbits of solutions with isotropy subgroups isomorphic (but not necessarily conjugate) to $\mathbf{D}_4$ and $\mathbf{D}_6$. In all cases the group orbit is diffeomorphic to a 2-torus, which we shall always denote by X_0. We now consider the following problem. What happens to X_0 when the vector field $\mathbf{f}$ is perturbed to the new system

$$\mathbf{F}(\mathbf{z}, \lambda, \varepsilon) = \mathbf{f}(\mathbf{z}, \lambda) + \varepsilon \mathbf{g}(\mathbf{z}),$$

where ε is real and small and $\mathbf{g}$ is equivariant with respect to only a subgroup of the symmetry group of the underlying lattice? Specifically, if $\Gamma = H \dot{+} \mathbf{T}^2$ is the symmetry group of the square or hexagonal lattice, so $H = \mathbf{D}_4$ or $\mathbf{D}_6$ respectively; the map $\mathbf{g}$ is chosen to be equivariant with respect to a non-trivial subgroup of H which is not isomorphic to $\mathbf{Z}_2$. This rather strange condition ensures that our new vector field $\mathbf{F}$ still has equilibria.

We study the square lattice problem in Chapter 4 and the hexagonal problem in Chapter 5. In each case we perform the following analysis of the perturbed vector field $\mathbf{F}$ on the group orbit X_0. For each subgroup $\Delta \subset H$ satisfying the criterion above we calculate the skeleton and its symmetry properties. In the four and six-dimensional representations of the square and hexagonal lattices respectively, the flow formulas are computed for some perturbations, and we investigate conditions on the perturbation term $\mathbf{g}$ for admissible flows and the existence of heteroclinic cycles and networks between equilibria on the skeleton. For the higher eight and twelve-dimensional representations our results are limited due to the complexities of the invariants and equivariants. For this reasons we give only partial results concerning the flow induced on the skeleton by the perturbation $\mathbf{g}$. In particular we could not exhibit any admissible perturbations $\mathbf{g}$—even though we know that they must exist. Finally we complete our analysis by presenting some planforms.

Chapter 4

Forced Symmetry Breaking on the Square Lattice

4.1 Introduction

Many authors have studied steady-state symmetry-breaking on the square lattice. In particular, Dionne and Golubitsky [20] gave a group theoretic analysis of the bifurcation problem, proving the existence of three different translation free axial planforms. Dionne *et al.* [21] gave a collection of stability results for the axial solution branches, which occur in the eight-dimensional problem. In this chapter we analyse the forced symmetry breaking of the three translation free axial solutions.

Let us recall the methods of Section 1.6 applied to the square lattice. Define two linearly independent vectors $\boldsymbol{\ell}_1 = (1,0)$ and $\boldsymbol{\ell}_2 = (0,1)$. The square lattice is defined by

$$\mathcal{L}_s = \{n_1\boldsymbol{\ell}_1 + n_2\boldsymbol{\ell}_2 | n_1,\ n_2 \in \mathbb{Z}\}.$$

The symmetry group of $\mathcal{L}_s$ is given by $\Gamma_s = \mathbf{D}_4 \dot{+} \mathbf{T}^2$. Here $\mathbf{D}_4$ is the dihedral group of order eight generated by a rotation ρ by $\pi/2$ anti-clockwise about the origin, κ a reflection in the line $x = y$ and $\mathbf{T}^2 = \mathbb{R}^2/\mathcal{L}_s$ is the translational symmetry of the lattice. We seek functions $\mathbf{u} \in \mathcal{X}$ which are doubly periodic with respect to the square lattice $\mathcal{L}_s$, and so are members of $\mathcal{X}_{\mathcal{L}_s}$. Define $\mathbf{k}_1 = (1,0)$ and $\mathbf{k}_2 = (0,1)$. The dual lattice to $\mathcal{L}_s$ is defined by

$$\mathcal{L}_s^* = \{n_1\mathbf{k}_1 + n_2\mathbf{k}_2 | n_1,\ n_2 \in \mathbb{Z}\}.$$

Now we may write a function $\mathbf{u} \in \mathcal{X}_{\mathcal{L}_s}$ in the form

$$\mathbf{u}(\mathbf{x},t) = \sum_{j=1}^{t} z_j e^{2\pi i \mathbf{K}_j \cdot \mathbf{x}} \mathbf{u}_j + c.c., \tag{4.1}$$

where $z_j \in \mathbb{C}$, the $\mathbf{K}_j$'s are the dual lattice vectors which meet the critical sphere of radius $k_c = |\mathbf{K}_j| = \sqrt{\alpha^2 + \beta^2}$ for integers α and β and *c.c.* denotes complex conjugate. Dionne and Golubitsky [20] show that $t = 2$ or 4. The case $t = 2$ occurs, for example when $k_c = 1$, with $(\alpha,\beta) = (1,0)$ and the case $t = 4$ when $k_c = \sqrt{5}$ and $(\alpha,\beta) = (2,1)$. Note that there are several special cases given by, for example, $(\alpha,\beta) = (5,0)$ and $(\alpha,\beta) = (4,3)$; these occur in mode interactions as studied by Crawford [13] and will not concern us. The expansion in (4.1) allows the bifurcation problem to be identified with $\mathbb{C}^t$. The representation of Γ_s on $\mathbb{C}^t$ is determined by its action on the complex amplitudes z_j in (4.1). In addition we note that all the representations are translation free. Our problem is now in the standard form, and we study the ODE

$$\dot{\mathbf{z}} = \mathbf{f}(\mathbf{z},\lambda), \tag{4.2}$$

where $\mathbf{f} : \mathbb{C}^t \times \mathbb{R} \to \mathbb{C}^t$ is Γ_s-equivariant. With this machinery in place we know, by the work of Dionne and Golubitsky [20], that there exist three translation free axial solutions, one in the four-dimensional representation ($t = 2$) and two in the eight-dimensional representation ($t = 4$). The group orbit of each of these solutions is diffeomorphic to a 2-torus, which we denote by X_0. We study the behaviour of X_0 when symmetry breaking terms with symmetry (isomorphic to) $\mathbf{D}_4$, $\mathbf{D}_2[\rho^2, \kappa\rho]$ and $\mathbf{D}_2[\rho^2, \kappa]$ are added to (4.2). Since X_0 is (generically) normally hyperbolic the methods of Chapter 2 become available to us. In particular for each problem under consideration we seek admissible perturbations and examine the possible existence of heteroclinic cycles and networks.

We now review the contents of the chapter and its organisation. In Section 4.2 we study the four-dimensional representation of the group Γ_s acting on $\mathbb{C}^2$. In this case there exists one translation free axial subgroup with $\mathbf{D}_4$ isotropy. Within Subsection 4.2.2 we examine the behaviour of the group orbit X_0 under forced symmetry breaking to the subgroup $\mathbf{D}_4$. Our analysis follows the lines of Chapter 2; we construct the skeleton and study its symmetry properties. These symmetry properties allow us to construct the projected skeleton and thus classify the number of "different" admissible flows on the skeleton. We then consider the invariant theory for the group $\mathbf{D}_4$ and calculate the flow formulas for a general quadratic $\mathbf{D}_4$-equivariant perturbation $\mathbf{g}$. This allows us to produce nondegeneracy conditions on the quadratic coefficients of $\mathbf{g}$ for the perturbation to be admissible. In addition we consider the behaviour of the flow on the perturbed skeleton in the nondegenerate and degenerate cases. Next in Subsection 4.2.3 we consider forced symmetry breaking to the subgroup $\mathbf{D}_2[\rho^2, \kappa\rho]$. This case has already been studied by Hou and Golubitsky [50]. The $\mathbf{D}_2[\rho^2, \kappa\rho]$ problem is in some sense "less degenerate" than the $\mathbf{D}_4$ problem. By "less degenerate" we mean that the conditions on the perturbation term $\mathbf{g}$ are of only linear order for both stability and for the flow to be admissible, whilst the $\mathbf{D}_4$ problem requires complex (and only implicitly given) conditions on the quadratic terms and the stability issues are complex. Finally, in Subsection 4.2.4 we complete our analysis of the four-dimensional representation by considering forced symmetry breaking to the subgroup $\mathbf{D}_2[\rho^2, \kappa]$. The analysis follows identical lines to the $\mathbf{D}_4$ case. Following the four-dimensional representation we continue our analysis in Section 4.3 with the eight-dimensional representation of Γ_s. The results concerning the skeleton and its symmetry properties are identical, for the square and anti-square solutions, to those for squares in the four-dimensional representation. From this point we encounter difficulties with the invariant theory. The complexity of the group representation means the invariants and equivariants are very complex and obviously different from those in the four-dimensional representation—which changes the flow formulas. For this reason we consider those perturbations arising from the primary invariants and present only an illustrative example. This makes our results rather incomplete in comparison with the four-dimensional representation, but interesting nonetheless. Finally, we finish by presenting a summary of the main results.

4.2 Four-Dimensional Representation

In this section we consider the forced symmetry breaking of a system of differential equations posed on the square lattice, when the symmetry group Γ_s is in its four-dimensional absolutely irreducible representation. More precisely, the representation of Γ_s on $\mathbb{C}^2$ corresponds to the following action. Choose coordinates $\mathbf{z} = (z_1, z_2)$ on $\mathbb{C}^2$. Then the action of Γ_s is generated by,

$$\begin{aligned} \rho(z_1, z_2) &= (\overline{z_2}, z_1), \\ \kappa(z_1, z_2) &= (z_2, z_1), \\ \theta(z_1, z_2) &= (e^{\mathrm{i}\theta_1} z_1, e^{\mathrm{i}\theta_2} z_2), \end{aligned} \tag{4.3}$$

where $\theta = (\theta_1, \theta_2) \in \mathbf{T}^2$. Consider the Γ_s-equivariant system of differential equations

$$\dot{\mathbf{z}} = \mathbf{f}(\mathbf{z}, \lambda), \tag{4.4}$$

where $\mathbf{f} : \mathbb{C}^2 \times \mathbb{R} \to \mathbb{C}^2$ is Γ_s-equivariant. In this section we investigate the behaviour of group orbits of solutions to equation (4.4) under forced symmetry breaking to the subgroups $\mathbf{D}_4$, $\mathbf{D}_2[\rho^2, \kappa]$ and $\mathbf{D}_2[\rho^2, \kappa\rho]$ of Γ_s.

This section is organised as follows. We begin in Subsection 4.2.1 by proving the existence of a bifurcating translation free axial solution to the equation (4.4). In Subsection 4.2.2 we investigate the behaviour of X_0 under forced symmetry breaking to the group $\mathbf{D}_4$. We construct the skeleton, knots and projected skeleton for this problem. In order to study the flow formulas we require knowledge of the $\mathbf{D}_4$-invariants and equivariants, and these are then discussed. Using the invariant theory, we compute the flow formula along the connections on the skeleton. This allows us to find nondegeneracy conditions for the nonexistence of additional equilibria on the connections of the skeleton. Using Theorem 2.38 we deduce the behaviour of $\mathbf{D}_4$-equivariant flows on the perturbed group orbit X_ε. We also briefly discuss the degenerate behaviour. In Subsection 4.2.3 we study the problem of forced symmetry breaking with $\mathbf{D}_2[\rho^2, \kappa\rho]$-symmetry. This problem has been studied previously by Hou and Golubitsky [50]. Finally, in Subsection 4.2.4 we consider forced symmetry breaking to $\mathbf{D}_2[\rho^2, \kappa]$.

4.2.1 Existence of the Translation Free Axial Solution

The following section closely follows that of Hou and Golubitsky [50], but the contents are repeated briefly for completeness. The action of Γ_s has four conjugacy classes of isotropy subgroups given by: Γ_s, $\mathbf{D}_2 \dot{+} \mathbf{S}^1$, $\mathbf{D}_4$ and $\mathbf{D}_2$. We shall focus exclusively on the translation free axial subgroup $\Sigma = \mathbf{D}_4$. A general Γ_s-equivariant mapping has the form

$$\mathbf{f}(\mathbf{z}, \lambda) = \left(P(|z_1|^2, |z_2|^2, \lambda), P(|z_2|^2, |z_1|^2, \lambda)\right), \tag{4.5}$$

where $P : \mathbb{R}^2 \times \mathbb{R} \to \mathbb{R}$ is a Γ_s-invariant function. Assume that $P_\lambda(0,0,0) \neq 0$; then the third order truncation of (4.5) is

$$\mathbf{K}(\mathbf{z}, \lambda) = \left((a|z_1|^2 + b|z_2|^2 - \lambda)z_1, (b|z_1|^2 + a|z_2|^2 - \lambda)z_2\right),$$

where a, $b \in \mathbb{R}$. The map $\mathbf{K}$ is the *normal form* of $\mathbf{f}$. We say that a Γ_s-equivariant vector field $\mathbf{f}$ is *nondegenerate* if $a \neq 0$ and $a \neq \pm b$. In this case the existence and stability of solutions to (4.5) is determined by $\mathbf{K}$.

Theorem 4.1
Let $\mathbf{f} : \mathbb{C}^2 \times \mathbb{R} \to \mathbb{C}^2$ be a Γ_s-equivariant bifurcation problem. Then, generically, there exists a branch of steady-state solutions bifurcating from the origin with Σ-symmetry. Furthermore, if $a > |b|$ in the normal form $\mathbf{K}$, then this branch of solutions is asymptotically stable.

Proof. See Hou and Golubitsky [50]. □

4.2.2 Forced Symmetry Breaking to $\mathbf{D}_4$

In this subsection we study the behaviour of the group orbit of bifurcating solutions given by Theorem 4.1, when symmetry breaking terms with $\mathbf{D}_4$ symmetry are added to equation (4.5). The group orbit of these solutions is a 2-torus, which we denote by X_0. Moreover, this 2-torus is normally hyperbolic. Let $\mathbf{g} : \mathbb{C}^2 \to \mathbb{C}^2$ be a $\mathbf{D}_4$-equivariant mapping with $\mathbf{g}(\mathbf{0}) = \mathbf{0}$. Let ε be real and small. Consider the perturbed vector field $\mathbf{F} : \mathbb{C}^2 \times \mathbb{R}^2 \to \mathbb{C}^2$ defined by

$$\mathbf{F}(\mathbf{z}, \lambda, \varepsilon) = \mathbf{f}(\mathbf{z}, \lambda) + \varepsilon \mathbf{g}(\mathbf{z}). \tag{4.6}$$

The normal hyperbolicity of X_0 guarantees, by the equivariant persistence theorem, the existence of a manifold X_ε diffeomorphic to X_0 and invariant under the dynamics of $\mathbf{F}$. Therefore we can study the dynamics of $\mathbf{D}_4$-equivariant vector fields on X_ε by considering their behaviour on the known space X_0.

The action of the group $\mathbf{D}_4$ on the space $\mathbb{C}^2$ is given by:

$$\begin{array}{llll} \rho(z_1,z_2) &= (\overline{z_2},z_1), & \rho^2(z_1,z_2) &= (\overline{z_1},\overline{z_2}), \\ \rho^3(z_1,z_2) &= (z_2,\overline{z_1}), & \kappa(z_1,z_2) &= (z_2,z_1), \\ \kappa\rho(z_1,z_2) &= (z_1,\overline{z_2}), & \kappa\rho^2(z_1,z_2) &= (\overline{z_2},\overline{z_1}), \\ \kappa\rho^3(z_1,z_2) &= (\overline{z_1},z_2). & & \end{array} \tag{4.7}$$

This action is essential for calculating the fixed-point submanifolds of the subgroups of $\mathbf{D}_4$ required for the computation of the skeleton.

Calculation of the Skeleton

Here we calculate the skeleton of X_0. The skeleton supports nontrivial and interesting flows for $\mathbf{D}_4$-equivariant vector fields on X_0. To begin we calculate the set $\mathscr{C}_{\mathbf{D}_4}$, for which we require:

Lemma 4.2
There are ten closed subgroups of $\mathbf{D}_4$ *given by:* $\mathbf{D}_4$, $\mathbf{Z}_4[\rho]$, $\mathbf{D}_2[\rho^2,\kappa\rho]$, $\mathbf{D}_2[\rho^2,\kappa]$, $\mathbf{Z}_2[\rho^2]$, $\mathbf{Z}_2[\kappa]$, $\mathbf{Z}_2[\kappa\rho]$, $\mathbf{Z}_2[\kappa\rho^2]$, $\mathbf{Z}_2[\kappa\rho^3]$ *and the trivial subgroup.*

Proof. Use standard results from any elementary algebra text, or a straightforward calculation. □

We fix some notation for the rest of this work. We denote an n-torus by $\mathbf{T}^n$ and use coordinates $\theta = (\theta_1,\ldots,\theta_n)$, where $\theta_j \in [0,2\pi)$, for $j = 1,\ldots,n$.

Using these coordinates on $\mathbf{T}^2$ we make the following definitions to simplify the presentation.

Definition 4.3
Define the following subsets of X_0:

$$\begin{array}{lll} e_1 = \{(0,0)\}, & e_2 = \{(\pi,0)\}, & e_3 = \{(0,\pi)\}, \\ e_4 = \{(\pi,\pi)\}, & c_1 = \{(\theta,\theta)\big|\theta \in [0,2\pi)\}, & c_2 = \{(\theta,0)\big|\theta \in [0,2\pi)\}, \\ c_3 = \{(\theta,\pi)\big|\theta \in [0,2\pi)\}, & c_4 = \{(0,\theta)\big|\theta \in [0,2\pi)\}, & c_5 = \{(\pi,\theta)\big|\theta \in [0,2\pi)\}, \\ c_6 = \{(\theta,-\theta)\big|\theta \in [0,2\pi)\}. & & \end{array}$$

Proposition 4.4
Let $\mathbf{D}_4$ *act on* X_0 *with the action induced from (4.3). Then*

$$\mathscr{C}_{\mathbf{D}_4} = \{e_1,e_2,e_3,e_4,c_1,c_2,c_3,c_4,c_5,c_6\}.$$

To prove this proposition we compute the fixed-point submanifolds for each subgroup of $\mathbf{D}_4$, this is the content of the following proposition:

Proposition 4.5
Let $\mathbf{D}_4$ *act on* X_0 *with the action induced from (4.3). Then the fixed-point submanifolds for each subgroup of* $\mathbf{D}_4$ *are contained in Table 4.1.*

Proof.

Case 1: $\mathbf{D}_4$ and $\mathbf{Z}_4[\rho]$. We calculate the set $N_\Gamma(\mathbf{D}_4,\Sigma) = \{\gamma \in \Gamma\big|\gamma\mathrm{Fix}(\Sigma) \subseteq \mathrm{Fix}(\mathbf{D}_4)\}$. This calculation requires us to find those $\gamma \in \Gamma_s$ such that $\gamma(x,x) \in \mathrm{Fix}(\mathbf{D}_4)$. Since $\mathrm{Fix}(\mathbf{D}_4) = \{(x,x)\big|x \in \mathbb{R}\}$, it follows that $\gamma = (0,0)$, (π,π) or $\gamma \in \mathbf{D}_4$. Therefore, $\mathrm{Fix}_{X_0}(\mathbf{D}_4) = N_\Gamma(\mathbf{D}_4,\Sigma)/\Sigma = e_1 \cup e_4$. Similarly, since the action of ρ implies $\mathrm{Fix}(\mathbf{Z}_4[\rho]) = \mathrm{Fix}(\mathbf{D}_4)$ the result for $\mathbf{Z}_4[\rho]$ follows.

Case 2: $\mathbf{D}_2[\rho^2,\kappa\rho]$ and $\mathbf{D}_2[\rho^2,\kappa]$. The action given in (4.7) shows $\mathrm{Fix}(\mathbf{D}_2[\rho^2,\kappa])$ and $\mathrm{Fix}(\mathbf{D}_2[\rho^2,\kappa\rho])$ are both given by $\{(x,y)\big|x,y \in \mathbb{R}\}$. Thus it suffices to calculate the set $N_\Gamma(\mathbf{D}_2[\rho^2,\kappa\rho],\Sigma) =$

Table 4.1: Fixed-point submanifolds for nontrivial subgroups of $\mathbf{D}_4$.

Group	Fixed-Point Submanifold
$\mathbf{D}_4$	e_1, e_4
$\mathbf{Z}_4$	e_1, e_4
$\mathbf{D}_2[\rho^2, \kappa]$	e_1, e_2, e_3, e_4
$\mathbf{D}_2[\rho^2, \kappa\rho]$	e_1, e_2, e_3, e_4
$\mathbf{Z}_2[\rho^2]$	e_1, e_2, e_3, e_4
$\mathbf{Z}_2[\kappa]$	c_1
$\mathbf{Z}_2[\kappa\rho]$	$c_2 \cup c_3$
$\mathbf{Z}_2[\kappa\rho^2]$	$c_4 \cup c_5$
$\mathbf{Z}_2[\kappa\rho^3]$	c_6

$\{\gamma \in \Gamma | \gamma \mathrm{Fix}(\Sigma) \subseteq \mathrm{Fix}(\mathbf{D}_2[\rho^2, \kappa])\}$. So we need the elements of $\gamma \in \Gamma_s$ such that $\gamma(x, x) \in \{(x, y) | x, y \in \mathbb{R}\}$. Therefore $\gamma = (0, 0), (\pi, 0), (0, \pi), (\pi, \pi)$ or $\gamma \in \Sigma$, so

$$\mathrm{Fix}_{X_0}(\mathbf{D}_2[\rho^2, \kappa\rho]) = N_\Gamma(\mathbf{D}_2[\rho^2, \kappa\rho], \Sigma)/\Sigma = e_1 \cup e_2 \cup e_3 \cup e_4,$$

Case 3: $\mathbf{Z}_2[\rho^2]$. From the action (4.7) we have $\mathrm{Fix}(\mathbf{Z}_2[\rho^2]) = \mathrm{Fix}(\mathbf{D}_2[\rho^2, \kappa\rho])$. Therefore $\mathrm{Fix}_{X_0}(\mathbf{Z}_2[\rho^2]) = e_1 \cup e_2 \cup e_3 \cup e_4$.

Case 4: $\mathbf{Z}_2[\kappa]$. From the action given in (4.7) we have $\kappa(z_1, z_2) = (z_2, z_1)$. Thus $\mathrm{Fix}(\mathbf{Z}_2[\kappa]) = \{(z, z) | z \in \mathbb{C}\}$. Hence, we need to find those $\gamma \in \Gamma_s$ such that $\gamma(x, x) \in \{(z, z) | z \in \mathbb{C}\}$. Therefore $\gamma \in \{(\theta, \theta) | \theta \in [0, 2\pi)\}$, or $\gamma \in \Sigma$, so $\mathrm{Fix}_{X_0}(\mathbf{Z}_2[\kappa]) = c_1$.

Case 5: $\mathbf{Z}_2[\kappa\rho]$. Again by using the action defined in (4.7) we have $\mathrm{Fix}(\mathbf{Z}_2[\kappa\rho]) = \{(z, y) | y \in \mathbb{R} \text{ and } z \in \mathbb{C}\}$. We now need to find those $\gamma \in \Gamma_s$ such that $\gamma(x, x) \in \mathrm{Fix}(\mathbf{Z}_2[\kappa\rho])$. Thus we require

$$\gamma \in \{(\theta, 0) | \theta \in [0, 2\pi)\} \cup \{(\theta, \pi) | \theta \in [0, 2\pi)\},$$

or $\gamma \in \Sigma$. Therefore $\mathrm{Fix}_{X_0}(\mathbf{Z}_2[\kappa\rho]) = c_2 \cup c_3$.

Case 6: $\mathbf{Z}_2[\kappa\rho^2]$. From the action given in (4.7) we find that, $\mathrm{Fix}(\mathbf{Z}_2[\kappa\rho^2]) = \{(z, \bar{z}) | z \in \mathbb{C}\}$. Performing the calculation of the set $N_\Gamma(\mathbf{Z}_2[\kappa\rho^2], \Sigma)$, which follows identical lines as those for the group $\mathbf{Z}_2[\kappa]$, we find that $\mathrm{Fix}_{X_0}(\mathbf{Z}_2[\kappa\rho^2]) = c_6$.

Case 7: $\mathbf{Z}_2[\kappa\rho^3]$. The action in (4.7) implies that $\mathrm{Fix}(\mathbf{Z}_2[\kappa\rho^3]) = \{(x, z) | x \in \mathbb{R} \text{ and } z \in \mathbb{C}\}$. Performing the calculations of the set $N_\Gamma(\mathbf{Z}_2[\kappa\rho^3], \Sigma)$, which are identical to the corresponding calculations for the group $\mathbf{Z}_2[\kappa\rho]$, we find that $\mathrm{Fix}_{X_0}(\mathbf{Z}_2[\kappa\rho^3]) = c_4 \cup c_5$. □

We have now calculated the fixed-point submanifolds for all nontrivial closed subgroups of $\mathbf{D}_4$. Since $\mathrm{Fix}_{X_0}(\{1\}) = X_0$,

$$\mathscr{C}_{\mathbf{D}_4} = \{e_1, e_2, e_3, e_4, c_1, c_2, c_3, c_4, c_5, c_6\}.$$

This completes the proof of Proposition 4.4. Now we have calculated $\mathscr{C}_{\mathbf{D}_4}$ it is a trivial task to calculate the skeleton $\mathbb{X}_{\mathbf{D}_4}$ of X_0. We find that

$$\begin{aligned} \mathbb{X}_{\mathbf{D}_4} &= \bigcup_{C \in \mathscr{C}_{\mathbf{D}_4}} C \\ &= c_1 \cup c_2 \cup c_3 \cup c_4 \cup c_5 \cup c_6 \\ &\subset X_0. \end{aligned}$$

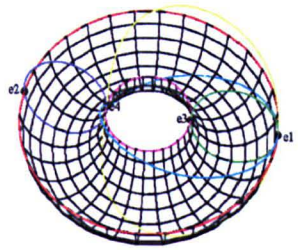

Figure 4.1: The skeleton $\mathbf{X}_{\mathbf{D}_4}$ within the 2-torus X_0. Here c_1 is yellow, c_2 red, c_3 purple, c_4 green, c_5 blue, and c_6 cyan.

In Figure 4.1 we illustrate $\mathbf{X}_{\mathbf{D}_4}$. The next step we perform is to determine the smooth stratification of $\mathbf{X}_{\mathbf{D}_4}$. Recall that $\mathbf{X}_{\mathbf{D}_4}$ is not (in general) a smooth manifold, but does have a smooth stratification into the sets $E_{(\mathbf{D}_4,X_0)}$, $H_{(\mathbf{D}_4,X_0)}$ and $P_{(\mathbf{D}_4,X_0)}$, in our case $P_{(\mathbf{D}_4,X_0)} = \emptyset$. We make the following definitions to simplify notation.

Definition 4.6
Define the following subsets of X_0:

$$\begin{array}{lll} h_1 = \{(\theta,\theta)\big|\theta \in (0,\pi)\}, & h_2 = \{(\theta,\theta)\big|\theta \in (\pi,2\pi)\}, & h_3 = \{(\theta,0)\big|\theta \in (0,\pi)\}, \\ h_4 = \{(\theta,0)\big|\theta \in (\pi,2\pi)\}, & h_5 = \{(\theta,\pi)\big|\theta \in (0,\pi)\}, & h_6 = \{(\theta,\pi)\big|\theta \in (\pi,2\pi)\}, \\ h_7 = \{(0,\theta)\big|\theta \in (0,\pi)\}, & h_8 = \{(0,\theta)\big|\theta \in (\pi,2\pi)\}, & h_9 = \{(\pi,\theta)\big|\theta \in (0,\pi)\}, \\ h_{10} = \{(\pi,\theta)\big|\theta \in (\pi,2\pi)\}, & h_{11} = \{(\theta,-\theta)\big|\theta \in (0,\pi)\}, & h_{12} = \{(\theta,-\theta)\big|\theta \in (\pi,2\pi)\}. \end{array}$$

Then we have the following stratification of $\mathbf{X}_{\mathbf{D}_4}$ into subsets, and each element of $E_{(\mathbf{D}_4,X_0)}$ and $H_{(\mathbf{D}_4,X_0)}$ is a manifold:

$$\begin{aligned} E_{(\mathbf{D}_4,X_0)} &= e_1 \cup e_2 \cup e_3 \cup e_4, \\ H_{(\mathbf{D}_4,X_0)} &= h_1 \cup h_2 \cup h_3 \cup h_4 \cup h_5 \cup h_6 \cup h_7 \cup h_8 \cup h_9 \cup h_{10} \cup h_{11}. \end{aligned}$$

This completes the calculation of the skeleton. At this point we may use the calculation performed above to deduce the following important existence result.

Theorem 4.7
Let $\Gamma = \mathbf{D}_4 \dotplus \mathbf{T}^2$, $\Sigma = \mathbf{D}_4$ and $\Delta = \mathbf{D}_4$. Let Γ act on $\mathbb{C}^2$ as in (4.3). Let $\mathbf{f} \in \vec{\mathcal{E}}_\Gamma$ be a Γ-equivariant bifurcation problem. Let $\mathbf{g} \in \vec{\mathcal{E}}_\Delta$ be Δ-equivariant and satisfy $\mathbf{g}(\mathbf{0}) = \mathbf{0}$. Let $\mathbf{F}(\mathbf{z},\lambda,\varepsilon) = \mathbf{f}(\mathbf{z},\lambda) + \varepsilon\mathbf{g}(\mathbf{z})$. Then there exists a steady-state solution to $\mathbf{f}(\mathbf{z},\lambda) = 0$ bifurcating from $(\mathbf{0},0)$ with Σ-isotropy. Let $X_0 \cong \mathbf{T}^2$ be the group orbit of steady states. Then for sufficiently small ε, X_0 persists to give a new $\mathbf{F}$-invariant manifold X_ε which is Δ-equivariantly diffeomorphic to X_0. Moreover, there exists $\mathbf{g} \in \vec{\mathcal{E}}_\Delta$ such that the elements in $E_{(\Delta,X_0)}$ are equilibria for the new flow and those of $H_{(\Delta,X_0)}$ are heteroclinic connections between equilibria.

Proof. The existence of the bifurcating solution follows the previous discussion. Theorem 2.3 implies the that group orbit of solutions persists and that there exists an equivariant diffeomorphism. Theorem 2.28 guarantees the existence of a Δ-equivariant vector field $\mathbf{g}$ with elements of $E_{(\Delta,X_0)}$ as equilibria and element of $H_{(\Delta,X_0)}$ as heteroclinic connections between equilibria. □

The above result demonstrate only the existence of vector fields $\mathbf{g}$ with the property that elements of $E_{(\mathbf{D}_4,X_0)}$ are equilibria and elements of $H_{(\mathbf{D}_4,X_0)}$ are heteroclinic connection between

them. The main problem is to exhibit simple $\mathbf{D}_4$-equivariant vector fields with these properties. Indeed, it will be shown that it is "very difficult" to find such vector fields. A natural question is how the $\mathbf{D}_4$ symmetry restricts the flows along the connections between the elements of $E_{(\mathbf{D}_4,X_0)}$. The presence of symmetry, as always, greatly simplifies the analysis.

Symmetry Properties of $\mathbb{X}_{\mathbf{D}_4}$

We concern ourselves with the symmetry properties of $\mathbb{X}_{\mathbf{D}_4}$. More precisely, given $C \in \mathscr{C}_{\mathbf{D}_4}$ we calculate the setwise and the pointwise isotropy, $\mathrm{Stab}(C)$ and $\mathrm{stab}(C)$, respectively. Using the groups $\mathrm{Stab}(C)$ and $\mathrm{stab}(C)$ we may form the factor group $\mathrm{S}(C) = \mathrm{Stab}(C)/\mathrm{stab}(C)$. This group acts naturally on the elements $h \in H_{(\mathbf{D}_4,X_0)}$ which are subsets of C. By Lemma 2.19 we have for any $x \in C - E_{(\mathbf{D}_4,X_0)}$ that $\mathbf{D}_4 x \cap C = \mathrm{S}(C)x$. Hence using the group $\mathrm{S}(C)$ we can determine which points of C lie on the same group orbit. It will turn out that $\mathrm{S}(C) \cong \mathbf{Z}_2$ for all $C \in \mathscr{C}_{\mathbf{D}_4}$. This group acts by reflection about an axis (which is yet to be determined) on C. In addition, we may compute the knots relative to a given $C \in \mathscr{C}_{\mathbf{D}_4}$—that is, the axis of symmetry alluded to above, for flows on C and hence $\mathbb{X}_{\mathbf{D}_4}$. This symmetry information restricts the types of flows that are possible on $\mathbb{X}_{\mathbf{D}_4}$. Furthermore, it simplifies the calculation of the projected skeleton, allowing us to classify the different types of behaviour to be expected on the skeleton.

Pointwise and Setwise Isotropy Subgroups. The action (4.7) of $\mathbf{D}_4$ on $\mathbb{C}^2$ induces a natural action on X_0, given by

$$\begin{array}{llll} \rho(\theta_1,\theta_2) = (-\theta_2,\theta_1), & \rho^2(\theta_1,\theta_2) = -(\theta_1,\theta_2), \\ \rho^3(\theta_1,\theta_2) = (\theta_2,-\theta_1), & \kappa(\theta_1,\theta_2) = (\theta_2,\theta_1), \\ \kappa\rho(\theta_1,\theta_2) = (\theta_1,-\theta_2), & \kappa\rho^2(\theta_1,\theta_2) = (-\theta_2,-\theta_1), \\ \kappa\rho^3(\theta_1,\theta_2) = (-\theta_1,\theta_2). & \end{array} \tag{4.8}$$

This action is straightforward to calculate. Let $(\theta_1,\theta_2) \in X_0$; this corresponds to the point $(e^{\mathrm{i}\theta_1}x, e^{\mathrm{i}\theta_2}x) \in \mathbb{C}^2$. The action of any element of $\gamma \in \mathbf{D}_4$ gives a new point $\gamma\mathbf{z} \in \mathbb{C}^2$. This in turn corresponds to a new point in X_0, giving the induced action on X_0. For example, the action of $\rho \in \mathbf{D}_4$ is given by $\rho(e^{\mathrm{i}\theta_1}x, e^{\mathrm{i}\theta_2}x) = (e^{-\mathrm{i}\theta_2}x, e^{\mathrm{i}\theta_1}x)$, so $\rho(\theta_1,\theta_2) = (-\theta_2,\theta_1)$. The action of $\mathbf{D}_4$ on X_0 in turn induces an action of $\mathbf{D}_4$ on $\mathscr{C}_{\mathbf{D}_4}$ by permutation of its elements. Again this action is straightforward to compute, and the results are given in Table 4.2. As an example, consider $c_1 \in \mathscr{C}_{\mathbf{D}_4}$. Then

$$\begin{aligned} \rho c_1 &= \rho\{(\theta,\theta)\big|\theta \in [0,2\pi)\} \\ &= \{(-\theta,\theta)\big|\theta \in [0,2\pi)\} \\ &= c_6. \end{aligned}$$

Using this action we deduce:

Proposition 4.8
Let $\mathbf{D}_4$ act on $\mathscr{C}_{\mathbf{D}_4}$ as in Table 4.2 and on X_0 with the action in (4.8). Then given $C \in \mathscr{C}_{\mathbf{D}_4}$, the setwise isotropy Stab(C), pointwise isotropy stab(C) and the group $S(C) = \mathrm{Stab}(C)/\mathrm{stab}(C)$ are given in Table 4.3.

Proof. The calculations for $\mathrm{Stab}(C)$ follow immediately from the action given in Table 4.2. To compute $\mathrm{stab}(C)$ we need consider only the elements of $\mathrm{Stab}(C)$ and check those that act trivially on C. □

Knots. Given any $C \in \mathscr{C}_{\mathbf{D}_4}$, with $C \cong \mathbf{S}^1$, a knot relative to C gives an axis of symmetry of C. This axis of symmetry places great restrictions on the types of flow possible on the skeleton $\mathbb{X}_{\mathbf{D}_4}$. We calculate the knots for those C's that are topological circles. Since $S(C) \cong \mathbf{Z}_2$ for those C that are circles, and each such C contains exactly two equilibria, it follows that these equilibria are the knots. The knots relative to each C are contain in Table 4.4.

Table 4.2: Induced action of $\mathbf{D}_4$ on $\mathscr{C}_{\mathbf{D}_4}$.

Element of $\mathscr{C}_{\mathbf{D}_4}$	Elements of $\mathbf{D}_4$ acting nontrivially	Action
e_1	none	
e_2	$\rho, \rho^3, \kappa, \kappa\rho^2$	e_3
e_3	$\rho, \rho^3, \kappa, \kappa\rho^2$	e_2
e_4	none	
c_1	$\rho, \rho^3, \kappa\rho, \kappa\rho^3$	c_6
c_2	$\rho, \rho^3, \kappa, \kappa\rho^2$	c_4
c_3	$\rho, \rho^3, \kappa, \kappa\rho^2$	c_5
c_4	$\rho, \rho^3, \kappa, \kappa\rho^2$	c_2
c_5	$\rho, \rho^3, \kappa, \kappa\rho^2$	c_3
c_6	$\rho, \rho^3, \kappa\rho, \kappa\rho^3$	c_1

It is important to realise that the symmetry results are independent of the perturbation term $\mathbf{g}$ and remain true for *any* $\mathbf{D}_4$-equivariant flow. Thus at this point we have some very general restrictions on the flows on $\mathbb{X}_{\mathbf{D}_4}$. To compute flows and conditions for the existence of admissible flows on the skeleton, we must consider the form of a general perturbation term $\mathbf{g}$.

Projected Skeleton $\mathbb{X}^p_{\mathbf{D}_4}$

Using the symmetry information, we are in a position to construct the projected skeleton $\mathbb{X}^p_{\mathbf{D}_4}$ of the skeleton $\mathbb{X}_{\mathbf{D}_4}$. Each $C \in \mathscr{C}_{\mathbf{D}_4} - E_{(\mathbf{D}_4, X_0)}$ has two knots, and so one axis of reflection symmetry, for any $\mathbf{D}_4$-equivariant flow. Using the action of $\mathbf{D}_4$ on $\mathscr{C}_{\mathbf{D}_4}$, see Table 4.2, it follows that there are three orbit representatives for the elements of $E_{(\mathbf{D}_4, X_0)}$ and similarly three representatives for the connections in $H_{(\mathbf{D}_4, X_0)}$. We choose the following representatives for the equilibria: e_1, e_3, e_4 and the following orbit representative for the connections: h_1, h_3 and h_9. The element h_1 connects e_1 to e_3, h_3 connects e_3 to e_4 and h_9 connects e_1 to e_4. In Figure 4.2 we illustrate the projected skeleton with two different types of flows on it. Each of these flows corresponds to a possible flow on the skeleton. Thus we can determine an optimal upper bound for the qualitatively different admissible flows on $\mathbb{X}^p_{\mathbf{D}_4}$ and hence $\mathbb{X}_{\mathbf{D}_4}$. Two flows on the (projected) skeleton are qualitatively different if they flow in opposite directions. Note that although we can arrange for heteroclinic cycles on the projected skeleton, it is not true that these cycles pull back to give heteroclinic cycles on the skeleton. Consider Figure 4.2(b). The pullback of this flow gives a flow on the skeleton where the unstable manifold of e_1 is

Table 4.3: Isotropy data for $\mathscr{C}_{\mathbf{D}_4}$.

$C \in \mathscr{C}_{\mathbf{D}_4}$	stab(C)	Stab(C)	$S(C)$ = Stab(C)/stab(C)
e_1	$\mathbf{D}_4$	$\mathbf{D}_4$	$\mathbf{1}$
e_2	$\mathbf{D}_2[\rho^2, \kappa\rho]$	$\mathbf{D}_2[\rho^2, \kappa\rho]$	$\mathbf{1}$
e_3	$\mathbf{D}_2[\rho^2, \kappa\rho]$	$\mathbf{D}_2[\rho^2, \kappa\rho]$	$\mathbf{1}$
e_4	$\mathbf{D}_4$	$\mathbf{D}_4$	$\mathbf{1}$
c_1	$\mathbf{Z}_2[\kappa]$	$\mathbf{D}_2[\rho^2, \kappa]$	$\mathbf{Z}_2$
c_2	$\mathbf{Z}_2[\kappa\rho]$	$\mathbf{D}_2[\rho^2, \kappa\rho]$	$\mathbf{Z}_2$
c_3	$\mathbf{Z}_2[\kappa\rho]$	$\mathbf{D}_2[\rho^2, \kappa\rho]$	$\mathbf{Z}_2$
c_4	$\mathbf{Z}_2[\kappa\rho^3]$	$\mathbf{D}_2[\rho^2, \kappa\rho]$	$\mathbf{Z}_2$
c_5	$\mathbf{Z}_2[\kappa\rho^3]$	$\mathbf{D}_2[\rho^2, \kappa\rho]$	$\mathbf{Z}_2$
c_6	$\mathbf{Z}_2[\kappa\rho^2]$	$\mathbf{D}_2[\rho^2, \kappa]$	$\mathbf{Z}_2$

Table 4.4: Knots relative to $C \in \mathscr{C}_{\mathbf{D}_4}$, for C a topological circle.

$C \in \mathscr{C}_{\mathbf{D}_4}$	Knots
c_1	e_1, e_4
c_2	e_1, e_2
c_3	e_3, e_4
c_4	e_1, e_3
c_5	e_2, e_4
c_6	e_1, e_4

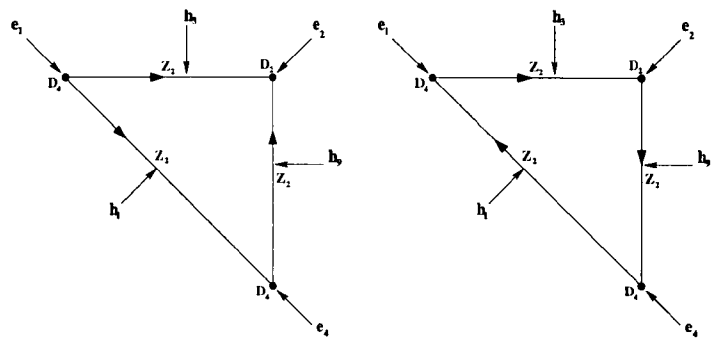

(a) (b)

Figure 4.2: The projected skeleton $\mathbb{X}^p_{\mathbf{D}_4}$. (a) One possible flow where the flow is directed to the equilibrium e_2. (b) A possible heteroclinic cycle.

contained in the stable manifold of e_2 and e_3. However, we do have a heteroclinic network. The dynamics of such a network would prove interesting in light of the work of Kirk and Silber [55]. But we shall not pursue this issue. It is easy to see that there is a maximum of eight different admissible flows on the projected skeleton, hence the same number on the skeleton.

Remark 4.9
In the remainder of this work we shall often encounter heteroclinic cycles and networks on the projected skeletons. The comments made above still hold in these cases. These cycles and networks do not (necessarily) pullback to give cycles and networks on the skeleton.

Invariant Theory for $\mathbf{D}_4$

To determine the flow formulas we must compute the general form of a $\mathbf{D}_4$-equivariant mapping. We calculate a set of generators for the ring of $\mathbf{D}_4$-invariants functions $\mathcal{E}_{\mathbf{D}_4}$ and the module of $\mathbf{D}_4$-equivariant mappings $\vec{\mathcal{E}}_{\mathbf{D}_4}$. By the theorems of Schwarz (Theorem 1.4) and Poénaru (Theorem 1.5) it is sufficient to consider the ring $\mathcal{P}_{\mathbf{D}_4}$ of polynomial invariants and the module $\vec{\mathcal{P}}_{\mathbf{D}_4}$ of polynomial equivariants. The problem of finding a generating set is, in general, difficult. For this reason we adopt a systematic approach using a computer algebra package, the details of which are contained in Appendix A. Using this information we compute the general form of a $\mathbf{D}_4$-equivariant vector field with degree less than or equal to two. It is possible using the results of this section to compute higher order terms, but these are not required for our future work.

We begin with the invariants.

Lemma 4.10
Let $\mathbf{D}_4$ *act on* $\mathbb{C}^2$ *with the action given by (4.7). Then the Poincaré series for the invariants is*

$$\begin{aligned}\Upsilon(t) &= \frac{t^2-t+1}{(1-t^4)(1-t^2)(1-t)^2} \\ &= 1+t+3t^2+4t^3+8t^4+10t^5+16t^6+\ldots,\end{aligned}$$

where ... *denotes higher order terms.*

Proof. See Appendix A. □

Using the Poincaré series we may calculate a set of generating invariant polynomials for the ring $\mathcal{P}_{\mathbf{D}_4}$.

Lemma 4.11
Let $\mathbf{D}_4$ *act on* $\mathbb{C}^2$ *with the action given by (4.7). Then the polynomials*

$$\begin{aligned}u_1 &= z_1+\overline{z_1}+z_2+\overline{z_2}, \\ u_2 &= z_1^2+\overline{z_1}^2+z_2^2+\overline{z_2}^2, \\ u_3 &= z_1z_2+\overline{z_1}z_2+z_1\overline{z_2}+\overline{z_1z_2}, \\ u_4 &= z_1^4+\overline{z_1}^4+z_2^4+\overline{z_2}^2,\end{aligned}$$

are invariant under the action of $\mathbf{D}_4$ *and are linearly independent. Moreover, they generate the ring* $\mathcal{P}_{\mathbf{D}_4}$.

Proof. See Appendix A. □

We have now produced a set of generators for the ring $\mathcal{P}_{\mathbf{D}_4}$, so we consider the module $\vec{\mathcal{P}}_{\mathbf{D}_4}$ of equivariant polynomial mappings.

Lemma 4.12
Let $\mathbf{D}_4$ *act on* $\mathbb{C}^2$ *with the action given by (4.7). Then the Poincaré series for the equivariants is*

$$\begin{aligned}\Xi(t) &= \frac{1}{(1-t^2)(1-t)^3} \\ &= 1+3t+7t^2+13t^3+22t^4+34t^5+50t^6+\ldots,\end{aligned}$$

where ... *denotes higher order terms.*

Proof. See Appendix A. □

With the Poincaré series at hand we may calculate a set of generating equivariant polynomial mappings for the module $\vec{\mathcal{P}}_{\mathbf{D}_4}$.

Lemma 4.13
Let $\mathbf{D}_4$ *act on* $\mathbb{C}^2$ *with the action given by (4.7). Then the module of equivariant polynomial mappings is generated over the ring* $\mathcal{P}_{\mathbf{D}_4}$ *by the mappings*

$$e_1=\begin{bmatrix}1\\1\end{bmatrix},\qquad e_2=\begin{bmatrix}z_1\\z_2\end{bmatrix},\qquad e_3=\begin{bmatrix}z_2+\overline{z_2}\\z_1+\overline{z_1}\end{bmatrix},$$

$$e_4=\begin{bmatrix}z_1^2\\z_2^2\end{bmatrix},\qquad e_5=\begin{bmatrix}z_2^2+\overline{z_2}^2\\z_1^2+\overline{z_1}^2\end{bmatrix},\qquad e_6=\begin{bmatrix}z_1^3\\z_2^3\end{bmatrix},$$

$$e_7=\begin{bmatrix}z_2^3+\overline{z_2}^3\\z_1^3+\overline{z_1}^3\end{bmatrix},\qquad e_8=\begin{bmatrix}z_1^4\\z_2^4\end{bmatrix}.$$

Proof. See Appendix A. □

Let $\mathbf{g} : \mathbb{C}^2 \to \mathbb{C}^2$ be $\mathbf{D}_4$-equivariant mapping. Write $\mathbf{g} = (g_1, g_2)$; then by Lemmas 4.11 and 4.13 the general form of a $\mathbf{D}_4$-equivariant mapping is

$$\begin{aligned} g_1(\mathbf{z}) &= p_1(\mathbf{u}) + p_2(\mathbf{u})z_1 + p_3(\mathbf{u})(z_2 + \overline{z_2}) + p_4(\mathbf{u})z_1^2 \\ &+ p_5(\mathbf{u})(z_2^2 + \overline{z_2}^2) + p_6(\mathbf{u})z_1^3 + p_7(\mathbf{u})(z_2^3 + \overline{z_2}^3) + p_8(\mathbf{u})z_1^4, \\ g_2(\mathbf{z}) &= p_1(\mathbf{u}) + p_2(\mathbf{u})z_2 + p_3(\mathbf{u})(z_1 + \overline{z_1}) + p_4(\mathbf{u})z_2^2 \\ &+ p_5(\mathbf{u})(z_1^2 + \overline{z_1}^2) + p_6(\mathbf{u})z_2^3 + p_7(\mathbf{u})(z_1^3 + \overline{z_1}^3) + p_8(\mathbf{u})z_2^4, \end{aligned}$$

where the p_j's are smooth functions of the invariants $\mathbf{u} = (u_1, u_2, u_3, u_4)$.

Flow Formulas

The aim of this section is twofold. We begin by calculating, for a general quadratic order $\mathbf{D}_4$-equivariant perturbation $\mathbf{g}$, the directions of flows along the connections of the skeleton. We need consider only three orbit representatives h_1, h_3 and h_9. The invariant theory shows that the general form of a $\mathbf{D}_4$-equivariant map $\mathbf{g}$, to quadratic order, is

$$\begin{aligned} g_1(\mathbf{z}) &= p_{1,u_1}u_1 + p_{1,u_2}u_2 + p_{1,u_1^2}u_1^2 + p_2 z_1 \\ &+ p_{2,u_1}z_1u_1 + p_3(z_2 + \overline{z_2}) + p_{3,u_1}(z_2 + \overline{z_2})u_1 + p_4 z_1^2 + p_5(z_2^2 + \overline{z_2}^2), \\ g_2(\mathbf{z}) &= p_{1,u_1}u_1 + p_{1,u_2}u_2 + p_{1,u_1^2}u_1^2 + p_2 z_2 \\ &+ p_{2,u_1}z_2u_1 + p_3(z_1 + \overline{z_1}) + p_{3,u_1}(z_2 + \overline{z_2})u_1 + p_4 z_2^2 + p_5(z_1^2 + \overline{z_1}^2). \end{aligned} \tag{4.9}$$

For notational simplicity, we have not explicitly written that the coefficients are evaluated at zero, so for example, $p_5 = p_5(0)$.

Given a perturbation (4.9) we wish to know the direction of flow along the connections h_1, h_3 and h_9. Let h_j, where $j = 1, 3, 9$, be a connection parametrised by the function $\omega_j : [0, \pi] \to X_0$, then the flow along h_j is given by

$$\mathcal{F}(t) = < \mathbf{g}(\omega(t)), \mathcal{T}(t) >,$$

where $\mathcal{T}(t) = d/dt\ \omega_j(t)$.

Next, we find conditions on the coefficients of (4.9) so that no additional equilibria lie on the connections $h \in H_{(\mathbf{D}_4, X_0)}$. We thereby obtain a collection of nondegeneracy conditions on the perturbation term required, so that we may apply Theorem 2.38 to deduce the behaviour of the flow on the perturbed skeleton.

We begin by parametrising the connections on the skeleton. There are only three distinct group orbits of connections given by h_1, h_3 and h_9. We parametrise the connection h_1 using the function $\omega_{h_1} : [0, \pi] \to X_0$ defined by $\omega_{h_1}(t) = (e^{it}x, e^{it}x)$. The connection h_3 is parametrised by $\omega_{h_3} : [0, \pi] \to X_0$ defined by $\omega_{h_3}(t) = (e^{it}x, x)$ and finally the connection h_9 is parametrised by $\omega_{h_9}(t) = (-x, e^{it}x)$. The tangent vectors to each of these connections are:

$$\begin{aligned} \mathcal{T}_{h_1}(t) &= (-\sin t, \cos t, -\sin t, \cos t), \\ \mathcal{T}_{h_3}(t) &= (-\sin t, \cos t, 0, 0), \\ \mathcal{T}_{h_9}(t) &= (0, 0, -\sin t, \cos t). \end{aligned}$$

Here we have used real coordinates, so for $(z_1, z_2) \in \mathbb{C}^2$ we write $(x_1, y_1, x_2, y_2) \in \mathbb{R}^4$ where $z_j = x_j + iy_j$, for $j = 1, 2$. The next series of lemmas constructs the flow formulas for each of the individual equivariant terms in (4.9). Using these flow formulas, linearity allows us to compute the flow formula for any perturbation $\mathbf{g}$ up to quadratic order. In each case we use the notation $\mathcal{F}^{\mathbf{g}}(t) = (\mathcal{F}^{\mathbf{g}}_{h_1}(t), \mathcal{F}^{\mathbf{g}}_{h_3}(t), \mathcal{F}^{\mathbf{g}}_{h_9}(t))$, where $\mathcal{F}^{\mathbf{g}}_{h_j}(t)$ is the flow along h_j.

Lemma 4.14
Define $\mathbf{g} : \mathbb{C}^2 \to \mathbb{C}^2$ *by* $\mathbf{g}(\mathbf{z}) = (u_1, u_1)$. *Then the flow formula for this perturbation is*

$$\mathcal{F}^{\mathbf{g}}(t) = -2x^2(4\sin t\cos t, \sin t(\cos t + 1), \sin t(\cos t - 1)).$$

The perturbation $\mathbf{g}$ *is a simple degenerate perturbation. Moreover, the flow on the perturbed skeleton induced by* $\mathbf{g}$ *is* $\mathcal{F}^{\mathbf{g}}(t)$.

Proof. Let $\mathbf{g}(\mathbf{z}) = (u_1, u_1)$, where $u_1 = z_1 + \overline{z_1} + z_2 + \overline{z_2}$. Evaluating the invariant u_1 along each of the connections h_1, h_3 and h_9 gives:

$$\begin{aligned} u_1(\omega_{h_1}(t)) &= 4x\cos t, \\ u_1(\omega_{h_3}(t)) &= 2x(\cos t + 1), \\ u_1(\omega_{h_9}(t)) &= 2x(\cot t - 1). \end{aligned}$$

To calculate the flow formulas along the connections h_1, h_3 and h_9 we form the inner product of $u_1(\omega_{h_j})$ with $\mathcal{T}_{h_j}(t)$ where $j = 1, 3, 9$. This straightforward calculation yields:

$$\begin{aligned} \mathcal{F}^{\mathbf{g}}_{h_1}(t) &= -8x^2\sin t\cos t, \\ \mathcal{F}^{\mathbf{g}}_{h_3}(t) &= -2x^2\sin t(\cos t + 1), \\ \mathcal{F}^{\mathbf{g}}_{h_9}(t) &= -2x^2\sin t(\cos t - 1). \end{aligned}$$

Collecting together these results we have $\mathcal{F}^{\mathbf{g}}(t) = (\mathcal{F}^{\mathbf{g}}_{h_1}(t), \mathcal{F}^{\mathbf{g}}_{h_3}(t), \mathcal{F}^{\mathbf{g}}_{h_9}(t))$, as required.

Since $\mathcal{F}^{\mathbf{g}}_{h_1}(t)$ has only a simple zero at $t = \pi/2$, and $\mathcal{F}^{\mathbf{g}}_{h_3}(t)$ and $\mathcal{F}^{\mathbf{g}}_{h_9}(t)$ are non-zero for all $t \in (0, \pi)$, the perturbation $\mathbf{g}$ is a simple degenerate perturbation. Hence by Theorem 2.38 the behaviour of the flow on the perturbed skeleton is qualitatively the same as that on the skeleton, which is $\mathcal{F}^{\mathbf{g}}(t)$. □

Lemma 4.15
Define $\mathbf{g} : \mathbb{C}^2 \to \mathbb{C}^2$ *by* $\mathbf{g}(\mathbf{z}) = (u_2, u_2)$. *Then the flow formula for this perturbation is*

$$\mathcal{F}^{\mathbf{g}}(t) = -2x^3(4\sin t\cos 2t, \sin t(\cos 2t + 1), \sin t(\cos 2t + 1)).$$

The perturbation $\mathbf{g}$ *is a degenerate perturbation. The flow formula along* h_1 *has only simple zeros at* $\pi/4$ *and* $3\pi/4$. *The flow formulas along* h_3 *and* h_9 *have degenerate zeros at* $\pi/2$. *The flow on the perturbed skeleton is not the same as that on the skeleton, but by Theorem 2.41 there are only two possible types of behaviour for the zeros on the connections* h_3 *and* h_9. *Therefore, there is a total of four different types of behaviour on the perturbed skeleton.*

Proof. Let $\mathbf{g}(\mathbf{z}) = (u_2, u_2)$, where $u_2 = z_1^2 + \overline{z_1}^2 + z_2^2 + \overline{z_2}^2$. The evaluation of the invariant u_2 along the connections h_1, h_3 and h_9 gives:

$$\begin{aligned} u_2(\omega_{h_1}(t)) &= 4x^2\cos 2t, \\ u_2(\omega_{h_3}(t)) &= 2x^2(\cos 2t + 1), \\ u_2(\omega_{h_9}(t)) &= 2x^2(\cos 2t + 1). \end{aligned}$$

The flow formulas along each connection are now trivial to calculate, and we find that

$$\begin{aligned} \mathcal{F}^{\mathbf{g}}_{h_1}(t) &= -8x^3\sin t\cos 2t, \\ \mathcal{F}^{\mathbf{g}}_{h_3}(t) &= -4x^2\sin t(\cos 2t + 1), \\ \mathcal{F}^{\mathbf{g}}_{h_9}(t) &= -4x^2\sin t(\cos 2t + 1). \end{aligned}$$

Clearly $\mathcal{F}^{\mathbf{g}}_{h_1}$ has only simple zeros at $\pi/4$ and $3\pi/4$, Whereas $\mathcal{F}^{\mathbf{g}}_{h_3}$ and $\mathcal{F}^{\mathbf{g}}_{h_9}(t)$ both have zeros at $t = \pi/2$. A simple computation shows that the zero $\pi/2$ is first order degenerate. Thus the behaviour on the projected skeleton is determined by Theorem 2.41. This shows that the zero $t = \pi/2$ corresponds to either no zero or two zeros on the perturbed skeleton. This gives the four different types of behaviour on the perturbed skeleton. □

Lemma 4.16
Define $\mathbf{g} : \mathbb{C}^2 \to \mathbb{C}^2$ *by* $\mathbf{g}(\mathbf{z}) = (u_1^2, u_1^2)$. *Then the flow formula for this perturbation is*

$$\mathcal{F}^{\mathbf{g}}(t) = -4x^3(8\sin t\cos^2 t, \sin t(\cos t + 1)^2, \sin t(\cos t - 1)^2).$$

The perturbation $\mathbf{g}$ *is degenerate. The flow formula along* h_1 *has a degenerate zero at* $\pi/2$. *The flow formulas along* h_3 *and* h_9 *have no zeros. The flow on the perturbed skeleton is not the same as that on the skeleton, but by Theorem 2.41 there are only two possible types of behaviour for the zeros on the connection* h_1. *Therefore, there is a total of two different types of behaviour on the perturbed skeleton.*

Proof. The flow formulas follow from the proof of Lemma 4.14 by just squaring the results of evaluating the invariants along the connections on the skeleton. Furthermore, it is easy to see that the flow formulas along the connections h_3 and h_9 have no zeros, so by Theorem 2.38 the flow on the perturbed skeleton is the same. A simple computation shows that the flow formula for the connection h_1 has a degenerate first order zero at $t = \pi/2$, and so Theorem 2.41 implies that there are two different types of behaviour possible on the perturbed skeleton: the zero corresponds to no zero, or two zeros on the perturbed skeleton. □

There is no need to consider the flow formulas for the equivariant (z_1, z_2) since it is equivariant with respect to the torus action and thus induce a trivial flow. The equivariant (z_1u_1, z_2u_1) also induces trivial flow and so we shall not consider this perturbation.

Lemma 4.17
Define $\mathbf{g} : \mathbb{C}^2 \to \mathbb{C}^2$ *by* $\mathbf{g}(\mathbf{z}) = (z_2 + \overline{z_2}, z_1 + \overline{z_1})$. *Then the flow formula for this perturbation is*

$$\mathcal{F}^{\mathbf{g}}(t) = -2x^2(2\sin t\cos t, \sin t, \sin t\cos t).$$

The perturbation $\mathbf{g}$ *is a simple degenerate perturbation. The flow on the perturbed skeleton is the same as the flow on the skeleton*

Proof. Let $\mathbf{g}(\mathbf{z}) = (z_2 + \overline{z_2}, z_1 + \overline{z_1})$. Then $\mathbf{g}$ evaluated along the connections h_1, h_3 and h_9 gives

$$\begin{aligned}
\mathbf{g}(\omega_{h_1}(t)) &= 2x(\cos t, \cos t),\\
\mathbf{g}(\omega_{h_3}(t)) &= 2x(1, \cos t),\\
\mathbf{g}(\omega_{h_9}(t)) &= 2x(\cos t, -1).
\end{aligned}$$

From these equations the flow formulas are immediate. Further, the flow formulas show that $\mathbf{g}$ is a simple degenerate perturbation, and by Theorem 2.38 the behaviour of the flow on the skeleton and perturbed skeleton is the same. □

Lemma 4.18
Define $\mathbf{g} : \mathbb{C}^2 \to \mathbb{C}^2$ *by* $\mathbf{g}(\mathbf{z}) = ((z_2 + \overline{z_2})u_1, (z_1 + \overline{z_1})u_1)$. *Then the flow formula for this perturbation is*

$$\mathcal{F}^{\mathbf{g}}(t) = -4x^3(4\sin t\cos^2 t, \sin t(\cos t + 1), \sin t(\cos t - 1)).$$

The perturbation $\mathbf{g}$ *is degenerate. The flow formula has a degenerate zero at* $t = \pi/2$ *along the branch* h_1; *there are two different possibilities for the behaviour on the perturbed skeleton, either* $t = \pi/2$ *corresponds to no zero or to two different zeros near* $\pi/2$.

Proof. Let $\mathbf{g}(\mathbf{z}) = ((z_2 + \overline{z_2})u_1, (z_1 + \overline{z_1})u_1)$. Then $\mathbf{g}$ evaluated along the connections h_1, h_3 and h_9 gives:

$$\begin{aligned}
\mathbf{g}(\omega_{h_1}(t)) &= 8x^2(\cos^2 t, \cos^2 t),\\
\mathbf{g}(\omega_{h_3}(t)) &= 4x^2((\cos t + 1), (\cos t + 1)),\\
\mathbf{g}(\omega_{h_9}(t)) &= 4x^2((\cos t - 1), (\cos t - 1)).
\end{aligned}$$

From these equations the flow formulas along the connections h_1, h_3 and h_9 follow immediately. In addition it is obvious that the flow formulas along the connections h_3 and h_9 have no zeros, so Theorem 2.38 implies that the behaviour on the skeleton is the same as that on the projected skeleton. Now the flow formula along the connection h_1 has a degenerate zero at $\pi/2$, so by Theorem 2.41 this zero corresponds either to no zero, or to two different zeros on the perturbed skeleton. □

Lemma 4.19
Define $\mathbf{g} : \mathbb{C}^2 \to \mathbb{C}^2$ *by* $\mathbf{g}(\mathbf{z}) = (z_1^2, z_2^2)$. *Then the flow formula for this perturbation is*

$$\mathcal{F}^{\mathbf{g}}(t) = x^3(2\sin t, \sin t, \sin t).$$

The perturbation $\mathbf{g}$ *is admissible. The behaviour of the flow on the perturbed skeleton is the same as the skeleton.*

Proof. Let $\mathbf{g}(\mathbf{z}) = (z_1^2, z_2^2)$. Evaluating $\mathbf{g}$ along the connections h_1, h_3 and h_9 gives (in real coordinates),

$$\begin{aligned}
\mathbf{g}(\omega_{h_1}(t)) &= (\cos 2t, \sin 2t, \cos 2t, \sin 2t)x^2, \\
\mathbf{g}(\omega_{h_3}(t)) &= (\cos 2t, \sin 2t, 1, 0)x^2, \\
\mathbf{g}(\omega_{h_9}(t)) &= (1, 0, \cos 2t, \sin 2t)x^2.
\end{aligned}$$

The flow formulas are

$$\begin{aligned}
\mathcal{F}_{h_1}^{\mathbf{g}}(t) &= 2x^3(-\sin t \cos 2t + \cos t \sin 2t), \\
\mathcal{F}_{h_3}^{\mathbf{g}}(t) &= x^3(-\sin t \cos 2t + \cos t \sin 2t), \\
\mathcal{F}_{h_9}^{\mathbf{g}}(t) &= x^3(-\sin t \cos 2t + \cos t \sin 2t).
\end{aligned}$$

Simplification gives the stated flow formulas. Each flow formula has no zeros in the interval $(0, \pi)$, so $\mathbf{g}$ is an admissible perturbation. By Theorem 2.38, the flows on the skeleton and perturbed skeleton are the same. □

Finally we come to the last perturbation at quadratic order.

Lemma 4.20
Define $\mathbf{g} : \mathbb{C}^2 \to \mathbb{C}^2$ *by* $\mathbf{g}(\mathbf{z}) = (z_2^2 + \overline{z_2}^2, z_1^2 + \overline{z_1}^2)$. *Then the flow formula for this perturbation is*

$$\mathcal{F}^{\mathbf{g}}(t) = -2x^3(2\sin t \cos 2t, \sin t, \sin t).$$

The perturbation $\mathbf{g}$ *is simple degenerate . The behaviour of the flow on the perturbed skeleton is the same as on the skeleton.*

Proof. Let $\mathbf{g}(\mathbf{z}) = (z_2^2 + \overline{z_2}^2, z_1^2 + \overline{z_1}^2)$. Then $\mathbf{g}$ evaluated along the connections h_1, h_3 and h_9 gives:

$$\begin{aligned}
\mathbf{g}(\omega_{h_1}(t)) &= 2x^2(\cos 2t, \cos 2t), \\
\mathbf{g}(\omega_{h_3}(t)) &= 2x^2(1, \cos 2t), \\
\mathbf{g}(\omega_{h_9}(t)) &= 2x^2(\cos 2t, 1).
\end{aligned}$$

From these equations the flow formulas follow easily, as does the conclusion of the theorem. □

It is possible to combine each of the flow formulas above, using the linearity of the flow function $\mathcal{F}$, into a collective flow formula for a general quadratic order perturbation. However, this is really not that instructive—the formula is too complex to be of much use. We

Table 4.5: Eigenvalues at equilibria in directions tangent to X_ε.

Equilibria	Sign of eigenvalues
e_1	$-\text{sgn}(\varepsilon)\text{sgn}(g_{1,\overline{z_1}}(0,0) + g_{1,\overline{z_2}}(0,0))$ $-\text{sgn}(\varepsilon)\text{sgn}(g_{2,\overline{z_2}}(0,0) + g_{2,\overline{z_1}}(0,0))$
e_2	$-\text{sgn}(\varepsilon)\text{sgn}(g_{1,\overline{z_1}}(0,0) - g_{1,\overline{z_2}}(0,0))$ $-\text{sgn}(\varepsilon)\text{sgn}(g_{2,\overline{z_2}}(0,0) - g_{2,\overline{z_1}}(0,0))$
e_3	$-\text{sgn}(\varepsilon)\text{sgn}(g_{1,\overline{z_1}}(0,0) - g_{1,\overline{z_2}}(0,0))$ $-\text{sgn}(\varepsilon)\text{sgn}(g_{2,\overline{z_2}}(0,0) - g_{2,\overline{z_1}}(0,0))$
e_4	$-\text{sgn}(\varepsilon)\text{sgn}(g_{1,\overline{z_1}}(0,0) + g_{1,\overline{z_2}}(0,0))$ $-\text{sgn}(\varepsilon)\text{sgn}(g_{2,\overline{z_2}}(0,0) + g_{2,\overline{z_1}}(0,0))$

do make some general comments about the flow formulas. Firstly, there exist linear perturbations, for example (u_1, u_1), for which the flows along the connections h_3 and h_9 have no additional zeros. So any combinations of $\mathbf{D}_4$-equivariants will give an admissible perturbation along h_3 and h_9 provided the admissible part dominates the perturbation. In contrast, along the connection h_1 only the perturbation (z_1^2, z_2^2) is admissible, but again if we take any linear combination of $\mathbf{D}_4$-equivariants the resultant perturbation is admissible provided the term (z_1^2, z_2^2) dominates. Therefore, a general $\mathbf{D}_4$-equivariant perturbation $\mathbf{g}$, is admissible provided the individual admissible term is dominant. Due to the complexities involved in the general quadratic $\mathbf{D}_4$-equivariant vector field, we cannot give precise conditions on the coefficients to guarantee that a perturbation is admissible: we can say only that such a perturbation exists.

What happens in the degenerate case. In Lemmas 4.14 to 4.20 we computed the flow formulas for all $\mathbf{D}_4$-equivariants up to and including quadratic order. Above we addressed the question of when a perturbation $\mathbf{g}$ is admissible. Consider what happens when a general quadratic order perturbation $\mathbf{g}$ is not admissible. Obviously it is degenerate, but to what order? Since we have seen above that a single perturbation term is no worse that first order degenerate, we would expect (under generic conditions on the coefficients) that any linear combination of the perturbation terms considered in Lemmas 4.14 to 4.20 would give a simple degenerate perturbation. Why? The first order degenerate behaviour of a single perturbation term would be (generically) destroyed by the addition of any term which does not share this first order degeneracy at the same point. The problem then becomes: how many zeros are there of the vector field along a general connection h_1, h_3 or h_9? This is a question that cannot be answered in general, but only in a specific case. Here we have ignored the end points of the connection where more complex degenerate behaviour can occur. Although there exist first order degenerate perturbation at quadratic order, generically they do no persist when additional terms are considered. Therefore, we generically expect only simple degenerate behaviour on the skeleton, an occurrence that can easily be dealt with using Theorem 2.38.

4.2.3 Forced Symmetry Breaking to $\mathbf{D}_2[\rho^2, \kappa\rho]$

Hou and Golubitsky [50] have performed a study of forced symmetry breaking on the square lattice to the group $\mathbf{D}_2[\rho^2, \kappa\rho]$. They prove that there exists an open set of perturbations which not only give heteroclinic cycles on the skeleton, but moreover these cycles can be asymptotically stable. They prove that $\mathscr{C}_{\mathbf{D}_2[\rho^2,\kappa\rho]} = \{e_1, e_2, e_3, e_4, c_2, c_3, c_4, c_5\}$ and for a general $\mathbf{D}_2[\rho^2, \kappa]$-equivariant perturbation the eigenvalues (in tangential directions) at the equilibria are as in Table 4.5. Importantly, the existence and stability of heteroclinic cycles requires only linear order conditions. Let $u_1 = z_1 + \overline{z_1}$, $u_2 = z_2 + \overline{z_2}$. Let p and q be $\mathbf{D}_2[\rho^2, \kappa\rho]$-invariant functions, then a linear order $\mathbf{D}_2[\rho^2, \kappa\rho]$-equivariant map has the form $\mathbf{g}(\mathbf{z}) = (p_{1,u_1}u_1 + p_{1,u_2}u_2 + p_2 z_1, q_{1,u_1}u_1 + q_{1,u_2}u_2 + q_2 z_2)$, where each term is evaluated at zero, so for example, $p_{1,u_2} = p_{1,u_2}(\mathbf{0})$. To summarise, the main result of Hou and Golubitsky [50] is:

Theorem 4.21
Let $\Gamma = \mathbf{D}_4 \dot{+} \mathbf{T}^2$, $\Sigma = \mathbf{D}_4$ and $\Delta = \mathbf{D}_2[\rho^2, \kappa\rho]$. Let Γ act on $\mathbb{C}^2$ with the action given in (4.3). Let $\mathbf{f} \in \vec{\mathcal{E}}_\Gamma$ be a Γ-equivariant bifurcation problem. Let $\mathbf{g} \in \vec{\mathcal{E}}_\Delta$ be Δ-equivariant and satisfy $\mathbf{g}(\mathbf{0}) = \mathbf{0}$. Let $\mathbf{F}(\mathbf{z}, \lambda, \varepsilon) = \mathbf{f}(\mathbf{z}, \lambda) + \varepsilon\mathbf{g}(\mathbf{z})$. Then there exists a steady-state solution to $\mathbf{f}(\mathbf{z}, \lambda) = 0$ bifurcating from $(\mathbf{0}, 0)$ with Σ-isotropy. Let $X_0 \cong \mathbf{T}^2$ be the group orbit of steady states. Then for sufficiently small ε, X_0 persists to give a new $\mathbf{F}$-invariant manifold X_ε which is Δ-equivariantly diffeomorphic to X_0. Suppose that the coefficients of $\mathbf{g}$ satisfy the following conditions:

$$\begin{aligned} K_1 = \operatorname{sgn}(p_{1,u_1} + p_{1,u_2}) &= -\operatorname{sgn}(p_{1,u_1} - p_{1,u_2}) = -K_2, \\ L_1 = \operatorname{sgn}(q_{1,u_1} + q_{1,u_2}) &= -\operatorname{sgn}(p_{1,u_1} + p_{1,u_2}) = -K_1, \\ L_2 = \operatorname{sgn}(p_{1,u_1} + p_{1,u_2}) &= -\operatorname{sgn}(q_{1,u_1} - q_{1,u_2}) = K_1. \end{aligned}$$

Then there exists a heteroclinic cycle connecting the equilibria. Moreover, if $\operatorname{sgn}(\varepsilon) = \operatorname{sgn}(L_1K_2 - K_1L_2)\operatorname{sgn}(K_1)$, then the cycle is asymptotically stable.

4.2.4 Forced Symmetry Breaking to $\mathbf{D}_2[\rho^2, \kappa]$

In this section we consider the behaviour of the group orbit X_0, when symmetry-breaking terms with $\mathbf{D}_2[\rho^2, \kappa]$ symmetry are added to equation (4.5). The action of the group $\mathbf{D}_2[\rho^2, \kappa]$ on the space $\mathbb{C}^2$ is the restriction of the action (4.7):

$$\begin{aligned} \rho^2(z_1, z_2) &= (\overline{z_1}, \overline{z_2}), \\ \kappa(z_1, z_2) &= (z_2, z_1), \\ \kappa\rho^2(z_1, z_2) &= (\overline{z_2}, \overline{z_1}). \end{aligned} \tag{4.10}$$

Calculation of the Skeleton

First we the calculate the skeleton. X_0 is a 2-torus, $\mathbf{T}^2$. Our notation is the same as in Definition 4.3. The group $\mathbf{D}_2[\rho^2, \kappa]$ has four nontrivial subgroups: $\mathbf{D}_2[\rho^2, \kappa]$, $\mathbf{Z}_2[\rho^2]$, $\mathbf{Z}_2[\kappa]$, and $\mathbf{Z}_2[\kappa\rho^2]$. We have:

Proposition 4.22
Let $\mathbf{D}_2[\rho^2, \kappa]$ act on $\mathbb{C}^2$ with the action (4.10). Then $\mathscr{C}_{\mathbf{D}_2[\rho^2,\kappa]} = \{e_1, e_2, e_3, e_4, c_1, c_6\}$.

Proof. This follows from the entries of Table 4.1. □

The skeleton $\mathbb{X}_{\mathbf{D}_2[\rho^2,\kappa]}$ of X_0 is

$$\begin{aligned} \mathbb{X}_{\mathbf{D}_2[\rho^2,\kappa]} &= \bigcup_{C \in \mathscr{C}_{\mathbf{D}_2[\rho^2,\kappa]}} C \\ &= c_1 \cup c_6 \\ &\subset X_0. \end{aligned}$$

Figure 4.3 illustrates $\mathbb{X}_{\mathbf{D}_2[\rho^2,\kappa]}$. The next step is to determine the smooth stratification of $\mathbb{X}_{\mathbf{D}_2[\rho^2,\kappa]}$. We use the terminology of Definition 4.6. Then we have the following stratification of $\mathbb{X}_{\mathbf{D}_2[\rho^2,\kappa]}$, in which each element of $E_{(\mathbf{D}_4,X_0)}$ and $H_{(\mathbf{D}_4,X_0)}$ is a manifold:

$$\begin{aligned} E_{(\mathbf{D}_4,X_0)} &= e_1 \cup e_2 \cup e_3 \cup e_4, \\ H_{(\mathbf{D}_4,X_0)} &= h_1 \cup h_2 \cup h_{11} \cup h_{12}. \end{aligned}$$

This completes the calculation of the skeleton. At this point we may use the above calculation to deduce the following existence result.

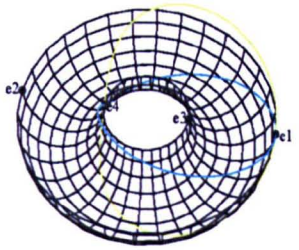

Figure 4.3: The skeleton $\mathbf{X}_{\mathbf{D}_2[\rho^2,\kappa]}$ within the 2-torus X_0, Here c_1 is yellow, and c_6 is cyan.

Theorem 4.23
Let $\Gamma = \mathbf{D}_4 \dot{+} \mathbf{T}^2$, $\Sigma = \mathbf{D}_4$ and $\Delta = \mathbf{D}_2[\rho^2, \kappa]$. Let Γ act on $\mathbb{C}^2$ with the action given in (4.3). Let $\mathbf{f} \in \vec{\mathcal{E}}_\Gamma$ be a Γ-equivariant bifurcation problem. Let $\mathbf{g} \in \vec{\mathcal{E}}_\Delta$ be Δ-equivariant and satisfy $\mathbf{g}(\mathbf{0}) = \mathbf{0}$. Let $\mathbf{F}(\mathbf{z}, \lambda, \varepsilon) = \mathbf{f}(\mathbf{z}, \lambda) + \varepsilon \mathbf{g}(\mathbf{z})$. Then there exists a steady-state solution to $\mathbf{f}(\mathbf{z}, \lambda) = 0$ bifurcating from $(\mathbf{0}, 0)$ with Σ-isotropy. Let $X_0 \cong \mathbf{T}^2$ be the group orbit of steady states. Then for sufficiently small ε, X_0 persists to give a new $\mathbf{F}$-invariant manifold X_ε, which is Δ-equivariantly diffeomorphic to X_0. Moreover, there exists $g \in \vec{\mathcal{E}}_\Delta$ such that the elements in $E_{(\Delta, X_0)}$ are equilibria for the new flow and those of $H_{(\Delta, X_0)}$ are heteroclinic connections between equilibria.

As was the case for the subgroup $\mathbf{D}_4$ we wish to consider the restrictions placed on the skeleton by the action of the symmetry group $\mathbf{D}_2[\rho^2, \kappa]$ on X_0.

Symmetry Properties of $\mathbf{X}_{\mathbf{D}_2[\rho^2,\kappa]}$

Here we concern ourselves with the symmetry properties of $\mathbf{X}_{\mathbf{D}_2[\rho^2,\kappa]}$. More precisely, given $C \in \mathscr{C}_{\mathbf{D}_2[\rho^2,\kappa]}$ we calculate the setwise and pointwise isotropy subgroups. This symmetry information restricts the types of flows that are possible on $\mathbf{X}_{\mathbf{D}_2[\rho^2,\kappa]}$. In addition, it simplifies the calculation of the projected skeleton, allowing us to classify the different types of behaviour to be expected on the skeleton.

Pointwise and Setwise Isotropy Subgroups. The action of $\mathbf{D}_2[\rho^2, \kappa]$ on $\mathbb{C}^2$ given by (4.10) induces a natural action on X_0. This action is given by

$$\begin{aligned} \rho^2(\theta_1, \theta_2) &= (\theta_1, \theta_2), \\ \kappa(\theta_1, \theta_2) &= (\theta_2, \theta_1), \\ \kappa\rho^2(\theta_1, \theta_2) &= (-\theta_2, -\theta_1). \end{aligned} \tag{4.11}$$

This action is easy to calculate: it is the restriction of the $\mathbf{D}_4$ action (4.8). The action of $\mathbf{D}_2[\rho^2, \kappa]$ on X_0 in turn induces an action on $\mathscr{C}_{\mathbf{D}_2[\rho^2,\kappa]}$ by permutation. Again this action is the restriction of the action in Table 4.2, the results of which are contained in Table 4.6. Note that the group $\mathbf{D}_2[\rho^2, \kappa]$ acts trivially on c_1 and c_6. Using this action we may deduce the following result

Proposition 4.24
Let $\mathbf{D}_2[\rho^2, \kappa]$ act on $\mathscr{C}_{\mathbf{D}[\rho^2,\kappa]}$ as in Table 4.6 and on X_0 with the action in (4.11). Then given $C \in \mathscr{C}_{\mathbf{D}_2[\rho^2,\kappa]}$, the setwise isotropy $Stab(C)$, the pointwise isotropy $stab(C)$ and the group $S(C) = Stab(C)/stab(C)$ are given in Table 4.7.

Table 4.6: Induced action of $\mathbf{D}_2[\rho^2,\kappa]$ on $\mathscr{C}_{\mathbf{D}_2[\rho^2,\kappa]}$.

Element of $\mathscr{C}_{\mathbf{D}_2[\rho^2,\kappa]}$	Elements of $\mathbf{D}_2[\rho^2,\kappa]$ acting nontrivially	Action
e_1	none	
e_2	$\kappa, \kappa\rho^2$	e_3
e_3	$\kappa, \kappa\rho^2$	e_2
e_4	none	
c_1	none	
c_6	none	

Table 4.7: Isotropy data for $C \in \mathscr{C}_{\mathbf{D}_2[\rho^2,\kappa]}$

$C \in \mathscr{C}_{\mathbf{D}_2[\rho^2,\kappa]}$	stab(C)	Stab(C)	$S(C) = \text{Stab}(C)/\text{stab}(C)$
e_1	$\mathbf{D}_2[\rho^2,\kappa]$	$\mathbf{D}_2[\rho^2,\kappa]$	$\mathbf{1}$
e_2	$\mathbf{Z}_2[\rho^2]$	$\mathbf{Z}_2[\rho^2]$	$\mathbf{1}$
e_3	$\mathbf{Z}_2[\rho^2]$	$\mathbf{Z}_2[\rho^2]$	$\mathbf{1}$
e_4	$\mathbf{D}_2[\rho^2,\kappa]$	$\mathbf{D}_2[\rho^2,\kappa]$	$\mathbf{1}$
c_1	$\mathbf{Z}_2[\kappa]$	$\mathbf{D}_2[\rho^2,\kappa]$	$\mathbf{Z}_2$
c_6	$\mathbf{Z}_2[\kappa\rho^2]$	$\mathbf{D}_2[\rho^2,\kappa]$	$\mathbf{Z}_2$

Proof. Use Proposition 4.8. □

Knots. Given any $C \in \mathscr{C}_{\mathbf{D}_2[\rho^2,\kappa]}$, where C is a topological circle, a knot relative to C gives an axis of symmetry of C. This axis of symmetry places great restrictions on the types of flow that are possible on the skeleton $\mathbb{X}_{\mathbf{D}_2[\rho^2,\kappa]}$. We have seen that $S(C) \cong \mathbf{Z}_2$ for $C = c_1$, c_6 and that each C contains the two equilibria e_1 and e_4, thus these equilibria are the knots relative to c_1 and c_6.

Projected Skeleton $\mathbb{X}^p_{\mathbf{D}_2[\rho^2,\kappa]}$

We can now construct the projected skeleton $\mathbb{X}^p_{\mathbf{D}_2[\rho^2,\kappa]}$ of the skeleton $\mathbb{X}_{\mathbf{D}_2[\rho^2,\kappa]}$. Both c_1 and c_6 have two knots and so one axis of reflection symmetry for any $\mathbf{D}_2[\rho^2,\kappa]$-equivariant flow. We choose the following orbit representatives for the equilibria: e_1, e_3 and e_4. We choose the following orbit representative for the connections: h_1 and h_{11}. The element h_1 connects e_1 to e_4 and h_{11} connects e_4 to e_1. Figure 4.4 illustrates the projected skeleton with two different types of flow, each corresponding to a possible flow on the skeleton $\mathbb{X}_{\mathbf{D}_2[\rho^2,\kappa]}$. From the projected skeleton we can see that there is a maximum of four different admissible flows, of which two can give heteroclinic cycles between the equilibria e_1 and e_4.

Invariant Theory for $\mathbf{D}_2[\rho^2,\kappa]$

To determine the flow formulas we must compute the general form of a $\mathbf{D}_2[\rho^2,\kappa]$-equivariant mapping. Here we determine a set of generators for the ring of $\mathbf{D}_2[\rho^2,\kappa]$-invariant functions $\mathcal{E}_{\mathbf{D}_2[\rho^2,\kappa]}$ and the module of $\mathbf{D}_2[\rho^2,\kappa]$-equivariant mappings $\vec{\mathcal{E}}_{\mathbf{D}_2[\rho^2,\kappa]}$. By the theorems of Schwarz (Theorem 1.4) and Poénaru (Theorem 1.5) it is sufficient to consider the ring $\mathcal{P}_{\mathbf{D}_2[\rho^2,\kappa]}$ of polynomial invariants and the module $\vec{\mathcal{P}}_{\mathbf{D}_2[\rho^2,\kappa]}$ of polynomial equivariants.

We begin with the invariants.

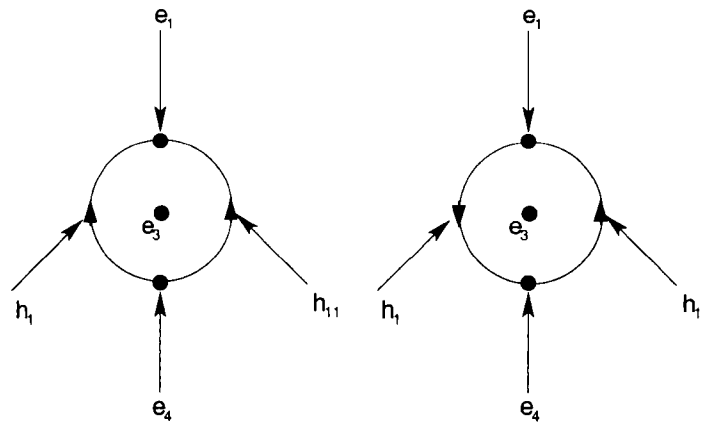

Figure 4.4: Projected skeleton $\mathbb{X}^{p}_{\mathbf{D}_2[\rho^2,\kappa]}$ with two possible flows.

Lemma 4.25
Let $\mathbf{D}_2[\rho^2,\kappa]$ act on $\mathbb{C}^2$ with the action given by equation (4.10). Then the Poincaré series for the invariants is

$$\begin{aligned}\Upsilon(t) &= \frac{t^2-t+1}{(1-t^2)^2(1-t)^2} \\ &= 1+t+4t^2+5t^3+11t^4+14t^5+24t^6+\ldots,\end{aligned}$$

where ... denotes higher order terms.

Proof. See Appendix A. □

Using the Poincaré series we may calculate a set of generating invariant polynomials for the ring $\mathcal{P}_{\mathbf{D}_2[\rho^2,\kappa]}$.

Lemma 4.26
Let $\mathbf{D}_2[\rho^2,\kappa]$ act on $\mathbb{C}^2$ with the action given by equation (4.10). Then the polynomials

$$\begin{aligned}u_1 &= z_1+\overline{z_1}+z_2+\overline{z_2}, \\ u_2 &= z_1^2+\overline{z_1}^2+z_2^2+\overline{z_2}^2, \\ u_3 &= z_1z_2+\overline{z_1}\,\overline{z_2}, \\ u_4 &= z_1\overline{z_1}+z_2\overline{z_2},\end{aligned}$$

are invariant under the action of $\mathbf{D}_2[\rho^2,\kappa]$ and are linearly independent. Moreover they generate the ring $\mathcal{P}_{\mathbf{D}_2[\rho^2,\kappa]}$.

Proof. See Appendix A. □

We have now produced a set of generators for the ring $\mathcal{P}_{\mathbf{D}_2[\rho^2,\kappa]}$, we move on to consider the module $\vec{\mathcal{P}}_{\mathbf{D}_2[\rho^2,\kappa]}$ of equivariant polynomial mappings.

Lemma 4.27
Let $\mathbf{D}_2[\rho^2,\kappa]$ act on $\mathbb{C}^2$ with the action given by equation (4.10). Then the Poincaré series for

the equivariants is

$$\begin{aligned}\Xi(t) &= \frac{1}{(1-t)^4} \\ &= 1 + 4t + 10t^2 + 20t^3 + 35t^4 + 56t^5 + 84t^6 + \ldots,\end{aligned}$$

where ... denotes higher order terms.

Proof. See Appendix A. □

With the Poincaré series at hand we may calculate a set of generating equivariant polynomial mappings for the module $\vec{\mathcal{P}}_{\mathbf{D}_2[\rho^2,\kappa]}$.

Lemma 4.28
Let $\mathbf{D}_2[\rho^2,\kappa]$ act on $\mathbb{C}^2$ with the action given by equation (4.10). Then the module of equivariant polynomial mappings is generated over the ring $\mathcal{P}_{\mathbf{D}_2[\rho^2,\kappa]}$ by the mappings

$$e_1 = \begin{bmatrix} 1 \\ 1 \end{bmatrix}, \quad e_2 = \begin{bmatrix} z_1 \\ z_2 \end{bmatrix}, \quad e_3 = \begin{bmatrix} z_2 \\ z_1 \end{bmatrix},$$

$$e_4 = \begin{bmatrix} \overline{z_1} \\ \overline{z_2} \end{bmatrix}, \quad e_5 = \begin{bmatrix} z_1^2 \\ z_2^2 \end{bmatrix}, \quad e_6 = \begin{bmatrix} z_2^2 \\ z_1^2 \end{bmatrix},$$

$$e_7 = \begin{bmatrix} \overline{z_1}^2 \\ \overline{z_2}^2 \end{bmatrix}, \quad e_8 = \begin{bmatrix} z_1^3 \\ z_2^3 \end{bmatrix},$$

Proof. See Appendix A. □

Let $\mathbf{g}$ be $\mathbf{D}_2[\rho^2,\kappa]$-equivariant mapping. Write $\mathbf{g} = (g_1, g_2)$, then by Lemmas 4.26 and 4.28 the general form of a $\mathbf{D}_2[\rho^2,\kappa]$-equivariant mapping is given by

$$\begin{aligned} g_1(\mathbf{z}) &= p_1(\mathbf{u}) + p_2(\mathbf{u})z_1 + p_3(\mathbf{u})z_2 + p_4(\mathbf{u})\overline{z_1} \\ &+ p_5(\mathbf{u})z_1^2 + p_6(\mathbf{u})z_2^2 + p_7(\mathbf{u})\overline{z_1}^2 + p_8(\mathbf{u})z_1^3, \\ g_2(\mathbf{z}) &= p_1(\mathbf{u}) + p_2(\mathbf{u})z_2 + p_3(\mathbf{u})z_1 + p_4(\mathbf{u})\overline{z_2} \\ &+ p_5(\mathbf{u})z_2^2 + p_6(\mathbf{u})z_1^2 + p_7(\mathbf{u})\overline{z_2}^2 + p_8(\mathbf{u})z_2^3. \end{aligned}$$

where the p_j's are smooth functions of the invariants $\mathbf{u} = (u_1, u_2, u_3, u_4)$.

Flow Formulas

The aim of this section is twofold. We begin by calculating, for a general quadratic order $\mathbf{D}_2[\rho^2,\kappa]$-equivariant perturbation $\mathbf{g}$, the direction of flow along the connections of the skeleton. We need only consider two orbit types of connections given by h_1 and h_{11}. The general form of a $\mathbf{D}_2[\rho^2,\kappa]$-equivariant map $\mathbf{g}$ on $\mathbb{C}^2$, is given to quadratic order by

$$\begin{aligned} g_1(\mathbf{z}) &= p_{1,u_1}u_1 + p_{1,u_2}u_2 + p_{1,u_3}u_3 + p_{1,u_4}u_4 + p_{1,u_1^2}u_1^2 \\ &+ p_2z_1 + p_{2,u_1}z_1u_1 + p_3z_2 + p_{2,u_1}z_2u_1 + p_4\overline{z_1} + p_{4,u_1}\overline{z_1}u_1 \\ &+ p_5z_1^2 + p_6z_2^2 + p_7\overline{z_1}^2, \\ g_2(\mathbf{z}) &= p_{1,u_1}u_1 + p_{1,u_2}u_2 + p_{1,u_3}u_3 + p_{1,u_4}u_4 + p_{1,u_1^2}u_1^2 \\ &+ p_2z_2 + p_{2,u_1}z_2u_1 + p_3z_1 + p_{2,u_1}z_1u_1 + p_4\overline{z_2} + p_{4,u_1}\overline{z_2}u_1 \\ &+ p_5z_2^2 + p_6z_1^2 + p_7\overline{z_2}^2. \end{aligned} \tag{4.12}$$

For notational simplicity, we have not explicitly written that the coefficients are evaluated at zero, so for example, $p_5 = p_5(0)$. Given a perturbation (4.12) we wish to know the direction of flow along the connections h_1 and h_{11}.

With the flow formulas calculated, we find conditions on the coefficients of (4.12) so that no additional equilibria lie on the connections $h \in H_{(\mathbf{D}_2[\rho^2,\kappa],X_0)}$. These conditions form a collection of nondegeneracy condition on the perturbation term required, so that we may apply Theorem 2.38 to deduce the behaviour of the flow on the perturbed skeleton.

There are only two group orbits of connections in $H_{(\mathbf{D}_2[\rho^2,\kappa],X_0)}$. These are given by h_1 and h_{11}. These connections are parametrised by the functions ω_{h_1}, $\omega_{h_{11}} : [0,\pi] \to X_0$ defined by $\omega_{h_1}(t) = (e^{it}, e^{it})x$ and $\omega_{h_{11}}(t) = (e^{it}, e^{-it})x$. Using these parametrisations we find the tangent vectors to the connections are given by:

$$\begin{aligned} \mathcal{T}_{h_1}(t) &= (-\sin t, \cos t, -\sin t, \cos t), \\ \mathcal{T}_{h_{11}}(t) &= (-\sin t, \cos t, -\sin t, -\cos t). \end{aligned}$$

Here we have used real coordinates to express the tangent vectors, and the notation $\mathcal{F}^{\mathbf{g}}(t) = (\mathcal{F}^{\mathbf{g}}_{h_1}(t), \mathcal{F}^{\mathbf{g}}_{h_{11}}(t))$.

Lemma 4.29
Define $\mathbf{g} : \mathbb{C}^2 \to \mathbb{C}^2$ by $\mathbf{g}(\mathbf{z}) = (u_1, u_1)$, where $u_1 = z_1 + \overline{z_1} + z_2 + \overline{z_2}$. The flow formula for the perturbation $\mathbf{g}$ on $\mathbb{X}_{\mathbf{D}_2[\rho^2,\kappa]}$ is

$$\mathcal{F}^{\mathbf{g}}(t) = (-8x^2 \sin t \cos t, -8x^2 \sin t \cos t).$$

The flow along the connections h_1 and h_{11} has a simple zero at $t = \pi/2$, and the flow on the perturbed skeleton is qualitatively the same as on the skeleton.

Proof. Define $\mathbf{g} : \mathbb{C}^2 \to \mathbb{C}^2$ by $\mathbf{g}(\mathbf{z}) = (u_1, u_1)$. Then

$$\mathbf{g}(\omega_{h_1}(t)) = \mathbf{g}(\omega_{h_{11}}(t)) = (4\cos t, 4\cos t)x.$$

Therefore the flow formulas along the connections h_1 and h_{11} are:

$$\begin{aligned} \mathcal{F}^{\mathbf{g}}_{h_1}(t) &= -8x^2 \sin t \cos t, \\ \mathcal{F}^{\mathbf{g}}_{h_{11}}(t) &= -8x^2 \sin t \cos t. \end{aligned}$$

It is now easy to see that the flow formulas have a simple zero at $t = \pi/2$. Therefore, by Theorem 2.38 the flow on the perturbed skeleton is qualitatively the same as the flow on the skeleton. □

Lemma 4.30
Define $\mathbf{g} : \mathbb{C}^2 \to \mathbb{C}^2$ by $\mathbf{g}(\mathbf{z}) = (u_2, u_2)$, where $u_2 = z_1^2 + \overline{z_1}^2 + z_2^2 + \overline{z_2}^2$. The flow formula for the perturbation $\mathbf{g}$ on $\mathbb{X}_{\mathbf{D}_2[\rho^2,\kappa]}$ is

$$\mathcal{F}^{\mathbf{g}}(t) = -8x^3(\sin t \cos 2t, \sin t \cos 2t).$$

The flow along the connections h_1 and h_{11} have simple zeros at $t = \pi/4$ and $t = 3\pi/4$, and the flow on the perturbed skeleton is qualitatively the same as on the skeleton.

Proof. Define $\mathbf{g} : \mathbb{C}^2 \to \mathbb{C}^2$ by $\mathbf{g}(\mathbf{z}) = (u_2, u_2)$. Then

$$\mathbf{g}(\omega_{h_1}(t)) = \mathbf{g}(\omega_{h_{11}}(t)) = (4\cos 2t, 4\cos 2t)x^2.$$

Therefore the flow formulas along the connections h_1 and h_{11} are:

$$\begin{aligned} \mathcal{F}^{\mathbf{g}}_{h_1}(t) &= -8x^3 \sin t \cos 2t, \\ \mathcal{F}^{\mathbf{g}}_{h_{11}}(t) &= -8x^3 \sin t \cos 2t. \end{aligned}$$

It is now easy to see that the flow formulas have simple zeros at $t = \pi/4$ and $t = 3\pi/4$. Therefore, by Theorem 2.38 the flow on the perturbed skeleton is qualitatively the same as the flow on the skeleton. □

Lemma 4.31
Define $\mathbf{g} : \mathbb{C}^2 \to \mathbb{C}^2$ *by* $\mathbf{g}(\mathbf{z}) = (u_3, u_3)$, *where* $u_3 = z_1 z_2 + \overline{z_1 z_2}$. *The flow formula for the perturbation* $\mathbf{g}$ *on* $\mathbb{X}_{\mathbf{D}_2[\rho^2,\kappa]}$ *is*

$$\mathcal{F}^{\mathbf{g}}(t) = -4x^3(\sin t \cos 2t, \sin t).$$

The flow along the connections h_1 *has simple zeros at* $t = \pi/4$ *and* $t = 3\pi/4$, *whilst along the connection* h_{11} *there are no zeros, and the flow on the perturbed skeleton is qualitatively the same as on the skeleton.*

Proof. Define $\mathbf{g} : \mathbb{C}^2 \to \mathbb{C}^2$ by $\mathbf{g}(\mathbf{z}) = (u_3, u_3)$. Then

$$\begin{aligned} \mathbf{g}(\omega_{h_1}(t)) &= (2\cos 2t, 2\cos 2t)x^2, \\ \mathbf{g}(\omega_{h_{11}}(t)) &= (2,2)x^2. \end{aligned}$$

Therefore the flow formulas along the connections h_1 and h_{11} are:

$$\begin{aligned} \mathcal{F}^{\mathbf{g}}_{h_1}(t) &= -4x^3 \sin t \cos 2t, \\ \mathcal{F}^{\mathbf{g}}_{h_{11}}(t) &= -4x^3 \sin t. \end{aligned}$$

It is now easy to see that the flow formula along h_1 has simple zeros at $t = \pi/4$ and $t = 3\pi/4$. Therefore, by Theorem 2.38 the flow on the perturbed skeleton is qualitatively the same as the flow on the skeleton. □

We now give the first example of a perturbation which gives no additional zeros along *both* connections h_1 and h_{11}.

Lemma 4.32
Define $\mathbf{g} : \mathbb{C}^2 \to \mathbb{C}^2$ *by* $\mathbf{g}(\mathbf{z}) = (u_4, u_4)$, *where* $u_4 = z_1\overline{z_1} + z_2\overline{z_2}$. *The flow formula for the perturbation* $\mathbf{g}$ *on* $\mathbb{X}_{\mathbf{D}_2[\rho^2,\kappa]}$ *is*

$$\mathcal{F}^{\mathbf{g}}(t) = -4x^3(\sin t, \sin t).$$

The flow along the connections h_1 *and* h_{11} *have no zeros. The flow on the perturbed skeleton is qualitatively the same as the skeleton.*

Proof. Define $\mathbf{g} : \mathbb{C}^2 \to \mathbb{C}^2$ by $\mathbf{g}(\mathbf{z}) = (u_4, u_4)$. Then $\mathbf{g}(\omega_{h_1})(t) = \mathbf{g}(\omega_{h_{11}})(t) = (2,2)x^2$. Therefore the flow formulas along the connections h_1 and h_{11} are:

$$\begin{aligned} \mathcal{F}^{\mathbf{g}}_{h_1}(t) &= -4x^3 \sin t, \\ \mathcal{F}^{\mathbf{g}}_{h_{11}}(t) &= -4x^3 \sin t. \end{aligned}$$

Therefore, by Theorem 2.38, the flow on the perturbed skeleton is qualitatively the same as the flow on the skeleton. □

Lemma 4.33
Define $\mathbf{g} : \mathbb{C}^2 \to \mathbb{C}^2$ *by* $\mathbf{g}(\mathbf{z}) = (u_1^2, u_1^2)$, *where* $u_1 = z_1 + \overline{z_1} + z_2 + \overline{z_2}$. *The flow formula for the perturbation* $\mathbf{g}$ *on* $\mathbb{X}_{\mathbf{D}_2[\rho^2,\kappa]}$ *is*

$$\mathcal{F}^{\mathbf{g}}(t) = -32x^3(\sin t \cos^2 t, \sin t \cos^2 t).$$

The flow along the connections h_1 *and* h_{11} *have a first order degenerate zero at* $t = \pi/2$. *The flow on the perturbed skeleton near* $t = \pi/2$ *has either no zero or two different zeros.*

Proof. Define $\mathbf{g} : \mathbb{C}^2 \to \mathbb{C}^2$ by $\mathbf{g}(\mathbf{z}) = (u_1^2, u_1^2)$. Then

$$\mathbf{g}(\omega_{h_1}(t)) = \mathbf{g}(\omega_{h_{11}}(t)) = (16\cos^2 t, 16\cos^2 t)x^2.$$

Therefore the flow formulas along the connections h_1 and h_{11} are:

$$\begin{aligned}\mathcal{F}^{\mathbf{g}}_{h_1}(t) &= -32x^3 \sin t \cos^2 t,\\ \mathcal{F}^{\mathbf{g}}_{h_{11}}(t) &= -32x^3 \sin t \cos^2 t.\end{aligned}$$

From which we see $t = \pi/2$ is a zero of the flow formula and also a first order degenerate zero. Therefore, by Theorem 2.41 the flow on the perturbed skeleton either has no zero near $t = \pi/2$ and hence the flow is admissible or there are two distinct zeros near $\pi/2$. □

There is no need the consider the perturbation term (z_1, z_2), since this is actually Γ_s-equivariant and so induces only a trivial flow on X_0.

Lemma 4.34
Define $\mathbf{g} : \mathbb{C}^2 \to \mathbb{C}^2$ *by* $\mathbf{g}(\mathbf{z}) = (z_2, z_1)$. *The flow formula for the perturbation* $\mathbf{g}$ *on* $\mathbb{X}_{\mathbf{D}_2[\rho^2,\kappa]}$ *is*

$$\mathcal{F}^{\mathbf{g}}(t) = (0, -4x^3 \sin t \cos t).$$

The flow along the connection h_{11} *has a zero at* $t = \pi/2$. *Since the flow along the connection* h_1 *is trivial we can conclude only that the behaviour on the perturbed connection* h^{ε}_{11} *is the same as the connection* h_{11}. *It is not possible to say how the flow behaves along on the connection* h_1.

Proof. Define $\mathbf{g} : \mathbb{C}^2 \to \mathbb{C}^2$ by $\mathbf{g}(\mathbf{z}) = (z_2, z_1)$. Then $\mathbf{g}(\omega_{h_1}(t)) = (\cos t, \sin t, \cos t, \sin t)x$ and $\mathbf{g}(\omega_{h_{11}})(t) = (\cos t, -\sin t, \cos t, \sin t)x$, where real coordinates have been used. Therefore the flow formulas along the connections h_1 and h_{11} are:

$$\begin{aligned}\mathcal{F}^{\mathbf{g}}_{h_1}(t) &= 0,\\ \mathcal{F}^{\mathbf{g}}_{h_{11}}(t) &= -4x^2 \sin t \cos t.\end{aligned}$$

It is easily seen that $t = \pi/2$ is a simple zero of the flow formula for the connection h_{11} Therefore, by Theorem 2.38 the flow on the perturbed connection h^{ε}_{11} is the same as on h_{11}. □

Lemma 4.35
Define $\mathbf{g} : \mathbb{C}^2 \to \mathbb{C}^2$ *by* $\mathbf{g}(\mathbf{z}) = (z_2u_1, z_1u_1)$. *The flow formula for the perturbation* $\mathbf{g}$ *on* $\mathbb{X}_{\mathbf{D}_2[\rho^2,\kappa]}$ *is*

$$\mathcal{F}^{\mathbf{g}}(t) = (0, -16x^3 \sin t \cos^2 t).$$

The flow along the connection h_{11} *has a degenerate zero at* $t = \pi/2$. *Since the flow along the connection* h_1 *is trivial we can conclude only that the behaviour on the perturbed connection* h^{ε}_{11} *has either no zeros or two distinct zeros.*

Proof. Define $\mathbf{g} : \mathbb{C}^2 \to \mathbb{C}^2$ by $\mathbf{g}(\mathbf{z}) = (z_2u_1, z_1u_1)$. Then

$$\begin{aligned}\mathbf{g}(\omega_{h_1}(t)) &= (4\cos^2 t, 4\cos t \sin t, 4\cos^2 t, 4\cos t \sin t)x^2,\\ \mathbf{g}(\omega_{h_{11}}(t) &= (4\cos^2 t, -3\cos t \sin t, 4\cos^2 t, 4\cos t \sin t)x^2,\end{aligned}$$

where real coordinates have been used. Therefore the flow formulas along the connections h_1 and h_{11} are:

$$\begin{aligned}\mathcal{F}^{\mathbf{g}}_{h_1}(t) &= 0,\\ \mathcal{F}^{\mathbf{g}}_{h_{11}}(t) &= -16x^3 \sin t \cos^2 t.\end{aligned}$$

It is easily seen that $t = \pi/2$ is a degenerate zero of the flow formula for the connection h_{11}. Therefore, by Theorem 2.41 the flow on the perturbed connection h^{ε}_{11} has either no zero or two zeros near $t = \pi/2$. □

Lemma 4.36
Define $\mathbf{g} : \mathbb{C}^2 \to \mathbb{C}^2$ *by* $\mathbf{g}(\mathbf{z}) = (\overline{z_1}, \overline{z_2})$. *The flow formula for the perturbation* $\mathbf{g}$ *on* $\mathbb{X}_{\mathbf{D}_2[\rho^2,\kappa]}$ *is*

$$\mathcal{F}^{\mathbf{g}}(t) = (-4x^2 \sin t \cos t, -4x^2 \sin t \cos t).$$

The flow formula has a simple zero at $t = \pi/2$. *The flow on the perturbed skeleton is qualitatively the same as the flow on the skeleton.*

Proof. Define $\mathbf{g} : \mathbb{C}^2 \to \mathbb{C}^2$ by $\mathbf{g}(\mathbf{z}) = (\overline{z_1}, \overline{z_2})$. Then

$$\begin{aligned} \mathbf{g}(\omega_{h_1}(t)) &= (\cos t, -\sin t, \cos t, -\sin t)x, \\ \mathbf{g}(\omega_{h_{11}}(t)) &= (\cos t, -\sin t, \cos t, \sin t)x, \end{aligned}$$

where real coordinates have been used. Therefore the flow formulas along the connections h_1 and h_{11} are:

$$\begin{aligned} \mathcal{F}^{\mathbf{g}}_{h_1}(t) &= -4x^2 \sin t \cos t, \\ \mathcal{F}^{\mathbf{g}}_{h_{11}}(t) &= -4x^2 \sin t \cos t. \end{aligned}$$

It is easily seen that $t = \pi/2$ is a simple zero of the flow formula Therefore, by Theorem 2.38 the flow on the perturbed skeleton is the same as on the skeleton. □

Lemma 4.37
Define $\mathbf{g} : \mathbb{C}^2 \to \mathbb{C}^2$ *by* $\mathbf{g}(\mathbf{z}) = (\overline{z_1}u_1, \overline{z_2}u_1)$. *The flow formula for the perturbation* $\mathbf{g}$ *on* $\mathbb{X}_{\mathbf{D}_2[\rho^2,\kappa]}$ *is*

$$\mathcal{F}^{\mathbf{g}}(t) = -16x^3(\sin t \cos^2 t, \sin t \cos^2 t).$$

The flow formula has a degenerate zero at $t = \pi/2$. *And the flow on the perturbed skeleton has either no zero or two distinct zeros near* $t = \pi/2$.

Proof. Define $\mathbf{g} : \mathbb{C}^2 \to \mathbb{C}^2$ by $\mathbf{g}(\mathbf{z}) = (\overline{z_1}, \overline{z_2})$. Then

$$\begin{aligned} \mathbf{g}(\omega_{h_1}(t)) &= (4\cos^2 t, -4\sin t \cos t, 4\cos^2 t, -4\cos t \sin t)x, \\ \mathbf{g}(\omega_{h_{11}}(t)) &= (4\cos^2 t, -4\cos t \sin t, 4\cos^2 t, 4\cos t \sin t)x, \end{aligned}$$

where real coordinates have been used. Therefore the flow formulas along the connections h_1 and h_{11} are:

$$\begin{aligned} \mathcal{F}^{\mathbf{g}}_{h_1}(t) &= -16x^2 \sin t \cos^2 t, \\ \mathcal{F}^{\mathbf{g}}_{h_{11}}(t) &= -16x^2 \sin t \cos^2 t. \end{aligned}$$

It is easily seen that $t = \pi/2$ is a degenerate zero of the flow formula. Therefore, by Theorem 2.38 the flow on the perturbed skeleton is the same as on the skeleton. □

Next we give our second example of an admissible perturbation.

Lemma 4.38
Define $\mathbf{g} : \mathbb{C}^2 \to \mathbb{C}^2$ *by* $\mathbf{g}(\mathbf{z}) = (z_1^2, z_2^2)$. *The flow formula for the perturbation* $\mathbf{g}$ *on* $\mathbb{X}_{\mathbf{D}_2[\rho^2,\kappa]}$ *is*

$$\mathcal{F}^{\mathbf{g}}(t) = 2x^3(\sin t, \sin t).$$

The flow formula has no zeros along either of the connections h_1 *or* h_{11}. *The flow on the perturbed skeleton is the same as on the skeleton.*

Proof. Define $\mathbf{g} : \mathbb{C}^2 \to \mathbb{C}^2$ by $\mathbf{g}(\mathbf{z}) = (z_1^2, z_2^2)$. Then

$$\begin{aligned} \mathbf{g}(\omega_{h_1}(t)) &= (\cos 2t, \sin 2t, \cos 2t, \sin 2t)x, \\ \mathbf{g}(\omega_{h_{11}}(t)) &= (\cos 2t, \sin 2t, \cos 2t, -\sin 2t)x, \end{aligned}$$

where real coordinates have been used. Therefore the flow formulas along the connections h_1 and h_{11} are:

$$\begin{aligned} \mathcal{F}^{\mathbf{g}}_{h_1}(t) &= (-2\cos 2t \sin t + 2\cos t \sin 2t)x^3 = 2x^2 \sin t, \\ \mathcal{F}^{\mathbf{g}}_{h_{11}}(t) &= (-\sin t \cos 2t + 2\cos t \sin 2t)x^3 = 2x^3 \sin t. \end{aligned}$$

Therefore, by Theorem 2.38 the flow on the perturbed skeleton is the same as on the skeleton. □

Lemma 4.39
Define $\mathbf{g} : \mathbb{C}^2 \to \mathbb{C}^2$ *by* $\mathbf{g}(\mathbf{z}) = (z_2^2, z_1^2)$. *The flow formula for the perturbation* $\mathbf{g}$ *on* $\mathbb{X}_{\mathbf{D}_2[\rho^2,\kappa]}$ *is*

$$\mathcal{F}^{\mathbf{g}}(t) = 2x^2(\sin t, -\sin 3t).$$

The flow formula has no zeros along either of the connections h_1 *or* h_{11}. *The flow on the perturbed skeleton is the same as on the skeleton.*

Proof. Define $\mathbf{g} : \mathbb{C}^2 \to \mathbb{C}^2$ by $\mathbf{g}(\mathbf{z}) = (z_2^2, z_1^2)$. Then

$$\begin{aligned} \mathbf{g}(\omega_{h_1}(t)) &= (\cos 2t, \sin 2t, \cos 2t, \sin 2t)x, \\ \mathbf{g}(\omega_{h_{11}}(t)) &= (\cos 2t, -\sin 2t, \cos 2t, \sin 2t)x, \end{aligned}$$

where real coordinates have been used. Therefore the flow formulas along the connections h_1 and h_{11} are:

$$\begin{aligned} \mathcal{F}^{\mathbf{g}}_{h_1}(t) &= (-2\cos 2t \sin t + 2\cos t \sin 2t)x^3 = 2x^2 \sin t, \\ \mathcal{F}^{\mathbf{g}}_{h_{11}}(t) &= (-2\sin t \cos 2t - 2\cos t \sin 2t)x^3 = -2x^3 \sin 3t. \end{aligned}$$

Therefore, by Theorem 2.38 the flow on the perturbed skeleton is the same as on the skeleton. □

Lemma 4.40
Define $\mathbf{g} : \mathbb{C}^2 \to \mathbb{C}^2$ *by* $\mathbf{g}(\mathbf{z}) = (\overline{z_1}^2, \overline{z_2}^2)$. *The flow formula for the perturbation* $\mathbf{g}$ *on* $\mathbb{X}_{\mathbf{D}_2[\rho^2,\kappa]}$ *is*

$$\mathcal{F}^{\mathbf{g}}(t) = (-2x^3 \sin t \cos 2t, -2x^3 \sin 2t \cos t).$$

The flow formula has a simple zeros at $t = \pi/4$ *and* $3\pi/4$. *The flow on the perturbed skeleton is the same as on the skeleton.*

Proof. Define $\mathbf{g} : \mathbb{C}^2 \to \mathbb{C}^2$ by $\mathbf{g}(\mathbf{z}) = (\overline{z_1}^2, \overline{z_2}^2)$. Then

$$\begin{aligned} \mathbf{g}(\omega_{h_1}(t)) &= (\cos 2t, -\sin 2t, \cos 2t, -\sin 2t)x, \\ \mathbf{g}(\omega_{h_{11}}(t)) &= (\cos 2t, -\sin 2t, \cos 2t, \sin 2t)x, \end{aligned}$$

where real coordinates have been used. Therefore the flow formulas along the connections h_1 and h_{11} are:

$$\begin{aligned} \mathcal{F}^{\mathbf{g}}_{h_1}(t) &= -2x^3 \sin t \cos 2t, \\ \mathcal{F}^{\mathbf{g}}_{h_{11}}(t) &= -2x^3 \sin 2t \cos t. \end{aligned}$$

Therefore, by Theorem 2.38 the flow on the perturbed skeleton is the same as on the skeleton. □

This completes the computation of the flow formulas for all $\mathbf{D}_2[\rho^2,\kappa]$-equivariant perturbations up to quadratic order. We have exhibited two admissible perturbations given by (u_4,u_4) and (z_1^2,z_2^2). Therefore, we can exhibit as many admissible flows as we wish by taking a combination of the admissible perturbations with any $\mathbf{D}_2[\rho^2,\kappa]$ provided the admissible perturbation dominates.

Example 4.41
Here we present two illustrative examples. The first, which can be seen as a prototype for the second, gives an example where the equilibria contained in $E_{(\mathbf{D}_2[\rho^2,\kappa],X_0)}$ are degenerate. The second example gives a heteroclinic cycle on $\mathbb{X}_{\mathbf{D}_2[\rho^2,\kappa]}$.

1. Let $\mathbf{g}:\mathbb{C}^2\to\mathbb{C}^2$ be the $\mathbf{D}_2[\rho^2,\kappa]$-equivariant map defined by

$$\begin{aligned} g_1(\mathbf{z}) &= Az_2^2+Bu_3,\\ g_2(\mathbf{z}) &= Az_1^2+Bu_3. \end{aligned} \tag{4.13}$$

The flow formulas are:

$$\begin{aligned} \mathcal{F}_{h_1}(t) &= 2x^3\sin t(A-2B\cos 2t),\\ \mathcal{F}_{h_{11}}(t) &= -2x^3(A\sin 3t+2B\sin t). \end{aligned}$$

If we choose $A=2$ and $B=1$ (or in general $A=2B$), then the flow formulas have the form illustrated in Figure 4.5. Observe that the flow along h_1 is admissible and the flow along h_{11} is degenerate at $t=\pi/2$. Interestingly the flow formula for h_1 is degenerate at $t=0$ and $t=\pi$, having saddle points. If we perturb (4.13) we do not (necessarily) get an admissible flow along h_1 (although the points $t=0$ and $t=\pi$ will still be equilibria). Instead we get (possible) additional equilibria near $t=0$ and $t=\pi$, so the heteroclinic connection is destroyed.

2. The problem with the previous example is the degenerate nature of the points $t=0$ and $t=\pi$. We now choose $A=0.3$ and $B=0.2$. In this case the flow along h_1 is admissible and the equilibria in $E_{(\mathbf{D}_2[\rho^2,\kappa],X_0)}$ are not degenerate. To find heteroclinic cycles we must find a perturbation which gives different flows along h_1 and h_{11}. At quadratic order the only suitable term is $(\overline{z_1}^2,\overline{z_2}^2)$. Thus we now have the perturbations

$$\begin{aligned} g_1(\mathbf{z}) &= Az_2^2+Bu_3+C\overline{z_1}^2,\\ g_2(\mathbf{z}) &= Az_1^2+Bu_3+C\overline{z_2}^2. \end{aligned} \tag{4.14}$$

The flow formulas are:

$$\begin{aligned} \mathcal{F}_{h_1}(t) &= 2x^3\sin t(A-(2B+C)\cos 2t),\\ \mathcal{F}_{h_{11}}(t) &= -2x^3(A\sin 3t+2B\sin t+C\sin 2t\cos t). \end{aligned}$$

If we choose (say) $A=0.3$, $B=0.2$ and $C=-0.3$ then we get the flows illustrated in Figure 4.6 and hence heteroclinic cycles between the equilibria.

4.2.5 Conclusion and Perturbed Planforms

In this section we have investigated the behaviour of the group orbit X_0 of $\mathbf{D}_4$ equilibria guaranteed to exist by Theorem 4.2.1, when symmetry breaking terms with $\mathbf{D}_4$, $\mathbf{D}_2[\rho^2,\kappa\rho]$ or $\mathbf{D}_2[\rho^2,\kappa]$ symmetry are added to a general Γ_s-equivariant map. It was shown that there always exist four equilibria on X_0. In addition, there exist (possible) heteroclinic connections between these equilibria. Indeed, it was shown that there exist open sets in the parameter space such that there are heteroclinic connections between these equilibria. The $\mathbf{D}_2[\rho^2,\kappa]$ case is different: the equilibria e_2 and e_3 are isolated and there exist only (possible) heteroclinic connection between

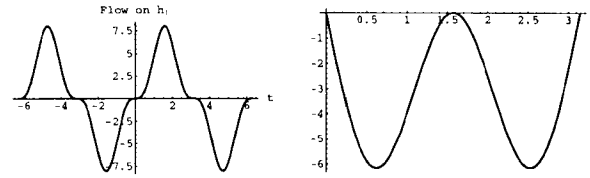

(a) Flow along h_1 (b) Flow along h_{11}

Figure 4.5: Flows along the connections h_1 and h_{11} for the perturbation (4.13).

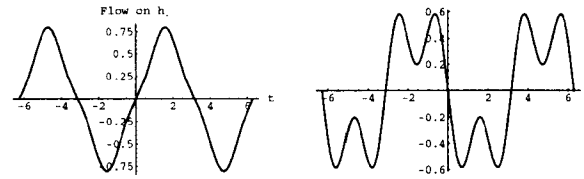

(a) Flow along h_1 (b) Flow along h_{11}

Figure 4.6: Flows along the connections h_1 and h_{11} for the perturbation (4.14).

the equilibria e_1 and e_4. It was shown (by example) that these heteroclinic connections can be arranged to form a heteroclinic cycle, but such cycles always require quadratic order terms. However, in the $\mathbf{D}_2[\rho^2, \kappa\rho]$ case there exists an open set of perturbations, which give heteroclinic cycles between the equilibria on X_0. Furthermore, these cycles can be stable.

Planforms. Here we present examples of the planforms associated with the forced symmetry breaking of the square solution. Specifically we choose perturbed lattices $\mathcal{L}^\varepsilon$ with symmetry group $\mathbf{D}_4$, $\mathbf{D}_2[\rho^2, \kappa\rho]$ or $\mathbf{D}_2[\rho^2, \kappa]$ and present a density plot of the eigenfunction $\mathbf{u}(\mathbf{x})$ for representative points on the skeleton. There are obviously a large number of different perturbed lattices that we can choose, all of which achieve the same aim. For forced symmetry breaking to the group $\mathbf{D}_4$ we define a function Ψ such that the symmetry group of $\mathcal{L}^\varepsilon = \Psi(\mathcal{L})$ is $\mathbf{D}_4$. An interesting choice is the following function: Define $\Psi((x,y)) = (\tanh(x-0.75)+1, \tanh(y-0.75)+1)$. The perturbed eigenfunction is given by

$$\mathbf{u}(\mathbf{x}) = \sum_{j=1}^{2} z_j \exp\left(\mathrm{i}\mathbf{K}_i \cdot (\Psi^{-1}(\mathbf{x}))\right).$$

Figure 4.7 (a) presents a rendering of $\mathbf{u}(\mathbf{x})$. Notice that the boundary of the domain chosen for the rendering is emulating a real boundary in experiments. The planform is greatly distorted within a finite healing zone close to the boundary, but regains its normal form further from the boundary. Ideally, we would want a function Ψ which makes the healing zone smaller (this would fit better with experimental results), but it is not easy to find such a function which can be expressed in such an elementary form. However, it is clear that such functions exist with a healing zone of any desired thickness.

To break the symmetry of the system to the group $\mathbf{D}_2[\rho^2, \kappa\rho]$ we could choose a function like that used for the $\mathbf{D}_4$ case with the slight alteration to the scaling in one of the x or y directions. Such a function would emulate the existence of different boundary conditions on different walls. We take a different approach. Define a function $\Psi(x,y) = ((1+\varepsilon)^{-1}x, (1+\varepsilon/7)^{-1}y)$, where ε is small. This transformation linearly stretches the x and y axis, but by differing amounts. The

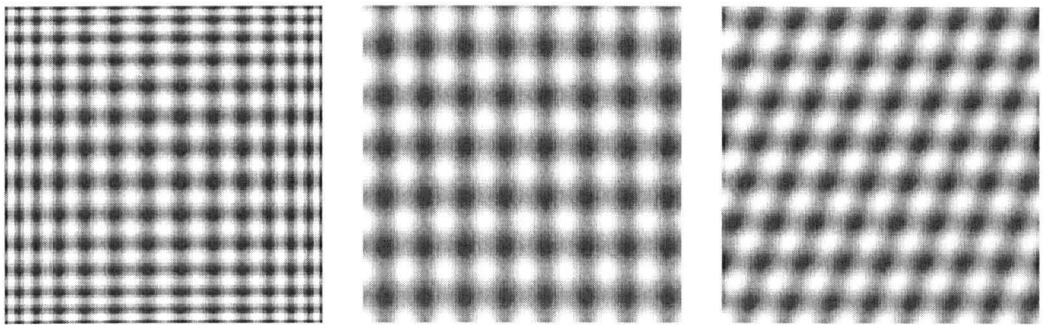

(a) (b) (c)

Figure 4.7: Perturbations of the square planform. (a) One possible effect of breaking the symmetry to $\mathbf{D}_4$. (b) Breaking the symmetry to $\mathbf{D}_2[\rho^2, \kappa\rho]$. (c) Breaking the symmetry to $\mathbf{D}_2[\rho^2, \kappa]$.

eigenfunction is given by

$$\mathbf{u}(\mathbf{x}) = \cos((1+\varepsilon)x) + \cos((1+\varepsilon/7)y).$$

Figure 4.7 (b) presents a rendering of this planform. Finally, to consider forced symmetry breaking to the group $\mathbf{D}_2[\rho^2, \kappa]$ we define a function $\Psi(x,y) = ((1+\varepsilon)^{-1}x + \varepsilon y, (1+\varepsilon)^{-1}y)$. The eigenfunction is given by

$$\mathbf{u}(\mathbf{x}) = \cos((1+\varepsilon)x + \varepsilon y) + \cos((1+\varepsilon)y).$$

Figure 4.7 (c) presents a rendering of this planform; notice that it has a rhombic structure. In all the cases above we must remember that each of these planforms in physical space can exhibit heteroclinic behaviour which will manifest itself as motion of the planform. In addition it should be noted that we have presented only examples of how to perturbed the lattice, so as to realise the appropriate forced symmetry breaking problem. There are actually infinitely many different perturbations that could be used. Finally, the points used to render the planforms are from the skeleton, not the perturbed skeleton. To give a better idea of how these planforms would appear, the equilibria on the perturbed skeleton corresponding to the equilibria on the skeleton should be used.

4.3 Eight-Dimensional Representation

In this section we consider the forced symmetry breaking of a system of differential equations posed on the square lattice, when the symmetry group Γ_s is in its eight-dimensional absolutely irreducible representation. This representation of Γ_s on $\mathbb{C}^4$ corresponds to the following action. Choose coordinates $\mathbf{z} = (z_1, z_2, z_3, z_4)$ on $\mathbb{C}^4$ and let α and β be integers that are relatively prime, not both odd and satisfy $\alpha > \beta > 0$. Then

$$\begin{aligned}
\rho(z_1,z_2,z_3,z_4) &= (\overline{z_2}, z_1, \overline{z_4}, z_3),\\
\kappa(z_1,z_2,z_3,z_4) &= (z_3, \overline{z_4}, z_1, \overline{z_2}),\\
\theta(z_1,z_2,z_3,z_4) &= (e^{\mathrm{i}(\alpha\theta_1+\beta\theta_2)}z_1, e^{\mathrm{i}(-\beta\theta_1+\alpha\theta_2)}z_2,\\
&\qquad e^{\mathrm{i}(\beta\theta_1+\alpha\theta_2)}z_3, e^{\mathrm{i}(-\alpha\theta_1+\beta\theta_2)}z_4).
\end{aligned} \tag{4.15}$$

Consider the Γ_s-equivariant system of differential equations

$$\dot{\mathbf{z}} = \mathbf{f}(\mathbf{z}, \lambda), \tag{4.16}$$

where $\mathbf{f} : \mathbb{C}^4 \times \mathbb{R} \to \mathbb{C}^4$ is Γ_s-equivariant. In this section we investigate, as we did for the four-dimensional representation, the behaviour of the group orbit of solutions to equation (4.16) under forced symmetry breaking. The main difference between the eight and four-dimensional representations is the existence of two translation free axial subgroups, $\mathbf{D}_4$ and $\widetilde{\mathbf{D}}_4[\rho, \kappa\rho(\pi/2, \pi/2)]$. This initial complication is actually no complication at all; the calculation of the skeleton, its symmetry properties, and knots, all reduce to the four-dimensional representation. Beyond this success, our results concerning this representation are not as complete as they are for the four-dimensional representation. There are two reasons for this. The first is the additional complexities introduced in the invariant theory by considering the higher dimensional representation. This means that it is very difficult to find admissible perturbations—in fact, we could not find any. The second reason, which is closely related to the first, is that the lack of admissible flows immediately implies that the connections on the skeleton have additional equilibria. If these additional equilibria arise from simple degenerate perturbations, then we know by Theorem 2.38 that the flow on the skeleton is the same as that on the perturbed skeleton. However, if the additional equilibria arise from degenerate perturbations, then we must apply Theorem 2.41 to classify the different types of behaviour that can occur on the perturbed skeleton.

4.3.1 Existence of Translation Free Axial Solutions

In this section we show that there exist two translation free axial solutions to the bifurcation problem (4.16). This section uses results from Dionne *et al.* [21] and Dionne and Golubitsky [20].

The action of the group Γ_s has six conjugacy classes of axial subgroups, of which we shall consider only the translation free axial subgroups $\mathbf{D}_4$ and $\widetilde{\mathbf{D}}_4[\rho, \kappa\rho(\pi/2, \pi/2)]$[1].

A general Γ_s-equivariant mapping is far too difficult to find, so to leading order we find that (first component only)

$$f_1(\mathbf{z}, \lambda) = z_1 p(|z_1|^2, |z_2|^2, |z_3|^2, |z_4|^2) + b_1 \overline{z_1}^{\beta-1} \overline{z_2}^{\alpha} z_3^{\alpha} z_4^{\beta} + b_2 \overline{z_1}^{\alpha-1} z_2^{\beta} z_3^{\beta} \overline{z_4}^{\alpha} + \ldots,$$

where $\ldots$ denotes higher order terms, p is a real-valued function and b_1, $b_2 \in \mathbb{R}$. The cubic truncation is

$$f_1(\mathbf{z}, \lambda) = \lambda z_1 + z_1(a_1|z_1|^2 + a_2|z_2|^2 + a_3|z_3|^2 + a_4|z_4|^2) + \ldots$$

where $\ldots$ denotes higher order terms. The signs of the eigenvalues for the solutions $\mathbf{D}_4[\rho, \kappa]$ and $\widetilde{\mathbf{D}}_4[\rho, \kappa(\pi/2, \pi/2)\rho]$ are given in Table 4.8. From these eigenvalues it is easy to see that only one of these solutions can be stable at bifurcation.

Theorem 4.42
Let $\mathbf{f} : \mathbb{C}^4 \times \mathbb{R} \to \mathbb{C}^4$ be a Γ_s-equivariant bifurcation problem. Then, generically, there exist two branches of steady-state solutions bifurcating from the origin with $\mathbf{D}_4$ and $\widetilde{\mathbf{D}}_4[\rho, \kappa\rho(\pi/2, \pi/2)]$-symmetry. Furthermore, these branches can be stable, but if one branch is stable then the other is not.

Proof. The existence of these branches follows from Dionne and Golubitsky [20]. The stability follows from the above discussion of the eigenvalues. □

We shall refer to the solution with $\mathbf{D}_4$ isotropy as the *super square* solution and the solution with $\widetilde{\mathbf{D}}_4[\rho, \kappa\rho(\pi/2, \pi/2)]$ isotropy as the *anti-square* solution.

[1]The element that we denote by $\kappa\rho$ corresponds to the element τ in Dionne *et al.* [21].

Table 4.8: Eigenvalues of the two translation free axial solutions.

Translation Free Axial Solution	Eigenvalues
$\mathbf{D}_4$	$\mathrm{sgn}(a_1+a_2+a_3+a_4)$, $\mathrm{sgn}(a_1+a_2-a_3-a_4)$, $\mathrm{sgn}(a_1-a_2+a_3-a_4)$, $\mathrm{sgn}(a_1-a_2-a_3+a_4)$, $\mathrm{sgn}(-b_1\beta-b_2\alpha)$,
$\widetilde{\mathbf{D}}_4[\rho,\kappa\rho(\pi/2,\pi/2)]$	$\mathrm{sgn}(a_1+a_2+a_3+a_4)$, $\mathrm{sgn}(a_1+a_2-a_3-a_4)$, $\mathrm{sgn}(a_1-a_2+a_3-a_4)$, $\mathrm{sgn}(a_1-a_2-a_3+a_4)$, $\mathrm{sgn}(b_1\beta+b_2\alpha)$,

4.3.2 Forced Symmetry Breaking of Square and Anti-Square Solutions

In this subsection we discuss the behaviour of the group orbit of bifurcating solutions given by Theorem 4.42, when symmetry breaking terms are added to the equation (4.16). We shall show that the skeleton is unchanged from the four-dimensional case, and in this sense some of the results from the four-dimensional case carry over to the eight-dimensional representation.

The group orbits of solutions with $\mathbf{D}_4$ and $\widetilde{\mathbf{D}}_4$ isotropy are 2-tori, which we denote by X_0. These 2-tori are normally hyperbolic. It is trivial to see that the induced action of $\mathbf{D}_4$ on X_0 is identical to the four-dimensional action. However, it is not so obvious that the action of $\widetilde{\mathbf{D}}_4$ on X_0 is isomorphic to $\mathbf{D}_4$ on X_0. To show this we use the following lemma:

Lemma 4.43
Let Γ be a group acting on a set X. Let Σ and Σ' be isotropy subgroups. Let Δ and Δ' be subgroups of Σ and Σ', respectively. Suppose there exist an isomorphism $f:\Sigma\to\Sigma'$. Suppose there exist an isomorphism $g:\Gamma/\Sigma\to\Gamma/\Sigma'$. Then the action of Δ on Γ/Σ' is isomorphic to the action of Δ' on Γ/Σ.

Proof. Let f be the isomorphism between Σ and Σ'. Let g be the isomorphism between Γ/Σ and Γ/Σ'. Since $\Delta\subseteq\Sigma$ and $\Delta'\subseteq\Sigma'$, the isomorphism f induces an action of Δ' on Γ/Σ in a natural way. Indeed, for $\delta'\in\Delta'$ with $f(\delta)=\delta'$ for some $\delta\in\Delta$ and $\widetilde{\gamma}\in\Gamma/\Sigma$

$$\delta'\widetilde{\gamma}=f^{-1}(\delta')\widetilde{\gamma}=\delta\widetilde{\gamma}.$$

Moreover, the action of Δ' on Γ/Σ is isomorphic (via the isomorphism f) to the action of Δ on Γ/Σ. Similarly, there is an induced action of Δ on Γ/Σ'. This again is isomorphic to the action of Δ' on Γ/Σ'.

The isomorphism g, by reasoning identical to that above, induces an isomorphism between the action of Δ on Γ/Σ and Δ on Γ/Σ'. Moreover, there is also an induced isomorphism between the action of Δ' on Γ/Σ and Δ' on Γ/Σ'.

Combining all the above isomorphisms together gives the following commutative diagram

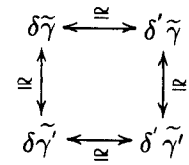

where $\delta \in \Delta$, $\delta' \in \Delta'$, $\tilde{\gamma} \in \Gamma/\Sigma$ and $\tilde{\gamma'} \in \Gamma/\Sigma'$. Therefore, the action of Δ on Γ/Σ is isomorphic to the action of Δ' on Γ/Σ'. □

This lemma shows the skeleton, pointwise and setwise isotropy subgroups and the knots are identical for forced symmetry breaking to $\mathbf{D}_4$ and $\widetilde{\mathbf{D}}_4$. We are now in a position to give our first existence result.

Theorem 4.44
Let $\Gamma = \mathbf{D}_4 \dot{+} \mathbf{T}^2$, $\Sigma = \mathbf{D}_4$ and $\Delta = \mathbf{D}_4$, $\mathbf{D}_2[\rho^2, \kappa\rho]$ or $\mathbf{D}_2[\rho^2, \kappa]$. Let Γ act on $\mathbb{C}^4$ with the action given in (4.15). Let $\mathbf{f} \in \vec{\mathcal{E}}_\Gamma$ be a Γ-equivariant bifurcation problem. Let $\mathbf{g} \in \vec{\mathcal{E}}_\Delta$ be Δ-equivariant and satisfy $\mathbf{g}(\mathbf{0}) = \mathbf{0}$. Let $\mathbf{F}(\mathbf{z}, \lambda, \varepsilon) = \mathbf{f}(\mathbf{z}, \lambda) + \varepsilon\mathbf{g}(\mathbf{z})$. Then there exists a steady-state solution to $\mathbf{f}(\mathbf{z}, \lambda) = 0$ bifurcating from $(\mathbf{0}, 0)$ with Σ-isotropy. Let $X_0 \cong \mathbf{T}^2$ be the group orbit of steady states. Then for sufficiently small ε, X_0 persists to give a new $\mathbf{F}$-invariant manifold X_ε which is Δ-equivariantly diffeomorphic to X_0. Moreover, there exists $g \in \vec{\mathcal{E}}_\Delta$ such that the elements in $E_{(\Delta, X_0)}$ are equilibria for the new flow and those of $H_{(\Delta, X_0)}$ are heteroclinic connections between equilibria.

Remark 4.45
By Lemma 4.43, the same theorem holds when $\Sigma = \widetilde{\mathbf{D}}_4$ and $\Delta = \widetilde{\mathbf{D}}_4$, $\widetilde{\mathbf{D}}_2[\rho^2, \kappa\rho]$ or $\widetilde{\mathbf{D}}_2[\rho^2, \kappa]$.

There is an important distinction between forced symmetry breaking in the four-dimensional and eight-dimensional representations. In the eight-dimensional case, the same point on X_0 can correspond to different points in $\mathbb{C}^4$, depending on α and β. More precisely, suppose that α is odd (and so by definition β is even), then the point $e_2 = (\pi, 0)$ on the skeleton corresponds to the point $(-x, x, x, -x) \in \mathbb{C}^4$ and the point $e_3 = (0, \pi)$ corresponds to the point $(x, -x, -x, x) \in \mathbb{C}^4$. Now suppose that α is even (and so β is odd) then e_2 corresponds to $(x, -x, -x, x)$ and e_3 to the point $(-x, x, x, -x)$. For this reason we must be cautious when interpreting our results.

Example Flow Formula for $\mathbf{D}_4$

We compute the flow formulas along the connections $h \in H_{(X_0, \mathbf{D}_4)}$ for an example $\mathbf{D}_4$-equivariant perturbation of the form $\mathbf{g}(\mathbf{z}) = u\mathbf{e}_1$, where u is the primary $\mathbf{D}_4$-invariant $z_2\overline{z_3} + z_1 z_4 + z_3\overline{z_2} + \overline{z_1 z_4}$ and $e_1 = (1, 1, 1, 1)$ is a constant equivariant. Although these perturbations obviously do not represent the breadth of general $\mathbf{D}_4$-equivariants, the behaviour that is exhibited is an illustration of how the dynamics of the four and eight-dimensional theory for $\mathbf{D}_4$ symmetry breaking differ.

Our initial task is to parametrise the connections h_1, h_3 and $h_9 \in H_{(X_0, \mathbf{D}_4)}$; these connections are the orbit representatives of the connections. Define ω_{h_1}, ω_{h_3} and $\omega_{h_9} : [0, \pi] \to X_0$ by

$$\begin{aligned}
\omega_{h_1}(t) &= (e^{\mathrm{i}(\alpha+\beta)t}, e^{\mathrm{i}(\alpha-\beta)t}, e^{\mathrm{i}(\alpha+\beta)t}, e^{\mathrm{i}(\beta-\alpha)t})x, \\
\omega_{h_3}(t) &= (e^{\mathrm{i}\alpha t}, e^{-\mathrm{i}\beta t}, e^{\mathrm{i}\beta t}, e^{-\mathrm{i}\alpha t})x, \\
\omega_{h_9}(t) &= (-e^{\mathrm{i}\beta t}, e^{-\mathrm{i}\alpha t}, e^{\mathrm{i}\alpha t}, -e^{-\mathrm{i}\beta t})x, \text{ when } \alpha \text{ is even and} \\
\omega_{h_9}(t) &= (e^{\mathrm{i}\beta t}, -e^{-\mathrm{i}\alpha t}, -e^{\mathrm{i}\alpha t}, e^{-\mathrm{i}\beta t})x, \text{ when } \alpha \text{ is odd.}
\end{aligned}$$

Each of these parametrisations respects the change in equilibria e_2 and e_3 when α changes from odd to even. Using these parametrisations, we construct the tangent vectors $\mathcal{T}_{h_j}(t)$ to each function ω_{h_j}. For simplicity we employ a real coordinate system; this choice makes the

calculation of the flow formula more straightforward.

$$\begin{aligned}
\mathcal{T}_{h_1}(t) &= (-(\alpha+\beta)\sin(\alpha+\beta)t, (\alpha+\beta)\cos(\alpha+\beta)t, -(\alpha-\beta)\sin(\alpha-\beta)t,\\
&\quad (\alpha-\beta)\cos(\alpha-\beta)t, -(\alpha+\beta)\sin(\alpha+\beta)t, (\alpha+\beta)\cos(\alpha+\beta)t,\\
&\quad -(\alpha-\beta)\sin(\alpha-\beta)t, -(\alpha-\beta)\cos(\alpha-\beta)t)x,\\
\mathcal{T}_{h_3}(t) &= (-\alpha\sin\alpha t, \alpha\cos\alpha t, -\beta\sin\beta t, -\beta\cos\beta t, -\beta\sin\beta t, \beta\cos\beta t, -\alpha\sin\alpha t,\\
&\quad -\alpha\cos\alpha t)x,\\
\mathcal{T}_{h_9}(t) &= (-\beta\sin\beta t, \beta\cos\beta t, \alpha\sin\alpha t, -\alpha\cos\alpha t, \alpha\sin\alpha t, -\alpha\cos\alpha t,\\
&\quad -\beta\sin\beta t, \beta\cos\beta t)x, \text{ when } \alpha \text{ is odd and}\\
\mathcal{T}_{h_9}(t) &= (\beta\sin\beta t, -\beta\cos\beta t, -\alpha\sin\alpha t, \alpha\cos\alpha t, -\alpha\sin\alpha t, \alpha\cos\alpha t, \beta\sin\beta t,\\
&\quad -\beta\cos\beta t)x, \text{ when } \alpha \text{ is even.}
\end{aligned}$$

Proposition 4.46
The flow direction on the skeleton $\mathbb{X}_{\mathbf{D}_4}$ for the perturbation $\mathbf{g}(\mathbf{z}) = u\mathbf{e}_1$ is

$$\begin{aligned}
\mathcal{F}^{u\mathbf{e}_1}(t) &= -4x^2(4(\cos 2\alpha t + \cos 2\beta t)(\alpha\cos\beta t\sin\alpha t + \beta\cos\alpha t\sin\beta t),\\
&\quad (\cos 2\beta t + 1)(\alpha\sin\alpha t + \beta\sin\beta t),\\
&\quad (\cos 2\alpha t + 1)(\pm\alpha\sin\alpha t \mp \beta\sin\beta t),
\end{aligned}$$

where the top sign holds when α is even and the bottom when α is odd. The function $\mathcal{F}^{\mathbf{g}}_{h_1}(t)$ has a simple zero at $t = \pi/(2(\alpha+\beta))$, $\mathcal{F}^{\mathbf{g}}_{h_3}(t)$ has a degenerate zero at $t = \pi/(2\beta)$ and $\mathcal{F}^{\mathbf{g}}_{h_9}(t)$ has a zero at $t = \pi/(2\alpha)$.

Proof. Define $\mathbf{g} : \mathbb{C}^4 \to \mathbb{C}^4$ by $\mathbf{g}(\mathbf{z}) = (u, u, u, u)$, where $u = z_2\overline{z_3} + z_1 z_4 + z_3\overline{z_2} + \overline{z_1 z_4}$. Then evaluating $\mathbf{g}$ along the connections h_1, h_3 and h_9 gives

$$\begin{aligned}
\mathbf{g}(\omega_{h_1}(t)) &= 2x^2(\cos 2\alpha t + \cos 2\beta t),\\
\mathbf{g}(\omega_{h_3}(t)) &= 2x^2(\cos 2\beta t + 1),\\
\mathbf{g}(\omega_{h_9}(t)) &= 2x^2(\cos 2\alpha t + 1).
\end{aligned}$$

Therefore, the flow formulas along the connections h_1, h_3 and h_9 are

$$\begin{aligned}
\mathcal{F}^{u\mathbf{e}_1}_{h_1}(t) &= -16x^3(\cos 2\alpha t + \cos 2\beta t)(\alpha\cos\beta t\sin\alpha t + \beta\cos\alpha t\sin\beta t),\\
\mathcal{F}^{u\mathbf{e}_1}_{h_3}(t) &= -4x^3(\cos 2\beta t + 1)(\alpha\sin\alpha t + \beta\sin\beta t),\\
\mathcal{F}^{u\mathbf{e}_1}_{h_9}(t) &= -4x^3(\cos 2\alpha t + 1)(\pm\alpha\sin\alpha t \mp \beta\sin\beta t).
\end{aligned}$$

From these flow formulas we see that $t = \pi/(2(\alpha+\beta))$ is a zero of $\mathcal{F}^{u\mathbf{e}_1}_{h_1}(t)$, $t = \pi/(2\beta)$ is a zero of $\mathcal{F}^{u\mathbf{e}_1}_{h_3}(t)$, and $\mathcal{F}^{u\mathbf{e}_1}_{h_9}(t)$ has a zero at $t = \pi/(2\alpha)$. The nature of these zeros follows by differentiation. □

When $\alpha = 2$ and $\beta = 1$ we show in Figure 4.8 the flow formulas $\mathcal{F}^{u\mathbf{e}_1}_{h_3}(t)$ and $\mathcal{F}^{u\mathbf{e}_1}_{h_9}(t)$. This is an interesting example since we know that the unfolding of the degenerate zeros of $\mathcal{F}^{u\mathbf{e}_1}_{h_3}(t)$ and $\mathcal{F}^{u\mathbf{e}_1}_{h_9}(t)$ can produce admissible perturbations. However, we cannot produce heteroclinic cycles since the flow along h_1 has simple zeros, which persist under small perturbations. But even so we have exhibited an "almost" admissible perturbation.

This example completes our study of the eight-dimensional representation.

4.3.3 Conclusion

We have shown that the study of forced symmetry breaking for the squares and anti-squares solutions follows easily from the results for the four-dimensional problem. That is the skeleton, knots and symmetry properties are "identical", although the interpretation of the points on X_0

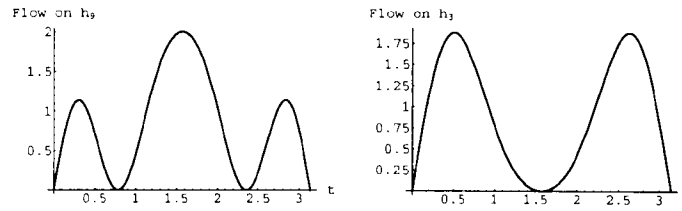

(a) $\mathcal{F}_{h_3}^{\mathbf{ue}_1}(t)$ (b) $\mathcal{F}_{h_9}^{\mathbf{ue}_1}(t)$

Figure 4.8: Flow formulas $\mathcal{F}_{h_9}^{\mathbf{ue}_1}(t)$ and $\mathcal{F}_{h_3}^{\mathbf{ue}_1}(t)$.

is different, with the same point on X_0 representing a different point in $\mathbb{C}^4$ depending on α and β. This illustrates the power of the techniques involved, for all the symmetry properties of the skeleton are not dependent on the form of the perturbation term $\mathbf{g}$, just its symmetry. At this point the similarities between the four and eight-dimensional case vanish. The structure of the rings of invariants and modules of equivariants make a determination of a general flow formulas (even at quadratic order) too computationally intense to perform. Thus we have contented ourselves with an example. In particular we show the existence of an "almost" admissible flow. That is a perturbation $\mathbf{g}$ where a suitable unfolding gives an admissible flow. However, we could not find any examples of admissible perturbations. These difficulties should not be taken too critically for they reflect what in some sense we would naturally expect—the eight-dimensional case should be more complex than the four-dimensional case.

4.4 Review

In this chapter we have investigated the forced symmetry breaking of group orbits of square planforms which arise from steady-state symmetry-breaking bifurcations of $\mathbf{E}(2)$-equivariant PDEs. We consider separately the four and eight-dimensional representations of the group $\Gamma_s = \mathbf{D}_4 \dot{+} \mathbf{T}^2$. For each representation we consider the behaviour of the group orbit of translation free axial solutions guaranteed to exist by the equivariant branching lemma, and (partially) classify their behaviour when terms with symmetry (isomorphic) to $\mathbf{D}_4$, $\mathbf{D}_2[\rho^2, \kappa]$ or $\mathbf{D}_2[\rho^2, \kappa]$ are added to the underlying ODEs.

The previous study in this area performed by Hou and Golubitsky [50] considered only the four-dimensional $\mathbf{D}_2[\rho^2, \kappa\rho]$ problem. In this chapter we have generalised this result to all translation free irreducible representations of Γ_s and also to the groups $\mathbf{D}_4$ and $\mathbf{D}_2[\rho^2, \kappa]$. The eight-dimensional problem gives a classification for a countable set of planforms. In the four-dimensional case it is shown that the $\mathbf{D}_4$ and $\mathbf{D}_2[\rho^2, \kappa]$ are considerably more complex than the $\mathbf{D}_2[\rho^2, \kappa\rho]$ case—requiring quadratic terms in the perturbation for admissible flows. We now review the main results of the chapter.

$\mathbf{D}_4$ For forced symmetry breaking to $\mathbf{D}_4$ it is possible to exhibit admissible perturbations at quadratic order; indeed the term (z_1^2, z_2^2) is admissible. So there exists an open set of perturbations which give admissible perturbations; all that is required is that the term (z_1^2, z_2^2) dominates the perturbation.

$\mathbf{D}_2[\rho^2, \kappa\rho]$ This case was studied by Hou and Golubitsky [50] and is shown to exhibit stable heteroclinic cycles for an open set of perturbations.

$\mathbf{D}_2[\rho^2, \kappa]$ This case yields behaviour not seen before: the skeleton contains isolated equilibria. We provide two examples, the first shows that the equilibria contained in $E_{(\mathbf{D}_2[\rho^2,\kappa],X_0)}$ can be degenerate, the second gives a perturbation of this example which produces heteroclinic cycles. This heteroclinic cycle is produced using quadratic terms in the perturbation.

The eight-dimensional representation is naturally more complex than for the four-dimensional one and general results are difficult to achieve. In each case the behaviour of the skeleton is the same as in the four-dimensional case.

Chapter 5

Forced Symmetry Breaking on the Hexagonal Lattice

5.1 Introduction

In contrast to the square lattice, steady-state symmetry-breaking problems on the hexagonal lattice have been the subject of many studies, see for example Bosch Vivancos *et al.* [3], Buzano and Golubitsky [6], Dionne *et al.* [21], Dionne and Golubitsky [20], Golubitsky *et al.* [36], Golubitsky and Stewart [32] and the references contain therein. The reason for the enormous amount of literature on this problem is easy to trace: we see hexagonal patterns more often than we see square patterns. The observed preference for hexagonal structures can be explained (intuitively) by reasoning that a hexagonal pattern represents a minimal energy and maximal packing solution to the problem. We must stress that this *ad hoc* reasoning does in no way offer a concrete solution. Of all the studies performed on the hexagonal lattice we focus on work of Dionne and Golubitsky [20], where a group theoretic classification of the translation free axial planforms expected on the hexagonal lattice was performed. The authors prove that there exist two translation free axial solutions, both with $\mathbf{D}_6$ symmetry. Following this work Dionne *et al.* [21] performed a stability analysis for the axial solutions in the twelve-dimensional bifurcation problem. Previous to this work, Buzano and Golubitsky [6] considered the six-dimensional problem. In this chapter we analyse the forced symmetry breaking behaviour that may be expected from these solutions.

Let us recall the methods of Section 1.6 applied to the hexagonal lattice. Define two linearly independent vectors $\boldsymbol{\ell}_1 = (\frac{2}{\sqrt{3}}, 0)$ and $\boldsymbol{\ell}_2 = (\frac{1}{\sqrt{3}}, 1)$. The hexagonal lattice is defined by

$$\mathcal{L}_h = \{n_1\boldsymbol{\ell}_1 + n_2\boldsymbol{\ell}_2 | n_1,\ n_2 \in \mathbb{Z}\},$$

with symmetry group $\Gamma_h = \mathbf{D}_6 \dot{+} \mathbf{T}^2$. Here $\mathbf{D}_6$ is the dihedral group of order twelve generated by a rotation ρ by $\pi/3$ anticlockwise and a reflection κ in the line $x = 0$. We seek functions $\mathbf{u} \in \mathcal{X}$ which are doubly periodic with respect to the hexagonal lattice $\mathcal{L}_h$, and so are members of $\mathcal{X}_{\mathcal{L}_h}$. Define $\mathbf{k}_1 = (1, 0)$ and $\mathbf{k}_2 = (\frac{1}{2}\sqrt{3}, -\frac{1}{2})$. Then the dual lattice to $\mathcal{L}_h$ is defined by

$$\mathcal{L}_h^* = \{n_1\mathbf{k}_1 + n_2\mathbf{k}_2 | n_1,\ n_2 \in \mathbb{Z}\}.$$

Now we may write a function $\mathbf{u} \in \mathcal{X}_{\mathcal{L}_h}$ in the form

$$\mathbf{u}(\mathbf{x}, t) = \sum_{j=1}^{s} z_j e^{2\pi i \mathbf{K}_j \cdot \mathbf{x}} \mathbf{u}_j + c.c., \tag{5.1}$$

where $z_j \in \mathbb{C}$ and $k_c = |\mathbf{K}_j| = \sqrt{\alpha^2 + \beta^2 - \alpha\beta}$ for integers α and β. Dionne and Golubitsky [20] show that $s = 3$ or 6. The case $s = 3$ occurs, for example, when $k_c = 1$, and $(\alpha, \beta) = (1, 0)$, and

$s = 6$ when $k_c = \sqrt{7}$ and $(\alpha, \beta) = (3, 2)$. The bifurcation problem may then be identified with $\mathbb{C}^s$. The representation of Γ_h on $\mathbb{C}^s$ is determined by its action on the complex amplitudes z_j in (5.1). All representations are translation free. Our problem is now in the standard form; we consider the system of ODEs

$$\dot{\mathbf{z}} = \mathbf{f}(\mathbf{z}, \lambda), \tag{5.2}$$

where $\mathbf{f} : \mathbb{C}^s \times \mathbb{R} \to \mathbb{C}^s$ is Γ_h-equivariant. With this set-up in place we know by Dionne and Golubitsky [20] that there exist two translation free axial solutions, one in the six-dimensional representation ($s = 3$) and one in the twelve-dimensional representation ($s = 6$). The group orbit of each of these solutions is diffeomorphic to the 2-torus, denoted by X_0. We study the behaviour of X_0 when symmetry breaking terms with symmetry $\mathbf{D}_6$, $\mathbf{D}_3[\rho^2, \kappa\rho]$, $\mathbf{D}_3[\rho^2, \kappa]$, $\mathbf{D}_2[\rho^3, \kappa]$, $\mathbf{D}_2[\rho^3, \kappa\rho]$ or $\mathbf{D}_2[\rho^3, \kappa\rho^2]$ are added to equation (5.2). Since X_0 is (generically) normally hyperbolic the methods of Chapter 2 become available to us. In particular for each problem under consideration we seek admissible perturbations and examine the possible existence of heteroclinic cycles and networks.

We now review the contents of the chapter and its organisation. In Section 5.2 we study the six-dimensional representation of the group Γ_h acting on $\mathbb{C}^3$. In this case there exists a translation free axial solution with $\mathbf{D}_6$ isotropy. Within Subsection 5.2.2 we examine the behaviour of the group orbit X_0 under forced symmetry breaking to the subgroup $\mathbf{D}_6$. Our analysis follows the lines of Chapter 2: we construct the skeleton and study its symmetry properties. In the process we answer a question posed by Lauterbach *et al.* [62]. These symmetry properties allow us to construct the projected skeleton and thus classify the number of "different" admissible flows on the skeleton. Following this, we perform the same operations for the groups $\mathbf{D}_3[\rho^2, \kappa\rho]$, $\mathbf{D}_3[\rho^2, \kappa]$, $\mathbf{D}_2[\rho^3, \kappa]$, $\mathbf{D}_2[\rho^3, \kappa\rho]$ and $\mathbf{D}_2[\rho^3, \kappa\rho^2]$. In particular, we exhibit heteroclinic cycles for the group $\mathbf{D}_3[\rho^2, \kappa\rho]$. We conclude with an example planform. In Section 5.3 we generalise our presentation to the twelve-dimensional representation. As was the case for the square lattice, many of the results can be deduced from the six-dimensional representation. We conclude with some sample planforms. Finally, in Section 5.4, we review our results.

5.2 Six-Dimensional Representation

In this section we consider the six-dimensional representation of the group Γ_h. This representation occurs when the wavelength of the instabilities coincides with the periodicity of the functions in $\mathcal{X}_{\mathcal{L}_h}$. The representation of Γ_h on $\mathbb{C}^3$ corresponds to the following action. Choose coordinates $\mathbf{z} = (z_1, z_2, z_3)$ on $\mathbb{C}^3$. Then the action of Γ_h is generated by

$$\begin{aligned} \rho(z_1, z_2, z_3) &= (\overline{z_2}, \overline{z_3}, \overline{z_1}), \\ \kappa(z_1, z_2, z_3) &= (z_1, z_3, z_2), \\ \theta(z_1, z_2, z_3) &= (e^{\mathrm{i}\theta_1} z_1, e^{\mathrm{i}\theta_2} z_2, e^{-\mathrm{i}(\theta_1+\theta_2)} z_3), \end{aligned} \tag{5.3}$$

where $(\theta_1, \theta_2) \in \mathbf{T}^2$. Consider the Γ_h-equivariant system of differential equations

$$\dot{\mathbf{z}} = \mathbf{f}(\mathbf{z}, \lambda), \tag{5.4}$$

where $\mathbf{f} : \mathbb{C}^3 \times \mathbb{R} \to \mathbb{C}^3$ is Γ_h-equivariant. We investigate the behaviour of the group orbit of solutions to (5.4) under forced symmetry breaking to the subgroups $\mathbf{D}_6$, $\mathbf{D}_3[\rho^2, \kappa]$, $\mathbf{D}_3[\rho^2, \kappa\rho]$, $\mathbf{D}_2[\rho^3, \kappa]$, $\mathbf{D}_2[\rho^2, \kappa\rho]$ and $\mathbf{D}_2[\rho^2, \kappa\rho^2]$ of Γ_h. In particular we are interested in the existence of equilibria and heteroclinic connections on X_0.

This section is organised as follows. We begin in Subsection 5.2.1 by summarising some existence results for bifurcating solutions. Then in Subsection 5.2.2 we consider forced symmetry breaking to the subgroup $\mathbf{D}_6$; this subsection is the backbone of the section, and all further results depend on it. The derivations of the results contained in this subsection are performed in the usual manner: the skeleton is computed, its symmetry properties analysed and the projected skeleton discussed. Using the results of Subsection 5.2.2 we proceed in Subsections 5.2.3

to 5.2.7 to study the behaviour of the hexagonal solution under forced symmetry breaking to the subgroups $\mathbf{D}_3[\rho^2, \kappa]$, $\mathbf{D}_3[\rho^2, \kappa\rho]$, $\mathbf{D}_2[\rho^3, \kappa]$, $\mathbf{D}_2[\rho^2, \kappa\rho]$ and $\mathbf{D}_2[\rho^2, \kappa\rho^2]$.

5.2.1 Existence of Translation Free Axial Solution

Here we summarise the important results we require for our future work. The results presented here have appeared in many different works, by several authors (see the references in the introduction to this chapter). It is important to realise those bifurcation problems on the hexagonal lattice have been studied in two different ways. Firstly, a general Γ_h-equivariant bifurcation problem possess a quadratic equivariant, which implies that all bifurcating solutions are unstable. Hence a singularity theory approach (specifically normal forms and universal unfoldings) must be undertaken, see Buzano and Golubitsky [6]. The second approach is computationally more straightforward, we consider a $\Gamma_h \oplus \mathbf{Z}_2$-equivariant bifurcation problem. The additional $\mathbf{Z}_2$ symmetry implies that the bifurcation problem contains only odd terms, see Golubitsky *et al.* [36]. We shall consider only the pure Γ_h problem. The action of Γ_h on $\mathbb{C}^3$ has eight conjugacy classes of isotropy subgroups, see Buzano and Golubitsky [6]. Of these subgroups the only translation free axial subgroup is $\Sigma = \mathbf{D}_6$ and we shall focus exclusively on this group. A general Γ_h-equivariant mapping has the form (first component only)

$$f_1(\mathbf{z}, \lambda) = z_1 \left(p_1 + p_2 u_1 + p_3 u_1^2\right) + \overline{z_2 z_3} \left(q_1 + u_1 q_2 + u_1^2 q_3\right), \tag{5.5}$$

where the p_i's and q_i's are functions of λ and of the invariants

$$\begin{aligned} \sigma_1 &= u_1 + u_2 + u_3, \\ \sigma_2 &= u_1 u_2 + u_2 u_3 + u_3 u_1, \\ \sigma_3 &= u_1 u_2 u_3, \\ q &= z_1 z_2 z_3 + \overline{z_1 z_2 z_3}, \end{aligned}$$

where $u_j = z_j \overline{z_j}$. The equations for f_2 and f_3 are given by equivariance. Then we have the following:

Theorem 5.1
Let $\mathbf{f} : \mathbb{C}^3 \times \mathbb{R} \to \mathbb{C}^3$ be a Γ_h-equivariant bifurcation problem. Then, generically, there exists a branch of steady-state solutions bifurcating from the origin with Σ-isotropy.

Proof. See Buzano and Golubitsky [6] or Dionne and Golubitsky [20]. □

Buzano and Golubitsky [6] show that an unfolding of the quadratic degeneracy can yield stable solutions. The solution given by Theorem 5.1 are referred to in the literature as hexagons, we shall adopt the same convention.

5.2.2 Forced Symmetry Breaking to $\mathbf{D}_6$

In this subsection we study forced symmetry breaking of the hexagonal solution which generically exists for a general Γ_h-equivariant bifurcation problem. The methods which we employ are now familiar and standard. The group orbit of hexagon solutions to (5.5) is a 2-torus, which as always we denote by X_0. The manifold X_0 is normally hyperbolic and so is amenable to the results of Chapter 2. The precise formulation of our problem is as follows. Let $\mathbf{g} : \mathbb{C}^3 \to \mathbb{C}^3$ be a $\mathbf{D}_6$-equivariant mapping which satisfies $\mathbf{g}(\mathbf{z}) = \mathbf{0}$. Let ε be real and small. Consider the $\mathbf{D}_6$-equivariant perturbation of (5.5), $\mathbf{F} : \mathbb{C}^3 \times \mathbb{R}^2 \to \mathbb{C}^3$ defined by

$$\mathbf{F}(\mathbf{z}, \lambda, \varepsilon) = \mathbf{f}(\mathbf{z}, \lambda) + \varepsilon \mathbf{g}(\mathbf{z}).$$

Since X_0 is normally hyperbolic, by the Equivariant Persistence Theorem, there exists an $\mathbf{F}$ and a $\mathbf{D}_6$-invariant manifold X_ε which is $\mathbf{D}_6$-equivariantly diffeomorphic to X_0. We shall study

the $\mathbf{D}_6$ action on X_0, which via the diffeomorphism allows us to study X_ε. We begin with the action of $\mathbf{D}_6$ on $\mathbb{C}^3$; this action is given by the restriction of the Γ_h action on $\mathbb{C}^3$. More precisely, we have:

$$\begin{array}{llllll} \rho\mathbf{z} & = & (\overline{z_2},\overline{z_3},\overline{z_1}), & \rho^2\mathbf{z} & = & (z_3,z_1,z_2), \\ \rho^3\mathbf{z} & = & (\overline{z_1},\overline{z_2},\overline{z_3}), & \rho^4\mathbf{z} & = & (z_2,z_3,z_1), \\ \rho^5\mathbf{z} & = & (\overline{z_3},\overline{z_1},\overline{z_2}), & \kappa\mathbf{z} & = & (z_1,z_3,z_2), \\ \kappa\rho\mathbf{z} & = & (\overline{z_2},\overline{z_1},\overline{z_3}), & \kappa\rho^2\mathbf{z} & = & (z_3,z_2,z_1), \\ \kappa\rho^3\mathbf{z} & = & (\overline{z_1},\overline{z_3},\overline{z_2}), & \kappa\rho^4\mathbf{z} & = & (z_2,z_1,z_3), \\ \kappa\rho^5\mathbf{z} & = & (\overline{z_3},\overline{z_2},\overline{z_1}) & & & . \end{array} \tag{5.6}$$

This action induces a natural action of $\mathbf{D}_6$ on $X_0 \cong \Gamma_h/\Sigma$.

Calculation of the Skeleton

Using the action (5.6) of $\mathbf{D}_6$ on $\mathbb{C}^3$ we compute the skeleton of X_0. The skeleton is our critical tool in understanding the behaviour of $\mathbf{D}_6$-equivariant vector field on X_0 in a sensible and manageable way. Firstly we require knowledge of the subgroups of $\mathbf{D}_6$.

Lemma 5.2
There are sixteen closed subgroups of $\mathbf{D}_6$. *These groups are:*

$$\begin{array}{llll} \mathbf{D}_6, & \mathbf{Z}_6[\rho], & \mathbf{D}_3[\rho^2,\kappa], & \mathbf{D}_3[\rho^2,\kappa\rho], \\ \mathbf{D}_2[\rho^3,\kappa], & \mathbf{D}_2[\rho^3,\kappa\rho], & \mathbf{D}_2[\rho^3,\kappa\rho^2], & \mathbf{Z}_3[\rho^2], \\ \mathbf{Z}_2[\rho^3], & \mathbf{Z}_2[\kappa], & \mathbf{Z}_2[\kappa\rho], & \mathbf{Z}_2[\kappa\rho^2], \\ \mathbf{Z}_2[\kappa\rho^3], & \mathbf{Z}_2[\kappa\rho^4], & \mathbf{Z}_2[\kappa\rho^5], & \end{array}$$

and the trivial subgroup.

Proof. See Armstrong [1]. □

We make the following definitions that prevent some rather tedious and cumbersome repetition later. It should be noted that we are still using the notation from Definition 4.3 explaining the numbering used below.

Definition 5.3
Define the following subsets of X_0:

$$\begin{array}{ll} e_5 = \{(2\pi/3, 2\pi/3)\}, & e_6 = \{(4\pi/3, 4\pi/3)\}, \\ c_7 = \{(2\theta, -\theta) \big| \theta \in [0, 2\pi)\}, & c_8 = \{(-\theta, 2\theta) \big| \theta \in [0, 2\pi)\}. \end{array}$$

The next step is the calculation of the set $\mathscr{C}_{\mathbf{D}_6}$.

Proposition 5.4
Let $\mathbf{D}_6$ *act on* $\mathbb{C}^3$ *as in (5.6). Then*

$$\mathscr{C}_{\mathbf{D}_6} = \{e_1, e_2, e_3, e_4, e_5, e_6, c_1, c_2, c_4, c_6, c_7, c_8\}.$$

We separate the proof of Proposition 5.4 into a series of Lemmas, each of which is useful later when studying forced symmetry breaking to other subgroups of $\mathbf{D}_6$. In all cases we shall require the trivial fact that $\mathrm{Fix}(\Sigma) = \{(x,x,x) \big| x \in \mathbb{R}\}$.

Lemma 5.5
Let the groups $\mathbf{D}_6$, $\mathbf{Z}_6[\rho]$ *and* $\mathbf{D}_3[\rho^2, \kappa\rho]$ *act on* X_0 *with the natural action induced from the action of* $\mathbb{C}^3$. *Then the fixed-point submanifold in* X_0 *of each group is* e_1.

Proof. We begin by showing that $\mathrm{Fix}(\Sigma) = \mathrm{Fix}(\Delta)$ where $\Delta = \mathbf{D}_6$, $\mathbf{Z}_6[\rho]$ or $\mathbf{D}_3[\rho^2, \kappa\rho]$. This shows that we may treat all these cases together. The case $\Delta = \mathbf{D}_6$ is trivial. Next, consider the group $\mathbf{Z}_6[\rho]$. The action of ρ in (5.6) shows that $\mathrm{Fix}(\mathbf{Z}_6[\rho]) = \{(x,x,x)\big|x \in \mathbb{R}\}$. Finally, consider the case $\Delta = \mathbf{D}_3[\rho^2, \kappa\rho]$. The action of ρ^2 and ρ^4 implies that any point $\mathbf{z} = (z,z,z) \in \mathbb{C}^3$ is fixed by Δ. In addition the action of $\kappa\rho$ implies that $z = \overline{z}$, it follows that $\mathrm{Fix}(\mathbf{D}_3[\rho^2, \kappa\rho]) = \mathrm{Fix}(\Sigma)$. Hence to prove the lemma it is sufficient to prove it for $\mathbf{D}_6$, say. Now

$$\mathrm{Fix}_{X_0}(\mathbf{D}_6) = N_{\Gamma_h}(\mathbf{D}_6, \Sigma)/\Sigma.$$

So we must calculate those elements $\gamma \in \Gamma_h$ such that $\gamma(x,x,x) \in \mathrm{Fix}(\mathbf{D}_6)$. Clearly any $\gamma \in \mathbf{D}_6$ satisfies this requirement. Let $\gamma \in \mathbf{T}^2 \subset \Gamma_h$. Then

$$\gamma(x,x,x) = (e^{\mathrm{i}\theta_1}, e^{\mathrm{i}\theta_2}, e^{-\mathrm{i}(\theta_1+\theta_2)})x \in \mathrm{Fix}(\Sigma)$$

if and only if $(\theta_1, \theta_2) = (0,0)$. Therefore, $\mathrm{Fix}_{X_0}(\mathbf{D}_6) = e_1$ as required. □

Lemma 5.6
Let the groups $\mathbf{D}_3[\rho^2, \kappa]$ and $\mathbf{Z}_3[\rho^2]$ act naturally on X_0 with the action induced from the action (5.6) on $\mathbb{C}^3$. Then the fixed-point submanifolds in X_0 of these two groups are both $e_1 \cup e_5 \cup e_6$.

Proof. We begin by claiming

$$\mathrm{Fix}(\mathbf{D}_3[\rho^2, \kappa]) = \mathrm{Fix}(\mathbf{Z}_3[\rho^2]) = \{(z,z,z)\big|z \in \mathbb{C}\}.$$

To prove this, we observe that the action of the elements ρ^2 and ρ^4 implies that a point $\mathbf{z} = (z_1, z_2, z_3) \in \mathbb{C}^3$ is fixed by the group $\mathbf{Z}_3[\rho^2]$ if and only if $z_1 = z_2 = z_3$. The action of κ places no additional restrictions on $\mathbf{z}$, so this proves the claim. Now we must calculate (say)

$$\begin{aligned} \mathrm{Fix}_{X_0}(\mathbf{D}_3[\rho^2, \kappa]) &= N_{\Gamma_h}(\mathbf{D}_3[\rho^2, \kappa], \Sigma)/\Sigma \\ &= \{\gamma \in \Gamma_h \big| \gamma(x,x,x) \subset \mathrm{Fix}(\mathbf{D}_3[\rho^2, \kappa])\}/\Sigma. \end{aligned}$$

Clearly any $\gamma \in \mathbf{D}_6$ is contained in $N_{\Gamma_h}(\mathbf{D}_3[\rho^2, \kappa])$. So let $\gamma = (\theta_1, \theta_2) \in \mathbf{T}^2$. Then $\gamma \in N_{\Gamma_h}(\mathbf{D}_3[\rho^2, \kappa], \Sigma)$ if and only if

$$\theta_1 = \theta_2 = -(\theta_1 + \theta_2) \mathrm{mod}\ 2\pi.$$

Solving this equation gives the three solutions e_1, e_5 and e_6, as required. □

We now consider the subgroups of $\mathbf{D}_6$ that are isomorphic to the subgroup $\mathbf{D}_2$, of which there are three.

Lemma 5.7
Let $\mathbf{D}_2[\rho^3, \kappa]$, $\mathbf{D}_2[\rho^3, \kappa\rho]$ and $\mathbf{D}_2[\rho^3, \kappa\rho^2]$ act on X_0 with the natural action induced from the action (5.6) on $\mathbb{C}^3$. Then

$$\begin{aligned} \mathrm{Fix}_{X_0}(\mathbf{D}_2[\rho^3, \kappa]) &= e_1 \cup e_3, \\ \mathrm{Fix}_{X_0}(\mathbf{D}_2[\rho^3, \kappa\rho]) &= e_1 \cup e_4, \\ \mathrm{Fix}_{X_0}(\mathbf{D}_2[\rho^3, \kappa\rho^2]) &= e_1 \cup e_2. \end{aligned}$$

Proof.

Case 1: $\mathbf{D}_2[\rho^3, \kappa]$. The action given in (5.6) shows that an element $\mathbf{z} = (z_1, z_2, z_3)$ is fixed by $\mathbf{D}_2[\rho^2, \kappa]$ if and only if $z_1 \in \mathbb{R}$ and $z_2 = z_3 \in \mathbb{R}$, that is $\mathrm{Fix}(\mathbf{D}_2[\rho^3, \kappa]) = \{(x,y,y)\big|x,y \in \mathbb{R}\}$. Thus $N_{\Gamma_h}(\mathbf{D}_2[\rho^3, \kappa], \Sigma)/\Sigma$, we require $\gamma = (\theta_1, \theta_2) \in \mathbf{T}^2 \subset \Gamma_h$, where θ_1 and θ_2 satisfy

$$\begin{aligned} \theta_1 &= 0 \quad \text{or} \quad \pi \bmod 2\pi, \\ \theta_2 &= -(\theta_1 + \theta_2) = 0 \quad \text{or} \quad \pi \bmod 2\pi. \end{aligned} \tag{5.7}$$

If $\theta_1 = 0$, then clearly the only solution to (5.7) is $\theta_2 = 0$ or $\theta_2 = \pi$. Now suppose that $\theta_1 = \pi$; then (5.7) implies that there are no solutions. Therefore, $\mathrm{Fix}_{X_0}(\mathbf{D}_2[\rho^3, \kappa]) = e_1 \cup e_3$.

Case 2: $\mathbf{D}_2[\rho^3, \kappa\rho]$. Using the action (5.6) it follows that $(z_1, z_2, z_3) \in \mathbb{C}^3$ is fixed by $\mathbf{D}_2[\rho^3, \kappa\rho]$ if and only if $z_1 = z_2 \in \mathbb{R}$ and $z_3 \in \mathbb{R}$. So $\mathrm{Fix}(\mathbf{D}_2[\rho^3, \kappa\rho]) = \{(x, y, y) | x, y \in \mathbb{R}\}$. Now an element γ is contained in $N_{\Gamma_h}(\mathbf{D}_3[\rho^2, \kappa\rho], \Sigma)$ if and only if $\gamma \in \mathbf{D}_6$ or $\gamma = (\theta_1, \theta_2)$ and θ_1, θ_2 satisfy

$$\begin{aligned} \theta_1 = \theta_2 &= 0 \quad \text{or} \quad \pi \bmod 2\pi, \\ \theta_1 + \theta_2 &= 0 \quad \text{or} \quad \pi \bmod 2\pi. \end{aligned}$$

Clearly, the only solutions are given by $(\theta_1, \theta_2) = (0, 0)$ or (π, π). Therefore, $\mathrm{Fix}_{X_0}(\mathbf{D}_3[\rho^3, \kappa\rho]) = e_1 \cup e_4$.

Case 3: $\mathbf{D}_2[\rho^3, \kappa\rho^2]$. By (5.6) $\mathrm{Fix}(\mathbf{D}_2[\rho^2, \kappa\rho^2]) = \{(x, y, x) | x, y \in \mathbb{R}\}$. Next we compute the set $N_{\Gamma_h}(\mathbf{D}_2[\rho^3, \kappa\rho], \Sigma)$. Clearly any $\gamma \in \mathbf{D}_6$ is also contained in $N_{\Gamma_h}(\mathbf{D}_2[\rho^3, \kappa\rho], \Sigma)$. So let $\gamma = (\theta_1, \theta_2) \in \mathbf{T}^2 \subset \Gamma_h$. Then $\gamma \in N_{\Gamma_h}(\mathbf{D}_2[\rho^2, \kappa\rho^2], \Sigma)$ if and only if γ satisfies

$$\begin{aligned} \theta_1 = -(\theta_1 + \theta_2) &= 0 \quad \text{or } \pi \mod 2\pi, \\ \theta_2 &= 0 \quad \text{or } \pi \bmod 2\pi. \end{aligned} \tag{5.8}$$

Suppose $\theta_2 = 0$. Then either $\theta_1 = 0$ or π, giving the solutions $(\theta_1, \theta_2) = (0, 0)$ or $(\pi, 0)$. Now suppose $\theta_2 = \pi$; by (5.8) there is no solution. Therefore $\mathrm{Fix}_{X_0}(\mathbf{D}_2[\rho^3, \kappa\rho^2]) = e_1 \cup e_2$. □

Now we consider the subgroups of $\mathbf{D}_6$ which are isomorphic to $\mathbf{Z}_2$.

Lemma 5.8
The fixed-point submanifolds in X_0 of the subgroups of $\mathbf{D}_6$ isomorphic to $\mathbf{Z}_2$ are

$$\begin{aligned} \mathrm{Fix}_{X_0}(\mathbf{Z}_2[\rho^3]) &= e_1 \cup e_2 \cup e_3 \cup e_4, \\ \mathrm{Fix}_{X_0}(\mathbf{Z}_2[\kappa]) &= c_7, \\ \mathrm{Fix}_{X_0}(\mathbf{Z}_2[\kappa\rho]) &= c_6, \\ \mathrm{Fix}_{X_0}(\mathbf{Z}_2[\kappa\rho^2]) &= c_8, \\ \mathrm{Fix}_{X_0}(\mathbf{Z}_2[\kappa\rho^3]) &= c_4, \\ \mathrm{Fix}_{X_0}(\mathbf{Z}_2[\kappa\rho^4]) &= c_1, \\ \mathrm{Fix}_{X_0}(\mathbf{Z}_2[\kappa\rho^5]) &= c_2. \end{aligned}$$

Proof.

Case 1: $\mathbf{Z}_2[\rho^3]$. The action of ρ^3 on $\mathbb{C}^3$ shows that $\mathrm{Fix}(\mathbf{Z}_2[\rho^3]) = \{(w, x, y) | w, x, y \in \mathbb{R}\}$. Next we may calculate the set $N_{\Gamma_h}(\mathbf{Z}_2[\rho^3], \Sigma)$. As always $\gamma \in \mathbf{D}_6$ or $\gamma = (\theta_1, \theta_2) \in \mathbf{T}^2$ where θ_1 and θ_2 satisfy the conditions:

$$\begin{aligned} \theta_1 &= 0 \quad \text{or} \quad \pi \bmod 2\pi, \\ \theta_2 &= 0 \quad \text{or} \quad \pi \bmod 2\pi, \\ \theta_1 + \theta_2 &= 0 \quad \text{or} \quad \pi \bmod 2\pi. \end{aligned}$$

Solving these equations gives the conditions $(\theta_1, \theta_2) = (0, 0)$, $(\pi, 0)$, $(0, \pi)$ or (π, π). Therefore, $\mathrm{Fix}_{X_0}(\mathbf{Z}_2[\rho^3]) = e_1 \cup e_2 \cup e_3 \cup e_4$.

Case 2: $\mathbf{Z}_2[\kappa]$. The action of the element κ on $\mathbb{C}^3$ shows that $\mathrm{Fix}(\mathbf{Z}_2[\kappa]) = \{(z_1, z_2, z_2) | z_i \in \mathbb{C}\}$.

Now we compute the set $N_{\Gamma_h}(\mathbf{Z}_2[\kappa], \Sigma)$. Clearly any $\gamma \in \mathbf{D}_6$ is contained in $N_{\Gamma_h}(\mathbf{Z}_2[\kappa], \Sigma)$. Let $\gamma = (\theta_1, \theta_2) \in \mathbf{T}^2 \subset \Gamma_h$. Then $\gamma \in N_{\Gamma_h}(\mathbf{Z}_2[\kappa], \Sigma)$ if and only if

$$\theta_2 = -(\theta_1 + \theta_2).$$

Solving this equation gives $(\theta_1, \theta_2) = (2\theta, -\theta)$ where $\theta \in [0, 2\pi)$. Therefore $\mathrm{Fix}_{X_0}(\mathbf{Z}_2[\kappa]) = c_7$.

Case 3: $\mathbf{Z}_2[\kappa\rho]$. The action of the element $\kappa\rho$ on $\mathbb{C}^3$ shows that $\mathrm{Fix}(\mathbf{Z}_2[\kappa\rho]) = \{(z, \overline{z}, x) | z \in \mathbb{C} \text{ and } x \in \mathbb{R}\}$. Now we compute the set $N_{\Gamma_h}(\mathbf{Z}_2[\kappa\rho], \Sigma)$. Clearly any $\gamma \in \mathbf{D}_6$ is contained in $N_{\Gamma_h}(\mathbf{Z}_2[\kappa\rho], \Sigma)$. Let $\gamma = (\theta_1, \theta_2) \in \mathbf{T}^2 \subset \Gamma_h$. Then $\gamma \in N_{\Gamma_h}(\mathbf{Z}_2[\kappa\rho], \Sigma)$ if and only if

$$\begin{aligned} \theta_1 + \theta_2 &= 0 \text{ or } \pi \bmod 2\pi, \\ \theta_2 &= -\theta_1. \end{aligned}$$

Solving this equation gives $(\theta_1, \theta_2) = (\theta, -\theta)$ where $\theta \in [0, 2\pi)$. Therefore $\mathrm{Fix}_{X_0}(\mathbf{Z}_2[\kappa]) = c_6$.

Case 4: $\mathbf{Z}_2[\kappa\rho^2]$. The action of the element $\kappa\rho^2$ on $\mathbb{C}^3$ shows that $\mathrm{Fix}(\mathbf{Z}_2[\kappa]) = \{(z_1, z_2, z_1) | z_i \in \mathbb{C}\}$. Now we compute the set $N_{\Gamma_h}(\mathbf{Z}_2[\kappa\rho^2], \Sigma)$. Clearly any $\gamma \in \mathbf{D}_6$ is contained in $N_{\Gamma_h}(\mathbf{Z}_2[\kappa\rho^2], \Sigma)$. Let $\gamma = (\theta_1, \theta_2) \in \mathbf{T}^2 \subset \Gamma_h$. Then $\gamma \in N_{\Gamma_h}(\mathbf{Z}_2[\kappa\rho^2], \Sigma)$ if and only if

$$\theta_1 = -(\theta_1 + \theta_2),$$

Solving this equation gives $(\theta_1, \theta_2) = (\theta, -2\theta)$ where $\theta \in [0, 2\pi)$. Therefore $\mathrm{Fix}_{X_0}(\mathbf{Z}_2[\kappa\rho^2]) = c_8$.

Case 5: $\mathbf{Z}_2[\kappa\rho^3]$. The action of the element $\kappa\rho^3$ shows that $\mathrm{Fix}(\mathbf{Z}_2[\kappa\rho^3]) = \{(x, z, \overline{z}) | z \in \mathbb{C} \text{ and } x \in \mathbb{R}\}$. Now we compute the set $N_{\Gamma_h}(\mathbf{Z}_2[\kappa\rho^3], \Sigma)$. Clearly any $\gamma \in \mathbf{D}_6$ is contained in $N_{\Gamma_h}(\mathbf{Z}_2[\kappa\rho^3], \Sigma)$. Let $\gamma = (\theta_1, \theta_2) \in \mathbf{T}^2 \subset \Gamma_h$. Then $\gamma \in N_{\Gamma_h}(\mathbf{Z}_2[\kappa\rho^3], \Sigma)$ if and only if

$$\begin{aligned} \theta_1 &= 0 \text{ or } \pi \bmod 2\pi, \\ \theta_2 &= (\theta_1 + \theta_2). \end{aligned}$$

Solving this equation gives $(\theta_1, \theta_2) = (0, \theta)$ where $\theta \in [0, 2\pi)$. Therefore $\mathrm{Fix}_{X_0}(\mathbf{Z}_2[\kappa\rho^3]) = c_4$.

Case 6: $\mathbf{Z}_2[\kappa\rho^4]$. The action of the element $\kappa\rho^4$ on $\mathbb{C}^3$ shows that $\mathrm{Fix}(\mathbf{Z}_2[\kappa\rho^4]) = \{(z_1, z_1, z_2) | z_i \in \mathbb{C}\}$. Now we compute the set $N_{\Gamma_h}(\mathbf{Z}_2[\kappa\rho^4], \Sigma)$. Clearly any $\gamma \in \mathbf{D}_6$ is contained in $N_{\Gamma_h}(\mathbf{Z}_2[\kappa\rho^4], \Sigma)$. Let $\gamma = (\theta_1, \theta_2) \in \mathbf{T}^2 \subset \Gamma_h$. Then $\gamma \in N_{\Gamma_h}(\mathbf{Z}_2[\kappa\rho^4], \Sigma)$ if and only if $\theta_1 = \theta_2$. Solving this equation gives $(\theta_1, \theta_2) = (\theta, \theta)$ where $\theta \in [0, 2\pi)$. Therefore $\mathrm{Fix}_{X_0}(\mathbf{Z}_2[\kappa\rho^4]) = c_1$.

Case 7: $\mathbf{Z}_2[\kappa\rho^5]$. The action of the element $\kappa\rho^5$ on $\mathbb{C}^3$ shows that $\mathrm{Fix}(\mathbf{Z}_2[\kappa\rho^5]) = \{(z, x, \overline{z}) | z \in \mathbb{C},\ x \in \mathbb{R}\}$. Now we compute the set $N_{\Gamma_h}(\mathbf{Z}_2[\kappa\rho^5], \Sigma)$. Clearly any $\gamma \in \mathbf{D}_6$ is contained in $N_{\Gamma_h}(\mathbf{Z}_2[\kappa\rho^5], \Sigma)$. Let $\gamma = (\theta_1, \theta_2) \in \mathbf{T}^2 \subset \Gamma_h$. Then $\gamma \in N_{\Gamma_h}(\mathbf{Z}_2[\kappa\rho^5], \Sigma)$ if and only if

$$\begin{aligned} \theta_2 &= 0 \text{ or } \pi \bmod 2\pi, \\ \theta_1 &= \theta_1 + \theta_2 \bmod 2\pi. \end{aligned}$$

Solving this equation gives $(\theta_1, \theta_2) = (\theta, 0)$ where $\theta \in [0, 2\pi)$. Therefore $\mathrm{Fix}_{X_0}(\mathbf{Z}_2[\kappa\rho^5]) = c_3$. □

Using the calculation $\mathscr{C}_{\mathbf{D}_6}$ we may now compute the skeleton $\mathbb{X}_{\mathbf{D}_6}$. We find that

$$\begin{aligned} \mathbb{X}_{\mathbf{D}_6} &= \bigcup_{C \in \mathscr{C}_{\mathbf{D}_6}} C \\ &= c_1 \cup c_2 \cup c_4 \cup c_6 \cup c_7 \cup c_8. \end{aligned}$$

Figure 5.1 illustrates $\mathbb{X}_{\mathbf{D}_6}$; we show $\mathbb{X}_{\mathbf{D}_6}$ contained in a cutaway of X_0. Given the set $\mathbb{X}_{\mathbf{D}_6}$ the next step is to define the smooth stratification of $\mathbb{X}_{\mathbf{D}_6}$ into the sets $E_{(X_0, \mathbf{D}_6)}$ and $H_{(X_0, \mathbf{D}_6)}$. Recall the definition of $h_1, \ldots, h_{12}$ in Definition 4.6, and make the following additional definitions:

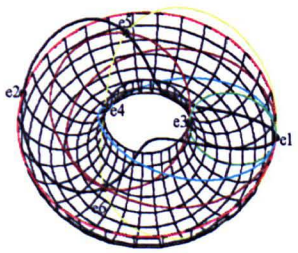

Figure 5.1: The skeleton $\mathbf{X}_{\mathbf{D}_6}$ in the 2-torus X_0. Here c_1 is yellow, c_2 is red, c_4 is green, c_6 is cyan, c_7 is brown, and c_8 is black.

Definition 5.9
Define the following subsets of X_0:

$$\begin{aligned}
h_{13} &= \{(\theta,\theta)\,|\,\theta \in (0,2\pi/3)\}, & h_{14} &= \{(\theta,\theta)\,|\,\theta \in (2\pi/3,\pi)\},\\
h_{15} &= \{(\theta,\theta)\,|\,\theta \in (\pi,4\pi/3)\}, & h_{16} &= \{(\theta,\theta)\,|\,\theta \in (4\pi/3,2\pi)\},\\
h_{17} &= \{(-\theta,2\theta)\,|\,\theta \in (0,2\pi/3)\}, & h_{18} &= \{(-\theta,2\theta)\,|\,\theta \in (2\pi/3,\pi)\},\\
h_{19} &= \{(-\theta,2\theta)\,|\,\theta \in (\pi,4\pi/3)\}, & h_{20} &= \{(-\theta,2\theta)\,|\,\theta \in (4\pi/3,2\pi)\},\\
h_{21} &= \{(2\theta,-\theta)\,|\,\theta \in (0,4\pi/3)\}, & h_{22} &= \{(2\theta,-\theta)\,|\,\theta \in (4\pi/3,2\pi)\},\\
h_{24} &= \{(2\theta,-\theta)\,|\,\theta \in (0,2\pi/3)\}, & h_{25} &= \{(2\theta,-\theta)\,|\,\theta \in (2\pi/3,2\pi)\}.
\end{aligned}$$

Using these subsets we may stratify $\mathbf{X}_{\mathbf{D}_6}$ as follows:

$$\begin{aligned}
E_{(\mathbf{D}_6,X_0)} &= e_1 \cup e_2 \cup e_3 \cup e_4,\\
H_{(\mathbf{D}_6,X_0)} &= h_3 \cup h_4 \cup h_7 \cup h_8 \cup h_{11} \cup h_{12} \cup h_{13} \cup h_{14}\\
&\quad \cup h_{15} \cup h_{16} \cup h_{17} \cup h_{18} \cup h_{19} \cup h_{20}\\
&\quad \cup h_{21} \cup h_{22} \cup h_{23}.
\end{aligned}$$

This complete the computation of the skeleton. Using the stratification of $\mathbf{X}_{\mathbf{D}_6}$ we deduce the following existence result.

Theorem 5.10
Let $\Gamma = \mathbf{D}_6 \dot{+} \mathbf{T}^2$, $\Sigma = \mathbf{D}_6$ and $\Delta = \mathbf{D}_6$. Let Γ act on $\mathbb{C}^3$ as in (5.6). Let $\mathbf{f} \in \vec{\mathcal{E}}_\Gamma$ be a Γ-equivariant bifurcation problem. Let $\mathbf{g} \in \vec{\mathcal{E}}_\Delta$ be Δ-equivariant and satisfy $\mathbf{g}(\mathbf{0}) = \mathbf{0}$. Let $\mathbf{F}(\mathbf{z},\lambda,\varepsilon) = \mathbf{f}(\mathbf{z},\lambda) + \varepsilon\mathbf{g}(\mathbf{z})$. Then there exists a steady-state solution to $\mathbf{f}(\mathbf{z},\lambda) = 0$ bifurcating from $(\mathbf{0},0)$ with Σ-isotropy. Let $X_0 \cong \mathbf{T}^2$ be the group orbit of steady states. Then for sufficiently small ε, X_0 persists to give a new $\mathbf{F}$-invariant manifold X_ε which is Δ-equivariantly diffeomorphic to X_0. Moreover, there exists $g \in \vec{\mathcal{E}}_\Delta$ such that the elements in $E_{(\Delta,X_0)}$ are equilibria for the new flow and those of $H_{(\Delta,X_0)}$ are heteroclinic connections between equilibria.

As always, the problem with this existence result is that it is only an existence result. We have no way of knowing what type of $\mathbf{D}_6$-equivariant perturbation $\mathbf{g}$ gives rise to heteroclinic connections between the equilibria in $E_{(\mathbf{D}_6,X_0)}$. We must use the $\mathbf{D}_6$ symmetry to gain a better understanding of how flows behave on $\mathbf{X}_{\mathbf{D}_6}$.

Symmetry Properties of $\mathbf{X}_{\mathbf{D}_6}$

The action of the group $\mathbf{D}_6$ on X_0, and consequently on $\mathbf{X}_{\mathbf{D}_6}$, has a strong influence on the flows that are permitted on $\mathbf{X}_{\mathbf{D}_6}$. Here we calculate for any $C \in \mathscr{C}_{\mathbf{D}_6}$ the setwise and pointwise

isotropy subgroups. From these two groups we may calculate the group $S(C)$ which gives information on the projected skeleton $\mathbb{X}^p_{\mathbf{D}_6}$. In particular we may use the group $S(C)$ to compute the axes of symmetry (if any) on $C \in \mathscr{C}_{\mathbf{D}_6}$. These axes of symmetry are given by the knots relative to C—which are always elements of $E_{(\mathbf{D}_6, X_0)}$.

Pointwise and Setwise Isotropy Subgroups. The action (5.6) of the group $\mathbf{D}_6$ on $\mathbb{C}^3$ induces a natural action on X_0. Using coordinates (θ_1, θ_2) on X_0, this action is:

$$\begin{array}{llll} \rho(\theta_1,\theta_2) &= (-\theta_2, \theta_1+\theta_2), & \rho^2(\theta_1,\theta_2) &= (-\theta_1-\theta_2, \theta_1), \\ \rho^3(\theta_1,\theta_2) &= (-\theta_1, -\theta_2), & \rho^4(\theta_1,\theta_2) &= (\theta_2, -\theta_1-\theta_2), \\ \rho^5(\theta_1,\theta_2) &= (\theta_1+\theta_2, -\theta_1), & \kappa(\theta_1,\theta_2) &= (\theta_1, -(\theta_1+\theta_2)), \\ \kappa\rho(\theta_1,\theta_2) &= (-\theta_2, -\theta_1), & \kappa\rho^2(\theta_1,\theta_2) &= (-\theta_1-\theta_2, \theta_2), \\ \kappa\rho^3(\theta_1,\theta_2) &= (-\theta_1, \theta_1+\theta_2), & \kappa\rho^4(\theta_1,\theta_2) &= (\theta_2, \theta_1), \\ \kappa\rho^5(\theta_1,\theta_2) &= (\theta_1+\theta_2, -\theta_2). & & \end{array} \tag{5.9}$$

This action is derived as follows. Let $(\theta_1, \theta_2) \in X_0$. Then (θ_1, θ_2) corresponds (via the $\mathbf{T}^2$ action) to the point $\mathbf{z} = (e^{\mathrm{i}\theta_1}, e^{\mathrm{i}\theta_2}, e^{-\mathrm{i}(\theta_1+\theta_2)})x$ in $\mathbb{C}^3$. The action of ρ on $\mathbf{z}$ gives

$$\rho\mathbf{z} = (e^{-\mathrm{i}\theta_2}, e^{\mathrm{i}(\theta_1+\theta_2)}, e^{-\mathrm{i}\theta_1})x.$$

Comparing $\mathbf{z}$ with $\rho\mathbf{z}$ we see that $(\theta_1, \theta_2) \mapsto (-\theta_2, \theta_1 + \theta_2)$. Next we consider the action of the generator κ. The action of κ on $\mathbf{z}$ gives

$$\kappa\mathbf{z} = (e^{\mathrm{i}\theta_1}, e^{-\mathrm{i}(\theta_1+\theta_2)}, e^{\mathrm{i}\theta_2})x.$$

A quick comparison of $\kappa\mathbf{z}$ with $\mathbf{z}$ shows that $(\theta_1, \theta_2) \mapsto (\theta_1, -(\theta_1 + \theta_2))$. This gives the action of the generators of $\mathbf{D}_6$ on X_0 from which the whole action of $\mathbf{D}_6$ can be deduced.

The action of $\mathbf{D}_6$ on X_0 induces an action on $\mathscr{C}_{\mathbf{D}_6}$ by permutation of its elements. This action is derived as follows. Let $C \in \mathscr{C}_{\mathbf{D}_6}$ then the action of (say) ρ on the set C is given by applying ρ to all elements of C, the results set will then be another element of $\mathscr{C}_{\mathbf{D}_6}$. This action is given in Table 5.1. Using the action of $\mathbf{D}_6$ on $\mathscr{C}_{\mathbf{D}_6}$ we may compute the groups $\mathrm{Stab}(C)$ and $\mathrm{stab}(C)$. This is the content of the next proposition.

Proposition 5.11
Let $\mathbf{D}_6$ act on $\mathscr{C}_{\mathbf{D}_6}$ as in Table 5.1. Then given $C \in \mathscr{C}_{\mathbf{D}_6}$, the setwise isotropy $\mathrm{Stab}(C)$ and the pointwise isotropy $\mathrm{stab}(C)$ along with the factor group $S(C)$ as in Table 5.2.

Proof. The computations of $\mathrm{Stab}(C)$ are trivial and follow directly from the entries in Table 5.1. To compute $\mathrm{stab}(C)$ we just check to see which elements of $\mathrm{Stab}(C)$ act pointwise trivially. □

We have now completed the computations of the setwise and pointwise isotropy subgroups of $C \in \mathscr{C}_{\mathbf{D}_6}$. These computations reveal that $S(C) \cong \mathbf{Z}_2$ for all $C \in \mathscr{C}_{\mathbf{D}_6}$, with $C \cong \mathbf{S}^1$ and so there is one axis of symmetry along every such C. We must now determine where these axes lie.

Knots Relative to C. Given $C \in \mathscr{C}_{\mathbf{D}_6}$ a knot relative to C gives an axis of symmetry for any $\mathbf{D}_6$-equivariant flow on C.

Proposition 5.12
Let $C \in \mathscr{C}_{\mathbf{D}_6}$ and suppose $K(C) \neq \emptyset$. Then the knots relative to C are as in Table 5.3.

Proof. Now the $\mathbf{D}_6$ action shows that there are only three orbit representatives for the connections between the equilibria. For the connections with only two equilibria, it follows immediately that these equilibria are knots. Now only the representative for c_1 contains more that two equilibria, so we must use a more direct method to find the knots. Suppose that $C \in \mathscr{C}_{\mathbf{D}_6}$ and $k \in C \cap E_{(\mathbf{D}_6, X_0)}$. Then k is a knot relative to C if and only if

$$B(k) = (\mathrm{Stab}(k) - \mathrm{stab}(C)) \cap N_\Delta(\mathrm{stab}(C)) \neq \emptyset.$$

Table 5.1: Action of $\mathbf{D}_6$ induced on $\mathscr{C}_{\mathbf{D}_6}$.

Element of $\mathscr{C}_{\mathbf{D}_6}$	Elements of $\mathbf{D}_6$ acting nontrivially	Action
e_1	none	
e_2	ρ, ρ^4, $\kappa\rho$, $\kappa\rho^4$	e_3
	ρ^2, ρ^5, κ, $\kappa\rho^3$	e_4
e_3	ρ, ρ^4, $\kappa\rho^2$, $\kappa\rho^5$	e_4
	ρ^2, ρ^5, $\kappa\rho$, $\kappa\rho^4$	e_2
e_4	ρ, ρ^4, $\kappa\rho^3$, κ	e_2
	ρ^2, ρ^5, $\kappa\rho^2$, $\kappa\rho^5$	e_3
e_5	ρ, ρ^3, ρ^5, $\kappa\rho$, $\kappa\rho^3$, $\kappa\rho^5$.	e_6
e_6	ρ, ρ^3, ρ^5, $\kappa\rho$, $\kappa\rho^3$, $\kappa\rho^5$.	e_5
c_1	ρ^2, ρ^5, $\kappa\rho^2$, $\kappa\rho^5$	c_7
	ρ, ρ^4, κ, $\kappa\rho^3$, ρ^5	c_8
c_2	ρ, ρ^4, $\kappa\rho$, $\kappa\rho^4$	c_4
	ρ^2, ρ^5, κ, $\kappa\rho^3$	c_6
c_4	ρ, ρ^4, $\kappa\rho^2$, $\kappa\rho^5$	c_6
	ρ^2, ρ^5, $\kappa\rho$, $\kappa\rho^4$	c_2
c_6	ρ, ρ^4, κ, $\kappa\rho^3$	c_2
	ρ^2, ρ^5, $\kappa\rho^2$, $\kappa\rho^5$	c_4
c_7	ρ, ρ^4, $\kappa\rho^2$, $\kappa\rho^5$	c_1
	ρ^2, ρ^5, $\kappa\rho$, $\kappa\rho^4$	c_8
c_8	ρ, ρ^4, $\kappa\rho$, $\kappa\rho^4$	c_7
	κ, ρ^2, ρ^5, $\kappa\rho^3$	c_1

Table 5.2: Isotropy data for $C \in \mathscr{C}_{\mathbf{D}_6}$.

Element of $\mathscr{C}_{\mathbf{D}_6}$	Stab(C)	stab(C)	$S(C)$
e_1	$\mathbf{D}_6$	$\mathbf{D}_6$	$\mathbf{1}$
e_2	$\mathbf{D}_2[\rho^3, \kappa\rho^2]$	$\mathbf{D}_2[\rho^3, \kappa\rho^2]$	$\mathbf{1}$
e_3	$\mathbf{D}_2[\rho^3, \kappa]$	$\mathbf{D}_2[\rho^3, \kappa]$	$\mathbf{1}$
e_4	$\mathbf{D}_2[\rho^3, \kappa\rho]$	$\mathbf{D}_2[\rho^3, \kappa\rho]$	$\mathbf{1}$
e_5	$\mathbf{D}_3[\rho^2, \kappa]$	$\mathbf{D}_3[\rho^2, \kappa]$	$\mathbf{1}$
e_6	$\mathbf{D}_3[\rho^2, \kappa]$	$\mathbf{D}_3[\rho^2, \kappa]$	$\mathbf{1}$
c_1	$\mathbf{D}_2[\rho^3, \kappa\rho]$	$\mathbf{Z}_2[\kappa\rho^4]$	$\mathbf{Z}_2$
c_2	$\mathbf{D}_2[\rho^3, \kappa\rho^2]$	$\mathbf{Z}_2[\kappa\rho^5]$	$\mathbf{Z}_2$
c_4	$\mathbf{D}_2[\rho^3, \kappa]$	$\mathbf{Z}_2[\kappa\rho^3]$	$\mathbf{Z}_2$
c_6	$\mathbf{D}_2[\rho^3, \kappa\rho]$	$\mathbf{Z}_2[\kappa\rho]$	$\mathbf{Z}_2$
c_7	$\mathbf{D}_2[\rho^3, \kappa]$	$\mathbf{Z}_2[\kappa]$	$\mathbf{Z}_2$
c_8	$\mathbf{D}_2[\rho^3, \kappa\rho^2]$	$\mathbf{Z}_2[\kappa\rho^2]$	$\mathbf{Z}_2$

Table 5.3: Knots relative to $C \in \mathscr{C}_{\mathbf{D}_6}$ when C is a topological circle.

Element of $\mathscr{C}_{\mathbf{D}_6}$	Knots
c_1	e_1, e_4
c_2	e_1, e_2
c_4	e_1, e_3
c_6	e_1, e_4
c_7	e_1, e_2
c_8	e_1, e_3

By Proposition 5.11, $\text{stab}(c_1) = \mathbf{Z}_2[\kappa\rho^4]$. On c_1 either $k = e_1$, e_4, e_5 or e_6. Now $\text{Stab}(e_1) = \mathbf{D}_6$. So $\text{Stab}(e_1) - \text{stab}(c_1) = \mathbf{D}_6 - \mathbf{Z}_2[\kappa\rho^4]$. Now $N_{\mathbf{D}_6}(\mathbf{Z}_2[\kappa\rho^4]) = \mathbf{D}_2[\rho^3, \kappa\rho]$. Hence

$$B(e_1) = (\mathbf{D}_6 - \mathbf{Z}_2[\kappa\rho^4]) \cap \mathbf{D}_2[\rho^3, \kappa\rho] \neq \emptyset.$$

Therefore e_1 is a knot relative to c_1. Next consider e_4, then $\text{Stab}(e_4) = \mathbf{D}_2[\rho^3, \kappa\rho]$. Hence

$$B(e_4) = (\mathbf{D}_2[\rho^3, \kappa\rho] - \mathbf{Z}_2[\kappa\rho^4]) \cap \mathbf{D}_2[\rho^3, \kappa\rho] \neq \emptyset.$$

Therefore, e_4 is a knot relative to c_1. Next we consider the cases e_5 and e_6 together. We can do this since $\text{Stab}(e_5) = \text{Stab}(e_6) = \mathbf{D}_3[\rho^2, \kappa]$. Hence

$$B(k) = (\mathbf{D}_3[\rho^2, \kappa] - \mathbf{Z}_2[\kappa\rho^4]) \cap \mathbf{D}_2[\rho^3, \kappa\rho] = \emptyset.$$

Therefore, e_5 and e_6 are not knots relative to c_1. Alternatively, we can argue that since $S(C) \cong \mathbf{Z}_2$ there are two knots on c_1, and we have seen that e_1 and e_4 are knots, so e_5 and e_6 cannot be knots. □

Remark 5.13
Not all of the elements of $E_{(\mathbf{D}_6, X_0)}$ are knots. The two points e_5 and e_6 are not knots relative to any $C \in \mathscr{C}_{\mathbf{D}_6}$ with $C \cong \mathbf{S}^1$. So symmetry places no restrictions on the types of flow to be expected along (say) c_1 between e_1 and e_4. This answers a question of Lauterbach et al. *[62] p. 895. The authors ask whether for general Γ, Σ and Δ all nonisolated elements of $E_{(\mathbf{D}_6, \Gamma/\Sigma)}$ are knots relative to at least one element of $\mathscr{C}_{(\Delta, \Gamma/\Sigma)}$. The authors show for $\Gamma = \mathbf{SO(3)}$ this is always true; our analysis shows in general it is false.*

It was shown in Proposition 5.11 that for any $C \in \mathscr{C}_{\mathbf{D}_6}$ which is a topological circle, the group $S(C) \cong \mathbf{Z}_2$. The group $S(C)$ acts on C by reflection about the (two) knots, and by Proposition 5.12 we know their location. Hence we have some very powerful restrictions on the behaviour of $\mathbf{D}_6$-equivariant flows on $\mathbb{X}_{\mathbf{D}_6}$. These results apply to *any* $\mathbf{D}_6$-equivariant perturbation, and not just some truncation at finite order.

Projected Skeleton

Here we compute the projected skeleton $\mathbb{X}^p_{\mathbf{D}_6}$. We have already calculated the action of $\mathbf{D}_6$ on $\mathscr{C}_{\mathbf{D}_6}$, the pointwise and setwise isotropy subgroups and the knots relative to each $C \in \mathscr{C}_{\mathbf{D}_6}$. Using this information we may construct the projected skeleton. The action of $\mathbf{D}_6$ on $\mathscr{C}_{\mathbf{D}_6}$ shows that there are three orbit representatives for points in $E_{(\mathbf{D}_6, X_0)}$. These are given by (say) e_1, e_2 and e_5. By Proposition 5.12 there are two knots relative to any $C \in \mathscr{C}_{\mathbf{D}_6}$, thus each C has an axis of reflection symmetry. Hence, each C projects into the orbit space as a line joining the two knots relative to C. Furthermore, the action of $\mathbf{D}_6$ on $\mathscr{C}_{\mathbf{D}_6}$ shows that there are three orbit representatives for the elements of $H_{(\mathbf{D}_6, X_0)}$. These are given by (say) $h_3 = \{(\theta, 0) | \theta \in (0, \pi)\}$,

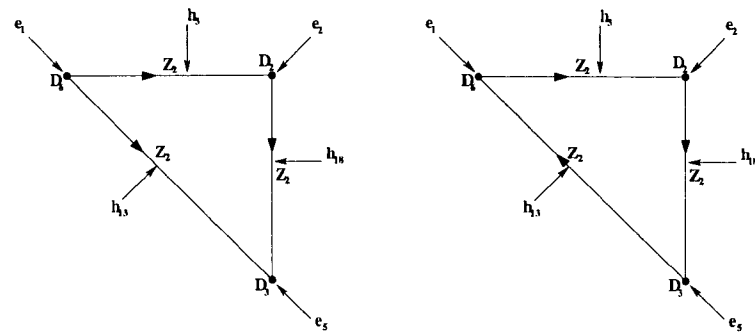

Figure 5.2: Two flows on the projected skeleton $\mathbb{X}^p_{\mathbf{D}_6}$. (a) An admissible flow where the flow is directed to the equilibria e_5. In this situation all the equilibria are hyperbolic. (b) A heteroclinic cycle on $\mathbb{X}^p_{\mathbf{D}_6}$. In this case, the equilibrium e_5 is not hyperbolic.

$h_{13} = \{(\theta,\theta)|\theta \in (0,2\pi/3)\}$ and $h_{18} = \{(\theta,-2\theta)|\theta \in (2\pi/3,\pi)\}$. The element h_3 connects e_1 to e_2, whilst h_{13} and h_{18} connect e_1 to e_5 and e_5 to e_2, respectively.

Figure 5.2 illustrates the projected skeleton. (a) Present an admissible flow on $\mathbb{X}^p_{\mathbf{D}_6}$ in which the flow is directed to the equilibrium e_5. (b) Illustrates a (possible) heteroclinic cycle on $\mathbb{X}^p_{\mathbf{D}_6}$. This flow requires the equilibrium e_5 to be non-hyperbolic, a situation that cannot be realised generically.

The presence of the equilibrium e_5 yields problems. Since e_5 is not a knot, there exist flows for which this equilibrium is not hyperbolic, which is not a generic situation. It is possible to exhibit flows for which all the equilibria are hyperbolic, but we shall not pursue this issue.

5.2.3 Forced Symmetry Breaking to $\mathbf{D}_3[\rho^2,\kappa]$

In this subsection we study forced symmetry breaking of the hexagonal solution which generically exists for a general Γ_h-equivariant bifurcation problem. The normal hyperbolicity of X_0 guarantees, by the Equivariant Persistence Theorem, the existence an invariant manifold X_ε that is $\mathbf{D}_3[\rho^2,\kappa]$-equivariantly diffeomorphic to X_0. We shall study the $\mathbf{D}_3[\rho^2,\kappa]$ action on X_0, which via the diffeomorphism allows us to study X_ε. We begin with the action of $\mathbf{D}_3[\rho^2,\kappa]$ on $\mathbb{C}^3$; this action is given by the restriction of the $\mathbf{D}_6$ action on $\mathbb{C}^3$ given in (5.6). More precisely, we have:

$$\begin{array}{lcllcl} \rho^2\mathbf{z} & = & (z_3,z_1,z_2), & \rho^4\mathbf{z} & = & (z_2,z_3,z_1), \\ \kappa\mathbf{z} & = & (z_1,z_3,z_2), & \kappa\rho^2\mathbf{z} & = & (z_3,z_2,z_1), \\ \kappa\rho^4\mathbf{z} & = & (z_2,z_1,z_3). & & & \end{array}$$

This action induces a natural action of $\mathbf{D}_3[\rho^2,\kappa]$ on $X_0 \cong \Gamma_h/\Sigma$.

Calculation of the Skeleton

Using the action (5.10) of $\mathbf{D}_3[\rho^2,\kappa]$ on $\mathbb{C}^3$ we compute the skeleton of X_0. Firstly we require knowledge of the subgroups of $\mathbf{D}_3[\rho^2,\kappa]$. There are six closed subgroups $\mathbf{D}_3[\rho^2,\kappa]$, given by $\mathbf{D}_3[\rho^2,\kappa]$, $\mathbf{Z}_3[\rho^2]$, $\mathbf{Z}_2[\kappa]$, $\mathbf{Z}_2[\kappa\rho^2]$, $\mathbf{Z}_2[\kappa\rho^4]$, and the trivial subgroup. Since X_0 is a 2-torus we have standard coordinates (θ_1,θ_2). The next step is the calculation of the set $\mathscr{C}_{\mathbf{D}_3[\rho^2,\kappa]}$.

Proposition 5.14
Let $\mathbf{D}_3[\rho^2,\kappa]$ act on $\mathbb{C}^3$ as in (5.10). Then $\mathscr{C}_{\mathbf{D}_3[\rho^2,\kappa]} = \{e_1,e_5,e_6,c_1,c_7,c_8\}$.

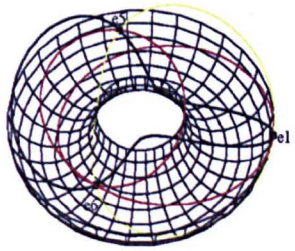

Figure 5.3: The skeleton $\mathbf{X}_{\mathbf{D}_3[\rho^2,\kappa]}$. Here c_1 is yellow, c_7 is brown, and c_8 is black.

Proof. The proof follows from Lemmas 5.6 and 5.8. □

Using the calculation $\mathscr{C}_{\mathbf{D}_3[\rho^2,\kappa]}$ we may now compute the skeleton $\mathbf{X}_{\mathbf{D}_3[\rho^2,\kappa]}$. We find that

$$\begin{aligned}\mathbf{X}_{\mathbf{D}_3[\rho^2,\kappa]} &= \bigcup_{C\in\mathscr{C}_{\mathbf{D}_3[\rho^2,\kappa]}} C \\ &= c_1 \cup c_7 \cup c_8.\end{aligned}$$

Figure 5.3 shows $\mathbf{X}_{\mathbf{D}_3[\rho^2,\kappa]}$.

Symmetry Properties of $\mathbf{X}_{\mathbf{D}_3[\rho^2,\kappa]}$

The action of the group $\mathbf{D}_3[\rho^2,\kappa]$ on X_0 and consequently on $\mathbf{X}_{\mathbf{D}_3[\rho^2,\kappa]}$, has a strong influence on the flows that are permitted on $\mathbf{X}_{\mathbf{D}_3[\rho^2,\kappa]}$. Here we calculate for any $C \in \mathscr{C}_{\mathbf{D}_3[\rho^2,\kappa]}$ the setwise and pointwise isotropy subgroups. From these two groups we calculate the group $S(C)$ which gives information on the projected skeleton $\mathbf{X}^p_{\mathbf{D}_3[\rho^2,\kappa]}$.

Pointwise and Setwise Isotropy Subgroups. The action (5.10) of $\mathbf{D}_3[\rho^2,\kappa]$ on $\mathbb{C}^3$ induces a natural action on X_0. Using coordinates (θ_1,θ_2) on X_0, this action is given by the restriction of the $\mathbf{D}_6$ action on X_0 in (5.9):

$$\begin{array}{lllllll}\rho^2(\theta_1,\theta_2) &=& (-\theta_1-\theta_2,\theta_1), & \rho^4(\theta_1,\theta_2) &=& (\theta_2,-\theta_1-\theta_2),\\ \kappa(\theta_1,\theta_2) &=& (\theta_1,-(\theta_1+\theta_2)), & \kappa\rho^2(\theta_1,\theta_2) &=& (-\theta_1-\theta_2,\theta_2),\\ \kappa\rho^4(\theta_1,\theta_2) &=& (\theta_2,\theta_1).\end{array} \tag{5.10}$$

The action of $\mathbf{D}_3[\rho^2,\kappa]$ on X_0 induces an action on $\mathscr{C}_{\mathbf{D}_3[\rho^2,\kappa]}$ by permutation of its elements. This action is given in Table 5.4. Using the action of $\mathbf{D}_3[\rho^2,\kappa]$ on $\mathscr{C}_{\mathbf{D}_3[\rho^2,\kappa]}$ we may compute the groups $\mathrm{Stab}(C)$ and $\mathrm{stab}(C)$.

Proposition 5.15
Let $\mathbf{D}_3[\rho^2,\kappa]$ act on $\mathscr{C}_{\mathbf{D}_3[\rho^2,\kappa]}$ as in Table 5.4 and on X_0 with the action in (5.10). Then given $C \in \mathscr{C}_{\mathbf{D}_3[\rho^2,\kappa]}$, the setwise isotropy $\mathrm{Stab}(C)$ and the pointwise isotropy $\mathrm{stab}(C)$ and the group $S(C)$ are given in Table 5.5.

Proof. The proof follows directly from Proposition 5.11. □

We have now completed the computations of the setwise and pointwise isotropy subgroups of $C \in \mathscr{C}_{\mathbf{D}_3[\rho^2,\kappa]}$. These computations reveal that $S(C) \cong \mathbf{1}$ for all $C \in \mathscr{C}_{\mathbf{D}_3[\rho^2,\kappa]}$. Hence there are no knots relative to any $C \in \mathscr{C}_{\mathbf{D}_3[\rho^2,\kappa]}$.

Table 5.4: Action of $\mathbf{D}_3[\rho^2, \kappa]$ induced on $\mathscr{C}_{\mathbf{D}_3[\rho^2,\kappa]}$.

Element of $\mathscr{C}_{\mathbf{D}_3[\rho^2,\kappa]}$	Elements of $\mathbf{D}_3[\rho^2, \kappa]$ acting nontrivially	Action
e_1	none	
e_5	none	
e_6	none	
c_1	ρ^2, $\kappa\rho^2$	c_7
	ρ^4, κ	c_8
c_7	ρ^4, $\kappa\rho^2$	c_1
	ρ^2, $\kappa\rho^4$	c_8
c_8	ρ^4,$\kappa\rho^4$	c_7
	ρ^2,κ	c_1

Table 5.5: Isotropy data for $C \in \mathscr{C}_{\mathbf{D}_3[\rho^2,\kappa]}$.

Element of $\mathscr{C}_{\mathbf{D}_3[\rho^2,\kappa]}$	Stab(C)	stab(C)	$S(C)$
e_1	$\mathbf{D}_3[\rho^2, \kappa]$	$\mathbf{D}_3[\rho^2, \kappa]$	1
e_5	$\mathbf{D}_3[\rho^2, \kappa]$	$\mathbf{D}_3[\rho^2, \kappa]$	1
e_6	$\mathbf{D}_3[\rho^2, \kappa]$	$\mathbf{D}_3[\rho^2, \kappa]$	1
c_1	$\mathbf{Z}_2[\kappa\rho^4]$	$\mathbf{Z}_2[\kappa\rho^4]$	1
c_7	$\mathbf{Z}_2[\kappa]$	$\mathbf{Z}_2[\kappa]$	1
c_8	$\mathbf{Z}_2[\kappa\rho^2]$	$\mathbf{Z}_2[\kappa\rho^2]$	1

Projected Skeleton

Here we compute the projected skeleton $\mathbb{X}^p_{\mathbf{D}_3[\rho^2,\kappa]}$. The action of $\mathbf{D}_3[\rho^2, \kappa]$ on $\mathscr{C}_{\mathbf{D}_3[\rho^2,\kappa]}$ shows that there are three orbit representatives for points in $E_{(\mathbf{D}_3[\rho^2,\kappa],X_0)}$. These are e_1, e_5 and e_6. There are no knots relative to any $C \in \mathscr{C}_{\mathbf{D}_3[\rho^2,\kappa]}$, thus there are no restrictions on the flows about the equilibria. Furthermore, the action of $\mathbf{D}_3[\rho^2, \kappa]$ on $\mathscr{C}_{\mathbf{D}_3[\rho^2,\kappa]}$ shows that there are three orbit representatives for the elements of $H_{(\mathbf{D}_3[\rho^2,\kappa],X_0)}$. These are $h_{13} = \{(\theta,\theta)|\theta \in (0, 2\pi/3)\}$, $h_{16} = \{(\theta,\theta)|\theta \in (4\pi/3, 2\pi)\}$ and $h_{26} = \{(\theta,\theta)|\theta \in (2\pi/3, 4\pi/3)\}$. The element h_{13} connects e_1 to e_5, h_{16} connects e_5 to e_6 and h_{26} connects e_6 to e_1.

Figure 5.4 illustrates the projected skeleton, which is a topological circle with three equilibria. It is not possible to find any generic admissible perturbations; there is always one equilibrium that is not hyperbolic.

The computations of the projected skeleton $\mathbb{X}^p_{\mathbf{D}_3[\rho^2,\kappa]}$ show that any admissible flow gives rise to equilibria on the skeleton which are not hyperbolic, which is not a generic situation. Since we seek behaviour expected to occur physically, only generic behaviour is of interest. For this reason we do not compute the flow formulas for this perturbation.

5.2.4 Forced Symmetry Breaking to $\mathbf{D}_3[\rho^2, \kappa\rho]$

In this subsection we study forced symmetry breaking of the group orbit X_0, when terms with $\mathbf{D}_3[\rho^2, \kappa\rho]$ symmetry are present. Since X_0 is normally hyperbolic, it persists by the Equivariant Persistence Theorem to give a new invariant manifold X_ε.

We begin with the action of $\mathbf{D}_3[\rho^2, \kappa\rho]$ on $\mathbb{C}^3$. This action is the restriction of the $\mathbf{D}_6$ action

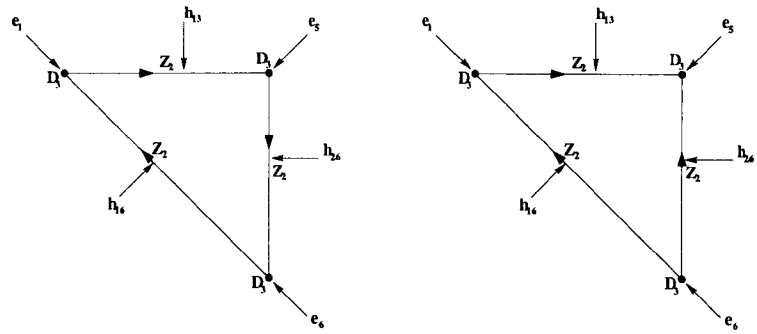

Figure 5.4: Two flows on $\mathbb{X}^p_{\mathbf{D}_3[\rho^2,\kappa]}$ for forced symmetry breaking on the hexagonal lattice.

on $\mathbb{C}^3$ in (5.6). More precisely, we have:

$$\begin{array}{lllllll} \rho^2\mathbf{z} & = & (z_3,z_1,z_2), & \rho^4\mathbf{z} & = & (z_2,z_3,z_1), \\ \kappa\rho\mathbf{z} & = & (\overline{z_2},\overline{z_1},\overline{z_3}), & \kappa\rho^3\mathbf{z} & = & (\overline{z_1},\overline{z_3},\overline{z_2}), \\ \kappa\rho^5\mathbf{z} & = & (\overline{z_3},\overline{z_2},\overline{z_1}). & & & \end{array} \tag{5.11}$$

Calculation of the Skeleton

Using the action (5.11) of $\mathbf{D}_3[\rho^2,\kappa\rho]$ on $\mathbb{C}^3$ we compute the skeleton of X_0. There are six closed subgroups $\mathbf{D}_3[\rho^2,\kappa\rho]$, namely: $\mathbf{D}_3[\rho^2,\kappa\rho]$, $\mathbf{Z}_3[\rho^2]$, $\mathbf{Z}_2[\kappa\rho]$, $\mathbf{Z}_2[\kappa\rho^3]$, $\mathbf{Z}_2[\kappa\rho^5]$, and the trivial subgroup. Since X_0 is a 2-torus and has the standard coordinates (θ_1,θ_2). The next step is the calculation of the set $\mathscr{C}_{\mathbf{D}_3[\rho^2,\kappa\rho]}$.

Proposition 5.16
Let $\mathbf{D}_3[\rho^2,\kappa\rho]$ act on $\mathbb{C}^3$ as in (5.11). Then $\mathscr{C}_{\mathbf{D}_3[\rho^2,\kappa\rho]} = \{e_1,e_5,e_6,c_2,c_4,c_6\}$.

Proof. The proof follows from Lemmas 5.5 and 5.8. □

Using the calculation $\mathscr{C}_{\mathbf{D}_3[\rho^2,\kappa\rho]}$ we may now compute the skeleton $\mathbb{X}_{\mathbf{D}_3[\rho^2,\kappa\rho]}$. We find that

$$\begin{aligned} \mathbb{X}_{\mathbf{D}_3[\rho^2,\kappa\rho]} &= \bigcup_{C\in\mathscr{C}_{\mathbf{D}_3[\rho^2,\kappa\rho]}} C \\ &= c_2 \cup c_4 \cup c_6. \end{aligned}$$

Figure 5.5 illustrates $\mathbb{X}_{\mathbf{D}_3[\rho^2,\kappa\rho]}$.

Symmetry Properties of $\mathbb{X}_{\mathbf{D}_3[\rho^2,\kappa\rho]}$

Here we calculate for any $C \in \mathscr{C}_{\mathbf{D}_3[\rho^2,\kappa\rho]}$ the setwise and pointwise isotropy.

Pointwise and Setwise Isotropy Subgroups. The action of $\mathbf{D}_3[\rho^2,\kappa\rho]$ on $\mathbb{C}^3$ in (5.11) induces a natural action on X_0. Using the coordinates (θ_1,θ_2) on X_0 this action is given by the restriction of the $\mathbf{D}_6$ action on X_0 in (5.12).

$$\begin{array}{lllllll} \rho^2(\theta_1,\theta_2) & = & (-\theta_1-\theta_2,\theta_1), & \rho^4(\theta_1,\theta_2) & = & (\theta_2,-\theta_1-\theta_2), \\ \kappa\rho(\theta_1,\theta_2) & = & (-\theta_2,-\theta_1), & \kappa\rho^3(\theta_1,\theta_2) & = & (-\theta_1,\theta_1+\theta_2), \\ \kappa\rho^5(\theta_1,\theta_2) & = & (\theta_1+\theta_2,-\theta_2). & & & \end{array} \tag{5.12}$$

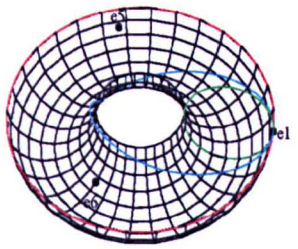

Figure 5.5: The skeleton $\mathbf{X}_{\mathbf{D}_3[\rho^2,\kappa\rho]}$. Here c_2 is red, c_4 is green and, c_6 is cyan.

Table 5.6: Action of $\mathbf{D}_3[\rho^2, \kappa\rho]$ induced on $\mathscr{C}_{\mathbf{D}_3[\rho^2,\kappa\rho]}$.

Element of $\mathscr{C}_{\mathbf{D}_3[\rho^2,\kappa\rho]}$	Elements of $\mathbf{D}_3[\rho^2, \kappa\rho]$ acting nontrivially	Action
e_1	none	
e_5	$\kappa\rho$,$\kappa\rho^3$, $\kappa\rho^5$	e_6
e_6	$\kappa\rho$,$\kappa\rho^3$, $\kappa\rho^5$	e_5
c_2	ρ^4, $\kappa\rho$, ρ^2, $\kappa\rho^3$	c_4 c_6
c_4	ρ^4, $\kappa\rho^3$ ρ^2, $\kappa\rho$,	c_6 c_2
c_6	ρ^4,$\kappa\rho^3$ ρ^2,$\kappa\rho^5$	c_2 c_4

Table 5.7: Isotropy data for $C \in \mathscr{C}_{\mathbf{D}_3[\rho^2,\kappa\rho]}$.

Element of $\mathscr{C}_{\mathbf{D}_3[\rho^2,\kappa\rho]}$	Stab(C)	stab(C)	$S(C)$
e_1	$\mathbf{D}_3[\rho^2,\kappa]$	$\mathbf{D}_3[\rho^2,\kappa]$	$\mathbf{1}$
e_5	$\mathbf{Z}_3[\rho^2]$	$\mathbf{Z}_3[\rho^2]$	$\mathbf{1}$
e_6	$\mathbf{Z}_3[\rho^2]$	$\mathbf{Z}_3[\rho^2]$	$\mathbf{1}$
c_2	$\mathbf{Z}_2[\kappa\rho^5]$	$\mathbf{Z}_2[\kappa\rho^5]$	$\mathbf{1}$
c_4	$\mathbf{Z}_2[\kappa\rho^3]$	$\mathbf{Z}_2[\kappa\rho^3]$	$\mathbf{1}$
c_6	$\mathbf{Z}_2[\kappa\rho]$	$\mathbf{Z}_2[\kappa\rho]$	$\mathbf{1}$

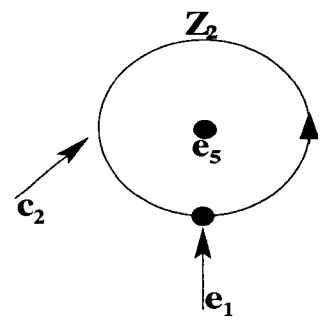

Figure 5.6: A heteroclinic cycle on the projected skeleton $\mathbb{X}^p_{\mathbf{D}_3[\rho^2,\kappa\rho]}$.

The action of $\mathbf{D}_3[\rho^2,\kappa\rho]$ on X_0 induces an action on $\mathscr{C}_{\mathbf{D}_3[\rho^2,\kappa\rho]}$ by permutation. This action is given in Table 5.6. Using the action of $\mathbf{D}_3[\rho^2,\kappa\rho]$ on $\mathscr{C}_{\mathbf{D}_3[\rho^2,\kappa\rho]}$ we may compute the groups Stab(C) and stab(C). This is the content of the next proposition.

Proposition 5.17
Let $\mathbf{D}_3[\rho^2,\kappa\rho]$ act on $\mathscr{C}_{\mathbf{D}_3[\rho^2,\kappa\rho]}$ as in Table 5.6 and on X_0 with the action (5.12). Then given $C \in \mathscr{C}_{\mathbf{D}_3[\rho^2,\kappa\rho]}$, the setwise isotropy Stab(C) and the pointwise isotropy stab(C) and the group $S(C)$ are given in Table 5.7.

Proof. The proof follows directly from Proposition 5.11. □

We have now completed the computations of the setwise and pointwise isotropy subgroups of $C \in \mathscr{C}_{\mathbf{D}_3[\rho^2,\kappa\rho]}$. These computations reveal that $S(C) \cong \mathbf{1}$, for all $C \in \mathscr{C}_{\mathbf{D}_3[\rho^2,\kappa\rho]}$. Hence there are no knots relative to any $C \in \mathscr{C}_{\mathbf{D}_3[\rho^2,\kappa\rho]}$.

Projected Skeleton

Here we compute the projected skeleton $\mathbb{X}^p_{\mathbf{D}_3[\rho^2,\kappa\rho]}$. We have already calculated the action of $\mathbf{D}_3[\rho^2,\kappa\rho]$ on $\mathscr{C}_{\mathbf{D}_3[\rho^2,\kappa\rho]}$, the pointwise and setwise isotropy subgroups and the knots relative to each $C \in \mathscr{C}_{\mathbf{D}_3[\rho^2,\kappa\rho]}$. Using this information we may construct the projected skeleton. The action of $\mathbf{D}_3[\rho^2,\kappa\rho]$ on $\mathscr{C}_{\mathbf{D}_3[\rho^2,\kappa\rho]}$ shows that there are two orbit representatives for points in $E_{(\mathbf{D}_3[\rho^2,\kappa\rho],X_0)}$. These are e_1 and e_5. There are no knots relative to any $C \in \mathscr{C}_{\mathbf{D}_3[\rho^2,\kappa\rho]}$, thus there are no restrictions on the flows about the equilibria . Furthermore, the action of $\mathbf{D}_3[\rho^2,\kappa\rho]$ on $\mathscr{C}_{\mathbf{D}_3[\rho^2,\kappa\rho]}$ shows that there is one orbit representative for the elements of $H_{(\mathbf{D}_3[\rho^2,\kappa\rho],X_0)}$, say $c_2 = \{(\theta,0)|\theta \in (0,2\pi)\}$. (Here we have changed the definition of c_2 slightly so that it is contained in $H_{(\mathbf{D}_3[\rho^2,\kappa\rho],X_0)}$, this makes no difference to the results.) The element c_2 connects e_1 to e_1 and passes through no other equilibria.

Figure 5.6 illustrates the projected skeleton. Since there are no knots along any $C \in \mathscr{C}_{\mathbf{D}_3[\rho^2,\kappa\rho]}$, we see that heteroclinic cycles can occur.

Invariant Theory for $\mathbf{D}_3[\rho^2, \kappa\rho]$

To determine the conditions on a general $\mathbf{D}_3[\rho^2, \kappa\rho]$-equivariant map for no additional equilibria on the connections of the skeleton, we must consider the invariant functions and equivariant maps. Here we compute a set of generators for $\mathcal{E}_{\mathbf{D}_3[\rho^2,\kappa\rho]}$ of invariant functions and $\overrightarrow{\mathcal{E}}_{\mathbf{D}_3[\rho^2,\kappa\rho]}$ of equivariant mappings. By the theorems of Schwarz (Theorem 1.4) and Poénaru (Theorem 1.5) it is sufficient to consider the polynomial ring $\mathcal{P}_{\mathbf{D}_3[\rho^2,\kappa\rho]}$ of invariant polynomial functions and the module $\overrightarrow{\mathcal{P}}_{\mathbf{D}_3[\rho^2,\kappa\rho]}$ of equivariant polynomial mappings. The task of giving a general set of generating equivariant polynomial is too long, so we only consider the equivariants up to quadratic order, which is sufficient for our needs.

We begin with the invariants.

Lemma 5.18
Let $\mathbf{D}_3[\rho^2, \kappa\rho]$ act on $\mathbb{C}^3$ as in (5.11). Then the Poincaré series for the invariants is

$$\begin{aligned}\Upsilon(t) &= \frac{t^6 + t^5 + 5t^4 + 3t^3 + t^2 + 1}{(1-t^3)^2(1-t^2)^3(1-t)} \\ &= 1 + t + 5t^2 + 10t^3 + 24t^4 + 42t^5 + \ldots,\end{aligned}$$

where ... denotes higher order terms.

Proof. See Appendix A. □

Using the Poincaré series we may calculate a set of generating primary invariant polynomials for the ring $\mathcal{P}_{\mathbf{D}_3[\rho^2,\kappa\rho]}$.

Lemma 5.19
Let $\mathbf{D}_3[\rho^2, \kappa\rho]$ act on $\mathbb{C}^3$ as in (5.11). Then the polynomials

$$\begin{aligned}u_1 &= z_1 + z_2 + z_3 + \overline{z_1} + \overline{z_2} + \overline{z_3}, \\ u_2 &= z_1^2 + z_2^2 + z_3^2 + \overline{z_1}^2 + \overline{z_2}^2 + \overline{z_3}^2, \\ u_3 &= z_1z_3 + \overline{z_2z_3} + z_1z_2 + \overline{z_1z_3} + z_2z_3 + \overline{z_1z_2}, \\ u_4 &= z_1\overline{z_1} + z_2\overline{z_2} + z_3\overline{z_3}, \\ u_5 &= z_1^3 + \overline{z_1}^3 + z_2^3 + \overline{z_2}^2 + z_3^3 + \overline{z_3}^3, \\ u_6 &= z_1^2z_2 + z_1z_3^2 + \overline{z_1z_2}^2 + z_2^2z_3 + \overline{z_2z_3}^2 + \overline{z_1}^2\overline{z_3},\end{aligned}$$

are invariant under the action of $\mathbf{D}_3[\rho^2, \kappa\rho]$ and are linearly independent, so they are the primary invariants.

Proof. See Appendix A. □

We have now produce a generating set of primary invariants, we shall not consider the secondary invariants, which are too complex. However, we now consider the polynomial equivariant mappings up to quadratic order.

Lemma 5.20
Let $\mathbf{D}_3[\rho^2, \kappa\rho]$ act on $\mathbb{C}^3$ was in (5.11). Then the Poincaré series for the equivariants is

$$\begin{aligned}\Xi(t) &= \frac{1}{(1-t)^6} \\ &= 1 + 6t + 21t^2 + 56t^3 + 126t^4 + 252t^5 + \ldots,\end{aligned}$$

where ... denotes higher order terms.

Proof. See Appendix A. □

Using the Poincaré series we may construct a generating set of quadratic order generators for the ring $\vec{\mathcal{P}}_{\mathbf{D}_3[\rho^2,\kappa\rho]}$.

Lemma 5.21
Let $\mathbf{D}_3[\rho^2,\kappa\rho]$ act on $\mathbb{C}^3$ as in (5.11). Then the polynomial maps

$$e_1 = \begin{bmatrix} 1 \\ 1 \\ 1 \end{bmatrix}, \quad e_2 = \begin{bmatrix} z_1 \\ z_2 \\ z_3 \end{bmatrix}, \quad e_3 = \begin{bmatrix} wz_2 + \overline{w}z_3 \\ wz_3 + \overline{w}z_1 \\ wz_1 + \overline{w}z_2 \end{bmatrix},$$

$$e_4 = \begin{bmatrix} \overline{z_1} \\ \overline{z_2} \\ \overline{z_3} \end{bmatrix}, \quad e_5 = \begin{bmatrix} w\overline{z_2} + \overline{w}\overline{z_3} \\ w\overline{z_3} + \overline{w}\overline{z_1} \\ w\overline{z_1} + \overline{w}\overline{z_2} \end{bmatrix}, \quad e_6 = \begin{bmatrix} z_1^2 \\ z_2^2 \\ z_3^2 \end{bmatrix},$$

$$e_7 = \begin{bmatrix} wz_2^2 + \overline{w}z_3^2 \\ wz_1^2 + \overline{w}z_3^2 \\ wz_1^2 + \overline{w}z_2^2 \end{bmatrix}, \quad e_8 = \begin{bmatrix} \overline{z_1}^2 \\ \overline{z_2}^2 \\ \overline{z_3}^2 \end{bmatrix}, \quad e_9 = \begin{bmatrix} z_1z_2 + z_1z_3 \\ z_1z_2 + z_2z_3 \\ z_1z_3 + z_2z_3 \end{bmatrix},$$

$$e_{10} = \begin{bmatrix} \overline{z_1z_2} + \overline{z_1z_3} \\ \overline{z_1z_2} + \overline{z_2z_3} \\ \overline{z_1z_3} + \overline{z_2z_3} \end{bmatrix}, \quad e_{11} = \begin{bmatrix} z_1\overline{z_1} \\ z_2\overline{z_2} \\ z_3\overline{z_3} \end{bmatrix},$$

where $w \in \mathbb{C}$ are equivariant under the $\mathbf{D}_3[\rho^2,\kappa]$ action. Furthermore, they generate the module $\vec{\mathcal{P}}_{\mathbf{D}_3[\rho^2,\kappa]}$ over the primary invariants, up to quadratic order.

Proof. See Appendix A. □

It would appear from the Poincaré series for the equivariants that there is a linear order equivariant missing; this is not so, but results from the choice of coordinates used to compute the Poincaré series.

Flow Formula

Here we compute the flow formulas for low order $\mathbf{D}_3[\rho^2,\kappa\rho]$-equivariant perturbations. The $\mathbf{D}_3[\rho^2,\kappa\rho]$-equivariance conditions allow some of the coefficients of the vector field to be complex. Indeed at linear order we have

$$\begin{aligned} g_1(\mathbf{z}) &= p_{1,u_1}u_1 + p_2z_1 + p_3\overline{z_1} + p_4z_2 + \overline{p_4}z_3 + p_5\overline{z_2} + \overline{p_5}\overline{z_3}, \\ g_2(\mathbf{z}) &= p_{1,u_1}u_1 + p_2z_2 + p_3\overline{z_2} + p_4z_3 + \overline{p_4}z_1 + p_5\overline{z_3} + \overline{p_5}\overline{z_1}, \\ g_3(\mathbf{z}) &= p_{1,u_1}u_1 + p_2z_3 + p_3\overline{z_3} + p_4z_1 + \overline{p_4}z_2 + p_5\overline{z_1} + \overline{p_5}\overline{z_2}, \end{aligned}$$

where p_4 and p_5 are complex and all other coefficients are real. We need consider only a linear order perturbation, since that is sufficient to admit heteroclinic cycles. We can safely ignore the equivariant (z_1,z_2,z_3) since only trivial flow is induced. This leaves a total of four equivariants. The only connection we need consider is c_2 (say), which is parametrised by

$$\omega_{c_2}(t) = (e^{it}, 1, e^{-it})$$

for $t \in [0,2\pi]$ and gives the tangent vector

$$\mathcal{T}_{c_2}(t) = (-\sin t, \cos t, 0, 0, -\sin t, -\cos t).$$

It is important to emphasise that our flow formulas are now defined for $t \in [0, 2\pi]$ (rather than just $[0, \pi]$ as in all other previous cases) and so the presence of a "$\sin t$ like term" is not sufficient to guarantee an admissible flow. It is interesting to ask whether there are any general restrictions on the coefficients which allow us to deduce whether a perturbation is admissible or not. Such a condition does exist.

Proposition 5.22
Let $\mathbf{g} \in \vec{\mathcal{E}}_{\mathbf{D}_3[\rho^2,\kappa\rho]}$. Suppose all the coefficients of $\mathbf{g}$ are real. Then $\mathbf{g}$ is not an admissible perturbation.

Proof. Let $\mathbf{g} \in \vec{\mathcal{E}}_{\mathbf{D}_3[\rho^2,\kappa\rho]}$. Then $\mathbf{g}$ may be written in the form (first component only)

$$g_1(\mathbf{z}) = \sum a_{\alpha\beta} z_1^{\alpha_1} z_2^{\alpha_2} z_3^{\alpha_3} \overline{z_1}^{\beta_1} \overline{z_2}^{\beta_2} \overline{z_3}^{\beta_3},$$

where $a_{\alpha\beta} \in \mathbb{R}$, α_i, β_i are integers. Equivariance implies that $g_2(\mathbf{z}) = g_1(z_2, z_3, z_1)$ and $g_3(\mathbf{z}) = g_1(z_3, z_1, z_2)$. Write $\mathbf{g}$ as its real and imaginary parts, so $g_i = g_i^r + \mathrm{i} g_i^I$ where g_i^r and g_i^I are real and $i = 1, 2, 3$. Then

$$\begin{aligned} \mathbf{g}(\mathbf{z}) &= (g_1^r, g_1^I, g_2^r, g_2^I, g_3^r, g_3^I) \\ &= (g_1^r(z_1, z_2, z_3), g_1^I(z_1, z_2, z_3), g_1^r(z_2, z_3, z_1), g_1^I(z_2, z_3, z_1), g_1^r(z_3, z_1, z_2), g_1^I(z_3, z_1, z_2)), \end{aligned}$$

where the second equality follows from equivariance. Evaluating $\mathbf{g}$ along the connection c_2 we find that

$$\begin{aligned} g_1(e^{\mathrm{i}t}, 1, e^{-\mathrm{i}t}) &= \sum a_{\alpha\beta}(\cos(\alpha_1 - \alpha_3)t + \mathrm{i}\sin(\beta_1 - \beta_3)t), \\ g_1(e^{-\mathrm{i}t}, e^{\mathrm{i}t}, 1) &= \sum a_{\alpha\beta}(\cos(-\alpha_1 + \alpha_2)t + \mathrm{i}\sin(-\beta_1 + \beta_2)t). \end{aligned}$$

We have not evaluated g_2 since this term makes no contribution to the flow formula. Since $a_{\alpha\beta} \in \mathbb{R}$,

$$g_1(e^{\mathrm{i}t}, 1, e^{-\mathrm{i}t}) = \sum a_{\alpha\beta}(\cos(\alpha_1 - \alpha_3)t) + \mathrm{i}\sum \sin((\beta_1 - \beta_3)t),$$

so $g_1^r(\mathbf{z}) = \sum a_{\alpha\beta}(\cos(\alpha_1 - \alpha_3)t)$ and $g_1^I(\mathbf{z}) = \sum a_{\alpha\beta}\sin((\beta_1 - \beta_3)t)$. Similar reasoning shows that

$$\begin{aligned} g_1^r(e^{-\mathrm{i}t}, e^{\mathrm{i}t}, 1) &= \sum a_{\alpha\beta}\cos(-\alpha_1 + \alpha_2)t \\ g_1^I(e^{-\mathrm{i}t}, e^{\mathrm{i}t}, 1) &= \sum a_{\alpha\beta}\sin(-\beta_1 + \beta_2)t. \end{aligned}$$

Therefore the flow formula is

$$\begin{aligned} \mathcal{F}(t) &= \langle \mathbf{g}(\omega_{c_2}(t)), \mathcal{T}_{c_2}(t) \rangle \\ &= -\sin t \sum a_{\alpha\beta}\cos(\alpha_1 - \alpha_3)t + \cos t \sum a_{\alpha\beta}\sin(\beta_1 - \beta_3)t \\ &\quad -\sin t \sum a_{\alpha\beta}\cos(-\alpha_1 + \alpha_2)t - \cos t \sum a_{\alpha\beta}\sin(-\beta_1 + \beta_2)t. \\ &= -\sin t \left(\sum a_{\alpha\beta}\cos(\alpha_1 - \alpha_3)t + \cos(-\alpha_1 + \alpha_2)t\right) \\ &\quad -\cos t \left(\sum a_{\alpha\beta}\sin(\beta_1 - \beta_3)t + \sin(-\beta_1 + \beta_2)t\right). \end{aligned}$$

Since $a_{\alpha\beta} \in \mathbb{R}$, α_i and β_i are integers, $\mathcal{F}(\pi) = 0$, so the perturbation is not admissible. □

Remark 5.23
This proposition holds for any $\mathbf{D}_3[\rho^2, \kappa\rho]$-equivariant map, and not just some low order truncation. So, if we want to see heteroclinic cycles, the perturbation term must have some non-real coefficients.

In the rest of this section we develop a classification of those perturbations $\mathbf{g}$ which are admissible—and by implication give heteroclinic cycles. We shall consider only a single equivariant at a time, which by the linearity of $\mathcal{F}^{\mathbf{g}}(t)$ gives the flow formulas for any perturbation involving these terms. Since the Poincaré series shows that there is a total of 27 linear and quadratic equivariants, no attempt will be made to determine all types of behaviour up to quadratic order. This is not really that limiting; linear perturbations are sufficient to find admissible perturbations. Furthermore, the equivariance condition $\overline{g_1(z_1,z_2,z_3)} = g_1(\overline{z_1},\overline{z_3},\overline{z_2})$ shows that the coefficients of the perturbations (u_1,u_1,u_1) and $(\overline{z_1},\overline{z_2},\overline{z_3})$ are all real and hence by Proposition 5.22 they do not induce admissible flows. This leaves only two different equivariants to consider.

Proposition 5.24
Define $\mathbf{g}:\mathbb{C}^3\to\mathbb{C}^3$ *by* $\mathbf{g}(\mathbf{z}) = (cz_2+\bar{c}z_3, cz_1+\bar{c}z_3, cz_2+\bar{c}z_1)$, *where* $c = a+\mathrm{i}b \in \mathbb{C}$. *Then the flow formula is*

$$\mathcal{F}^{\mathbf{g}}(t) = 4x^2\sin(3t/2)\left(-a\cos\left(\frac{t}{2}\right)+b\sin\left(\frac{t}{2}\right)\right).$$

This flow has additional zeros at $t = 2\pi/3$ *and* $t = 4\pi/3$ *and so is not admissible.*

Proof. Define $\mathbf{g}(\mathbf{z}) = (cz_2+\bar{c}z_3, cz_3+\bar{c}z_1, cz_2+\bar{c}z_1)$. Then (not evaluating the g_2 component, which is not required)

$$\begin{aligned}\mathbf{g}(\omega_{c_2}(t)) &= ((a+\mathrm{i}b)+(a-\mathrm{i}b)(\cos t-\mathrm{i}\sin t), g_2, (a+\mathrm{i}b)(\cos t+\mathrm{i}\sin t)+(a-\mathrm{i}b))\\ &= (a+a\cos t-b\sin t, b-b\cos t-a\sin t, g_2, a\cos t-b\sin t+a, b\cos t+a\sin t-b).\end{aligned}$$

Hence the flow formula is

$$\begin{aligned}\mathcal{F}(t) &= (-\sin t(a+a\cos t-b\sin t)+\cos t(b-b\cos t-a\sin t)-\sin t(a\cos t-b\sin t+a)\\ &\quad -\cos t(b\cos t+a\sin t-b))x^2\\ &= (-2a\sin t+2b\cos t-4a\sin t\cos t+2b\sin^2 t-2b\cos^2 t)x^2\\ &= 4x^2\sin(3t/2)\left(-a\cos\left(\frac{t}{2}\right)+b\sin\left(\frac{t}{2}\right)\right),\end{aligned}$$

with the final equality following from some tedious algebra. The location of the additional zeros is easily seen from the $\sin(3t/2)$ term. □

There is one linear perturbation remaining as a candidate for an admissible perturbation.

Proposition 5.25
Define $\mathbf{g}:\mathbb{C}^3\to\mathbb{C}^3$ *by* $\mathbf{g}(\mathbf{z}) = (d\overline{z_3}+\bar{d}\overline{z_2}, d\overline{z_1}+\bar{d}\overline{z_3}, d\overline{z_2}+\bar{d}\overline{z_1})$, *where* $d = a+\mathrm{i}b \in \mathbb{C}$. *Then the flow formula is*

$$\mathcal{F}^{\mathbf{g}}(t) = -2x^2(a\sin t+b(\cos t-1)).$$

If $|b| > a$ *then the flow formula has no additional zeros and the perturbation is admissible.*

Proof. Define $\mathbf{g}(\mathbf{z}) = (d\overline{z_3}+\bar{d}\overline{z_2}, d\overline{z_1}+\bar{d}\overline{z_3}, d\overline{z_2}+\bar{d}\overline{z_1})$. Then (not evaluating the g_2 component, which is not required) we find

$$\begin{aligned}\mathbf{g}(\omega_{c_1}(t)) &= ((a-\mathrm{i}b)+(a+\mathrm{i}b)(\cos t+\mathrm{i}\sin t), g_2, (a-\mathrm{i}b)(\cos t-\mathrm{i}\sin t)+(a+\mathrm{i}b))\\ &= (a+a\cos t-b\sin t, -b+b\cos t+a\sin t, g_2,\\ &\quad a\cos t-b\sin t+a, -b\cos t-a\sin t+b).\end{aligned}$$

Hence the flow formula is

$$\begin{aligned}\mathcal{F}(t) &= (-\sin t(a+a\cos t-b\sin t)+\cos t(-b+b\cos t+a\sin t)-\sin t(a\cos t-b\sin t+a)\\ &\quad -\cos t(-b\cos t-a\sin t+b))x^2\\ &= -2x^2(a\sin t+b(\cos t-1)).\end{aligned}$$

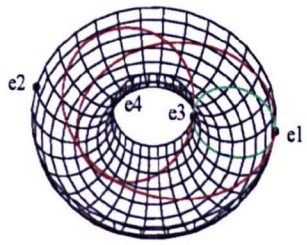

Figure 5.7: The skeleton $\mathbf{X}_{\mathbf{D}_2[\rho^3,\kappa]}$. Here c_4 is green and c_7 is brown.

Now $(\cos t - 1) < 0$ for all $t \in (0, 2\pi)$, so if $|b| > a$ we have no additional zeros. □

Thus we have found the linear admissible perturbation alluded to earlier. As always, this allows us to create as many admissible perturbations as desired, each giving a heteroclinic cycle.

5.2.5 Forced Symmetry Breaking to $\mathbf{D}_2[\rho^3, \kappa]$

In this subsection we study forced symmetry breaking of the group orbit X_0 when terms with $\mathbf{D}_2[\rho^3, \kappa]$ symmetry are used to perturbed (5.5). Since X_0 is normally hyperbolic, by the Equivariant Persistence Theorem, there exists a new invariant manifold X_ε which is $\mathbf{D}_2[\rho^3, \kappa]$-equivariantly diffeomorphic to X_0. We shall study the $\mathbf{D}_2[\rho^3, \kappa]$ action on X_0, which via the diffeomorphism allows us to study X_ε. The action of $\mathbf{D}_2[\rho^3, \kappa]$ on $\mathbb{C}^3$ is

$$\begin{aligned} \rho^3 \mathbf{z} &= (\overline{z_1}, \overline{z_2}, \overline{z_3}), \\ \kappa \mathbf{z} &= (z_1, z_3, z_2), \\ \kappa\rho^3 \mathbf{z} &= (\overline{z_1}, \overline{z_3}, \overline{z_2}). \end{aligned} \tag{5.13}$$

Calculation of the Skeleton

Using the action (5.13) of $\mathbf{D}_2[\rho^3, \kappa]$ on $\mathbb{C}^3$ we compute the skeleton of X_0. There are five closed subgroups of $\mathbf{D}_2[\rho^3, \kappa]$, namely $\mathbf{D}_2[\rho^3, \kappa]$, $\mathbf{Z}_2[\rho^3]$, $\mathbf{Z}_2[\kappa]$, $\mathbf{Z}_2[\kappa\rho^3]$ and the trivial subgroup. Since X_0 is a 2-torus we have standard coordinates (θ_1, θ_2). The next step is the calculation of the set $\mathscr{C}_{\mathbf{D}_2[\rho^3,\kappa]}$.

Proposition 5.26
Let $\mathbf{D}_2[\rho^3, \kappa]$ act on $\mathbb{C}^3$ as in (5.13). Then $\mathscr{C}_{\mathbf{D}_2[\rho^3,\kappa]} = \{e_1, e_2, e_3, e_4, c_4, c_7\}$.

Proof. The proof follows from Lemmas 5.7 and 5.8. □

Using the calculation $\mathscr{C}_{\mathbf{D}_2[\rho^3,\kappa]}$ we may now compute the skeleton $\mathbf{X}_{\mathbf{D}_2[\rho^3,\kappa]}$. We find that

$$\begin{aligned} \mathbf{X}_{\mathbf{D}_2[\rho^3,\kappa]} &= \bigcup_{C \in \mathscr{C}_{\mathbf{D}_2[\rho^3,\kappa]}} C \\ &= e_1 \cup e_2 \cup e_3 \cup e_4 \cup c_4 \cup c_7. \end{aligned}$$

Figure 5.7 shows $\mathbf{X}_{\mathbf{D}_2[\rho^3,\kappa]}$.

Table 5.8: Action of $\mathbf{D}_2[\rho^3,\kappa]$ induced on $\mathscr{C}_{\mathbf{D}_2[\rho^3,\kappa]}$.

Element of $\mathscr{C}_{\mathbf{D}_2[\rho^3,\kappa]}$	Elements of $\mathbf{D}_2[\rho^3,\kappa]$ acting nontrivially	Action
e_1	none	
e_2	κ,$\kappa\rho^3$	e_4
e_3	none	
e_4	κ, $\kappa\rho^3$	e_2
c_4	none	
c_7	none	

Table 5.9: Isotropy data for $C \in \mathscr{C}_{\mathbf{D}_2[\rho^3,\kappa]}$.

Element of $\mathscr{C}_{\mathbf{D}_2[\rho^3,\kappa]}$	Stab(C)	stab(C)	$S(C)$
e_1	$\mathbf{D}_2[\rho^3,\kappa]$	$\mathbf{D}_2[\rho^3,\kappa]$	$\mathbf{1}$
e_2	$\mathbf{Z}_2[\rho^3]$	$\mathbf{Z}_2[\rho^3]$	$\mathbf{1}$
e_3	$\mathbf{D}_2[\rho^3,\kappa]$	$\mathbf{D}_2[\rho^3,\kappa]$	$\mathbf{1}$
e_4	$\mathbf{Z}_2[\rho^3]$	$\mathbf{Z}_2[\rho^3]$	$\mathbf{1}$
c_4	$\mathbf{D}_2[\rho^3,\kappa]$	$\mathbf{Z}_2[\kappa\rho^3]$	$\mathbf{Z}_2$
c_7	$\mathbf{D}_2[\rho^3,\kappa]$	$\mathbf{Z}_2[\kappa]$	$\mathbf{Z}_2$

Symmetry Properties of $\mathbb{X}_{\mathbf{D}_2[\rho^3,\kappa]}$

Here we calculate for any $C \in \mathscr{C}_{\mathbf{D}_2[\rho^3,\kappa]}$ the setwise and pointwise isotropy.

Pointwise and Setwise Isotropy Subgroups. The action (5.13) of $\mathbf{D}_2[\rho^3,\kappa]$ on $\mathbb{C}^3$ induces a natural action on X_0. This action is given by the restriction of the $\mathbf{D}_6$ action on X_0 in (5.9):

$$\begin{aligned} \rho^3(\theta_1,\theta_2) &= (-\theta_1,-\theta_2), \\ \kappa(\theta_1,\theta_2) &= (\theta_1,-\theta_1-\theta_2), \\ \kappa\rho^3(\theta_1,\theta_2) &= (-\theta_1,\theta_1+\theta_2). \end{aligned} \tag{5.14}$$

The action of $\mathbf{D}_2[\rho^3,\kappa]$ on X_0 induces an action on $\mathscr{C}_{\mathbf{D}_2[\rho^3,\kappa]}$ by permutation of its elements. This action is given in Table 5.8. Using the action of $\mathbf{D}_2[\rho^3,\kappa]$ on $\mathscr{C}_{\mathbf{D}_2[\rho^3,\kappa]}$ we may compute the groups Stab(C) and stab(C). This is the content of the next proposition.

Proposition 5.27
Let $\mathbf{D}_2[\rho^3,\kappa]$ act on $\mathscr{C}_{\mathbf{D}_2[\rho^3,\kappa]}$ as in Table 5.8. Then given $C \in \mathscr{C}_{\mathbf{D}_2[\rho^3,\kappa]}$, the setwise isotropy Stab(C) and the pointwise isotropy stab(C) and the group $S(C)$ are given in Table 5.9.

Proof. The proof follows directly from Proposition 5.11. □

We have now completed the computations of the setwise and pointwise isotropy subgroups of $C \in \mathscr{C}_{\mathbf{D}_2[\rho^3,\kappa]}$. These computations reveal that $S(C) \cong \mathbf{Z}_2$, for all $C \in \mathscr{C}_{\mathbf{D}_2[\rho^3,\kappa]}$, with $C \cong \mathbf{S}^1$. Therefore, each such C has two knots, these knots are given by the two equilibria which lie on C. So the knots are e_1 and e_3 for both C's.

Projected Skeleton

The action of $\mathbf{D}_2[\rho^3,\kappa]$ on $\mathscr{C}_{\mathbf{D}_2[\rho^3,\kappa]}$ shows that there are three orbit representatives for points in $E_{(\mathbf{D}_2[\rho^3,\kappa],X_0)}$. These are e_1, e_3, and e_4. There are knots on c_4 and c_7. Furthermore, the action of $\mathbf{D}_2[\rho^3,\kappa]$ on $\mathscr{C}_{\mathbf{D}_2[\rho^3,\kappa]}$ shows that there are two orbit representative for the elements of

$H_{(\mathbf{D}_2[\rho^3,\kappa],X_0)}$. These are $h_7 = \{(0,\theta)|\theta \in [0,\pi)\}$ and $h_{27} = \{(2\theta,-\theta)|\theta \in [0,\pi)\}$. The element h_7 connects e_1 to e_3 and h_{27} connects e_1 to e_3. Figure 5.8 illustrates the projected skeleton with two flows.

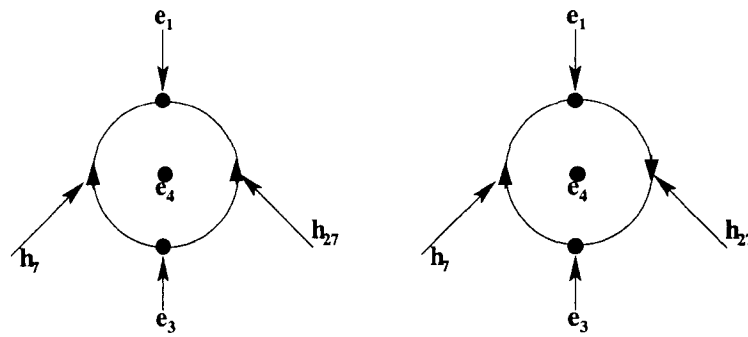

Figure 5.8: Two flows on $\mathbb{X}^p_{\mathbf{D}_2[\rho^3,\kappa]}$.

Flow Formula

A general classification of the flow formulas is too complex to undertake; there are just too many different possibilities even at quadratic order, the main problem being that the first component of the vector field is unrelated to the second and third. For this reason we consider an example which illustrates how admissible flows, and in particular heteroclinic cycles, exist for an open set of perturbations.

Example 5.28
Define $\mathbf{g} : \mathbb{C}^3 \to \mathbb{C}^3$ by $\mathbf{g}(\mathbf{z}) = (g_1, g_2, g_3) = (az_1(z_2 + z_3), b(z_2\overline{z_2} + z_3\overline{z_3}), b(z_2\overline{z_2} + z_3\overline{z_3}))$. Then $\mathbf{g}$ is $\mathbf{D}_2[\rho^3, \kappa]$-equivariant. The connections on the skeleton are h_7 and h_{27}. Along h_7 the g_1 component of the vector field does not contribute to the flow formula. Hence

$$\mathbf{g}(\omega_{h_7}(t)) = (\star, 2b, 2b)x^2,$$

where $\star$ denotes an entry that is not required. From this we get $\mathcal{F}^{\mathbf{g}}_{h_7}(t) = -4x^3 b \sin t$. Next we consider the flow along h_{27}, we find that

$$\mathbf{g}(\omega_{h_{27}}(t)) = (2ae^{it}, 2b, 2b)x^2,$$

Hence the flow formula is given by $\mathcal{F}^{\mathbf{g}}_{h_{27}}(t) = -4x^3(a(\sin 2t \cos t + \sin t \cos 2t - b \sin t) = -4x^3(a + b) \sin t$. Now the flow along h_7 is admissible if $b \neq 0$, the flow along h_{27} is admissible provided $(a + b) \neq 0$, for heteroclinic cycles we require $\mathrm{sgn}(b) = -\mathrm{sgn}(a + b)$. By taking suitable linear combinations with other $\mathbf{D}_2[\rho^3, \kappa]$-equivariants we can exhibit as many different heteroclinic cycles as we please, provided the perturbation $\mathbf{g}$ dominates.

5.2.6 Forced Symmetry Breaking to $\mathbf{D}_2[\rho^3, \kappa\rho]$

In this subsection we study forced symmetry breaking of the group orbit X_0 under a $\mathbf{D}_3[\rho^3, \kappa\rho]$-equivariant perturbation. Since X_0 is normally hyperbolic, by the Equivariant Persistence Theorem, there exists an invariant manifold X_ϵ which is $\mathbf{D}_2[\rho^3, \kappa\rho]$-equivariantly diffeomorphic

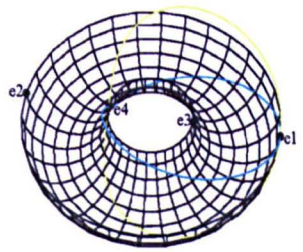

Figure 5.9: The skeleton $\mathbf{X}_{\mathbf{D}_2[\rho^2,\kappa\rho]}$. Here c_1 is yellow and c_6 is cyan.

to X_0. The action of $\mathbf{D}_2[\rho^3,\kappa\rho]$ on $\mathbb{C}^3$ is:

$$\begin{aligned} \rho^3\mathbf{z} &= (\overline{z_1},\overline{z_2},\overline{z_3}), \\ \kappa\rho\mathbf{z} &= (\overline{z_2},\overline{z_1},\overline{z_3}), \\ \kappa\rho^4\mathbf{z} &= (z_2,z_1,z_3). \end{aligned} \tag{5.15}$$

(5.16)

Calculation of the Skeleton

Using the action (5.15) of $\mathbf{D}_2[\rho^3,\kappa\rho]$ on $\mathbb{C}^3$ we compute the skeleton of X_0. There are five closed subgroups of $\mathbf{D}_2[\rho^3,\kappa\rho]$, namely: $\mathbf{D}_2[\rho^3,\kappa\rho]$, $\mathbf{Z}_2[\rho^3]$, $\mathbf{Z}_2[\kappa\rho]$, $\mathbf{Z}_2[\kappa\rho^4]$ and the trivial subgroup. The next step is the calculation of the set $\mathscr{C}_{\mathbf{D}_2[\rho^3,\kappa\rho]}$.

Proposition 5.29
Let $\mathbf{D}_2[\rho^3,\kappa\rho]$ act on $\mathbb{C}^3$ as in (5.15). Then $\mathscr{C}_{\mathbf{D}_2[\rho^3,\kappa\rho]} = \{e_1,e_2,e_3,e_4,c_1,c_6\}$.

Proof. The proof follows from Lemmas 5.7 and 5.8. □

Using the calculation $\mathscr{C}_{\mathbf{D}_2[\rho^3,\kappa\rho]}$ we may now compute the skeleton $\mathbf{X}_{\mathbf{D}_2[\rho^3,\kappa\rho]}$. We find that

$$\begin{aligned} \mathbf{X}_{\mathbf{D}_2[\rho^3,\kappa\rho]} &= \bigcup_{C\in\mathscr{C}_{\mathbf{D}_2[\rho^3,\kappa\rho]}} C \\ &= e_1\cup e_2\cup e_3\cup e_4\cup c_1\cup c_6. \end{aligned}$$

Figure 5.9 illustrates $\mathbf{X}_{\mathbf{D}_2[\rho^3,\kappa\rho]}$.

Symmetry Properties of $\mathbf{X}_{\mathbf{D}_2[\rho^3,\kappa\rho]}$

Here we calculate, for any $C\in\mathscr{C}_{\mathbf{D}_2[\rho^3,\kappa\rho]}$, the setwise and pointwise isotropy. From these two groups we may calculate the group $S(C)$ which gives information on the projected skeleton $\mathbf{X}^p_{\mathbf{D}_2[\rho^3,\kappa\rho]}$. In particular we may use the group $S(C)$ to compute the axis of symmetry (if any) on $C\in\mathscr{C}_{\mathbf{D}_2[\rho^3,\kappa\rho]}$.

Pointwise and Setwise Isotropy Subgroups. The action (5.15) of $\mathbf{D}_2[\rho^3,\kappa\rho]$ on $\mathbb{C}^3$ induces a natural action on X_0. Using the coordinates (θ_1,θ_2) on X_0 this action is given by the restriction of the $\mathbf{D}_6$ action on X_0 in (5.17).

$$\begin{aligned} \rho^3(\theta_1,\theta_2) &= (-\theta_1,-\theta_2), && (5.17)\\ \kappa\rho(\theta_1,\theta_2) &= (-\theta_2,-\theta_1), && (5.18)\\ \kappa\rho^4(\theta_1,\theta_2) &= (\theta_2,\theta_1). && (5.19) \end{aligned}$$

Table 5.10: Action of $\mathbf{D}_2[\rho^3, \kappa\rho]$ induced on $\mathscr{C}_{\mathbf{D}_2[\rho^3,\kappa\rho]}$.

Element of $\mathscr{C}_{\mathbf{D}_2[\rho^3,\kappa\rho]}$	Elements of $\mathbf{D}_2[\rho^3, \kappa\rho]$ acting non-trivially	Action
e_1	none	
e_2	$\kappa\rho^4$,$\kappa\rho$	e_3
e_3	$\kappa\rho^4$,$\kappa\rho$	e_2
e_4	none	
c_1	none	
c_6	none	

Table 5.11: Isotropy data for $C \in \mathscr{C}_{\mathbf{D}_2[\rho^3,\kappa\rho]}$.

Element of $\mathscr{C}_{\mathbf{D}_2[\rho^3,\kappa\rho]}$	Stab(C)	stab(C)	$S(C)$
e_1	$\mathbf{D}_2[\rho^3, \kappa\rho]$	$\mathbf{D}_2[\rho^3, \kappa\rho]$	$\mathbf{1}$
e_2	$\mathbf{Z}_2[\rho^3]$	$\mathbf{Z}_2[\rho^3]$	$\mathbf{1}$
e_3	$\mathbf{Z}_2[\rho^3]$	$\mathbf{Z}_2[\rho^3]$	$\mathbf{1}$
e_4	$\mathbf{D}_2[\rho^3, \kappa\rho]$	$\mathbf{D}_2[\rho^3, \kappa\rho]$	$\mathbf{1}$
c_1	$\mathbf{D}_2[\rho^3, \kappa\rho]$	$\mathbf{Z}_2[\kappa\rho^4]$	$\mathbf{Z}_2$
c_6	$\mathbf{D}_2[\rho^3, \kappa\rho]$	$\mathbf{Z}_2[\kappa\rho]$	$\mathbf{Z}_2$

The action of $\mathbf{D}_2[\rho^3, \kappa\rho]$ on X_0 induces an action on $\mathscr{C}_{\mathbf{D}_2[\rho^3,\kappa\rho]}$ by permutation. This action is given in Table 5.10. Using the action of $\mathbf{D}_2[\rho^3, \kappa\rho]$ on $\mathscr{C}_{\mathbf{D}_2[\rho^3,\kappa\rho]}$ we may compute the groups Stab(C) and stab(C).

Proposition 5.30
Let $\mathbf{D}_2[\rho^3, \kappa\rho]$ act on $\mathscr{C}_{\mathbf{D}_2[\rho^3,\kappa\rho]}$ as in Table 5.10 and on X_0 with the action in (5.17). Then given $C \in \mathscr{C}_{\mathbf{D}_2[\rho^3,\kappa\rho]}$, the setwise isotropy Stab(C) and the pointwise isotropy stab(C) and group $S(C)$ are given in Table 5.11.

Proof. The proof follows directly from Proposition 5.11. □

We have now completed the computations of the setwise and pointwise isotropy subgroups of $C \in \mathscr{C}_{\mathbf{D}_2[\rho^3,\kappa\rho]}$. These computations reveal that $S(C) \cong \mathbf{Z}_2$, for all $C \in \mathscr{C}_{\mathbf{D}_2[\rho^3,\kappa\rho]}$ with $C \cong \mathbf{S}^1$. Hence there are knots on c_1 and c_6, and these must be the equilibria e_1 and e_4.

Projected Skeleton

We have calculated the action of $\mathbf{D}_2[\rho^3, \kappa\rho]$ on $\mathscr{C}_{\mathbf{D}_2[\rho^3,\kappa\rho]}$, the pointwise and setwise isotropy subgroups and the knots relative to each $C \in \mathscr{C}_{\mathbf{D}_2[\rho^3,\kappa\rho]}$. Using this information we may construct the projected skeleton.

The action of $\mathbf{D}_2[\rho^3, \kappa\rho]$ on $\mathscr{C}_{\mathbf{D}_2[\rho^3,\kappa\rho]}$ shows that there are three orbit representatives for points in $E_{(\mathbf{D}_2[\rho^3,\kappa\rho],X_0)}$. These are e_1, e_2 and e_4. There are knots relative to any $C \in \mathscr{C}_{\mathbf{D}_2[\rho^3,\kappa\rho]}$, with $C \cong \mathbf{S}^1$, thus there are restrictions on the flows about the equilibria. Furthermore, the action of $\mathbf{D}_2[\rho^3, \kappa\rho]$ on $\mathscr{C}_{\mathbf{D}_2[\rho^3,\kappa\rho]}$ shows that there are two orbit representatives for the elements of $H_{(\mathbf{D}_2[\rho^3,\kappa\rho],X_0)}$. These are $h_1 = \{(\theta,\theta)|\theta \in [0,\pi)\}$ and $h_{11} = \{(\theta,-\theta)|\theta \in [0,\pi)\}$. The elements h_1 and h_{11} connect e_1 to e_4. Figure 5.10 we illustrates the projected skeleton, with two flows.

Flow Formula

Here we present an example of a $\mathbf{D}_2[\rho^3, \kappa\rho]$-equivariant perturbation which gives a heteroclinic cycle on $\mathbb{X}_{\mathbf{D}_2[\rho^3,\kappa]}$.

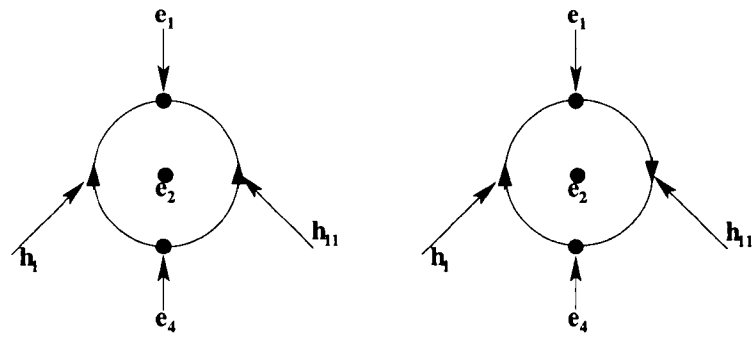

Figure 5.10: Two flows on the projected skeleton $\mathbb{X}^p_{\mathbf{D}_2[\rho^3,\kappa\rho]}$.

Example 5.31
The function defined by

$$\mathbf{g}(\mathbf{z}) = (a(z_1\overline{z_1} + z_2\overline{z_2}), a(z_1\overline{z_1} + z_2\overline{z_2}), b(z_3(z_1 + z_2)),$$

where a and b are real, is $\mathbf{D}_2[\rho^3, \kappa\rho]$-equivariant. The connections on $\mathbb{X}_{\mathbf{D}_2[\rho^3,\kappa\rho]}$ are given by h_1 and h_{11}. Along the h_1 connection we find that $\mathbf{g}(\omega_{h_1}(t)) = (2a, 2a, 2be^{-it})x^2$. Hence the flow formula is

$$\begin{aligned} \mathcal{F}^{\mathbf{g}}_{h_1}(t) &= -4ax^3 \sin t - 4bx^3(\sin 2t \cos t - \sin t \cos 2t) \\ &= -4x^3(a+b)\sin t. \end{aligned}$$

The flow along h_{11} is very simple to compute since the third component of g_3 makes no contribution. We find that $\mathcal{F}^{\mathbf{g}}_{h_{11}}(t) = -4x^3 a \sin t$. From here it is easy to arrange for heteroclinic cycles; we only require $\mathrm{sgn}(a) = -\mathrm{sgn}(a+b)$. Such cycles exist for any combination of $\mathbf{g}$ with other $\mathbf{D}_2[\rho^3, \kappa\rho]$-equivariant perturbations provided the $\mathbf{g}$ term dominates.

5.2.7 Forced Symmetry Breaking to $\mathbf{D}_2[\rho^3, \kappa\rho^2]$

In this final subsection we study forced symmetry breaking of the group orbit X_0 when perturbed by a $\mathbf{D}_2[\rho^3, \kappa\rho^2]$-equivariant mapping. Since X_0 is normally hyperbolic, by the Equivariant Persistence Theorem, there exists an invariant manifold X_ε which is $\mathbf{D}_2[\rho^3, \kappa\rho^2]$-equivariantly diffeomorphic to X_0. The action of $\mathbf{D}_2[\rho^3, \kappa\rho^2]$ on $\mathbb{C}^3$ is

$$\begin{aligned} \rho^3\mathbf{z} &= (\overline{z_1}, \overline{z_2}, \overline{z_3}), \\ \kappa\rho^2\mathbf{z} &= (z_3, z_2, z_1), \\ \kappa\rho^5\mathbf{z} &= (\overline{z_3}, \overline{z_2}, \overline{z_1}). \end{aligned} \tag{5.20}$$

Calculation of the Skeleton

Using the action of $\mathbf{D}_2[\rho^3, \kappa\rho^2]$ on $\mathbb{C}^3$ in (5.20) we compute the skeleton of X_0. There are five closed subgroups of $\mathbf{D}_2[\rho^3, \kappa\rho^2]$, namely: $\mathbf{D}_2[\rho^3, \kappa\rho^2]$, $\mathbf{Z}_2[\rho^3]$, $\mathbf{Z}_2[\kappa\rho^2]$, $\mathbf{Z}_2[\kappa\rho^5]$ and the trivial subgroup. The next step is the calculation of the set $\mathscr{C}_{\mathbf{D}_2[\rho^3,\kappa\rho^2]}$.

Proposition 5.32
Let $\mathbf{D}_2[\rho^3, \kappa\rho^2]$ act on $\mathbb{C}^3$ as in (5.20). Then $\mathscr{C}_{\mathbf{D}_2[\rho^3,\kappa\rho^2]} = \{e_1, e_2, e_3, e_4, c_2, c_8\}$.

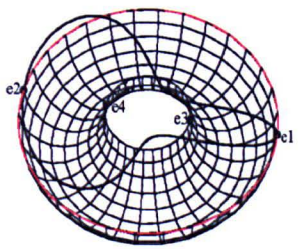

Figure 5.11: The skeleton $\mathbf{X}_{\mathbf{D}_2[\rho^2,\kappa\rho^2]}$. Here c_2 is red and c_8 is black.

Table 5.12: Action of $\mathbf{D}_2[\rho^3, \kappa\rho^2]$ induced on $\mathscr{C}_{\mathbf{D}_2[\rho^3,\kappa\rho^2]}$.

Element of $\mathscr{C}_{\mathbf{D}_2[\rho^3,\kappa\rho^2]}$	Elements of $\mathbf{D}_2[\rho^4, \kappa\rho^2]$ acting non-trivially	Action
e_1	none	
e_2	none	
e_3	$\kappa\rho^2$, $\kappa\rho^5$	e_4
e_4	$\kappa\rho^2$, $\kappa\rho^5$	e_3
c_2	none	
c_8	none	

Proof. The proof follows from Lemmas 5.7 and 5.8. □

Using the calculation $\mathscr{C}_{\mathbf{D}_2[\rho^3,\kappa\rho^2]}$ we may now compute the skeleton $\mathbf{X}_{\mathbf{D}_2[\rho^3,\kappa\rho^2]}$. We find that

$$\begin{aligned}\mathbf{X}_{\mathbf{D}_2[\rho^3,\kappa\rho^2]} &= \bigcup_{C\in\mathscr{C}_{\mathbf{D}_2[\rho^3,\kappa\rho]}} C \\ &= e_1 \cup e_2 \cup e_3 \cup e_4 \cup c_2 \cup c_8.\end{aligned}$$

Figure 5.11 illustrates of $\mathbf{X}_{\mathbf{D}_2[\rho^3,\kappa\rho^2]}$.

Symmetry Properties of $\mathbf{X}_{\mathbf{D}_2[\rho^3,\kappa\rho^2]}$

Here we calculate, for any $C \in \mathscr{C}_{\mathbf{D}_2[\rho^3,\kappa\rho^2]}$, the setwise and pointwise isotropy.

Pointwise and Setwise Isotropy Subgroups. The action (5.20) of $\mathbf{D}_2[\rho^3, \kappa\rho^2]$ on $\mathbb{C}^3$ induces a natural action on X_0. Using the coordinates (θ_1, θ_2) on X_0 this action is given by the restriction of the $\mathbf{D}_6$ action on X_0 in (5.21).

$$\rho^3(\theta_1,\theta_2) = (-\theta_1,-\theta_2), \tag{5.21}$$
$$\kappa\rho^2(\theta_1,\theta_2) = (-\theta_1-\theta_2,\theta_2), \tag{5.22}$$
$$\kappa\rho^5(\theta_1,\theta_2) = (\theta_1+\theta_2,-\theta_2). \tag{5.23}$$

The action of $\mathbf{D}_2[\rho^3, \kappa\rho^2]$ on X_0 induces an action on $\mathscr{C}_{\mathbf{D}_2[\rho^3,\kappa\rho^2]}$ by permutation. This action is given in Table 5.12. Using the action of $\mathbf{D}_2[\rho^3, \kappa\rho^2]$ on $\mathscr{C}_{\mathbf{D}_2[\rho^3,\kappa\rho^2]}$ we may compute the groups Stab(C) and stab(C). This is the content of the next proposition.

Table 5.13: Isotropy data for $C \in \mathscr{C}_{\mathbf{D}_2[\rho^3,\kappa\rho^2]}$.

Element of $\mathscr{C}_{\mathbf{D}_2[\rho^3,\kappa\rho^2]}$	Stab(C)	stab(C)	$S(C)$
e_1	$\mathbf{D}_2[\rho^3,\kappa\rho^2]$	$\mathbf{D}_2[\rho^3,\kappa\rho^2]$	$\mathbf{1}$
e_2	$\mathbf{D}_2[\rho^3,\kappa\rho^2]$	$\mathbf{D}_2[\rho^3,\kappa\rho^2]$	$\mathbf{1}$
e_3	$\mathbf{Z}_2[\rho^3]$	$\mathbf{Z}_2[\rho^3]$	$\mathbf{1}$
e_4	$\mathbf{Z}_2[\rho^3]$	$\mathbf{Z}_2[\rho^3]$	$\mathbf{1}$
c_2	$\mathbf{D}_2[\rho^3,\kappa\rho^2]$	$\mathbf{Z}_2[\kappa\rho^5]$	$\mathbf{Z}_2$
c_8	$\mathbf{D}_2[\rho^3,\kappa\rho^2]$	$\mathbf{Z}_2[\kappa\rho^2]$	$\mathbf{Z}_2$

Proposition 5.33
Let $\mathbf{D}_2[\rho^3,\kappa\rho^2]$ act on $\mathscr{C}_{\mathbf{D}_2[\rho^3,\kappa\rho]}$ as in Table 5.12 and on X_0 with the action in (5.21). Then given $C \in \mathscr{C}_{\mathbf{D}_2[\rho^3,\kappa\rho^2]}$, the setwise isotropy Stab(C) and the pointwise isotropy stab(C) and the group $S(C)$ are given in Table 5.13.

Proof. The proof follows directly from Proposition 5.11. □

We have now completed the computations of the setwise and pointwise isotropy subgroups of $C \in \mathscr{C}_{\mathbf{D}_2[\rho^3,\kappa\rho^2]}$. Since $S(c_2) = S(c_8) \cong \mathbf{Z}_2$, there are two knots on c_2 and c_8 given by e_1 and e_2.

Projected Skeleton

Here we compute the projected skeleton $\mathbb{X}^p_{\mathbf{D}_2[\rho^3,\kappa\rho^2]}$. We have calculated the action of $\mathbf{D}_2[\rho^3,\kappa\rho^2]$ on $\mathscr{C}_{\mathbf{D}_2[\rho^3,\kappa\rho^2]}$, the pointwise and setwise isotropy subgroups and the knots relative to each $C \in \mathscr{C}_{\mathbf{D}_2[\rho^3,\kappa\rho^2]}$.

The action of $\mathbf{D}_2[\rho^3,\kappa\rho^2]$ on $\mathscr{C}_{\mathbf{D}_2[\rho^3,\kappa\rho^2]}$ shows that there are three orbit representatives for points in $E_{(\mathbf{D}_2[\rho^3,\kappa\rho^2],X_0)}$. These are e_1, e_2 and e_3. Furthermore, the action of $\mathbf{D}_2[\rho^3,\kappa\rho^2]$ on $\mathscr{C}_{\mathbf{D}_2[\rho^3,\kappa\rho^2]}$ shows that there are two orbit representatives for the elements of $H_{(\mathbf{D}_2[\rho^3,\kappa\rho^2],X_0)}$. These are $h_3 = \{(\theta,0)|\theta \in [0,\pi)\}$ and $h_{28} = \{(-\theta,2\theta)|\theta \in [0,\pi)\}$. The element h_3 connects e_1 to e_2 and h_{28} connects e_1 to e_2. Figure 5.12 illustrates the projected skeleton.

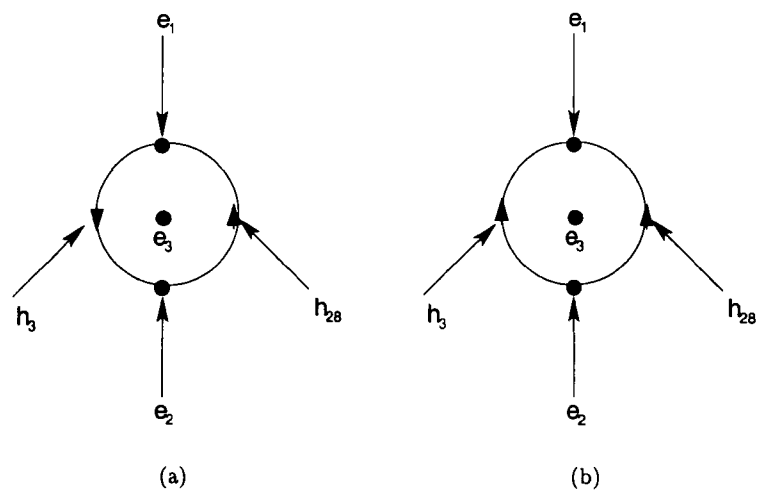

Figure 5.12: Two flows on the projected skeleton $\mathbb{X}^p_{\mathbf{D}_2[\rho^3,\kappa\rho^2]}$.

Flow Formula

As was the case with the other $\mathbf{D}_2$ subgroups of $\mathbf{D}_6$, it is too complex to give a complete list of all possible flow formulas, so again we present an example perturbation which gives rise to a heteroclinic cycle.

Example 5.34
It is easy to see that the map defined by $\mathbf{g}(\mathbf{z}) = (a(z_1\overline{z_1} + z_3\overline{z_3}), (z_2(z_1 + z_3), a(z_1\overline{z_1} + z_3\overline{z_3}))$ is $\mathbf{D}_2[\rho^3, \kappa\rho^2]$-equivariant. The two connections on the skeleton are h_3 and h_{28}. The flow along h_3 is $\mathcal{F}^{\mathbf{g}}_{h_3}(t) = -4x^3 a \sin t$, and the flow along h_{28} is $\mathcal{F}^{\mathbf{g}}_{h_{28}}(t) = -4x^3(a+b)\sin t$. Again, heteroclinic cycles can be arranged by choosing $a \neq 0$ and $\mathrm{sgn}(a) = -\mathrm{sgn}(a+b)$.

5.2.8 Conclusion and Planforms

In this section an investigation was undertaken of the behaviour expected from the group orbit of hexagons guaranteed to exist by Theorem 5.1, when symmetry breaking terms with $\mathbf{D}_6$, $\mathbf{D}_3[\rho^2, \kappa]$, $\mathbf{D}_3[\rho^2, \kappa\rho]$, $\mathbf{D}_2[\rho^3, \kappa]$, $\mathbf{D}_2[\rho^3, \kappa\rho]$ and $\mathbf{D}_2[\rho^3, \kappa\rho^2]$-symmetry are added to a general Γ_h-equivariant map. It was shown in the $\mathbf{D}_6$ case that some admissible perturbations are not generic, since one of the equilibria is not hyperbolic. This type of behaviour is in contrast with the square lattice, where all equilibria are hyperbolic. The reason for this difference can be traced to the symmetry properties of the skeleton. Two of the equilibria on the skeleton are not knots, thus they are not forced by symmetry to be axes of symmetry for the flow.

Forced symmetry breaking to the group $\mathbf{D}_3[\rho^2, \kappa]$ is even more interesting. It is not possible to find admissible perturbations, that give generic flow; one equilibrium on the skeleton is forced to be non-hyperbolic. Forced symmetry breaking to the group $\mathbf{D}_3[\rho^2, \kappa\rho]$ is different; any admissible flow must give a heteroclinic cycle (or more precisely a homoclinic cycle in the orbit space). To find such cycles we must choose non-real coefficients for the vector field (which the group action allow us to do). Finally, we exhibited a heteroclinic cycle for each of the $\mathbf{D}_2$ subgroups, but a more general classification was not performed.

Planforms. Here we present an example planform associated with the forced symmetry breaking of the hexagonal solution. Specifically we choose a perturbed lattice $\mathcal{L}^\epsilon$ with symmetry group $\mathbf{D}_2[\rho^3, \kappa]$ and present a density plot of the eigenfunction $\mathbf{u}(\mathbf{x})$ for representative points on X_0. There is obviously a large number of different perturbed lattices that we can choose, all of which achieve the same aim. Define $\Psi((x,y)) = (\tanh(x - 0.75) + 1, \tanh(y - 0.75) + 1)$. The perturbed eigenfunction is

$$\mathbf{u}(\mathbf{x}) = \sum_{j=1}^{3} z_j \exp\left(\mathrm{i}\mathbf{K}_j \cdot (\Psi^{-1}(\mathbf{x}))\right).$$

In Figure 5.13 we present a rendering of $\mathbf{u}(\mathbf{x})$. Notice that the boundary of the domain chosen for the rendering is emulating a real boundary in experiments. The planform is greatly distorted within a finite healing zone close to the boundary, but regains its normal form further from the boundary. Ideally, we would want a function Ψ which makes the healing zone smaller (this would fit better with experimental results), but it is not easy to find such a function which can be expressed in such an elementary form. However, it is clear that such functions exist with a healing zone of any desired thickness.

5.3 Twelve-Dimensional Representation

In this section we consider the twelve-dimensional representation of the group Γ_h. The representation of Γ_h on $\mathbb{C}^6$ corresponds to the following action, see Dionne and Golubitsky [20]. Choose coordinates $\mathbf{z} = (z_1, z_2, z_3, z_4, z_5, z_6)$ on $\mathbb{C}^6$. Let α and β be integers which satisfy the

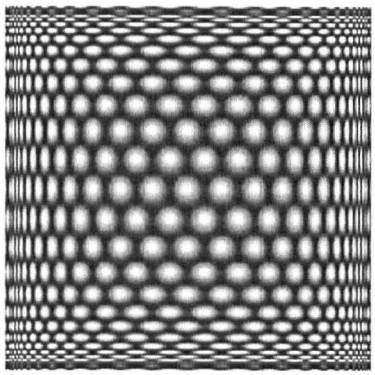

Figure 5.13: Perturbation of the hexagonal planform, showing one possible effect of breaking the symmetry to $\mathbf{D}_2[\rho^3, \kappa]$.

conditions: (1) $\alpha > \beta > \alpha/2 > 0$, (2) α and β are relatively prime, (3) $\alpha + \beta$ is not a multiple of 3. Then

$$\begin{aligned} \rho(z_1, z_2, z_3, z_4, z_5, z_6) &= (\overline{z_2}, \overline{z_3}, \overline{z_1}, \overline{z_5}, \overline{z_6}, \overline{z_4}), \\ \kappa(z_1, z_2, z_3, z_4, z_5, z_6) &= (z_6, z_5, z_4, z_3, z_2, z_1), \end{aligned}$$

and

$$\begin{aligned} \theta(z_1, z_2, z_3, z_4, z_5, z_6) = (&e^{-\mathrm{i}(\alpha\theta_1+\beta\theta_1)}z_1, e^{-\mathrm{i}((-\alpha+\beta)\theta_1-\alpha\theta_2)}z_2, \\ &e^{-\mathrm{i}((-\beta\theta_1+(\alpha-\beta)\theta_2)}z_3, e^{-\mathrm{i}(\alpha\theta_1+(\alpha-\beta)\theta_2)}z_4, e^{-\mathrm{i}(-\beta\theta_1-\alpha\theta_2)}z_5, e^{-\mathrm{i}((-\alpha+\beta)\theta_1+\beta\theta_2)}z_6). \end{aligned} \quad (5.24)$$

Consider the Γ_h-equivariant system of differential equations

$$\dot{\mathbf{z}} = \mathbf{f}(\mathbf{z}, \lambda), \quad (5.25)$$

where $\mathbf{f} : \mathbb{C}^6 \times \mathbb{R} \to \mathbb{C}^6$ is Γ_h-equivariant. In this section we investigate the behaviour of the group orbits of solutions to $\mathbf{f}(\mathbf{z}, \lambda) = 0$ when symmetry breaking terms with $\mathbf{D}_6$, $\mathbf{D}_3[\rho^2, \kappa]$, $\mathbf{D}_3[\rho^2, \kappa\rho]$, $\mathbf{D}_2[\rho^2, \kappa]$, $\mathbf{D}_2[\rho^2, \kappa\rho]$ and $\mathbf{D}_2[\rho^2, \kappa\rho^2]$ symmetry are added. As for the eight-dimensional representation of the square lattice, we may reduce the twelve-dimensional representation of Γ_h to the six-dimensional representation considered in Section 5.2. Indeed, the number of translation free axial subgroups is the same for both representations of Γ_h—each being one with $\mathbf{D}_6$-symmetry. Beyond this correspondence we do not consider this case in more detail. The invariant theory is too complex—even with the use of computers—to attempt the computations of the flow formulas, although we do present one example just to illustrate ideas. Our main result is Theorem 5.37, which is an existence result for admissible flows, classifying all the types of admissible flows.

This section is organised as follows. In Subsection 5.3.1 we show there exists a translation free axial solution with $\mathbf{D}_6$ isotropy. This solution is generically unstable at bifurcation, but we show (using the results of Dionne *et al.* [20]) that there exists a parameter region where this solution can be stable. Next in Subsection 5.3.2 we show the results for the twelve-dimensional representation of Γ_h are essentially the same as the six-dimensional representation. By essentially, we mean the skeleton, knots and symmetry properties are identical. We then present our classification, Theorem 5.37, and finally in Subsection 5.3.3 an example of a planform.

5.3.1 Existence of Translation Free Axial Solution

In this subsection we show there exists one translation free axial solution to the bifurcation problem (5.25). This subsection uses the results from Dionne *et al.* [20] and Dionne and Golubitsky [21].

The action of the group Γ_h on $\mathbb{C}^6$ has six conjugacy classes of axial subgroups, see Table 4, p. 331 of Dionne *et al.* [21], of which the only translation free subgroup is $\Sigma = \mathbf{D}_6$. A general Γ_h-equivariant map is too difficult to construct; however, a low order truncation is possible. To the lowest order required to determine the stability of the bifurcating solutions we have (first component only)

$$\begin{aligned} f_1(\mathbf{z},\lambda) &= \lambda z_1 + q\overline{z_2 z_3} + z_1(a_1|z_1|^2 + a_2|z_2|^2 + a_3|z_3|^2 + a_4|z_4|^2 + a_5|z_5|^2 + a_6|z_6|^2) \\ &+ \overline{z_2 z_3}(b_1|z_1|^2 + b_2|z_2|^2 + b_3|z_3|^2 + b_4|z_4|^2 + b_5|z_5|^2 + b_6|z_6|^2) \\ &+ z_1(c_1 z_1 z_2 z_3 + c_2 z_4 z_5 z_6 + c_3\overline{z_4 z_5 z_6}) + e_1\overline{z_1}^{\alpha-\beta-1} z_3^{\beta} z_4^{\beta}\overline{z_6}^{\alpha-\beta} \\ &+ e_2\overline{z_1}^{\beta-1} z_2^{\alpha-\beta} z_4^{\alpha-\beta}\overline{z_5}^{\beta} + \ldots, \end{aligned}$$

where $\ldots$ denotes higher order terms and a_j, b_j, c_j and e_j are all real. The presence of the quadratic term $q\overline{z_2 z_3}$ implies that, generically, all axial solutions are unstable at bifurcation. Dionne *et al.* [20] show that in the degenerate problem $q = 0$ any solution, in particular the $\mathbf{D}_6$-symmetric solution, can be stable.

Remark 5.35
Dionne et al. *[20] consider the $\Gamma_h \oplus \mathbf{Z}_2$ bifurcation problem. Here there are four translation free axial solutions each with non-conjugate $\mathbf{D}_6$ isotropy. These solutions are referred to as super hexagons, anti hexagons, super triangles and anti triangles. It is possible for these solutions to be stable at bifurcation, see Dionne* et al. *[20]. We shall not consider this case.*

Summarising we have the following.

Proposition 5.36
Let $\mathbf{f} : \mathbb{C}^6 \times \mathbb{R} \to \mathbb{C}^6$ be a Γ_h-equivariant bifurcation problem. Then, generically, there exists a branch of solutions bifurcating from the origin with $\mathbf{D}_6$-isotropy. In the nondegenerate problem this branch is unstable.

There is a problem; the solutions are unstable at bifurcation. Dionne *et al.* [20] show that if the degenerate problem $q = 0$ is weakly unfolded, so $|q| \ll 1$, then many secondary transitions are possible along the $\mathbf{D}_6$ branch of solutions. In particular the branch can gain stability at a secondary saddle-node bifurcation, (Dionne *et al.* [20] p. 343). Therefore, for sufficiently small $|q|$ and a suitable small range of values for λ, the bifurcating $\mathbf{D}_6$ solution given by Proposition 5.36 is stable. We denote this group orbit by X_0. Generically, X_0 is normally hyperbolic and is a 2-torus.

5.3.2 Forced Symmetry Breaking of Super Hexagons

In this subsection we classify the behaviour of the group orbit of solutions X_0 given by Proposition 5.36, when symmetry breaking terms are added. The space Γ/Σ is the same in both representations, as is the natural action of a subgroup Δ on Γ/Σ. So the skeleton, knots, setwise and pointwise isotropy subgroups are identical. Thus we may construct the skeletons for the subgroups $\mathbf{D}_6$, $\mathbf{D}_3[\rho^2,\kappa]$, $\mathbf{D}_3[\rho^2,\kappa\rho]$, $\mathbf{D}_2[\rho^3,\kappa]$, $\mathbf{D}_2[\rho^2,\kappa\rho]$ and $\mathbf{D}_2[\rho^2,\kappa\rho^2]$. Indeed we find, using the same definitions of the c_i's and e_i's as before (Definitions 4.3, 4.6 and 5.3), that

$$\begin{aligned} \mathbb{X}_{\mathbf{D}_6} &= \bigcup_{i=1\ldots8} c_i - (c_3 \cup c_5), \\ \mathbb{X}_{\mathbf{D}_3[\rho^2,\kappa]} &= c_1 \cup c_7 \cup c_8, \\ \mathbb{X}_{\mathbf{D}_3[\rho^2,\kappa\rho]} &= c_2 \cup c_4 \cup c_6 \cup e_5 \cup e_6, \\ \mathbb{X}_{\mathbf{D}_2[\rho^3,\kappa]} &= c_4 \cup c_7 \cup e_2 \cup e_4, \\ \mathbb{X}_{\mathbf{D}_2[\rho^2,\kappa\rho]} &= c_1 \cup c_6 \cup e_2 \cup e_3, \\ \mathbb{X}_{\mathbf{D}_2[\rho^2,\kappa\rho^2]} &= c_2 \cup c_8 \cup e_3 \cup e_4. \end{aligned}$$

Using this construction we now give the fundamental existence result for this section.

Theorem 5.37
Let $\Gamma = \mathbf{D}_6 \dot{+} \mathbf{T}^2$, $\Sigma = \mathbf{D}_6$ and Δ be one of the groups $\mathbf{D}_6$, $\mathbf{D}_3[\rho^2, \kappa]$, $\mathbf{D}_3[\rho^2, \kappa\rho]$, $\mathbf{D}_2[\rho^3, \kappa]$, $\mathbf{D}_2[\rho^3, \kappa\rho]$, $\mathbf{D}_2[\rho^3, \kappa\rho^2]$. Let Γ act on $\mathbb{C}^6$ as in (5.24), or on $\mathbb{C}^3$ as in (5.3). Let $\mathbf{f} \in \vec{\mathcal{E}}_\Gamma$ be a Γ-equivariant bifurcation problem. Let $\mathbf{g} \in \vec{\mathcal{E}}_\Delta$ be a Δ-equivariant vector field which satisfies $\mathbf{g}(\mathbf{0}) = \mathbf{0}$. Then there exists a branch of steady-state solutions to $\mathbf{f}(\mathbf{z}, \lambda) = \mathbf{0}$ bifurcating from $(\mathbf{0}, 0)$ with Σ-isotropy. Let $X_0 \cong \mathbf{T}^2$ be the group orbit of steady states. Consider the perturbed vector field $\mathbf{F}(\mathbf{z}, \lambda, \varepsilon) = \mathbf{f}(\mathbf{z}, \lambda) + \varepsilon\mathbf{g}(\mathbf{z})$, where ε is real and small. Then for sufficiently small ε, X_0 persists to give a new $\mathbf{F}$-invariant manifold X_ε, which is Δ-equivariantly diffeomorphic to X_0. The behaviour of the vector field on X_0 is characterised by:

1. *If $\Delta = \mathbf{D}_6$, then there exist three group orbits of equilibria e_1, e_2 and e_5, and three group orbits of heteroclinic connections between them.*
2. *If $\Delta = \mathbf{D}_3[\rho^2, \kappa]$, then any admissible flow must give an equilibrium which is not hyperbolic. Therefore, generically, we expect to find additional equilibria on the skeleton that are not contained in $E_{(\mathbf{D}_3[\rho^2,\kappa], X_0)}$.*
3. *If $\Delta = \mathbf{D}_3[\rho^2, \kappa\rho]$, then there are two group orbits of equilibria e_1 and e_5, where e_5 is isolated and e_1 is connected to itself by a heteroclinic connection. Thus any admissible perturbation gives rise to a heteroclinic cycle between the equilibria e_1.*
4. *If $\Delta = \mathbf{D}_2[\rho^3, \kappa]$, then there exist three group orbits of equilibria e_1, e_3 and e_4. The equilibrium e_4 is isolated. The other two equilibria are connected together by two heteroclinic connections. There exist possible heteroclinic cycles from e_1 to e_3 and back to e_1.*
5. *If $\Delta = \mathbf{D}_2[\rho^3, \kappa\rho]$, then there exist three group orbits of equilibrium e_1, e_2 and e_4. The equilibria e_2 is isolated. The other two equilibria are connected together by two heteroclinic connection. There exist possible heteroclinic cycles from e_1 to e_4 and back to e_1.*
6. *If $\Delta = \mathbf{D}_2[\rho^3, \kappa\rho^2]$, then there exist three group orbits of equilibria e_1, e_2 and e_3. The equilibrium e_3 is isolated. The other two equilibria are connected together by two heteroclinic connection. There exist possible heteroclinic cycles from e_1 to e_2 and back to e_1.*

Unfortunately this classification is as far as we can go with the twelve-dimensional representation. It is worth emphasising that we have shown for symmetry breaking to $\mathbf{D}_3[\rho^2, \kappa\rho]$, there exist perturbations giving heteroclinic cycles on the skeleton. The invariant theory of this representation is too complex to make any further general statements.

5.3.3 Examples

Here we present examples the types of flow that may arise on the skeleton and an example of a planform that occurs in the forced symmetry breaking problem.

Flow Formula. Here we present an example of the flow formula for a particular $\mathbf{D}_3[\rho^2, \kappa\rho]$-equivariant perturbation. The perturbation we consider is $\mathbf{g}(\mathbf{z}) = u(1, 1, 1, 1, 1, 1)$, where

$$u = \sum_{j=1}^{6} (z_j + \overline{z_j}). \tag{5.26}$$

The skeleton has one orbit representative for elements of $H_{(\mathbf{D}_3[\rho^2,\kappa\rho], X_0)}$, c_2 say. This connection is parametrised by the function $\omega_{c_2} : [0, 2\pi] \to X_0$ defined by

$$\omega_{c_2}(t) = (e^{-\mathrm{i}(\alpha t)} z_1, e^{-\mathrm{i}(-\alpha+\beta)t}, e^{-\mathrm{i}(-\beta t)}, e^{-\mathrm{i}(\alpha t)}, e^{-\mathrm{i}(-\beta t)}, e^{-\mathrm{i}((-\alpha+\beta)t)}) x,$$

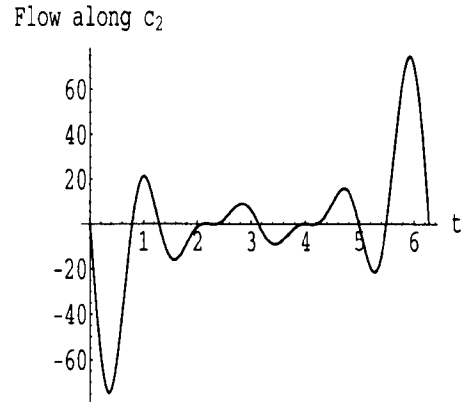

Figure 5.14: The flow formula along the connection c_2 for the perturbation in (5.26). There are eleven additional simple zeros along the connection.

where $x > 0$. From which the tangent vector is given by

$$\begin{aligned}\mathcal{T}_{c_2}(t) &= (-\alpha\sin\alpha t, -\alpha\cos\alpha t, -(-\alpha+\beta)\sin(-\alpha+\beta)t, -(-\alpha+\beta)\cos(-\alpha+\beta)t,\\ &\quad -\beta\sin\beta t, \beta\cos\beta t, -\alpha\sin\alpha t, -\alpha\cos\alpha t, -\beta\sin\beta t, \beta\cos\beta t,\\ &\quad -(-\alpha+\beta)\sin(-\alpha+\beta)t, -(-\alpha+\beta)\cos(-\alpha+\beta)t)x.\end{aligned}$$

Evaluating the u along the connection c_2 gives

$$u(\omega_{c_2}(t)) = 4(\cos\alpha t + \cos\beta t + \cos(-\alpha+\beta)t)x.$$

Thus the flow formula is given by

$$\begin{aligned}\mathcal{F}(t) &= 4x^2(\cos\alpha t + \cos\beta t + \cos(-\alpha+\beta)t)(-\alpha\sin\alpha t - (-\alpha+\beta)\sin(-\alpha+\beta)t\\ &\quad -\beta\sin\beta t - \alpha\sin\alpha t - \beta\sin\beta t - (-\alpha+\beta)\sin(-\alpha+\beta)t)\\ &= -8x^2(\cos\alpha t + \cos\beta t + \cos(-\alpha+\beta)t)(\alpha\sin\alpha t + \beta\sin\beta t + (-\alpha+\beta)\sin(-\alpha+\beta)t).\end{aligned}$$

The simplest example of when α and β satisfy the defining conditions on the representation is $(\alpha,\beta) = (3,2)$. In this case the flow formula has the form

$$\mathcal{F}(t) = -8x^2(\cos t + \cos 2t + \cos 3t)(\sin t + 2\sin 2t + 3\sin 3t).$$

Figure 5.14 presents a rendering of the flow formula. Notice that there are eleven additional equilibria along the connection. The zeros of the flow formula located near 2 and 4 are not inflection points, but really three zeros in close proximity. This example illustrates how complex the flows on the skeleton can be.

Planforms. Here we present an example planform associated with the forced symmetry breaking of the super hexagon solution to the group $\mathbf{D_2}[\rho^2,\kappa]$. Such a forced symmetry breaking problem can be realised in physical space as breaking the symmetry to that of a rectangular (almost square) container.

Define $\Psi((x,y)) = (\tanh(x)+1, \tanh(y)+1)$. The perturbed eigenfunction is given by

$$\mathbf{u}(\mathbf{x}) = \sum_{j=1}^{6} z_j \exp(\mathrm{i}\mathbf{K}_j \cdot (\Psi^{-1}(\mathbf{x})). \tag{5.27}$$

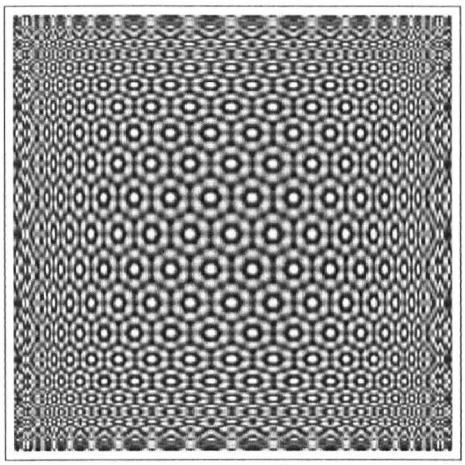

Figure 5.15: Sample planform associated with forced symmetry breaking of the super hexagon solution to the subgroup $\mathbf{D}_2[\rho^2, \kappa]$.

Figure 5.15 presents a density plot of $\mathbf{u}(\mathbf{x})$. As before the boundary of the rendered domain emulates a real boundary and features a healing zone where the planform is distorted, but further from this zone the planform retains its original unperturbed shape. The size of this healing zone can be chosen to be any size desired; we just need to define a suitable function Ψ.

Comments. The construction of the planforms requires the (rather large) assumption that the equilibria on the skeleton are in exactly the same position as those on the perturbed skeleton. This assumption is rather difficult to justify; in fact, we really can't. We now consider what happens to the planforms if this assumption is dropped.

The equilibrium e_1^ε on the perturbed skeleton has the form $e_1 + \varepsilon\hat{\mathbf{z}}$ where $\hat{\mathbf{z}}$ is an unknown point in $\mathbb{C}^6$. Writing $\hat{\mathbf{z}}$ in polar coordinates gives $\hat{\mathbf{z}} = (r_1 e^{\mathrm{i}\phi_1}, r_2 e^{\mathrm{i}\phi_2}, r_3 e^{\mathrm{i}\phi_3}, r_4 e^{\mathrm{i}\phi_4}, r_5 e^{\mathrm{i}\phi_5}, r_6 e^{\mathrm{i}\phi_6})$, where $r_j \in \mathbb{R}^+$ and $\phi_j \in [0, 2\pi)$. Then the resulting eigenfunction now has the form

$$\mathbf{u}(\mathbf{x}) = \sum_{j=1}^{6} r_j e^{\mathrm{i}\phi_j} \exp(\mathrm{i}\mathbf{K}_j \cdot (\Psi^{-1}(\mathbf{x})).$$

To realise $\mathbf{u}(\mathbf{x})$ in physical space we must compute its real part; this gives

$$\mathbf{u}(\mathbf{x}) = \sum_{j=1}^{6} r_j \left(\cos\phi_j \cos(\mathbf{K}_j \cdot \Psi^{-1}(\mathbf{x})) - \sin\phi_j \sin(\mathbf{K}_j \cdot \Psi^{-1}(\mathbf{x}))\right). \tag{5.28}$$

For the equilibrium e_1 (or any equilibria) the values of r_j and ϕ_j are fixed (provided ε is fixed). We make the slightly more valid assumption that e_1^ε is close to e_1, so ε is small. Figure 5.16 (a) presents a density plot of the eigenfunction $\mathbf{u}(\mathbf{x})$ in (5.28). The values for the r_j's and ϕ_j's were chosen at random. Figure 5.16 (b) presents the difference between the two eigenfunctions used to illustrate the planforms. It can easily be seen that the changes to the eigenfunction does not make much of a difference to the appearance of the planform; only a change in amplitude can be seen.

5.4 Review

In this chapter we have investigated the forced symmetry breaking behaviour of the hexagonal and super hexagon solutions to a Γ_h-equivariant system of differential equations. This problem

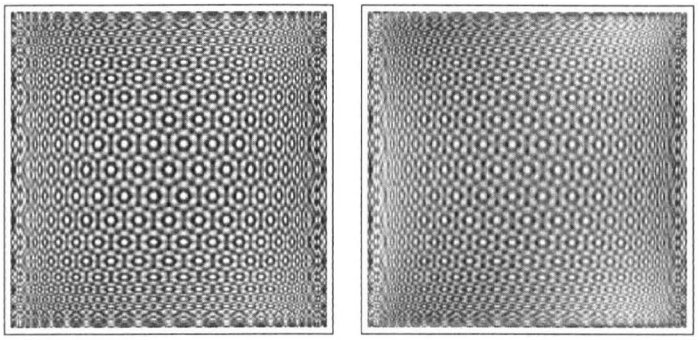

(a) (b)

Figure 5.16: A possible planform associated with forced symmetry breaking of the super hexagon solution. (a) Using the eigenfunction in (5.28). The values of r_j and ϕ_j were chosen at random. (b) The difference between the planforms using the eigenfunctions (5.28) and (5.27).

shares many of the characteristics exhibited in the square lattice case: the existence of equilibria both isolated and not, and heteroclinic connections between them. However, we also have seen new types of behaviour. The $\mathbf{D}_3[\rho^2, \kappa]$ problem leads to equilibria which are not hyperbolic. The existence of heteroclinic cycles is established in the $\mathbf{D}_3[\rho^2, \kappa\rho]$ case. The main result of the chapter is Theorem 5.37 which gives a partial classification for the behaviour of hexagons and super hexagons when certain symmetry breaking effects are considered.

Part III

Forced Symmetry Breaking of Planforms in Three Dimensions

Chapter 6

Steady-State Bifurcation with Three-Dimensional Euclidean Symmetry

Unlike pattern formation in two-dimensional systems, three-dimensional systems have only recently become the focus of attention. There are several reason for this. Firstly, three-dimensional patterns are more complex—there is a great number of three-dimensional lattices. This complexity manifests itself in the bifurcation problems which have high dimension and so are more difficult to study. Secondly, and more importantly, from an applied point of view, few truly three-dimensional patterns have been observed in experiments, making the relevance of theoretical studies dubious. However, recent work on pattern forming systems, both experimental [10, 73, 85, 81] and theoretical [86, 17], have shown the relevance of three-dimensional patterns. In addition, Gomes [39] demonstrated that the orientation of a three-dimensional pattern can have a dramatic effect on its appearance—exhibiting patterns which would otherwise only be seen in complex two-dimensional problems.

In this part we perform a partial classification of the behaviour associated with some three-dimensional structures under forced symmetry breaking. Specifically we focus on the cubic lattices, leaving the other (experimentally) less relevant lattices for future work.

As two dimensions, the three-dimensional Euclidean group $\mathbf{E}(3)$ is not compact, so we employ the techniques of Section 1.6 and reduce the $\mathbf{E}(3)$-equivariant bifurcation problem to that of finding spatially triply periodic solutions. There are fourteen three-dimensional lattices with which we can choose the periodicity of the solutions. Dionne [19] classified the translation free axial solutions guaranteed to exist by the equivariant branching lemma for each of these lattices. From this classification we select those solutions arising from the cubic lattices. The cubic lattices are: The Simple Cubic (SC), Face Centred Cubic (FCC) and Body Centred Cubic (BCC). Each of these, via the methods of Section 1.6, gives rise to a $\mathbb{O} \oplus \mathbf{Z}_2^c \dotplus \mathbf{T}^3$-equivariant bifurcation problem, but with a different representation of the group. The group $\mathbb{O}$ is the orientation preserving symmetries of the cube, $\mathbf{Z}_2^c$ is inversion through the origin, and $\mathbf{T}^3$ is translations. Dionne [19] classified all translation free irreducible representation of the SC, FCC and BCC lattices. We address each lattice in turn.

The irreducible representations of the SC lattice have dimensions six, twenty-four of types 1 and 2 and forty-eight. The two twenty-four-dimensional representations are not the same and give different planforms. Indeed, the classification of Dionne [19] proves that in the six-dimensional representation there is one translation free axial solution, called Simple Cubic (SC), in the twenty-four type 1 representation there are (up to) five (depending on the defining conditions on the representation) and in the twenty-four type 2 and forty-eight-dimensional representations there are four. Further to this study, Callahan and Knobloch [8] performed a detailed stability analysis of the six-dimensional representation, showing that the SC solution

ferent solutions; and in the forty-eight-dimensional representation there are either two or three, again depending on the defining conditions of the representation. In addition to this classification Callahan and Knobloch [8] consider the twelve-dimensional representation in detail. Their study is very complex for one simple reason: the general form of the vector field has a quadratic term, implying that all axial solutions are unstable at bifurcation. For this reason the authors consider the $\mathbb{O} \oplus \mathbf{Z}_2^c \oplus \mathbf{Z}_2 \dotplus \mathbf{T}^3$ bifurcation problem, where the additional $\mathbf{Z}_2$ symmetry acts as minus the identity. This $\mathbf{Z}_2$ action removes all even terms from the vector field allowing the bifurcation problem to be solved more easily. The $\mathbb{O} \oplus \mathbf{Z}_2^c \oplus \mathbf{Z}_2 \dotplus \mathbf{T}^3$ bifurcation problem is then "weakly" unfolded; that is, the coefficient of the quadratic term (and only the quadratic term) is made nonzero. The authors present several important results:

1. With the additional $\mathbf{Z}_2$ symmetry there exist ten axial branches of solutions, of which seven can be stable.
2. In addition to the axial solutions, there exist five submaximal solutions.
3. When the $\mathbf{Z}_2$ symmetry is weakly broken, two branches, BCC and hexagons, are unstable at bifurcation but regain stability at a secondary saddle-node bifurcation. Some of the previous axial branches become secondary branches, and some of the submaximal branches merge to a single branch.

This leads to highly elaborate bifurcating behaviour with many secondary bifurcations and changes in stability, for more details see Callahan and Knobloch [8]. To summarise, the three translation free axial solutions have the following properties:

1. The BCC solution is unstable at bifurcation, but gains stability at a secondary saddle-node bifurcation.
2. The BCCI solution can be stable at bifurcation, but if it is stable then the BCC branch cannot be stable.
3. The A solution is always unstable[1].

Figure 6.3 shows these three solutions. Further to the theoretical discussion of Callahan and Knobloch [8], they perform a centre manifold analysis of the Brusselator and Lengyel–Epstein models for three-dimensional reaction-diffusion systems [9].

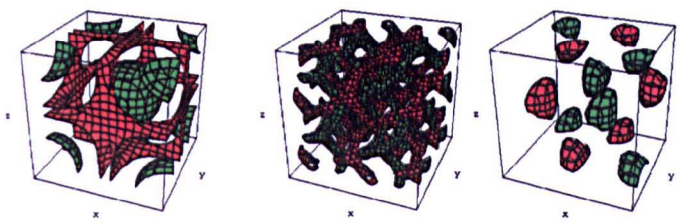

(a) BCC (b) BCCI (c) A

Figure 6.3: Rendering of the BCC solutions.

In this part we study the forced symmetry breaking of group orbits of the translation free axial solutions which occur on the cubic lattices. The approach we take is the same as for the two-dimensional systems considered in Part II. In Chapter 7 we consider the behaviour of the

[1]Interestingly, the solution A occurs as an axial solution on the Body Centred Tetragonal (BCT) Lattice. This lattice is the BCC lattice with one direction elongated so the full symmetry of the cube is lost and only the symmetry of a square remains. In this case the A solution can be stable, see Parker [74].

can be stable at bifurcation. Figure 6.1 presents the SC solution in three-dimensional projection. The figure shows a periodic cube with maxima rendered in green and minima in red. The coloured regions represent small areas around the maxima and minima.

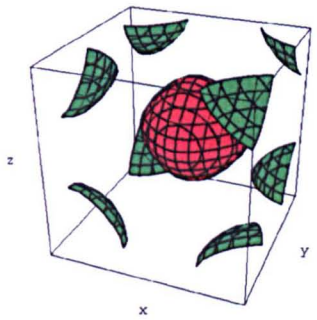

Figure 6.1: The SC solution.

The FCC lattice has three irreducible representations of dimensions eight, twenty-four and forty-eight. Dionne [19] proved; there are two translation free axial planforms in the eight-dimensional representation, called FCC and Double-Diamond in the literature. In addition there are up to five translation free axial solutions in the twenty-four-dimensional case; the precise number depends on the exact form of the representation. In the forty-eight-dimensional case there are always four. Again this classification was extended by Callahan and Knobloch [8] in the eight-dimensional case. They show the existence of an unstable submaximal solution, and give the stability assignments for the axial solutions. Furthermore, they consider the normal form and classify the bifurcation diagrams that can occur. In particular the FCC and Double-Diamond solutions can never be simultaneously stable, but it is possible for one of the solutions to be stable. Figure 6.2 renders the FCC and Double Diamond structure, using the same colour scheme as for the SC case.

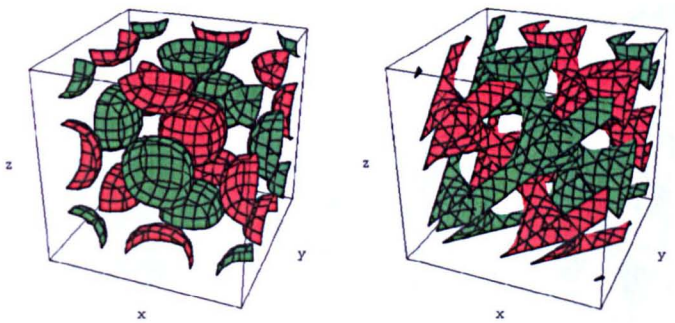

(a) FCC Solution (b) Double Diamond

Figure 6.2: Rendering of the FCC solutions. (a) The FCC solution. (b) The double diamond.

Finally, we come to the BCC lattice. The translation free irreducible representations have the following dimensions: twelve, twenty-four of type 1 and type 2, and forty-eight. Dionne proved the number of translation free axial solutions is: three in the twelve-dimensional representation called BCC, BCCI and A (here we use the terminology of Callahan and Knobloch [8]); in the twenty-four-dimensional representation of type 1 there are two or up to five depending on the conditions on the irreducible representation; the type 2 representation exhibits three dif-

translation free axial solutions supported on the SC lattice. This is the easiest case we consider in this part. Next in Chapter 8 we emulate our study of the SC lattice by considering the FCC lattice, and finally in Chapter 9 we consider the BCC lattice. Due to the complexities introduced by the high dimensionality of these three-dimensional problems we cannot consider these problem in as much depth as was possible for the two-dimensional cases. However, we find that the dynamical possibilities are much greater. From Appendix B we know that the group $\mathbb{O}$ has 30 subgroups; there is no way that we can sensibly consider the behaviour of all of these subgroups. However, this is not necessary. We consider the forced symmetry breaking of the group orbits to the following subgroups of $\mathbb{O}$: $\mathbb{O}$ itself, $\mathbb{T}$, $\mathbf{D}_4[\rho_x^2, \kappa_6]$, $\mathbf{D}_3[\tau_1, \kappa_5]$ (except on the BCC lattice where we consider the group $\mathbf{D}_3[\tau_3, \kappa_3]$), $\mathbf{D}_2[\rho_x^2, \kappa_6]$, and $\mathbf{D}_2[\rho_x^2, \rho_y^2]$. The reason for selecting only these groups is as follows. Consider the forced symmetry breaking problem to one of the $\mathbf{D}_4$ subgroups of $\mathbb{O}$. The construction of the skeleton, its symmetry properties and knots is related to the $\mathbf{D}_4$ action on the group orbit. It can be shown the skeletons for each of the three $\mathbf{D}_4$ subgroups are the same, up to an element of $\mathbb{O}$. The same holds in general for the groups selected above: they are representatives for their classes.

Chapter 7

Forced Symmetry Breaking on the Simple Cubic Lattice

7.1 Introduction

It was only recently that steady-state symmetry-breaking on the Simple Cubic (SC) lattice was studied. The work of Dionne [19] classified all translation free axial solutions supported by the SC lattice. Callahan and Knobloch later extended this work [8], giving stability criterion for the solutions supported by the fundamental SC lattice. Motivated by Turing patterns, Callahan and Knobloch [9] generalised these results to reaction-diffusion systems. In this chapter we continue this classification in a new direction, giving a partial classification of the behaviour that may be expected from the axial solutions supported on the SC lattice, when certain forced symmetry breaking effects are taken into account.

Let us recall the methods of Section 1.6 applied to the SC lattice. Define three linearly independent vectors $\boldsymbol{\ell}_1 = (1,0,0)$, $\boldsymbol{\ell}_2 = (0,1,0)$ and $\boldsymbol{\ell}_3 = (0,0,1)$. The SC lattice is defined by

$$\mathcal{L}_{SC} = \{n_1\boldsymbol{\ell}_1 + n_2\boldsymbol{\ell}_2 + n_3\boldsymbol{\ell}_3 | n_1, n_2, n_3 \in \mathbb{Z}\}.$$

The symmetry group of $\mathcal{L}_{SC}$ is given by $\Gamma = \mathbb{O} \oplus \mathbf{Z}_2^c \dotplus \mathbf{T}^3$. Where $\mathbb{O}$ is the orientation preserving symmetries of the cube, $\mathbf{Z}_2^c$ is inversion through the origin, and $\mathbf{T}^3$ is the translational symmetries of the lattice, which is the group $\mathbb{R}^3/\mathcal{L}_{SC}$. We seek functions $\mathbf{u} \in \mathcal{X}$ that are triply periodic with respect to the SC lattice and so are members of $\mathcal{X}_{\mathcal{L}_{SC}}$. Define $\mathbf{k}_1 = (1,0,0)$, $\mathbf{k}_2 = (0,1,0)$ and $\mathbf{k}_3 = (0,0,1)$. Then the dual lattice to $\mathcal{L}_{SC}$ is defined by

$$\mathcal{L}_{SC}^* = \{n_1\mathbf{k}_1 + n_2\mathbf{k}_2 + n_3\mathbf{k}_3 | n_1, n_2, n_3 \in \mathbb{Z}\}.$$

Now we may write a function $\mathbf{u} \in \mathcal{X}_{\mathcal{L}_{SC}}$ in the form

$$\mathbf{u}(\mathbf{x},t) = \sum_{j=1}^{s} z_j e^{2\pi i \mathbf{K}_j \cdot \mathbf{x}} \mathbf{u}_j + c.c., \tag{7.1}$$

where $z_j \in \mathbb{C}$, $|\mathbf{K}_j|$ are wave vectors on the dual lattice of length k_c—the critical radius. Dionne [19] shows that $s = 3$, 12 or 24. The case $s = 3$ occurs, for example, when $k_c = 1$, the case $s = 12$ has two different types: type 1 occurs when $k_c = \sqrt{17}$ and type 2 occurs when $k_c = \sqrt{13}$. Finally the forty-eight-dimensional case occurs when $k_c = \sqrt{14}$. The expression (7.1) shows that the domain of the bifurcation problem can be identified with $\mathbb{C}^s$. The representation of Γ on $\mathbb{C}^s$ is determined by its action on the complex coordinates z_j in (7.1). All representations that we consider satisfy the translation free hypothesis of Dionne [19]. Our problem is now in standard form; we have reduced the situation to the study of the ODE

$$\dot{\mathbf{z}} = \mathbf{f}(\mathbf{z}, \lambda), \tag{7.2}$$

where $\mathbf{f} : \mathbb{C}^s \times \mathbb{R} \to \mathbb{C}^s$ is Γ-equivariant. The work of Dionne [19] now tells us that there are (up to) 14 different translation free axial solutions, the precise number being determined by the defining conditions of the representations. In this chapter we study the behaviour of a selection of these 14 solutions when symmetry-breaking effects are considered in the underlying equation (7.2). We employ the techniques of Chapter 2 to examine this problem systematically; in particular we are interested in the persistence of equilibria and the occurrence of heteroclinic cycles and other intermittent behaviour.

We now review the contents of the chapter and its organisation. In Section 7.2 we study the six-dimensional representation. This representation (generically) has one translation free axial solution; the existence of this solution is considered in Subsection 7.2.1. We then proceed in Subsection 7.2.2 to study forced symmetry breaking of this solution when terms with $\mathbb{O}$ symmetry are present. This study follows our standard approach: we compute the skeleton, its symmetry properties, and the projected skeleton. By invoking results of Chapter 2 we deduce results concerning the persistence of equilibria and heteroclinic connections between equilibria. The projected skeleton is more important than in any previous case; the skeleton is a subset of a 3-torus and so is too complex an object to render in a illuminating way, but in contrast the projected skeleton is much simpler. We then discuss flows on the skeleton. In Subsections 7.2.3 to 7.2.7 the above process is repeated for the groups $\mathbf{D}_4[\rho_x, \kappa_6]$, $\mathbb{T}$, $\mathbf{D}_3[\tau_1, \kappa_5]$, $\mathbf{D}_2[\rho_x^2, \kappa_6]$ and $\mathbf{D}_2[\rho_x^2, \rho_y^2]$. In Sections 7.3 we consider the two twenty-four and the one forty-eight-dimensional representations. These representations possess a great many translation free axial solutions and we study only a selection, specifically those whose results can be deduced from the six-dimensional case. Finally in Section 7.4 we make some concluding remarks.

7.2 Six-Dimensional Representation

In this section we consider the six-dimensional representation of the group Γ. This representation occurs when the wavelength of instabilities coincides with the periodicity of the functions in $\mathcal{X}_{\mathcal{L}_{SC}}$. We begin in Subsection 7.2.1 by showing that there exists a group orbit of solutions with $\mathbb{O} \oplus \mathbf{Z}_2^c$ symmetry. Using this result, we then study its behaviour under perturbations equivariant with respect to the groups $\mathbb{O}$, $\mathbf{D}_4[\rho_x, \kappa_6]$, $\mathbb{T}$, $\mathbf{D}_3[\tau_1, \kappa_5]$, $\mathbf{D}_2[\rho_x^2, \kappa_6]$ and $\mathbf{D}_2[\rho_x^2, \rho_y^2]$. All computations follow identical lines: we calculate the skeleton, study the group action on the skeleton, compute the projected skeleton and make comments about the behaviour of flows on the projected and usual skeletons.

The representation of Γ on $\mathbb{C}^3$ corresponds to the following action. Choose coordinates $\mathbf{z} = (z_1, z_2, z_3)$ on $\mathbb{C}^3$. The action of Γ is generated by

$$\begin{aligned} \rho_x(\mathbf{z}) &= (z_1, \overline{z_3}, z_2), \\ \rho_y(\mathbf{z}) &= (z_3, z_2, z_1), \\ c(\mathbf{z}) &= (\overline{z_1}, \overline{z_2}, \overline{z_3}), \\ \theta(\mathbf{z}) &= (e^{\mathrm{i}\theta_1} z_1, e^{\mathrm{i}\theta_2} z_2, e^{\mathrm{i}\theta_3} z_3). \end{aligned}$$

Here ρ_x and ρ_y are the generators of $\mathbb{O}$, c generates the group $\mathbf{Z}_2^c$, and $\theta \in \mathbf{T}^3$. Consider the Γ-equivariant system of differential equations

$$\dot{\mathbf{z}} = \mathbf{f}(\mathbf{z}, \lambda), \tag{7.3}$$

where $\mathbf{f} : \mathbb{C}^3 \times \mathbb{R} \to \mathbb{C}^3$ is Γ_h-equivariant. Our primary interest is finding heteroclinic type behaviour on the different skeletons, we shall see that the possibilities are much richer for the SC lattice compared to either the square or hexagonal lattices. In particular we can exhibit very complex heteroclinic networks and other more elaborate networks.

7.2.1 Existence of Translation Free Axial Solution

The action of Γ on $\mathbb{C}^3$ has seven conjugacy classes of isotropy subgroups [8]. Of these subgroups only three are axial, and furthermore there is only one conjugacy class of translation free axial

subgroups given by $\mathbb{O} \oplus \mathbf{Z}_2^c$ [19]. We focus exclusively on this translation free axial subgroup, for which we introduce the notation $\Sigma = \mathbb{O} \oplus \mathbf{Z}_2^c$.

By [8] a general Γ-equivariant vector field has the form (first component only)

$$f_1(\mathbf{z}, \lambda) = (h_1 + u_1 h_3 + u_1^2 h_5) z_1, \tag{7.4}$$

where h is an arbitrary real-valued function of the three Γ-invariants

$$\begin{aligned} \sigma_1 &= u_1 + u_2 + u_3, \\ \sigma_2 &= u_1 u_2 + u_2 u_3 + u_1 u_3, \\ \sigma_3 &= u_1 u_2 u_3, \end{aligned}$$

and $u_j = z_j \overline{z}_j$. Callahan and Knobloch [8] show that if certain nondegeneracy conditions hold on the coefficients of the Taylor expansion of (7.4) up to third order, then the bifurcation problem is fully determined by the third-order truncation of (7.4). In particular, they show that the Σ symmetric solution can be stable at bifurcation. For the Σ symmetric solution to be stable we require $h_3(0) > 0$ and $3h_{1,\sigma_1}(0) + h_3(0) > 0$. Summarising, we have

Theorem 7.1
Let $f : \mathbb{C}^3 \times \mathbb{R} \to \mathbb{C}^3$ be a Γ-equivariant bifurcation problem. Then generically there exists a branch of steady-state solutions bifurcating from the origin with Σ-symmetry. Furthermore, if suitable nondegeneracy conditions hold, the bifurcation problem is fully determined by the third order truncation of the vector field. In particular, the solution can be stable at bifurcation.

Proof. See Callahan and Knobloch [8]. □

The group orbit of solutions with Σ symmetry is a 3-torus, which we denote throughout by X_0. The coordinate system on X_0 is $\theta = (\theta_1, \theta_2, \theta_3)$ introduced previously. The manifold X_0 is normally hyperbolic.

7.2.2 Forced Symmetry Breaking to $\mathbb{O}$

In this subsection we study the behaviour of the group orbit of bifurcating solutions given by Theorem 7.1, when symmetry-breaking terms with $\mathbb{O}$ symmetry are added to the vector field (7.4). More precisely, let $\mathbf{g} : \mathbb{C}^3 \times \mathbb{R} \to \mathbb{C}^3$ be a $\mathbb{O}$-equivariant vector field which satisfies $\mathbf{g}(\mathbf{0}) = \mathbf{0}$. Let ε be real and small. Consider the perturbed vector field $\mathbf{F} : \mathbb{C}^3 \times \mathbb{R}^2 \to \mathbb{C}^3$ defined by

$$\mathbf{F}(\mathbf{z}, \lambda, \varepsilon) = \mathbf{f}(\mathbf{z}, \lambda) + \varepsilon \mathbf{g}(\mathbf{z}).$$

The normal hyperbolicity of X_0 guarantees, by the Equivariant Persistence Theorem, the existence of a manifold X_ε $\mathbb{O}$-equivariantly diffeomorphic to X_0 and invariant under the dynamics of $\mathbf{F}$. Thus we can consider the behaviour of the $\mathbb{O}$-equivariant vector field on X_ε by considering its behaviour on X_0. The action of the group $\mathbb{O}$ on the space $\mathbb{C}^3$ is given in Table 7.1. This action is computed in the standard way. We compute the action of the elements of $\mathbb{O}$, as given in Appendix B, on the generators $\mathbf{K}_j$, $j = 1, \ldots, 3$ for the dual lattice; this computation is straightforward. We require this action for all future computations involving the subgroups of $\mathbb{O}$.

Calculation of the Skeleton

Each subgroup of $\mathbb{O}$ leaves certain submanifolds of X_0 fixed. These submanifolds are very important when trying to understand how $\mathbb{O}$-equivariant flows behave on X_0. Here we calculate the skeleton of X_0 under the action of $\mathbb{O}$. Our starting point is the computation of the set $\mathscr{C}_\mathbb{O}$, for which we require the following fundamental lemma.

Table 7.1: Action of the elements of $\mathbb{O}$ on $\mathbb{C}^3$ for the SC lattice.

Element of $\mathbb{O}$	Action on $\mathbb{C}^3$	Element of $\mathbb{O}$	Action on $\mathbb{C}^3$
ρ_x	$(z_1, \overline{z_3}, z_2)$	τ_2^2	$(\overline{z_3}, \overline{z_1}, z_2)$
ρ_x^2	$(z_1, \overline{z_2}, \overline{z_3})$	τ_3	$(\overline{z_3}, z_1, \overline{z_2})$
ρ_x^3	$(z_1, z_3, \overline{z_2})$	τ_3^2	$(z_2, \overline{z_3}, \overline{z_1})$
ρ_y	$(z_3, z_2, \overline{z_1})$	τ_4	$(\overline{z_2}, \overline{z_3}, z_1)$
ρ_y^2	$(\overline{z_1}, z_2, \overline{z_3})$	τ_4^2	$(z_3, \overline{z_1}, \overline{z_2})$
ρ_y^3	$(\overline{z_3}, z_2, z_1)$	κ_1	$(z_2, z_1, \overline{z_3})$
ρ_z	$(\overline{z_2}, z_1, z_3)$	κ_2	$(\overline{z_2}, \overline{z_1}, \overline{z_3})$
ρ_z^2	$(\overline{z_1}, \overline{z_2}, z_3)$	κ_3	$(z_3, \overline{z_2}, z_1)$
ρ_z^3	$(z_2, \overline{z_1}, z_3)$	κ_4	$(\overline{z_1}, z_3, z_2)$
τ_1	(z_3, z_1, z_2)	κ_5	$(\overline{z_3}, \overline{z_2}, \overline{z_1})$
τ_1^2	(z_2, z_3, z_1)	κ_6	$(\overline{z_1}, \overline{z_3}, \overline{z_2})$
τ_2	$(\overline{z_2}, z_3, \overline{z_1})$		

Lemma 7.2
There are 30 subgroups of $\mathbb{O}$. They are:

$\mathbb{O}$, $\mathbb{T}$, $\mathbf{D}_4[\rho_x, \kappa_6]$, $\mathbf{D}_4[\rho_y, \kappa_5]$, $\mathbf{D}_4[\rho_z, \kappa_1]$, $\mathbf{D}_3[\tau_1, \kappa_5]$,
$\mathbf{D}_3[\tau_4, \kappa_5]$, $\mathbf{D}_3[\tau_3, \kappa_3]$, $\mathbf{D}_3[\tau_2, \kappa_1]$, $\mathbf{Z}_4[\rho_x]$, $\mathbf{Z}_4[\rho_y]$, $\mathbf{Z}_4[\rho_z]$,
$\mathbf{D}_2[\rho_x^2, \kappa_4]$, $\mathbf{D}_2[\rho_y^2, \kappa_5]$, $\mathbf{D}_2[\rho_z^2, \kappa_1]$, $\mathbf{D}_2[\rho_x^2, \rho_y^2]$, $\mathbf{Z}_3[\tau_1]$, $\mathbf{Z}_3[\tau_2]$,
$\mathbf{Z}_3[\tau_3]$, $\mathbf{Z}_3[\tau_4]$, $\mathbf{Z}_2[\rho_x^2]$, $\mathbf{Z}_2[\rho_y^2]$, $\mathbf{Z}_2[\rho_z^2]$, $\mathbf{Z}_2[\kappa_1]$,
$\mathbf{Z}_2[\kappa_2]$, $\mathbf{Z}_2[\kappa_3]$, $\mathbf{Z}_2[\kappa_4]$, $\mathbf{Z}_2[\kappa_5]$, $\mathbf{Z}_2[\kappa_6]$,

and the trivial subgroup.

Proof. See Appendix B. □

Using the coordinates $(\theta_1, \theta_2, \theta_3)$ on X_0, we can express the fixed-point submanifolds of $\mathbb{O}$ conveniently. The main problem we encounter at this point is notational. Since there is a (reasonably) large number of subgroups of $\mathbb{O}$, there is a large number of fixed-point submanifolds on X_0. To help with this problem we introduce some notation; although the list is large, we shall see when considering the projected skeleton that we can make great simplifications. However, for the moment we must consider the full list of all zero and one-dimensional fixed-point submanifolds.

Definition 7.3
Define the following subsets of X_0:

$e_1 = \{(0,0,0)\}$, $e_2 = \{(0,0,\pi)\}$, $e_3 = \{(0,\pi,0)\}$,
$e_4 = \{(\pi,0,0)\}$, $e_5 = \{(\pi,\pi,0)\}$, $e_6 = \{(\pi,0,\pi)\}$,
$e_7 = \{(0,\pi,\pi)\}$, $e_8 = \{(\pi,\pi,\pi)\}$.
$c_1 = \{(\theta,0,0) \mid \theta \in [0,2\pi)\}$, $c_2 = \{(\theta,\pi,\pi) \mid \theta \in [0,2\pi)\}$, $c_3 = \{(0,\theta,0) \mid \theta \in [0,2\pi)\}$,
$c_4 = \{(\pi,\theta,\pi) \mid \theta \in [0,2\pi)\}$, $c_5 = \{(0,0,\theta) \mid \theta \in [0,2\pi)\}$, $c_6 = \{(\pi,\pi,\theta) \mid \theta \in [0,2\pi)\}$,
$c_7 = \{(\theta,\theta,0) \mid \theta \in [0,2\pi)\}$, $c_8 = \{(\theta,\theta,\pi) \mid \theta \in [0,2\pi)\}$, $c_9 = \{(\theta,-\theta,0) \mid \theta \in [0,2\pi)\}$,
$c_{10} = \{(\theta,-\theta,\pi) \mid \theta \in [0,2\pi)\}$, $c_{11} = \{(\theta,0,\theta) \mid \theta \in [0,2\pi)\}$, $c_{12} = \{(\theta,\pi,\theta) \mid \theta \in [0,2\pi)\}$,
$c_{13} = \{(\theta,0,-\theta) \mid \theta \in [0,2\pi)\}$, $c_{14} = \{(\theta,\pi,-\theta) \mid \theta \in [0,2\pi)\}$, $c_{15} = \{(0,\theta,\theta) \mid \theta \in [0,2\pi)\}$,
$c_{16} = \{(\pi,\theta,\theta) \mid \theta \in [0,2\pi)\}$, $c_{17} = \{(0,\theta,-\theta) \mid \theta \in [0,2\pi)\}$, $c_{18} = \{(\pi,\theta,-\theta) \mid \theta \in [0,2\pi)\}$,
$c_{19} = \{(\theta,\theta,\theta) \mid \theta \in [0,2\pi)\}$, $c_{20} = \{(\theta,-\theta,-\theta) \mid \theta \in [0,2\pi)\}$, $c_{21} = \{(\theta,\theta,-\theta) \mid \theta \in [0,2\pi)\}$,
$c_{22} = \{(\theta,-\theta,\theta) \mid \theta \in [0,2\pi)\}$, $c_{23} = \{(\theta,\pi,0) \mid \theta \in [0,2\pi)\}$, $c_{24} = \{(\theta,0,\pi) \mid \theta \in [0,2\pi)\}$,
$c_{25} = \{(\pi,\theta,0) \mid \theta \in [0,2\pi)\}$, $c_{26} = \{(0,\theta,\pi) \mid \theta \in [0,2\pi)\}$, $c_{27} = \{(0,\pi,\theta) \mid \theta \in [0,2\pi)\}$,
$c_{28} = \{(\pi,0,\theta) \mid \theta \in [0,2\pi)\}$

Using these definitions we may state the following fundamental proposition.

Proposition 7.4
Let $\mathbb{O}$ act on X_0 as induced from Table 7.1. Then

$$\begin{aligned}\mathscr{C}_{\mathbb{O}} = \{&e_1, e_2, e_3, e_4, e_5, e_6, e_7, e_8, c_1, c_2, c_3, c_4, c_5, c_6, c_7, c_8, c_9, c_{10}, c_{11}, c_{12},\\ &c_{13}, c_{14}, c_{15}, c_{16}, c_{17}, c_{18}, c_{19}, c_{20}, c_{21}, c_{22}, c_{23}, c_{24}, c_{25}, c_{26}, c_{27}, c_{28}\}.\end{aligned}$$

We divide the proof of this proposition into a series of lemmas. Each of these lemmas is useful for our later work on forced symmetry breaking to other subgroups of $\mathbb{O}$. We recall the trivial fact that $\mathrm{Fix}(\Sigma) = \{(x,x,x)\big|x \in \mathbb{R}\}$, and Lemma 2.8 which states that for a subgroup $\Delta \subseteq \mathbb{O}$

$$\mathrm{Fix}_{X_0}(\Delta) = \{\gamma \in \Gamma\big|\gamma\mathrm{Fix}(\Sigma) \subseteq \mathrm{Fix}(\Delta)\}/\Sigma,$$

where $\mathrm{Fix}(\Sigma)$ and $\mathrm{Fix}(\Delta) \subseteq \mathbb{C}^3$. Both of these results are used in the proofs of all the lemmas.

Lemma 7.5
Let the groups $\mathbb{O}$, $\mathbb{T}$, $\mathbf{D}_3[\tau_1, \kappa_5]$, $\mathbf{D}_3[\tau_4, \kappa_5]$, $\mathbf{D}_3[\tau_3, \kappa_3]$ and $\mathbf{D}_3[\tau_2, \kappa_1]$ act on X_0 with the action induced from Table 7.1. Then the fixed-point submanifolds in X_0 of each of these groups is $e_1 \cup e_8$.

Proof. Let Δ be any of $\mathbb{O}$, $\mathbb{T}$, $\mathbf{D}_3[\tau_1, \kappa_5]$, $\mathbf{D}_3[\tau_4, \kappa_5]$, $\mathbf{D}_3[\tau_3, \kappa_3]$ or $\mathbf{D}_3[\tau_2, \kappa_1]$. We begin by showing that $\mathrm{Fix}(\Delta) = \mathrm{Fix}(\mathbb{O})$. To finish the proof we need consider only the group $\mathbb{O}$. The case $\Delta = \mathbb{O}$ is trivial.

Case 1: $\mathbb{T}$. Since τ_1 and τ_1^2 are contained in $\mathbb{T}$, it follows that $\mathrm{Fix}(\mathbb{T}) \subset \{(z,z,z)\big|z \in \mathbb{C}^3\}$. Since $\rho_z^2 \in \mathbb{T}$, $z = \overline{z}$, so $\mathrm{Fix}(\mathbb{T}) = \mathrm{Fix}(\mathbb{O})$.

Case 2: $\mathbf{D}_3[\tau_1, \kappa_5]$. As for the group $\mathbb{T}$, since $\tau_1 \in \mathbf{D}_3[\tau_1, \kappa_5]$, $\mathrm{Fix}(\mathbf{D}_3[\tau_1, \kappa_5]) \subset \{(z,z,z)\big|z \in \mathbb{C}^3\}$. Furthermore, since $\kappa_5 \in \mathbf{D}_3[\tau_1, \kappa_5]$ $z = \overline{z}$ and so $\mathrm{Fix}(\mathbf{D}_3[\tau_1, \kappa_5]) = \mathrm{Fix}(\mathbb{O})$.

Case 3: $\mathbf{D}_3[\tau_2, \kappa_1]$. Since $\tau_2 \in \mathbf{D}_3[\tau_2, \kappa_1]$, $\mathrm{Fix}(\mathbf{D}_3[\tau_2, \kappa_1]) \subset \{(z,\overline{z},\overline{z})\big|z \in \mathbb{C}^3\}$. Furthermore, $\kappa_1 \in \mathbf{D}_3[\tau_2, \kappa_1]$ implies $z = \overline{z}$. So $\mathrm{Fix}(\mathbf{D}_3[\tau_2, \kappa_1]) = \mathrm{Fix}(\mathbb{O})$.

Case 4: $\mathbf{D}_3[\tau_3, \kappa_3]$. Since $\tau_3 \in \mathbf{D}_3[\tau_3, \kappa_3]$, $\mathrm{Fix}(\mathbf{D}_3[\tau_3, \kappa_3]) \subset \{(z,z,\overline{z})\big|z \in \mathbb{C}^3\}$. Furthermore, $\kappa_3 \in \mathbf{D}_3[\tau_3, \kappa_3]$ implies $z = \overline{z}$, whence $\mathrm{Fix}(\mathbf{D}_3[\tau_3, \kappa_3]) = \mathrm{Fix}(\mathbb{O})$.

Case 5: $\mathbf{D}_3[\tau_4, \kappa_5]$. Finally, $\tau_4 \in \mathbf{D}_3[\tau_4, \kappa_5]$, implies $\mathrm{Fix}(\mathbf{D}_3[\tau_4, \kappa_5]) \subset \{(z,\overline{z},z)\big|z \in \mathbb{C}^3\}$. Since $\kappa_5 \in \mathbf{D}_3[\tau_4, \kappa_5]$ we have $z = \overline{z}$. So $\mathrm{Fix}(\mathbf{D}_3[\tau_4, \kappa_5]) = \mathrm{Fix}(\mathbb{O})$.

To complete the proof we compute $\mathrm{Fix}_{X_0}(\mathbb{O})$. There is the equality

$$\mathrm{Fix}_{X_0}(\mathbb{O}) = N_\Gamma(\mathbb{O}, \mathbb{O} \oplus \mathbf{Z}_2^c)/\mathbb{O} \oplus \mathbf{Z}_2^c,$$

where $N_\Gamma(\mathbb{O}, \mathbb{O} \oplus \mathbf{Z}_2^c) = \{\gamma \in \Gamma\big|\gamma\mathrm{Fix}(\mathbb{O} \oplus \mathbf{Z}_2^c) \subseteq \mathrm{Fix}(\mathbb{O})\}$. A simple calculation shows that $\mathrm{Fix}_{X_0}(\mathbb{O}) = e_1 \cup e_8$. By our initial observations, this completes the proof. □

We now analyse the subgroups of order eight, that is, those isomorphic to $\mathbf{D}_4$.

Lemma 7.6
Let $\mathbf{D}_4[\rho_x, \kappa_6]$, $\mathbf{D}_4[\rho_y, \kappa_5]$ and $\mathbf{D}_4[\rho_z, \kappa_1]$ act on X_0 with the action induced from Table 7.1. Then

$$\begin{aligned}\mathrm{Fix}_{X_0}(\mathbf{D}_4[\rho_x, \kappa_6]) &= e_1 \cup e_4 \cup e_7 \cup e_8,\\ \mathrm{Fix}_{X_0}(\mathbf{D}_4[\rho_y, \kappa_5]) &= e_1 \cup e_3 \cup e_6 \cup e_8,\\ \mathrm{Fix}_{X_0}(\mathbf{D}_4[\rho_z, \kappa_1]) &= e_1 \cup e_2 \cup e_5 \cup e_8.\end{aligned}$$

Proof.

Case 1: $\mathbf{D}_4[\rho_x, \kappa_6]$. Since $\rho_x \in \mathbf{D}_4[\rho_x, \kappa_6]$, $\mathrm{Fix}(\mathbf{D}_4[\rho_x, \kappa_6]) \subset \{(z, x, x) | x \in \mathbb{R}, z \in \mathbb{C}\}$. Furthermore, the action of κ_6 shows that $z = \overline{z}$. So $\mathrm{Fix}(\mathbf{D}_4[\rho_x, \kappa_6]) = \{(y, x, x) | x \in \mathbb{R}, y \in \mathbb{C}\}$. Next compute

$$N_\Gamma(\mathbf{D}_4[\rho_x, \kappa_6], \mathbb{O} \oplus \mathbf{Z}_2^c) = \{\gamma \in \Gamma | \gamma \mathrm{Fix}(\mathbb{O} \oplus \mathbf{Z}_2^c) \subseteq \mathrm{Fix}(\mathbf{D}_4[\rho_x, \kappa_6])\}.$$

Clearly $\mathbb{O} \oplus \mathbf{Z}_2^c \subset N_\Gamma(\mathbf{D}_4[\rho_x, \kappa_6], \mathbb{O} \oplus \mathbf{Z}_2^c)$. The other elements of Γ contained in $N_\Gamma(\mathbf{D}_4[\rho_x, \kappa_6], \mathbb{O} \oplus \mathbf{Z}_2^c)$ are those in $\mathbf{T}^3$. Clearly $(\theta_1, \theta_2, \theta_3) \in \mathbf{T}^3$ is contained in $N_\Gamma(\mathbf{D}_4[\rho_x, \kappa_6], \mathbb{O} \oplus \mathbf{Z}_2^c)$ if and only if $\theta_1 = 0$ or π mod 2π and $\theta_2 = \theta_3 = 0$ or π mod 2π. Thus $N_\Gamma(\mathbf{D}_4[\rho_x, \kappa_6], \mathbb{O} \oplus \mathbf{Z}_2^c) = \mathbb{O} \oplus \mathbf{Z}_2^c \cup e_1 \cup e_4 \cup e_7 \cup e_8$. Since

$$\mathrm{Fix}_{X_0}(\mathbf{D}_4[\rho_x, \kappa_6]) = N_\Gamma(\mathbf{D}_4[\rho_x, \kappa_6], \mathbb{O} \oplus \mathbf{Z}_2^c)/\mathbb{O} \oplus \mathbf{Z}_2^c,$$

the result follows.

Case 2: $\mathbf{D}_4[\rho_y, \kappa_5]$. This case is very similar to $\mathbf{D}_4[\rho_x, \kappa_6]$. Since $\rho_y \in \mathbf{D}_4[\rho_y, \kappa_5]$ it follows that $\mathrm{Fix}(\mathbf{D}_4[\rho_y, \kappa_5]) \subset \{(x, z, x) | x \in \mathbb{R}, z \in \mathbb{C}\}$. The action of κ_5 shows that $z = \overline{z}$, hence $\mathrm{Fix}(\mathbf{D}_4[\rho_y, \kappa_5]) = \{(x, y, x) | x \in \mathbb{R}, y \in \mathbb{C}\}$. Next compute

$$N_\Gamma(\mathbf{D}_4[\rho_y, \kappa_5], \mathbb{O} \oplus \mathbf{Z}_2^c) = \{\gamma \in \Gamma | \gamma \mathrm{Fix}(\mathbb{O} \oplus \mathbf{Z}_2^c) \subseteq \mathrm{Fix}(\mathbf{D}_4[\rho_y, \kappa_5])\}.$$

Clearly $\mathbb{O} \oplus \mathbf{Z}_2^c \subset N_\Gamma(\mathbf{D}_4[\rho_y, \kappa_5], \mathbb{O} \oplus \mathbf{Z}_2^c)$. A simple computation show that $(\theta_1, \theta_2, \theta_3) \in \mathbf{T}^3$ is contained in $N_\Gamma(\mathbf{D}_4[\rho_y, \kappa_5], \mathbb{O} \oplus \mathbf{Z}_2^c)$ if and only if $\theta_2 = 0$ or π mod 2π and $\theta_1 = \theta_3 = 0$ or π mod 2π. Hence $N_\Gamma(\mathbf{D}_4[\rho_y, \kappa_5], \mathbb{O} \oplus \mathbf{Z}_2^c) = \mathbb{O} \oplus \mathbf{Z}_2^c \cup e_1 \cup e_3 \cup e_6 \cup e_8$. Since

$$\mathrm{Fix}_{X_0}(\mathbf{D}_4[\rho_y, \kappa_5]) = N_\Gamma(\mathbf{D}_4[\rho_y, \kappa_5], \mathbb{O} \oplus \mathbf{Z}_2^c)/\mathbb{O} \oplus \mathbf{Z}_2^c,$$

the result follows.

Case 3: $\mathbf{D}_4[\rho_z, \kappa_1]$. This case follows identical lines. Since $\rho_z \in \mathbf{D}_4[\rho_z, \kappa_1]$, $\mathrm{Fix}(\mathbf{D}_4[\rho_z, \kappa_1]) \subset \{(x, x, z) | x \in \mathbb{R}, z \in \mathbb{C}\}$. In addition the action of κ_1 shows that $z = \overline{z}$, thus $\mathrm{Fix}(\mathbf{D}_4[\rho_z, \kappa_1]) = \{(x, x, y) | x \in \mathbb{R}, y \in \mathbb{C}\}$. Next compute

$$N_\Gamma(\mathbf{D}_4[\rho_z, \kappa_1], \mathbb{O} \oplus \mathbf{Z}_2^c) = \{\gamma \in \Gamma | \gamma \mathrm{Fix}(\mathbb{O} \oplus \mathbf{Z}_2^c) \subseteq \mathrm{Fix}(\mathbf{D}_4[\rho_z, \kappa_1])\}.$$

Clearly $\mathbb{O} \oplus \mathbf{Z}_2^c \subset N_\Gamma(\mathbf{D}_4[\rho_z, \kappa_1], \mathbb{O} \oplus \mathbf{Z}_2^c)$. To complete the computation we must find the other elements of Γ that are contained in $N_\Gamma(\mathbf{D}_4[\rho_z, \kappa_1], \mathbb{O} \oplus \mathbf{Z}_2^c)$. These must be elements of $\mathbf{T}^3$. Clearly $(\theta_1, \theta_2, \theta_3) \in \mathbf{T}^3$ is contained in $N_\Gamma(\mathbf{D}_4[\rho_z, \kappa_1], \mathbb{O} \oplus \mathbf{Z}_2^c)$ if and only if $\theta_3 = 0$ or π mod 2π and $\theta_1 = \theta_2 = 0$ or π mod 2π. Thus $N_\Gamma(\mathbf{D}_4[\rho_z, \kappa_1], \mathbb{O} \oplus \mathbf{Z}_2^c) = \mathbb{O} \oplus \mathbf{Z}_2^c \cup e_1 \cup e_2 \cup e_5 \cup e_8$. Since

$$\mathrm{Fix}_{X_0}(\mathbf{D}_4[\rho_z, \kappa_1]) = N_\Gamma(\mathbf{D}_4[\rho_z, \kappa_1], \mathbb{O} \oplus \mathbf{Z}_2^c)/\mathbb{O} \oplus \mathbf{Z}_2^c,$$

the result follows. □

Next consider the groups $\mathbf{Z}_4[\rho_x]$, $\mathbf{Z}_4[\rho_y]$, and $\mathbf{Z}_4[\rho_z]$.

Lemma 7.7
Let $\mathbf{Z}_4[\rho_x]$, $\mathbf{Z}_4[\rho_y]$, and $\mathbf{Z}_4[\rho_z]$ act on X_0 with the action induced from Table 7.1. Then

$$\begin{aligned} \mathrm{Fix}_{X_0}(\mathbf{Z}_4[\rho_x]) &= c_1 \cup c_2, \\ \mathrm{Fix}_{X_0}(\mathbf{Z}_4[\rho_y]) &= c_3 \cup c_4, \\ \mathrm{Fix}_{X_0}(\mathbf{Z}_4[\rho_z]) &= c_5 \cup c_6. \end{aligned}$$

Proof.

Case 1: $\mathbf{Z}_4[\rho_x]$. The action of $\rho_x \in \mathbf{Z}_4[\rho_x]$ implies that $\mathrm{Fix}(\mathbf{Z}_4[\rho_x]) = \{(z,x,x)\big|x \in \mathbb{R}, z \in \mathbb{C}\}$. Using this we compute,

$$N_\Gamma(\mathbf{Z}_4[\rho_x], \mathbb{O} \oplus \mathbf{Z}_2^c) = \{\gamma \in \Gamma\big|\gamma\mathrm{Fix}(\mathbb{O} \oplus \mathbf{Z}_2^c) \subseteq \mathrm{Fix}(\mathbf{Z}_4[\rho_x])\}.$$

Trivially $\mathbb{O} \oplus \mathbf{Z}_2^c \subset N_\Gamma(\mathbf{Z}_4[\rho_x], \mathbb{O} \oplus \mathbf{Z}_2^c)$. Now we find those elements of $\mathbf{T}^3$ contained in $N_\Gamma(\mathbf{Z}_4[\rho_x], \mathbb{O} \oplus \mathbf{Z}_2^c)$. Clearly $(\theta_1, \theta_2, \theta_3) \in \mathbf{T}^3$ is contained in $N_\Gamma(\mathbf{Z}_4[\rho_x], \mathbb{O} \oplus \mathbf{Z}_2^c)$ if and only if $\theta_1 \in [0, 2\pi)$ and $\theta_2 = \theta_3 = 0$ or $\pi \bmod 2\pi$. Thus $N_\Gamma(\mathbf{Z}_4[\rho_x], \mathbb{O} \oplus \mathbf{Z}_2^c) = \mathbb{O} \oplus \mathbf{Z}_2^c \cup c_1 \cup c_2$. Since

$$\mathrm{Fix}_{X_0}(\mathbf{Z}_4[\rho_x]) = N_\Gamma(\mathbf{Z}_4[\rho_x], \mathbb{O} \oplus \mathbf{Z}_2^c)/\mathbb{O} \oplus \mathbf{Z}_2^c,$$

the result follows.

Case 2: $\mathbf{Z}_4[\rho_y]$. Since $\rho_y \in \mathbf{Z}_4[\rho_x]$, $\mathrm{Fix}(\mathbf{Z}_4[\rho_y]) = \{(x,z,x)\big|x \in \mathbb{R}, z \in \mathbb{C}\}$. To compute the fixed-point submanifold we must calculate

$$N_\Gamma(\mathbf{Z}_4[\rho_y], \mathbb{O} \oplus \mathbf{Z}_2^c) = \{\gamma \in \Gamma\big|\gamma\mathrm{Fix}(\mathbb{O} \oplus \mathbf{Z}_2^c) \subseteq \mathrm{Fix}(\mathbf{Z}_4[\rho_y])\}.$$

As always $\mathbb{O} \oplus \mathbf{Z}_2^c \subset N_\Gamma(\mathbf{Z}_4[\rho_y], \mathbb{O} \oplus \mathbf{Z}_2^c)$. A computation shows that $(\theta_1, \theta_2, \theta_3) \in \mathbf{T}^3$ is contained in $N_\Gamma(\mathbf{Z}_4[\rho_y], \mathbb{O} \oplus \mathbf{Z}_2^c)$ if and only if $\theta_2 \in [0, 2\pi)$ and $\theta_1 = \theta_3 = 0$ or $\pi \bmod 2\pi$. Thus $N_\Gamma(\mathbf{Z}_4[\rho_y], \mathbb{O} \oplus \mathbf{Z}_2^c) = \mathbb{O} \oplus \mathbf{Z}_2^c \cup c_3 \cup c_4$. Using the equation

$$\mathrm{Fix}_{X_0}(\mathbf{Z}_4[\rho_y]) = N_\Gamma(\mathbf{Z}_4[\rho_y], \mathbb{O} \oplus \mathbf{Z}_2^c)/\mathbb{O} \oplus \mathbf{Z}_2^c,$$

the result follows.

Case 3: $\mathbf{Z}_4[\rho_z]$. This case follows identical lines. The action of $\rho_z \in \mathbf{Z}_4[\rho_z]$ shows $\mathrm{Fix}(\mathbf{Z}_4[\rho_z]) = \{(x,x,z)\big|x \in \mathbb{R}, z \in \mathbb{C}\}$. TO compute the fixed-point submanifold of $\mathbf{Z}_4[\rho_z]$ in X_0, we find the elements of

$$N_\Gamma(\mathbf{Z}_4[\rho_z], \mathbb{O} \oplus \mathbf{Z}_2^c) = \{\gamma \in \Gamma\big|\gamma\mathrm{Fix}(\mathbb{O} \oplus \mathbf{Z}_2^c) \subseteq \mathrm{Fix}(\mathbf{Z}_4[\rho_z])\}.$$

Obviously $\mathbb{O} \oplus \mathbf{Z}_2^c \subset N_\Gamma(\mathbf{Z}_4[\rho_z], \mathbb{O} \oplus \mathbf{Z}_2^c)$. A calculation shows that $(\theta_1, \theta_2, \theta_3) \in \mathbf{T}^3$ is contained in $N_\Gamma(\mathbf{Z}_4[\rho_z], \mathbb{O} \oplus \mathbf{Z}_2^c)$ if and only if $\theta_3 \in [0, 2\pi)$ and $\theta_1 = \theta_2 = 0$ or $\pi \bmod 2\pi$. Thus $N_\Gamma(\mathbf{Z}_4[\rho_z], \mathbb{O} \oplus \mathbf{Z}_2^c) = \mathbb{O} \oplus \mathbf{Z}_2^c \cup c_5 \cup c_6$. Since

$$\mathrm{Fix}_{X_0}(\mathbf{Z}_4[\rho_z]) = N_\Gamma(\mathbf{Z}_4[\rho_z], \mathbb{O} \oplus \mathbf{Z}_2^c)/\mathbb{O} \oplus \mathbf{Z}_2^c,$$

the result follows. □

Next we consider the subgroups $\mathbf{D}_2[\rho_x^2, \kappa_4]$, $\mathbf{D}_2[\rho_y^2, \kappa_5]$, $\mathbf{D}_2[\rho_z^2, \kappa_1]$, and $\mathbf{D}_2[\rho_x^2, \rho_y^2]$.

Lemma 7.8
Let $\mathbf{D}_2[\rho_x^2, \kappa_4]$, $\mathbf{D}_2[\rho_y^2, \kappa_5]$, $\mathbf{D}_2[\rho_z^2, \kappa_1]$, and $\mathbf{D}_2[\rho_x^2, \rho_y^2]$ act on X_0 with the action induced from Table 7.1. Then

$$\begin{aligned}
\mathrm{Fix}_{X_0}(\mathbf{D}_2[\rho_x^2, \kappa_6]) &= e_1 \cup e_4 \cup e_7 \cup e_8, \\
\mathrm{Fix}_{X_0}(\mathbf{D}_2[\rho_y^2, \kappa_5]) &= e_1 \cup e_3 \cup e_6 \cup e_8, \\
\mathrm{Fix}_{X_0}(\mathbf{D}_2[\rho_z^2, \kappa_1]) &= e_1 \cup e_2 \cup e_5 \cup e_8, \\
\mathrm{Fix}_{X_0}(\mathbf{D}_2[\rho_x^2, \rho_y^2]) &= \bigcup_{i=1,\ldots,8} e_i.
\end{aligned}$$

Proof. It should be noted immediately that the $\mathbf{D}_2$ subgroups which contain an element κ_i for some i have the same fixed-point submanifolds as the $\mathbf{D}_4$ subgroups in which they are contained. We begin by proving this assertion. Consider the group $\mathbf{D}_2[\rho_x^2, \kappa_6]$.

Since $\rho_x^2 \in \mathbf{D}_2[\rho_x^2, \kappa_6]$, an element $\mathbf{z} = (z_1, z_2, z_3) \in \mathbb{C}^3$ is fixed by ρ_x^2 if and only if z_2 and z_3 are real. Furthermore, $\kappa_6 \in \mathbf{D}_2[\rho_x^2, \kappa_6]$ implies z_1 must be real and $z_2 = z_3$. So $\mathrm{Fix}(\mathbf{D}_2[\rho_x^2, \kappa_6]) = \mathrm{Fix}(\mathbf{D}_4[\rho_x, \kappa_6])$, which proves the first assertion. Similarly, since ρ_y^2 and κ_5 are contained in $\mathbf{D}_2[\rho_y^2, \kappa_5]$, $\mathrm{Fix}(\mathbf{D}_2[\rho_y^2, \kappa_5]) = \mathrm{Fix}(\mathbf{D}_4[\rho_y, \kappa_5])$. Also, since ρ_z^2 and κ_1 are contained in $\mathbf{D}_2[\rho_z^2, \kappa_1]$, $\mathrm{Fix}(\mathbf{D}_2[\rho_z^2, \kappa_1]) = \mathrm{Fix}(\mathbf{D}_4[\rho_z, \kappa_1])$. This completes the proof of the first three fixed-point submanifolds.

To finish the proof, consider the group $\mathbf{D}_2[\rho_x^2, \rho_y^2]$. Since ρ_x^2 and ρ_y^2 are contained in $\mathbf{D}_2[\rho_x^2, \rho_y^2]$, an element $\mathbf{z} = (z_1, z_2, z_3) \in \mathbb{C}^3$ is fixed by $\mathbf{D}_2[\rho_x^2, \rho_y^2]$ if and only if z_1, z_2, z_3 are all real. Therefore,

$$N_\Gamma(\mathbf{D}_2[\rho_x^2, \rho_y^2], \mathbb{O} \oplus \mathbf{Z}_2^c) = \{\gamma \in \Gamma \big| \gamma \mathrm{Fix}(\mathbb{O} \oplus \mathbf{Z}_2^c) \subseteq \mathrm{Fix}(\mathbf{D}_2[\rho_x^2, \rho_y^2])\}$$

contains the elements $e_1, \ldots, e_8$ as well as $\mathbb{O} \oplus \mathbf{Z}_2^c$. So

$$\mathrm{Fix}_{X_0}(\mathbf{D}_2[\rho_x^2, \rho_y^2]) = \bigcup_{i=1,\ldots,8} e_i,$$

as required. □

Next we consider the groups $\mathbf{Z}_3[\tau_1]$, $\mathbf{Z}_3[\tau_2]$, $\mathbf{Z}_3[\tau_3]$, and $\mathbf{Z}_3[\tau_4]$.

Lemma 7.9
Let $\mathbf{Z}_3[\tau_1]$, $\mathbf{Z}_3[\tau_2]$, $\mathbf{Z}_3[\tau_3]$ and $\mathbf{Z}_3[\tau_4]$ act on X_0 with the action induced from their action on $\mathbb{C}^3$ given in Table 7.1. Then

$$\begin{aligned} \mathrm{Fix}_{X_0}(\mathbf{Z}_3[\tau_1]) &= c_{19}, \\ \mathrm{Fix}_{X_0}(\mathbf{Z}_3[\tau_2]) &= c_{20}, \\ \mathrm{Fix}_{X_0}(\mathbf{Z}_3[\tau_3]) &= c_{21}, \\ \mathrm{Fix}_{X_0}(\mathbf{Z}_4[\tau_4]) &= c_{22}. \end{aligned}$$

Proof. The proof follows standard lines.

Case 1: $\mathbf{Z}_3[\tau_1]$. Since τ_1 and τ_1^2 are contained in $\mathbf{Z}_3[\tau_1]$, any element $(z_1, z_2, z_3) \in \mathbb{C}^3$ is fixed by $\mathbf{Z}_3[\tau_1]$ if and only if $z_1 = z_2 = z_3$. Since $\mathrm{Fix}(\mathbf{Z}_3[\tau_1]) = \{(z, z, z) \big| z \in \mathbb{C}\}$, the element $(\theta_1, \theta_2, \theta_3) \in \mathbf{T}^3$ is contained in $N_\Gamma(\mathbf{Z}_3[\tau_1], \mathbb{O} \oplus \mathbf{Z}_2^c)$ if and only if $\theta_1 = \theta_2 = \theta_3 \in [0, 2\pi)$. So $\mathrm{Fix}(\mathbf{Z}_3[\tau_1]) = c_{19}$.

Case 2: $\mathbf{Z}_3[\tau_2]$. The actions of τ_2 and τ_2^2 show that any element $(z_1, z_2, z_3) \in \mathbb{C}^3$ is fixed by $\mathbf{Z}_3[\tau_2]$ if and only if $z_1 = \overline{z_2} = \overline{z_3}$. Since $\mathrm{Fix}(\mathbf{Z}_3[\tau_2]) = \{(z, \overline{z}, \overline{z}) \big| z \in \mathbb{C}\}$, the element $(\theta_1, \theta_2, \theta_3) \in \mathbf{T}^3$ is contained in $N_\Gamma(\mathbf{Z}_3[\tau_1], \mathbb{O} \oplus \mathbf{Z}_2^c)$ if and only if $\theta_1 = -\theta_2 = -\theta_3 \in [0, 2\pi)$. So $\mathrm{Fix}(\mathbf{Z}_3[\tau_2]) = c_{20}$.

Case 3: $\mathbf{Z}_3[\tau_3]$. Since τ_3 and $\tau_3^2 \in \mathbf{Z}_3[\tau_3]$ any vector $(z_1, z_2, z_3) \in \mathbb{C}^3$ is fixed by $\mathbf{Z}_3[\tau_3]$ if and only if $z_1 = z_2 = \overline{z_3}$. Since $\mathrm{Fix}(\mathbf{Z}_3[\tau_3]) = \{(z, z, \overline{z}) \big| z \in \mathbb{C}\}$, the element $(\theta_1, \theta_2, \theta_3) \in \mathbf{T}^3$ is contained in $N_\Gamma(\mathbf{Z}_3[\tau_3], \mathbb{O} \oplus \mathbf{Z}_2^c)$ if and only if $\theta_1 = \theta_2 = -\theta_3 \in [0, 2\pi)$. So $\mathrm{Fix}(\mathbf{Z}_3[\tau_3]) = c_{21}$.

Case 4: $\mathbf{Z}_3[\tau_4]$. The elements τ_4 and τ_4^2 act on $\mathbb{C}^3$ so that $(z_1, z_2, z_3) \in \mathbb{C}^3$ is fixed by $\mathbf{Z}_3[\tau_4]$ if and only if $z_1 = \overline{z_2} = z_3$. Since $\mathrm{Fix}(\mathbf{Z}_3[\tau_4]) = \{(z, \overline{z}, z) \big| z \in \mathbb{C}\}$, the element $(\theta_1, \theta_2, \theta_3) \in \mathbf{T}^3$ is contained in $N_\Gamma(\mathbf{Z}_3[\tau_4], \mathbb{O} \oplus \mathbf{Z}_2^c)$ if and only if $\theta_1 = -\theta_2 = \theta_3 \in [0, 2\pi)$. So $\mathrm{Fix}(\mathbf{Z}_3[\tau_4]) = c_{22}$. □

Finally we consider the groups $\mathbf{Z}_2[\rho_x^2]$, $\mathbf{Z}_2[\rho_y^2]$, $\mathbf{Z}_2[\rho_z^2]$, $\mathbf{Z}_2[\kappa_1]$, $\mathbf{Z}_2[\kappa_2]$, $\mathbf{Z}_2[\kappa_3]$, $\mathbf{Z}_2[\kappa_4]$, $\mathbf{Z}_2[\kappa_5]$, and $\mathbf{Z}_2[\kappa_6]$.

Lemma 7.10
Let $\mathbf{Z}_2[\rho_x^2]$, $\mathbf{Z}_2[\rho_y^2]$, $\mathbf{Z}_2[\rho_z^2]$, $\mathbf{Z}_2[\kappa_1]$, $\mathbf{Z}_2[\kappa_2]$, $\mathbf{Z}_2[\kappa_3]$, $\mathbf{Z}_2[\kappa_4]$, $\mathbf{Z}_2[\kappa_5]$, *and* $\mathbf{Z}_2[\kappa_6]$ *act on* X_0 *with the action induced from Table 7.1. Then*

$$\begin{aligned}
\mathrm{Fix}_{X_0}(\mathbf{Z}_2[\rho_x^2]) &= c_1 \cup c_2 \cup c_{23} \cup c_{24}, \\
\mathrm{Fix}_{X_0}(\mathbf{Z}_2[\rho_y^2]) &= c_3 \cup c_4 \cup c_{25} \cup c_{25}, \\
\mathrm{Fix}_{X_0}(\mathbf{Z}_2[\rho_z^2]) &= c_5 \cup c_6 \cup c_{27} \cup c_{28}, \\
\mathrm{Fix}_{X_0}(\mathbf{Z}_2[\kappa_1]) &= c_7 \cup c_8, \\
\mathrm{Fix}_{X_0}(\mathbf{Z}_2[\kappa_2]) &= c_9 \cup c_{10}, \\
\mathrm{Fix}_{X_0}(\mathbf{Z}_2[\kappa_3]) &= c_{11} \cup c_{12}, \\
\mathrm{Fix}_{X_0}(\mathbf{Z}_2[\kappa_4]) &= c_{15} \cup c_{16}, \\
\mathrm{Fix}_{X_0}(\mathbf{Z}_2[\kappa_5]) &= c_{13} \cup c_{14}, \\
\mathrm{Fix}_{X_0}(\mathbf{Z}_2[\kappa_6]) &= c_{17} \cup c_{18}.
\end{aligned}$$

Proof. The proof follows the standard approach.

Case 1: $\mathbf{Z}_2[\rho_x^2]$. We find that $\mathrm{Fix}(\mathbf{Z}_2[\rho_x^2]) = \{(z,x,y)\big|x,y \in \mathbb{R}, z \in \mathbb{C}\}$. An easy computation shows $(\theta_1,\theta_2,\theta_3)$ is contained in $N_\Gamma(\mathbf{Z}_2[\rho_x^2], \mathbb{O} \oplus \mathbf{Z}_2^c)$ if and only if $\theta_1 \in [0,2\pi)$ and $\theta_2 = 0$ or π mod 2π and $\theta_3 = 0$ or π mod 2π. Therefore, $\mathrm{Fix}(\mathbf{Z}_2[\rho_x^2]) = c_1 \cup c_2 \cup c_{23} \cup c_{24}$.

Case 2: $\mathbf{Z}_2[\rho_y]$. The action of the group ρ_y^2 shows $\mathrm{Fix}(\mathbf{Z}_2[\rho_y^2]) = \{(x,z,y)\big|x,y \in \mathbb{R}, z \in \mathbb{C}\}$. A computation shows $(\theta_1,\theta_2,\theta_3)$ is contained in $N_\Gamma(\mathbf{Z}_2[\rho_y^2], \mathbb{O} \oplus \mathbf{Z}_2^c)$ if and only if $\theta_2 \in [0,2\pi)$ and $\theta_1 = 0$ or π mod 2π and $\theta_3 = 0$ or π mod 2π. Therefore, $\mathrm{Fix}(\mathbf{Z}_2[\rho_x^2]) = c_3 \cup c_4 \cup c_{25} \cup c_{25}$.

Case 3: $\mathbf{Z}_2[\rho_z]$. Since $\rho_z^2 \in \mathbf{Z}_2[\rho_z^2]$, $\mathrm{Fix}(\mathbf{Z}_2[\rho_z^2]) = \{(x,y,z)\big|x,y \in \mathbb{R}, z \in \mathbb{C}\}$. The element $(\theta_1,\theta_2,\theta_3) \in N_\Gamma(\mathbf{Z}_2[\rho_z^2], \mathbb{O} \oplus \mathbf{Z}_2^c)$ if and only if $\theta_3 \in [0,2\pi)$ and $\theta_1 = 0$ or π mod 2π and $\theta_2 = 0$ or π mod 2π. Therefore, $\mathrm{Fix}(\mathbf{Z}_2[\rho_z^2]) = c_5 \cup c_6 \cup c_{27} \cup c_{28}$.

Case 4: $\mathbf{Z}_2[\kappa_1]$. The action of κ_1 shows $\mathrm{Fix}(\mathbf{Z}_2[\kappa_1]) = \{(z,z,x)\big|x,y \in \mathbb{R}, z \in \mathbb{C}\}$. Next $(\theta_1,\theta_2,\theta_3) \in N_\Gamma(\mathbf{Z}_2[\kappa_1], \mathbb{O} \oplus \mathbf{Z}_2^c)$ if and only if $\theta_1 = \theta_2 \in [0,2\pi)$ and $\theta_3 = 0$ or π mod 2π. Therefore, $\mathrm{Fix}(\mathbf{Z}_2[\kappa_1]) = c_7 \cup c_8$.

Case 5: $\mathbf{Z}_2[\kappa_2]$. The action of κ_2 shows that $\mathrm{Fix}(\mathbf{Z}_2[\kappa_2]) = \{(z,\overline{z},x)\big|x,y \in \mathbb{R}, z \in \mathbb{C}\}$. A simple computation shows $(\theta_1,\theta_2,\theta_3)$ is contained in $N_\Gamma(\mathbf{Z}_2[\kappa_2], \mathbb{O} \oplus \mathbf{Z}_2^c)$ if and only if $\theta_1 = -\theta_2 \in [0,2\pi)$ and $\theta_3 = 0$ or π mod 2π. Therefore, $\mathrm{Fix}(\mathbf{Z}_2[\kappa_2]) = c_9 \cup c_{10}$.

Case 6: $\mathbf{Z}_2[\kappa_3]$. The action of κ_3 shows that $\mathrm{Fix}(\mathbf{Z}_2[\kappa_3]) = \{(z,x,z)\big|x,y \in \mathbb{R}, z \in \mathbb{C}\}$. Observe that $(\theta_1,\theta_2,\theta_3)$ is contained in $N_\Gamma(\mathbf{Z}_2[\kappa_3], \mathbb{O} \oplus \mathbf{Z}_2^c)$ if and only if $\theta_1 = \theta_3 \in [0,2\pi)$ and $\theta_2 = 0$ or π. Therefore, $\mathrm{Fix}(\mathbf{Z}_2[\kappa_3]) = c_{11} \cup c_{12}$.

Case 7: $\mathbf{Z}_2[\kappa_4]$. The action of κ_4 shows that $\mathrm{Fix}(\mathbf{Z}_2[\kappa_4]) = \{(x,z,z)\big|x,y \in \mathbb{R}, z \in \mathbb{C}\}$. The element $(\theta_1,\theta_2,\theta_3)$ is contained in $N_\Gamma(\mathbf{Z}_2[\kappa_4], \mathbb{O} \oplus \mathbf{Z}_2^c)$ if and only if $\theta_2 = \theta_3 \in [0,2\pi)$ and $\theta_1 = 0$ or π mod 2π. Therefore, $\mathrm{Fix}(\mathbf{Z}_2[\kappa_4]) = c_{15} \cup c_{16}$.

Case 8: $\mathbf{Z}_2[\kappa_5]$. We find that $\mathrm{Fix}(\mathbf{Z}_2[\kappa_5]) = \{(z,x,\overline{z})\big|x,y \in \mathbb{R}, z \in \mathbb{C}\}$. The element $(\theta_1,\theta_2,\theta_3) \in N_\Gamma(\mathbf{Z}_2[\kappa_5], \mathbb{O} \oplus \mathbf{Z}_2^c)$ if and only if $\theta_1 = -\theta_3 \in [0,2\pi)$ and $\theta_2 = 0$ or π mod 2π. Therefore, $\mathrm{Fix}(\mathbf{Z}_2[\kappa_5]) = c_{13} \cup c_{14}$.

Case 9: $\mathbf{Z}_2[\kappa_6]$. Clearly $\mathrm{Fix}(\mathbf{Z}_2[\kappa_6]) = \{(x,z,\overline{z})\big|x,y \in \mathbb{R}, z \in \mathbb{C}\}$. A computation $(\theta_1,\theta_2,\theta_3)$ is contained in $N_\Gamma(\mathbf{Z}_2[\kappa_6], \mathbb{O} \oplus \mathbf{Z}_2^c)$ if and only if $\theta_2 = -\theta_3 \in [0,2\pi)$ and $\theta_1 = 0$ or π mod 2π. Therefore, $\mathrm{Fix}(\mathbf{Z}_2[\kappa_6]) = c_{17} \cup c_{18}$. □

This completes the computation of all the fixed-point submanifolds for all nontrivial subgroups of $\mathbb{O}$. It now follows that

$$\begin{aligned}\mathscr{C}_{\mathbb{O}} &= \{e_1, e_2, e_3, e_4, e_5, e_6, e_7, e_8, c_1, c_2, c_3, c_4, c_5, c_6, c_7, c_8, c_9, c_{10}, c_{11}, c_{12},\\ &\quad c_{13}, c_{14}, c_{15}, c_{16}, c_{17}, c_{18}, c_{19}, c_{20}, c_{21}, c_{22}, c_{23}, c_{24}, c_{25}, c_{26}, c_{27}, c_{28}\}.\end{aligned}$$

This completes the proof of Proposition 7.4. We can now use this information to form the skeleton

$$\mathbb{X}_{\mathbb{O}} = \bigcup_{C \in \mathscr{C}_{\mathbb{O}}} C \subset X_0.$$

Since X_0 is a 3-torus it is not very instructive to present a rendering of the skeleton, even if we consider X_0 as the cube $[0, 2\pi)^3$: there are so many different one-dimensional strata. For this reason we delay rendering any object related to the skeleton until we discuss the projected skeleton, for as we shall see upon projecting the skeleton into the orbit space the form of the skeleton is greatly simplified. It would also be possible to decompose $\mathbb{X}_{\mathbb{O}}$ into strata, but again the list of different strata is enormous (one only has to look at the number of one-dimensional components to realise this).

Symmetry Properties of $\mathbb{X}_{\mathbb{O}}$

The skeleton as calculated above is a very complex object, making it difficult to study. Here the $\mathbb{O}$ symmetry is used to isolated those parts of the skeleton that are "important" and "essentially different". By this we mean to study the $\mathbb{O}$ action induced on the skeleton to determine the different orbit representatives for the elements of $\mathscr{C}_{\mathbb{O}}$; that is, elements of $\mathscr{C}_{\mathbb{O}}$ that are not symmetrically related. This allows us to form the projected skeleton, which is a geometrically much simpler object than the skeleton, but still retains all the important information we require. To be more precise, we begin by calculating the action of $\mathbb{O}$ on each $C \in \mathscr{C}_{\mathbb{O}}$. This allows us to identify those C's that are not related by the $\mathbb{O}$ symmetry, which gives a list of orbit representatives for the $\mathbb{O}$ action on $\mathscr{C}_{\mathbb{O}}$. We can construct the setwise isotropy $\mathrm{Stab}(C)$ and pointwise isotropy $\mathrm{stab}(C)$. Using these two groups we may form the group $S(C)$ which provides information on possible knots present on the skeleton, providing axes of symmetry for $\mathbb{O}$-equivariant flows on the skeleton and more simplifications. With this information we can form the projected skeleton.

Pointwise and Setwise Isotropy Subgroups. The action of $\mathbb{O}$ on $\mathbb{C}^3$ in Table 7.1 induces a natural action on X_0 with respect to the coordinates $(\theta_1, \theta_2, \theta_3)$. The generators for $\mathbb{O}$ act as follows:

$$\begin{aligned}\rho_x(\theta_1, \theta_2, \theta_3) &= (\theta_1, -\theta_3, \theta_2),\\ \rho_y(\theta_1, \theta_2, \theta_3) &= (\theta_3, \theta_2, -\theta_1).\end{aligned}$$

The complete action of $\mathbb{O}$ on X_0 is given in Table 7.2. This action is straightforward to compute; we present the computations for ρ_x as an example. Let $(\theta_1, \theta_2, \theta_3) \in X_0$. This element corresponds to the point $\mathbf{z} = (e^{\mathrm{i}\theta_1}, e^{\mathrm{i}\theta_2}, e^{\mathrm{i}\theta_3})x$ in $\mathbb{C}^3$, where x is a positive real number. The action of ρ_x on $\mathbf{z}$ gives the new point $(e^{\mathrm{i}\theta_1}, e^{-\mathrm{i}\theta_3}, e^{\mathrm{i}\theta_2})x$, which when written in the $(\theta_1, \theta_2, \theta_3)$ coordinates on X_0 gives the required action. The action of $\mathbb{O}$ on X_0 in turn induces an action of $\mathbb{O}$ on the set $\mathscr{C}_{\mathbb{O}}$ by permutation of its elements. Again this action is easy (but longwinded) to compute. As an example we consider the action of ρ_y on c_1. In the coordinates on X_0 an element of c_1 is given by $(\theta, 0, 0)$ where $\theta \in [0, 2\pi)$. The element ρ_y takes $(\theta, 0, 0)$ to $(0, 0, -\theta)$ which is an element of the set c_5. So the induced action of ρ_y on c_1 is the permutation which changes c_1 to c_5. The actions of the other elements on a general $C \in \mathscr{C}_{\mathbb{O}}$ is similar to compute. We present this action in Table 7.3.

Table 7.2: Action of $\mathbb{O}$ induced on X_0 for the SC lattice.

Element of $\mathbb{O}$	Action on X_0	Element of $\mathbb{O}$	Action on X_0
ρ_x	$(\theta_1, -\theta_3, \theta_2)$	τ_2^2	$(-\theta_3, -\theta_1, \theta_2)$
ρ_x^2	$(\theta_1, -\theta_2, \theta_3)$	τ_3	$(-\theta_3, \theta_1, -\theta_2)$
ρ_x^3	$(\theta_1, \theta_3, -\theta_2)$	τ_3^2	$(\theta_2, -\theta_3, -\theta_1)$
ρ_y	$(\theta_3, \theta_2, -\theta_1)$	τ_4	$(-\theta_2, -\theta_3, \theta_1)$
ρ_y^2	$(-\theta_1, \theta_2, -\theta_3)$	τ_4^2	$(\theta_3, -\theta_1, -\theta_2)$
ρ_y^3	$(-\theta_3, \theta_2, \theta_1)$	κ_1	$(\theta_2, \theta_1, -\theta_3)$
ρ_z	$(-\theta_2, \theta_1, \theta_3)$	κ_2	$(-\theta_2, -\theta_1, -\theta_3)$
ρ_z^2	$(-\theta_1, -\theta_2, \theta_3)$	κ_3	$(\theta_3, -\theta_2, \theta_1)$
ρ_z^3	$(\theta_2, -\theta_1, \theta_3)$	κ_4	$(-\theta_1, \theta_3, \theta_2)$
τ_1	$(\theta_3, \theta_1, \theta_2)$	κ_5	$(-\theta_3, -\theta_2, -\theta_1)$
τ_1^2	$(\theta_2, \theta_3, \theta_1)$	κ_6	$(-\theta_1, -\theta_3, -\theta_2)$
τ_2	$(-\theta_2, \theta_3, -\theta_1)$		

Table 7.3: Action of $\mathbb{O}$ induced on $\mathscr{C}_\mathbb{O}$ for the SC lattice.

Element of $\mathscr{C}_\mathbb{O}$	Elements of $\mathbb{O}$ acting nontrivially	Action
e_1	None	
e_2	$\rho_x, \rho_x^3, \kappa_4, \kappa_6, \tau_1^2, \tau_2, \tau_3^2, \tau_4$	e_3
	$\rho_y, \rho_y^3, \kappa_3, \kappa_5, \tau_1, \tau_2^2, \tau_3, \tau_4^2$	e_4
e_3	$\rho_x, \rho_x^3, \kappa_4, \kappa_6, \tau_1, \tau_2^2, \tau_3, \tau_4^2$	e_2
	$\rho_z, \rho_z^3, \kappa_1, \kappa_2, \tau_1^2, \tau_2, \tau_3^2, \tau_4$	e_4
e_4	$\rho_y, \rho_y^3, \kappa_3, \kappa_5, \tau_1^2, \tau_2, \tau_3^2, \tau_4$	e_2
	$\rho_z, \rho_z^3, \kappa_1, \kappa_2, \tau_1, \tau_2^2, \tau_3, \tau_4^2$	e_3
e_5	$\rho_x, \rho_x^3, \kappa_4, \kappa_6, \tau_1^2, \tau_2, \tau_3^2, \tau_4$	e_6
	$\rho_y, \rho_y^3, \kappa_3, \kappa_5, \tau_1, \tau_2^2, \tau_3, \tau_4^2$	e_7
e_6	$\rho_x, \rho_x^3, \kappa_4, \kappa_6, \tau_1^2, \tau_2, \tau_3^2, \tau_4$	e_5
	$\rho_z, \rho_z^3, \kappa_1, \kappa_2, \tau_1^2, \tau_2, \tau_3^2, \tau_4$	e_7
e_7	$\rho_z, \rho_z^3, \kappa_1, \kappa_2, \tau_1^2, \tau_2, \tau_3^2, \tau_4$	e_6
	$\rho_y, \rho_y^3, \kappa_3, \kappa_5, \tau_1, \tau_2^2, \tau_3, \tau_4^2$	e_5
e_8	None	

Table 7.4: Table 7.3 continued

Element of $\mathscr{C}_{\mathbb{O}}$	Elements of $\mathbb{O}$ acting nontrivially	Action
c_1	$\rho_y, \rho_y^3, \kappa_3, \kappa_5, \tau_1^2, \tau_2, \tau_3^2, \tau_4$	c_5
	$\rho_z, \rho_z^3, \kappa_1, \kappa_2, \tau_1, \tau_2^2, \tau_3, \tau_4^2$	c_3
c_2	$\rho_y, \rho_y^3, \kappa_3, \kappa_5, \tau_1^2, \tau_2, \tau_3^2, \tau_4$	c_6
	$\rho_z, \rho_z^3, \kappa_1, \kappa_2, \tau_1, \tau_2^2, \tau_3, \tau_4^2$	c_4
c_3	$\rho_x, \rho_x^3, \kappa_4, \kappa_6, \tau_1, \tau_2^2, \tau_3, \tau_4^2$	c_5
	$\rho_z, \rho_z^3, \kappa_1, \kappa_2, \tau_1^2, \tau_2, \tau_3^2, \tau_4$	c_1
c_4	$\rho_x, \rho_x^3, \kappa_4, \kappa_6, \tau_1, \tau_2^2, \tau_3, \tau_4^2$	c_6
	$\rho_z, \rho_z^3, \kappa_1, \kappa_2, \tau_1^2, \tau_2, \tau_3^2, \tau_4$	c_2
c_5	$\rho_x, \rho_x^3, \kappa_4, \kappa_6, \tau_1^2, \tau_2, \tau_3^2, \tau_4$	c_3
	$\rho_y, \rho_y^3, \kappa_3, \kappa_5, \tau_1, \tau_2^2, \tau_3, \tau_4^2$	c_1
c_6	$\rho_x, \rho_x^3, \kappa_4, \kappa_6, \tau_1^2, \tau_2, \tau_3^2, \tau_4$	c_4
	$\rho_y, \rho_y^3, \kappa_3, \kappa_5, \tau_1, \tau_2^2, \tau_3, \tau_4^2$	c_2
c_7	$\rho_x, \kappa_6, \tau_1^2, \tau_2$	c_{11}
	$\rho_x^2, \rho_y^2, \rho_z, \rho_z^3$	c_9
	$\rho_x^3, \kappa_4, \tau_3^2, \tau_4$	c_{13}
	$\rho_y, \kappa_3, \tau_2^2, \tau_3$	c_{17}
	$\rho_y^3, \kappa_5, \tau_1, \tau_4^2$	c_{15}
c_8	$\rho_x, \kappa_6, \tau_1^2, \tau_2$	c_{12}
	$\rho_x^2, \rho_y^2, \rho_z, \rho_z^3$	c_{10}
	$\rho_x^3, \kappa_4, \tau_3^2, \tau_4$	c_{14}
	$\rho_y, \kappa_3, \tau_2^2, \tau_3$	c_{18}
	$\rho_y^3, \kappa_5, \tau_1, \tau_4^2$	c_{16}
c_9	$\rho_x, \kappa_6, \tau_1^2, \tau_2$	c_{13}
	$\rho_x^2, \rho_y^2, \rho_z, \rho_z^3$	c_7
	$\rho_x^3, \kappa_4, \tau_3^2, \tau_4$	c_{11}
	$\rho_y, \kappa_3, \tau_2^2, \tau_3$	c_{15}
	$\rho_y^3, \kappa_5, \tau_1, \tau_4^2$	c_{17}
c_{10}	$\rho_x, \kappa_6, \tau_1^2, \tau_2$	c_{14}
	$\rho_x^2, \rho_y^2, \rho_z, \rho_z^3$	c_8
	$\rho_x^3, \kappa_4, \tau_3^2, \tau_4$	c_{12}
	$\rho_y, \kappa_3, \tau_2^2, \tau_3$	c_{16}
	$\rho_y^3, \kappa_5, \tau_1, \tau_4^2$	c_{18}
c_{11}	$\rho_x, \kappa_4, \tau_4^2, \tau_3$	c_9
	$\rho_x^2, \rho_y, \rho_y^3, \rho_z^2$	c_{13}
	$\rho_x^3, \kappa_6, \tau_2^2, \tau_1$	c_7
	$\rho_z, \kappa_2, \tau_1^2, \tau_3^2$	c_{15}
	$\rho_z^3, \kappa_1, \tau_2, \tau_4$	c_{17}

Table 7.5: Table 7.3 continued

Element of $\mathscr{C}_{\mathbb{O}}$	Elements of $\mathbb{O}$ acting nontrivially	Action
c_{12}	$\rho_x, \kappa_4, \tau_4^2, \tau_3$	c_{10}
	$\rho_x^2, \rho_y, \rho_y^3, \rho_z^2$	c_{14}
	$\rho_x^3, \kappa_6, \tau_2^2, \tau_1$	c_8
	$\rho_z, \kappa_2, \tau_1^2, \tau_3^2$	c_{16}
	$\rho_z^3, \kappa_1, \tau_2, \tau_4$	c_{18}
c_{13}	$\rho_x, \kappa_4, \tau_4^2, \tau_3$	c_7
	$\rho_x^2, \rho_y, \rho_y^3, \rho_z^2$	c_{11}
	$\rho_x^3, \kappa_6, \tau_2^2, \tau_1$	c_9
	$\rho_z, \kappa_2, \tau_1^2, \tau_3^2$	c_{17}
	$\rho_z^3, \kappa_1, \tau_2, \tau_4$	c_{15}
c_{14}	$\rho_x, \kappa_4, \tau_4^2, \tau_3$	c_8
	$\rho_x^2, \rho_y, \rho_y^3, \rho_z^2$	c_{12}
	$\rho_x^3, \kappa_6, \tau_2^2, \tau_1$	c_{10}
	$\rho_z, \kappa_2, \tau_1^2, \tau_3^2$	c_{18}
	$\rho_z^3, \kappa_1, \tau_2, \tau_4$	c_{16}
c_{15}	$\rho_x, \rho_x^3, \rho_y^2, \rho_z^2$	c_{17}
	$\rho_y, \kappa_5, \tau_1^2, \tau_4$	c_7
	$\rho_y^3, \kappa_3, \tau_2, \tau_3^2$	c_9
	$\rho_z, \kappa_1, \tau_2^2, \tau_4^2$	c_{13}
	$\rho_z^3, \kappa_2, \tau_1^2, \tau_3$	c_{11}
c_{16}	$\rho_x, \rho_x^3, \rho_y^2, \rho_z^2$	c_{18}
	$\rho_y, \kappa_5, \tau_1^2, \tau_4$	c_8
	$\rho_y^3, \kappa_3, \tau_2, \tau_3^2$	c_{10}
	$\rho_z, \kappa_1, \tau_2^2, \tau_4^2$	c_{14}
	$\rho_z^3, \kappa_2, \tau_1^2, \tau_3$	c_{12}
c_{17}	$\rho_x, \rho_x^3, \rho_y^2, \rho_z^2$	c_{15}
	$\rho_y, \kappa_5, \tau_1^2, \tau_4$	c_9
	$\rho_y^3, \kappa_3, \tau_2, \tau_3^2$	c_7
	$\rho_z, \kappa_1, \tau_2^2, \tau_4^2$	c_{11}
	$\rho_z^3, \kappa_2, \tau_1^2, \tau_3$	c_{13}
c_{18}	$\rho_x, \rho_x^3, \rho_y^2, \rho_z^2$	c_{16}
	$\rho_y, \kappa_5, \tau_1^2, \tau_4$	c_{10}
	$\rho_y^3, \kappa_3, \tau_2, \tau_3^2$	c_8
	$\rho_z, \kappa_1, \tau_2^2, \tau_4^2$	c_{12}
	$\rho_z^3, \kappa_2, \tau_1^2, \tau_3$	c_{14}
c_{19}	$\rho_x, \rho_y^2, \rho_z^3, \kappa_3, \tau_2, \tau_3$	c_{22}
	$\rho_x^2, \rho_y^3, \rho_z, \kappa_4, \tau_3^2, \tau_4^2$	c_{20}
	$\rho_x^3, \rho_y, \rho_z^2, \kappa_1, \tau_2^2, \tau_4$	c_{21}

Table 7.6: Table 7.3 continued

Element of $\mathscr{C}_{\mathbb{O}}$	Elements of $\mathbb{O}$ acting nontrivially	Action
c_{20}	$\rho_x, \rho_y^2, \rho_z, \kappa_5, \tau_1^2, \tau_4^2$	c_{21}
	$\rho_x^2, \rho_y, \rho_z^3, \kappa_4, \tau_3, \tau_4$	c_{19}
	$\rho_x^3, \rho_y^3, \rho_z^2, \kappa_2, \tau_1, \tau_3^2$	c_{22}
c_{21}	$\rho_x, \rho_y^3, \rho_z^2, \kappa_1, \tau_2, \tau_4^2$	c_{19}
	$\rho_x^2, \rho_y, \rho_z, \kappa_6, \tau_1^2, \tau_2^2$	c_{22}
	$\rho_x^3, \rho_y^2, \rho_z^3, \kappa_5, \tau_1, \tau_4$	c_{20}
c_{22}	$\rho_x, \rho_y, \rho_z^2, \kappa_2, \tau_1^2, \tau_3$	c_{20}
	$\rho_x^2, \rho_y^3, \rho_z^3, \kappa_6, \tau_1, \tau_2$	c_{21}
	$\rho_x^3, \rho_y^2, \rho_z, \kappa_3, \tau_2^2, \tau_3^2$	c_{19}
c_{23}	$\rho_x, \rho_x^3, \kappa_4, \kappa_6$	c_{24}
	$\rho_y, \rho_y^3, \kappa_3, \kappa_5$	c_{27}
	$\rho_z, \rho_z^3, \kappa_1, \kappa_2$	c_{25}
	$\tau_1, \tau_2^2, \tau_3, \tau_4^2$	c_{26}
	$\tau_1^2, \tau_2, \tau_3^2, \tau_4$	c_{28}
c_{24}	$\rho_x, \rho_x^3, \kappa_4, \kappa_6$	c_{23}
	$\rho_y, \rho_y^3, \kappa_3, \kappa_5$	c_{28}
	$\rho_z, \rho_z^3, \kappa_1, \kappa_2$	c_{26}
	$\tau_1, \tau_2^2, \tau_3, \tau_4^2$	c_{25}
	$\tau_1^2, \tau_2, \tau_3^2, \tau_4$	c_{27}
c_{25}	$\rho_x, \rho_x^3, \kappa_4, \kappa_6$	c_{28}
	$\rho_y, \rho_y^3, \kappa_3, \kappa_5$	c_{26}
	$\rho_z, \rho_z^3, \kappa_1, \kappa_2$	c_{23}
	$\tau_1, \tau_2^2, \tau_3, \tau_4^2$	c_{27}
	$\tau_1^2, \tau_2, \tau_3^2, \tau_4$	c_{24}
c_{26}	$\rho_x, \rho_x^3, \kappa_4, \kappa_6$	c_{27}
	$\rho_y, \rho_y^3, \kappa_3, \kappa_5$	c_{26}
	$\rho_z, \rho_z^3, \kappa_1, \kappa_2$	c_{24}
	$\tau_1, \tau_2^2, \tau_3, \tau_4^2$	c_{28}
	$\tau_1^2, \tau_2, \tau_3^2, \tau_4$	c_{23}
c_{27}	$\rho_x, \rho_x^3, \kappa_4, \kappa_6$	c_{26}
	$\rho_y, \rho_y^3, \kappa_3, \kappa_5$	c_{23}
	$\rho_z, \rho_z^3, \kappa_1, \kappa_2$	c_{28}
	$\tau_1, \tau_2^2, \tau_3, \tau_4^2$	c_{24}
	$\tau_1^2, \tau_2, \tau_3^2, \tau_4$	c_{25}
c_{28}	$\rho_x, \rho_x^3, \kappa_4, \kappa_6$	c_{25}
	$\rho_y, \rho_y^3, \kappa_3, \kappa_5$	c_{24}
	$\rho_z, \rho_z^3, \kappa_1, \kappa_2$	c_{27}
	$\tau_1, \tau_2^2, \tau_3, \tau_4^2$	c_{23}
	$\tau_1^2, \tau_2, \tau_3^2, \tau_4$	c_{26}

Using this action we may deduce the following fundamental symmetry result.

Proposition 7.11
Let $\mathbb{O}$ act on $\mathscr{C}_{\mathbb{O}}$ as in Table 7.3 and on X_0 as in Table 7.2. Then given $C \in \mathscr{C}_{\mathbb{O}}$, the setwise isotropy $\mathrm{Stab}(C)$ *and pointwise isotropy* $\mathrm{stab}(C)$ *and the group $S(C)$ are given in Table 7.7.*

Proof. The calculation for $\mathrm{Stab}(C)$ follows immediately from the action given in Table 7.3. To compute $\mathrm{stab}(C)$, we consider the elements of the group $\mathrm{Stab}(C)$, then use the action of $\mathbb{O}$ on X_0 in Table 7.2 to see which elements act pointwise trivially on C. Finally, to compute $S(C)$ we need only to form the quotient $\mathrm{Stab}(C)/\mathrm{stab}(C)$. □

We now know the symmetries of the equilibria and connection on the skeleton, together with the induced action of $\mathbb{O}$ on the set $\mathscr{C}_{\mathbb{O}}$. These computations show that $S(C) \cong \mathbf{Z}_2$ for all $C \in \mathscr{C}_{\mathbb{O}}$, with the action of $\mathbf{Z}_2$ being by reflection, so there is an axis of symmetry along every C. We must now determine where this axis lies.

Knots Relative to C. Given $C \in \mathscr{C}_{\mathbb{O}}$, a knot relative to C gives an axis of symmetry for any $\mathbb{O}$-equivariant flow on C. The task of computing all knots relative to each C is a tedious task; there are 28 different $C \in \mathscr{C}_{\mathbb{O}}$ homeomorphic to $\mathbf{S}^1$. To reduce the computational effort we employ the $\mathbb{O}$ symmetry. The action of $\mathbb{O}$ on $\mathscr{C}_{\mathbb{O}}$ given in Table 7.3 shows that there are only six C's which are not symmetrically related, namely,

$$\begin{aligned}
c_1 &= \{(\theta,0,0)\big|\theta \in [0,2\pi)\},\\
c_2 &= \{(\theta,\pi,\pi)\big|\theta \in [0,2\pi)\},\\
c_7 &= \{(\theta,\theta,0)\big|\theta \in [0,2\pi)\},\\
c_8 &= \{(\theta,\theta,\pi)\big|\theta \in [0,2\pi)\},\\
c_{19} &= \{(\theta,\theta,\theta)\big|\theta \in [0,2\pi)\}\\
c_{23} &= \{(\theta,\pi,0)\big|\theta \in [0,2\pi)\}.
\end{aligned}$$

The representatives of the equilibria that lie on these C's are given by e_1, e_2, e_5 and e_8. The $\mathbb{O}$ symmetry allows us to prove a result about c_1 (say) and immediately deduce that it holds for all other C's which are symmetrically related to c_1. So we need only compute the knots relative to the orbit representatives of the C's given above. We know that any knot must be an equilibrium and since each C has two equilibria on it, it follows that these equilibria are the knots relative to that C. We present this information in Table 7.8. We have abused notation here (and shall do so in future); each entry of this table is an orbit representative.

Projected Skeleton

Here we compute the projected skeleton $\mathbb{X}^p_{\mathbb{O}}$. The projected skeleton is very important since it gives a simple geometric description of the connections between the equilibria. The computation of the projected skeleton is simplified by our work on the pointwise and setwise isotropy subgroups and the knots. The action of $\mathbb{O}$ on $\mathscr{C}_{\mathbb{O}}$ shows that there are six orbit representatives for the elements of $\mathscr{C}_{\mathbb{O}}$ homeomorphic to $\mathbf{S}^1$; these are c_1, c_2, c_7, c_8, c_{19} and c_{23}. The orbit representatives for the equilibria are e_1, e_2, e_5 and e_8. Each $C \cong \mathbf{S}^1$ has two knots, implying there is an axis of reflection symmetry. So these C's project into the orbit space as a line joining the two knots. More precisely, we have the following relations. The element c_1 connects e_1 to e_2, c_2 connects e_5 to e_8, c_7 connects e_1 to e_5, c_8 connects e_5 to e_8, c_{19} connects e_1 to e_8 and c_{23} connects e_2 to e_5. We have abused the notation here (and will do so in the future); by saying that c_1 connects e_1 to e_2, we mean that the connection on the projected skeleton with orbit representative c_1 connects the equilibria with representatives e_1 and e_2. In Figure 7.1 we illustrate the projected skeleton.

Table 7.7: Isotropy data for $C \in \mathscr{C}_{\mathbb{O}}$ on the SC lattice.

$C \in \mathscr{C}_{\mathbb{O}}$	stab(C)	Stab(C)	$S(C) = \text{Stab}(C)/\text{stab}(C)$
e_1	$\mathbb{O}$	$\mathbb{O}$	$\mathbf{1}$
e_2	$\mathbf{D}_4[\rho_z, \kappa_1]$	$\mathbf{D}_4[\rho_z, \kappa_1]$	$\mathbf{1}$
e_3	$\mathbf{D}_4[\rho_y, \kappa_5]$	$\mathbf{D}_4[\rho_y, \kappa_5]$	$\mathbf{1}$
e_4	$\mathbf{D}_4[\rho_x, \kappa_6]$	$\mathbf{D}_4[\rho_x, \kappa_6]$	$\mathbf{1}$
e_5	$\mathbf{D}_4[\rho_z, \kappa_1]$	$\mathbf{D}_4[\rho_z, \kappa_1]$	$\mathbf{1}$
e_6	$\mathbf{D}_4[\rho_y, \kappa_5]$	$\mathbf{D}_4[\rho_y, \kappa_5]$	$\mathbf{1}$
e_7	$\mathbf{D}_4[\rho_x, \kappa_6]$	$\mathbf{D}_4[\rho_x, \kappa_6]$	$\mathbf{1}$
e_8	$\mathbb{O}$	$\mathbb{O}$	$\mathbf{1}$
c_1	$\mathbf{Z}_4[\rho_x]$	$\mathbf{D}_4[\rho_x, \kappa_6]$	$\mathbf{Z}_2$
c_2	$\mathbf{Z}_4[\rho_x]$	$\mathbf{D}_4[\rho_x, \kappa_6]$	$\mathbf{Z}_2$
c_3	$\mathbf{Z}_4[\rho_y]$	$\mathbf{D}_4[\rho_y, \kappa_5]$	$\mathbf{Z}_2$
c_4	$\mathbf{Z}_4[\rho_y]$	$\mathbf{D}_4[\rho_y, \kappa_5]$	$\mathbf{Z}_2$
c_5	$\mathbf{Z}_4[\rho_z]$	$\mathbf{D}_4[\rho_z, \kappa_1]$	$\mathbf{Z}_2$
c_6	$\mathbf{Z}_4[\rho_z]$	$\mathbf{D}_4[\rho_z, \kappa_1]$	$\mathbf{Z}_2$
c_7	$\mathbf{Z}_2[\kappa_1]$	$\mathbf{D}_2[\rho_z^2, \kappa_1]$	$\mathbf{Z}_2$
c_8	$\mathbf{Z}_2[\kappa_1]$	$\mathbf{D}_2[\rho_z^2, \kappa_1]$	$\mathbf{Z}_2$
c_9	$\mathbf{Z}_2[\kappa_2]$	$\mathbf{D}_2[\rho_z^2, \kappa_1]$	$\mathbf{Z}_2$
c_{10}	$\mathbf{Z}_2[\kappa_2]$	$\mathbf{D}_2[\rho_z^2, \kappa_1]$	$\mathbf{Z}_2$
c_{11}	$\mathbf{Z}_2[\kappa_3]$	$\mathbf{D}_2[\rho_y^2, \kappa_3]$	$\mathbf{Z}_2$
c_{12}	$\mathbf{Z}_2[\kappa_3]$	$\mathbf{D}_2[\rho_y^2, \kappa_3]$	$\mathbf{Z}_2$
c_{13}	$\mathbf{Z}_2[\kappa_5]$	$\mathbf{D}_2[\rho_y^2, \kappa_3]$	$\mathbf{Z}_2$
c_{14}	$\mathbf{Z}_2[\kappa_5]$	$\mathbf{D}_2[\rho_y^2, \kappa_3]$	$\mathbf{Z}_2$
c_{15}	$\mathbf{Z}_2[\kappa_4]$	$\mathbf{D}_2[\rho_x^2, \kappa_6]$	$\mathbf{Z}_2$
c_{16}	$\mathbf{Z}_2[\kappa_4]$	$\mathbf{D}_2[\rho_x^2, \kappa_6]$	$\mathbf{Z}_2$
c_{17}	$\mathbf{Z}_2[\kappa_6]$	$\mathbf{D}_2[\rho_x^2, \kappa_6]$	$\mathbf{Z}_2$
c_{18}	$\mathbf{Z}_2[\kappa_6]$	$\mathbf{D}_2[\rho_x^2, \kappa_6]$	$\mathbf{Z}_2$
c_{19}	$\mathbf{Z}_3[\tau_1]$	$\mathbf{D}_3[\tau_1, \kappa_5]$	$\mathbf{Z}_2$
c_{20}	$\mathbf{Z}_3[\tau_2]$	$\mathbf{D}_3[\tau_2, \kappa_1]$	$\mathbf{Z}_2$
c_{21}	$\mathbf{Z}_3[\tau_3]$	$\mathbf{D}_3[\tau_3, \kappa_3]$	$\mathbf{Z}_2$
c_{22}	$\mathbf{Z}_3[\tau_4]$	$\mathbf{D}_3[\tau_4, \kappa_5]$	$\mathbf{Z}_2$
c_{23}	$\mathbf{Z}_2[\rho_x^2]$	$\mathbf{D}_2[\rho_x^2, \rho_y^2]$	$\mathbf{Z}_2$
c_{24}	$\mathbf{Z}_2[\rho_x^2]$	$\mathbf{D}_2[\rho_x^2, \rho_y^2]$	$\mathbf{Z}_2$
c_{25}	$\mathbf{Z}_2[\rho_y^2]$	$\mathbf{D}_2[\rho_x^2, \rho_y^2]$	$\mathbf{Z}_2$
c_{26}	$\mathbf{Z}_2[\rho_y^2]$	$\mathbf{D}_2[\rho_x^2, \rho_y^2]$	$\mathbf{Z}_2$
c_{27}	$\mathbf{Z}_2[\rho_z^2]$	$\mathbf{D}_2[\rho_x^2, \rho_y^2]$	$\mathbf{Z}_2$
c_{28}	$\mathbf{Z}_2[\rho_z^2]$	$\mathbf{D}_2[\rho_x^2, \rho_y^2]$	$\mathbf{Z}_2$

Table 7.8: Knots relative to the orbit representatives of the $C \in \mathscr{C}_{\mathbb{O}}$.

Element of $\mathscr{C}_{\mathbb{O}}$	Knots
c_1	e_1, e_2
c_2	e_5, e_8
c_7	e_1, e_5
c_8	e_2, e_8
c_{19}	e_1, e_8
c_{23}	e_2, e_5

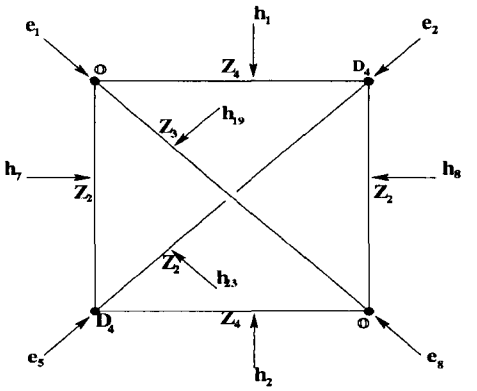

Figure 7.1: The projected skeleton $\mathbb{X}_0^p$. Here $h_1 = \{(\theta,0,0)|\theta \in (0,\pi)\}$, $h_2 = \{(\theta,\pi,\pi)|\theta \in (0,\pi)\}$, $h_7 = \{(\theta,\theta,0)|\theta \in (0,\pi)\}$, $h_8 = \{(\theta,\theta,\pi)|\theta \in (0,\pi)\}$, $h_{19} = \{(\theta,\theta,\theta)|\theta \in (0,\pi)\}$, and $h_{23} = \{(\theta,\pi,0)|\theta \in (0,\pi)\}$.

Remark 7.12
The structure of the projected skeleton shows that it does not support heteroclinic cycles in the usual sense. By this we mean that the definition of Krupa and Melbourne in Section 1.5 is not satisfied. The unstable manifold of a chosen equilibrium does not necessarily lie within the stable manifold of a single equilibrium on the (projected) skeleton. Such a situation has been previously studied by Kirk and Silber [55], under the name "heteroclinic network". However, even this generalisation is not appropriate for our situation; to obtain a heteroclinic network we would require that the projected skeleton could be written as the disjoint union of several heteroclinic cycles (in the usual sense), and this is not a condition that we can guarantee. We find that our problem falls outside the domain of previous studies of heteroclinic type behaviour, although the study of Kirk and Silber [55] is useful in demonstrating some of the complexities that could be encountered.

Example

In this section we exhibit interesting possible flows on the projected skeleton. We make no assertion that such flows can be realised.

To show how complex the dynamics could be Figure 7.2 (b) provides an illustrative example of a possible flow which has some interesting dynamical possibilities. This example is chosen since it illustrates how diverse the behaviour could be. On the projected skeleton there are three different heteroclinic cycles: $\mathcal{H}_1$ connecting e_1, e_5 and e_8, $\mathcal{H}_2$ connecting e_5, e_8 and e_2 and $\mathcal{H}_3$ connecting e_1, e_5, e_8 and e_2. Now $\mathcal{H}_i \cap \mathcal{H}_j \neq \emptyset$ for all i, j and the whole network can be written as $\mathcal{H} = \mathcal{H}_1 \cup \mathcal{H}_2 \cup \mathcal{H}_3$. These are the requirements for a heteroclinic network. Of course there are more general flows supported on the projected skeleton, which are not heteroclinic networks, see Figure 7.2 (a). It is worth applying some of the comments and questions of Kirk and Silber [55] to our network $\mathcal{H}$.

1. Do any of the cycles $\mathcal{H}_1$, $\mathcal{H}_2$ or $\mathcal{H}_3$ "dominate" in the network? By dominant cycle, we mean a cycle has strong attractivity properties, where any trajectory sufficiently near the network is eventually attracted to the dominate cycle, with the consequence that cyclic behaviour is still observed.

2. Can we observe more than one cycle?

3. Can there occur a sequence of apparently random visits to the equilibria?

Along with these questions it is worth noting that the stability criterion of Krupa and Melbourne [58] is not valid in such networks. In fact, the general stability properties of heteroclinic

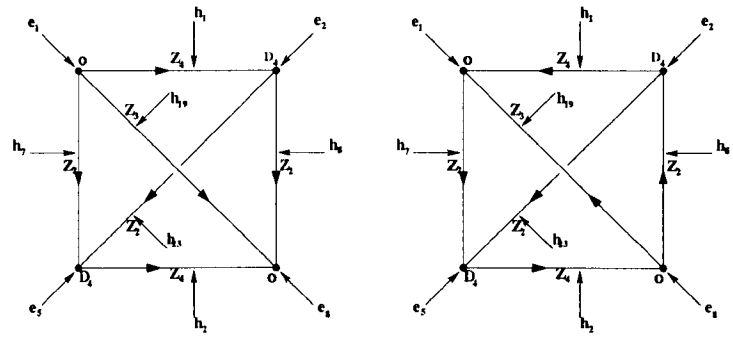

(a) (b)

Figure 7.2: Example flows on the projected skeleton $\mathbb{X}_{\mathbb{O}}^{p}$, showing two flows with interesting intermittency properties.

networks are very complex, as the example studied by Kirk and Silber [55] demonstrates. The network considered by Kirk and Silber [55] has some interesting dynamic properties:

1. A cycle in the network attracts nearly all trajectories that start near the cycle.
2. A cycle in the network attracts nearly all trajectories that start near one or more (but not all) of the heteroclinic connections that make up the cycle.
3. The cycle is unstable.

Our cycle $\mathcal{H}$ is more complex, but it is not unreasonable to expect it to show some of the above properties. And it is worth noting that the presence of higher order noise terms could alter the attracting and cycling dynamics leading to apparently random switching between $\mathcal{H}_1$, $\mathcal{H}_2$ and $\mathcal{H}_3$. The dynamics of $\mathcal{H}$ and general heteroclinic networks is an important and interesting issue for further study, but we shall not pursue this point any further.

The type of behaviour illustrated above is not specific to our example, but rather a "typical" feature of forced symmetry breaking on the SC lattice. We shall see far more elaborate structures in later subsections.

7.2.3 Forced Symmetry Breaking to $\mathbf{D}_4[\rho_x, \kappa_6]$

In this subsection we consider the behaviour of the group orbit of solutions X_0 when symmetry-breaking terms with $\mathbf{D}_4[\rho_x, \kappa_6]$ symmetry are added to equation (7.3). Since the manifold X_0 is normally hyperbolic, it persists by the Equivariant Persistence Theorem, to give a new invariant manifold X_ε $\mathbf{D}_4[\rho_x, \kappa_6]$-equivariantly diffeomorphic to X_0. To begin we require the action of the group $\mathbf{D}_4[\rho_x, \kappa_6]$ on $\mathbb{C}^3$. This is given in Table 7.9. This action is just the restriction of the action of the group $\mathbb{O}$ given in Table 7.1.

Table 7.9: Action of $\mathbf{D}_4[\rho_x, \kappa_6]$ on $\mathbb{C}^3$ for the SC lattice.

Element of $\mathbb{O}$	Action on $\mathbb{C}^3$	Element of $\mathbb{O}$	Action on $\mathbb{C}^3$
ρ_x	$(z_1, \overline{z_3}, z_2)$	ρ_x^2	$(z_1, \overline{z_2}, \overline{z_3})$
ρ_x^3	$(z_1, z_3, \overline{z_2})$	ρ_y^2	$(\overline{z_1}, z_2, \overline{z_3})$
ρ_z^2	$(\overline{z_1}, \overline{z_2}, z_3)$	κ_4	$(\overline{z_1}, z_3, z_2)$
κ_6	$(\overline{z_1}, \overline{z_3}, \overline{z_2})$		

Table 7.10: Action of $\mathbf{D}_4[\rho_x, \kappa_6]$ induced on X_0 for the SC lattice.

Element of $\mathbf{D}_4[\rho_x, \kappa_6]$	Action on X_0	Element of $\mathbf{D}_4[\rho_x, \kappa_6]$	Action on X_0
ρ_x	$(\theta_1, -\theta_3, \theta_2)$	ρ_x^2	$(\theta_1, -\theta_2, \theta_3)$
ρ_x^3	$(\theta_1, \theta_3, -\theta_2)$	ρ_y	$(\theta_3, \theta_2, -\theta_1)$
ρ_y^2	$(-\theta_1, \theta_2, -\theta_3)$	ρ_y^3	$(-\theta_3, \theta_2, \theta_1)$
κ_4	$(-\theta_1, \theta_3, \theta_2)$	κ_6	$(-\theta_1, -\theta_3, -\theta_2)$

Calculation of the Skeleton

Using the action of $\mathbf{D}_4[\rho_x, \kappa_6]$ in Table 7.9 we may compute the skeleton. The form of the skeleton is most conveniently described by choosing coordinates $(\theta_1, \theta_2, \theta_3)$ on X_0, where $\theta_j \in [0, 2\pi)$ for $j = 1, 2, 3$. The notation we employ is the same as used for the skeleton for forced symmetry breaking to $\mathbb{O}$. To begin, we calculate the set $\mathscr{C}_{\mathbf{D}_4[\rho_x, \kappa_6]}$, for which we recall there are eight subgroups of $\mathbf{D}_4[\rho_x, \kappa_6]$, namely: $\mathbf{D}_4[\rho_x, \kappa_6]$, $\mathbf{Z}_4[\rho_x]$, $\mathbf{D}_2[\rho_x^2, \kappa_4]$, $\mathbf{D}_2[\rho_x^2, \rho_y^2]$, $\mathbf{Z}_2[\rho_x^2]$, $\mathbf{Z}_2[\kappa_4]$, $\mathbf{Z}_2[\kappa_6]$ and the trivial subgroup.

Proposition 7.13
Let $\mathbf{D}_4[\rho_x, \kappa_6]$ act on X_0 with the action induced from Table 7.9. Then

$$\mathscr{C}_{\mathbf{D}_4[\rho_x, \kappa_6]} = \{e_1, e_2, e_3, e_4, e_5, e_6, e_7, e_8, c_1, c_2, c_3, c_4, c_5, c_6, c_{15}, c_{16}, c_{17}, c_{18}, c_{23}, c_{24}, c_{25}, c_{26}, c_{27}, c_{28}\}.$$

Proof. This follows from Lemmas 7.6, 7.7, 7.8 and 7.10. □

So the skeleton is now defined by

$$\mathbb{X}_{\mathbf{D}_4[\rho_x, \kappa_6]} = \bigcup_{C \in \mathscr{C}_{\mathbf{D}_4[\rho_x, \kappa_6]}} C \subset X_0.$$

At this point we encountered the same problem as for $\mathbb{X}_{\mathbb{O}}$. Since X_0 is a 3-torus, it is very difficult to rendered the skeleton $\mathbb{X}_{\mathbf{D}_4[\rho_x, \kappa_6]}$ as a subset X_0 in a way that is instructive. So rather than struggle with complex pictures, we shall postpone illustrating the interconnections between the equilibria until we can construct the projected skeleton. To perform this construction, we must consider the symmetry properties of the skeleton.

Symmetry Properties of $\mathbb{X}_{\mathbf{D}_4[\rho_x, \kappa_6]}$

Here we study the action of $\mathbf{D}_4[\rho_x, \kappa_6]$ induced on the skeleton. Using this action we may then construct a natural action of $\mathbf{D}_4[\rho_x, \kappa_6]$ on each $C \in \mathscr{C}_{\mathbf{D}_4[\rho_x, \kappa_6]}$. This allows us to compute the setwise isotropy $\mathrm{Stab}(C)$ and the pointwise isotropy $\mathrm{stab}(C)$.

Pointwise and Setwise Isotropy Subgroups. The action of $\mathbf{D}_4[\rho_x, \kappa_6]$ on $\mathbb{C}^3$ in Table 7.9 induces a natural action on X_0 with respect to coordinates $(\theta_1, \theta_2, \theta_3)$. The action of the generators for $\mathbf{D}_4[\rho_x, \kappa_6]$ is:

$$\begin{aligned} \rho_x(\theta_1, \theta_2, \theta_3) &= (\theta_1, -\theta_3, \theta_2), \\ \kappa_6(\theta_1, \theta_2, \theta_3) &= (-\theta_1, -\theta_3, -\theta_2). \end{aligned}$$

The complete action of $\mathbf{D}_4[\rho_x, \kappa_6]$ on X_0 is given in Table 7.10. This action is straightforward to compute; it is the restriction of the action of $\mathbb{O}$ on X_0 in Table 7.2. The action of $\mathbf{D}_4[\rho_x, \kappa_6]$ on X_0 in turn induces an action of $\mathbf{D}_4[\rho_x, \kappa_6]$ on the set $\mathscr{C}_{\mathbf{D}_4[\rho_x, \kappa_6]}$ by permutation of its elements; this action is the restriction of the $\mathbb{O}$ action in Table 7.3. We present the action of $\mathbf{D}_4[\rho_x, \kappa_6]$ on the set $\mathscr{C}_{\mathbf{D}_4[\rho_x, \kappa_6]}$ in Table 7.11. Using this action we may deduce the following fundamental symmetry result.

Table 7.11: Action of $\mathbf{D}_4[\rho_x, \kappa_6]$ induced on $\mathscr{C}_{\mathbf{D}_4[\rho_x,\kappa_6]}$ for the SC lattice.

Element of $\mathscr{C}_{\mathbf{D}_4[\rho_x,\kappa_6]}$	Elements of $\mathbf{D}_4[\rho_x, \kappa_6]$ acting nontrivially	Action
e_1	None	
e_2	ρ_x, ρ_x^3, κ_4, κ_6	e_3
e_3	ρ_x, ρ_x^3, κ_4, κ_6	e_2
e_4	None	
e_5	ρ_x, ρ_x^3, κ_4, κ_6	e_6
e_6	ρ_x, ρ_x^3, κ_4, κ_6	e_5
e_7	None	
e_8	None	
c_1	None	
c_2	None	
c_3	ρ_x, ρ_x^3, κ_4, κ_6	c_5
c_4	ρ_x, ρ_x^3, κ_4, κ_6	c_6
c_5	ρ_x, ρ_x^3, κ_4, κ_6	c_3
c_6	ρ_x, ρ_x^3, κ_4, κ_6	c_4
c_{15}	ρ_x, ρ_x^3, ρ_y^2, ρ_z^2	c_{17}
c_{16}	ρ_x, ρ_x^3, ρ_y^2, ρ_z^2	c_{18}
c_{17}	ρ_x, ρ_x^3, ρ_y^2, ρ_z^2	c_{15}
c_{18}	ρ_x, ρ_x^3, ρ_y^2, ρ_z^2	c_{16}
c_{23}	ρ_x, ρ_x^3, κ_4, κ_6	c_{24}
c_{24}	ρ_x, ρ_x^3, κ_4, κ_6	c_{23}
c_{25}	ρ_x, ρ_x^3, κ_4, κ_6	c_{28}
c_{26}	ρ_x, ρ_x^3, κ_4, κ_6	c_{27}
c_{27}	ρ_x, ρ_x^3, κ_4, κ_6	c_{26}
c_{28}	ρ_x, ρ_x^3, κ_4, κ_6	c_{25}

Table 7.12: Isotropy data for $C \in \mathscr{C}_{\mathbf{D}_4[\rho_x,\kappa_6]}$ for the SC lattice.

$C \in \mathscr{C}_{\mathbf{D}_4[\rho_x,\kappa_6]}$	stab(C)	Stab(C)	$S(C)$ = Stab(C)/stab(C)
e_1	$\mathbf{D}_4[\rho_x,\kappa_6]$	$\mathbf{D}_4[\rho_x,\kappa_6]$	$\mathbf{1}$
e_2	$\mathbf{D}_2[\rho_x^2,\rho_y^2]$	$\mathbf{D}_2[\rho_x^2,\rho_y^2]$	$\mathbf{1}$
e_3	$\mathbf{D}_2[\rho_x^2,\rho_y^2]$	$\mathbf{D}_2[\rho_x^2,\rho_y^2]$	$\mathbf{1}$
e_4	$\mathbf{D}_4[\rho_x,\kappa_6]$	$\mathbf{D}_4[\rho_x,\kappa_6]$	$\mathbf{1}$
e_5	$\mathbf{D}_2[\rho_x^2,\rho_y^2]$	$\mathbf{D}_2[\rho_x^2,\rho_y^2]$	$\mathbf{1}$
e_6	$\mathbf{D}_2[\rho_x^2,\rho_y^2]$	$\mathbf{D}_2[\rho_x^2,\rho_y^2]$	$\mathbf{1}$
e_7	$\mathbf{D}_4[\rho_x,\kappa_6]$	$\mathbf{D}_4[\rho_x,\kappa_6]$	$\mathbf{1}$
e_8	$\mathbf{D}_4[\rho_x,\kappa_6]$	$\mathbf{D}_4[\rho_x,\kappa_6]$	$\mathbf{1}$
c_1	$\mathbf{Z}_4[\rho_x]$	$\mathbf{D}_4[\rho_x,\kappa_6]$	$\mathbf{Z}_2$
c_2	$\mathbf{Z}_4[\rho_x]$	$\mathbf{D}_4[\rho_x,\kappa_6]$	$\mathbf{Z}_2$
c_3	$\mathbf{Z}_2[\rho_y^2]$	$\mathbf{D}_2[\rho_y^2,\rho_z^2]$	$\mathbf{Z}_2$
c_4	$\mathbf{Z}_2[\rho_y^2]$	$\mathbf{D}_2[\rho_y^2,\rho_z^2]$	$\mathbf{Z}_2$
c_5	$\mathbf{Z}_2[\rho_z^2]$	$\mathbf{D}_2[\rho_z^2,\rho_y^2]$	$\mathbf{Z}_2$
c_6	$\mathbf{Z}_2[\rho_z^2]$	$\mathbf{D}_2[\rho_z^2,\rho_y^2]$	$\mathbf{Z}_2$
c_{15}	$\mathbf{Z}_2[\kappa_4]$	$\mathbf{D}_2[\rho_x^2,\kappa_6]$	$\mathbf{Z}_2$
c_{16}	$\mathbf{Z}_2[\kappa_4]$	$\mathbf{D}_2[\rho_x^2,\kappa_6]$	$\mathbf{Z}_2$
c_{17}	$\mathbf{Z}_2[\kappa_6]$	$\mathbf{D}_2[\rho_x^2,\kappa_6]$	$\mathbf{Z}_2$
c_{18}	$\mathbf{Z}_2[\kappa_6]$	$\mathbf{D}_2[\rho_x^2,\kappa_6]$	$\mathbf{Z}_2$
c_{23}	$\mathbf{Z}_2[\rho_x^2]$	$\mathbf{D}_2[\rho_x^2,\rho_y^2]$	$\mathbf{Z}_2$
c_{24}	$\mathbf{Z}_2[\rho_x^2]$	$\mathbf{D}_2[\rho_x^2,\rho_y^2]$	$\mathbf{Z}_2$
c_{25}	$\mathbf{Z}_2[\rho_y^2]$	$\mathbf{D}_2[\rho_x^2,\rho_y^2]$	$\mathbf{Z}_2$
c_{26}	$\mathbf{Z}_2[\rho_y^2]$	$\mathbf{D}_2[\rho_x^2,\rho_y^2]$	$\mathbf{Z}_2$
c_{27}	$\mathbf{Z}_2[\rho_z^2]$	$\mathbf{D}_2[\rho_x^2,\rho_y^2]$	$\mathbf{Z}_2$
c_{28}	$\mathbf{Z}_2[\rho_z^2]$	$\mathbf{D}_2[\rho_x^2,\rho_y^2]$	$\mathbf{Z}_2$

Proposition 7.14
Let $\mathbf{D}_4[\rho_x,\kappa_6]$ *act on* $\mathscr{C}_{\mathbf{D}_4[\rho_x^2,\kappa_6]}$ *as in Table 7.11 and on* X_0 *as in Table 7.10. Then given* $C \in \mathscr{C}_{\mathbf{D}_4[\rho_x,\kappa_6]}$, *the setwise isotropy* Stab(C), *pointwise isotropy* stab(C) *and the group* $S(C)$ *are given in Table 7.12.*

Proof. Follow the standard lines given for Proposition 7.11. □

This completes the computations of the setwise and pointwise isotropy subgroups for all $C \in \mathscr{C}_{\mathbf{D}_4[\rho_x,\kappa_6]}$. These computations show that $S(C) \cong \mathbf{Z}_2$ for all $C \in \mathscr{C}_{\mathbf{D}_4[\rho_x,\kappa_6]}$, with $C \cong \mathbf{S}^1$, so there is an axis of symmetry along these C's.

Knots Relative to C. The action of $\mathbf{D}_4[\rho_x,\kappa_6]$ on $\mathscr{C}_{\mathbf{D}_4[\rho_x,\kappa_6]}$ in Table 7.11 shows that there are nine C's that are not symmetrically related; namely: c_1, c_2, c_3, c_4, c_{15}, c_{18}, c_{23}, c_{25}, and c_{26}. The representatives of the equilibria that lie on these C's are: e_1, e_2, e_4, e_5, e_7, and e_8. We need only compute the knots relative to the orbit representatives of the C's given above. The computation of the knots relative to each C is straightforward. Since there are only two equilibria on each $C \in \mathscr{C}_{\mathbf{D}_4[\rho_x,\kappa_6]}$, and $S(C) \cong \mathbf{Z}_2$, these equilibria are the knots. We summarise this information in Table 7.13.

Projected Skeleton

Here we compute the projected skeleton $\mathbb{X}^p_{\mathbf{D}_4[\rho_x,\kappa_6]}$. The projected skeleton is very important since it gives a simple geometric description of the connections between equilibria. The computation of the projected skeleton is made easy by our work on the pointwise and setwise isotropy subgroups and the knots.

Table 7.13: Knots relative to orbit representatives of each $C \in \mathscr{C}_{\mathbf{D}_4[\rho_x,\kappa_6]}$ for the SC lattice.

Element of $\mathscr{C}_{\mathbf{D}_4[\rho_x,\kappa_6]}$	Knots
c_1	e_1, e_4
c_2	e_7, e_8
c_3	e_1, e_2
c_4	e_5, e_8
c_{15}	e_1, e_7
c_{18}	e_4, e_8
c_{23}	e_2, e_5
c_{25}	e_4, e_5
c_{26}	e_2, e_7

The action of $\mathbf{D}_4[\rho_x, \kappa_6]$ on $\mathscr{C}_{\mathbf{D}_4[\rho_x,\kappa_6]}$ shows that there are nine orbit representatives for the elements of $\mathscr{C}_{\mathbf{D}_4[\rho_x,\kappa_6]}$ which are homeomorphic to $\mathbf{S}^1$. These are c_1, c_2, c_3, c_4, c_{15}, c_{18}, c_{23}, c_{25} and c_{26}. The orbit representatives for the equilibria are e_1, e_2, e_4, e_5, e_7 and e_8. We have seen also that each C has two knots; this implies that there is an axis of reflection symmetry on C. So each C projects into the orbit space as a line joining the two knots. More precisely, we have the following relations: the element c_1 connects e_1 to e_4, c_2 connects e_7 to e_8, c_3 connects e_1 to e_2, c_4 connects e_5 to e_8, c_{15} connects e_1 to e_7, c_{18} connects e_4 to e_8, c_{23} connects e_2 to e_5, c_{25} connects e_4 to e_5 and c_{26} connects e_2 to e_7. Figure 7.3 (a) illustrates the projected skeleton.

Remark 7.15
The projected skeleton $\mathbb{X}^p_{\mathbf{D}_4[\rho_x,\kappa_6]}$ shares many similarities with the projected skeleton $\mathbb{X}^p_{\mathbf{0}}$. In fact $\mathbb{X}^p_{\mathbf{D}_4[\rho_x,\kappa_6]}$ is the most complex projected skeleton we have yet encountered and the dynamical possibilities are huge.

Because of complexities involved in the projected skeleton, we do not attempt to find admissible perturbations. We end with an interesting possible flow on the projected skeleton. Figure 7.3 (b) illustrates a possible arrangement of connections between the equilibria. We are not stating that such a flow on the projected skeleton exists, but use it as an illustration of the complex dynamics that are possible. This heteroclinic network $\mathcal{H}$ consists of three separate

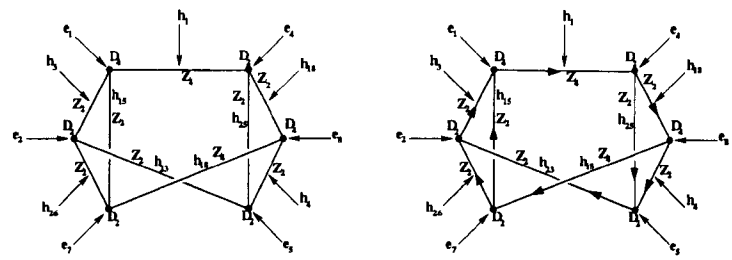

(a) (b)

Figure 7.3: The projected skeleton $\mathbb{X}^p_{\mathbf{D}_4[\rho_x,\kappa_6]}$. Here $h_1 = \{(\theta,0,0)|\theta \in (0,\pi)\}$, $h_2 = \{(\theta,\pi,\pi)|\theta \in (0,\pi)\}$, $h_3 = \{(0,\theta,0)|\theta \in (0,\pi)\}$, $h_4 = \{(\pi,\theta,\pi)|\theta \in (0,\pi)\}$, $h_{15} = \{(0,\theta,\theta)|\theta \in (0,\pi)\}$, $h_{18} = \{(\pi,\theta,-\theta)|\theta \in (0,\pi)\}$, $h_{23} = \{(\theta,\pi,0)|\theta \in (0,\pi)\}$, $h_{25} = \{(\pi,\theta,0)|\theta \in (0,\pi)\}$ and $h_{26} = \{(0,\theta,\pi)|\theta \in (0,\pi)\}$. (a) The projected skeleton. (b) An interesting flow on the projected skeleton.

cycles with the following connective behaviour: $\mathcal{H}_1$, $(e_1, e_4, e_8, e_7, e_2)$, $\mathcal{H}_2$, (e_1, e_4, e_5, e_2) and $\mathcal{H}_3$, (e_1, e_4, e_8, e_7), where we use the order tuples to indicate the equilibria in the cycle and the order in which they occur, so, for example, $\mathcal{H}_3$ is the cycle joining e_1 to e_4 to e_8 to e_7 and back to e_1, in that order. The dynamics to be expected from $\boldsymbol{\mathcal{H}}$ are complex, but should share some of the characteristics stated for the $\mathbb{O}$ example. As was the case for the $\mathbb{O}$ example, more general behaviour than a heteroclinic network is possible.

7.2.4 Forced Symmetry Breaking to $\mathbb{T}$

In this subsection we study the behaviour of the group orbit X_0 when symmetry-breaking terms with $\mathbb{T}$ symmetry are added to the vector field (7.4). The normal hyperbolicity of X_0 guarantees, by the Equivariant Persistence Theorem, the existence of a invariant manifold X_ε $\mathbb{T}$-equivariantly diffeomorphic to X_0. The action of the group $\mathbb{T}$ on the space $\mathbb{C}^3$ is in Table 7.14.

Table 7.14: Action of $\mathbb{T}$ on $\mathbb{C}^3$ for the SC lattice.

Element of $\mathbb{T}$	Action on $\mathbb{C}^3$	Element of $\mathbb{T}$	Action on $\mathbb{C}^3$
τ_1	(z_3, z_1, z_2)	τ_1^2	(z_2, z_3, z_1)
τ_2	$(\overline{z_2}, z_3, \overline{z_1})$	τ_2^2	$(\overline{z_3}, \overline{z_1}, z_2)$
τ_3	$(\overline{z_3}, z_1, \overline{z_2})$	τ_3^2	$(z_2, \overline{z_3}, \overline{z_1})$
τ_4	$(\overline{z_2}, \overline{z_3}, z_1)$	τ_4^2	$(z_3, \overline{z_1}, \overline{z_2})$
ρ_x^2	$(z_1, \overline{z_2}, \overline{z_3})$	ρ_y^2	$(\overline{z_1}, z_2, \overline{z_3})$
ρ_z^2	$(\overline{z_1}, \overline{z_2}, z_3)$		

Calculation of the Skeleton

Here we calculate the skeleton of X_0 under the action of $\mathbb{T}$. Recall, there are ten subgroups of $\mathbb{T}$. They are: $\mathbb{T}$, $\mathbf{Z}_3[\tau_1]$, $\mathbf{Z}_3[\tau_2]$, $\mathbf{Z}_3[\tau_3]$, $\mathbf{Z}_3[\tau_4]$, $\mathbf{D}_2[\rho_x^2, \rho_y^2]$, $\mathbf{Z}_2[\rho_x^2]$, $\mathbf{Z}_2[\rho_y^2]$, $\mathbf{Z}_2[\rho_z^2]$, and the trivial subgroup. Using the notation from Definition 7.3 we state the following fundamental proposition.

Proposition 7.16
Let $\mathbb{T}$ act on X_0 with the action induced from Table 7.14. Then

$$\begin{aligned}\mathscr{C}_{\mathbb{T}} \;=\; &\{e_1, e_2, e_3, e_4, e_5, e_6, e_7, e_8, c_1, c_2, c_3, c_4, c_5, c_6, c_{19}, c_{20}, c_{21}, c_{22}, c_{23},\\ &c_{24}, c_{25}, c_{26}, c_{27}, c_{28}\}.\end{aligned}$$

Proof. The proof follows from Lemmas 7.5, 7.8, 7.9 and 7.10. □

We can now use this information to form the skeleton

$$\mathbb{X}_{\mathbb{T}} = \bigcup_{C \in \mathscr{C}_{\mathbb{T}}} C \subset X_0.$$

As we saw for the $\mathbb{O}$ and $\mathbf{D}_4[\rho_x, \kappa_6]$ cases, it is not possible to render the skeleton in its current form. However, by considering the symmetry properties of the skeleton we can construct the projected skeleton, which is a simpler and more useful object.

Symmetry Properties of $\mathbb{X}_{\mathbb{T}}$

Here we study the $\mathbb{T}$ action induced on the skeleton to determine the setwise isotropy $\mathrm{Stab}(C)$ and pointwise isotropy $\mathrm{stab}(C)$. Using these two groups we may form the group $S(C)$ which provides information on possible knots present on the skeleton, giving axes of symmetry for

Table 7.15: Action of $\mathbb{T}$ induced on X_0 for the SC lattice.

Element of $\mathbb{T}$	Action on X_0	Element of $\mathbb{T}$	Action on X_0
τ_1	$(\theta_3, \theta_1, \theta_2)$	τ_1^2	$(\theta_2, \theta_3, \theta_1)$
τ_2	$(-\theta_2, \theta_3, -\theta_1)$	τ_2^2	$(-\theta_3, -\theta_1, \theta_2)$
τ_3	$(-\theta_3, \theta_1, -\theta_2)$	τ_3^2	$(\theta_2, -\theta_3, -\theta_1)$
τ_4	$(-\theta_2, -\theta_3, \theta_1)$	τ_4^2	$(\theta_3, -\theta_1, -\theta_2)$
ρ_x^2	$(\theta_1, -\theta_2, \theta_3)$	ρ_y^2	$(-\theta_1, \theta_2, -\theta_3)$
ρ_z^2	$(-\theta_1, -\theta_2, \theta_3)$		

Table 7.16: Action of $\mathbb{T}$ induced on $\mathscr{C}_\mathbb{T}$ for the SC lattice.

Element of $\mathscr{C}_\mathbb{T}$	Elements of $\mathbb{T}$ acting nontrivially	Action
e_1	None	
e_2	$\tau_1^2, \tau_2, \tau_3^2, \tau_4$	e_3
	$\tau_1, \tau_2^2, \tau_3, \tau_4^2$	e_4
e_3	$\tau_1, \tau_2^2, \tau_3, \tau_4^2$	e_2
	$\tau_1^2, \tau_2, \tau_3^2, \tau_4$	e_4
e_4	$\tau_1^2, \tau_2, \tau_3^2, \tau_4$	e_2
	$\tau_1, \tau_2^2, \tau_3, \tau_4^2$	e_3
e_5	$\tau_1^2, \tau_2, \tau_3^2, \tau_4$	e_6
	$\tau_1, \tau_2^2, \tau_3, \tau_4^2$	e_7
e_6	$\tau_1^2, \tau_2, \tau_3^2, \tau_4$	e_5
	$\tau_1^2, \tau_2, \tau_3^2, \tau_4$	e_7
e_7	$\tau_1^2, \tau_2, \tau_3^2, \tau_4$	e_6
	$\tau_1, \tau_2^2, \tau_3, \tau_4^2$	e_5
e_8	None	

$\mathbb{T}$-equivariant flows on the skeleton. With this information we can form the projected skeleton.

Pointwise and Setwise Isotropy Subgroups. The action of $\mathbb{T}$ on $\mathbb{C}^3$ in Table 7.14 induces a natural action on X_0 with respect to the coordinates $(\theta_1, \theta_2, \theta_3)$. The action of the generators for $\mathbb{T}$ is:

$$\begin{aligned} \rho_x(\theta_1, \theta_2, \theta_3) &= (\theta_1, -\theta_3, \theta_2), \\ \rho_y(\theta_1, \theta_2, \theta_3) &= (\theta_3, \theta_2, -\theta_1). \end{aligned}$$

The complete action of $\mathbb{T}$ on X_0 is given in Table 7.15. The action of $\mathbb{T}$ on X_0 in turn induces an action of $\mathbb{T}$ on the set $\mathscr{C}_\mathbb{T}$ by permutation. Again this action is straightforward to compute; it is the restriction of the action in Table 7.3. We present this action in Table 7.16. Using this action we may deduce the following fundamental symmetry result.

Proposition 7.17
Let $\mathbb{T}$ act on $\mathscr{C}_\mathbb{T}$ as in Table 7.16 and on X_0 as in Table 7.15. Then given $C \in \mathscr{C}_\mathbb{T}$, the setwise isotropy $\mathrm{Stab}(C)$, *pointwise isotropy* $\mathrm{stab}(C)$ *and the group $S(C)$ are given in Table 7.18.*

Proof. The proof follows the standard lines. □

Knots Relative to C. Given $C \in \mathscr{C}_\mathbb{T}$, a knot relative to C gives an axis of symmetry for any $\mathbb{T}$-equivariant flow on C. The action of $\mathbb{T}$ on $\mathscr{C}_\mathbb{T}$ in Table 7.16 shows that there are five C's that are not symmetrically related, namely: $c_1 = \{(\theta, 0, 0) | \theta \in [0, 2\pi)\}$, $c_2 = \{(\theta, \pi, \pi) | \theta \in [0, 2\pi)\}$, $c_{19} = \{(\theta, \theta, \theta) | \theta \in [0, 2\pi)\}$, $c_{23} = \{(\theta, \pi, 0) | \theta \in [0, 2\pi)\}$, and $c_{24} = \{(\theta, 0, \pi) | \theta \in [0, 2\pi)\}$. The

Table 7.17: Table 7.16 continued.

Element of $\mathscr{C}_{\mathbb{T}}$	Elements of $\mathbb{T}$ acting nontrivially	Action
c_1	$\tau_1^2, \tau_2, \tau_3^2, \tau_4$	c_5
	$\tau_1, \tau_2^2, \tau_3, \tau_4^2$	c_3
c_2	$\tau_1^2, \tau_2, \tau_3^2, \tau_4$	c_6
	$\tau_1, \tau_2^2, \tau_3, \tau_4^2$	c_4
c_3	$\tau_1, \tau_2^2, \tau_3, \tau_4^2$	c_5
	$\tau_1^2, \tau_2, \tau_3^2, \tau_4$	c_1
c_4	$\tau_1, \tau_2^2, \tau_3, \tau_4^2$	c_6
	$\tau_1^2, \tau_2, \tau_3^2, \tau_4$	c_2
c_5	$\tau_1^2, \tau_2, \tau_3^2, \tau_4$	c_3
	$\tau_1, \tau_2^2, \tau_3, \tau_4^2$	c_1
c_6	$\tau_1^2, \tau_2, \tau_3^2, \tau_4$	c_4
	$\tau_1, \tau_2^2, \tau_3, \tau_4^2$	c_2
c_{19}	ρ_y^2, τ_2, τ_3	c_{22}
	$\rho_x^2, \tau_3^2, \tau_4^2$	c_{20}
	$\rho_z^2, \tau_2^2, \tau_4$	c_{21}
c_{20}	$\rho_y^2, \tau_1^2, \tau_4^2$	c_{21}
	ρ_x^2, τ_3, τ_4	c_{19}
	$\rho_z^2, \tau_1, \tau_3^2$	c_{22}
c_{21}	$\rho_z^2, \tau_2, \tau_4^2$	c_{19}
	$\rho_x^2, \tau_1^2, \tau_2^2$	c_{22}
	ρ_y^2, τ_1, τ_4	c_{20}
c_{22}	$\rho_z^2, \tau_1^2, \tau_3$	c_{20}
	ρ_x^2, τ_1, τ_2	c_{21}
	$\rho_y^2, \tau_2^2, \tau_3^2$	c_{19}
c_{23}	$\tau_1, \tau_2^2, \tau_3, \tau_4^2$	c_{26}
	$\tau_1^2, \tau_2, \tau_3^2, \tau_4$	c_{28}
c_{24}	$\tau_1, \tau_2^2, \tau_3, \tau_4^2$	c_{25}
	$\tau_1^2, \tau_2, \tau_3^2, \tau_4$	c_{27}
c_{25}	$\tau_1, \tau_2^2, \tau_3, \tau_4^2$	c_{27}
	$\tau_1^2, \tau_2, \tau_3^2, \tau_4$	c_{24}
c_{26}	$\tau_1, \tau_2^2, \tau_3, \tau_4^2$	c_{28}
	$\tau_1^2, \tau_2, \tau_3^2, \tau_4$	c_{23}
c_{27}	$\tau_1, \tau_2^2, \tau_3, \tau_4^2$	c_{24}
	$\tau_1^2, \tau_2, \tau_3^2, \tau_4$	c_{25}
c_{28}	$\tau_1, \tau_2^2, \tau_3, \tau_4^2$	c_{23}
	$\tau_1^2, \tau_2, \tau_3^2, \tau_4$	c_{26}

representatives of the equilibria which lie on these C's are: e_1, e_4, e_5 and e_8. The computations of the group $S(C)$ show that that all connections, with the exception of c_{19}, c_{20}, c_{21}, and c_{22}, have knots relative to them, and we know that c_{19} is the orbit representative of these connections. For those connection with knots, the knots are straightforward to identify. Since each such C contains two equilibria, these equilibria must form the knots. In Table 7.19 we present the knots relative to each representative C, when such knots exist.

Projected Skeleton

Here we compute the projected skeleton $\mathbb{X}_{\mathbb{T}}^p$. The action of $\mathbb{T}$ on $\mathscr{C}_{\mathbb{T}}$ shows that there are five orbit representatives for the elements of $\mathscr{C}_{\mathbb{T}}$ which are homeomorphic to $\mathbf{S}^1$; these are c_1, c_2, c_{19}, c_{23}, and c_{24}. The orbit representatives for the equilibria are e_1, e_4, e_5 and e_8. We have seen also

Table 7.18: Isotropy data for $C \in \mathscr{C}_{\mathrm{T}}$ on the SC lattice.

$C \in \mathscr{C}_{\mathrm{T}}$	stab(C)	Stab(C)	$S(C) = \mathrm{Stab}(C)/\mathrm{stab}(C)$
e_1	$\mathbb{T}$	$\mathbb{T}$	$\mathbf{1}$
e_2	$\mathbf{D}_2[\rho_x^2, \rho_y^2]$	$\mathbf{D}_2[\rho_x^2, \rho_y^2]$	$\mathbf{1}$
e_3	$\mathbf{D}_2[\rho_x^2, \rho_y^2]$	$\mathbf{D}_2[\rho_x^2, \rho_y^2]$	$\mathbf{1}$
e_4	$\mathbf{D}_2[\rho_x^2, \rho_y^2]$	$\mathbf{D}_2[\rho_x^2, \rho_y^2]$	$\mathbf{1}$
e_5	$\mathbf{D}_2[\rho_x^2, \rho_y^2]$	$\mathbf{D}_2[\rho_x^2, \rho_y^2]$	$\mathbf{1}$
e_6	$\mathbf{D}_2[\rho_x^2, \rho_y^2]$	$\mathbf{D}_2[\rho_x^2, \rho_y^2]$	$\mathbf{1}$
e_7	$\mathbf{D}_2[\rho_x^2, \rho_y^2]$	$\mathbf{D}_2[\rho_x^2, \rho_y^2]$	$\mathbf{1}$
e_8	$\mathbb{T}$	$\mathbb{T}$	$\mathbf{1}$
c_1	$\mathbf{Z}_2[\rho_x^2]$	$\mathbf{D}_2[\rho_x^2, \rho_y^2]$	$\mathbf{Z}_2$
c_2	$\mathbf{Z}_4[\rho_x^2]$	$\mathbf{D}_4[\rho_x, \rho_y^2]$	$\mathbf{Z}_2$
c_3	$\mathbf{Z}_4[\rho_y^2]$	$\mathbf{D}_4[\rho_x, \rho_y^2]$	$\mathbf{Z}_2$
c_4	$\mathbf{Z}_4[\rho_y^2]$	$\mathbf{D}_4[\rho_x, \rho_y^2]$	$\mathbf{Z}_2$
c_5	$\mathbf{Z}_4[\rho_z^2]$	$\mathbf{D}_4[\rho_x, \rho_y^2]$	$\mathbf{Z}_2$
c_6	$\mathbf{Z}_4[\rho_z^2]$	$\mathbf{D}_4[\rho_x, \rho_y^2]$	$\mathbf{Z}_2$
c_{19}	$\mathbf{Z}_3[\tau_1]$	$\mathbf{Z}_3[\tau_1]$	$\mathbf{1}$
c_{20}	$\mathbf{Z}_3[\tau_2]$	$\mathbf{Z}_3[\tau_2]$	$\mathbf{1}$
c_{21}	$\mathbf{Z}_3[\tau_3]$	$\mathbf{Z}_3[\tau_3]$	$\mathbf{1}$
c_{22}	$\mathbf{Z}_3[\tau_4]$	$\mathbf{Z}_3[\tau_4]$	$\mathbf{1}$
c_{23}	$\mathbf{Z}_2[\rho_x^2]$	$\mathbf{D}_2[\rho_x^2, \rho_y^2]$	$\mathbf{Z}_2$
c_{24}	$\mathbf{Z}_2[\rho_x^2]$	$\mathbf{D}_2[\rho_x^2, \rho_y^2]$	$\mathbf{Z}_2$
c_{25}	$\mathbf{Z}_2[\rho_y^2]$	$\mathbf{D}_2[\rho_x^2, \rho_y^2]$	$\mathbf{Z}_2$
c_{26}	$\mathbf{Z}_2[\rho_y^2]$	$\mathbf{D}_2[\rho_x^2, \rho_y^2]$	$\mathbf{Z}_2$
c_{27}	$\mathbf{Z}_2[\rho_z^2]$	$\mathbf{D}_2[\rho_x^2, \rho_y^2]$	$\mathbf{Z}_2$
c_{28}	$\mathbf{Z}_2[\rho_z^2]$	$\mathbf{D}_2[\rho_x^2, \rho_y^2]$	$\mathbf{Z}_2$

Table 7.19: Knots relative to orbit representatives of $C \in \mathscr{C}_{\mathrm{T}}$.

Element of $\mathscr{C}_{\mathrm{T}}$	Knots
c_1	e_1, e_4
c_2	e_5, e_8
c_{23}	e_4, e_5
c_{24}	e_4, e_5

that c_1, c_2, c_{23}, and c_{24} have two knots; implying that there is an axis of reflection symmetry. So each C projects into the orbit space as a line joining the two knots. More precisely we have the following relations. The element c_1 connects e_1 to e_4, c_2 connects e_5 to e_8, c_{19} connects e_1 to e_8, c_{23} connects e_4 to e_5 and c_{24} connects e_4 to e_5. Figure 7.4 (a) illustrates the projected skeleton. Figure 7.4 (b) presents an example that shows interesting intermittency properties. This network $\mathcal{H}$ contains three cycles. Our previous discussion for the examples given in the $\mathbb{O}$ and $\mathbf{D}_4[\rho_x, \kappa_6]$ cases remains valid for the example presented here. This case is slightly different from the other cases we have considered, since the connection c_{19} has no knots on it. Symmetry does not place any restrictions on the flow directions either side of the equilibria on c_{19}; that is, the flow on c_{19} close to e_1 and e_8 can be in any direction we choose, which leads to some interesting possibilities. However, we must be wary that the network does not become structurally unstable given such freedom. Even the dynamics associated with this example merit further investigation, but we shall not consider this example further.

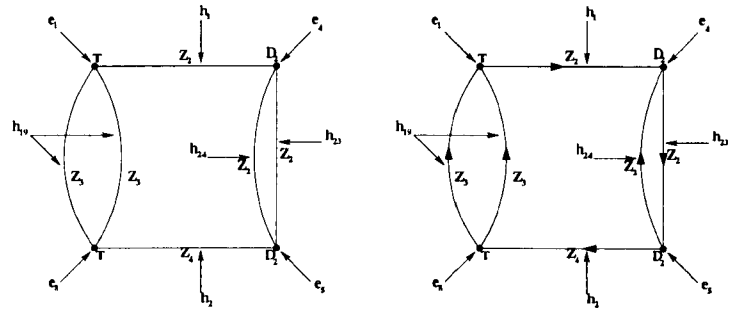

(a) (b)

Figure 7.4: The projected skeleton $\mathbb{X}_{\mathrm{T}}^{p}$. Here $h_1 = \{(\theta,0,0)|\theta \in (0,\pi)\}$, $h_2 = \{(\theta,\pi,\pi)|\theta \in (0,\pi)\}$, $c_{19} = \{(\theta,\theta,\theta)|\theta \in [0,2\pi)\}$, $h_{23} = \{(\theta,\pi,0)|\theta \in (0,\pi)\}$ and $h_{24} = \{(\theta,0,\pi)|\theta \in (0,\pi)\}$. (a) The projected skeleton showing how the equilibria are connected and related. (b) An example of a possible flow that can occur on the projected skeleton.

7.2.5 Forced Symmetry Breaking to $\mathbf{D}_3[\tau_1, \kappa_5]$

In this subsection we study the behaviour of the group orbit X_0 when symmetry breaking terms with $\mathbf{D}_3[\tau_1, \kappa_5]$ symmetry are used to perturbed the system. The normal hyperbolicity of X_0 guarantees, by the Equivariant Persistence Theorem, the existence of a manifold X_ε $\mathbf{D}_3[\tau_1, \kappa_5]$-equivariantly diffeomorphic to X_0 and invariant under the new dynamics. The action of the group $\mathbf{D}_3[\tau_1, \kappa_5]$ on the space $\mathbb{C}^3$ is in Table 7.20.

Table 7.20: Action of $\mathbf{D}_3[\tau_1, \kappa_5]$ on $\mathbb{C}^3$ for the SC lattice.

Element of $\mathbf{D}_3[\tau_1, \kappa_5]$	Action on $\mathbb{C}^3$	Element of $\mathbf{D}_3[\tau_1, \kappa_5]$	Action on $\mathbb{C}^3$
τ_1	(z_3, z_1, z_2)	τ_1^2	(z_2, z_3, z_1)
κ_2	$(\overline{z_2}, \overline{z_1}, \overline{z_3})$	κ_5	$(\overline{z_3}, \overline{z_2}, \overline{z_1})$
κ_6	$(\overline{z_1}, \overline{z_3}, \overline{z_2})$		

Calculation of the Skeleton

Here we calculate the skeleton of X_0 under the action of $\mathbf{D}_3[\tau_1, \kappa_5]$. To begin we calculate the set $\mathscr{C}_{\mathbf{D}_3[\tau_1,\kappa_5]}$, for which we recall, there are five subgroups of $\mathbf{D}_3[\tau_1, \kappa_5]$. They are: $\mathbf{D}_3[\tau_1, \kappa_5]$, $\mathbf{Z}_3[\tau_1]$, $\mathbf{Z}_2[\kappa_2]$, $\mathbf{Z}_2[\kappa_5]$, $\mathbf{Z}_2[\kappa_6]$ and the trivial subgroup.

Proposition 7.18
Let $\mathbf{D}_3[\tau_1, \kappa_5]$ act on X_0 with the action induced from Table 7.20. Then

$$\mathscr{C}_{\mathbf{D}_3[\tau_1,\kappa_5]} = \{e_1, e_8, c_9, c_{10}, c_{11}, c_{13}, c_{14}, c_{17}, c_{18}, c_{19}\}.$$

Proof. The proof follows from Lemmas 7.5, 7.8 and 7.9. □

We can now use this information to form the skeleton

$$\mathbb{X}_{\mathbf{D}_3[\tau_1,\kappa_5]} = \bigcup_{C \in \mathscr{C}_{\mathbf{D}_3[\tau_1,\kappa_5]}} C \subset \mathbf{T}^3 \cong X_0.$$

Table 7.21: Action of $\mathbf{D}_3[\tau_1, \kappa_5]$ induced on X_0 for the SC lattice.

Element of $\mathbf{D}_3[\tau_1, \kappa_5]$	Action on X_0	Element of $\mathbf{D}_3[\tau_1, \kappa_5]$	Action on X_0
τ_1	$(\theta_3, \theta_1, \theta_2)$	τ_1^2	$(\theta_2, \theta_3, \theta_1)$
κ_2	$(-\theta_2, -\theta_1, -\theta_3)$	κ_5	$(-\theta_3, -\theta_2, -\theta_1)$
κ_6	$(-\theta_1, -\theta_3, -\theta_2)$		

Table 7.22: Action of $\mathbf{D}_3[\tau_1, \kappa_5]$ induced on $\mathscr{C}_{\mathbf{D}_3[\tau_1,\kappa_5]}$ for the SC lattice.

Element of $\mathscr{C}_{\mathbf{D}_3[\tau_1,\kappa_5]}$	Elements of $\mathbf{D}_3[\tau_1, \kappa_5]$ acting nontrivially	Action
e_1	None	
e_8	None	
c_9	κ_6, τ_1^2,	c_{13}
	κ_5, τ_1,	c_{17}
c_{10}	κ_6, τ_1^2,	c_{14}
	κ_5, τ_1,	c_{18}
c_{13}	κ_6, τ_1	c_9
	κ_2, τ_1^2,	c_{17}
c_{14}	κ_6, τ_1	c_{10}
	κ_2, τ_1^2,	c_{18}
c_{17}	κ_5, τ_1^2,	c_9
	κ_2, τ_1^2,	c_{13}
c_{18}	κ_5, τ_1^2,	c_{10}
	κ_2, τ_1^2,	c_{14}
c_{19}	None	

Symmetry Properties of $\mathbb{X}_{\mathbf{D}_3[\tau_1,\kappa_5]}$

Here we study the $\mathbf{D}_3[\tau_1, \kappa_5]$ action induced on the skeleton to determine the different orbit representative for equilibria and heteroclinic connections present. This allows us to form the projected skeleton which is geometrically a simpler object than the skeleton and contains all the important information we require.

Pointwise and Setwise Isotropy Subgroups. The action of $\mathbf{D}_3[\tau_1, \kappa_5]$ on $\mathbb{C}^3$ in Table 7.20 induces a natural action on X_0 with respect to the coordinates $(\theta_1, \theta_2, \theta_3)$. The action of the generators is:

$$\begin{aligned} \tau_1(\theta_1, \theta_2, \theta_3) &= (\theta_3, \theta_1, \theta_2), \\ \kappa_5(\theta_1, \theta_2, \theta_3) &= (-\theta_3, -\theta_2, -\theta_1). \end{aligned}$$

The complete action of $\mathbf{D}_3[\tau_1, \kappa_5]$ on X_0 is given in Table 7.21. The action of $\mathbf{D}_3[\tau_1, \kappa_5]$ on X_0 in turn induces an action of $\mathbf{D}_3[\tau_1, \kappa_5]$ on the set $\mathscr{C}_{\mathbf{D}_3[\tau_1,\kappa_5]}$ by permutation. We present this action in Table 7.22. Using this action we may deduce the following fundamental symmetry result.

Proposition 7.19
Let $\mathbf{D}_3[\tau_1, \kappa_5]$ act on $\mathscr{C}_{\mathbf{D}_3[\tau_1,\kappa_5]}$ as in Table 7.22 and on X_0 as in Table 7.21. Then given $C \in \mathscr{C}_{\mathbf{D}_3[\tau_1,\kappa_5]}$, the setwise isotropy $\mathrm{Stab}(C)$, *pointwise isotropy* $\mathrm{stab}(C)$ *and the group $S(C)$ are given in Table 7.23.*

Proof. The proof follows the standard lines. □

Table 7.23: Isotropy data for $C \in \mathscr{C}_{\mathbf{D}_3[\tau_1,\kappa_5]}$ on the SC lattice.

$C \in \mathscr{C}_{\mathbf{D}_3[\tau_1,\kappa_5]}$	stab(C)	Stab(C)	$S(C) = \text{Stab}(C)/\text{stab}(C)$
e_1	$\mathbf{D}_3[\tau_1, \kappa_5]$	$\mathbf{D}_3[\tau_1, \kappa_5]$	**1**
e_2	$\mathbf{Z}_2[\kappa_2]$	$\mathbf{Z}_2[\kappa_2]$	**1**
e_3	$\mathbf{Z}_2[\kappa_5]$	$\mathbf{Z}_2[\kappa_5]$	**1**
e_4	$\mathbf{Z}_2[\kappa_6]$	$\mathbf{Z}_2[\kappa_6]$	**1**
e_5	$\mathbf{Z}_2[\kappa_2]$	$\mathbf{Z}_2[\kappa_2]$	**1**
e_6	$\mathbf{Z}_2[\kappa_5]$	$\mathbf{Z}_2[\kappa_5]$	**1**
e_7	$\mathbf{Z}_2[\kappa_6]$	$\mathbf{Z}_2[\kappa_6]$	**1**
e_8	$\mathbf{D}_3[\tau_1, \kappa_5]$	$\mathbf{D}_3[\tau_1, \kappa_5]$	**1**
c_9	$\mathbf{Z}_2[\kappa_2]$	$\mathbf{Z}_2[\kappa_2]$	**1**
c_{10}	$\mathbf{Z}_2[\kappa_2]$	$\mathbf{Z}_2[\kappa_2]$	**1**
c_{13}	$\mathbf{Z}_2[\kappa_5]$	$\mathbf{Z}_2[\kappa_5]$	**1**
c_{14}	$\mathbf{Z}_2[\kappa_5]$	$\mathbf{Z}_2[\kappa_5]$	**1**
c_{17}	$\mathbf{Z}_2[\kappa_6]$	$\mathbf{Z}_2[\kappa_6]$	**1**
c_{18}	$\mathbf{Z}_2[\kappa_6]$	$\mathbf{Z}_2[\kappa_6]$	**1**
c_{19}	$\mathbf{Z}_3[\tau_1]$	$\mathbf{D}_3[\tau_1, \kappa_5]$	$\mathbf{Z}_2$

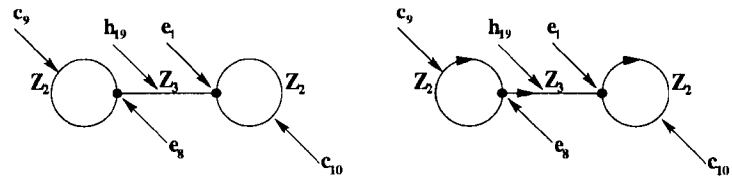

Figure 7.5: The projected skeleton $\mathbb{X}^p_{\mathbf{D}_3[\tau_1,\kappa_5]}$. Here $c_9 = \{(\theta, -\theta, 0) | \theta \in [0, 2\pi)\}$, $c_{10} = \{(\theta, -\theta, \pi) | \theta \in [0, 2\pi)\}$ and $h_{19} = \{(\theta, \theta, \theta) | \theta \in (0, \pi)\}$. (a) The projected skeleton. (b) An example of a heteroclinic cycle.

This completes the computations of the setwise and pointwise isotropy subgroups of all $C \in \mathscr{C}_{\mathbf{D}_3[\tau_1,\kappa_5]}$. These computations show that $S(c_{19}) \cong \mathbf{Z}_2$ and $S(C)$ is trivial otherwise, so there is an axis of symmetry along c_{19}.

Knots Relative to C. Given $C \in \mathscr{C}_{\mathbf{D}_3[\tau_1,\kappa_5]}$ a knot relative to C gives an axis of symmetry for any $\mathbf{D}_3[\tau_1, \kappa_5]$-equivariant flow on C. We know only c_{19} has knots, since the only two equilibria that lie on c_{19} are e_1 and e_8. These are the two knots relative to c_{19}.

Projected Skeleton

Here we compute the projected skeleton $\mathbb{X}^p_{\mathbf{D}_3[\tau_1,\kappa_5]}$. The action of $\mathbf{D}_3[\tau_1, \kappa_5]$ on $\mathscr{C}_{\mathbf{D}_3[\tau_1,\kappa_5]}$ shows that there are three orbit representatives for the elements of $\mathscr{C}_{\mathbf{D}_3[\tau_1,\kappa_5]}$ which are homeomorphic to $\mathbf{S}^1$. These are c_9, c_{10} and c_{19}. The orbit representatives for the equilibria are e_1 and e_8. The connection c_{19} has two knots; this implies that there is an axis of reflection symmetry. So c_{19} projects into the orbit space as a line joining the two knots. We denote the projection of c_{19} by h_{19}. More precisely, we have the following relations. The element c_9 connects e_1 to itself, c_{10} connects e_8 to itself and h_{19} connects e_1 to e_8. Figure 7.5 (a) illustrates the projected skeleton. The projected skeleton shows that heteroclinic cycles can exist provided that there are no additional equilibria along the (orbit representative) connections c_9 and c_{10}. We know

that such perturbations exist. We show an example in Figure 7.5 (b). This result in itself is significant, but we shall not attempt to find perturbations that give these heteroclinic cycles: instead we leave such a study for future work.

7.2.6 Forced Symmetry Breaking to $\mathbf{D}_2[\rho_x^2, \kappa_6]$

In this subsection we study the behaviour of the group orbit X_0, when symmetry-breaking terms with $\mathbf{D}_2[\rho_x^2, \kappa_6]$ symmetry are added to the vector field (7.4). The normal hyperbolicity of X_0 guarantees, by the Equivariant Persistence Theorem, the existence of a manifold X_ε diffeomorphic to X_0 and invariant under the dynamics. The action of the group $\mathbf{D}_2[\rho_x^2, \kappa_6]$ on the space $\mathbb{C}^3$ is in Table 7.24.

Table 7.24: Action of $\mathbf{D}_2[\rho_x^2, \kappa_6]$ on $\mathbb{C}^3$ for the SC lattice.

Element of $\mathbf{D}_2[\rho_x^2, \kappa_6]$	Action on $\mathbb{C}^3$
ρ_x^2	$(z_1, \overline{z_2}, \overline{z_3})$
κ_4	$(\overline{z_1}, z_3, z_2)$
κ_6	$(\overline{z_1}, \overline{z_3}, \overline{z_2})$

Calculation of the Skeleton

Here we calculate the skeleton of X_0 under the action of $\mathbf{D}_2[\rho_x^2, \kappa_6]$. To begin we calculate the set $\mathscr{C}_{\mathbf{D}_2[\rho_x^2,\kappa_6]}$, for which we recall, there are five subgroups of $\mathbf{D}_2[\rho_x^2, \kappa_6]$. They are: $\mathbf{D}_2[\rho_x^2, \kappa_4]$, $\mathbf{Z}_2[\rho_x^2]$, $\mathbf{Z}_2[\kappa_4]$, $\mathbf{Z}_2[\kappa_6]$ and the trivial subgroup.

Proposition 7.20
Let $\mathbf{D}_2[\rho_x^2, \kappa_6]$ act on X_0 with the action induced from Table 7.24. Then

$$\mathscr{C}_{\mathbf{D}_2[\rho_x^2,\kappa_6]} = \{e_1, e_4, e_7, e_8, c_1, c_2, c_{15}, c_{16}, c_{17}, c_{18}, c_{23}, c_{24}\}.$$

Proof. The proof follows from Lemmas 7.8 and 7.10. □

We can now use this information to form the skeleton

$$\mathbb{X}_{\mathbf{D}_2[\rho_x^2,\kappa_6]} = \bigcup_{C \in \mathscr{C}_{\mathbf{D}_2[\rho_x^2,\kappa_6]}} C \subset X_0.$$

Symmetry Properties of $\mathbb{X}_{\mathbf{D}_2[\rho_x^2,\kappa_6]}$

Here we use the $\mathbf{D}_2[\rho_x^2, \kappa_6]$ symmetry to determine the different orbit representatives for equilibria and heteroclinic connections. This allows us to form the projected skeleton.

Pointwise and Setwise Isotropy Subgroups. The action of $\mathbf{D}_2[\rho_x^2, \kappa_6]$ on $\mathbb{C}^3$ in Table 7.24 induces a natural action on X_0 with respect to the coordinates $(\theta_1, \theta_2, \theta_3)$. The action of the generators is:

$$\begin{aligned} \rho_x^2(\theta_1, \theta_2, \theta_3) &= (\theta_1, -\theta_2, \theta_3), \\ \kappa_6(\theta_1, \theta_2, \theta_3) &= (-\theta_1, -\theta_3, -\theta_2). \end{aligned}$$

The complete action of $\mathbf{D}_2[\rho_x^2, \kappa_6]$ on X_0 is given in Table 7.25. The action of $\mathbf{D}_2[\rho_x^2, \kappa_6]$ on X_0 in turn induces an action of $\mathbf{D}_2[\rho_x^2, \kappa_6]$ on the set $\mathscr{C}_{\mathbf{D}_2[\rho_x^2,\kappa_6]}$ by permutation. We present this action in Table 7.26. Using this action we may deduce the following fundamental symmetry result.

Table 7.25: Action of $\mathbf{D}_2[\rho_x^2, \kappa_6]$ induced on X_0 for the SC lattice.

Element of $\mathbf{D}_2[\rho_x^2, \kappa_6]$	Action on X_0
ρ_x^2	$(\theta_1, -\theta_2, \theta_3)$
κ_4	$(-\theta_1, \theta_3, \theta_2)$
κ_6	$(-\theta_1, -\theta_3, -\theta_2)$

Table 7.26: Action of $\mathbf{D}_2[\rho_x^2, \kappa_6]$ induced on $\mathscr{C}_{\mathbf{D}_2[\rho_x^2,\kappa_6]}$ for the SC lattice.

Element of $\mathscr{C}$	Elements of $\mathbf{D}_2[\rho_x^2, \kappa_6]$ acting nontrivially	Action
e_1	None	
e_4	None	
e_7	None	
e_8	None	
c_1	None	
c_2	None	
c_{15}	None	
c_{16}	None	
c_{17}	None	
c_{18}	None	
c_{23}	κ_4, κ_6	c_{24}
c_{24}	κ_4, κ_6	c_{23}

Table 7.27: Isotropy data for $C \in \mathscr{C}_{\mathbf{D}_2[\rho_x^2,\kappa_6]}$ on the SC lattice.

$C \in \mathscr{C}_{\mathbf{D}_2[\rho_x^2,\kappa_6]}$	stab(C)	Stab(C)	$S(C) = \text{Stab}(C)/\text{stab}(C)$
e_1	$\mathbf{D}_2[\rho_x^2, \kappa_6]$	$\mathbf{D}_2[\rho_x^2, \kappa_6]$	$\mathbf{1}$
e_4	$\mathbf{D}_2[\rho_x^2, \kappa_6]$	$\mathbf{D}_2[\rho_x^2, \kappa_6]$	$\mathbf{1}$
e_7	$\mathbf{D}_2[\rho_x^2, \kappa_6]$	$\mathbf{D}_2[\rho_x^2, \kappa_6]$	$\mathbf{1}$
e_8	$\mathbf{D}_2[\rho_x^2, \kappa_6]$	$\mathbf{D}_2[\rho_x^2, \kappa_6]$	$\mathbf{1}$
c_1	$\mathbf{Z}_2[\rho_x^2]$	$\mathbf{D}_2[\rho_x^2, \kappa_6^2]$	$\mathbf{Z}_2$
c_2	$\mathbf{Z}_2[\rho_x^2]$	$\mathbf{D}_2[\rho_x^2, \kappa_6^2]$	$\mathbf{Z}_2$
c_{15}	$\mathbf{Z}_2[\kappa_4]$	$\mathbf{D}_2[\rho_x^2, \kappa_6]$	$\mathbf{Z}_2$
c_{16}	$\mathbf{Z}_2[\kappa_4]$	$\mathbf{D}_2[\rho_x^2, \kappa_6]$	$\mathbf{Z}_2$
c_{17}	$\mathbf{Z}_2[\kappa_6]$	$\mathbf{D}_2[\rho_x^2, \kappa_6]$	$\mathbf{Z}_2$
c_{18}	$\mathbf{Z}_2[\kappa_6]$	$\mathbf{D}_2[\rho_x^2, \kappa_6]$	$\mathbf{Z}_2$
c_{23}	$\mathbf{Z}_2[\rho_x^2]$	$\mathbf{Z}_2[\rho_x^2]$	$\mathbf{1}$
c_{24}	$\mathbf{Z}_2[\rho_x^2]$	$\mathbf{Z}_2[\rho_x^2]$	$\mathbf{1}$

Proposition 7.21
Let $\mathbf{D}_2[\rho_x^2, \kappa_6]$ *act on* $\mathscr{C}_{\mathbf{D}_2[\rho_x^2,\kappa_6]}$ *as in Table 7.26 and on* X_0 *as in Table 7.25. Then given* $C \in \mathscr{C}_{\mathbf{D}_2[\rho_x^2,\kappa_6]}$, *the setwise isotropy* Stab(C), *pointwise isotropy* stab(C) *and the group* $S(C)$ *are given in Table 7.27.*

Proof. The proof follows the standard lines. □

This completes the computations of the setwise and pointwise isotropy subgroups of all $C \in \mathscr{C}_{\mathbf{D}_2[\rho_x^2,\kappa_6^2]}$. These computations show that $S(C) \cong \mathbf{Z}_2$ for all $C \in \mathscr{C}_{\mathbf{D}_2[\rho_x^2,\kappa_6^2]}$, with $C \cong \mathbf{S}^1$, except for c_{23} and c_{24}.

Table 7.28: Knots relative to orbit representatives of $C \in \mathscr{C}_{\mathbf{D}_2[\rho_x^2,\kappa_6^2]}$ for the SC lattice.

Element of $\mathscr{C}_{\mathbf{D}_2[\rho_x^2,\kappa_6^2]}$	Knots
c_1	e_1, e_4
c_2	e_7, e_8
c_{15}	e_1, e_7
c_{16}	e_4, e_8
c_{17}	e_7, e_1
c_{18}	e_4, e_8

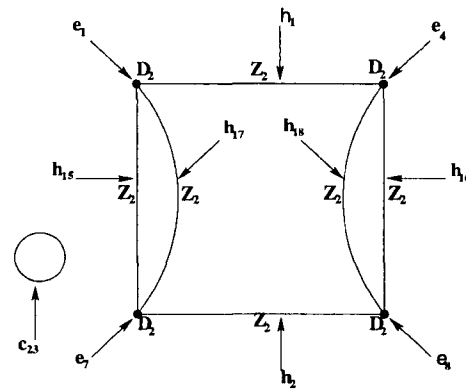

Figure 7.6: The projected skeleton $\mathbb{X}^p_{\mathbf{D}_2[\rho_x^2,\kappa_6]}$. Here $h_1 = \{(\theta,0,0)|\theta \in (0,\pi)\}$, $h_2 = \{(\theta,\pi,\pi)|\theta \in (0,\pi)\}$, $h_{15} = \{(0,\theta,\theta,)|\theta \in (0,\pi)\}$, $h_{16} = \{(\pi,\theta,\theta)|\theta \in (0,\pi)\}$, $h_{17} = \{(0,\theta,-\theta)|\theta \in (0,\pi)\}$, $h_{18} = \{(\pi,\theta,-\theta)|\theta \in (0,\pi)\}$ and $c_{23} = \{(\theta,\pi,0)|\theta \in [0,2\pi)\}$.

Knots Relative to C. The task of computing all knots relative to each C is not simplified by the $\mathbf{D}_2[\rho_x^2,\kappa_6^2]$ symmetry. However, since we know that $S(C) \cong \mathbf{Z}_2$ for each $C \cong \mathbf{S}^1$ except c_{23} and c_{24}, it follows that there are two knots relative to all such C's except c_{23} and c_{24}. These knots must be the two equilibria that are contained in C. We present this information in Table 7.28.

Projected Skeleton

Here we compute the projected skeleton $\mathbb{X}^p_{\mathbf{D}_2[\rho_x^2,\kappa_6]}$. The action of $\mathbf{D}_2[\rho_x^2,\kappa_6]$ on $\mathscr{C}_{\mathbf{D}_2[\rho_x^2,\kappa_6]}$ shows that there are six orbit representatives for the elements of $\mathscr{C}_{\mathbf{D}_2[\rho_x^2,\kappa_6]}$ that are homeomorphic to $\mathbf{S}^1$. These are c_1, c_2, c_{15}, c_{16}, c_{17}, c_{18} and c_{23}. The orbit representatives for the equilibria are e_1, e_4, e_7 and e_8. Each C apart from c_{23} has two knots; this implies that there is an axis of reflection symmetry. So each such C projects into the orbit space as a line joining the two knots. More precisely, we have the following relations. The element c_1 connects e_1 to e_4, c_2 connects e_7 to e_8, c_{15} connects e_1 to e_7, c_{16} connects e_4 to e_8, c_{17} connects e_1 to e_7, c_{18} connects e_4 to e_8 and c_{23} is a topological circle with no equilibria (forced by the group action). Figure 7.6 illustrates the projected skeleton.

The projected skeleton supports many different types of flows, but it is interesting to note that, not only is it disconnected, but also there is a periodic orbit. This is the first time we have exhibited a periodic orbit at the same time as equilibria and heteroclinic connections. The presence of a periodic orbit means that we cannot create a heteroclinic network, no matter how we choose the flow. Of course, if we ignore the periodic orbit then such a network can be created.

7.2.7 Forced Symmetry Breaking to $\mathbf{D}_2[\rho_x^2, \rho_y^2]$

In this subsection we study the behaviour of the group orbit X_0 when symmetry-breaking terms with $\mathbf{D}_2[\rho_x^2, \rho_y^2]$ symmetry are added to the vector field (7.4). The normal hyperbolicity of X_0 guarantees, by the Equivariant Persistence Theorem, the existence of a manifold X_ε diffeomorphic to X_0 and invariant under the dynamics. The action of the group $\mathbf{D}_2[\rho_x^2, \rho_y^2]$ on the space $\mathbb{C}^3$ is in Table 7.29.

Table 7.29: Action of $\mathbf{D}_2[\rho_x^2, \rho_y^2]$ on $\mathbb{C}^3$ for the SC lattice.

Element of $\mathbf{D}_2[\rho_x^2, \rho_y^2]$	Action on $\mathbb{C}^3$
ρ_x^2	$(z_1, \overline{z_2}, \overline{z_3})$
ρ_y^2	$(\overline{z_1}, z_2, \overline{z_3})$
ρ_z^2	$(\overline{z_1}, \overline{z_2}, z_3)$

Calculation of the Skeleton

Here we calculate the skeleton of X_0 under the action of $\mathbf{D}_2[\rho_x^2, \rho_y^2]$. To begin we calculate the set $\mathscr{C}_{\mathbf{D}_2[\rho_x^2,\rho_y^2]}$, for which we recall, there are five subgroups of $\mathbf{D}_2[\rho_x^2, \rho_y^2]$. They are: $\mathbf{D}_2[\rho_x^2, \rho_y^2]$, $\mathbf{Z}_2[\rho_x^2]$, $\mathbf{Z}_2[\rho_y^2]$, $\mathbf{Z}_2[\rho_z^2]$, and the trivial subgroup.

Proposition 7.22
Let $\mathbf{D}_2[\rho_x^2, \rho_y^2]$ act on X_0 with the action induced from Table 7.29. Then

$$\mathscr{C}_{\mathbf{D}_2[\rho_x^2,\rho_y^2]} = \{e_1, e_2, e_3, e_4, e_5, e_6, e_7, e_8, c_1, c_2, c_3, c_4, c_5, c_6, c_{23}, c_{24}, c_{25}, c_{26}, c_{27}, c_{28}\}.$$

Proof. Follows from Lemmas 7.8 and 7.10. □

We can now use this information to form the skeleton

$$\mathbb{X}_{\mathbf{D}_2[\rho_x^2,\rho_y^2]} = \bigcup_{C \in \mathscr{C}_{\mathbf{D}_2[\rho_x^2,\rho_y^2]}} C \subset \mathbf{T}^3 \cong X_0.$$

Symmetry Properties of $\mathbb{X}_{\mathbf{D}_2[\rho_x^2,\rho_y^2]}$

Here we study the $\mathbf{D}_2[\rho_x^2, \rho_y^2]$ action on each $C \in \mathscr{C}_{\mathbf{D}_2[\rho_x^2,\rho_y^2]}$. This allows us to construct the setwise isotropy $\mathrm{Stab}(C)$ and the pointwise isotropy $\mathrm{stab}(C)$.

Pointwise and Setwise Isotropy Subgroups. The action of $\mathbf{D}_2[\rho_x^2, \rho_y^2]$ on $\mathbb{C}^3$ in Table 7.29 induces a natural action on X_0 with respect to the coordinates $(\theta_1, \theta_2, \theta_3)$. The generators of $\mathbf{D}_2[\rho_x^2, \rho_y^2]$ act as follows:

$$\begin{aligned} \rho_x^2(\theta_1, \theta_2, \theta_3) &= (\theta_1, -\theta_2, \theta_3), \\ \rho_y^2(\theta_1, \theta_2, \theta_3) &= (-\theta_1, \theta_2, -\theta_3). \end{aligned}$$

The complete action of $\mathbf{D}_2[\rho_x^2, \rho_y^2]$ on X_0 is given in Table 7.30. In Table 7.30 we present the full action of $\mathbf{D}_2[\rho_x^2, \rho_y^2]$. The action of $\mathbf{D}_2[\rho_x^2, \rho_y^2]$ on X_0 in turn induces an action of $\mathbf{D}_2[\rho_x^2, \rho_y^2]$ on the set $\mathscr{C}_{\mathbf{D}_2[\rho_x^2,\rho_y^2]}$ by permutation of its elements; this action is trivial. Using this action we may deduce the following fundamental symmetry result.

Proposition 7.23
Let $\mathbf{D}_2[\rho_x^2, \rho_y^2]$ act on $\mathscr{C}_{\mathbf{D}_2[\rho_x^2,\rho_y^2]}$ with the induced trivial action and on X_0 as in Table 7.30. Then given $C \in \mathscr{C}_{\mathbf{D}_2[\rho_x^2,\rho_y^2]}$, the setwise isotropy $\mathrm{Stab}(C)$, pointwise isotropy $\mathrm{stab}(C)$ and the group $S(C)$ are given in Table 7.7.

Table 7.30: Action of $\mathbf{D}_2[\rho_x^2, \rho_y^2]$ induced on X_0 on the SC lattice.

Element of $\mathbf{D}_2[\rho_x^2, \rho_y^2]$	Action on X_0
ρ_x^2	$(\theta_1, -\theta_2, \theta_3)$
ρ_y^2	$(-\theta_1, \theta_2, -\theta_3)$
ρ_z^2	$(-\theta_1, -\theta_2, \theta_3)$

Table 7.31: Isotropy data for $C \in \mathscr{C}_{\mathbf{D}_2[\rho_x^2,\rho_y^2]}$ on the SC lattice.

$C \in \mathscr{C}_{\mathbf{D}_2[\rho_x^2,\rho_y^2]}$	stab(C)	Stab(C)	$S(C) = \text{Stab}(C)/\text{stab}(C)$
e_1	$\mathbf{D}_2[\rho_x^2, \rho_y^2]$	$\mathbf{D}_2[\rho_x^2, \rho_y^2]$	$\mathbf{1}$
e_2	$\mathbf{D}_2[\rho_x^2, \rho_y^2]$	$\mathbf{D}_2[\rho_x^2, \rho_y^2]$	$\mathbf{1}$
e_3	$\mathbf{D}_2[\rho_x^2, \rho_y^2]$	$\mathbf{D}_2[\rho_x^2, \rho_y^2]$	$\mathbf{1}$
e_4	$\mathbf{D}_2[\rho_x^2, \rho_y^2]$	$\mathbf{D}_2[\rho_x^2, \rho_y^2]$	$\mathbf{1}$
e_5	$\mathbf{D}_2[\rho_x^2, \rho_y^2]$	$\mathbf{D}_2[\rho_x^2, \rho_y^2]$	$\mathbf{1}$
e_6	$\mathbf{D}_2[\rho_x^2, \rho_y^2]$	$\mathbf{D}_2[\rho_x^2, \rho_y^2]$	$\mathbf{1}$
e_7	$\mathbf{D}_2[\rho_x^2, \rho_y^2]$	$\mathbf{D}_2[\rho_x^2, \rho_y^2]$	$\mathbf{1}$
e_8	$\mathbf{D}_2[\rho_x^2, \rho_y^2]$	$\mathbf{D}_2[\rho_x^2, \rho_y^2]$	$\mathbf{1}$
c_1	$\mathbf{Z}_2[\rho_x^2]$	$\mathbf{D}_2[\rho_x^2, \rho_y^2]$	$\mathbf{Z}_2$
c_2	$\mathbf{Z}_2[\rho_x^2]$	$\mathbf{D}_2[\rho_x^2, \rho_y^2]$	$\mathbf{Z}_2$
c_3	$\mathbf{Z}_2[\rho_y^2]$	$\mathbf{D}_2[\rho_x^2, \rho_y^2]$	$\mathbf{Z}_2$
c_4	$\mathbf{Z}_2[\rho_y^2]$	$\mathbf{D}_2[\rho_x^2, \rho_y^2]$	$\mathbf{Z}_2$
c_5	$\mathbf{Z}_2[\rho_z^2]$	$\mathbf{D}_2[\rho_x^2, \rho_y^2]$	$\mathbf{Z}_2$
c_6	$\mathbf{Z}_2[\rho_z^2]$	$\mathbf{D}_2[\rho_x^2, \rho_y^2]$	$\mathbf{Z}_2$
c_{23}	$\mathbf{Z}_2[\rho_x^2]$	$\mathbf{D}_2[\rho_x^2, \rho_y^2]$	$\mathbf{Z}_2$
c_{24}	$\mathbf{Z}_2[\rho_x^2]$	$\mathbf{D}_2[\rho_x^2, \rho_y^2]$	$\mathbf{Z}_2$
c_{25}	$\mathbf{Z}_2[\rho_y^2]$	$\mathbf{D}_2[\rho_x^2, \rho_y^2]$	$\mathbf{Z}_2$
c_{26}	$\mathbf{Z}_2[\rho_y^2]$	$\mathbf{D}_2[\rho_x^2, \rho_y^2]$	$\mathbf{Z}_2$
c_{27}	$\mathbf{Z}_2[\rho_z^2]$	$\mathbf{D}_2[\rho_x^2, \rho_y^2]$	$\mathbf{Z}_2$
c_{28}	$\mathbf{Z}_2[\rho_z^2]$	$\mathbf{D}_2[\rho_x^2, \rho_y^2]$	$\mathbf{Z}_2$

Proof. The proof follows standard lines. □

Knots Relative to C. Given $C \in \mathscr{C}_{\mathbf{D}_2[\rho_x^2,\rho_y^2]}$ a knot relative to C gives an axis of symmetry for any $\mathbf{D}_2[\rho_x^2, \rho_y^2]$-equivariant flow on C. We know that each $C \in \mathscr{C}_{\mathbf{D}_2[\rho_x^2,\rho_y^2]}$ with $C \cong \mathbf{S}^1$, satisfies $S(C) \cong \mathbf{Z}_2$. Thus each $C \cong \mathbf{S}^1$ has two knots, which must be equilibria; it follows that the knots are just those equilibria that lie on C. The knots relative to C are given in Table 7.32.

Projected Skeleton

Here we compute the projected skeleton $\mathbb{X}^p_{\mathbf{D}_2[\rho_x^2,\rho_y^2]}$. The action of $\mathbf{D}_2[\rho_x^2, \rho_y^2]$ on $\mathscr{C}_{\mathbf{D}_2[\rho_x^2,\rho_y^2]}$ shows that there are twelve orbit representatives for the elements of $\mathscr{C}_{\mathbf{D}_2[\rho_x^2,\rho_y^2]}$ that are homeomorphic to $\mathbf{S}^1$; that is, the symmetry does not simplify the calculations in this respect. However, we have seen also that each such C has two knots; this implies that there is an axis of reflection symmetry. So these C's project into the orbit space as a line joining the two knots. More precisely, each $C \in \mathscr{C}_{\mathbf{D}_2[\rho_x^2,\rho_y^2]}$ homeomorphic to $\mathbf{S}^1$ joins the two knots in Table 7.32. Figure 7.1 illustrates the projected skeleton. This is the most complex example of a projected skeleton that we have yet seen. In fact, the $\mathbf{D}_2[\rho_x^2, \rho_y^2]$ symmetry makes very few simplifications of the skeleton, only providing the location of the knots. The dynamics supported by the (projected) skeleton are not only interesting, but also very complex. It is possible to arrange to for highly

Table 7.32: Knots relative to the orbit representatives of the $C \in \mathscr{C}_{\mathbf{D}_2[\rho_x^2,\rho_y^2]}$ for the SC lattice.

Element of $\mathscr{C}_{\mathbf{D}_2[\rho_x^2,\rho_y^2]}$	Knots
c_1	e_1, e_4
c_2	e_1, e_8
c_3	e_1, e_3
c_4	e_6, e_8
c_5	e_1, e_2
c_6	e_5, e_8
c_{23}	e_3, e_5
c_{24}	e_2, e_6
c_{25}	e_4, e_5
c_{26}	e_2, e_7
c_{27}	e_3, e_7
c_{28}	e_4, e_6

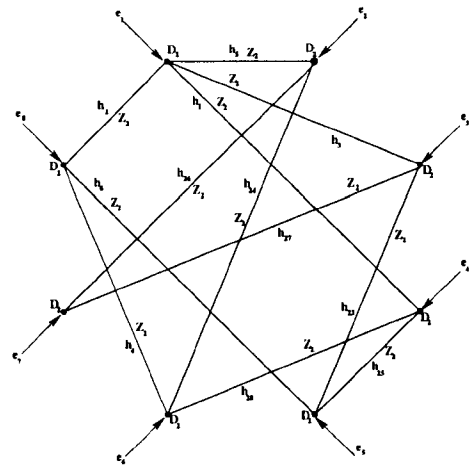

Figure 7.7: The projected skeleton $\mathbb{X}^p_{\mathbf{D}_2[\rho_x^2,\rho_y^2]}$. Here $h_1 = \{(\theta,0,0)|\theta \in (0,\pi)\}$, $h_2 = \{(\theta,\pi,\pi)|\theta \in (0,\pi)\}$ a, $h_3 = \{(0,\theta,0)|\theta \in (0,\pi)\}$, $h_4 = \{(\pi,\theta,\pi)|\theta \in (0,\pi)\}$, $h_5 = \{(0,0,\theta)|\theta \in (0,\pi)\}$, $h_6 = \{(\pi,\pi,\theta)|\theta \in (0,\pi)\}$, $h_{23} = \{(\theta,\pi,0)|\theta \in (0,\pi)\}$, $h_{24} = \{(\theta,0,\pi)|\theta \in (0,\pi)\}$, $h_{25} = \{(\pi,\theta,0)|\theta \in (0,\pi)\}$, $h_{26} = \{(0,\theta,\pi)|\theta \in (0,\pi)\}$, $h_{27} = \{(0,\pi,\theta)|\theta \in (0,\pi)\}$ and $h_{28} = \{(\pi,0,\theta)|\theta \in (0,\pi)\}$. None of the connection meet except at the equilibria.

elaborate cycling behaviour to occur, but we shall not take this avenue of investigation any further.

7.2.8 Example

In this subsection we present an example which illustrates how the structure of the planform is changed when forced symmetry breaking terms are considered. The example we consider is forced symmetry breaking to $\mathbb{O}$. Breaking the original Γ symmetry to $\mathbb{O}$ symmetry corresponds to a perturbation of the SC lattice in the three mutually perpendicular directions $\boldsymbol{\ell}_1$, $\boldsymbol{\ell}_2$ and $\boldsymbol{\ell}_3$. We define the perturbation by $\Psi(\mathbf{x}) = (\tanh^{-1} x, \tanh^{-1} y, \tanh^{-1} z)$. Using this perturbation

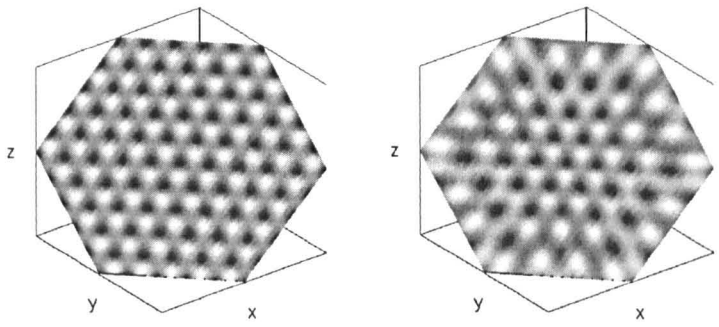

(a) (b)

Figure 7.8: Two density plots of the SC axial solution in a hexagonal cross section of the cube. (a) Planform when no forced symmetry breaking is present ($\varepsilon = 0$). (b) Planform when symmetry breaking terms are present.

the resulting eigenfunction is

$$\mathbf{u}(\mathbf{x}) = \sum_{j=1}^{3} z_j \exp\left(i\mathbf{K}_j \cdot (\Psi^{-1}(\mathbf{x}))\right). \tag{7.5}$$

To give a physical interpretation to this function we use the methods of Gomes [39] and consider a slice of the planform given by (7.5) in a plane $z = x + y$. Figure 7.8 presents two planforms. In (a) we show a density plot of the function (7.5) in a hexagonal cross section when $\Psi \equiv 1$, that is the unperturbed case $\varepsilon = 0$. In (b) we show how the planform in (a) is altered when $\varepsilon \neq 0$ but is still chosen small, in both cases $z_j = 1$ for all j. To render these figure we use a Matlab [67] program developed by Gomes [37], see Appendix C.

7.3 High Dimensional Representations

In this section we consider the high dimensional representations of the group Γ. These representations are much more complex than the previous six-dimensional case considered above. However, for a certain class of solutions the high dimensional problems may be identified with the six-dimensional problems and the results concerning the skeleton, symmetry properties and the projected skeleton are identical. Beyond these special solutions we do not consider these representation further.

Remark 7.24
The results of the six-dimensional case can be applied, in certain situations, to the higher dimensional representations. The symmetry group of all the bifurcation problems is $\Gamma = \mathbb{O} \oplus \mathbf{Z}_2^c \dotplus \mathbf{T}^3$. *Suppose there exist a bifurcating solution with* $\Sigma = \mathbb{O} \oplus \mathbf{Z}_2^c$ *symmetry. The group orbit* $X_0 = \Gamma x \cong \Gamma/\Sigma$ *is (topologically) unchanged from the six-dimensional case, and is still a 3-torus, but in coordinates the parametrisation of this torus is much more complex. The behaviour of the group orbit* Γ/Σ *under a* Δ*-equivariant perturbation is determined precisely by the action of* Δ *on* Γ/Σ. *This action is natural,* $(\delta, [\gamma]_\Sigma) \mapsto [\delta\gamma]_\Sigma$, *and is again unchanged from the six-dimensional representation. In particular, the action of the group* $\mathbb{O}$ *on* Γ/Σ *is the same, therefore all the results from the six-dimensional representation concerning the form of the skeleton, its symmetry properties, and the form of the projected skeleton are identical.*

We claim that the same is true for any solution with symmetry group isomorphic to Σ and isomorphic group orbit. Let Σ^a be the symmetry group of a solution, with $\Sigma^a \cong \Sigma$. Moreover, suppose $\Gamma/\Sigma \cong \Gamma/\Sigma^a$. Let Δ and Δ^a be subgroups of Σ and Σ^a, respectively. Suppose Δ^a satisfies $\Delta \cong \Delta^a$. By Lemma 4.43 there is a one-to-one correspondence between the results for the six-dimensional representation and the solutions in the higher dimensional representations with isomorphic isotropy subgroups.

7.3.1 Existence of Translation Free Axial Solutions

In this subsection we discuss the results of Dionne [19] concerning the existence of translation free axial solutions for the high dimensional representations of Γ. We recall that there are two twenty-four-dimensional representations and one forty-eight-dimensional representations. Dionne [19] proves the existence of 13 translation free axial solutions; they are given in Table 7.33. This table is taken from Dionne [19]. The superscripts on the subgroups are used to differentiate groups with different generators. The group $\widetilde{\mathbf{D}}_3 \oplus \mathbf{Z}_2^c$ occurs only in the twenty-four-dimensional type 1 representation when certain defining conditions on the representation are satisfied, see Dionne [19]. For each axial subgroup Σ isomorphic $\mathbb{O} \oplus \mathbf{Z}_2^c$, the group orbit is a 3-torus.

The construction of general equivariant mappings for the high dimensional representations is a task of incredible complexity and one we do not address. We content ourselves with the following classification theorem for those solutions in Table 7.33 with symmetry isomorphic to $\mathbb{O} \oplus \mathbf{Z}_2^c$.

Theorem 7.25
Let $\Gamma = \mathbb{O} \oplus \mathbf{Z}_2^c \dotplus \mathbf{T}^3$. Let $\Sigma \cong \mathbb{O} \oplus \mathbf{Z}_2^c$. Let Δ be isomorphic to one of the groups $\mathbb{O}$, $\mathbf{D}_4[\rho_x, \kappa_6]$, $\mathbb{T}$, $\mathbf{D}_3[\tau_1, \kappa_5]$, $\mathbf{D}_2[\rho_x^2, \kappa_6]$, $\mathbf{D}_2[\rho_x^2, \rho_y^2]$. Let Γ act on $\mathbb{C}^s$, where $s = 6$, 12 or 24 depending on the representation. Let $\mathbf{f} \in \vec{\mathcal{E}}_\Gamma$ be a Γ-equivariant bifurcation problem. Let $\mathbf{g} \in \vec{\mathcal{E}}_\Delta$ be a Δ-equivariant vector field that satisfies $\mathbf{g}(\mathbf{0}) = \mathbf{0}$. Then there exists branches of steady-state solutions to $\mathbf{f}(\mathbf{0}, \lambda) = \mathbf{0}$ bifurcating from the origin with isotropy Σ. The group orbit of these solutions is diffeomorphic to a standard 3-torus. Consider the perturbed system $\mathbf{F}(\mathbf{z}, \lambda, \varepsilon) = \mathbf{f}(\mathbf{z}, \lambda) + \varepsilon \mathbf{g}(\mathbf{z})$, where ε is real and small. Then for sufficiently small ε, X_0 persists to give a new $\mathbf{F}$-invariant manifold X_ε, which is Δ-equivariantly diffeomorphic to X_0. The behaviour of the vector field on X_0 is characterised by:

Table 7.33: Translation free axial subgroups of Γ.

Dimension	Axial Subgroup Σ
24 Type 1	$\mathbb{O} \oplus \mathbf{Z}_2^c$
	$\widetilde{\mathbb{O}} \oplus \mathbf{Z}_2^c$
	$\hat{\mathbb{O}}$
	$\widetilde{\mathbb{T}} \oplus \mathbf{Z}_2^c$
	$\widetilde{\mathbf{D}}_3 \oplus \mathbf{Z}_2^c$
24 Type 2	$\mathbb{O} \oplus \mathbf{Z}_2^c$
	$\widetilde{\mathbb{O}}^a \oplus \mathbf{Z}_2^c$
	$\hat{\mathbb{O}}$
	$\widetilde{\mathbb{T}}^a \oplus \mathbf{Z}_2^c$
48	$\mathbb{O} \oplus \mathbf{Z}_2^c$
	$\widetilde{\mathbb{O}} \oplus \mathbf{Z}_2^c$
	$\widetilde{\mathbb{O}}^a \oplus \mathbf{Z}_2^c$
	$\widetilde{\mathbb{O}}^b \oplus \mathbf{Z}_2^c$

1. *When* $\Delta \cong \mathbb{O}$ *there are four (group orbits of) equilibria given by:* e_1, e_2, e_5 *and* e_8, *together with nine (group orbits of) heteroclinic connections given by:* h_1, h_2, h_7, h_8, h_{19} *and* h_{23}. *The arrangement of these equilibria and connections is in Figure 7.1.*

2. *When* $\Delta \cong \mathbf{D}_4[\rho_x, \kappa_6]$ *there are six (group orbits of) equilibria given by:* e_1, e_2, e_4, e_5, e_7 *and* e_8, *together with six (group orbits of) heteroclinic connections given by:* h_1, h_2, h_3, h_4, h_{15}, h_{18}, h_{23}, h_{25} *and* h_{26}. *The arrangement of these equilibria and connections is in Figure 7.3.*

3. *When* $\Delta \cong \mathbb{T}$ *there are four (group orbits of) equilibria given by:* e_1, e_4, e_5 *and* e_8, *together with five (group orbits of) heteroclinic connections given by:* h_1, h_2, h_{19}, h_{23} *and* h_{24}. *The arrangement of these equilibria and connections is in Figure 7.4.*

4. *When* $\Delta \cong \mathbf{D}_3[\tau_1, \kappa_5]$ *there are two equilibria given by:* e_1 *and* e_8, *together with three (group orbits of) heteroclinic connections given by:* c_9, c_{10} *and* h_{19}. *The arrangement of these equilibria and connections is in Figure 7.5. There exist perturbations that give two heteroclinic cycles, the first between the equilibrium* e_1 *and the second between the equilibrium* e_8.

5. *When* $\Delta \cong \mathbf{D}_2[\rho_x^2, \kappa_6]$ *there are four equilibria given by:* e_1, e_4, e_7 *and* e_8, *together with six (group orbits of) heteroclinic connections given by:* h_1, h_2, h_{15}, h_{16}, h_{17}, h_{18} *and a periodic orbit given by* c_{23}. *The arrangement of these equilibria, connections and periodic orbit is in Figure 7.6. There exist perturbations that give periodic orbits along* c_{23}.

6. *When* $\Delta \cong \mathbf{D}_2[\rho_x^2, \rho_y^2]$ *there are eight equilibria given by:* e_1 *to* e_8, *together with twelve (group orbits of) heteroclinic connections given by:* h_1, h_2, h_3, h_4, h_5, h_6, h_{23}, h_{24}, h_{25}, h_{26}, h_{27} *and* h_{28}. *The arrangement of these equilibria and connections is in Figure 7.7.*

This classification theorem is as far as we can go; because of the complexities of the invariant theory we cannot make any further general statements.

7.3.2 Examples

Here we present examples of how the planforms associated with the solution with symmetry $\mathbb{O} \oplus \mathbf{Z}_2^c$ are changed when the symmetry is broken. Breaking of the original Γ symmetry of the system to $\mathbb{O}$ symmetry corresponds to a perturbation of the SC lattice in the three mutually perpendicular directions $\boldsymbol{\ell}_1$, $\boldsymbol{\ell}_2$ and $\boldsymbol{\ell}_3$. We define the perturbation by $\Psi(\mathbf{x}) = (\tanh^{-1} x, \tanh^{-1} y, \tanh^{-1} z)$; this was the same perturbation we used when presenting an example in the six-dimensional representation. Using this perturbation, the resulting eigenfunction is

$$\mathbf{u}(\mathbf{x}) = \sum_{j=1}^{s} z_j \exp\left(i\mathbf{K}_j \cdot (\Psi^{-1}(\mathbf{x}))\right), \tag{7.6}$$

where $s = 12$ or 24. As in the six-dimensional representation, we use the methods of Gomes [39] and consider a slice of the planform given by (7.6) in a plane $z = x + y$.

Twenty-four-Dimensional Type 1 Representation

Figure 7.9 presents an example of two planforms. In (a) we show a density plot of the function (7.6) in a hexagonal cross section of the cube of periodicity of the planform, when $\Psi \equiv 1$; that is, the unperturbed case $\varepsilon = 0$. This is the first time this planform has been rendered and it shows a highly developed structure. In (b) we show how the planform in (a) is altered when $\varepsilon \neq 0$ but is still chosen small; in both cases $z_j = 1$ for all j.

The planforms in Figure 7.9 show a dramatic difference between the unperturbed and perturbed cases: the pattern becomes distorted. A number of points are worth mentioning. We have rendered only one of the four equilibria on the skeleton, and have not indicated what the planforms look like along a connection between the equilibria. More importantly, we have

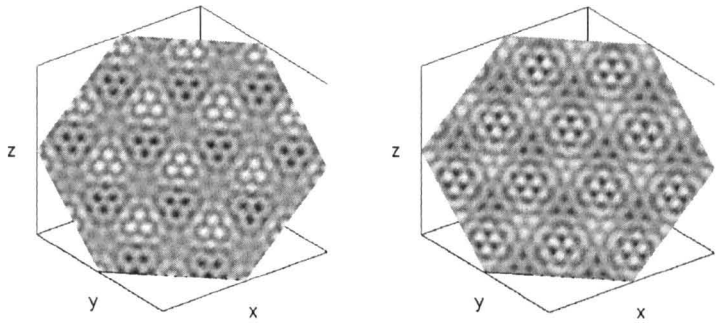

(a) (b)

Figure 7.9: Two density plots of the twenty-four-dimensional type 1 axial solution with $\mathbb{O} \oplus \mathbf{Z}_2^c$ symmetry, in a hexagonal cross section of the cube. (a) Planform when no forced symmetry breaking is present ($\varepsilon = 0$). (b) Planform when symmetry breaking terms are present.

plotted the planform as if it were on the manifold X_0, rather than the correct X_ε. To give a more realistic interpretation to our results, we should plot the equilibria on the manifold X_ε. On X_ε the equilibrium e_1 has the form $e_1^\varepsilon = e_1 + \varepsilon z_j$, where z_j is an unknown complex number. However, since z_j is unknown it is very difficult to say how the equilibria will behave. For this reason we shall not attempt to give a more precise rendering for the planform, leaving such cases to the more experimentally relevant cases.

Twenty-four-Dimensional Type 2 Representation

Figure 7.10 presents an example of two planforms. In (a) we show a density plot of the function (7.6) in a hexagonal cross section of the cube of periodicity of the planform, when $\Psi \equiv 1$; that is, the unperturbed case $\varepsilon = 0$. This is the first time this planform has been rendered and it shows very intricate periodicity. In (b) we show how the planform in (a) is altered when $\varepsilon \neq 0$ but is still chosen small; in both cases $z_j = 1$ for all j.

It is possible to break the symmetry in numerous other ways. The comments we have made previously concerning the six and twenty-four-dimensional type 1 representations still hold for this example.

Forty-eight-Dimensional Representation

Figure 7.11 presents an example of two planforms. In (a) we show a density plot of the function (7.6) in a hexagonal cross section of the cube, when $\phi \equiv 1$; that is, the unperturbed case $\varepsilon = 0$. This is the first time this planform has been rendered and it shows a highly elaborate structure. In (b) we show how the planform in (a) is altered when $\varepsilon \neq 0$ but is still chosen small; in both cases $z_j = 1$ for all j.

7.4 Conclusion

We have seen that the SC lattice is capable of supporting dynamics much richer than any of the two-dimensional lattices allowed; heteroclinic cycles and more generally networks are possible. In this chapter we have not considered the class II and III subgroups of $\mathbb{O} \oplus \mathbf{Z}_2^c$, but we make some comments on this issue. Firstly, we find it difficult to think of a situation where a Γ-equivariant system of equation could have its symmetry broken to a class III subgroup, so we

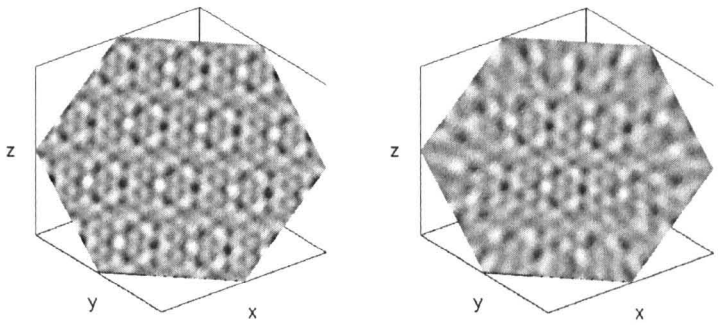

(a) (b)

Figure 7.10: Two density plots of the twenty-four-dimensional type 2 axial solution with $\mathbb{O}\oplus\mathbf{Z}_2^c$ in a hexagonal cross section of the cube. (a) Planform when no forced symmetry breaking is present ($\varepsilon = 0$). (b) Planform when symmetry breaking terms are present.

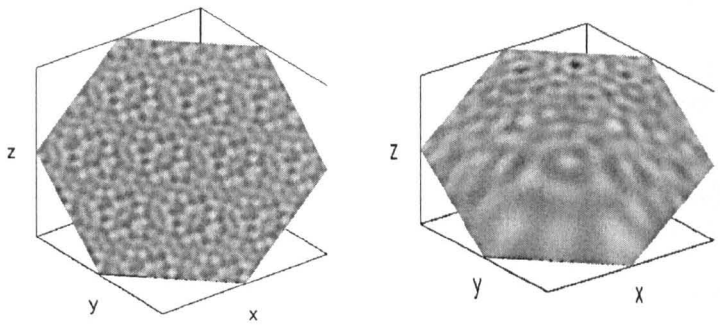

(a) (b)

Figure 7.11: Two density plots of the forty-eight-dimensional representation axial solution in a hexagonal cross section of the cube. (a) Planform when no forced symmetry breaking is present ($\varepsilon = 0$). (b) Planform when symmetry breaking terms are present.

do not consider this occurrence. Secondly, all class II subgroups have the form $H \oplus \mathbf{Z}_2^c$ where H is a class I subgroup. The action of $\mathbf{Z}_2^c$ on X_0 is given by $(\theta_1, \theta_2, \theta_3) \mapsto -(\theta_1, \theta_2, \theta_3)$. So a point $(\theta_1, \theta_2, \theta_3)$ is fixed by a group containing $\mathbf{Z}_2^c$ if and only if $\theta_j = 0$ or π. So the forced symmetry breaking of a Γ-equivariant system of equations where the perturbation term is equivariant with respect to a class II subgroup is effectively the same as the study we performed for the class I subgroups, except that the symmetry of the equilibria is different—they have an additional $\mathbf{Z}_2^c$ component.

Of major importance, and the main result of the chapter, is Theorem 7.25. This theorem gives a partial classification of the behaviour that we may expect from a solution with $\mathbb{O} \oplus \mathbf{Z}_2^c$ symmetry to a Γ-equivariant bifurcation problem when symmetry breaking effects are taken into account.

Chapter 8

Forced Symmetry Breaking on the Faced Centred Cubic Lattice

8.1 Introduction

The face centred cubic (FCC) lattice, like the SC lattice, was the subject of a group theoretical analysis by Dionne [19], which classifies all the translation free axial solutions supported by this lattice. This work was extended by Callahan and Knobloch [8] who studied the lowest (eight) dimensional bifurcation problem, providing stability criteria. Taking motivation from Turing patterns, this work was applied to models of reaction-diffusion systems [9]. In this chapter we perform a similar analysis to Chapter 7, extending the previous steady-state results further, partially classifying the types of behaviour exhibited by the FCC solution when symmetry-breaking terms are taken into account.

Let us recall the methods of Section 1.6 applied to the FCC lattice. Define three linearly independent vectors $\boldsymbol{\ell}_1 = (\frac{1}{2}, \frac{1}{2}, 0)$, $\boldsymbol{\ell}_2 = (-\frac{1}{2}, \frac{1}{2}, 0)$ and $\boldsymbol{\ell}_3 = (0, \frac{1}{2}, \frac{1}{2})$. The FCC lattice is defined by

$$\mathcal{L}_{FCC} = \{n_1\boldsymbol{\ell}_1 + n_2\boldsymbol{\ell}_2 + n_3\boldsymbol{\ell}_3 \big| n_1, n_2, n_3 \in \mathbb{Z}\}.$$

The symmetry group of $\mathcal{L}_{FCC}$ is $\Gamma = \mathbb{O} \oplus \mathbf{Z}_2^c \dot{+} \mathbf{T}^3$, where $\mathbb{O}$ is the orientation preserving symmetries of the cube, $\mathbf{Z}_2^c$ is inversion through the origin, and $\mathbf{T}^3$ is the translational symmetries of the lattice $\mathbb{R}^3/\mathcal{L}_{FCC}$. We seek functions $\mathbf{u} \in \mathcal{X}$ that are triply periodic with respect to the FCC lattice, and so are members of $\mathcal{X}_{\mathcal{L}_{FCC}}$. Define $\mathbf{k}_1 = (1, 1, -1)$, $\mathbf{k}_2 = (-1, 1, -1)$ and $\mathbf{k}_3 = (0, 0, 2)$. Then the dual lattice to $\mathcal{L}_{FCC}$ is

$$\mathcal{L}^*_{FCC} = \{n_1\mathbf{k}_1 + n_2\mathbf{k}_2 + n_3\mathbf{k}_3 \big| n_1, n_2, n_3 \in \mathbb{Z}\}.$$

We may write a function $\mathbf{u} \in \mathcal{X}_{\mathcal{L}_{FCC}}$ in the form

$$\mathbf{u}(\mathbf{x}, t) = \sum_{j=1}^{s} z_j e^{2\pi i \mathbf{K}_j \cdot \mathbf{x}} \mathbf{u}_j + c.c., \tag{8.1}$$

where $z_j \in \mathbb{C}$ and $\mathbf{K}_j$ are the wave vectors of the dual lattice which lie on the critical sphere of radius k_c. Dionne [19] shows that $s = 4$, 12 or 48. The domain of the bifurcation problem is then identified with $\mathbb{C}^s$. The representation of Γ on $\mathbb{C}^s$ is determined by its action on the complex coordinates z_j in (8.1). In addition we require, in line with Dionne [19], that our representations are translation free. Our problem is now in standard form, so we have reduce the situation to the study of the ODE

$$\dot{\mathbf{z}} = \mathbf{f}(\mathbf{z}, \lambda), \tag{8.2}$$

where $\mathbf{f} : \mathbb{C}^s \times \mathbb{R} \to \mathbb{C}^s$ is Γ-equivariant. Dionne [19] states that there are (up to) 11 different axial solutions[1]. In the eight-dimensional representation there are two solutions with symmetry $\mathbb{O} \oplus \mathbf{Z}_2^c$ and $\widetilde{\mathbb{O}} \oplus \mathbf{Z}_2^c$, respectively. The group orbit of these solutions is a 3-torus, which we denote by X_0. We study the behaviour of X_0 when symmetry-breaking terms equivariant with respect to certain subgroups are added to (8.2). We employ the methods of Chapter 2 to examine this problem systematically. In particular, for each problem we seek admissible perturbations, persistence of equilibria, the existence of heteroclinic cycles and networks and other more general dynamics.

This chapter is organised as follows. In Section 8.2 we consider the eight-dimensional representation of the group Γ. This is the representation studied by Callahan and Knobloch [8, 9]. The process we adopt is by now familiar: we construct the skeleton, study its symmetry properties, and construct the projected skeleton. Using the projected skeleton we make general comments about the behaviour of flows on the skeleton; identifying possible heteroclinic cycles and networks and more general dynamic properties. Following this section we apply the results in Section 8.3 to the twenty-four and forty-eight-dimensional representations of Γ, studying a selection of the axial solutions proved to exist by Dionne [19]. Finally, in Section 8.4, we make some general observation and comments.

8.2 Eight-Dimensional Representation

In this section we consider the eight-dimensional representation of the group Γ. This representation occurs when the wavelength of instabilities coincides with the periodicity of the functions in $\mathcal{X}_{\mathcal{L}_{FCC}}$. In this case the wave vectors of the dual lattice that are of the critical radius k_c are, by [19]

$$\begin{aligned} \mathbf{K}_1 &= (1,1,1), \\ \mathbf{K}_2 &= (1,-1,1), \\ \mathbf{K}_3 &= (1,-1,-1), \\ \mathbf{K}_4 &= (1,1,-1). \end{aligned}$$

The representation of Γ on $\mathbb{C}^4$ corresponds to the following action. Choose coordinates $\mathbf{z} = (z_1, z_2, z_3, z_4)$ on $\mathbb{C}^4$. The action of Γ is generated by

$$\begin{aligned} \rho_x(\mathbf{z}) &= (z_4, z_1, z_2, z_3), \\ \rho_y(\mathbf{z}) &= (\overline{z_3}, \overline{z_4}, z_2, z_1), \\ c(\mathbf{z}) &= (\overline{z_1}, \overline{z_2}, \overline{z_3}, \overline{z_4}), \\ \theta(\mathbf{z}) &= (e^{-\mathrm{i}(\theta_1+\theta_3)} z_1, e^{\mathrm{i}\theta_2} z_2, e^{\mathrm{i}(\theta_2+\theta_3)} z_3, e^{-\mathrm{i}\theta_1} z_4). \end{aligned}$$

Here ρ_x and ρ_y are the generators of $\mathbb{O}$, c generates the group $\mathbf{Z}_2^c$, and $\theta = (\theta_1, \theta_2, \theta_3) \in \mathbf{T}^3$. Consider the Γ-equivariant system of differential equations

$$\dot{\mathbf{z}} = \mathbf{f}(\mathbf{z}, \lambda), \tag{8.3}$$

where $\mathbf{f} : \mathbb{C}^4 \times \mathbb{R} \to \mathbb{C}^4$ is Γ-equivariant. In this section we investigate the behaviour of the group orbit of solutions to (8.3) with $\mathbb{O} \oplus \mathbf{Z}_2^c$ or $\widetilde{\mathbb{O}} \oplus \mathbf{Z}_2^c$ symmetry under forced symmetry breaking to the subgroups (isomorphic to) $\mathbb{O}$, $\mathbb{T}$, $\mathbf{D}_4[\rho_x, \kappa_6]$, $\mathbf{D}_3[\tau_1, \kappa_5]$, and two $\mathbf{D}_2$ subgroups $\mathbf{D}_2[\rho_x^2, \kappa_6]$ and $\mathbf{D}_2[\rho_x^2, \rho_y^2]$.

This section is organised as follows. We begin by summarising the results of Callahan and Knobloch [8] which show that there exist two group orbits of translation free axial solutions with $\mathbb{O} \oplus \mathbf{Z}_2^c$ and $\widetilde{\mathbb{O}} \oplus \mathbf{Z}_2^c$ symmetry. We then consider forced symmetry breaking of these solutions; this

[1] The twenty-four-dimensional representation can have between two and five translation free axial solutions depending on the defining conditions of the representation. This will not affect our work, since we shall consider only the two solutions that are always guaranteed to exist.

involves the computation of the skeleton, its symmetry properties, and the projected skeleton. Having completed the analysis of forced symmetry breaking to the group $\mathbb{O}$, we use these results to study forced symmetry breaking for the groups $\mathbb{T}$, $\mathbf{D}_4[\rho_x, \kappa_6]$, $\mathbf{D}_3[\tau_1, \kappa_5]$, $\mathbf{D}_2[\rho_x^2, \kappa_6]$, and $\mathbf{D}_2[\rho_x^2, \rho_y^2]$. We finish with an example.

8.2.1 Existence of Translation Free Axial Solution

The action of Γ on $\mathbb{C}^4$ has fifteen conjugacy classes of isotropy subgroups [8]. Of these subgroups, only four are axial, and furthermore there are only two conjugacy classes of translation free axial subgroup given by $\mathbb{O} \oplus \mathbf{Z}_2^c$ and $\widetilde{\mathbb{O}} \oplus \mathbf{Z}_2^c$ [19]. We focus exclusively on these two translation free axial subgroups.

By [8] a general Γ-equivariant vector field has the form (first component only)

$$f_1(\mathbf{z}, \lambda) = (h_1 + u_1 h_3 + u_1^2 h_5 + u_1^3 h_7) z_1 + \overline{z_2} z_3 \overline{z_4} (p_3 + u_1 p_5 + u_1^2 p_7 + u_1^3 p_9), \tag{8.4}$$

where h_j and p_j are arbitrary real-valued function of the four Γ-invariants

$$\begin{aligned} \sigma_1 &= u_1 + u_2 + u_3 + u_4, \\ \sigma_2 &= u_1 u_2 + u_1 u_3 + u_1 u_4 + u_2 u_3 + + u_2 u_4 + u_3 u_4, \\ \sigma_3 &= u_1 u_2 u_3 + u_1 u_2 u_4 + u_1 u_3 u_4 + u_2 u_3 u_4, \\ q &= z_1 z_2 z_3 z_4 + \overline{z_1 z_2 z_3 z_4}, \end{aligned}$$

and $u_j = z_j \overline{z}_j$. Callahan and Knobloch [8] show that if certain nondegeneracy conditions hold on the coefficients of the Taylor expansion of (8.4) up to third order, then the bifurcation problem is fully determined by the third-order truncation of (8.4). Indeed, they compute a normal form and classify the bifurcation diagrams. They show that the solutions with $\mathbb{O} \oplus \mathbf{Z}_2^c$ and $\widetilde{\mathbb{O}} \oplus \mathbf{Z}_2^c$ symmetry can be stable at bifurcation, but not at the same time. Summarising, we have:

Theorem 8.1
Let $f : \mathbb{C}^4 \times \mathbb{R} \to \mathbb{C}^4$ be a Γ-equivariant bifurcation problem. Then generically there exist branches of steady-state solutions bifurcating from the origin with isotropy $\mathbb{O} \oplus \mathbf{Z}_2^c$ and $\widetilde{\mathbb{O}} \oplus \mathbf{Z}_2^c$. Furthermore, if certain nondegeneracy conditions hold, the bifurcation problem is fully determined by the third order truncation of the vector field; in particular, the solutions can be stable at bifurcation, but not simultaneously.

Proof. See Callahan and Knobloch [8]. □

The group orbit of solutions with $\mathbb{O} \oplus \mathbf{Z}_2^c$ or $\widetilde{\mathbb{O}} \oplus \mathbf{Z}_2^c$ symmetry are 3-tori, denoted throughout by X_0. The manifold X_0 is normally hyperbolic. We begin by studying the group orbit of solutions with $\mathbb{O} \oplus \mathbf{Z}_2^c$ symmetry. By an argument identical to Remark 7.24, the $\widetilde{\mathbb{O}} \oplus \mathbf{Z}_2^c$ case can be reduced to the $\mathbb{O} \oplus \mathbf{Z}_2^c$ case and so does not need to be studied separately.

8.2.2 Forced Symmetry Breaking to $\mathbb{O}$

In this subsection we study the behaviour of the group orbit of bifurcating solutions given by Theorem 8.1 when symmetry-breaking terms with $\mathbb{O}$ symmetry are added to the vector field (8.4). More precisely, let $\mathbf{g} : \mathbb{C}^4 \times \mathbb{R} \to \mathbb{C}^4$ be $\mathbb{O}$-equivariant vector field that satisfies $\mathbf{g}(\mathbf{0}) = \mathbf{0}$. Let ε be real and small. Consider the perturbed vector field $\mathbf{F} : \mathbb{C}^4 \times \mathbb{R}^2 \to \mathbb{C}^4$ defined by

$$\mathbf{F}(\mathbf{z}, \lambda, \varepsilon) = \mathbf{f}(\mathbf{z}, \lambda) + \varepsilon \mathbf{g}(\mathbf{z}).$$

Normal hyperbolicity of X_0 guarantees, by the Equivariant Persistence Theorem, the existence of a manifold X_ε diffeomorphic to X_0 and invariant under the dynamics of $\mathbf{F}$. We can consider the behaviour of the $\mathbb{O}$-equivariant vector field on X_ε by considering its behaviour on X_0.

The action of the group $\mathbb{O}$ on the space $\mathbb{C}^4$ is given in Table 8.1. This action is computed in the standard way. We compute the action of the elements of $\mathbb{O}$, as given in Appendix B, on the vectors $\mathbf{K}_j$, $j = 1, \ldots, 4$ which lie on the critical sphere. Such a computation is straightforward.

Table 8.1: Action of $\mathbb{O}$ on $\mathbb{C}^4$ for the FCC lattice.

Element of $\mathbb{O}$	Action on $\mathbb{C}^4$	Element of $\mathbb{O}$	Action on $\mathbb{C}^4$
ρ_x	(z_4, z_1, z_2, z_3)	τ_2^2	$(\overline{z_4}, \overline{z_1}, z_3, z_2)$
ρ_x^2	(z_3, z_4, z_1, z_2)	τ_3	$(\overline{z_2}, \overline{z_3}, z_1, z_4)$
ρ_x^3	(z_2, z_3, z_4, z_1)	τ_3^2	$(z_3, \overline{z_1}, \overline{z_2}, z_4)$
ρ_y	$(\overline{z_3}, \overline{z_4}, z_2, z_1)$	τ_4	$(\overline{z_4}, z_2, z_1, \overline{z_3})$
ρ_y^2	$(\overline{z_2}, \overline{z_1}, \overline{z_4}, \overline{z_3})$	τ_4^2	$(z_3, z_2, \overline{z_4}, \overline{z_1})$
ρ_y^3	$(z_4, z_3, \overline{z_1}, \overline{z_2})$	κ_1	$(z_4, \overline{z_2}, \overline{z_3}, z_1)$
ρ_z	$(z_2, \overline{z_4}, \overline{z_1}, z_3)$	κ_2	$(\overline{z_1}, z_3, z_2, \overline{z_4})$
ρ_z^2	$(\overline{z_4}, \overline{z_3}, \overline{z_2}, \overline{z_1})$	κ_3	$(z_2, z_1, \overline{z_3}, \overline{z_4})$
ρ_z^3	$(\overline{z_3}, z_1, z_4, \overline{z_2})$	κ_4	$(\overline{z_3}, \overline{z_2}, \overline{z_1}, \overline{z_4})$
τ_1	$(z_1, z_4, \overline{z_2}, \overline{z_3})$	κ_5	$(\overline{z_1}, \overline{z_2}, z_4, z_3)$
τ_1^2	$(z_1, \overline{z_3}, \overline{z_4}, z_2)$	κ_6	$(\overline{z_1}, \overline{z_4}, \overline{z_3}, \overline{z_2})$
τ_2	$(\overline{z_2}, z_4, z_3, \overline{z_1})$		

Calculation of the Skeleton

Here we calculate the skeleton of X_0 under the action of $\mathbb{O}$. To begin we calculate the set $\mathscr{C}_{\mathbb{O}}$, for which we recall from Appendix B that there are 30 subgroups of $\mathbb{O}$. We use the standard coordinates $(\theta_1, \theta_2, \theta_3)$ on the 3-torus X_0, where θ_1, θ_2 and $\theta_3 \in [0, 2\pi)$. To simplify notation we make the following definitions, in addition to those already given in Definition 7.3 for the SC lattice.

Definition 8.2
Define the following subsets of X_0.

$$
\begin{aligned}
e_9 &= \{(3\pi/2, \pi/2, \pi)\}, & e_{10} &= \{(\pi/2, 3\pi/2, \pi)\},\\
c_{29} &= \{(\theta, -\theta, 2\theta) \,|\, \theta \in [0, 2\pi)\}, & c_{30} &= \{(\theta, -\theta, -2\theta) \,|\, \theta \in [0, 2\pi)\},\\
c_{31} &= \{(3\theta, \theta, -2\theta) \,|\, \theta \in [0, 2\pi)\}, & c_{32} &= \{(\theta, 3\theta, -2\theta) \,|\, \theta \in [0, 2\pi)\},\\
c_{33} &= \{(\theta, \theta, -2\theta) \,|\, \theta \in [0, 2\pi)\}, & c_{34} &= \{(\theta, \theta, \pi - \theta) \,|\, \theta \in [0, 2\pi)\},\\
c_{35} &= \{(\theta, \pi, \pi - \theta) \,|\, \theta \in [0, 2\pi)\}, & c_{36} &= \{(\pi, \theta, \pi - \theta) \,|\, \theta \in [0, 2\pi)\},\\
c_{37} &= \{(\theta + \pi, \theta, \pi) \,|\, \theta \in [0, 2\pi)\}, & c_{38} &= \{(\theta + \pi, \theta, -2\theta) \,|\, \theta \in [0, 2\pi)\}.
\end{aligned}
$$

We may now state the following fundamental proposition.

Proposition 8.3
Let $\mathbb{O}$ act on X_0 with the action induced from Table 8.1. Then

$$
\begin{aligned}
\mathscr{C}_{\mathbb{O}} = \{&e_1, e_2, e_3, e_4, e_5, e_6, e_7, e_8, e_9, e_{10}, c_1, c_3, c_5, c_6, c_7, c_9, c_{10}, c_{13}, c_{17}, c_{21}, c_{23}, c_{25}, c_{29},\\
&c_{30}, c_{31}, c_{32}, c_{33}, c_{34}, c_{35}, c_{36}, c_{37}, c_{38}\}.
\end{aligned}
$$

We divide the proof of this proposition into a series of lemmas; each of these is useful for later work on the other subgroups of $\mathbb{O}$. We recall the trivial fact that $\mathrm{Fix}(\Sigma) = \{(x, x, x, x) \,|\, x \in \mathbb{R}\}$, and in each case use the method of Lemma 2.8 to compute the fixed-point submanifolds.

Lemma 8.4
Let the groups $\mathbb{O}$, $\mathbb{T}$, $\mathbf{D}_4[\rho_x, \kappa_6]$, $\mathbf{D}_4[\rho_y, \kappa_5]$, $\mathbf{D}_4[\rho_z, \kappa_1]$, $\mathbf{D}_3[\tau_1, \kappa_5]$, $\mathbf{D}_3[\tau_4, \kappa_5]$, $\mathbf{D}_3[\tau_3, \kappa_3]$, and $\mathbf{D}_3[\tau_2, \kappa_1]$ act on X_0 with the action induced from the action in Table 8.1. Then the fixed-point submanifolds in X_0 of each of these groups is $e_1 \cup e_5$.

Proof. Let Δ be any of the groups $\mathbb{O}$, $\mathbf{D}_4[\rho_x, \kappa_6]$, $\mathbf{D}_4[\rho_y, \kappa_5]$ or $\mathbf{D}_4[\rho_z, \kappa_1]$. We begin by showing that $\mathrm{Fix}(\Delta) = \mathrm{Fix}(\mathbb{O})$. To finish the proof in these cases we need consider only the group $\mathbb{O}$. The case of $\Delta = \mathbb{O}$ is trivial.

Case 1: $\mathbf{D}_4[\rho_x, \kappa_6]$. Since ρ_x, ρ_x^2, and $\rho_x^3 \in \mathbf{D}_4[\rho_x, \kappa_6]$, it follows that $\mathrm{Fix}(\mathbf{D}_4[\rho_x, \kappa_6]) \subseteq \{(z, z, z, z) | z \in \mathbb{C}\}$. Furthermore, $\kappa_6 \in \mathbf{D}_4[\rho_x, \kappa_6]$ implies $\mathrm{Fix}(\mathbf{D}_4[\rho_x, \kappa_6]) = \{(x, x, x, x) | x \in \mathbb{C}\}$.

Case 2: $\mathbf{D}_4[\rho_y, \kappa_5]$. Since ρ_y, ρ_y^2, and $\rho_y^3 \in \mathbf{D}_4[\rho_y, \kappa_5]$, $\mathrm{Fix}(\mathbf{D}_4[\rho_y, \kappa_5]) \subseteq \{(z, \overline{z}, \overline{z}, z) | z \in \mathbb{C}\}$. Furthermore, the condition $\kappa_5 \in \mathbf{D}_4[\rho_y, \kappa_5]$ implies $\mathrm{Fix}(\mathbf{D}_4[\rho_y, \kappa_5]) = \{(x, x, x, x) | x \in \mathbb{C}\}$.

Case 3: $\mathbf{D}_4[\rho_z, \kappa_1]$. Since ρ_z, ρ_z^2, and $\rho_z^3 \in \mathbf{D}_4[\rho_z, \kappa_1]$, $\mathrm{Fix}(\mathbf{D}_4[\rho_z, \kappa_1]) \subseteq \{(z, z, \overline{z}, \overline{z}) | z \in \mathbb{C}\}$. Since $\kappa_1 \in \mathbf{D}_4[\rho_z, \kappa_1]$, we have $\mathrm{Fix}(\mathbf{D}_4[\rho_z, \kappa_1]) = \{(x, x, x, x) | x \in \mathbb{C}\}$.

Observe that

$$\mathrm{Fix}_{X_0}(\mathbb{O}) = N_\Gamma(\mathbb{O}, \mathbb{O} \oplus \mathbf{Z}_2^c)/\mathbb{O} \oplus \mathbf{Z}_2^c,$$

where $N_\Gamma(\mathbb{O}, \mathbb{O} \oplus \mathbf{Z}_2^c) = \{\gamma \in \Gamma | \gamma \mathrm{Fix}(\mathbb{O} \oplus \mathbf{Z}_2^c) \subseteq \mathrm{Fix}(\mathbb{O})\}$. Now $\gamma \in N_\Gamma(\mathbb{O}, \mathbb{O} \oplus \mathbf{Z}_2^c)$ if and only if $\gamma \in \mathbb{O} \oplus \mathbf{Z}_2^c$ or $\theta_1 + \theta_3 = -\theta_2 = -\theta_2 - \theta_3 = \theta_1 = 0$ or π mod 2π. Thus $\theta_1 = \theta_2 = 0$ or π and $\theta_3 = 0$. This gives $\mathrm{Fix}_{X_0}(\mathbb{O}) = e_1 \cup e_5$. This completes the proof for the groups $\mathbb{O}$, $\mathbf{D}_4[\rho_x, \kappa_6]$, $\mathbf{D}_4[\rho_y, \kappa_5]$, and $\mathbf{D}_4[\rho_z, \kappa_1]$.

Case 4: $\mathbb{T}$. Clearly $\mathrm{Fix}(\mathbb{T}) = \{(z, \overline{z}, z, \overline{z}) | z \in \mathbb{C}\}$. Now $\gamma \in N_\Gamma(\mathbb{T}, \mathbb{O} \oplus \mathbf{Z}_2^c)$ if and only if $-(\theta_1 + \theta_3) = -\theta_2 = \theta_2 + \theta_3 = \theta_1$. The only solutions are e_1 and e_5.

Case 5: $\mathbf{D}_3[\tau_1, \kappa_5]$. Since $\tau_1 \in \mathbf{D}_3[\tau_1, \kappa_5]$ it follows that $\mathrm{Fix}(\mathbf{D}_3[\tau_1, \kappa_5]) \subset \{(z, z_2, \overline{z}_2, z_2) | z, z_2 \in \mathbb{C}\}$. Furthermore, $\kappa_5 \in \mathbf{D}_3[\tau_1, \kappa_5]$, implies $z = \overline{z}$ and $z_2 = \overline{z_2}$, so $\mathrm{Fix}(\mathbf{D}_3[\tau_1, \kappa_5]) = \{(x, y, y, y) | x, y \in \mathbb{R}\}$. We must now compute t $N_\Gamma(\mathbf{D}_3[\tau_1, \kappa_5], \mathbb{O} \oplus \mathbf{Z}_2^c)$. Now $\gamma \in N_\Gamma(\mathbf{D}_3[\tau_1, \kappa_5], \mathbb{O} \oplus \mathbf{Z}_2^c)$ if and only if $\theta_1 + \theta_3 = 0$ or π mod 2π, $\theta_2 = \theta_2 + \theta_3 = -\theta_1 = 0$ or π mod 2π. Therefore, $\theta_3 = 0$ and $\theta_1 = \theta_2 = 0$ or π, so $\mathrm{Fix}_{X_0}(\mathbf{D}_3[\tau_1, \kappa_5]) = e_1 \cup e_5$.

Case 6: $\mathbf{D}_3[\tau_2, \kappa_1]$. Since $\tau_2 \in \mathbf{D}_3[\tau_2, \kappa_1]$, it follows that $\mathrm{Fix}(\mathbf{D}_3[\tau_2, \kappa_1])$ is contained in $\{(z, \overline{z}, z_3, \overline{z}) | z, z_3 \in \mathbb{C}\}$. Furthermore, $\kappa_1 \in \mathbf{D}_3[\tau_2, \kappa_1]$ implies $z = \overline{z}$ and $z_3 = \overline{z_3}$, so $\mathrm{Fix}(\mathbf{D}_3[\tau_1, \kappa_5]) = \{(x, x, y, x) | x, y \in \mathbb{R}\}$. Now $\gamma \in N_\Gamma(\mathbf{D}_3[\tau_2, \kappa_1], \mathbb{O} \oplus \mathbf{Z}_2^c)$ if and only if $\theta_2 + \theta_3 = 0$ or π mod 2π, $-\theta_1 - \theta_3 = \theta_2 = -\theta_1 = 0$ or π mod 2π. Therefore $\theta_3 = 0$ and $\theta_1 = \theta_2 = 0$ or π, so $\mathrm{Fix}_{X_0}(\mathbf{D}_3[\tau_2, \kappa_1]) = e_1 \cup e_5$.

Case 7: $\mathbf{D}_3[\tau_3, \kappa_3]$. Since $\tau_3 \in \mathbf{D}_3[\tau_3, \kappa_3]$ it follows that $\mathrm{Fix}(\mathbf{D}_3[\tau_3, \kappa_3])$ is contained in $\{(z, \overline{z}, z, z_4) | z, z_4 \in \mathbb{C}\}$. Furthermore $\kappa_3 \in \mathbf{D}_3[\tau_3, \kappa_3]$ implies $z = \overline{z}$ and $z_4 = \overline{z_4}$, so $\mathrm{Fix}(\mathbf{D}_3[\tau_3, \kappa_3]) = \{(x, x, x, y) | x, y \in \mathbb{R}\}$. Now $\gamma \in N_\Gamma(\mathbf{D}_3[\tau_3, \kappa_3], \mathbb{O} \oplus \mathbf{Z}_2^c)$ if and only if $\theta_1 = 0$ or π mod 2π, $\theta_1 + \theta_3 = \theta_2 + \theta_3 = \theta_2 = 0$ or π mod 2π. Therefore $\theta_3 = 0$ and $\theta_1 = \theta_2 = 0$ or π, so $\mathrm{Fix}_{X_0}(\mathbf{D}_3[\tau_3, \kappa_3]) = e_1 \cup e_5$.

Case 8: $\mathbf{D}_3[\tau_4, \kappa_5]$. Since $\tau_4 \in \mathbf{D}_3[\tau_4, \kappa_5]$ it follows that $\mathrm{Fix}(\mathbf{D}_3[\tau_4, \kappa_5]) \subset \{(z, z_2, z, \overline{z}) | z, z_2 \in \mathbb{C}\}$. Furthermore, $\kappa_5 \in \mathbf{D}_3[\tau_3, \kappa_3]$, implies $z = \overline{z}$ and $z_2 = \overline{z_2}$, so $\mathrm{Fix}(\mathbf{D}_3[\tau_4, \kappa_5]) = \{(x, y, x, x) | x, y \in \mathbb{R}\}$. Now $\gamma \in N_\Gamma(\mathbf{D}_3[\tau_4, \kappa_5], \mathbb{O} \oplus \mathbf{Z}_2^c)$ if and only if $\theta_2 = 0$ or π mod 2π, $-\theta_1 - \theta_3 = \theta_2 + \theta_3 = -\theta_1 = 0$ or π mod 2π. Therefore $\theta_3 = 0$ and $\theta_1 = \theta_2 = 0$ or π, so $\mathrm{Fix}_{X_0}(\mathbf{D}_3[\tau_4, \kappa_5]) = e_1 \cup e_5$. □

We now consider the groups $\mathbf{Z}_4[\rho_x]$, $\mathbf{Z}_4[\rho_y]$, and $\mathbf{Z}_4[\rho_z]$.

Lemma 8.5
Let $\mathbf{Z}_4[\rho_x]$, $\mathbf{Z}_4[\rho_y]$ and $\mathbf{Z}_4[\rho_z]$ act on X_0, with the action induced from Table 8.1. Then

$$\begin{aligned} \mathrm{Fix}_{X_0}(\mathbf{Z}_4[\rho_x]) &= c_9, \\ \mathrm{Fix}_{X_0}(\mathbf{Z}_4[\rho_y]) &= c_7, \\ \mathrm{Fix}_{X_0}(\mathbf{Z}_4[\rho_z]) &= c_{33}. \end{aligned}$$

Proof.

Case 1: $\mathbf{Z}_4[\rho_x]$. Since $\rho_x \in \mathbf{Z}_4[\rho_x]$, it follows that $\mathrm{Fix}(\mathbf{Z}_4[\rho_x]) \subset \{(z,z,z,z)\big|z \in \mathbb{C}\}$. Next we compute

$$N_\Gamma(\mathbf{Z}_4[\rho_x], \mathbb{O} \oplus \mathbf{Z}_2^c) = \{\gamma \in \Gamma\big|\gamma \mathrm{Fix}(\mathbb{O} \oplus \mathbf{Z}_2^c) \subseteq \mathrm{Fix}(\mathbf{Z}_4[\rho_x])\}.$$

Clearly $\mathbb{O} \oplus \mathbf{Z}_2^c \subset N_\Gamma(\mathbf{Z}_4[\rho_x], \mathbb{O} \oplus \mathbf{Z}_2^c)$ (and we shall not state this obvious fact for the rest of the proof). We now ask what other elements of Γ are contained in $N_\Gamma(\mathbf{Z}_4[\rho_x], \mathbb{O} \oplus \mathbf{Z}_2^c)$. Now $(\theta_1, \theta_2, \theta_3) \in \mathbf{T}^3$ is contained in $N_\Gamma(\mathbf{Z}_4[\rho_x], \mathbb{O} \oplus \mathbf{Z}_2^c)$ if and only if $-\theta_1 - \theta_3 = \theta_2 = \theta_2 + \theta_3 = -\theta_1$. Therefore $\theta_3 = 0$ and $\theta_1 = -\theta_2$, so $N_\Gamma(\mathbf{Z}_4[\rho_x], \mathbb{O} \oplus \mathbf{Z}_2^c) = \mathbb{O} \oplus \mathbf{Z}_2^c \cup c_9$. Since

$$\mathrm{Fix}_{X_0}(\mathbf{Z}_4[\rho_x]) = N_\Gamma(\mathbf{Z}_4[\rho_x], \mathbb{O} \oplus \mathbf{Z}_2^c)/\mathbb{O} \oplus \mathbf{Z}_2^c,$$

the result follows.

Case 2: $\mathbf{Z}_4[\rho_y]$. Since $\rho_y \in \mathbf{Z}_4[\rho_x]$ it follows that $\mathrm{Fix}(\mathbf{Z}_4[\rho_y]) \subset \{(z,\overline{z},\overline{z},z)\big|z \in \mathbb{C}\}$. Now $(\theta_1, \theta_2, \theta_3) \in \mathbf{T}^3$ is contained in $N_\Gamma(\mathbf{Z}_4[\rho_y], \mathbb{O} \oplus \mathbf{Z}_2^c)$ if and only if $-\theta_1 - \theta_3 = -\theta_2 = -\theta_2 - \theta_3 = -\theta_1$, so $\theta_3 = 0$ and $\theta_1 = \theta_2$. Thus $N_\Gamma(\mathbf{Z}_4[\rho_y], \mathbb{O} \oplus \mathbf{Z}_2^c) = \mathbb{O} \oplus \mathbf{Z}_2^c \cup c_7$. Since

$$\mathrm{Fix}_{X_0}(\mathbf{Z}_4[\rho_y]) = N_\Gamma(\mathbf{Z}_4[\rho_y], \mathbb{O} \oplus \mathbf{Z}_2^c)/\mathbb{O} \oplus \mathbf{Z}_2^c,$$

the result follows.

Case 3: $\mathbf{Z}_4[\rho_z]$. Since $\rho_z \in \mathbf{Z}_4[\rho_z]$ it follows that $\mathrm{Fix}(\mathbf{Z}_4[\rho_z]) \subset \{(z,z,\overline{z},\overline{z})\big|z \in \mathbb{C}\}$. Now $(\theta_1, \theta_2, \theta_3) \in \mathbf{T}^3$ is contained in $N_\Gamma(\mathbf{Z}_4[\rho_z], \mathbb{O} \oplus \mathbf{Z}_2^c)$ if and only if $-\theta_1 - \theta_3 = \theta_2 = -\theta_2 - \theta_3 = \theta_1$, so $\theta_1 = \theta_2$ and $\theta_3 = -2\theta_1$. Thus $N_\Gamma(\mathbf{Z}_4[\rho_z], \mathbb{O} \oplus \mathbf{Z}_2^c) = \mathbb{O} \oplus \mathbf{Z}_2^c \cup c_{33}$. Since

$$\mathrm{Fix}_{X_0}(\mathbf{Z}_4[\rho_z]) = N_\Gamma(\mathbf{Z}_4[\rho_z], \mathbb{O} \oplus \mathbf{Z}_2^c)/\mathbb{O} \oplus \mathbf{Z}_2^c,$$

the result follows. □

Next we consider the subgroups $\mathbf{D}_2[\rho_x^2, \kappa_4]$, $\mathbf{D}_2[\rho_y^2, \kappa_5]$, $\mathbf{D}_2[\rho_z^2, \kappa_1]$, and $\mathbf{D}_2[\rho_x^2, \rho_y^2]$.

Lemma 8.6
Let $\mathbf{D}_2[\rho_x^2, \kappa_4]$, $\mathbf{D}_2[\rho_y^2, \kappa_5]$, $\mathbf{D}_2[\rho_z^2, \kappa_1]$ and $\mathbf{D}_2[\rho_x^2, \rho_y^2]$ act on X_0, with the action induced from t Table 8.1. Then

$$\begin{aligned}
\mathrm{Fix}_{X_0}(\mathbf{D}_2[\rho_x^2, \kappa_6]) &= e_1 \cup e_2 \cup e_5 \cup e_8, \\
\mathrm{Fix}_{X_0}(\mathbf{D}_2[\rho_y^2, \kappa_5]) &= e_1 \cup e_5 \cup e_6 \cup e_7, \\
\mathrm{Fix}_{X_0}(\mathbf{D}_2[\rho_z^2, \kappa_1]) &= e_1 \cup e_3 \cup e_4 \cup e_5, \\
\mathrm{Fix}_{X_0}(\mathbf{D}_2[\rho_x^2, \rho_y^2]) &= e_1 \cup e_5 \cup e_9 \cup e_{10}.
\end{aligned}$$

Proof.

Case 1: $\mathbf{D}_2[\rho_x^2, \kappa_6]$. Since ρ_x^2 and $\kappa_6 \in \mathbf{D}_2[\rho_x^2, \kappa_6]$, it follows that $\mathrm{Fix}(\mathbf{D}_2[\rho_x^2, \kappa_6]) = \{(x,y,x,y)\big|x,y \in \mathbb{R}\}$. An element $(\theta_1, \theta_2, \theta_3) \in \mathbf{T}^3$ is contained in $N_\Gamma(\mathbf{D}_2[\rho_x^2, \kappa_6], \mathbb{O} \oplus \mathbf{Z}_2^c)$ if and only if $\theta_1 + \theta_3 = \theta_2 + \theta_3 = 0$ or $\pi \bmod 2\pi$ and $\theta_1 = \theta_2 = 0$ or $\pi \bmod 2\pi$. Therefore we obtain e_1, e_2, e_5, and e_8, so $\mathrm{Fix}(\mathbf{D}_2[\rho_x^2, \kappa_6]) = e_1 \cup e_2 \cup e_5 \cup e_8$.

Case 2: $\mathbf{D}_2[\rho_y^2, \kappa_5]$. Since ρ_y^2 and $\kappa_5 \in\in \mathbf{D}_2[\rho_y^2, \kappa_5]$ it follows that $\mathrm{Fix}(\mathbf{D}_2[\rho_y^2, \kappa_5]) = \{(x,x,y,y)\big|x,y \in \mathbb{R}\}$. An element $(\theta_1, \theta_2, \theta_3) \in \mathbf{T}^3$ is contained in $N_\Gamma(\mathbf{D}_2[\rho_y^2, \kappa_5], \mathbb{O} \oplus \mathbf{Z}_2^c)$ if and only if $\theta_1 + \theta_3 = \theta_2 = 0$ or $\pi \bmod 2\pi$ and $\theta_2 + \theta_3 = \theta_1 = 0$ or $\pi \bmod 2\pi$. Therefore we obtain $\mathrm{Fix}(\mathbf{D}_2[\rho_y^2, \kappa_5]) = e_1 \cup e_5 \cup e_6 \cup e_7$.

Case 3: $\mathbf{D}_2[\rho_z^2, \kappa_1]$. Since ρ_z^2 and $\kappa_1 \in \mathbf{D}_2[\rho_z^2, \kappa_1]$ it follows that $\mathrm{Fix}(\mathbf{D}_2[\rho_z^2, \kappa_1]) = \{(x,y,y,x)\big|x,y \in$

$\mathbb{R}\}$. An element $(\theta_1, \theta_2, \theta_3) \in \mathbf{T}^3$ is contained in $N_\Gamma(\mathbf{D}_2[\rho_z^2, \kappa_1], \mathbb{O} \oplus \mathbf{Z}_2^c)$ if and only if $\theta_1 + \theta_3 = \theta_1 = 0$ or π mod 2π and $\theta_2 + \theta_3 = \theta_2 = 0$ or π mod 2π. Therefore we obtain e_1, e_3, e_4, and e_5, and $\mathrm{Fix}(\mathbf{D}_2[\rho_z^2, \kappa_1]) = e_1 \cup e_3 \cup e_4 \cup e_5$.

Case 4: $\mathbf{D}_2[\rho_x^2, \rho_y^2]$. Since ρ_x^2, $\rho_y^2 \in \mathbf{D}_2[\rho_x^2, \rho_y^2]$ it follows that $\mathrm{Fix}(\mathbf{D}_2[\rho_x^2, \rho_y^2]) = \{(z, \overline{z}, z, \overline{z}) \big| z \in \mathbb{R}\}$. An element $(\theta_1, \theta_2, \theta_3) \in \mathbf{T}^3$ is contained in $N_\Gamma(\mathbf{D}_2[\rho_x^2, \rho_y^2], \mathbb{O} \oplus \mathbf{Z}_2^c)$ if and only if $\theta_1 + \theta_3 = \theta_2 = -\theta_2 - \theta_3 = \theta_1$, so $\theta_3 = 0$ and $\theta_1 = \theta_2 = 0$ or π. Thus we have the elements e_1, e_5, e_9, and e_{10} and $\mathrm{Fix}(\mathbf{D}_2[\rho_x^2, \rho_y^2]) = e_1 \cup e_5 \cup e_9 \cup e_{10}$. □

Next we consider the groups $\mathbf{Z}_3[\tau_1]$, $\mathbf{Z}_3[\tau_2]$, $\mathbf{Z}_3[\tau_3]$, and $\mathbf{Z}_3[\tau_4]$.

Lemma 8.7
Let $\mathbf{Z}_3[\tau_1]$, $\mathbf{Z}_3[\tau_2]$, $\mathbf{Z}_3[\tau_3]$ and $\mathbf{Z}_3[\tau_4]$ act on X_0, with the action induced from Table 8.1. Then

$$\begin{aligned} \mathrm{Fix}_{X_0}(\mathbf{Z}_3[\tau_1]) &= c_{29}, \\ \mathrm{Fix}_{X_0}(\mathbf{Z}_3[\tau_2]) &= c_{30}, \\ \mathrm{Fix}_{X_0}(\mathbf{Z}_3[\tau_3]) &= c_{31}, \\ \mathrm{Fix}_{X_0}(\mathbf{Z}_3[\tau_4]) &= c_{32}. \end{aligned}$$

Proof.

Case 1: $\mathbf{Z}_3[\tau_1]$. Since τ_1 and τ_1^2 are contained in $\mathbf{Z}_3[\tau_1]$, a vector $(z_1, z_2, z_3, z_4) \in \mathbb{C}^4$ is fixed by $\mathbf{Z}_3[\tau_1]$ if and only if $z_2 = \overline{z_3} = z_4$. Since $\mathrm{Fix}(\mathbf{Z}_3[\tau_1]) = \{(z_1, z_2, \overline{z_2}, z_2) \big| z \in \mathbb{C}\}$, it follows that $(\theta_1, \theta_2, \theta_3) \in \mathbf{T}^3$ is contained in $N_\Gamma(\mathbf{Z}_3[\tau_1], \mathbb{O} \oplus \mathbf{Z}_2^c)$ if and only if $\theta_2 = -\theta_2 - \theta_3 = -\theta_1$. Therefore $\mathrm{Fix}(\mathbf{Z}_3[\tau_1]) = c_{29}$.

Case 2: $\mathbf{Z}_3[\tau_2]$. Since τ_2 and τ_2^2 are contained in $\mathbf{Z}_3[\tau_2]$, a vector $(z_1, z_2, z_3, z_4) \in \mathbb{C}^4$ is fixed by $\mathbf{Z}_3[\tau_2]$ if and only if $z_1 = \overline{z_2} = \overline{z_4}$. Since $\mathrm{Fix}(\mathbf{Z}_3[\tau_2]) = \{(z, \overline{z}, z_3, \overline{z}) \big| z, z_3 \in \mathbb{C}\}$, it follows that $(\theta_1, \theta_2, \theta_3) \in \mathbf{T}^3$ is contained in $N_\Gamma(\mathbf{Z}_3[\tau_1], \mathbb{O} \oplus \mathbf{Z}_2^c)$ if and only if $-\theta_1 - \theta_3 = -\theta_2 = \theta_1 \in [0, 2\pi)$. Therefore $\mathrm{Fix}(\mathbf{Z}_3[\tau_2]) = c_{30}$.

Case 3: $\mathbf{Z}_3[\tau_3]$. Since τ_3 and τ_3^2 are contained in $\mathbf{Z}_3[\tau_3]$, a vector $(z_1, z_2, z_3, z_4) \in \mathbb{C}^4$ is fixed by $\mathbf{Z}_3[\tau_3]$ if and only if $z_1 = \overline{z_2} = z_3$. Since $\mathrm{Fix}(\mathbf{Z}_3[\tau_3]) = \{(z, \overline{z}, z, z_4) \big| z, z_4 \in \mathbb{C}\}$, it follows that $(\theta_1, \theta_2, \theta_3) \in \mathbf{T}^3$ is contained in $N_\Gamma(\mathbf{Z}_3[\tau_3], \mathbb{O})$ if and only if $\theta_1 + \theta_3 = -\theta_2 - \theta_3 = \theta_2$. Therefore $\mathrm{Fix}(\mathbf{Z}_3[\tau_3]) = c_{31}$.

Case 4: $\mathbf{Z}_3[\tau_4]$. Since τ_4 and τ_4^2 are contained in $\mathbf{Z}_3[\tau_4]$, a vector $(z_1, z_2, z_3, z_4) \in \mathbb{C}^4$ is fixed by $\mathbf{Z}_3[\tau_4]$ if and only if $z_1 = z_3 = \overline{z_4}$. Since $\mathrm{Fix}(\mathbf{Z}_3[\tau_4]) = \{(z, z_2, z, \overline{z}) \big| z, z_2 \in \mathbb{C}\}$, it follows that $(\theta_1, \theta_2, \theta_3) \in \mathbf{T}^3$ is contained in $N_\Gamma(\mathbf{Z}_3[\tau_4], \mathbb{O} \oplus \mathbf{Z}_2^c)$ if and only if $\theta_1 + \theta_3 = -\theta_2 - \theta_3 = -\theta_1$. Therefore $\mathrm{Fix}(\mathbf{Z}_3[\tau_4]) = c_{32}$. □

Finally we consider the groups $\mathbf{Z}_2[\rho_x^2]$, $\mathbf{Z}_2[\rho_y^2]$, $\mathbf{Z}_2[\rho_z^2]$, $\mathbf{Z}_2[\kappa_1]$, $\mathbf{Z}_2[\kappa_2]$, $\mathbf{Z}_2[\kappa_3]$, $\mathbf{Z}_2[\kappa_4]$, $\mathbf{Z}_2[\kappa_5]$, and $\mathbf{Z}_2[\kappa_6]$.

Lemma 8.8
Let $\mathbf{Z}_2[\rho_x^2]$, $\mathbf{Z}_2[\rho_y^2]$, $\mathbf{Z}_2[\rho_z^2]$, $\mathbf{Z}_2[\kappa_1]$, $\mathbf{Z}_2[\kappa_2]$, $\mathbf{Z}_2[\kappa_3]$, $\mathbf{Z}_2[\kappa_4]$, $\mathbf{Z}_2[\kappa_5]$ and $\mathbf{Z}_2[\kappa_6]$ act on X_0, with the action induced from Table 8.1. Then

$$\begin{aligned} \mathrm{Fix}_{X_0}(\mathbf{Z}_2[\rho_x^2]) &= c_9 \cup c_{10}, \\ \mathrm{Fix}_{X_0}(\mathbf{Z}_2[\rho_y^2]) &= c_7 \cup c_{37}, \\ \mathrm{Fix}_{X_0}(\mathbf{Z}_2[\rho_z^2]) &= c_{33} \cup c_{38}, \\ \mathrm{Fix}_{X_0}(\mathbf{Z}_2[\kappa_1]) &= c_1 \cup c_{23}, \end{aligned}$$

$$\begin{aligned}
\mathrm{Fix}_{X_0}(\mathbf{Z}_2[\kappa_2]) &= c_3 \cup c_{25}, \\
\mathrm{Fix}_{X_0}(\mathbf{Z}_2[\kappa_3]) &= c_{17} \cup c_{36}, \\
\mathrm{Fix}_{X_0}(\mathbf{Z}_2[\kappa_4]) &= c_5 \cup c_6, \\
\mathrm{Fix}_{X_0}(\mathbf{Z}_2[\kappa_5]) &= c_{13} \cup c_{35}, \\
\mathrm{Fix}_{X_0}(\mathbf{Z}_2[\kappa_6]) &= c_{21} \cup c_{34}.
\end{aligned}$$

Proof.

Case 1: $\mathbf{Z}_2[\rho_x^2]$. We find that $\mathrm{Fix}(\mathbf{Z}_2[\rho_x^2]) = \{(z,z,z,z) | z \in \mathbb{C}\}$. Now $(\theta_1,\theta_2,\theta_3)$ is contained in $N_\Gamma(\mathbf{Z}_2[\rho_x^2], \mathbb{O}\oplus\mathbf{Z}_2^c)$ if and only if $\theta_1+\theta_3 = -\theta_2-\theta_3 = \theta_2 = -\theta_1$. Therefore $\mathrm{Fix}(\mathbf{Z}_2[\rho_x^2]) = c_9 \cup c_{10}$.

Case 2: $\mathbf{Z}_2[\rho_y^2]$. We find that $\mathrm{Fix}(\mathbf{Z}_2[\rho_y^2]) = \{(z,\overline{z},z,\overline{z}) | z \in \mathbb{C}\}$. Now $(\theta_1,\theta_2,\theta_3)$ is contained in $N_\Gamma(\mathbf{Z}_2[\rho_y^2], \mathbb{O}\oplus\mathbf{Z}_2^c)$ if and only if $\theta_1+\theta_3 = \theta_2 = \theta_2+\theta_3 = \theta_1$. Therefore $\mathrm{Fix}(\mathbf{Z}_2[\rho_x^2]) = c_7 \cup c_{37}$.

Case 3: $\mathbf{Z}_2[\rho_z^2]$. We find that $\mathrm{Fix}(\mathbf{Z}_2[\rho_z^2]) = \{(z,z,\overline{z},\overline{z}) | z \in \mathbb{C}\}$. Now $(\theta_1,\theta_2,\theta_3)$ is contained in $N_\Gamma(\mathbf{Z}_2[\rho_z^2], \mathbb{O}\oplus\mathbf{Z}_2^c)$ if and only if $-\theta_1-\theta_3 = \theta_2 = \theta_1 = -\theta_2-\theta_3$. Therefore $\mathrm{Fix}(\mathbf{Z}_2[\rho_z^2]) = c_{33} \cup c_{38}$.

Case 4: $\mathbf{Z}_2[\kappa_1]$. We find that $\mathrm{Fix}(\mathbf{Z}_2[\kappa_1]) = \{(z,x_2,x_3,z) | x_2,x_3 \in \mathbb{R}, z \in \mathbb{C}\}$. Now $(\theta_1,\theta_2,\theta_3)$ is contained in $N_\Gamma(\mathbf{Z}_2[\kappa_1], \mathbb{O}\oplus\mathbf{Z}_2^c)$ if and only if $\theta_2 = 0$ or π, $\theta_2+\theta_3 = 0$ or $\pi \bmod 2\pi$ and $-\theta_1-\theta_3 = \theta_1$. Therefore, $\mathrm{Fix}(\mathbf{Z}_2[\kappa_1]) = c_1 \cup c_{23}$.

Case 5: $\mathbf{Z}_2[\kappa_2]$. We find that $\mathrm{Fix}(\mathbf{Z}_2[\kappa_2]) = \{(x_1,z,z,x_4) | x_1,x_4 \in \mathbb{R}, z \in \mathbb{C}\}$. Now $(\theta_1,\theta_2,\theta_3)$ is contained in $N_\Gamma(\mathbf{Z}_2[\kappa_2], \mathbb{O}\oplus\mathbf{Z}_2^c)$ if and only if $\theta_1+\theta_3 = 0$ or $\pi \bmod 2\pi$, $\theta_2 = \theta_2+\theta_3$ and $\theta_1 = 0$ or $\pi \bmod 2\pi$. Therefore $\mathrm{Fix}(\mathbf{Z}_2[\kappa_2]) = c_3 \cup c_{25}$.

Case 6: $\mathbf{Z}_2[\kappa_3]$. We find that $\mathrm{Fix}(\mathbf{Z}_2[\kappa_2]) = \{(z,z,x_3,x_4) | x_3,x_4 \in \mathbb{R}, z \in \mathbb{C}\}$. Now $(\theta_1,\theta_2,\theta_3)$ is contained in $N_\Gamma(\mathbf{Z}_2[\kappa_3], \mathbb{O}\oplus\mathbf{Z}_2^c)$ if and only if $\theta_1 = 0$ or $\pi \bmod 2\pi$, $\theta_2+\theta_3 = 0$ or $\pi \bmod 2\pi$ and $-\theta_1-\theta_3 = \theta_2$. Therefore $\mathrm{Fix}(\mathbf{Z}_2[\kappa_3]) = c_{17} \cup c_{36}$.

Case 7: $\mathbf{Z}_2[\kappa_4]$. We find that $\mathrm{Fix}(\mathbf{Z}_2[\kappa_4]) = \{(z,x_2,\overline{z},x_4) | x_2,x_4 \in \mathbb{R}, z \in \mathbb{C}\}$. Now $(\theta_1,\theta_2,\theta_3)$ is contained in $N_\Gamma(\mathbf{Z}_2[\kappa_4], \mathbb{O}\oplus\mathbf{Z}_2^c)$ if and only if $\theta_1+\theta_3 = \theta_2+\theta_3 \in [0,2\pi)$, $\theta_2 = 0$ or $\pi \bmod 2\pi$ and $\theta_1 = 0$ or $\pi \bmod 2\pi$. Therefore $\mathrm{Fix}(\mathbf{Z}_2[\kappa_4]) = c_5 \cup c_6$.

Case 8: $\mathbf{Z}_2[\kappa_5]$. We find that $\mathrm{Fix}(\mathbf{Z}_2[\kappa_5]) = \{(x_1,x_2,z,z) | x_1,x_2 \in \mathbb{R}, z \in \mathbb{C}\}$. Now $(\theta_1,\theta_2,\theta_3)$ is contained in $N_\Gamma(\mathbf{Z}_2[\kappa_5], \mathbb{O}\oplus\mathbf{Z}_2^c)$ if and only if $\theta_1+\theta_3 = 0$ or $\pi \bmod 2\pi$, $\theta_2 = 0$ or $\pi \bmod 2\pi$ and $\theta_2+\theta_3 = -\theta_1$. Therefore $\mathrm{Fix}(\mathbf{Z}_2[\kappa_5]) = c_{13} \cup c_{35}$.

Case 9: $\mathbf{Z}_2[\kappa_6]$. We find that $\mathrm{Fix}(\mathbf{Z}_2[\kappa_6]) = \{(x_1,z,x_3,\overline{z}) | x_1,x_3 \in \mathbb{R}, z \in \mathbb{C}\}$. Now $(\theta_1,\theta_2,\theta_3)$ is contained in $N_\Gamma(\mathbf{Z}_2[\kappa_6], \mathbb{O}\oplus\mathbf{Z}_2^c)$ if and only if $\theta_1+\theta_3 = 0$ or $\pi \bmod 2\pi$, $\theta_2+\theta_3 = 0$ or $\pi \bmod 2\pi$ and $\theta_1 = \theta_2$. Therefore $\mathrm{Fix}(\mathbf{Z}_2[\kappa_6]) = c_{21} \cup c_{34}$. □

This completes the computation of all the fixed-point submanifolds for all nontrivial subgroups of $\mathbb{O}$. It now follows that

$$\begin{aligned}
\mathscr{C}_{\mathbb{O}} = \{&e_1,e_2,e_3,e_4,e_5,e_6,e_7,e_8,e_9,e_{10}c_1,c_3,c_5,c_6,c_7,c_8,c_9,c_{10},c_{13},c_{17},c_{21},c_{23},c_{25},c_{29},c_{30},\\
&c_{31},c_{32},c_{33},c_{34},c_{35},c_{36},c_{37},c_{38}\}.
\end{aligned}$$

Which completes the proof of Proposition 8.3. We can now use this information to form the skeleton

$$\mathbb{X}_{\mathbb{O}} = \bigcup_{C \in \mathscr{C}_{\mathbb{O}}} C \subset X_0.$$

Since X_0 is a 3-torus we encounter the same problems as with the SC lattice studied in Chapter 7—the skeleton is too complex to be rendered in a meaningful and instructive way. To help

Table 8.2: Action of $\mathbb{O}$ induced on X_0 for the FCC lattice.

Element of $\mathbb{O}$	Action on X_0
ρ_x	$(-(\theta_2+\theta_3), -(\theta_1+\theta_3), (\theta_1+\theta_2+\theta_3))$
ρ_x^2	$(-\theta_2, -\theta_1, -\theta_3)$
ρ_x^3	$(\theta_1+\theta_3, \theta_2+\theta_3, -(\theta_1+\theta_2+\theta_3))$
ρ_y	$(\theta_1+\theta_3, \theta_1, -\theta_1+\theta_2)$
ρ_y^2	$(\theta_2+\theta_3, \theta_1+\theta_3, -\theta_3)$
ρ_y^3	$(\theta_2, \theta_2+\theta_3, \theta_1-\theta_2)$
ρ_z	$(-(\theta_2+\theta_3), \theta_1, \theta_3)$
ρ_z^2	$(-(\theta_1+\theta_3), -(\theta_2+\theta_3), \theta_3)$
ρ_z^3	$(\theta_2, -(\theta_1+\theta_3), \theta_3)$
τ_1	$(\theta_2+\theta_3, -\theta_1, \theta_1-\theta_2)$
τ_1^2	$(-\theta_2, -(\theta_2+\theta_3), \theta_1+\theta_2+\theta_3)$
τ_2	$(-\theta_1-\theta_3, -\theta_1, \theta_1+\theta_2+\theta_3)$
τ_2^2	$(-\theta_2, \theta_1+\theta_3, -\theta_1+\theta_2)$
τ_3	$(\theta_1, -\theta_2-\theta_3, \theta_2-\theta_1)$
τ_3^2	$(\theta_1, \theta_1+\theta_3, -(\theta_1+\theta_2+\theta_3))$
τ_4	$(\theta_2+\theta_3, \theta_2, -(\theta_1+\theta_2+\theta_3))$
τ_4^2	$(-\theta_1-\theta_3, \theta_2, -(-\theta_1+\theta_2))$
κ_1	$(\theta_1+\theta_3, -\theta_2, -\theta_3)$
κ_2	$(-\theta_1, \theta_2+\theta_3, -\theta_3)$
κ_3	$(-\theta_1, -(\theta_1+\theta_3), \theta_1-\theta_2)$
κ_4	$(-\theta_1, -\theta_2, \theta_1+\theta_2+\theta_3)$
κ_5	$(-(\theta_2+\theta_3), -\theta_2, \theta_2-\theta_1)$
κ_6	$(\theta_2, \theta_1, -(\theta_1+\theta_2+\theta_3))$

with this difficulty, we compute the symmetry properties of the skeleton; using this information we can construct the simpler geometric object, the projected skeleton, which contains all the important information about the equilibria and the interconnections between them.

Symmetry Properties of $\mathbb{X}_0$

To understand how the components of the skeleton are related, we simplify the skeleton. The best way to achieve this is to study the action of $\mathbb{O}$ on X_0, which, in turn, induces an action of $\mathbb{O}$ on the skeleton. Beginning with the action of $\mathbb{O}$ on X_0 and $\mathscr{C}_0$, it is easy to deduce the setwise Stab(C) and pointwise stab(C) isotropy subgroups of all $C \in \mathscr{C}_0$. These two pieces of information allow the construction of the group $S(C)$, giving information about the knots located on the skeleton. Combining all this information, we may construct the projected skeleton.

Pointwise and Setwise Isotropy Subgroups. The action of $\mathbb{O}$ on $\mathbb{C}^4$ in Table 8.1 induces a natural action on X_0 with respect to the coordinates $(\theta_1, \theta_2, \theta_3)$. The action of the generators for $\mathbb{O}$ is

$$\begin{aligned} \rho_x(\theta_1,\theta_2,\theta_3) &= (-\theta_2-\theta_3, -\theta_1-\theta_3, \theta_1+\theta_2+\theta_3), \\ \rho_y(\theta_1,\theta_2,\theta_3) &= (\theta_1+\theta_3, \theta_1, \theta_2-\theta_1). \end{aligned}$$

The complete action of $\mathbb{O}$ on X_0 is in Table 8.2. This action is calculated in the usual way; we present the computations for ρ_x as an example. Let $(\theta_1, \theta_2, \theta_3) \in X_0$. This element corresponds to the point $\mathbf{z} = (e^{-\mathrm{i}(\theta_1+\theta_3)}, e^{\mathrm{i}\theta_2}, e^{\mathrm{i}(\theta_2+\theta_3)}, e^{-\mathrm{i}\theta_1})x$, where $x > 0$ in $\mathbb{C}^4$. The action of ρ_x on $\mathbf{z}$ gives the new point $(e^{-\mathrm{i}\theta_1}, e^{-\mathrm{i}(\theta_1+\theta_3)}, e^{\mathrm{i}\theta_2}, e^{\mathrm{i}(\theta_2+\theta_3)})x$, which when written in $(\theta_1, \theta_2, \theta_3)$ coordinates on X_0 gives the required action. The action of $\mathbb{O}$ on X_0 in turn induces an action of $\mathbb{O}$ on the set $\mathscr{C}_0$ by permutation of its elements. Again this action is straightforward to compute.

Table 8.3: Action of $\mathbb{O}$ induced on $\mathscr{C}_{\mathbb{O}}$ for the FCC lattice.

Element of $\mathscr{C}_{\mathbb{O}}$	Elements of $\mathbb{O}$ acting nontrivially	Action
e_1	None	
e_2	ρ_x, κ_6, τ_1, τ_2^2	e_7
	ρ_x^2, ρ_y^2, ρ_z, ρ_z^3	e_3
	ρ_x^3, κ_4, τ_3, τ_4^2	e_6
	ρ_y, κ_3, τ_2, τ_3^2	e_8
	ρ_y^3, κ_5, τ_4, τ_1^2	e_3
e_3	ρ_x, κ_6, τ_1, τ_2^2	e_6
	ρ_x^2, ρ_y^2, ρ_z, ρ_z^3	e_4
	ρ_x^3, κ_4, τ_3, τ_4^2	e_7
	ρ_y, κ_3, τ_2, τ_3^2	e_2
	ρ_y^3, κ_5, τ_4, τ_1^2	e_8
e_4	ρ_x, ρ_x^3, ρ_y^2, ρ_z^2	e_8
	ρ_y, κ_5, τ_4^2, τ_1	e_4
	ρ_y^3, κ_3, τ_3, τ_2^2	e_3
	ρ_z, κ_1, τ_2, τ_4	e_6
	ρ_z^3, τ_1^2, τ_3^2, κ_2	e_7
e_5	None	
e_6	ρ_z^3, κ_1, τ_2^2, τ_4^2	e_2
	ρ_x^2, ρ_y, ρ_z^2, ρ_y^3	e_7
	ρ_x^3, κ_6, τ_1^2, τ_2	e_3
	ρ_z, κ_2, τ_1, τ_3	e_8
	ρ_x, κ_4, τ_3^2, τ_4	e_4

As an example, we consider the action of ρ_y^3 on c_1. In the coordinates on X_0 an element of c_1 is given by $(\theta,0,0)$ where $\theta \in [0,2\pi)$. The element ρ_y^3 takes $(\theta,0,0)$ to $(0,0,\theta)$, which is an element of the set c_5. So the induced action of ρ_y^3 on c_1 is the permutation that changes c_1 to c_5. The actions of the other elements on a general $C \in \mathscr{C}_{\mathbb{O}}$ are similar. We present this action in Table 8.3. The action of $\mathbb{O}$ on $\mathscr{C}_{\mathbb{O}}$ is the cornerstone of the symmetry properties of the skeleton. Using this action we can deduce the following fundamental symmetry result.

Proposition 8.9
Let $\mathbb{O}$ act on $\mathscr{C}_{\mathbb{O}}$ as in Table 8.3 and on X_0 as in Table 8.2. Then given $C \in \mathscr{C}_{\mathbb{O}}$, the setwise isotropy $\mathrm{Stab}(C)$, *pointwise isotropy* $\mathrm{stab}(C)$ *and the group $S(C)$ are given in Table 8.7.*

Proof. The proof follows the standard lines. □

We have now completed our symmetry analysis, based on the action of the group $\mathbb{O}$ on $C \in \mathscr{C}_{\mathbb{O}}$. This analysis has produced important pieces of information; $S(C) \cong \mathbf{Z}_2$ for all $C \in \mathscr{C}_{\mathbb{O}}$ with $C \cong \mathbf{S}^1$. This shows that each such C has two knots , and hence an axis of reflection symmetry. The presence of this symmetry again produces further simplifications.

Knots Relative to C. The symmetry analysis above shows that there are knots relative to each $C \in \mathscr{C}_{\mathbb{O}}$ with $C \cong \mathbf{S}^1$. It is important to locate these knots. Due to the complexity of the skeleton such a computation is tedious. However, it is possible to employ the $\mathbb{O}$ symmetry to simplify the task. The action of $\mathbb{O}$ on $\mathscr{C}_{\mathbb{O}}$ in Table 8.3 shows that there are five C's homeomorphic to $\mathbf{S}^1$ that are not related by $\mathbb{O}$ symmetry; that is, they are in different group orbits. The components are given by $c_1 = \{(\theta,0,0)|\theta \in [0,2\pi)\}$, $c_6 = \{(\pi,\pi,\theta)|\theta \in [0,2\pi)\}$, $c_7 = \{(\theta,\theta,0)|\theta \in [0,2\pi)\}$, $c_{10} = \{(\theta,-\theta,\pi)|\theta \in [0,2\pi)\}$, and $c_{29} = \{(\theta,-\theta,2\theta)|\theta \in [0,2\pi)\}$.

Table 8.4: Table 8.3 continued

Element of $\mathscr{C}_{\mathbb{O}}$	Elements of $\mathbb{O}$ acting nontrivially	Action
e_7	$\rho_z^3,\ \kappa_1,\ \tau_2^2,\ \tau_4^2$	e_8
	$\rho_x^2,\ \rho_y,\ \rho_z^2,\ \rho_y^3$	e_6
	$\rho_x^3,\ \kappa_6,\ \tau_1^2,\ \tau_2$	e_4
	$\rho_z,\ \kappa_2,\ \tau_1,\ \tau_3$	e_2
	$\rho_x,\ \kappa_4,\ \tau_3^2,\ \tau_4$	e_3
e_8	$\rho_x,\ \rho_x^3,\ \rho_y^2,\ \rho_z^2$	e_2
	$\rho_y,\ \kappa_5,\ \tau_4^2,\ \tau_1$	e_3
	$\rho_y^3,\ \kappa_3,\ \tau_3,\ \tau_2^2$	e_4
	$\rho_z,\ \kappa_1,\ \tau_2,\ \tau_4$	e_7
	$\rho_z^3,\ \tau_1^2,\ \tau_3^2,\ \kappa_2$	e_6
e_9	$\mathbb{O} - \mathbf{D}_2[\rho_x^2, \rho_y^2]$	e_{10}
e_{10}	$\mathbb{O} - \mathbf{D}_2[\rho_x^2, \rho_y^2]$	e_9
c_1	$\rho_x^2,\ \rho_y^2,\ \rho_z,\ \rho_z^3$	c_3
	$\rho_y^3,\ \kappa_5,\ \tau_1^2,\ \tau_4$	c_5
	$\rho_x^3,\ \kappa_4,\ \tau_3,\ \tau_4^2$	c_{13}
	$\rho_y,\ \kappa_3,\ \tau_2,\ \tau_3^2$	c_{21}
	$\rho_x,\ \kappa_6,\ \tau_1,\ \tau_2^2$	c_{17}
c_3	$\rho_x^2,\ \rho_y^2,\ \rho_z,\ \rho_z^3$	c_1
	$\rho_y,\ \kappa_3,\ \tau_2,\ \tau_3^2$	c_5
	$\rho_x,\ \kappa_6,\ \tau_1,\ \tau_2^2$	c_{13}
	$\rho_x^3,\ \kappa_4,\ \tau_3,\ \tau_4^2$	c_{17}
	$\rho_y^3,\ \kappa_5,\ \tau_1^2,\ \tau_4$	c_{21}
c_5	$\rho_x,\ \rho_x^3,\ \rho_y^2,\ \rho_z^2$	c_{21}
	$\rho_y,\ \kappa_5,\ \tau_1,\ \tau_4^2$	c_1
	$\rho_y^3,\ \kappa_3,\ \tau_2^2,\ \tau_3$	c_3
	$\rho_z,\ \kappa_1,\ \tau_2,\ \tau_4$	c_{13}
	$\rho_z^3,\ \kappa_2,\ \tau_1^2,\ \tau_3^2$	c_{17}
c_6	$\rho_x,\ \rho_x^3,\ \rho_y^2,\ \rho_z^2$	c_{34}
	$\rho_y,\ \kappa_5,\ \tau_1,\ \tau_4^2$	c_{23}
	$\rho_y^3,\ \kappa_3,\ \tau_2^2,\ \tau_3$	c_{25}
	$\rho_z,\ \kappa_1,\ \tau_2,\ \tau_4$	c_{35}
	$\rho_z^3,\ \kappa_2,\ \tau_1^2,\ \tau_3^2$	c_{36}

Table 8.5: Table 8.3 continued

Element of $\mathscr{C}_{\mathbb{O}}$	Elements of $\mathbb{O}$ acting nontrivially	Action
c_7	$\rho_x, \rho_x^3, \kappa_6, \kappa_4, \tau_1^2, \tau_2, \tau_3^2, \tau_4$	c_{33}
	$\rho_z, \rho_z^3, \kappa_2, \kappa_1, \tau_1, \tau_2^2, \tau_3, \tau_4^2$	c_9
c_9	$\rho_y, \rho_y^3, \kappa_3, \kappa_5, \tau_1, \tau_2^2, \tau_3, \tau_4^2$	c_{33}
	$\rho_z, \rho_z^3, \kappa_2, \kappa_1, \tau_1^2, \tau_2, \tau_3^2, \tau_4$	c_7
c_{10}	$\rho_y, \rho_y^3, \kappa_3, \kappa_5, \tau_1, \tau_2^2, \tau_3, \tau_4^2$	c_{38}
	$\rho_z, \rho_z^3, \kappa_2, \kappa_1, \tau_1^2, \tau_2, \tau_3^2, \tau_4$	c_{37}
c_{13}	$\rho_x, \kappa_4, \tau_3^2, \tau_4$	c_1
	$\rho_x^2, \rho_y, \rho_y^3, \rho_z^2$	c_{17}
	$\rho_x^3, \kappa_6, \tau_1^2, \tau_2$	c_3
	$\rho_z, \kappa_2, \tau_1, \tau_3$	c_{21}
	$\rho_z^3, \kappa_1, \tau_2^2, \tau_4^2$	c_{17}
c_{17}	$\rho_x, \kappa_4, \tau_3^2, \tau_4$	c_3
	$\rho_x^2, \rho_y, \rho_y^3, \rho_z^2$	c_{13}
	$\rho_x^3, \kappa_6, \tau_1^2, \tau_2$	c_1
	$\rho_z, \kappa_2, \tau_1, \tau_3$	c_5
	$\rho_z^3, \kappa_1, \tau_2^2, \tau_4^2$	c_{21}
c_{21}	$\rho_x, \rho_x^3, \rho_y^2, \rho_z^2$	c_5
	$\rho_y, \kappa_5, \tau_1, \tau_4^2$	c_3
	$\rho_y^3, \kappa_3, \tau_2^2, \tau_3$	c_1
	$\rho_z, \kappa_1, \tau_2, \tau_4$	c_{17}
	$\rho_z^3, \kappa_2, \tau_1^2, \tau_3^2$	c_{13}
c_{23}	$\rho_x, \kappa_6, \tau_1^2, \tau_2$	c_{36}
	$\rho_x^2, \rho_y^2, \rho_z, \rho_z^3$	c_{26}
	$\rho_x^3, \kappa_4, \tau_3, \tau_4^2$	c_{35}
	$\rho_y, \kappa_3, \tau_2, \tau_3^2$	c_{34}
	$\rho_y^3, \kappa_5, \tau_1^2, \tau_4$	c_6
c_{25}	$\rho_x, \kappa_6, \tau_1, \tau_2^2$	c_{35}
	$\rho_x^2, \rho_y^2, \rho_z, \rho_z^3$	c_{23}
	$\rho_x^3, \kappa_4, \tau_3, \tau_4^2$	c_{36}
	$\rho_y, \kappa_3, \tau_2, \tau_3^2$	c_6
	$\rho_y^3, \kappa_5, \tau_1^2, \tau_4$	c_{34}
c_{29}	$\rho_x, \rho_y^2, \rho_z^3, \kappa_3, \tau_2^2, \tau_3$	c_{32}
	$\rho_x^2, \rho_y^3, \rho_z, \kappa_4, \tau_3, \tau_4$	c_{30}
	$\rho_x^3, \rho_y, \rho_z^2, \kappa_1, \tau_2, \tau_4^2$	c_{31}
c_{30}	$\rho_x, \rho_y^2, \rho_z, \kappa_5, \tau_1, \tau_4$	c_{31}
	$\rho_x^2, \rho_y, \rho_z^3, \kappa_4, \tau_3^2, \tau_4^2$	c_{29}
	$\rho_x^3, \rho_y^3, \rho_z^2, \kappa_2, \tau_1^2, \tau_3$	c_{32}
c_{31}	$\rho_x, \rho_y^3, \rho_z^2, \kappa_1, \tau_2^2, \tau_4$	c_{29}
	$\rho_x^2, \rho_y, \rho_z, \kappa_6, \tau_1, \tau_2$	c_{32}
	$\rho_x^3, \rho_y^2, \rho_z^3, \kappa_5, \tau_1^2, \tau_4^2$	c_{30}
c_{32}	$\rho_x, \rho_y, \rho_z^2, \kappa_2, \tau_1, \tau_3^2$	c_{30}
	$\rho_x^2, \rho_y^3, \rho_z^3, \kappa_6, \tau_1^2, \tau_2^2$	c_{31}
	$\rho_x^3, \rho_y^2, \rho_z, \kappa_3, \tau_2, \tau_3$	c_{29}
c_{33}	$\rho_x, \rho_x^3, \kappa_6, \kappa_4, \tau_1, \tau_2^2, \tau_3, \tau_4^2$	c_7
	$\rho_y, \rho_y^3, \kappa_5, \kappa_3, \tau_1^2, \tau_2, \tau_3^2, \tau_4$	c_9
c_{34}	$\rho_x, \rho_x^3, \rho_y^2, \rho_z^2$	c_6
	$\rho_y, \kappa_5, \tau_1, \tau_4^2$	c_{25}
	$\rho_y^3, \kappa_3, \tau_2^2, \tau_3$	c_{23}
	$\rho_z, \kappa_1, \tau_2, \tau_4$	c_{36}
	$\rho_z^3, \kappa_2, \tau_1^2, \tau_3^2$	c_{35}

Table 8.6: Table 8.3 continued

Element of $\mathscr{C}_{\mathbb{O}}$	Elements of $\mathbb{O}$ acting nontrivially	Action
c_{35}	$\rho_x,\ \kappa_4,\ \tau_3^2,\ \tau_4$	c_{23}
	$\rho_x^2,\ \rho_y,\ \rho_y^3,\ \rho_z^2$	c_{36}
	$\rho_x^3,\ \kappa_6,\ \tau_1^2,\ \tau_2$	c_{25}
	$\rho_z,\ \kappa_1,\ \tau_2,\ \tau_4$	c_{34}
	$\rho_z^3,\ \kappa_1,\ \tau_2^2,\ \tau_4^2$	c_6
c_{36}	$\rho_x,\ \kappa_4,\ \tau_3^2,\ \tau_4$	c_{25}
	$\rho_x^2,\ \rho_y,\ \rho_y^3,\ \rho_z^2$	c_{35}
	$\rho_x^3,\ \kappa_6,\ \tau_1^2,\ \tau_2$	c_{23}
	$\rho_z,\ \kappa_1,\ \tau_2,\ \tau_4$	c_6
	$\rho_z^3,\ \kappa_1,\ \tau_2^2,\ \tau_4^2$	c_{34}
c_{37}	$\rho_x,\ \rho_x^3,\ \kappa_6,\ \kappa_4,\ \tau_1,\ \tau_2^2,\ \tau_3,\ \tau_4^2$	c_{38}
	$\rho_z,\ \rho_z^3,\ \kappa_2,\ \kappa_1,\ \tau_1,\ \tau_2^2,\ \tau_3,\ \tau_4^2$	c_{10}
c_{38}	$\rho_x,\ \rho_x^3,\ \kappa_6,\ \kappa_4,\ \tau_1,\ \tau_2^2,\ \tau_3,\ \tau_4^2$	c_{37}
	$\rho_z,\ \rho_z^3,\ \kappa_2,\ \kappa_1,\ \tau_1,\ \tau_2^2,\ \tau_3,\ \tau_4^2$	c_{10}

Table 8.7: Isotropy data for $C \in \mathscr{C}_{\mathbb{O}}$ on the FCC lattice.

$C \in \mathscr{C}_{\mathbb{O}}$	stab(C)	Stab(C)	$S(C) = \text{Stab}(C)/\text{stab}(C)$
e_1	$\mathbb{O}$	$\mathbb{O}$	$\mathbf{1}$
e_2	$\mathbf{D}_2[\rho_x^2, \kappa_6]$	$\mathbf{D}_2[\rho_x^2, \kappa_6]$	$\mathbf{1}$
e_3	$\mathbf{D}_2[\rho_z^2, \kappa_1]$	$\mathbf{D}_2[\rho_x^2, \kappa_1]$	$\mathbf{1}$
e_4	$\mathbf{D}_2[\rho_z^2, \kappa_1]$	$\mathbf{D}_2[\rho_z^2, \kappa_1]$	$\mathbf{1}$
e_5	$\mathbb{O}$	$\mathbb{O}$	$\mathbf{1}$
e_6	$\mathbf{D}_2[\rho_y^2, \kappa_5]$	$\mathbf{D}_2[\rho_y^2, \kappa_5]$	$\mathbf{1}$
e_7	$\mathbf{D}_2[\rho_y^2, \kappa_5]$	$\mathbf{D}_2[\rho_y^2, \kappa_5]$	$\mathbf{1}$
e_8	$\mathbf{D}_2[\rho_x^2, \kappa_6]$	$\mathbf{D}_2[\rho_x^2, \kappa_6]$	$\mathbf{1}$
c_1	$\mathbf{Z}_2[\kappa_1]$	$\mathbf{D}_2[\rho_z^2, \kappa_2]$	$\mathbf{Z}_2$
c_3	$\mathbf{Z}_2[\kappa_2]$	$\mathbf{D}_2[\rho_z^2, \kappa_2]$	$\mathbf{Z}_2$
c_5	$\mathbf{Z}_2[\kappa_4]$	$\mathbf{D}_2[\rho_x^2, \kappa_4]$	$\mathbf{Z}_2$
c_6	$\mathbf{Z}_2[\kappa_4]$	$\mathbf{D}_2[\rho_x^2, \kappa_4]$	$\mathbf{Z}_2$
c_7	$\mathbf{Z}_4[\rho_y]$	$\mathbf{D}_4[\rho_y, \kappa_5]$	$\mathbf{Z}_2$
c_9	$\mathbf{Z}_4[\rho_x]$	$\mathbf{D}_4[\rho_x, \kappa_6]$	$\mathbf{Z}_2$
c_{10}	$\mathbf{Z}_2[\rho_x^2]$	$\mathbf{D}_4[\rho_x, \kappa_6]$	$\mathbf{Z}_2$
c_{13}	$\mathbf{Z}_2[\kappa_5]$	$\mathbf{D}_2[\rho_y^2, \kappa_3]$	$\mathbf{Z}_2$
c_{17}	$\mathbf{Z}_2[\kappa_3]$	$\mathbf{D}_2[\rho_y^2, \kappa_3]$	$\mathbf{Z}_2$
c_{21}	$\mathbf{Z}_3[\kappa_4]$	$\mathbf{D}_2[\rho_x^2, \kappa_6]$	$\mathbf{Z}_2$
c_{23}	$\mathbf{Z}_2[\kappa_1]$	$\mathbf{D}_2[\rho_z^2, \kappa_2]$	$\mathbf{Z}_2$
c_{25}	$\mathbf{Z}_2[\kappa_2]$	$\mathbf{D}_2[\rho_z^2, \kappa_2]$	$\mathbf{Z}_2$
c_{29}	$\mathbf{Z}_3[\tau_1]$	$\mathbf{D}_3[\tau_1, \kappa_6]$	$\mathbf{Z}_2$
c_{30}	$\mathbf{Z}_3[\tau_2]$	$\mathbf{D}_3[\tau_2, \kappa_3]$	$\mathbf{Z}_2$
c_{31}	$\mathbf{Z}_3[\tau_3]$	$\mathbf{D}_3[\tau_3, \kappa_4]$	$\mathbf{Z}_2$
c_{32}	$\mathbf{Z}_3[\tau_4]$	$\mathbf{D}_3[\tau_4, \kappa_5]$	$\mathbf{Z}_2$
c_{33}	$\mathbf{Z}_4[\rho_z]$	$\mathbf{D}_4[\rho_z, \kappa_2]$	$\mathbf{Z}_2$
c_{34}	$\mathbf{Z}_2[\kappa_6]$	$\mathbf{D}_2[\rho_x^2, \kappa_6]$	$\mathbf{Z}_2$
c_{35}	$\mathbf{Z}_2[\kappa_5]$	$\mathbf{D}_2[\rho_y^2, \kappa_5]$	$\mathbf{Z}_2$
c_{36}	$\mathbf{Z}_2[\kappa_3]$	$\mathbf{D}_2[\rho_y^2, \kappa_3]$	$\mathbf{Z}_2$
c_{37}	$\mathbf{Z}_2[\rho_y^2]$	$\mathbf{D}_2[\rho_y^2, \kappa_5]$	$\mathbf{Z}_2$
c_{38}	$\mathbf{Z}_2[\kappa_5]$	$\mathbf{D}_2[\rho_y^2, \kappa_5]$	$\mathbf{Z}_2$

Table 8.8: Knots relative to orbit representatives of $C \in \mathscr{C}_{\mathbb{O}}$ for the FCC lattice.

Element of $\mathscr{C}_{\mathbb{O}}$	Knots
c_1	e_1, e_4
c_6	e_4, e_5
c_7	e_1, e_5
c_{10}	e_4, e_9
c_{29}	e_1, e_9

We must also consider the orbit representatives for the equilibria, given by e_1, e_4, e_5, and e_9. Here we adopt the same abuse of notation as for the SC lattice, each of these representatives actually represents an entire class of C's which are all contained in the same group orbit. The computation of the knots is straightforward, since $S(C) \cong \mathbf{Z}_2$ for each $C \in \mathscr{C}_{\mathbb{O}}$ with $C \cong \mathbf{S}^1$; it follows that any C has two knots. All knots are equilibria, and since each C contains only two equilibria, these equilibria are the knots we seek. We summarise this information in Table 8.8.

Projected Skeleton

Here we compute the projected skeleton $\mathbb{X}^p_{\mathbb{O}}$. The action of $\mathbb{O}$ on $\mathscr{C}_{\mathbb{O}}$ shows that there are five orbit representatives for the elements of $\mathscr{C}_{\mathbb{O}}$ that are homeomorphic to $\mathbf{S}^1$. These are c_1, c_6, c_7, c_{10}, and c_{29}. The orbit representatives for the equilibria are e_1, e_4, e_5, and e_9. We have seen also that each C has two knots; this implies that there is an axis of reflection symmetry. So each C projects into the orbit space as a line joining the two knots. More precisely, we have the following relations. The element c_1 connects e_1 to e_4, c_6 connects e_5 to e_4, c_7 connects e_1 to e_5, c_{10} connects e_4 to e_9 and c_{29} connects e_1 to e_9. Figure 8.1 (a) illustrates the projected skeleton. From the projected skeleton we may deduce there exist at most $2^5 = 32$ qualitatively different

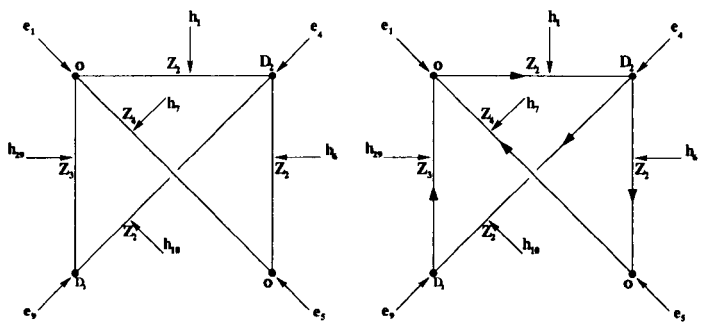

(a) (b)

Figure 8.1: (a) The projected skeleton $\mathbb{X}^p_{\mathbb{O}}$. Here $h_1 = \{(\theta,0,0)|\theta \in (0,\pi)\}$, $h_6 = \{(\pi,\pi,\theta)|\theta \in (0,\pi)\}$, $h_7 = \{(\theta,\theta,\pi)|\theta \in (0,\pi)\}$, $h_{10} = \{(\theta,-\theta,\pi)|\theta \in (0,\pi)\}$ and $h_{29} = \{(\theta,-\theta,2\theta)|\theta \in (0,\pi)\}$. (b) A heteroclinic network on the projected skeleton.

$\mathbb{O}$-equivariant flows on $\mathbb{X}_{\mathbb{O}}$. The structure of the projected skeleton, whilst being different from the projected skeleton encountered for the SC lattice, has similarities. By this we mean that the projected skeleton supports an arrangement of flows that give a heteroclinic network. We illustrate such a network in Figure 8.1 (b), which consists of two heteroclinic cycles that share a common connection. This network is very close to the network studied by Kirk and Silber [55], and it is not unreasonable to expect some of the properties of their network to hold. This illustrates some interesting dynamics that are possible on the projected skeleton.

8.2.3 Forced Symmetry Breaking to $\mathbf{D}_4[\rho_x, \kappa_6]$

In this subsection we consider the behaviour of X_0 when symmetry breaking terms with $\mathbf{D}_4[\rho_x, \kappa_6]$ symmetry are added to (8.3). Since the manifold X_0 is normally hyperbolic, by the Equivariant Persistence Theorem, there is an invariant manifold X_ε, $\mathbf{D}_4[\rho_x, \kappa_6]$-equivariantly diffeomorphic to X_0. The action of the group $\mathbf{D}_4[\rho_x, \kappa_6]$ on $\mathbb{C}^4$ is in Table 8.9.

Table 8.9: Action of $\mathbf{D}_4[\rho_x, \kappa_6]$ on $\mathbb{C}^4$ for the FCC lattice.

Element of $\mathbb{O}$	Action on $\mathbb{C}^4$	Element of $\mathbb{O}$	Action on $\mathbb{C}^4$
ρ_x	(z_4, z_1, z_2, z_3)	ρ_x^2	(z_3, z_4, z_1, z_2)
ρ_x^3	(z_2, z_3, z_4, z_1)	ρ_y^2	$(\overline{z_2}, \overline{z_1}, \overline{z_4}, \overline{z_3})$
ρ_z^2	$(\overline{z_4}, \overline{z_3}, \overline{z_2}, \overline{z_1})$	κ_4	$(\overline{z_3}, \overline{z_2}, \overline{z_1}, \overline{z_4})$
κ_6	$(\overline{z_1}, \overline{z_4}, \overline{z_3}, \overline{z_2})$		

Calculation of the Skeleton

Using the action of $\mathbf{D}_4[\rho_x, \kappa_6]$ in Table 8.9 we may compute the skeleton. To begin, we calculate the set $\mathscr{C}_{\mathbf{D}_4[\rho_x,\kappa_6]}$, for which we recall there are eight subgroups of $\mathbf{D}_4[\rho_x, \kappa_6]$.

Proposition 8.10
Let $\mathbf{D}_4[\rho_x, \kappa_6]$ act on X_0 with the action induced from Table 8.9. Then

$$\mathscr{C}_{\mathbf{D}_4[\rho_x,\kappa_6]} = \{e_1, e_2, e_5, e_8, e_9, e_{10}, c_5, c_6, c_7, c_9, c_{10}, c_{21}, c_{33}, c_{34}, c_{37}, c_{38}\}.$$

Proof. The proof follows from Lemmas 8.4, 8.5, 8.6 and 8.8. □

We can now use this information to form the skeleton

$$\mathbb{X}_{\mathbf{D}_4[\rho_x,\kappa_6]} = \bigcup_{C \in \mathscr{C}_{\mathbf{D}_4[\rho_x,\kappa_6]}} C \subset \mathbf{T}^3 \cong X_0.$$

The complexity of the skeleton again means that we shall not render this object until we have a better understanding of how the action of the group $\mathbf{D}_4[\rho_x, \kappa_6]$ restricts the types of flow.

Symmetry Properties of $\mathbf{D}_4[\rho_x, \kappa_6]$

Here we study the $\mathbf{D}_4[\rho_x, \kappa_6]$ action induced on the skeleton, and determine orbit representative for equilibria and heteroclinic connections.

Pointwise and Setwise Isotropy Subgroups. The action of $\mathbf{D}_4[\rho_x, \kappa_6]$ on $\mathbb{C}^4$ in Table 8.9 induces a natural action on X_0 with respect to the coordinates $(\theta_1, \theta_2, \theta_3)$. The action of the generators for $\mathbf{D}_4[\rho_x, \kappa_6]$ is

$$\begin{aligned} \rho_x(\theta_1, \theta_2, \theta_3) &= (-\theta_2 - \theta_3, -\theta_1 - \theta_3, \theta_1 + \theta_2 + \theta_3), \\ \kappa_6(\theta_1, \theta_2, \theta_3) &= (\theta_2, \theta_1, -(\theta_1 + \theta_2 + \theta_3)). \end{aligned}$$

The complete action of $\mathbf{D}_4[\rho_x, \kappa_6]$ on X_0 is in Table 8.10. The action of $\mathbf{D}_4[\rho_x, \kappa_6]$ on X_0 in turn induces an action of $\mathbf{D}_4[\rho_x, \kappa_6]$ on the set $\mathscr{C}_{\mathbf{D}_4[\rho_x,\kappa_6]}$ by permutation. We present the action of $\mathbf{D}_4[\rho_x, \kappa_6]$ on the set $\mathscr{C}_{\mathbf{D}_4[\rho_x,\kappa_6]}$ in Table 7.11. Using this action we may deduce the following fundamental symmetry result.

Proposition 8.11
Let $\mathbf{D}_4[\rho_x, \kappa_6]$ act on $\mathscr{C}_{\mathbf{D}_4[\rho_x,\kappa_6]}$ as in Table 8.11 and on X_0 as in Table 8.10. Then given $C \in \mathscr{C}_{\mathbf{D}_4[\rho_x,\kappa_6]}$, the setwise isotropy Stab(C), *pointwise isotropy* stab(C) *and the group $S(C)$ are given in Table 8.12.*

Table 8.10: Action of $\mathbf{D}_4[\rho_x, \kappa_6]$ induced on X_0 for the FCC lattice.

Element of $\mathbf{D}_4[\rho_x, \kappa_6]$	Action on X_0
ρ_x	$(-(\theta_2+\theta_3), -(\theta_1+\theta_3), (\theta_1+\theta_2+\theta_3))$
ρ_x^2	$(-\theta_2, -\theta_1, -\theta_3)$
ρ_x^3	$(\theta_1+\theta_3, \theta_2+\theta_3, -(\theta_1+\theta_2+\theta_3))$
ρ_y^2	$(\theta_2+\theta_3, \theta_1+\theta_3, -\theta_3)$
ρ_z^2	$(-(\theta_1+\theta_3), -(\theta_2+\theta_3), \theta_3)$
κ_4	$(-\theta_1, -\theta_2, \theta_1+\theta_2+\theta_3)$
κ_6	$(\theta_2, \theta_1, -(\theta_1+\theta_2+\theta_3))$

Table 8.11: Action of $\mathbf{D}_4[\rho_x, \kappa_6]$ induced on $\mathscr{C}_{\mathbf{D}_4[\rho_x,\kappa_6]}$ for the FCC lattice.

Element of $\mathscr{C}_{\mathbf{D}_4[\rho_x,\kappa_6]}$	Elements of $\mathbf{D}_4[\rho_x, \kappa_6]$ acting nontrivially	Action
e_1	None	
e_2	ρ_x, ρ_x^3, ρ_y^2, ρ_z^2	e_8
e_5	None	
e_8	ρ_x, ρ_x^3, ρ_y^2, ρ_z^2	e_2
e_9	$\mathbf{D}_4[\rho_x, \kappa_6] - \mathbf{D}_2[\rho_x^2, \rho_y^2]$	e_{10}
e_{10}	$\mathbf{D}_4[\rho_x, \kappa_6] - \mathbf{D}_2[\rho_x^2, \rho_y^2]$	e_9
c_5	ρ_x, ρ_x^3, ρ_y^2, ρ_z^2	c_{21}
c_6	ρ_x, ρ_x^3, ρ_y^2, ρ_z^2	c_{34}
c_7	ρ_x, ρ_x^3, κ_6, κ_4,	c_{33}
c_9	None	
c_{10}	None	
c_{21}	ρ_x, ρ_x^3, ρ_y^2, ρ_z^2	c_5
c_{33}	ρ_x, ρ_x^3, κ_6, κ_4,	c_7
c_{34}	ρ_x, ρ_x^3, ρ_y^2, ρ_z^2	c_6
c_{37}	ρ_x, ρ_x^3, κ_6, κ_4,	c_{38}
c_{38}	ρ_x, ρ_x^3, κ_6, κ_4,	c_{37}

Proof. This is a simple calculation. □

This completes the computations of the setwise and pointwise isotropy subgroups of all $C \in \mathscr{C}_{\mathbf{D}_4[\rho_x,\kappa_6]}$. We have now computed almost all the information required, but we still need to compute the knots relative to each C.

Knots Relative to C. Here we compute the knots relative to each $C \in \mathscr{C}_{\mathbf{D}_4[\rho_x,\kappa_6]}$. The action of $\mathbf{D}_4[\rho_x, \kappa_6]$ on $\mathscr{C}_{\mathbf{D}_4[\rho_x,\kappa_6]}$ in Table 8.11 shows that there are six C's homeomorphic to $\mathbf{S}^1$ that are not symmetrically related, namely: c_5, c_6, c_7, c_9, c_{10}, and c_{37}. The representatives of the equilibria are e_1, e_2, e_5, and e_9. Since $S(C) \cong \mathbf{Z}_2$ for each $C \in \mathscr{C}_{\mathbf{D}_4[\rho_x,\kappa_6]}$, with $C \cong \mathbf{S}^1$, there are two knots relative to each such C. Since all knots are equilibria, and each C contain two equilibria, these equilibria are knots. We present this information in Table 8.13. The connection c_{37} is interesting; it has two knots e_9 and e_{10}, but since these points lie in the same group orbit, on projection, the representative c_{37} connects the class representative e_9 to itself.

Projected Skeleton

Here we compute the projected skeleton $\mathbb{X}^p_{\mathbf{D}_4[\rho_x,\kappa_6]}$. The action of $\mathbf{D}_4[\rho_x, \kappa_6]$ on $\mathscr{C}_{\mathbf{D}_4[\rho_x,\kappa_6]}$ shows that there are six orbit representatives for the elements of $\mathscr{C}_{\mathbf{D}_4[\rho_x,\kappa_6]}$ which are homeomorphic to $\mathbf{S}^1$. These are c_5, c_6, c_7, c_9, c_{10}, and c_{37}. The orbit representatives for the equilibria are e_1, e_2,

Table 8.12: Isotropy data for $C \in \mathscr{C}_{\mathbf{D}_4[\rho_x,\kappa_6]}$ on the FCC lattice.

$C \in \mathscr{C}_{\mathbf{D}_4[\rho_x,\kappa_6]}$	stab(C)	Stab(C)	$S(C) = \text{Stab}(C)/\text{stab}(C)$
e_1	$\mathbf{D}_4[\rho_x, \kappa_6]$	$\mathbf{D}_4[\rho_x, \kappa_6]$	$\mathbf{1}$
e_2	$\mathbf{D}_2[\rho_x^2, \rho_y^2]$	$\mathbf{D}_2[\rho_x^2, \rho_y^2]$	$\mathbf{1}$
e_5	$\mathbf{D}_4[\rho_x, \kappa_6]$	$\mathbf{D}_4[\rho_x, \kappa_6]$	$\mathbf{1}$
e_8	$\mathbf{D}_2[\rho_x^2, \kappa_6]$	$\mathbf{D}_2[\rho_x^2, \rho_y^2]$	$\mathbf{1}$
e_9	$\mathbf{D}_2[\rho_x^2, \rho_y^2]$	$\mathbf{D}_2[\rho_x^2, \rho_y^2]$	$\mathbf{1}$
e_{10}	$\mathbf{D}_2[\rho_x^2, \rho_y^2]$	$\mathbf{D}_2[\rho_x^2, \rho_y^2]$	$\mathbf{1}$
c_5	$\mathbf{Z}_2[\kappa_4]$	$\mathbf{D}_2[\rho_x^2, \kappa_4]$	$\mathbf{Z}_2$
c_6	$\mathbf{Z}_2[\kappa_4]$	$\mathbf{D}_2[\rho_x^2, \kappa_4]$	$\mathbf{Z}_2$
c_7	$\mathbf{Z}_2[\rho_y^2]$	$\mathbf{D}_2[\rho_x^2, \rho_y^2]$	$\mathbf{Z}_2$
c_9	$\mathbf{Z}_4[\rho_x]$	$\mathbf{D}_4[\rho_x, \kappa_6]$	$\mathbf{Z}_2$
c_{10}	$\mathbf{Z}_2[\rho_x^2]$	$\mathbf{D}_4[\rho_x, \kappa_6]$	$\mathbf{Z}_2$
c_{21}	$\mathbf{Z}_2[\kappa_6]$	$\mathbf{D}_2[\rho_x^2, \kappa_6]$	$\mathbf{Z}_2$
c_{33}	$\mathbf{Z}_2[\rho_z^2]$	$\mathbf{D}_2[\rho_x^2, \rho_y^2]$	$\mathbf{Z}_2$
c_{34}	$\mathbf{Z}_2[\kappa_6]$	$\mathbf{D}_2[\rho_x^2, \kappa_6]$	$\mathbf{Z}_2$
c_{37}	$\mathbf{Z}_2[\rho_y^2]$	$\mathbf{D}_2[\rho_x^2, \rho_y^2]$	$\mathbf{Z}_2$
c_{38}	$\mathbf{Z}_2[\rho_y^2]$	$\mathbf{D}_2[\rho_x^2, \rho_y^2]]$	$\mathbf{Z}_2$

Table 8.13: Knots relative to orbit representatives of $C \in \mathscr{C}_{\mathbf{D}_4[\rho_x,\kappa_6]}$ for the FCC lattice.

Element of $\mathscr{C}_{\mathbf{D}_4[\rho_x,\kappa_6]}$	Knots
c_5	e_1, e_2
c_6	e_5, e_2
c_7	e_1, e_5
c_9	e_1, e_5
c_{10}	e_2, e_9
c_{37}	e_9, e_9

e_5, and e_9. Each $C \cong \mathbf{S}^1$ has two knots; this implies that there is an axis of reflection symmetry. So each such C projects into the orbit space as a line joining the two knots. More precisely, we have the following relations: c_5 connects e_1 to e_2, c_6 connects e_2 to e_5, c_7 connects e_1 to e_5, c_9 connects e_1 to e_5, c_{10} connects e_2 to e_9, and c_{37} connects e_9 to e_9. Figure 8.2 (a) illustrates the projected skeleton. From the projected skeleton we may deduce there exist at most $2^6 = 64$ qualitatively different $\mathbf{D}_4[\rho_x, \kappa_6]$-equivariant flows on $\mathbb{X}_{\mathbf{D}_4[\rho_x,\kappa_6]}$. In particular there exist flows that give heteroclinic cycles along h_{37}. It is not possible to arrange for any admissible flow to give a heteroclinic network on the projected skeleton, because of the connection h_{10}. However, there do exist interesting arrangements of flows on the projected skeleton; one such example is presented in Figure 8.2 (b). This flow exhibits three different heteroclinic cycles, but is not a heteroclinic network since the whole network is not the union of heteroclinic cycles. It would be interesting to consider the attracting properties of this network, but we shall not consider this issue here.

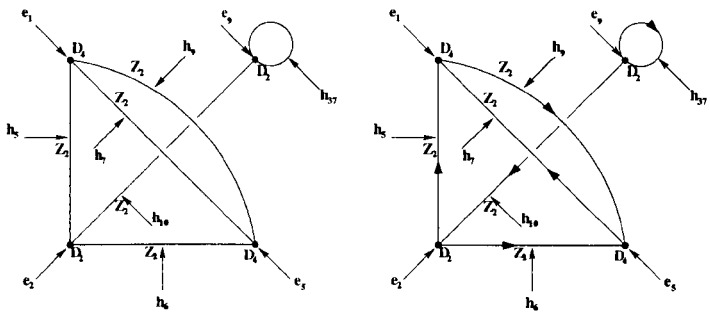

(a) (b)

Figure 8.2: (a) The projected skeleton $\mathbb{X}^p_{\mathbf{D}_4[\rho_x,\kappa_6]}$.Here $h_5 = \{(0,0,\theta)|\theta \in (0,\pi)\}$,$h_6 = \{(\pi,\pi,\theta)|\theta \in (0,\pi)\}$ $h_7 = \{(\theta,\theta,0)|\theta \in (0,\pi)\}$, $h_9 = \{(\theta,-\theta,0)|\theta \in (0,\pi)\}$, $h_{10} = \{(\theta,-\theta,\pi)|\theta \in (0,\pi)\}$ and $h_{37} = \{(\theta+\pi,\theta,\pi)|\theta \in (0,\pi)\}$. (b) An interesting example flow.

8.2.4 Forced Symmetry Breaking to $\mathbb{T}$

In this subsection we study the behaviour of X_0 when symmetry breaking terms with $\mathbb{T}$ symmetry are added to the vector field (8.4). The normal hyperbolicity of X_0 guarantees, by the Equivariant Persistence Theorem, the existence of a manifold X_ε diffeomorphic to X_0 and invariant under the new dynamics. We can consider the behaviour of the $\mathbb{T}$-equivariant vector field on X_ε by considering its behaviour on X_0. The action of the group $\mathbb{T}$ on $\mathbb{C}^4$ is in Table 8.14.

Table 8.14: Action of $\mathbb{T}$ on $\mathbb{C}^4$ for the FCC lattice.

Element of $\mathbb{T}$	Action on $\mathbb{C}^4$
τ_1	$(z_1, z_4, \overline{z_2}, \overline{z_3})$
τ_1^2	$(z_1, \overline{z_3}, \overline{z_4}, z_2)$
τ_2	$(\overline{z_2}, z_4, z_3, \overline{z_1})$
τ_2^2	$(\overline{z_4}, \overline{z_1}, z_3, z_2)$
τ_3	$(\overline{z_2}, \overline{z_3}, z_1, z_4)$
τ_3^2	$(z_3, \overline{z_1}, \overline{z_2}, z_4)$
τ_4	$(\overline{z_4}, z_2, z_1, \overline{z_3})$
τ_4^2	$(z_3, z_2, \overline{z_4}, \overline{z_1})$
ρ_x^2	(z_3, z_4, z_1, z_2)
ρ_y^2	$(\overline{z_2}, \overline{z_1}, \overline{z_4}, \overline{z_3})$
ρ_z^2	$(\overline{z_4}, \overline{z_3}, \overline{z_2}, \overline{z_1})$

Calculation of the Skeleton

Here we calculate the skeleton of X_0 under the action of $\mathbb{T}$. To begin we recall that there are ten subgroups of $\mathbb{T}$.

Proposition 8.12
Let $\mathbb{T}$ act on X_0 with the action induced from Table 8.14. Then

$$\mathscr{C}_{\mathbb{T}} = \{e_1, e_5, e_9, e_{10}, c_7, c_9, c_{10}, c_{29}, c_{30}, c_{31}, c_{32}, c_{33}, c_{37}, c_{38}\}.$$

Proof. The proof follows from Lemmas 8.4, 8.7, 8.6 and 8.8. □

We can now use this information to form the skeleton, this is given by

$$\mathbb{X}_{\mathbb{T}} = \bigcup_{C \in \mathscr{C}_{\mathbb{T}}} C \subset \mathbf{T}^3 \cong X_0.$$

We now consider the action of the group $\mathbb{T}$ on $\mathbb{X}_{\mathbb{T}}$ and discuss what simplifications can be made using this action.

Symmetry Properties of $\mathbb{X}_{\mathbb{T}}$

Here we study the $\mathbb{T}$ action induced on the skeleton to determine the orbit representative for equilibria and heteroclinic connections.

Pointwise and Setwise Isotropy Subgroups. The action of $\mathbb{T}$ on $\mathbb{C}^4$ in Table 8.14 induces a natural action on X_0 with respect to the coordinates $(\theta_1, \theta_2, \theta_3)$. The generators for $\mathbb{T}$ act as follows:

$$\begin{aligned} \tau_1(\theta_1, \theta_2, \theta_3) &= (\theta_2 + \theta_3, -\theta_1, \theta_1 - \theta_2), \\ \tau_2(\theta_1, \theta_2, \theta_3) &= (-(\theta_1 + \theta_3), -\theta_1, \theta_1 + \theta_2 + \theta_3). \end{aligned}$$

The complete action of $\mathbb{T}$ on X_0 is in Table 8.15. The action of $\mathbb{T}$ on X_0 in turn induces an

Table 8.15: Action of $\mathbb{T}$ induced on X_0 for the FCC lattice.

Element of $\mathbb{T}$	Action on X_0
τ_1	$(\theta_2 + \theta_3, -\theta_1, \theta_1 - \theta_2)$
τ_1^2	$(-\theta_2, -(\theta_2 + \theta_3), \theta_1 + \theta_2 + \theta_3)$
τ_2	$(\theta_2 + \theta_3, -\theta_1, \theta_1 + \theta_2 + \theta_3)$
τ_2^2	$(-\theta_2, \theta_1 + \theta_3, -\theta_2 + \theta_2)$
τ_3	$(\theta_1, -\theta_2 - \theta_3, \theta_2 - \theta_1)$
τ_3^2	$(\theta_1, \theta_1 + \theta_3, -(\theta_1 + \theta_2 + \theta_3))$
τ_4	$(\theta_2 + \theta_3, \theta_2, -(\theta_1 + \theta_2 + \theta_3))$
τ_4^2	$(-\theta_1 - \theta_3, \theta_2, -(-\theta_1 + \theta_2))$
ρ_x^2	$(-\theta_2, -\theta_1, -\theta_3)$
ρ_y^2	$(\theta_2 + \theta_3, \theta_1 + \theta_3, -(\theta_1 + \theta_2 + \theta_3))$
ρ_z^2	$(-(\theta_1 + \theta_3), -(\theta_2 + \theta_3), \theta_3)$

action of $\mathbb{T}$ on the set $\mathscr{C}_{\mathbb{T}}$ by permutation. We present this action in Table 8.16. Using this action we may deduce the following fundamental symmetry result.

Proposition 8.13
Let $\mathbb{T}$ act on $\mathscr{C}_{\mathbb{T}}$ as in Table 8.16 on X_0 as in Table 8.15. Then given $C \in \mathscr{C}_{\mathbb{T}}$, the setwise isotropy $\mathrm{Stab}(C)$, *pointwise isotropy* $\mathrm{stab}(C)$ *and the group $S(C)$ are given in Table 8.17.*

Proof. This is a simple calculation. □

This completes the computations of the setwise and pointwise isotropy subgroups for all $C \in \mathscr{C}_{\mathbb{T}}$. The connections c_7, c_9, c_{10}, c_{33}, c_{37}, and c_{38} all have $S(C) \cong \mathbf{Z}_2$, so there is an axis of reflection symmetry present on these C's.

Table 8.16: Action of $\mathbb{T}$ induced on $\mathscr{C}_{\mathbb{T}}$ for the FCC lattice.

Element of $\mathscr{C}_{\mathbb{T}}$	Elements of $\mathbb{T}$ acting nontrivially	Action
e_1	None	
e_5	None	
e_9	$\mathbb{T} - \mathbf{D}_2[\rho_x^2, \rho_y^2]$	e_{10}
e_{10}	$\mathbb{T} - \mathbf{D}_2[\rho_x^2, \rho_y^2]$	e_9
c_7	$\tau_1^2, \tau_2, \tau_3^2, \tau_4$	c_{33}
	$\tau_1, \tau_2^2, \tau_3, \tau_4^2$	c_9
c_9	$\tau_1, \tau_2^2, \tau_3, \tau_4^2$	c_{33}
	$\tau_1^2, \tau_2, \tau_3^2, \tau_4$	c_7
c_{10}	$\tau_1, \tau_2^2, \tau_3, \tau_4^2$	c_{38}
	$\tau_1^2, \tau_2, \tau_3^2, \tau_4$	c_{37}
c_{29}	$\rho_y^2, \tau_2^2, \tau_3$	c_{32}
	ρ_x^2, τ_3, τ_4	c_{30}
	$\rho_z^2, \tau_2, \tau_4^2$	c_{31}
c_{30}	ρ_y^2, τ_1, τ_4	c_{31}
	$\rho_x^2, \tau_3^2, \tau_4^2$	c_{29}
	$\rho_z^2, \tau_1^2, \tau_3$	c_{32}
c_{31}	$\rho_z^2, \tau_2^2, \tau_4$	c_{29}
	ρ_x^2, τ_1, τ_2	c_{32}
	$\rho_y^2, \tau_1^2, \tau_4^2$	c_{30}
c_{32}	$\rho_z^2, \tau_1, \tau_3^2$	c_{30}
	$\rho_x^2, \tau_1^2, \tau_2^2$	c_{31}
	ρ_y^2, τ_2, τ_3	c_{29}
c_{33}	$\tau_1, \tau_2^2, \tau_3, \tau_4^2$	c_7
	$\tau_1^2, \tau_2, \tau_3^2, \tau_4$	c_9
c_{37}	$\tau_1, \tau_2^2, \tau_3, \tau_4^2$	c_{38}
	$\tau_1, \tau_2^2, \tau_3, \tau_4^2$	c_{10}
c_{38}	$\tau_1, \tau_2^2, \tau_3, \tau_4^2$	c_{37}
	$\tau_1, \tau_2^2, \tau_3, \tau_4^2$	c_{10}

Table 8.17: Isotropy data for $C \in \mathscr{C}_{\mathbb{T}}$ on the FCC lattice.

$C \in \mathscr{C}_{\mathbb{T}}$	stab(C)	Stab(C)	$S(C) = \text{Stab}(C)/\text{stab}(C)$
e_1	$\mathbb{T}$	$\mathbb{T}$	$\mathbf{1}$
e_5	$\mathbb{T}$	$\mathbb{T}$	$\mathbf{1}$
e_9	$\mathbf{D}_2[\rho_x^2, \rho_y^2]$	$\mathbf{D}_2[\rho_x^2, \rho_y^2]$	$\mathbf{1}$
e_{10}	$\mathbf{D}_2[\rho_x^2, \rho_y^2]$	$\mathbf{D}_2[\rho_x^2, \rho_y^2]$	$\mathbf{1}$
c_7	$\mathbf{Z}_2[\rho_x^2]$	$\mathbf{D}_2[\rho_x^2, \rho_y^2]$	$\mathbf{Z}_2$
c_9	$\mathbf{Z}_2[\rho_x^2]$	$\mathbf{D}_2[\rho_x^2, \rho_y^2]$	$\mathbf{Z}_2$
c_{10}	$\mathbf{Z}_2[\rho_x^2]$	$\mathbf{D}_2[\rho_x^2, \rho_y^2]$	$\mathbf{Z}_2$
c_{29}	$\mathbf{Z}_3[\tau_1]$	$\mathbf{Z}_3[\tau_1]$	$\mathbf{1}$
c_{30}	$\mathbf{Z}_3[\tau_2]$	$\mathbf{Z}_3[\tau_2]$	$\mathbf{1}$
c_{31}	$\mathbf{Z}_3[\tau_3]$	$\mathbf{Z}_3[\tau_3]$	$\mathbf{1}$
c_{32}	$\mathbf{Z}_3[\tau_4]$	$\mathbf{Z}_3[\tau_4]$	$\mathbf{1}$
c_{33}	$\mathbf{Z}_2[\rho_z^2]$	$\mathbf{D}_2[\rho_x^2, \rho_y^2]$	$\mathbf{Z}_2$
c_{37}	$\mathbf{Z}_2[\rho_y^2]$	$\mathbf{D}_2[\rho_x^2, \rho_y^2]$	$\mathbf{Z}_2$
c_{38}	$\mathbf{Z}_2[\rho_z^2]$	$\mathbf{D}_2[\rho_x^2, \rho_y^2]$	$\mathbf{Z}_2$

Table 8.18: Knots relative to orbit representatives of $C \in \mathscr{C}_{\mathbb{T}}$ for the FCC lattice.

Element of $\mathscr{C}_{\mathbb{T}}$	Knots
c_7	e_1, e_5
c_{10}	e_9, e_{10}

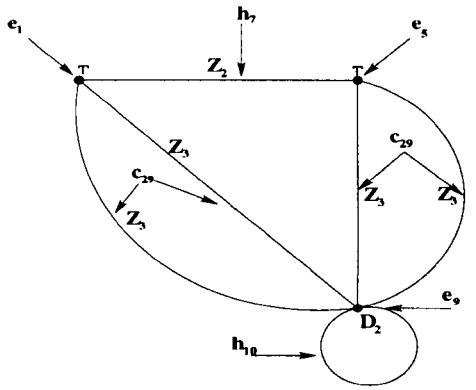

Figure 8.3: The projected skeleton $\mathbb{X}_{\mathbb{T}}^{p}$.Here $h_7 = \{(\theta,\theta,0)|\theta \in (0,\pi)\}$, $h_{10} = \{(\theta,-\theta,\pi)|\theta \in (0,\pi)\}$, and $c_{29} = \{(\theta,-\theta,2\theta)|\theta \in (0,\pi)\}$.

Knots Relative to C. The action of $\mathbb{T}$ on $\mathscr{C}_{\mathbb{T}}$ in Table 8.16 shows that there are three C's that are not symmetrically related, namely: $c_7 = \{(\theta,\theta,0)|\theta \in [0,2\pi)\}$, $c_{10} = \{(\theta,-\theta,\pi)|\theta \in [0,2\pi)\}$, and $c_{29} = \{(\theta,-\theta,2\theta)|\theta \in [0,2\pi)\}$. The representatives of the equilibria are given by e_1, e_5, and e_9. The orbit representative c_{29} has no knots, since $S(c_{29}) \cong \mathbf{1}$. The computation of the knots is straightforward since each remaining connection contains two equilibria. We present this information in Table 8.18.

Projected Skeleton

The action of $\mathbb{T}$ on $\mathscr{C}_{\mathbb{T}}$ shows that there are three orbit representatives for the elements of $\mathscr{C}_{\mathbb{T}}$ that are homeomorphic to $\mathbf{S}^1$; these are c_7, c_{10} and c_{29}. The orbit representatives for the equilibria are e_1, e_5 and e_9. Furthermore c_7 and c_{10} have two knots; this implies that there is an axis of reflection symmetry. Therefore these C's project into the orbit space as a line joining the two knots. More precisely, we have the following relations. The element c_7 connects e_1 to e_5, c_{10} connects e_9 to e_9, c_{29} connects e_1 to e_9 then to e_5, back to e_9 and finally returns to e_1. It is worth noting that c_{10} connects e_9 to e_9 since the equilibrium e_{10} projects to the same representative as e_9 in the orbit space. Figure 8.3 (a) illustrates the projected skeleton. From the projected skeleton we deduce that there exist at most $2^6 = 64$ qualitatively different $\mathbb{T}$-equivariant flows on $\mathbb{X}_{\mathbb{T}}$. The projected skeleton has some interesting properties. The first and most important is that the connection c_{29} has no restrictions on the flow imposed by symmetry. For this reason this connection joins each of the equilibria in a (topological) circle. This allows for some interesting dynamic possibilities, not all of which are generic.

8.2.5 Forced Symmetry Breaking to $\mathbf{D}_3[\tau_1, \kappa_5]$

In this subsection we study the behaviour of the group orbit X_0 when symmetry breaking terms with $\mathbf{D}_3[\tau_1, \kappa_5]$ symmetry are added to the vector field (8.4). Normal hyperbolicity of X_0 guarantees, by the Equivariant Persistence Theorem, the existence of a manifold X_ε diffeomorphic to X_0 and invariant under the new dynamics. The action of the group $\mathbf{D}_3[\tau_1, \kappa_5]$ on $\mathbb{C}^4$ is in Table 8.19.

Table 8.19: Action of $\mathbf{D}_3[\tau_1, \kappa_5]$ on $\mathbb{C}^4$ for the FCC lattice.

Element of $\mathbb{O}$	Action on $\mathbb{C}^4$
τ_1	$(z_1, z_4, \overline{z_2}, \overline{z_3})$
τ_1^2	$(z_1, \overline{z_3}, \overline{z_4}, z_2)$
κ_2	$(\overline{z_1}, z_3, z_2, \overline{z_4})$
κ_5	$(\overline{z_1}, \overline{z_2}, z_4, z_3)$
κ_6	$(\overline{z_1}, \overline{z_4}, \overline{z_3}, \overline{z_2})$

Table 8.20: Action of $\mathbf{D}_3[\tau_1, \kappa_5]$ induced on X_0 for the FCC lattice.

Element of $\mathbf{D}_3[\tau_1, \kappa_5]$	Action on X_0
τ_1	$(\theta_2 + \theta_3, -\theta_1, \theta_1 - \theta_2)$
τ_1^2	$(-\theta_2, -(\theta_2 + \theta_3), \theta_1 + \theta_2 + \theta_3)$
κ_2	$(-\theta_1, \theta_2 + \theta_3, -\theta_3)$
κ_5	$(-(\theta_2 + \theta_3), -\theta_2, \theta_2 - \theta_1)$
κ_6	$(\theta_2, \theta_1, -(\theta_1 + \theta_2 + \theta_3))$

Calculation of the Skeleton

Here we calculate the skeleton of X_0 under the action of $\mathbf{D}_3[\tau_1, \kappa_5]$. To begin, we calculate the set $\mathscr{C}_{\mathbf{D}_3[\tau_1,\kappa_5]}$, for which we recall there are six subgroups of $\mathbf{D}_3[\tau_1, \kappa_5]$.

Proposition 8.14
Let $\mathbf{D}_3[\tau_1, \kappa_5]$ act on X_0 with the action induced from Table 8.19. Then

$$\mathscr{C}_{\mathbf{D}_3[\tau_1,\kappa_5]} = \{e_1, e_5, c_3, c_{13}, c_{21}, c_{25}, c_{29}, c_{34}, c_{35}\}.$$

Proof. The proof follows from Lemmas 8.4, 8.7 and 8.6. □

We can now use this information to form the skeleton

$$\mathbb{X}_{\mathbf{D}_3[\tau_1,\kappa_5]} = \bigcup_{C \in \mathscr{C}_{\mathbf{D}_3[\tau_1,\kappa_5]}} C \subset \mathbf{T}^3 \cong X_0.$$

Symmetry Properties of $\mathbb{X}_{\mathbf{D}_3[\tau_1,\kappa_5]}$

The action of $\mathbf{D}_3[\tau_1, \kappa_5]$ given in Table 8.19 induces a natural action on X_0 with respect to the coordinates $(\theta_1, \theta_2, \theta_3)$. The action of the generators for $\mathbf{D}_3[\tau_1, \kappa_5]$ is

$$\begin{aligned} \tau_1(\theta_1, \theta_2, \theta_3) &= (-\theta_2, -(\theta_2 + \theta_3), \theta_1 + \theta_2 + \theta_3), \\ \kappa_5(\theta_1, \theta_2, \theta_3) &= (-(\theta_2 + \theta_3), -\theta_2, \theta_2 - \theta_1). \end{aligned}$$

The complete action of $\mathbf{D}_3[\tau_1, \kappa_5]$ on X_0 is in Table 8.20. The action of $\mathbf{D}_3[\tau_1, \kappa_5]$ on X_0 in turn induces an action of $\mathbf{D}_3[\tau_1, \kappa_5]$ on the set $\mathscr{C}_{\mathbf{D}_3[\tau_1,\kappa_5]}$ by permutation of its elements. We present this action in Table 8.21.

Proposition 8.15
Let $\mathbf{D}_3[\tau_1, \kappa_5]$ act on $\mathscr{C}_{\mathbf{D}_3[\tau_1,\kappa_5]}$ as in Table 8.21 and on X_0 as in Table 8.20. Then given $C \in \mathscr{C}_{\mathbf{D}_3[\tau_1,\kappa_5]}$, the setwise isotropy $\mathrm{Stab}(C)$, *pointwise isotropy* $\mathrm{stab}(C)$ *and $S(C)$ are in Table 8.22.*

Proof. This is a simple calculation. □

Table 8.21: Action of $\mathbf{D}_3[\tau_1, \kappa_5]$ induced on $\mathscr{C}_{\mathbf{D}_3[\tau_1,\kappa_5]}$ for the FCC lattice.

Element of $\mathscr{C}_{\mathbf{D}_3[\tau_1,\kappa_5]}$	Elements of $\mathbf{D}_3[\tau_1, \kappa_5]$	Action
e_1	None	
e_5	None	
c_3	κ_6, τ_1,	c_{13}
	τ_1^2, κ_5	c_{21}
c_{13}	κ_6, τ_1^2	c_3
	κ_2, τ_1	c_{21}
c_{21}	κ_5, τ_1	c_3
	κ_2, τ_1^2	c_{13}
c_{25}	κ_6, τ_1	c_{35}
	κ_5, τ_1^2	c_{34}
c_{29}	None	
c_{34}	κ_5, τ_1	c_{25}
	κ_2, τ_1^2	c_{35}
c_{35}	κ_6, τ_1^2	c_{25}
	κ_2, τ_1	c_{34}

This completes the computations of the setwise and pointwise isotropy subgroups for all $C \in \mathscr{C}_{\mathbf{D}_3[\tau_1,\kappa_5]}$. These computations show that $S(c_{29}) \cong \mathbf{Z}_2$ and $S(C)$ is trivial otherwise, so there is an axis of symmetry along c_{29}. This axis is given by the knots, which are e_1 and e_5.

Projected Skeleton

Here we compute the projected skeleton $\mathbb{X}^p_{\mathbf{D}_3[\tau_1,\kappa_5]}$. The action of $\mathbf{D}_3[\tau_1, \kappa_5]$ on $\mathscr{C}_{\mathbf{D}_3[\tau_1,\kappa_5]}$ shows that there are three orbit representatives for the elements of $\mathscr{C}_{\mathbf{D}_3[\tau_1,\kappa_5]}$ that are homeomorphic to $\mathbf{S}^1$, these are c_3, c_{25}, and c_{29}. The orbit representatives for the equilibria are e_1 and e_5. Furthermore, c_{29} has two knots; this implies that there is an axis of reflection symmetry. So c_{29} projects into the orbit space as a line joining the two knots. More precisely, we have the following relations. The element c_3 connects e_1 to itself, c_{25} connects e_5 to itself, and c_{29} connects e_1 to e_5. Figure 8.4 illustrates the projected skeleton. From the projected skeleton we deduce there exist at most $2^3 = 8$ qualitatively different $\mathbf{D}_3[\tau_1, \kappa_5]$-equivariant flows on $\mathbb{X}_{\mathbf{D}_3[\tau_1,\kappa_5]}$. Clearly, there exist perturbations which give heteroclinic cycles between the equilibria e_1 and itself and the equilibria e_5 and itself.

Table 8.22: Isotropy data for $C \in \mathscr{C}_{\mathbf{D}_3[\tau_1,\kappa_5]}$ on the FCC lattice.

$C \in \mathscr{C}_{\mathbf{D}_3[\tau_1,\kappa_5]}$	stab(C)	Stab(C)	$S(C) = \text{Stab}(C)/\text{stab}(C)$
e_1	$\mathbf{D}_3[\tau_1, \kappa_5]$	$\mathbf{D}_3[\tau_1, \kappa_5]$	$\mathbf{1}$
e_5	$\mathbf{D}_3[\tau_1, \kappa_5]$	$\mathbf{D}_3[\tau_1, \kappa_5]$	$\mathbf{1}$
c_3	$\mathbf{Z}_2[\kappa_2]$	$\mathbf{Z}_2[\kappa_2]$	$\mathbf{1}$
c_{13}	$\mathbf{Z}_2[\kappa_5]$	$\mathbf{Z}_2[\kappa_5]$	$\mathbf{1}$
c_{21}	$\mathbf{Z}_2[\kappa_6]$	$\mathbf{Z}_2[\kappa_6]$	$\mathbf{1}$
c_{25}	$\mathbf{Z}_2[\kappa_2]$	$\mathbf{Z}_2[\kappa_2]$	$\mathbf{1}$
c_{29}	$\mathbf{Z}_3[\tau_1]$	$\mathbf{D}_3[\tau_1, \kappa_5]$	$\mathbf{Z}_2$
c_{34}	$\mathbf{Z}_2[\kappa_6]$	$\mathbf{Z}_2[\kappa_6]$	$\mathbf{1}$
c_{35}	$\mathbf{Z}_2[\kappa_5]$	$\mathbf{Z}_2[\kappa_5]$	$\mathbf{1}$

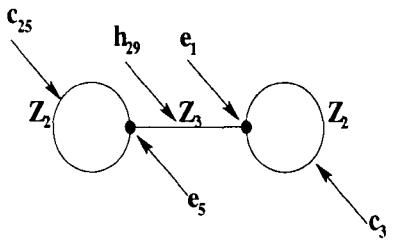

Figure 8.4: The projected skeleton $\mathbb{X}^p_{\mathbf{D}_3[\tau_1,\kappa_5]}$. Here $c_3 = \{(0,\theta,0)|\theta \in (0,2\pi)\}$, $c_{25} = \{(\pi,\theta,0)|\theta \in (0.2\pi)\}$ and $h_{29} = \{(\theta,-\theta,2\theta)|\theta \in (0,\pi)\}$.

8.2.6 Forced Symmetry Breaking to $\mathbf{D}_2[\rho_x^2,\kappa_6]$

In this subsection we study the behaviour of the group orbit X_0 when symmetry breaking terms with $\mathbf{D}_2[\rho_x^2,\kappa_6]$ symmetry are added to the vector field (8.4). Normal hyperbolicity of X_0 guarantees, by the Equivariant Persistence Theorem, the existence of a manifold X_ε diffeomorphic to X_0 and invariant under the new dynamics. The action of the group $\mathbf{D}_2[\rho_x^2,\kappa_6]$ on $\mathbb{C}^4$ is in Table 8.23.

Table 8.23: Action of $\mathbf{D}_2[\rho_x^2,\kappa_6]$ on $\mathbb{C}^4$ for the FCC lattice.

Element of $\mathbf{D}_2[\rho_x^2,\kappa_6]$	Action on $\mathbb{C}^4$
ρ_x^2	(z_3,z_4,z_1,z_2)
κ_4	$(\overline{z_3},\overline{z_2},\overline{z_1},\overline{z_4})$
κ_6	$(\overline{z_1},\overline{z_4},\overline{z_4},\overline{z_2})$

Calculation of the Skeleton

Here we calculate the skeleton of X_0 under the action of $\mathbf{D}_2[\rho_x^2,\kappa_6]$. To begin, we calculate the set $\mathscr{C}_{\mathbf{D}_2[\rho_x^2,\kappa_6]}$, for which we recall that there are five subgroups of $\mathbf{D}_2[\rho_x^2,\kappa_6]$.

Proposition 8.16
Let $\mathbf{D}_2[\rho_x^2,\kappa_6]$ act on X_0 with the action induced from Table 8.23. Then

$$\mathscr{C}_{\mathbf{D}_2[\rho_x^2,\kappa_6]} = \{e_1,e_2,e_5,e_8,c_5,c_6,c_9,c_{21},c_{34}\}.$$

Proof. The proof follows from Lemmas 8.6 and 8.8. □

From this the skeleton is

$$\mathbb{X}_{\mathbf{D}_2[\rho_x^2,\kappa_6]} = \bigcup_{C\in\mathscr{C}_{\mathbf{D}_2[\rho_x^2,\kappa_6]}} C \subset \mathbf{T}^3 \cong X_0.$$

Symmetry Properties of $\mathbb{X}_{\mathbf{D}_2[\rho_x^2,\kappa_6]}$

Here we use the $\mathbf{D}_2[\rho_x^2,\kappa_6]$ symmetry to study the $\mathbf{D}_2[\rho_x^2,\kappa_6]$ action induced on the skeleton.

Pointwise and Setwise Isotropy Subgroups. The action of the generators for $\mathbf{D}_2[\rho_x^2,\kappa_6]$ on X_0 is

$$\begin{aligned}\rho_x^2(\theta_1,\theta_2,\theta_3) &= (-\theta_2,-\theta_1,-\theta_3),\\ \kappa_6(\theta_1,\theta_2,\theta_3) &= (\theta_2,\theta_1,-(\theta_1+\theta_2+\theta_3)).\end{aligned}$$

Table 8.24: Action of $\mathbf{D}_2[\rho_x^2, \kappa_6]$ induced on X_0 for the FCC lattice.

Element of $\mathbf{D}_2[\rho_x^2, \kappa_6]$	Action on X_0
ρ_x^2	$(-\theta_2, -\theta_1, -\theta_3)$
κ_4	$(-\theta_1, -\theta_2, \theta_1 + \theta_2 + \theta_3)$
κ_6	$(\theta_2, \theta_1, -(\theta_1 + \theta_2 + \theta_3))$

The complete action of $\mathbf{D}_2[\rho_x^2, \kappa_6]$ on X_0 is in Table 8.24. The action of $\mathbf{D}_2[\rho_x^2, \kappa_6]$ on X_0 induces an action of $\mathbf{D}_2[\rho_x^2, \kappa_6]$ on $\mathscr{C}_{\mathbf{D}_2[\rho_x^2, \kappa_6]}$ by permutation; this action is trivial.

Proposition 8.17
Let $\mathbf{D}_2[\rho_x^2, \kappa_6]$ act on $\mathscr{C}_{\mathbf{D}_2[\rho_x^2, \kappa_6]}$ with its induced trivial action and on X_0 as in Table 8.24. Then given $C \in \mathscr{C}_{\mathbf{D}_2[\rho_x^2, \kappa_6]}$, the setwise isotropy Stab(C), *pointwise isotropy* stab(C) *and the group $S(C)$ are given in Table 8.25.*

Proof. The simple calculations follow the standard pattern. □

Table 8.25: Isotropy data for $C \in \mathscr{C}_{\mathbf{D}_2[\rho_x^2, \kappa_6]}$ on the FCC lattice.

$C \in \mathscr{C}_{\mathbf{D}_2[\rho_x^2, \kappa_6]}$	stab(C)	Stab(C)	$S(C) =$ Stab(C)/stab(C)
e_1	$\mathbf{D}_2[\rho_x^2, \kappa_6]$	$\mathbf{D}_2[\rho_x^2, \kappa_6]$	$\mathbf{1}$
e_2	$\mathbf{D}_2[\rho_x^2, \kappa_6]$	$\mathbf{D}_2[\rho_x^2, \kappa_6]$	$\mathbf{1}$
e_5	$\mathbf{D}_2[\rho_x^2, \kappa_6]$	$\mathbf{D}_2[\rho_x^2, \kappa_6]$	$\mathbf{1}$
e_8	$\mathbf{D}_2[\rho_x^2, \kappa_6]$	$\mathbf{D}_2[\rho_x^2, \kappa_6]$	$\mathbf{1}$
c_5	$\mathbf{Z}_2[\kappa_4]$	$\mathbf{D}_2[\rho_x^2, \kappa_6^2]$	$\mathbf{Z}_2$
c_6	$\mathbf{Z}_2[\kappa_4]$	$\mathbf{D}_2[\rho_x^2, \kappa_6^2]$	$\mathbf{Z}_2$
c_9	$\mathbf{Z}_2[\rho_x^2]$	$\mathbf{D}_2[\rho_x^2, \kappa_6]$	$\mathbf{Z}_2$
c_{21}	$\mathbf{Z}_2[\kappa_6]$	$\mathbf{D}_2[\rho_x^2, \kappa_6]$	$\mathbf{Z}_2$
c_{34}	$\mathbf{Z}_2[\kappa_6]$	$\mathbf{D}_2[\rho_x^2, \kappa_6]$	$\mathbf{Z}_2$

These computations show that $S(C) \cong \mathbf{Z}_2$ for all $C \in \mathscr{C}_{\mathbf{D}_2[\rho_x^2, \kappa_6^2]}$ homeomorphic to $\mathbf{S}^1$.

Knots Relative to C. The $\mathbf{D}_2[\rho_x^2, \kappa_6^2]$ symmetry does not give any simplify the computation of the knots, but since $S(C) \cong \mathbf{Z}_2$, each C has two knots relative to itself, and since each connection has two equilibria, these are the knots. The knots relative to C are given in Table 8.26.

Projected Skeleton

The action of $\mathbf{D}_2[\rho_x^2, \kappa_6]$ on $\mathscr{C}_{\mathbf{D}_2[\rho_x^2, \kappa_6]}$ shows that there are six orbit representatives for the elements of $\mathscr{C}_{\mathbf{D}_2[\rho_x^2, \kappa_6]}$ that are homeomorphic to $\mathbf{S}^1$; these are c_5, c_6, c_9, c_{10}, c_{21}, and c_{34}. The orbit representatives for the equilibria are e_1, e_2, e_5, and e_8. Each $C \cong \mathbf{S}^1$ has two knots, so there is an axis of reflection symmetry. Each C projects into the orbit space as a line joining the two knots. More precisely, we have the following relations: c_5 connects e_1 to e_2, c_6 connects e_5 to e_8, c_9 connects e_1 to e_5, c_{21} connects e_1 to e_8, and c_{34} connects e_2 to e_5. Figure 8.5 illustrates the projected skeleton. From the projected skeleton we deduce that there exist at most $2^6 = 64$ qualitatively different $\mathbf{D}_2[\rho_x^2, \kappa_6]$-equivariant flows on $\mathbb{X}_{\mathbf{D}_2[\rho_x^2, \kappa_6]}$.

Table 8.26: Knots relative to orbit representatives of $C \in \mathscr{C}_{\mathbf{D}_2[\rho_x^2,\kappa_6^2]}$ for the FCC lattice.

Element of $\mathscr{C}_{\mathbf{D}_2[\rho_x^2,\kappa_6^2]}$	Knots
c_5	e_1, e_2
c_6	e_5, e_8
c_9	e_1, e_5
c_{10}	e_2, e_8
c_{21}	e_1, e_8
c_{34}	e_2, e_5

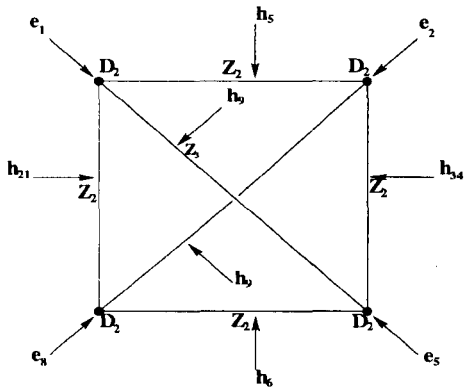

Figure 8.5: The projected skeleton $\mathbb{X}^p_{\mathbf{D}_2[\rho_x^2,\kappa_6]}$. Here $h_5 = \{(0,0,\theta)|\theta \in (0,\pi)\}$, $h_6 = \{(\pi,\pi,\theta)|\theta \in (0,\pi)\}$, $h_9 = \{(\theta,-\theta,0)|\theta \in (0,\pi)\}$, $h_{21} = \{(\theta,\theta,-\theta)|\theta \in (0,\pi)\}$ and $h_{34} = \{(\theta,\theta,\pi-\theta)|\theta \in (0,\pi)\}$.

8.2.7 Forced Symmetry Breaking to $\mathbf{D}_2[\rho_x^2, \rho_y^2]$

In this subsection we study the behaviour of X_0 when symmetry breaking terms with $\mathbf{D}_2[\rho_x^2, \rho_y^2]$ symmetry are added to the vector field (8.4). Normal hyperbolicity of X_0 guarantees, by the Equivariant Persistence Theorem, the existence of a manifold X_ε diffeomorphic to X_0 and invariant under the new dynamics. The action of the group $\mathbf{D}_2[\rho_x^2, \rho_y^2]$ on $\mathbb{C}^4$ is given in Table 8.27.

Table 8.27: Action of $\mathbf{D}_2[\rho_x^2, \rho_y^2]$ on $\mathbb{C}^4$ for the FCC lattice.

Element of $\mathbf{D}_2[\rho_x^2, \rho_y^2]$	Action on $\mathbb{C}^4$
ρ_x^2	(z_3, z_4, z_1, z_2)
ρ_y^2	$(\overline{z_2}, \overline{z_1}, \overline{z_4}, \overline{z_3})$
ρ_z^2	$(\overline{z_4}, \overline{z_3}, \overline{z_2}, \overline{z_1})$

Calculation of the Skeleton

Here we calculate the skeleton of X_0 under the action of $\mathbf{D}_2[\rho_x^2, \rho_y^2]$. To begin, we calculate $\mathscr{C}_{\mathbf{D}_2[\rho_x^2,\rho_y^2]}$, recalling the subgroups of $\mathbf{D}_2[\rho_x^2, \rho_y^2]$.

Proposition 8.18
Let $\mathbf{D}_2[\rho_x^2, \rho_y^2]$ act on X_0 with the action induced from Table 8.27. Then

$$\mathscr{C}_{\mathbf{D}_2[\rho_x^2,\rho_y^2]} = \{e_1, e_5, e_9, e_{10}, c_7, c_9, c_{10}, c_{33}, c_{37}, c_{38}\}.$$

Table 8.28: Action of $\mathbf{D}_2[\rho_x^2, \rho_y^2]$ induced on X_0.

Element of $\mathbf{D}_2[\rho_x^2, \rho_y^2]$	Action on X_0
ρ_x^2	$(-\theta_2, -\theta_1, -\theta_3)$
ρ_y^2	$(\theta_2 + \theta_3, \theta_1 + \theta_3, -\theta_3)$
ρ_z^2	$(-(\theta_1 + \theta_3), -(\theta_2 + \theta_3), \theta_3)$

Table 8.29: Isotropy data for $C \in \mathscr{C}_{\mathbf{D}_2[\rho_x^2, \rho_y^2]}$ on the FCC lattice.

$C \in \mathscr{C}_{\mathbf{D}_2[\rho_x^2, \rho_y^2]}$	stab(C)	Stab(C)	$S(C) = \text{Stab}(C)/\text{stab}(C)$
e_1	$\mathbf{D}_2[\rho_x^2, \rho_y^2]$	$\mathbf{D}_2[\rho_x^2, \rho_y^2]$	$\mathbf{1}$
e_5	$\mathbf{D}_2[\rho_x^2, \rho_y^2]$	$\mathbf{D}_2[\rho_x^2, \rho_y^2]$	$\mathbf{1}$
e_9	$\mathbf{D}_2[\rho_x^2, \rho_y^2]$	$\mathbf{D}_2[\rho_x^2, \rho_y^2]$	$\mathbf{1}$
e_{10}	$\mathbf{D}_2[\rho_x^2, \rho_y^2]$	$\mathbf{D}_2[\rho_x^2, \rho_y^2]$	$\mathbf{1}$
c_7	$\mathbf{Z}_2[\rho_y^2]$	$\mathbf{D}_2[\rho_x^2, \rho_y^2]$	$\mathbf{Z}_2$
c_9	$\mathbf{Z}_2[\rho_x^2]$	$\mathbf{D}_2[\rho_x^2, \rho_y^2]$	$\mathbf{Z}_2$
c_{10}	$\mathbf{Z}_2[\rho_x^2]$	$\mathbf{D}_2[\rho_x^2, \rho_y^2]$	$\mathbf{Z}_2$
c_{33}	$\mathbf{Z}_2[\rho_z^2]$	$\mathbf{D}_2[\rho_x^2, \rho_y^2]$	$\mathbf{Z}_2$
c_{37}	$\mathbf{Z}_2[\rho_y^2]$	$\mathbf{D}_2[\rho_x^2, \rho_y^2]$	$\mathbf{Z}_2$
c_{38}	$\mathbf{Z}_2[\rho_z^2]$	$\mathbf{D}_2[\rho_x^2, \rho_y^2]$	$\mathbf{Z}_2$

Proof. The proof follows from Lemmas 8.6 and 8.8. □

Therefore the skeleton is

$$\mathbb{X}_{\mathbf{D}_2[\rho_x^2, \rho_y^2]} = \bigcup_{C \in \mathscr{C}_{\mathbf{D}_2[\rho_x^2, \rho_y^2]}} C \subset X_0.$$

Symmetry Properties of $\mathbb{X}_{\mathbf{D}_2[\rho_x^2, \rho_y^2]}$

Here we use the $\mathbf{D}_2[\rho_x^2, \rho_y^2]$ symmetry to determine the different orbit representatives for equilibria and heteroclinic connections.

Pointwise and Setwise Isotropy Subgroups. The generators for $\mathbf{D}_2[\rho_x^2, \rho_y^2]$ act on X_0 as

$$\begin{aligned} \rho_x^2(\theta_1, \theta_2, \theta_3) &= (-\theta_2, -\theta_1, -\theta_3), \\ \rho_y^2(\theta_1, \theta_2, \theta_3) &= (\theta_2 + \theta_3, \theta_1 + \theta_3, -\theta_3). \end{aligned}$$

The complete action of $\mathbf{D}_2[\rho_x^2, \rho_y^2]$ on X_0 is in Table 8.28. The action of $\mathbf{D}_2[\rho_x^2, \rho_y^2]$ on X_0 induces the trivial action $\mathscr{C}_{\mathbf{D}_2[\rho_x^2, \rho_y^2]}$. We obtain:

Proposition 8.19
Let $\mathbf{D}_2[\rho_x^2, \rho_y^2]$ act on $\mathscr{C}_{\mathbf{D}_2[\rho_x^2, \rho_y^2]}$ with the induced trivial action and on X_0 as in Table 8.28. Then given $C \in \mathscr{C}_{\mathbf{D}_2[\rho_x^2, \rho_y^2]}$, the setwise isotropy Stab(C), *pointwise isotropy* stab(C) *and $S(C)$ are given in Table 8.7.*

Proof. This is a simple calculation. □

Knots Relative to C. Since all knots are equilibria and each C contains two equilibria, it follows that the knots are exactly the equilibria which are contained in C. This information is contained in Table 8.30.

Table 8.30: Knots relative to orbit representatives of $C \in \mathscr{C}_{\mathbf{D}_2[\rho_x^2,\rho_y^2]}$ for the FCC lattice.

Element of $\mathscr{C}_{\mathbf{D}_2[\rho_x^2,\rho_y^2]}$	Knots
c_7	e_1, e_5
c_9	e_1, e_5
c_{33}	e_1, e_5
c_{37}	e_9, e_{10}
c_{38}	e_9, e_{10}

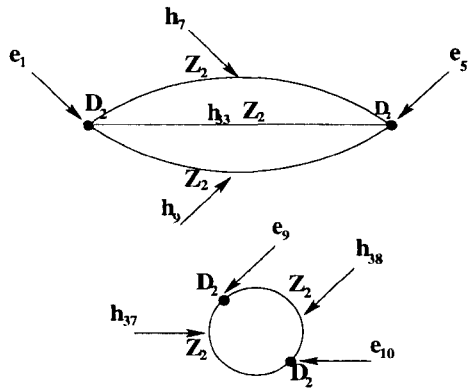

Figure 8.6: The projected skeleton $\mathbb{X}^p_{\mathbf{D}_2[\rho_x^2,\rho_y^2]}$. Here $h_7 = \{(\theta,-\theta,0)|\theta \in (0,\pi)\}$, $h_9 = \{(\theta,-\theta,\pi)|\theta \in (0,\pi)\}$, $h_{33} = \{(\theta,\theta,-2\theta)|\theta \in (0,\pi)\}$, $h_{37} = \{(\theta+\pi,\theta,-2\theta)|\theta \in (0,\pi)\}$, and $h_{38} = \{(\theta+\pi,\theta,\pi)|\theta \in (0,\pi)\}$.

Projected Skeleton

Here we compute the projected skeleton $\mathbb{X}^p_{\mathbf{D}_2[\rho_x^2,\rho_y^2]}$. The action of $\mathbf{D}_2[\rho_x^2,\rho_y^2]$ on $\mathscr{C}_{\mathbf{D}_2[\rho_x^2,\rho_y^2]}$ shows that there are five orbit representatives for the elements of $\mathscr{C}_{\mathbf{D}_2[\rho_x^2,\rho_y^2]}$ that are homeomorphic to $\mathbf{S}^1$. Each $C \cong \mathbf{S}^1$ has two knots; this implies that there is an axis of reflection symmetry. So each C projects into the orbit space as a line joining the two knots in Table 8.30. Figure 8.1 illustrates the projected skeleton. From the projected skeleton we deduce that there exist at most $2^5 = 32$ qualitatively different $\mathbf{D}_2[\rho_x^2,\rho_y^2]$-equivariant flows on $\mathbb{X}_{\mathbf{D}_2[\rho_x^2,\rho_y^2]}$. The projected skeleton has some interesting properties, which are worth commenting on. Firstly, the projected skeleton is disconnected. This is not a new phenomenon, but it is the first time that we have seen a projected skeleton consisting of two disjoint networks. Secondly, there exist perturbations that give heteroclinic cycles between the equilibria e_9 and e_{10} along the connections h_{37} and h_{38}. Finally, it is possible to exhibit admissible flows, which give the projected skeleton the structure of two disjoint heteroclinic networks.

8.2.8 Example

In this subsection we present an example illustrating how the structure of the planforms with $\mathbb{O}\oplus\mathbf{Z}_2^c$ and $\widetilde{\mathbb{O}}\oplus\mathbf{Z}_2^c$ symmetry are altered when forced symmetry breaking terms are taken into account. We consider forced symmetry breaking to $\mathbb{O}$, since this is the simplest case.

Breaking the original Γ symmetry of the system to $\mathbb{O}$ symmetry corresponds to a perturbation of the FCC lattice in the three mutually perpendicular directions $\boldsymbol{\ell}_1$, $\boldsymbol{\ell}_2$ and $\boldsymbol{\ell}_3$. We define

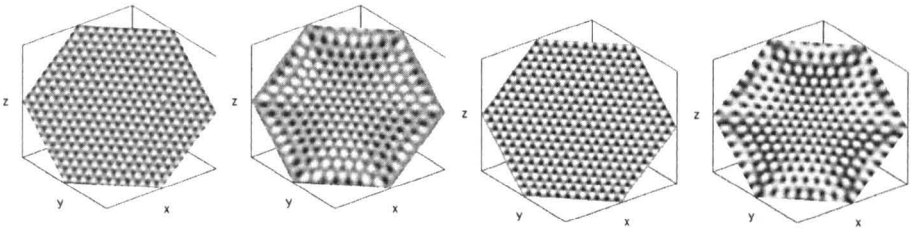

(a) (b) (c) (d)

Figure 8.7: Density plots of the unperturbed planforms with $\mathbb{O} \oplus \mathbf{Z}_2^c$ and $\widetilde{\mathbb{O}} \oplus \mathbf{Z}_2^c$ symmetry (a) and (c), and their corresponding perturbations (b) and (d).

the perturbation by $\Psi(\mathbf{x}) = (\tanh^{-1} x, \tanh^{-1} y, \tanh^{-1} z)$. The resulting eigenfunction is

$$\mathbf{u}(\mathbf{x}) = \sum_{j=1}^{4} z_j \exp\left(i\mathbf{K}_j \cdot (\Psi^{-1}(\mathbf{x}))\right). \tag{8.5}$$

To give a physical interpretation we employ the methods used to render the planforms on the SC lattice: we consider a slice in the $z = x + y$ direction. Figure 8.7 presents examples of two planforms. (a) Shows a density plot of (8.5) in a hexagonal cross section of the cube of periodicity of the planform when $\Psi \equiv 1$; that is. the unperturbed case $\varepsilon = 0$. (b) Shows how the planform in (a) is altered when $\varepsilon \neq 0$ but is still chosen small; in both cases $z_j = 1$ for all j, which corresponds to the solution with $\mathbb{O} \oplus \mathbf{Z}_2^c$ symmetry. (c) and (d) show the same plots, but now for the solutions with $\widetilde{\mathbb{O}} \oplus \mathbf{Z}_2^c$ symmetry.

8.3 High Dimensional Representations

In this section the high dimensional representations of the group Γ are considered. The reasoning of Remark 7.24 lets us use the results of the eight-dimensional representation in the higher dimensional cases. More precisely, if Σ is the isotropy of a solution in the twenty-four or forty-eight-dimensional representation and $\Sigma \cong \mathbb{O} \oplus \mathbf{Z}_2^c$, then the results for the eight-dimensional representation hold.

8.3.1 Existence of Translation Free Axial Solutions

In this subsection we discuss the existence of translation free axial solutions to the high dimensional bifurcation problems. Dionne [19] showed that there exist up to nine translation free axial solutions to the twenty-four and forty-eight-dimensional bifurcation problems. The symmetry groups of these solutions are presented in Table 8.31.

As for the SC lattice, we cannot determine the form of a general Γ-equivariant vector field, or even a finite order truncation, for either of the high dimensional representations. Thus stability and direction of branching are two issues that we do not address. However, we can present the following classification theorem for those solutions in Table 8.31 that have symmetry isomorphic to $\mathbb{O} \oplus \mathbf{Z}_2^c$.

Theorem 8.20
Let $\Gamma = \mathbb{O} \oplus \mathbf{Z}_2^c \dotplus \mathbf{T}^3$. Let Σ be isomorphic to $\mathbb{O} \oplus \mathbf{Z}_2^c$. Let $\Delta \subseteq \Sigma$ be isomorphic to: $\mathbb{O}$, $\mathbf{D}_4[\rho_x, \kappa_6]$, $\mathbb{T}$, $\mathbf{D}_3[\tau_1, \kappa_5]$, $\mathbf{D}_2[\rho_x^2, \kappa_6]$, or $\mathbf{D}_2[\rho_x^2, \rho_y^2]$. Let Γ act on $\mathbb{C}^s$, where $s = 8$, 12 or 24. Let $\mathbf{f} \in \overrightarrow{\mathcal{E}}_\Gamma$ be a Γ-equivariant bifurcation problem. Let $\mathbf{g} \in \overrightarrow{\mathcal{E}}_\Delta$ be a Δ-equivariant vector

Table 8.31: The translation free axial subgroups of Γ. Superscripts distinguish groups with different generators. The groups $\widetilde{\mathbf{D}}_4 \oplus \mathbf{Z}_2^c$, $\widetilde{\mathbf{D}}_4^{\,a} \oplus \mathbf{Z}_2^c$ and $\widetilde{\mathbf{D}}_3 \oplus \mathbf{Z}_2^c$ occur only in the twenty-four-dimensional representation when certain defining conditions on the representation are satisfied [19].

Dimension	Axial Subgroup Σ
24	$\mathbb{O} \oplus \mathbf{Z}_2^c$
	$\widetilde{\mathbb{O}} \oplus \mathbf{Z}_2^c$
	$\widetilde{\mathbf{D}}_4 \oplus \mathbf{Z}_2^c$
	$\widetilde{\mathbf{D}}_4^{\,a} \oplus \mathbf{Z}_2^c$
	$\widetilde{\mathbf{D}}_3 \oplus \mathbf{Z}_2^c$
48	$\mathbb{O} \oplus \mathbf{Z}_2^c$
	$\widetilde{\mathbb{O}} \oplus \mathbf{Z}_2^c$
	$\widetilde{\mathbb{O}}^a \oplus \mathbf{Z}_2^c$
	$\widetilde{\mathbb{O}}^b \oplus \mathbf{Z}_2^c$

field that satisfies $\mathbf{g}(\mathbf{0}) = \mathbf{0}$. *Then there exist branches of steady-state solutions to* $\mathbf{f}(\mathbf{0}, \lambda) = \mathbf{0}$ *bifurcating from the origin with isotropy* Σ. *The group orbit of these solutions is diffeomorphic to a standard 3-torus. Consider the perturbed system* $\mathbf{F}(\mathbf{z}, \lambda, \varepsilon) = \mathbf{f}(\mathbf{z}, \lambda) + \varepsilon \mathbf{g}(\mathbf{z})$, *where* ε *is real and small. Then for sufficiently small* ε, X_0 *persists to give a new* $\mathbf{F}$*-invariant manifold* X_ε, *which is* Δ*-equivariantly diffeomorphic to* X_0. *The behaviour of the vector field on* X_0 *is characterised by:*

1. *When* $\Delta \cong \mathbb{O}$ *there are four (group orbits of) equilibria:* e_1, e_4, e_5, *and* e_9, *together with five (group orbits of) heteroclinic connections given by:* h_1, h_6, h_7, h_{10} *and* h_{29}. *Figure 8.1 shows how they are arranged.*

2. *When* $\Delta \cong \mathbf{D}_4[\rho_x, \kappa_6]$ *there are four (group orbits of) equilibria:* e_1, e_2, e_5, *and* e_9, *and six (group orbits of) heteroclinic connections given by:* h_5, h_6, h_7, h_9, h_{10}, *and* h_{37}. *Figure 8.2 shows how they are arranged.*

3. *When* $\Delta \cong \mathbb{T}$ *there are three (group orbits of) equilibria given by:* e_1, e_5, *and* e_9, *and three (group orbits of) heteroclinic connections given by:* h_7, h_{10} *and* c_{29}. *Figure 8.3 shows how they are arranged.*

4. *When* $\Delta \cong \mathbf{D}_3[\tau_1, \kappa_5]$ *there are two equilibria given by:* e_1, *and* e_5, *and three (group orbits of) heteroclinic connections given by:* c_3, c_{25} *and* h_{29}. *Figure 8.4 shows how they are arranged. There exist perturbation which give two heteroclinic cycles, the first between the equilibria* e_1 *and the second* e_8.

5. *When* $\Delta \cong \mathbf{D}_2[\rho_x^2, \kappa_6]$ *there are four equilibria given by:* e_1, e_2, e_5, *and* e_8, *and six (group orbits of) heteroclinic connections given by:* h_5, h_6, h_9, h_{10}, h_{21} *and* h_{34}. *Figure 8.5 shows how they are arranged.*

6. *When* $\Delta \cong \mathbf{D}_2[\rho_x^2, \rho_y^2]$ *there are four equilibria given by:* e_1, e_5, e_9, *and* e_{10}, *and five (group orbits of) heteroclinic connections given by:* h_7, h_9, h_{33}, h_{37} *and* h_{38}. *Figure 8.6 shows how they are arranged.*

8.3.2 Examples

In this subsection we present an example to illustrate how the structure of a planform is altered when forced symmetry breaking terms are taken into account. The example we consider is forced symmetry breaking to $\mathbb{O}$. Breaking the original Γ symmetry of the system to $\mathbb{O}$ corresponds to a perturbation of the FCC lattice in the three mutually perpendicular directions $\boldsymbol{\ell}_1, \boldsymbol{\ell}_2$ and $\boldsymbol{\ell}_3$. We

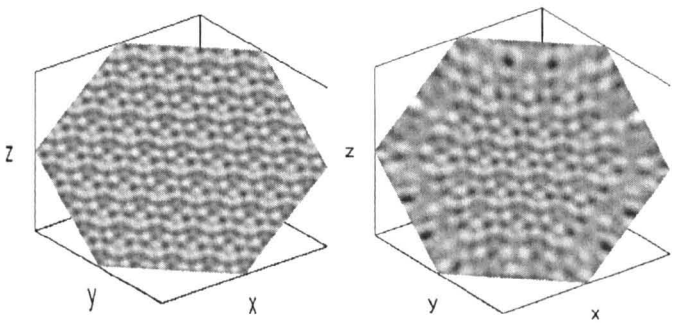

(a) (b)

Figure 8.8: Density plots of the unperturbed planforms with $\mathbb{O} \oplus \mathbf{Z}_2^c$ symmetry (a), and their corresponding perturbations (b).

define the perturbation by $\Psi(\mathbf{x}) = (\tanh^{-1} x, \tanh^{-1} y, \tanh^{-1} z)$. The resulting eigenfunction is

$$\mathbf{u}(\mathbf{x}) = \sum_{j=1}^{s} z_j \exp\left(i\mathbf{K}_j \cdot (\Psi^{-1}(\mathbf{x}))\right), \tag{8.6}$$

where $s = 12$ or 24. To give a physical interpretation we employ the methods used to render the planforms on the SC lattice; we consider a slice in the $z = x + y$ direction.

Twenty-four-Dimensional Representation

Figure 8.8 presents examples of two planforms. (a) Shows a density plot of (8.6) in a hexagonal cross section of the cube of periodicity of the planform, when $\Psi \equiv 1$; that is, the unperturbed case $\varepsilon = 0$. (b) Shows how the planform in (a) is altered when $\varepsilon \neq 0$ but is still chosen small; in both cases $z_j = 1$ for all j, which corresponds to the solution with $\mathbb{O} \oplus \mathbf{Z}_2^c$ symmetry.

We shall not consider the planforms associated with the forty-eight-dimensional representation.

8.4 Conclusion

We have seen that the FCC, like the SC lattice, is capable of supporting dynamics much richer than those supported by any two-dimensional lattice; heteroclinic cycles and more generally networks are possible. In this chapter we have not considered the class II and III subgroups of $\mathbb{O} \oplus \mathbf{Z}_2^c$; the reasons are identical to those for the SC lattice. The forced symmetry breaking of a Γ-equivariant system of equations, where the perturbation term is equivariant with respect to a class II subgroup, is effectively the same as the study performed for the class I subgroups, except that the symmetry of the equilibria is different—they have an additional $\mathbf{Z}_2^c$ component.

The main result of the chapter is Theorem 8.20. This theorem gives a partial classification of the behaviour that we may expect from solutions with symmetry isomorphic to $\mathbb{O} \oplus \mathbf{Z}_2^c$ of a Γ-equivariant bifurcation problem, when symmetry breaking effects are taken into account.

Chapter 9

Forced Symmetry Breaking on the Body Centred Cubic Lattice

9.1 Introduction

Bifurcation problems on the Body Centred Cubic (BCC) lattice, like those on the hexagonal lattice, are of great interest because of their experimental relevance. The theoretical work of De Wit *et al.* [17] showed, numerically, the existence of three-dimensional BCC structures in reaction-diffusion systems. Understanding the behaviour of approximate BCC bifurcations is important in resolving the issue of black-eye instabilities. We shall study this problem in detail in Part IV.

We now review some recent work. Dionne [19] classified all the translation free axial solutions supported by the BCC lattice. Motivated by Turing patterns, Callahan and Knobloch [8] generalised these results, giving stability criteria for the simplest (twelve-dimensional) representation. The presence of a quadratic equivariant leads to complexities that are not encountered for the SC and FCC problems. An ideal resolution to this problem is a singularity theory approach, but this is just too complex. Callahan and Knobloch tackled the problem via the use of additional $\mathbf{Z}_2[-I]$ symmetry, which removes all even terms from the bifurcation problem: then they considered a weak unfolding of this new bifurcation problem. In this chapter we shall extend the previous steady-state results by partially classifying the types of behaviour exhibited by some BCC solutions under forced symmetry breaking.

Recall the methods of Section 1.6, applied to the BCC lattice. Define three linearly independent vectors $\boldsymbol{\ell}_1 = (1,0,0)$, $\boldsymbol{\ell}_2 = (0,1,0)$ and $\boldsymbol{\ell}_3 = (\frac{1}{2},\frac{1}{2},\frac{1}{2})$. The BCC lattice is

$$\mathcal{L}_{BCC} = \{n_1\boldsymbol{\ell}_1 + n_2\boldsymbol{\ell}_2 + n_3\boldsymbol{\ell}_3 \big| n_1, n_2, n_3 \in \mathbb{Z}\}.$$

The symmetry group of $\mathcal{L}_{BCC}$ is $\Gamma = \mathbb{O} \oplus \mathbf{Z}_2^c \dot{+} \mathbf{T}^3$. Here $\mathbb{O}$ and $\mathbf{Z}_2^c$ are as for the SC and FCC lattices, and $\mathbf{T}^3 = \mathbb{R}^3/\mathcal{L}_{BCC}$. We seek functions $\mathbf{u} \in \mathcal{X}$ that are triply periodic with respect to the BCC lattice, and so are members of $\mathcal{X}_{\mathcal{L}_{BCC}}$. Define $\mathbf{k}_1 = (1,0,-1)$, $\mathbf{k}_2 = (0,1,-1)$, and $\mathbf{k}_3 = (0,0,2)$. Then the dual lattice to $\mathcal{L}_{BCC}$ is

$$\mathcal{L}^*_{BCC} = \{n_1\mathbf{k}_1 + n_2\mathbf{k}_2 + n_3\mathbf{k}_3 \big| n_1, n_2, n_3 \in \mathbb{Z}\}.$$

We may write a function $\mathbf{u} \in \mathcal{X}_{\mathcal{L}_{BCC}}$ in the form

$$\mathbf{u}(\mathbf{x},t) = \sum_{j=1}^{s} z_j e^{2\pi i \mathbf{K}_j \cdot \mathbf{x}} \mathbf{u}_j + c.c., \tag{9.1}$$

where $z_j \in \mathbb{C}$ and $\mathbf{K}_j$ are the dual lattice vectors that intersect the critical sphere of radius k_c. These vectors give rise to an irreducible representation of Γ. Dionne [19] shows that for

the representation of Γ to be translation free, either $s = 6$, 12 (two different types) or $s = 24$. The domain of the bifurcation problem is then identified with $\mathbb{C}^s$. The representation of Γ on $\mathbb{C}^s$ is determined by its action on the complex coordinates z_j in (9.1). Our problem is in the standard form: we have reduced the situation to the study of the ODE

$$\dot{\mathbf{z}} = \mathbf{f}(\mathbf{z}, \lambda), \tag{9.2}$$

where $\mathbf{f} : \mathbb{C}^s \times \mathbb{R} \to \mathbb{C}^s$ is Γ-equivariant. Dionne [19] proves that there are (up to) 15 different axial solutions[1]. In the twelve-dimensional representation there are three translation free axial solutions with $\mathbb{O} \oplus \mathbf{Z}_2^c$, $\widetilde{\mathbb{O}}$, and $\widetilde{\mathbf{D}}_4 \oplus \mathbf{Z}_2^c$ symmetry. The group orbit of the $\mathbb{O} \oplus \mathbf{Z}_2^c$ solution is a 3-torus which we denote by X_0, whilst the other group orbits have a more complex form. We study the behaviour of X_0 when symmetry breaking terms equivariant with respect to certain subgroups are added to (9.2). Employing the methods of Chapter 2 we seek admissible perturbations, heteroclinic cycles and networks between equilibria, and other more elaborate structures.

We now review the contents of the chapter and its organisation. Section 9.2 studies the forced symmetry breaking of the twelve-dimensional representation. Subsection 9.2.1 considers the existence of the three translation free axial solutions and their stability. Subsection 9.2.2 studies the forced symmetry breaking of the group orbit of the $\mathbb{O} \oplus \mathbf{Z}_2^c$ symmetric solution. From this subsection all other results in this section are derived; in particular, the behaviour of forced symmetry breaking to the subgroups $\mathbb{O}$, $\mathbb{T}$, $\mathbf{D}_4[\rho_x, \kappa_6]$, $\mathbf{D}_3[\tau_3, \kappa_3]$, $\mathbf{D}_2[\rho_x^2, \kappa_4]$, and $\mathbf{D}_2[\rho_x^2, \rho_y^2]$. Section 9.3 discusses the behaviour of (a selection of) the solutions that occur in the higher dimensional representations under forced symmetry breaking. Section 9.4 provides some concluding remarks.

9.2 Twelve-Dimensional Representation

In this section we consider the twelve-dimensional representation of the group Γ. This representation occurs when the wavelength of instabilities coincides with the periodicity of the functions in $\mathcal{X}_{\mathcal{L}_{BCC}}$. The representation of Γ on $\mathbb{C}^6$ corresponds to the following action. Choose coordinates $\mathbf{z} = (z_1, z_2, z_3, z_4, z_5, z_6)$ on $\mathbb{C}^6$. The action of Γ is generated by

$$\begin{aligned}
\rho_x(\mathbf{z}) &= (z_4, z_1, z_2, z_3, , \overline{z_6}, z_5), \\
\rho_y(\mathbf{z}) &= (z_5, \overline{z_4}, z_6, z_2, \overline{z_3}, z_1), \\
c(\mathbf{z}) &= (\overline{z_1}, \overline{z_2}, \overline{z_3}, \overline{z_4}, \overline{z_5}, \overline{z_6}), \\
\theta(\mathbf{z}) &= (e^{-\mathrm{i}(\theta_1+\theta_2+\theta_3)} z_1, e^{-\mathrm{i}(\theta_1+\theta_3)} z_2, e^{-\mathrm{i}(\theta_1-\theta_2)} z_3, e^{-\mathrm{i}\theta_1} z_4, e^{-\mathrm{i}(\theta_2+\theta_3)} z_5, e^{-\mathrm{i}\theta_2} z_6).
\end{aligned}$$

Here ρ_x and ρ_y are the generators of $\mathbb{O}$, c generates $\mathbf{Z}_2^c$, and $\theta \in \mathbf{T}^3$. Consider the Γ-equivariant system of differential equations

$$\dot{\mathbf{z}} = \mathbf{f}(\mathbf{z}, \lambda), \tag{9.3}$$

where $\mathbf{f} : \mathbb{C}^6 \times \mathbb{R} \to \mathbb{C}^6$ is Γ-equivariant. In this section we investigate the behaviour of the group orbit of solutions to (9.3) under forced symmetry breaking to the subgroups $\mathbb{O}$, $\mathbb{T}$, $\mathbf{D}_4[\rho_x, \kappa_6]$, $\mathbf{D}_3[\tau_3, \kappa_3]$, and two $\mathbf{D}_2$ subgroups given by $\mathbf{D}_2[\rho_x^2, \kappa_6]$ and $\mathbf{D}_2[\rho_x^2, \rho_y^2]$. Our primary interest is heteroclinic type behaviour on the different skeletons.

9.2.1 Existence of Translation Free Axial Solutions

The action of Γ on $\mathbb{C}^6$ has a large number of conjugacy classes of isotropy subgroups; there are 16 with fixed-point subspace of dimension two or less [8]. Of these subgroups, only six are axial; furthermore only three conjugacy classes are translation free. These are $\mathbb{O} \oplus \mathbf{Z}_2^c$, $\widetilde{\mathbb{O}}$, and $\widetilde{\mathbf{D}}_4 \oplus \mathbf{Z}_2^c$ [19]. We focus exclusively on these translation free axial subgroups, which we denote by BCC, BCCI and A respectively[2].

[1] The twenty-four-dimensional type 1 representation has either four or five solutions, depending on the defining conditions of the representation.

[2] This notation is that of Callahan and Knobloch [8].

By [8] a general Γ-equivariant vector field up to cubic order has the form (first component only),

$$\begin{aligned} f_1(\mathbf{z},\lambda) &= \lambda z_1 + \frac{1}{2}a_1(z_2\overline{z_6} + z_4 z_5) + a_2|z_1|^2 z_1 + a_3|z_3|^2 z_1 + \frac{1}{2}a_4(\overline{z_3}z_4\overline{z_6} + z_2 z_3 z_5) \\ &+ \frac{1}{4}a_5(|z_2|^2 + |z_4|^2 + |z_5|^2 + |z_6|^2)z_1, \end{aligned} \tag{9.4}$$

where the a_j's are real[3]. The quadratic term immediately leads to problems: local to the origin, all solutions are unstable at bifurcation. For this reason it is necessary to understand an unfolding of the degeneracy $a_1 = 0$. A singularity theory approach to this question is too complex, so Callahan and Knobloch [8] adopt a well-known alternative: they introduce an extra $\mathbf{Z}_2[-I]$ symmetry which removes all even order terms. Then the $a_1 = 0$ term is weakly unfolded, so $0 < a_1 \ll 1$. Callahan and Knobloch [8] show that the bifurcation problem with the extra $\mathbf{Z}_2[-I]$ symmetry has stable solutions BCC and BCCI, but not at the same time. In addition, the solution A can *never* be stable. The question now arises, what happens when the degeneracy $a_1 = 0$ is weakly unfolded? In this case the solutions BCCI and A are independent of the a_1 term, so their stability and bifurcation behaviour does not change; importantly, the solution A remains unstable. In contrast, the BCC solution does depend on the a_1 term, and the solution is unstable at bifurcation but regains stability at a secondary saddle-node bifurcation. So there exists a region of the parameter space for which the BCC and BCCI solutions are stable, but not simultaneously. Summarising:

Theorem 9.1
Let $f : \mathbb{C}^6 \times \mathbb{R} \to \mathbb{C}^6$ be a Γ-equivariant bifurcation problem. Then, generically there exist branches of steady-state solutions bifurcating from the origin with isotropy $\mathbb{O} \oplus \mathbf{Z}_2^c$, $\widetilde{\mathbb{O}}$ and $\widetilde{\mathbf{D}}_4 \oplus \mathbf{Z}_2^c$. Furthermore, if certain nondegeneracy conditions hold on the third order truncation of the vector field in (9.4), the solution with $\widetilde{\mathbf{D}}_4 \oplus \mathbf{Z}_2^c$ symmetry is always unstable. The solutions with $\mathbb{O} \oplus \mathbf{Z}_2^c$ and $\widetilde{\mathbb{O}}$ symmetry can be stable at bifurcation, but never *at the same time.*

Proof. See Callahan and Knobloch [8]. □

The group orbit of solutions with $\mathbb{O} \oplus \mathbf{Z}_2^c$ symmetry is a 3-torus which we denote throughout by X_0. The manifold X_0 is normally hyperbolic. The solution with $\widetilde{\mathbb{O}}$ symmetry has a group orbit composed of two 3-tori; we shall not consider this solution further, since our intended applications in Part IV concern the $\mathbb{O} \oplus \mathbf{Z}_2^c$ solution only.

9.2.2 Forced Symmetry Breaking to $\mathbb{O}$

In this subsection we study the behaviour of the group orbit X_0 of bifurcating solutions with $\mathbb{O} \oplus \mathbf{Z}_2^c$ symmetry given by Theorem 9.1, when symmetry breaking terms with $\mathbb{O}$ symmetry are added to the vector field (9.4). The normal hyperbolicity of X_0 guarantees, by the Equivariant Persistence Theorem, the existence of a manifold X_ε diffeomorphic to X_0 and invariant under the new dynamics. The action of $\mathbb{O}$ on $\mathbb{C}^6$ is given in Table 9.1.

Calculation of the Skeleton

Here we calculate the skeleton of X_0 under the action of $\mathbb{O}$. To begin we calculate $\mathscr{C}_0$. We introduce some new notation:

[3]The form (and notation) used here is different from that in Callahan and Knobloch [8], which was

$$\begin{aligned} f_1(\mathbf{z},\lambda) &= \lambda z_1 + \frac{1}{2}a_{12}(\overline{z_3}z_4 + z_2\overline{z_6}) + a_1|z_1|^2 z_1 + a_8|z_5|^2 z_1 + \frac{1}{2}a_{16}(z_4 z_5\overline{z_6} + z_2\overline{z_3}\,\overline{z_5}) \\ &+ \frac{1}{4}a_3(|z_2|^2 + |z_3|^2 + |z_4|^2 + |z_6|^2)z_1. \end{aligned}$$

The reason for this difference is the slightly different action of the generators for $\mathbb{O}$; this has no computational effect.

Table 9.1: Action of $\mathbb{O}$ on $\mathbb{C}^6$ for the BCC lattice.

Element of $\mathbb{O}$	Action on $\mathbb{C}^6$
ρ_x	$(z_4, z_1, z_2, z_3, \overline{z_6}, z_5)$
ρ_x^2	$(z_3, z_4, z_1, z_2, \overline{z_5}, \overline{z_6})$
ρ_x^3	$(z_2, z_3, z_4, z_1, z_6, \overline{z_5})$
ρ_y	$(z_5, \overline{z_4}, z_6, z_2, \overline{z_3}, \overline{z_1})$
ρ_y^2	$(\overline{z_3}, \overline{z_2}, \overline{z_1}, \overline{z_4}, \overline{z_6}, \overline{z_5})$
ρ_y^3	$(\overline{z_6}, z_4, \overline{z_5}, \overline{z_2}, z_1, z_3)$
ρ_z	$(z_3, z_6, \overline{z_1}, \overline{z_5}, z_2, \overline{z_4})$
ρ_z^2	$(\overline{z_1}, \overline{z_4}, \overline{z_3}, \overline{z_2}, z_6, z_5)$
ρ_z^3	$(\overline{z_3}, z_5, z_1, \overline{z_6}, \overline{z_4}, z_2)$
τ_1	$(z_2, z_5, \overline{z_4}, z_6, z_1, \overline{z_3})$
τ_1^2	$(z_5, z_1, \overline{z_6}, \overline{z_3}, z_2, z_4)$
τ_2	$(\overline{z_2}, \overline{z_6}, z_4, \overline{z_5}, \overline{z_3}, z_1)$
τ_2^2	$(z_6, \overline{z_1}, \overline{z_5}, z_3, \overline{z_4}, \overline{z_2})$
τ_3	$(z_4, \overline{z_5}, \overline{z_2}, \overline{z_6}, z_3, \overline{z_1})$
τ_3^2	$(\overline{z_6}, \overline{z_3}, z_5, z_1, \overline{z_2}, \overline{z_4})$
τ_4	$(\overline{z_5}, z_3, z_6, \overline{z_1}, z_4, z_2)$
τ_4^2	$(\overline{z_4}, z_6, z_2, z_5, \overline{z_1}, z_3)$
κ_1	$(z_1, \overline{z_6}, \overline{z_3}, z_5, z_4, \overline{z_2})$
κ_2	$(\overline{z_1}, \overline{z_5}, z_3, z_6, \overline{z_2}, z_4)$
κ_3	$(z_6, z_2, z_5, \overline{z_4}, z_3, z_1)$
κ_4	$(\overline{z_4}, \overline{z_3}, \overline{z_2}, \overline{z_1}, z_5, \overline{z_6})$
κ_5	$(\overline{z_5}, \overline{z_2}, \overline{z_6}, z_4, \overline{z_1}, \overline{z_3})$
κ_6	$(\overline{z_2}, \overline{z_1}, \overline{z_4}, \overline{z_3}, \overline{z_5}, z_6)$

Definition 9.2
Define the following subsets of X_0:

$$
\begin{aligned}
e_{11} &= \{(\pi/2, \pi, 0)\} & e_{12} &= \{(3\pi/2, \pi, 0)\} \\
e_{13} &= \{(\pi, \pi/2, 0)\} & e_{14} &= \{(\pi, 3\pi/2, 0)\} \\
e_{15} &= \{(\pi/2, 3\pi/2, \pi)\} & e_{16} &= \{(3\pi/2, \pi/2, \pi)\}, \\
c_{39} &= \{(0, \theta, -2\theta) \,|\, \theta \in [0, 2\pi)\} & c_{40} &= \{(\pi, \theta, \pi - 2\theta) \,|\, \theta \in [0, 2\pi)\}, \\
c_{41} &= \{(\theta, 0, -2\theta) \,|\, \theta \in [0, 2\pi)\} & c_{42} &= \{(\theta, \pi, \pi - 2\theta) \,|\, \theta \in [0, 2\pi)\}, \\
c_{43} &= \{(2\theta, \theta - 2\theta) \,|\, \theta \in [0, 2\pi)\} & c_{44} &= \{(2\theta, \theta, \pi - 2\theta) \,|\, \theta \in [0, 2\pi)\} \\
c_{45} &= \{(\theta, 2\theta, -2\theta) \,|\, \theta \in [0, 2\pi)\} & c_{46} &= \{(\theta, 2\theta, \pi - 2\theta) \,|\, \theta \in [0, 2\pi)\}.
\end{aligned}
$$

Then we have:

Proposition 9.3
Let $\mathbb{O}$ act on X_0 with the action induced from Table 9.1. Then

$$
\begin{aligned}
\mathscr{C}_{\mathbb{O}} = \{&e_1, e_2, e_3, e_4, e_5, e_6, e_7, e_8, e_{11}, e_{12}, e_{13}, e_{14}, e_{15}, e_{16}, c_1, c_3, c_5, c_7, c_9, c_{10}, c_{13}, c_{17}, \\
&c_{21}, c_{23}, c_{25}, c_{33}, c_{37}, c_{38}, c_{39}, c_{40}, c_{41}, c_{42}, c_{43}, c_{44}, c_{45}, c_{46}\}.
\end{aligned}
$$

We divide the proof of this proposition into a series of lemmas, each of which is useful for our later work on forced symmetry breaking to other subgroups of $\mathbb{O}$. Recall that $\mathrm{Fix}(\Sigma) = \{(x, x, x, x, x, x) \,|\, x \in \mathbb{R}\}$.

Lemma 9.4
Let $\mathbb{O}$ and $\mathbb{T}$ act on X_0 with the action induced from Table 9.1. Then the fixed-point submanifold in X_0 of each of these groups is e_1.

Proof. We begin by showing that $\mathrm{Fix}(\mathbb{T}) = \mathrm{Fix}(\mathbb{O})$. To finish the proof we need only consider the group $\mathbb{O}$. A look at the action of each of the elements of $\mathbb{T}$ on $\mathbb{C}^6$ shows that any vector $(z_1, z_2, z_3, z_4, z_5, z_6) \in \mathbb{C}^6$ fixed by $\mathbb{T}$ must satisfy $z_j = z_i$ for all $i, j = 1, \ldots, 6$. Furthermore the action of $\mathbb{T}$ implies $z_1 = \overline{z_1}$; this shows that $\mathrm{Fix}(\mathbb{T}) = \mathrm{Fix}(\mathbb{O})$.

To complete the proof we compute $\mathrm{Fix}_{X_0}(\mathbb{O})$. We have

$$\mathrm{Fix}_{X_0}(\mathbb{O}) = N_\Gamma(\mathbb{O}, \mathbb{O} \oplus \mathbf{Z}_2^c)/\mathbb{O} \oplus \mathbf{Z}_2^c,$$

where $N_\Gamma(\mathbb{O}, \mathbb{O} \oplus \mathbf{Z}_2^c) = \{\gamma \in \Gamma | \gamma \mathrm{Fix}(\mathbb{O} \oplus \mathbf{Z}_2^c) \subseteq \mathrm{Fix}(\mathbb{O})\}$. We seek those elements of $\mathbf{T}^3$ that are contained in $N_\Gamma(\mathbb{O}, \mathbb{O} \oplus \mathbf{Z}_2^c)$. Now $\gamma = (\theta_1, \theta_2, \theta_3) \in N_\Gamma(\mathbb{O}, \mathbb{O} \oplus \mathbf{Z}_2^c)$ if and only if $\theta_1 + \theta_2 + \theta_3 = \theta_1 + \theta_3 = \theta_1 - \theta_2 = \theta_1 = \theta_2 + \theta_3 = \theta_2 \equiv 0$ or π mod 2π. This equation has only one solution $(\theta_1, \theta_2, \theta_3) = (0, 0, 0)$, so $\mathrm{Fix}_{X_0}(\mathbb{O}) = e_1$. □

We now analyse the subgroups of order eight; that is, those isomorphic to $\mathbf{D}_4$.

Lemma 9.5
Let $\mathbf{D}_4[\rho_x, \kappa_6]$, $\mathbf{D}_4[\rho_y, \kappa_5]$, and $\mathbf{D}_4[\rho_z, \kappa_1]$ act on X_0 with the action induced from Table 9.1. Then

$$\begin{aligned} \mathrm{Fix}_{X_0}(\mathbf{D}_4[\rho_x, \kappa_6]) &= e_1 \cup e_4, \\ \mathrm{Fix}_{X_0}(\mathbf{D}_4[\rho_y, \kappa_5]) &= e_1 \cup e_3, \\ \mathrm{Fix}_{X_0}(\mathbf{D}_4[\rho_z, \kappa_1]) &= e_1 \cup e_5. \end{aligned}$$

Proof.

Case 1: $\mathbf{D}_4[\rho_x, \kappa_6]$. Since $\rho_x \in \mathbf{D}_4[\rho_x, \kappa_6]$, we have $\mathrm{Fix}(\mathbf{D}_4[\rho_x, \kappa_6]) \subset \{(z, z, z, z, x, x) | x \in \mathbb{R}, z \in \mathbb{C}\}$. Furthermore, the action of κ_6 implies that $z = \overline{z}$. Hence $\mathrm{Fix}(\mathbf{D}_4[\rho_x, \kappa_6]) = \{(x, x, x, x, y, y) | x \in \mathbb{R}, y \in \mathbb{R}\}$. We must now compute the fixed-point submanifold of $\mathbf{D}_4[\rho_x, \kappa_6]$ in X_0 we compute

$$N_\Gamma(\mathbf{D}_4[\rho_x, \kappa_6], \mathbb{O} \oplus \mathbf{Z}_2^c) = \{\gamma \in \Gamma | \gamma \mathrm{Fix}(\mathbb{O} \oplus \mathbf{Z}_2^c) \subseteq \mathrm{Fix}(\mathbf{D}_4[\rho_x, \kappa_6])\}.$$

The element $(\theta_1, \theta_2, \theta_3) \in \mathbf{T}^3$ is contained in $N_\Gamma(\mathbf{D}_4[\rho_x, \kappa_6], \mathbb{O} \oplus \mathbf{Z}_2^c)$ if and only if $\theta_1 + \theta_2 + \theta_3 = \theta_1 + \theta_3 = \theta_1 - \theta_2 = \theta_1 \equiv 0$ or π mod 2π and $\theta_2 + \theta = -\theta_2 \equiv 0$ or π mod 2π. Solving these equations yields $N_\Gamma(\mathbf{D}_4[\rho_x, \kappa_6], \mathbb{O} \oplus \mathbf{Z}_2^c) = \mathbb{O} \oplus \mathbf{Z}_2^c \cup e_1 \cup e_4$. Since

$$\mathrm{Fix}_{X_0}(\mathbf{D}_4[\rho_x, \kappa_6]) = N_\Gamma(\mathbf{D}_4[\rho_x, \kappa_6], \mathbb{O} \oplus \mathbf{Z}_2^c)/\mathbb{O} \oplus \mathbf{Z}_2^c,$$

the result follows.

Case 2: $\mathbf{D}_4[\rho_y, \kappa_5]$. Since $\rho_y \in \mathbf{D}_4[\rho_y, \kappa_5]$, we have $\mathrm{Fix}(\mathbf{D}_4[\rho_y, \kappa_5]) \subset \{(z, x, \overline{z}, x, z, \overline{z}) | x \in \mathbb{R}, z \in \mathbb{C}\}$. Furthermore, the action of κ_5 implies that $z = \overline{z}$. So $\mathrm{Fix}(\mathbf{D}_4[\rho_y, \kappa_5]) = \{(x, y, x, y, x, x) | x \in \mathbb{R}, y \in \mathbb{C}\}$. The element $(\theta_1, \theta_2, \theta_3) \in \mathbf{T}^3$ is contained in $N_\Gamma(\mathbf{D}_4[\rho_y, \kappa_5], \mathbb{O} \oplus \mathbf{Z}_2^c)$ if and only if $\theta_1 + \theta_2 + \theta_3 = \theta_1 - \theta_2 = \theta_2 + \theta_3 = -\theta_2 \equiv 0$ or π mod 2π and $\theta_1 + \theta_3 = \theta_1 \equiv 0$ or π mod 2π. Thus $N_\Gamma(\mathbf{D}_4[\rho_y, \kappa_5], \mathbb{O} \oplus \mathbf{Z}_2^c) = \mathbb{O} \oplus \mathbf{Z}_2^c \cup e_1 \cup e_3$. Since

$$\mathrm{Fix}_{X_0}(\mathbf{D}_4[\rho_y, \kappa_5]) = N_\Gamma(\mathbf{D}_4[\rho_y, \kappa_5], \mathbb{O})/\mathbb{O} \oplus \mathbf{Z}_2^c,$$

the result follows.

Case 3: $\mathbf{D}_4[\rho_z, \kappa_1]$. Since $\rho_z \in \mathbf{D}_4[\rho_z, \kappa_1]$, we have $\mathrm{Fix}(\mathbf{D}_4[\rho_z, \kappa_1]) \subset \{(x, z, x, \overline{z}, z, z) | x \in \mathbb{R}, z \in \mathbb{C}\}$. Furthermore, the action of κ_1 implies that $z = \overline{z}$. Therefore, $\mathrm{Fix}(\mathbf{D}_4[\rho_z, \kappa_1]) = \{(x, y, x, y, y, y) | x \in \mathbb{R}, y \in \mathbb{R}\}$. The element $(\theta_1, \theta_2, \theta_3) \in \mathbf{T}^3$ is contained in $N_\Gamma(\mathbf{D}_4[\rho_z, \kappa_1], \mathbb{O} \oplus \mathbf{Z}_2^c)$ if and only if $\theta_1 + \theta_2 + \theta_3 = \theta_1 - \theta_2 \equiv 0$ or π mod 2π and $\theta_1 + \theta_3 = \theta_1 = \theta_2 + \theta_3 = -\theta_2 \equiv 0$ or π mod 2π. Whence $N_\Gamma(\mathbf{D}_4[\rho_z, \kappa_1], \mathbb{O} \oplus \mathbf{Z}_2^c) = \mathbb{O} \oplus \mathbf{Z}_2^c \cup e_1 \cup e_5$. Since

$$\mathrm{Fix}_{X_0}(\mathbf{D}_4[\rho_z, \kappa_1]) = N_\Gamma(\mathbf{D}_4[\rho_z, \kappa_1], \mathbb{O} \oplus \mathbf{Z}_2^c)/\mathbb{O} \oplus \mathbf{Z}_2^c,$$

the result follows. □

Next we consider the groups isomorphic to $\mathbf{D}_3$.

Lemma 9.6
Let $\mathbf{D}_3[\tau_3,\kappa_3]$, $\mathbf{D}_3[\tau_2,\kappa_1]$, $\mathbf{D}_3[\tau_3,\kappa_3]$ *and* $\mathbf{D}_3[\tau_4,\kappa_5]$ *act on* X_0 *with the action induced from Table 9.1. Then*

$$\begin{aligned}
\mathrm{Fix}_{X_0}(\mathbf{D}_3[\tau_3,\kappa_3]) &= e_1 \cup e_2,\\
\mathrm{Fix}_{X_0}(\mathbf{D}_3[\tau_2,\kappa_1]) &= e_1 \cup e_6,\\
\mathrm{Fix}_{X_0}(\mathbf{D}_3[\tau_3,\kappa_3]) &= e_1 \cup e_8,\\
\mathrm{Fix}_{X_0}(\mathbf{D}_3[\tau_4,\kappa_5]) &= e_1 \cup e_7.
\end{aligned}$$

Proof.

Case 1: $\mathbf{D}_3[\tau_3,\kappa_3]$. Since $\tau_1 \in \mathbf{D}_3[\tau_3,\kappa_3]$, we have $\mathrm{Fix}(\mathbf{D}_3[\tau_3,\kappa_3]) \subset \{(z,z,z_3,\overline{z_3},z,\overline{z_3})\big|z_3 \in \mathbb{C}, z \in \mathbb{C}\}$. Furthermore $\kappa_5 \in \mathbf{D}_3[\tau_3,\kappa_3]$ implies that $\mathrm{Fix}(\mathbf{D}_3[\tau_3,\kappa_3]) \subset \{(x,x,z_3,\overline{z_3},x,\overline{z_3})\big|z_3 \in \mathbb{C}, x \in \mathbb{R}\}$. The element $(\theta_1,\theta_2,\theta_3) \in \mathbf{T}^3$ is contained in $N_\Gamma(\mathbf{D}_3[\tau_3,\kappa_3],\mathbb{O}\oplus\mathbf{Z}_2^c)$ if and only if $\theta_1+\theta_2+\theta_3 = \theta_1+\theta_3 = \theta_2+\theta_3 \equiv 0$ or π mod 2π and $-\theta_1+\theta_2 = \theta_1 = -\theta_2 \in [0,2\pi)$. Whence $N_\Gamma(\mathbf{D}_3[\tau_3,\kappa_3],\mathbb{O}\oplus\mathbf{Z}_2^c) = \mathbb{O}\oplus\mathbf{Z}_2^c \cup e_1 \cup e_2$. Since

$$\mathrm{Fix}_{X_0}(\mathbf{D}_3[\tau_3,\kappa_3]) = N_\Gamma(\mathbf{D}_3[\tau_3,\kappa_3],\mathbb{O}\oplus\mathbf{Z}_2^c)/\mathbb{O}\oplus\mathbf{Z}_2^c,$$

the result follows.

Case 2: $\mathbf{D}_3[\tau_2,\kappa_1]$. Since $\tau_2 \in \mathbf{D}_3[\tau_2,\kappa_1]$, we have $\mathrm{Fix}(\mathbf{D}_3[\tau_2,\kappa_1]) \subset \{(z,\overline{z},z_3,z_3,\overline{z_3},z)\big|z_3 \in \mathbb{C}, z \in \mathbb{C}\}$. Furthermore $\kappa_1 \in \mathbf{D}_3[\tau_2,\kappa_1]$ implies that $\mathrm{Fix}(\mathbf{D}_3[\tau_2,\kappa_1]) \subset \{(z,z,x,x,x,z)\big|z \in \mathbb{C}, x \in \mathbb{R}\}$. The element $(\theta_1,\theta_2,\theta_3) \in \mathbf{T}^3$ is contained in $N_\Gamma(\mathbf{D}_3[\tau_2,\kappa_1],\mathbb{O}\oplus\mathbf{Z}_2^c)$ if and only if $\theta_1+\theta_2+\theta_3 = \theta_1+\theta_3 = -\theta_2 \in [0,2\pi)$ and $\theta_2+\theta_3 = \theta_1-\theta_2 = \theta_1 \equiv 0$ or π mod 2π. Therefore $N_\Gamma(\mathbf{D}_3[\tau_2,\kappa_1],\mathbb{O}\oplus\mathbf{Z}_2^c) = \mathbb{O}\oplus\mathbf{Z}_2^c \cup e_1 \cup e_6$. Since

$$\mathrm{Fix}_{X_0}(\mathbf{D}_3[\tau_2,\kappa_1]) = N_\Gamma(\mathbf{D}_3[\tau_2,\kappa_1],\mathbb{O}\oplus\mathbf{Z}_2^c)/\mathbb{O}\oplus\mathbf{Z}_2^c,$$

the result follows.

Case 3: $\mathbf{D}_3[\tau_3,\kappa_3]$. Since $\tau_3 \in \mathbf{D}_3[\tau_2,\kappa_1]$, we have $\mathrm{Fix}(\mathbf{D}_3[\tau_3,\kappa_3]) \subset \{(z,z_2,\overline{z_2},z,\overline{z_2},\overline{z})\big|z_2 \in \mathbb{C}, z \in \mathbb{C}\}$. Furthermore $\kappa_3 \in \mathbf{D}_3[\tau_3,\kappa_3]$ implies that $\mathrm{Fix}(\mathbf{D}_3[\tau_3,\kappa_3]) \subset \{(x,z,z,x,z,x)\big|z \in \mathbb{C}, x \in \mathbb{R}\}$. The element $(\theta_1,\theta_2,\theta_3) \in \mathbf{T}^3$ is contained in $N_\Gamma(\mathbf{D}_3[\tau_3,\kappa_3],\mathbb{O}\oplus\mathbf{Z}_2^c)$ if and only if $\theta_1+\theta_2+\theta_3 = \theta_1 = -\theta_2 \equiv 0$ or π mod 2π and $\theta_1+\theta_3 = \theta_1-\theta_2 = \theta_2+\theta_3 \in [0,2\pi)$. Therefore $N_\Gamma(\mathbf{D}_3[\tau_3,\kappa_3],\mathbb{O}\oplus\mathbf{Z}_2^c) = \mathbb{O}\oplus\mathbf{Z}_2^c \cup e_1 \cup e_8$. Since

$$\mathrm{Fix}_{X_0}(\mathbf{D}_3[\tau_3,\kappa_3]) = N_\Gamma(\mathbf{D}_3[\tau_3,\kappa_3],\mathbb{O}\oplus\mathbf{Z}_2^c)/\mathbb{O}\oplus\mathbf{Z}_2^c,$$

the result follows.

Case 4: $\mathbf{D}_3[\tau_4,\kappa_5]$. Since $\tau_4 \in \mathbf{D}_3[\tau_4,\kappa_5]$, we have $\mathrm{Fix}(\mathbf{D}_3[\tau_4,\kappa_5]) \subset \{(z,z_2,z_2,\overline{z},\overline{z},z_2)\big|z_2 \in \mathbb{C}, z \in \mathbb{C}\}$. Furthermore $\kappa_3 \in \mathbf{D}_3[\tau_4,\kappa_5]$ implies that $\mathrm{Fix}(\mathbf{D}_3[\tau_4,\kappa_5]) \subset \{(z,x,x,\overline{z},\overline{z},x)\big|z \in \mathbb{C}, x \in \mathbb{R}\}$. The element $(\theta_1,\theta_2,\theta_3) \in \mathbf{T}^3$ is contained in $N_\Gamma(\mathbf{D}_3[\tau_4,\kappa_5],\mathbb{O}\oplus\mathbf{Z}_2^c)$ if and only if $\theta_1+\theta_2+\theta_3 = \theta_1 = \theta_2+\theta_3 \in [0,2\pi)$ and $\theta_1+\theta_3 = \theta_1-\theta_2 = -\theta_2 \equiv 0$ or π mod 2π. Therefore, $N_\Gamma(\mathbf{D}_3[\tau_4,\kappa_5],\mathbb{O}\oplus\mathbf{Z}_2^c) = \mathbb{O}\oplus\mathbf{Z}_2^c \cup e_1 \cup e_8$. Since

$$\mathrm{Fix}_{X_0}(\mathbf{D}_3[\tau_4,\kappa_5]) = N_\Gamma(\mathbf{D}_3[\tau_4,\kappa_5],\mathbb{O}\oplus\mathbf{Z}_2^c)/\mathbb{O}\oplus\mathbf{Z}_2^c,$$

the result follows. □

We now consider the groups $\mathbf{Z}_4[\rho_x]$, $\mathbf{Z}_4[\rho_y]$, and $\mathbf{Z}_4[\rho_z]$.

Lemma 9.7
Let $\mathbf{Z}_4[\rho_x]$, $\mathbf{Z}_4[\rho_y]$ *and* $\mathbf{Z}_4[\rho_z]$ *act on* X_0 *with the action induced from Table 9.1. Then*

$$\begin{aligned}\mathrm{Fix}_{X_0}(\mathbf{Z}_4[\rho_x]) &= c_1,\\ \mathrm{Fix}_{X_0}(\mathbf{Z}_4[\rho_y]) &= c_3,\\ \mathrm{Fix}_{X_0}(\mathbf{Z}_4[\rho_z]) &= c_{33}.\end{aligned}$$

Proof.

Case 1: $\mathbf{Z}_4[\rho_x]$. Since $\rho_x \in \mathbf{Z}_4[\rho_x]$, we have $\mathrm{Fix}(\mathbf{Z}_4[\rho_x]) = \{(z,z,z,z,x,x)\big|x \in \mathbb{R}, z \in \mathbb{C}\}$. The element $(\theta_1,\theta_2,\theta_3) \in \mathbf{T}^3$ is contained in $N_\Gamma(\mathbf{Z}_4[\rho_x], \mathbb{O} \oplus \mathbf{Z}_2^c)$ if and only if $\theta_1+\theta_2+\theta_3 = \theta_1+\theta_3 = \theta_1-\theta_2 = \theta_1$ and $\theta_2+\theta_3 = -\theta_2 \equiv 0$ or $\pi \bmod 2\pi$. Therefore $N_\Gamma(\mathbf{Z}_4[\rho_x], \mathbb{O}\oplus\mathbf{Z}_2^c) = \mathbb{O}\cup c_1$. Since

$$\mathrm{Fix}_{X_0}(\mathbf{Z}_4[\rho_x]) = N_\Gamma(\mathbf{Z}_4[\rho_x], \mathbb{O} \oplus \mathbf{Z}_2^c)/\mathbb{O} \oplus \mathbf{Z}_2^c,$$

the result follows.

Case 2: $\mathbf{Z}_4[\rho_y]$. Since $\rho_y \in \mathbf{Z}_4[\rho_y]$, we have $\mathrm{Fix}(\mathbf{Z}_4[\rho_y]) = \{(z,x,\overline{z},x,z,\overline{z})\big|x \in \mathbb{R}, z \in \mathbb{C}\}$. The element $(\theta_1,\theta_2,\theta_3) \in \mathbf{T}^3$ is contained in $N_\Gamma(\mathbf{Z}_4[\rho_y], \mathbb{O}\oplus\mathbf{Z}_2^c)$ if and only if $\theta_1+\theta_2+\theta_3 = -(\theta_1+\theta_2) = \theta_2+\theta_3 = \theta_2$ and $\theta_1+\theta_3 = \theta_1 \equiv 0$ or $\pi \bmod 2\pi$. Thus $N_\Gamma(\mathbf{Z}_4[\rho_y], \mathbb{O} \oplus \mathbf{Z}_2^c) = \mathbb{O} \oplus \mathbf{Z}_2^c \cup c_3$. Since

$$\mathrm{Fix}_{X_0}(\mathbf{Z}_4[\rho_y]) = N_\Gamma(\mathbf{Z}_4[\rho_y], \mathbb{O} \oplus \mathbf{Z}_2^c)/\mathbb{O} \oplus \mathbf{Z}_2^c,$$

the result follows.

Case 3: $\mathbf{Z}_4[\rho_z]$. Since $\rho_z \in \mathbf{Z}_4[\rho_z]$, we have $\mathrm{Fix}(\mathbf{Z}_4[\rho_z]) \subset \{(x,z,x,\overline{z},z,z)\big|x \in \mathbb{R}, z \in \mathbb{C}\}$. The element $(\theta_1,\theta_2,\theta_3) \in \mathbf{T}^3$ is contained in $N_\Gamma(\mathbf{Z}_4[\rho_z], \mathbb{O}\oplus\mathbf{Z}_2^c)$ if and only if $\theta_1+\theta_2+\theta_3 = \theta_1-\theta_2 \equiv 0$ or $\pi \bmod 2\pi$ and $\theta_1+\theta_3 = -\theta_1 = \theta_2+\theta_3 = -\theta_2$. Therefore $N_\Gamma(\mathbf{Z}_4[\rho_z], \mathbb{O}\oplus\mathbf{Z}_2^c) = \mathbb{O}\oplus\mathbf{Z}_2^c \cup c_{33}$. Since

$$\mathrm{Fix}_{X_0}(\mathbf{Z}_4[\rho_z]) = N_\Gamma(\mathbf{Z}_4[\rho_z], \mathbb{O} \oplus \mathbf{Z}_2^c)/\mathbb{O} \oplus \mathbf{Z}_2^c,$$

the result follows. □

Next we consider the subgroups $\mathbf{D}_2[\rho_x^2,\kappa_4]$, $\mathbf{D}_2[\rho_y^2,\kappa_5]$, $\mathbf{D}_2[\rho_z^2,\kappa_1]$, and $\mathbf{D}_2[\rho_x^2,\rho_y^2]$.

Lemma 9.8
Let $\mathbf{D}_2[\rho_x^2,\kappa_4]$, $\mathbf{D}_2[\rho_y^2,\kappa_5]$, $\mathbf{D}_2[\rho_z^2,\kappa_1]$ *and* $\mathbf{D}_2[\rho_x^2,\rho_y^2]$ *act on* X_0 *with the action induced from Table 9.1. Then*

$$\begin{aligned}\mathrm{Fix}_{X_0}(\mathbf{D}_2[\rho_x^2,\kappa_6]) &= e_1 \cup e_4 \cup e_{11} \cup e_{12},\\ \mathrm{Fix}_{X_0}(\mathbf{D}_2[\rho_y^2,\kappa_5]) &= e_1 \cup e_3 \cup e_{13} \cup e_{14},\\ \mathrm{Fix}_{X_0}(\mathbf{D}_2[\rho_z^2,\kappa_1]) &= e_1 \cup e_5 \cup e_{15} \cup e_{16},\\ \mathrm{Fix}_{X_0}(\mathbf{D}_2[\rho_x^2,\rho_y^2]) &= e_1 \cup e_3 \cup e_4 \cup e_5.\end{aligned}$$

Proof.

Case 1: $\mathbf{D}_2[\rho_x^2,\kappa_6]$. Since $\rho_x^2, \kappa_6 \in \mathbf{D}_2[\rho_x^2,\kappa_6]$, we have $\mathrm{Fix}(\mathbf{D}_2[\rho_x^2,\kappa_6]) \subset \{(z,\overline{z},z,\overline{z},x_5,x_6)\big|x_5,x_6 \in \mathbb{R}, z \in \mathbb{C}\}$. The element $(\theta_1,\theta_2,\theta_3) \in \mathbf{T}^3$ is contained in $N_\Gamma(\mathbf{D}_2[\rho_x^2,\kappa_6], \mathbb{O} \oplus \mathbf{Z}_2^c)$ if and only if $\theta_1+\theta_2+\theta_3 = -\theta_1-\theta_3 = \theta_1-\theta_2 = -\theta_1 \in [0,2\pi)$ and θ_2, $\theta_2+\theta_3 \equiv 0$ or $\pi \bmod 2\pi$. Whence $N_\Gamma(\mathbf{D}_2[\rho_x^2,\kappa_6], \mathbb{O} \oplus \mathbf{Z}_2^c) = \mathbb{O} \oplus \mathbf{Z}_2^c \cup e_1 \cup e_4 \cup e_{11} \cup e_{12}$. Since

$$\mathrm{Fix}_{X_0}(\mathbf{D}_2[\rho_x^2,\kappa_6]) = N_\Gamma(\mathbf{D}_2[\rho_x^2,\kappa_6], \mathbb{O} \oplus \mathbf{Z}_2^c)/\mathbb{O} \oplus \mathbf{Z}_2^c,$$

the result follows.

Case 2: $\mathbf{D}_2[\rho_y^2,\kappa_5]$. Since $\rho_y^2, \kappa_5 \in \mathbf{D}_2[\rho_y^2,\kappa_5]$, we have $\mathrm{Fix}(\mathbf{D}_2[\rho_y^2,\kappa_5]) \subset \{(z,x_2,\overline{z},x_4,\overline{z},z)\big|x_2,x_4 \in$

$\mathbb{R}, z \in \mathbb{C}\}$. The element $(\theta_1, \theta_2, \theta_3) \in \mathbf{T}^3$ is contained in $N_\Gamma(\mathbf{D}_2[\rho_y^2, \kappa_5], \mathbb{O} \oplus \mathbf{Z}_2^c)$ if and only if $\theta_1 + \theta_2 + \theta_3 = -\theta_2 = -\theta_1 + \theta_2 = -\theta_2 - \theta_3 \in [0, 2\pi)$ and θ_1, $\theta_1 + \theta_3 \equiv 0$ or π mod 2π. Therefore, $N_\Gamma(\mathbf{D}_2[\rho_y^2, \kappa_5], \mathbb{O} \oplus \mathbf{Z}_2^c) = \mathbb{O} \oplus \mathbf{Z}_2^c \cup e_1 \cup e_3 \cup e_{13} \cup e_{14}$. Since

$$\mathrm{Fix}_{X_0}(\mathbf{D}_2[\rho_y^2, \kappa_5]) = N_\Gamma(\mathbf{D}_2[\rho_y^2, \kappa_5], \mathbb{O} \oplus \mathbf{Z}_2^c)/\mathbb{O} \oplus \mathbf{Z}_2^c,$$

the result follows.

Case 3: $\mathbf{D}_2[\rho_z^2, \kappa_1]$. Since ρ_z^2, $\kappa_1 \in \mathbf{D}_2[\rho_y^2, \kappa_5]$, we have $\mathrm{Fix}(\mathbf{D}_2[\rho_z^2, \kappa_1]) \subset \{(x_1, z, x_3, \overline{z}, \overline{z}, \overline{z}) \big| x_1, x_3 \in \mathbb{R}, z \in \mathbb{C}\}$. The element $(\theta_1, \theta_2, \theta_3) \in \mathbf{T}^3$ is contained in $N_\Gamma(\mathbf{D}_2[\rho_z^2, \kappa_1], \mathbb{O} \oplus \mathbf{Z}_2^c)$ if and only if $\theta_1 + \theta_3 = -\theta_1 = -\theta_2 - \theta_3 = \theta_2 \in [0, 2\pi)$ and $\theta_1 + \theta_2 + \theta_3$, $\theta_1 - \theta_2 \equiv 0$ or π mod 2π. Therefore $N_\Gamma(\mathbf{D}_2[\rho_z^2, \kappa_1], \mathbb{O} \oplus \mathbf{Z}_2^c) = \mathbb{O} \oplus \mathbf{Z}_2^c \cup e_1 \cup e_3 \cup e_{15} \cup e_{16}$. Since

$$\mathrm{Fix}_{X_0}(\mathbf{D}_2[\rho_z^2, \kappa_1]) = N_\Gamma(\mathbf{D}_2[\rho_z^2, \kappa_1], \mathbb{O} \oplus \mathbf{Z}_2^c)/\mathbb{O} \oplus \mathbf{Z}_2^c,$$

the result follows.

Case 4: $\mathbf{D}_2[\rho_x^2, \rho_y^2]$. Since ρ_x^2, $\rho_y^2 \in \mathbf{D}_2[\rho_x^2, \rho_y^2]$ an element $\mathbf{z} = (z_1, z_2, z_3, z_4, z_5, z_6) \in \mathbb{C}^3$ is fixed by $\mathbf{D}_2[\rho_x^2, \rho_y^2]$ if and only if $z_1 = z_3$, $z_2 = z_4$, z_5 and z_6 are all real. Therefore,

$$N_\Gamma(\mathbf{D}_2[\rho_x^2, \rho_y^2], \mathbb{O} \oplus \mathbf{Z}_2^c) = \{\gamma \in \Gamma \big| \gamma \mathrm{Fix}(\mathbb{O} \oplus \mathbf{Z}_2^c) \subseteq \mathrm{Fix}(\mathbf{D}_2[\rho_x^2, \rho_y^2])\},$$

contains the elements e_1, e_3, e_4, e_5 as well as $\mathbb{O} \oplus \mathbf{Z}_2^c$. Therefore

$$\mathrm{Fix}_{X_0}(\mathbf{D}_2[\rho_x^2, \rho_y^2]) = e_1 \cup e_3 \cup e_4 \cup e_5,$$

as required. □

Next we consider the groups $\mathbf{Z}_3[\tau_1]$, $\mathbf{Z}_3[\tau_2]$, $\mathbf{Z}_3[\tau_3]$, and $\mathbf{Z}_3[\tau_4]$.

Lemma 9.9
Let $\mathbf{Z}_3[\tau_1]$, $\mathbf{Z}_3[\tau_2]$, $\mathbf{Z}_3[\tau_3]$ and $\mathbf{Z}_3[\tau_4]$ act on X_0 with the action induced from Table 9.1. Then

$$\begin{aligned} \mathrm{Fix}_{X_0}(\mathbf{Z}_3[\tau_1]) &= c_5, \\ \mathrm{Fix}_{X_0}(\mathbf{Z}_3[\tau_2]) &= c_{13}, \\ \mathrm{Fix}_{X_0}(\mathbf{Z}_3[\tau_3]) &= c_{21}, \\ \mathrm{Fix}_{X_0}(\mathbf{Z}_4[\tau_4]) &= c_{17}. \end{aligned}$$

Proof.

Case 1: $\mathbf{Z}_3[\tau_1]$. Since τ_1, $\tau_1^2 \in \mathbf{Z}_3[\tau_1]$, a vector $(z_1, z_2, z_3, z_4, z_5, z_6) \in \mathbb{C}^6$ is fixed by $\mathbf{Z}_3[\tau_1]$ if and only if $z_1 = z_2 = z_5$ and $z_3 = \overline{z_4} = \overline{z_6}$. Therefore $\mathrm{Fix}(\mathbf{Z}_3[\tau_1]) = \{(z, z, z_3, \overline{z_3}, \overline{z_3}, z) \big| z, z_3 \in \mathbb{C}\}$. The element $(\theta_1, \theta_2, \theta_3) \in \mathbf{T}^3$ is contained in $N_\Gamma(\mathbf{Z}_3[\tau_1], \mathbb{O} \oplus \mathbf{Z}_2^c)$ if and only if $\theta_1 + \theta_2 + \theta_3 = \theta_1 + \theta_3 = \theta_2 + \theta_3$ and $\theta_1 - \theta_2 = -\theta_1 = \theta_2$. Therefore $\mathrm{Fix}(\mathbf{Z}_3[\tau_1]) = c_5$.

Case 2: $\mathbf{Z}_3[\tau_2]$. Since τ_2, $\tau_2^2 \in \mathbf{Z}_3[\tau_2]$, a vector $(z_1, z_2, z_3, z_4, z_5, z_6) \in \mathbb{C}^6$ is fixed by $\mathbf{Z}_3[\tau_2]$ if and only if $z_1 = \overline{z_2} = z_6$, $z_3 = z_4 = \overline{z_5}$. Therefore $\mathrm{Fix}(\mathbf{Z}_3[\tau_2]) = \{(z, \overline{z}, z_3, z_3, \overline{z_3}, z) \big| z \in \mathbb{C}\}$. A $(\theta_1, \theta_2, \theta_3) \in \mathbf{T}^3$ is contained in $N_\Gamma(\mathbf{Z}_3[\tau_1], \mathbb{O} \oplus \mathbf{Z}_2^c)$ if and only if $\theta_1 + \theta_2 + \theta_3 = -\theta_1 - \theta_3 = -\theta_2$ and $\theta_1 - \theta_2 = \theta_1 = -\theta_2 - \theta_3$. Therefore $\mathrm{Fix}(\mathbf{Z}_3[\tau_2]) = c_{13}$.

Case 3: $\mathbf{Z}_3[\tau_3]$. Since τ_3, $\tau_3^2 \in \mathbf{Z}_3[\tau_3]$, a vector $(z_1, z_2, z_3, z_4, z_5, z_6) \in \mathbb{C}^6$ is fixed by $\mathbf{Z}_3[\tau_3]$ if and only if $z_1 = z_4 = \overline{z_6}$ and $z_2 = \overline{z_3} = \overline{z_5}$. Therefore $\mathrm{Fix}(\mathbf{Z}_3[\tau_3]) = \{(z, z_2, \overline{z_2}, z, \overline{z_2}, \overline{z}) \big| z, z_2 \in \mathbb{C}\}$. The element $(\theta_1, \theta_2, \theta_3) \in \mathbf{T}^3$ is contained in $N_\Gamma(\mathbf{Z}_3[\tau_3], \mathbb{O} \oplus \mathbf{Z}_2^c)$ if and only if $\theta_1 + \theta_2 + \theta_3 = \theta_1 = \theta_2$ and $\theta_1 + \theta_3 = -\theta_1 + \theta_2 = -\theta_2 - \theta_3$. Therefore $\mathrm{Fix}(\mathbf{Z}_3[\tau_3]) = c_{21}$.

Case 4: $\mathbf{Z}_3[\tau_4]$. Since τ_4 and τ_4^2 are contained in $\mathbf{Z}_3[\tau_4]$, a vector $(z_1, z_2, z_3, z_4, z_5, z_6) \in \mathbb{C}^6$ is fixed by $\mathbf{Z}_3[\tau_4]$ if and only if $z_1 = \overline{z_4} = \overline{z_5}$ and $z_2 = z_3 = z_6$. Therefore $\mathrm{Fix}(\mathbf{Z}_3[\tau_4]) = \{(z, z_2, z_2, \overline{z}, \overline{z}, z_2) | z, z_2 \in \mathbb{C}\}$. The element $(\theta_1, \theta_2, \theta_3) \in \mathbf{T}^3$ is contained in $N_\Gamma(\mathbf{Z}_3[\tau_4], \mathbb{O} \oplus \mathbf{Z}_2^c)$ if and only if $\theta_1 + \theta_2 + \theta_3 = \theta_1 = \theta_2 + \theta_3$ and $\theta_1 + \theta_3 = \theta_1 - \theta_2 = -\theta_2$. Therefore $\mathrm{Fix}(\mathbf{Z}_3[\tau_4]) = c_{17}$. □

Finally we consider the groups $\mathbf{Z}_2[\rho_x^2]$, $\mathbf{Z}_2[\rho_y^2]$, $\mathbf{Z}_2[\rho_z^2]$, $\mathbf{Z}_2[\kappa_1]$, $\mathbf{Z}_2[\kappa_2]$, $\mathbf{Z}_2[\kappa_3]$, $\mathbf{Z}_2[\kappa_4]$, $\mathbf{Z}_2[\kappa_5]$, and $\mathbf{Z}_2[\kappa_6]$.

Lemma 9.10
Let $\mathbf{Z}_2[\rho_x^2]$, $\mathbf{Z}_2[\rho_y^2]$, $\mathbf{Z}_2[\rho_z^2]$, $\mathbf{Z}_2[\kappa_1]$, $\mathbf{Z}_2[\kappa_2]$, $\mathbf{Z}_2[\kappa_3]$, $\mathbf{Z}_2[\kappa_4]$, $\mathbf{Z}_2[\kappa_5]$, and $\mathbf{Z}_2[\kappa_6]$ act on X_0 with the action induced from Table 9.1. Then

$$\begin{aligned}
\mathrm{Fix}_{X_0}(\mathbf{Z}_2[\rho_x^2]) &= c_1 \cup c_{23}, \\
\mathrm{Fix}_{X_0}(\mathbf{Z}_2[\rho_y^2]) &= c_3 \cup c_{25}, \\
\mathrm{Fix}_{X_0}(\mathbf{Z}_2[\rho_z^2]) &= c_{33} \cup c_{38}, \\
\mathrm{Fix}_{X_0}(\mathbf{Z}_2[\kappa_1]) &= c_7 \cup c_{37}, \\
\mathrm{Fix}_{X_0}(\mathbf{Z}_2[\kappa_2]) &= c_9 \cup c_{10}, \\
\mathrm{Fix}_{X_0}(\mathbf{Z}_2[\kappa_3]) &= c_{39} \cup c_{40}, \\
\mathrm{Fix}_{X_0}(\mathbf{Z}_2[\kappa_4]) &= c_{41} \cup c_{42}, \\
\mathrm{Fix}_{X_0}(\mathbf{Z}_2[\kappa_5]) &= c_{43} \cup c_{44}, \\
\mathrm{Fix}_{X_0}(\mathbf{Z}_2[\kappa_6]) &= c_{45} \cup c_{46}.
\end{aligned}$$

Proof.

Case 1: $\mathbf{Z}_2[\rho_x^2]$. The action of ρ_x^2 implies that $\mathrm{Fix}(\mathbf{Z}_2[\rho_x^2]) = \{(z_1, z_2, z_1, z_2, x_5, x_6) | z_1, z_2 \in \mathbb{C}, x_5, x_6 \in \mathbb{R}\}$, so $N_\Gamma(\mathbf{Z}_2[\rho_x^2], \mathbb{O} \oplus \mathbf{Z}_2^c) = \mathbb{O} \oplus \mathbf{Z}_2^c \cup c_1 \cup c_{23}$. Indeed, $(\theta_1, \theta_2, \theta_3)$ is contained in $N_\Gamma(\mathbf{Z}_2[\rho_x^2], \mathbb{O} \oplus \mathbf{Z}_2^c)$ if and only if $\theta_1 + \theta_2 + \theta_3 = \theta_1 - \theta_2$, $\theta_1 + \theta_3 = \theta_1$ and $\theta_2 + \theta_3$, $\theta_2 = 0$ or $\pi \bmod 2\pi$. Therefore $\mathrm{Fix}(\mathbf{Z}_2[\rho_x^2]) = c_1 \cup c_{23}$.

Case 2: $\mathbf{Z}_2[\rho_y^2]$. A straightforward computations shows $\mathrm{Fix}(\mathbf{Z}_2[\rho_y^2]) = \{(z, x_2, \overline{z}, x_4, z_4, \overline{z_5}) | x_2, x_4 \in \mathbb{R}, z_2, z_5 \in \mathbb{C}\}$. The element $(\theta_1, \theta_2, \theta_3)$ is contained in $N_\Gamma(\mathbf{Z}_2[\rho_y^2], \mathbb{O} \oplus \mathbf{Z}_2^c)$ if and only if $\theta_1 + \theta_2 + \theta_3 = -\theta_1 + \theta_2$, $\theta_2 + \theta_3 = \theta_2$ and $\theta_1 + \theta_3$, $\theta_1 = 0$ or $\pi \bmod 2\pi$. Therefore $\mathrm{Fix}(\mathbf{Z}_2[\rho_x^2]) = c_3 \cup c_{25}$.

Case 3: $\mathbf{Z}_2[\rho_z^2]$. A standard computations shows $\mathrm{Fix}(\mathbf{Z}_2[\rho_z^2]) = \{(x_1, z_2, x_3, \overline{z_2}, z_5, z_5) | x_1, x_3 \in \mathbb{R}, z_2, z_5 \in \mathbb{C}\}$. The element $(\theta_1, \theta_2, \theta_3)$ is contained in $N_\Gamma(\mathbf{Z}_2[\rho_z^2], \mathbb{O} \oplus \mathbf{Z}_2^c)$ if and only if $\theta_1 + \theta_3 = -\theta_1$, $\theta_2 + \theta_3 = -\theta_2$ and $\theta_1 + \theta_2 + \theta_3$, $\theta_1 - \theta_2 = 0$ or $\pi \bmod 2\pi$ Therefore $\mathrm{Fix}(\mathbf{Z}_2[\rho_z^2]) = c_{33} \cup c_{38}$.

Case 4: $\mathbf{Z}_2[\kappa_1]$. A standard computation shows $\mathrm{Fix}(\mathbf{Z}_2[\kappa_1]) = \{(z, z_2, x_3, z_4, z_4, \overline{z_2}) | x_3 \in \mathbb{R}, z, z_2, z_4 \in \mathbb{C}\}$. The element $(\theta_1, \theta_2, \theta_3)$ is contained in $N_\Gamma(\mathbf{Z}_2[\kappa_1], \mathbb{O} \oplus \mathbf{Z}_2^c)$ if and only if $\theta_1 + \theta_3 = \theta_2$, $\theta_1 = \theta_2 + \theta_3$ and $\theta_1 - \theta_2 = 0$ or $\pi \bmod 2\pi$. Therefore $\mathrm{Fix}(\mathbf{Z}_2[\kappa_1]) = c_7 \cup c_{37}$.

Case 5: $\mathbf{Z}_2[\kappa_2]$. A computation shows $\mathrm{Fix}(\mathbf{Z}_2[\kappa_2]) = \{(x_1, z_2, z_3, z_4, \overline{z_2}, z_4) | x_1 \in \mathbb{R}, z_2, z_3, z_4 \in \mathbb{C}\}$. The element $(\theta_1, \theta_2, \theta_3)$ is contained in $N_\Gamma(\mathbf{Z}_2[\kappa_2], \mathbb{O} \oplus \mathbf{Z}_2^c)$ if and only if $\theta_1 + \theta_3 = -\theta_2 - \theta_3$, $\theta_1 = -\theta_2$ and $\theta_1 + \theta_2 + \theta_3 \equiv 0$ or $\pi \bmod 2\pi$. Therefore $\mathrm{Fix}(\mathbf{Z}_2[\kappa_2]) = c_9 \cup c_{10}$.

Case 6: $\mathbf{Z}_2[\kappa_3]$. A computation shows $\mathrm{Fix}(\mathbf{Z}_2[\kappa_3]) = \{(z_1, z_2, z_3, x_4, z_3, z_1) | x_4 \in \mathbb{R}, z_1, z_2, z_3 \in \mathbb{C}\}$. The element $(\theta_1, \theta_2, \theta_3)$ is contained in $N_\Gamma(\mathbf{Z}_2[\kappa_3], \mathbb{O} \oplus \mathbf{Z}_2^c)$ if and only if $\theta_1 + \theta_2 + \theta_3 = -\theta_2$, $\theta_1 - \theta_2 = \theta_2 + \theta_3$ and $\theta_1 = 0$ or $\pi \bmod 2\pi$. Therefore $\mathrm{Fix}(\mathbf{Z}_2[\kappa_3]) = c_{39} \cup c_{40}$.

Case 7: $\mathbf{Z}_2[\kappa_4]$.A computation shows $\mathrm{Fix}(\mathbf{Z}_2[\kappa_4]) = \{(z_1, z_2, \overline{z_2}, \overline{z_1}, z_5, x_6) | x_6 \in \mathbb{R}, z_1, z_2, z_5 \in$

$\mathbb{C}\}$. The element $(\theta_1, \theta_2, \theta_3)$ is contained in $N_\Gamma(\mathbf{Z}_2[\kappa_4], \mathbb{O} \oplus \mathbf{Z}_2^c)$ if and only if $\theta_1 + \theta_2 + \theta_3 = -\theta_2 - \theta_3$, $\theta_1 - \theta_2 = \theta_2$ and $\theta_1 + \theta_3 = 0$ or π mod 2π. Therefore $\mathrm{Fix}(\mathbf{Z}_2[\kappa_4]) = c_{41} \cup c_{42}$.

Case 8: $\mathbf{Z}_2[\kappa_5]$. A computation shows $\mathrm{Fix}(\mathbf{Z}_2[\kappa_5]) = \{(z_1, x_2, z_3, z_4, \overline{z_1}, \overline{z_3}) | x_2 \in \mathbb{R}, z_1, z_3, z_4 \in \mathbb{C}\}$. The element $(\theta_1, \theta_2, \theta_3)$ is contained in $N_\Gamma(\mathbf{Z}_2[\kappa_5], \mathbb{O} \oplus \mathbf{Z}_2^c)$ if and only if $\theta_1 + \theta_2 + \theta_3 = -\theta_2 - \theta_3$, $\theta_1 - \theta_2 = \theta_2$ and $\theta_1 + \theta_3 = 0$ or π mod 2π. Therefore $\mathrm{Fix}(\mathbf{Z}_2[\kappa_5]) = c_{43} \cup c_{44}$.

Case 9: $\mathbf{Z}_2[\kappa_6]$. A computation shows $\mathrm{Fix}(\mathbf{Z}_2[\kappa_6]) = \{(z_1, \overline{z_1}, z_3, \overline{z_3}, x_5, z_6) | x_5 \in \mathbb{R}, z_1, z_3, z_6 \in \mathbb{C}\}$. The element $(\theta_1, \theta_2, \theta_3)$ is contained in $N_\Gamma(\mathbf{Z}_2[\kappa_6], \mathbb{O} \oplus \mathbf{Z}_2^c)$ if and only if $\theta_1 + \theta_2 + \theta_3 = -\theta_1 - \theta_3$, $\theta_1 - \theta_2 = -\theta_1$ and $\theta_2 + \theta_3 = 0$ or π mod 2π. Therefore $\mathrm{Fix}(\mathbf{Z}_2[\kappa_6]) = c_{45} \cup c_{46}$. □

This completes the computation of all the fixed-point submanifolds for all non-trivial subgroups of $\mathbb{O}$. It now follows that

$$\begin{aligned}\mathscr{C}_{\mathbb{O}} = \{&e_1, e_2, e_3, e_4, e_5, e_6, e_7, e_8, e_{11}, e_{12}, e_{13}, e_{14}, e_{15}, e_{16}, c_1, c_3, c_5, c_7, c_9, c_{10},\\ &c_{13}, c_{17}, c_{21}, c_{23}, c_{25}, c_{33}, c_{37}, c_{38}, c_{39}, c_{40}, c_{41}, c_{42}, c_{43}, c_{44}, c_{45}, c_{46}\}.\end{aligned}$$

Which completes the proof of Proposition 9.3. We use this information to form the skeleton

$$\mathbb{X}_{\mathbb{O}} = \bigcup_{C \in \mathscr{C}_{\mathbb{O}}} C \subset \mathbf{T}^3 \cong X_0.$$

At this point we meet our by now familiar problem: the skeleton is too complex to be meaningful. Thus we use the $\mathbb{O}$ symmetry to simplify the geometry.

Symmetry Properties of $\mathbb{X}_{\mathbb{O}}$

Here using the $\mathbb{O}$ action induced on X_0 we compute the setwise isotropy $\mathrm{Stab}(C)$ and the pointwise isotropy $\mathrm{stab}(C)$. This provides restrictions on $\mathbb{O}$-equivariant flows on the skeleton and simplifications of the skeletons geometry. Using this information we form the projected skeleton.

Pointwise and Setwise Isotropy Subgroups. The action of $\mathbb{O}$ in Table 9.1 induces a natural action on X_0. The generators for $\mathbb{O}$ act as follows:

$$\begin{aligned}\rho_x(\theta_1, \theta_2, \theta_3) &= (\theta_1 - \theta_2, -\theta_2 - \theta_3, 2\theta_2 + \theta_3),\\ \rho_y(\theta_1, \theta_2, \theta_3) &= (\theta_1 + \theta_3, -\theta_2, -\theta_3).\end{aligned}$$

The complete action of $\mathbb{O}$ on X_0 is given in Table 9.2. The action of $\mathbb{O}$ on X_0 induces an action of $\mathbb{O}$ on $\mathscr{C}_{\mathbb{O}}$ by permutation. We present this action in Table 9.3.

Proposition 9.11
Let $\mathbb{O}$ act on $\mathscr{C}_{\mathbb{O}}$ as in Table 9.3 and on X_0 as in Table 9.2. Then given $C \in \mathscr{C}_{\mathbb{O}}$, the setwise isotropy $\mathrm{Stab}(C)$, pointwise isotropy $\mathrm{stab}(C)$ and the group $S(C)$ are given in Table 9.7.

Proof. Perform the usual calculations. □

It is interesting to observe that we have several C's with $S(C) \cong \mathbf{D}_2$. The implications of this will be discussed later.

Knots Relative to C. The action of $\mathbb{O}$ on $\mathscr{C}_{\mathbb{O}}$ in Table 9.3 shows that there are five C's that are not symmetrically related, namely: $c_1 = \{(\theta, 0, 0) | \theta \in [0, 2\pi)\}$, $c_5 = \{(0, 0, \theta) | \theta \in [0, 2\pi)\}$, $c_7 = \{(\theta, \theta, 0) | \theta \in [0, 2\pi)\}$, $c_{10} = \{(\theta, -\theta, \pi) | \theta \in [0, 2\pi)\}$, and $c_{23} = \{(\theta, \pi, 0) | \theta \in [0, 2\pi)\}$. The representatives of the equilibria that lie on these C's are: e_1, e_2, e_4 and e_{11}.

For those (orbit representatives) C's that satisfy $S(C) \cong \mathbf{Z}_2$ or $\mathbf{D}_2$, it follows that there is at least one axis of reflection symmetry on C. These axes are given by the knots relative to C.

Table 9.2: Action of $\mathbb{O}$ induced on X_0 for the BCC lattice.

Element of $\mathbb{O}$	Action on X_0
ρ_x	$(\theta_1 - \theta_2, -\theta_2 - \theta_3, 2\theta_2 + \theta_3)$
ρ_x^2	$(\theta_1 + \theta_3, -\theta_2, -\theta_3)$
ρ_x^3	$(\theta_1 + \theta_2 + \theta_3, \theta_2 + \theta_3, -2\theta_2 - \theta_3)$
ρ_y	$(\theta_1 + \theta_3, -\theta_2, -\theta_3)$
ρ_y^2	$(-\theta_1, \theta_2 + \theta_3, -\theta_3)$
ρ_y^3	$(-\theta_1 - \theta_3, \theta_2 + \theta_3, -\theta_3)$
ρ_z	$(-\theta_2 - \theta_3, \theta_1, \theta_3)$
ρ_z^2	$(-\theta_1 - \theta_3, -\theta_2 - \theta_3, \theta_3)$
ρ_z^3	$(\theta_2, -\theta_1 - \theta_3, \theta_3)$
τ_1	$(-\theta_2, \theta_1 - \theta_2, 2\theta_2 + \theta_3)$
τ_1^2	$(\theta_2 - \theta_1, -\theta_1, 2\theta_1 + \theta_3)$
τ_2	$(\theta_1 - \theta_2, \theta_1 + \theta_3, -2\theta_1 - \theta_3)$
τ_2^2	$(-\theta_2 - \theta_3, -\theta_1 - \theta_2 - \theta_3, 2\theta_2 + \theta_3)$
τ_3	$(\theta_2, \theta_1 + \theta_2 + \theta_3, -2\theta_2 - \theta_3)$
τ_3^2	$(\theta_1 + \theta_2 + \theta_3, \theta_1, -2\theta_1 - \theta_3)$
τ_4	$(-\theta_1 - \theta_2 - \theta_3, -\theta_1 - \theta_3, 2\theta_1 + \theta_3)$
τ_4^2	$(\theta_2 + \theta_3, -\theta_1 + \theta_2, -2\theta_2 - \theta_3)$
κ_1	$(\theta_2 + \theta_3, \theta_1 + \theta_3, -\theta_3)$
κ_2	$(-\theta_2, -\theta_1, -\theta_3)$
κ_3	$(-\theta_1, -\theta_1 - \theta_2 - \theta_3, 2\theta_1 + \theta_3)$
κ_4	$(-\theta_1 - \theta_2 - \theta_3, -\theta_2, 2\theta_2 + \theta_3)$
κ_5	$(\theta_1, \theta_1 - \theta_2, -2\theta_1 - \theta_3)$
κ_6	$(-\theta_1 + \theta_2, \theta_2, 2\theta_2 - \theta_3)$

Table 9.3: Action of $\mathbb{O}$ induced on $\mathscr{C}_\mathbb{O}$ for the BCC lattice.

Element of $\mathscr{C}_\mathbb{O}$	Elements of $\mathbb{O}$ acting nontrivially	Action
e_1	None	
e_2	$\rho_x, \rho_y^2, \rho_z^3, \kappa_3, \tau_2, \tau_3$	e_7
	$\rho_x^2, \rho_y^3, \rho_z, \kappa_4, \tau_3^2, \tau_4^2$	e_6
	$\rho_x^3, \rho_y^3, \rho_z^2, \kappa_2, \tau_1, \tau_3^2$	e_8
e_3	$\rho_x, \rho_x^3, \kappa_4, \kappa_6, \tau_1, \tau_2^2, \tau_3, \tau_4^2$	e_5
	$\rho_z, \rho_z^3, \kappa_1, \kappa_2, \tau_1^2, \tau_2, \tau_3^2, \tau_4$	e_4
e_4	$\rho_y, \rho_y^3, \kappa_3, \kappa_5, \tau_1^2, \tau_2, \tau_3^2, \tau_4$	e_5
	$\rho_z, \rho_z^3, \kappa_1, \kappa_2, \tau_1, \tau_2^2, \tau_3, \tau_4^2$	e_3
e_5	$\rho_x, \rho_x^3, \kappa_4, \kappa_6, \tau_1^2, \tau_2, \tau_3^2, \tau_4$	e_3
	$\rho_y, \rho_y^3, \kappa_3, \kappa_5, \tau_1, \tau_2^2, \tau_3, \tau_4^2$	e_4
e_6	$\rho_x, \rho_y^2, \rho_z^3, \kappa_6, \tau_1^2, \tau_4^2$	e_8
	$\rho_x^2, \rho_y^3, \rho_z, \kappa_4, \tau_3, \tau_4$	e_2
	$\rho_x^3, \rho_y^3, \rho_z^2, \kappa_2, \tau_1, \tau_3^2$	e_7
e_7	$\rho_x, \rho_y, \rho_z^2, \kappa_2, \tau_1^2, \tau_3$	e_6
	$\rho_x^2, \rho_y^3, \rho_z^3, \kappa_6, \tau_1, \tau_2$	e_8
	$\rho_x^3, \rho_y^2, \rho_z, \kappa_3, \tau_2^2, \tau_3^2$	e_2
e_8	$\rho_x, \rho_y^3, \rho_z^2, \kappa_1, \tau_2, \tau_4^2$	e_2
	$\rho_x^2, \rho_y, \rho_z, \kappa_6, \tau_1^2, \tau_2^2$	e_7
	$\rho_x^3, \rho_y^2, \rho_z^3, \kappa_5, \tau_1, \tau_4$	e_6

Table 9.4: Table 9.3 continued

Element of $\mathscr{C}_0$	Elements of $\mathbb{O}$ acting nontrivially	Action
e_{11}	$\rho_x, \rho_x^3, \rho_z^2, \rho_y^2$	e_{12}
	$\rho_y, \kappa_5, \tau_1^2, \tau_4$	e_{15}
	$\rho_y^3, \kappa_3, \tau_2, \tau_3^2$	e_{16}
	$\rho_z, \kappa_1, \tau_2^2, \tau_4^2$	e_{13}
	$\rho_z^3, \kappa_2, \tau_1, \tau_3$	e_{14}
e_{12}	$\rho_x, \rho_x^3, \rho_z^2, \rho_y^2$	e_{11}
	$\rho_y, \kappa_5, \tau_1^2, \tau_4$	e_{16}
	$\rho_y^3, \kappa_3, \tau_2, \tau_3^2$	e_{15}
	$\rho_z, \kappa_1, \tau_2^2, \tau_4^2$	e_{14}
	$\rho_z^3, \kappa_2, \tau_1, \tau_3$	e_{13}
e_{13}	$\rho_x, \kappa_4, \tau_3, \tau_4^2$	e_{12}
	$\rho_x^2, \rho_y, \rho_y^3, \rho_z^2$	e_{16}
	$\rho_x^3, \kappa_6, \tau_1, \tau_2^2$	e_{15}
	$\rho_z, \kappa_2, \tau_1^2, \tau_3^2$	e_{14}
	$\rho_z^3, \kappa_1, \tau_2, \tau_4$	e_{13}
e_{14}	$\rho_x, \kappa_4, \tau_3, \tau_4^2$	e_{15}
	$\rho_x^2, \rho_y, \rho_y^3, \rho_z^2$	e_{13}
	$\rho_x^3, \kappa_6, \tau_1, \tau_2^2$	e_{16}
	$\rho_z, \kappa_2, \tau_1^2, \tau_3^2$	e_{12}
	$\rho_z^3, \kappa_1, \tau_2, \tau_4$	e_{11}
e_{15}	$\rho_x, \kappa_6, \tau_2, \tau_1^2$	e_{14}
	$\rho_x^2, \rho_y^2, \rho_z, \rho_z^3$	e_{16}
	$\rho_x^3, \kappa_4, \tau_3^2, \tau_4$	e_{13}
	$\rho_y, \kappa_3, \tau_2^2, \tau_3$	e_{12}
	$\rho_y^3, \kappa_5, \tau_4^2, \tau_1$	e_{11}
e_{16}	$\rho_x, \kappa_6, \tau_2, \tau_1^2$	e_{13}
	$\rho_x^2, \rho_y^2, \rho_z, \rho_z^3$	e_{15}
	$\rho_x^3, \kappa_4, \tau_3^2, \tau_4$	e_{14}
	$\rho_y, \kappa_3, \tau_2^2, \tau_3$	e_{11}
	$\rho_y^3, \kappa_5, \tau_4^2, \tau_1$	e_{12}
c_1	$\rho_y, \rho_y^3, \kappa_3, \kappa_5, \tau_1^2, \tau_2, \tau_3^2, \tau_4$	c_{33}
	$\rho_z, \rho_z^3, \kappa_1, \kappa_2, \tau_1, \tau_2^2, \tau_3, \tau_4^2$	c_3
c_3	$\rho_x, \rho_x^3, \kappa_4, \kappa_6, \tau_1, \tau_2^2, \tau_3, \tau_4^2$	c_{33}
	$\rho_z, \rho_z^3, \kappa_1, \kappa_2, \tau_1^2, \tau_2, \tau_3^2, \tau_4$	c_1

Table 9.5: Table 9.3 continued

Element of $\mathscr{C}_{\mathbb{O}}$	Elements of $\mathbb{O}$ acting nontrivially	Action
c_5	$\rho_x, \rho_x^3, \kappa_4, \kappa_6, \tau_2, \tau_3$	c_{17}
	$\rho_x^2, \rho_y^3, \rho_z, \kappa_4, \tau_3^2, \tau_4^2$	c_{13}
	$\rho_x^3, \rho_y, \rho_z^2, \kappa_1, \tau_2^2, \tau_4$	c_{21}
c_7	$\rho_x, \kappa_6, \tau_1^2, \tau_2$	c_{39}
	$\rho_x^2, \rho_y^2, \rho_z, \rho_z^3$	c_9
	$\rho_x^3, \kappa_4, \tau_3^2, \tau_4$	c_{43}
	$\rho_y, \kappa_3, \tau_2^2, \tau_3$	c_{45}
	$\rho_y^3, \kappa_5, \tau_1, \tau_4^2$	c_{41}
c_9	$\rho_x, \kappa_6, \tau_1^2, \tau_2$	c_{43}
	$\rho_x^2, \rho_y^2, \rho_z, \rho_z^3$	c_7
	$\rho_x^3, \kappa_4, \tau_3^2, \tau_4$	c_{39}
	$\rho_y, \kappa_3, \tau_2^2, \tau_3$	c_{41}
	$\rho_y^3, \kappa_5, \tau_1, \tau_4^2$	c_{45}
c_{10}	$\rho_x, \kappa_6, \tau_1^2, \tau_2$	c_{44}
	$\rho_x^2, \rho_y^2, \rho_z, \rho_z^3$	c_{37}
	$\rho_x^3, \kappa_4, \tau_3^2, \tau_4$	c_{40}
	$\rho_y, \kappa_3, \tau_2^2, \tau_3$	c_{42}
	$\rho_y^3, \kappa_5, \tau_1, \tau_4^2$	c_{46}
c_{13}	$\rho_x, \rho_y^2, \rho_z, \kappa_5, \tau_1^2, \tau_4^2$	c_{21}
	$\rho_x^2, \rho_y, \rho_z^3, \kappa_4, \tau_3, \tau_4$	c_5
	$\rho_x^3, \rho_y^3, \rho_z^2, \kappa_2, \tau_1, \tau_3^2$	c_{17}
c_{17}	$\rho_x, \rho_y, \rho_z^2, \kappa_2, \tau_1^2, \tau_3$	c_{13}
	$\rho_x^2, \rho_y^3, \rho_z^3, \kappa_6, \tau_1, \tau_2$	c_{21}
	$\rho_x^3, \rho_y^2, \rho_z, \kappa_3, \tau_2^2, \tau_3^2$	c_5
c_{21}	$\rho_x, \rho_y^3, \rho_z^2, \kappa_1, \tau_2, \tau_4^2$	c_5
	$\rho_x^2, \rho_y, \rho_z, \kappa_6, \tau_1^2, \tau_2^2$	c_{17}
	$\rho_x^3, \rho_y^2, \rho_z^3, \kappa_5, \tau_1, \tau_4$	c_{13}
c_{23}	$\rho_y, \rho_y^3, \kappa_3, \kappa_5, \tau_1^2, \tau_2, \tau_3^2, \tau_4$	c_{38}
	$\rho_z, \rho_z^3, \kappa_1, \kappa_2, \tau_1, \tau_2^2, \tau_3, \tau_4^2$	c_{25}
c_{25}	$\rho_x, \rho_x^3, \kappa_4, \kappa_6, \tau_1, \tau_2^2, \tau_3, \tau_4^2$	c_{38}
	$\rho_z, \rho_z^3, \kappa_1, \kappa_2, \tau_1^2, \tau_2, \tau_3^2, \tau_4$	c_{23}
c_{33}	$\rho_x, \rho_x^3, \kappa_4, \kappa_6, \tau_1^2, \tau_2, \tau_3^2, \tau_4$	c_3
	$\rho_y, \rho_y^3, \kappa_3, \kappa_5, \tau_1, \tau_2^2, \tau_3, \tau_4^2$	c_1
c_{37}	$\rho_x, \tau_1, \tau_1^2, \tau_2$	c_{40}
	$\rho_x^2, \rho_y^2, \rho_z, \rho_z^3$	c_{10}
	$\rho_x^3, \kappa_4, \tau_3^2, \tau_4$	c_{44}
	$\rho_y, \kappa_3, \tau_2^2, \tau_3$	c_{46}
	$\rho_y^3, \kappa_5, \tau_1, \tau_4^2$	c_{42}

Table 9.6: Table 9.3 continued

Element of $\mathscr{C}_{\mathbb{O}}$	Elements of $\mathbb{O}$ acting nontrivially	Action
c_{38}	$\rho_x, \rho_x^3, \kappa_4, \kappa_6, \tau_1^2, \tau_2, \tau_3^2, \tau_4$	c_{25}
	$\rho_y, \rho_y^3, \kappa_3, \kappa_5, \tau_1, \tau_2^2, \tau_3, \tau_4^2$	c_{23}
c_{39}	$\rho_x, \kappa_4, \tau_3, \tau_4^2$	c_9
	$\rho_x^2, \rho_y, \rho_y^3, \rho_z^2$	c_{43}
	$\rho_x^3, \kappa_6, \tau_1, \tau_2^2$	c_7
	$\rho_z, \kappa_2, \tau_1^2, \tau_3^2$	c_{41}
	$\rho_z^3, \kappa_1, \tau_2, \tau_4$	c_{45}
c_{40}	$\rho_x, \kappa_4, \tau_3, \tau_4^2$	c_{10}
	$\rho_x^2, \rho_y, \rho_y^3, \rho_z^2$	c_{44}
	$\rho_x^3, \kappa_6, \tau_1, \tau_2^2$	c_{37}
	$\rho_z, \kappa_2, \tau_1^2, \tau_3^2$	c_{38}
	$\rho_z^3, \kappa_1, \tau_2, \tau_4$	c_{46}
c_{41}	$\rho_x, \rho_x^3, \rho_y^2, \rho_z^2$	c_{45}
	$\rho_y, \kappa_5, \tau_1^2, \tau_4$	c_7
	$\rho_y^3, \kappa_3, \tau_2, \tau_3^2$	c_9
	$\rho_z, \kappa_1, \tau_2^2, \tau_4^2$	c_{43}
	$\rho_z^3, \kappa_2, \tau_1^2, \tau_3$	c_{39}
c_{42}	$\rho_x, \rho_x^3, \rho_y^2, \rho_z^2$	c_{46}
	$\rho_y, \kappa_5, \tau_1^2, \tau_4$	c_{37}
	$\rho_y^3, \kappa_3, \tau_2, \tau_3^2$	c_{10}
	$\rho_z, \kappa_1, \tau_2^2, \tau_4^2$	c_{44}
	$\rho_z^3, \kappa_2, \tau_1^2, \tau_3$	c_{40}
c_{43}	$\rho_x, \kappa_4, \tau_3, \tau_4^2$	c_7
	$\rho_x^2, \rho_y, \rho_y^3, \rho_z^2$	c_{39}
	$\rho_x^3, \kappa_6, \tau_1, \tau_2^2$	c_9
	$\rho_z, \kappa_2, \tau_1^2, \tau_3^2$	c_{41}
	$\rho_z^3, \kappa_1, \tau_2, \tau_4$	c_{45}
c_{44}	$\rho_x, \kappa_4, \tau_3, \tau_4^2$	c_{37}
	$\rho_x^2, \rho_y, \rho_y^3, \rho_z^2$	c_{40}
	$\rho_x^3, \kappa_6, \tau_1, \tau_2^2$	c_{10}
	$\rho_z, \kappa_2, \tau_1^2, \tau_3^2$	c_{46}
	$\rho_z^3, \kappa_1, \tau_2, \tau_4$	c_{42}
c_{45}	$\rho_x, \rho_x^3, \rho_y^2, \rho_z^2$	c_{41}
	$\rho_y, \kappa_5, \tau_1^2, \tau_4$	c_9
	$\rho_y^3, \kappa_3, \tau_2, \tau_3^2$	c_7
	$\rho_z, \kappa_1, \tau_2^2, \tau_4^2$	c_{39}
	$\rho_z^3, \kappa_2, \tau_1^2, \tau_3$	c_{43}
c_{46}	$\rho_x, \rho_x^3, \rho_y^2, \rho_z^2$	c_{42}
	$\rho_y, \kappa_5, \tau_1^2, \tau_4$	c_{10}
	$\rho_y^3, \kappa_3, \tau_2, \tau_3^2$	c_{37}
	$\rho_z, \kappa_1, \tau_2^2, \tau_4^2$	c_{40}
	$\rho_z^3, \kappa_2, \tau_1^2, \tau_3$	c_{44}

Table 9.7: Isotropy data for $C \in \mathscr{C}_{\mathbb{O}}$ for the BCC lattice.

$C \in \mathscr{C}_{\mathbb{O}}$	stab(C)	Stab(C)	$S(C) = \text{Stab}(C)/\text{stab}(C)$
e_1	$\mathbb{O}$	$\mathbb{O}$	$\mathbf{1}$
e_2	$\mathbf{D}_3[\tau_3, \kappa_3]$	$\mathbf{D}_3[\tau_3, \kappa_3]$	$\mathbf{1}$
e_3	$\mathbf{D}_3[\tau_3, \kappa_3]$	$\mathbf{D}_3[\tau_3, \kappa_3]$	$\mathbf{1}$
e_4	$\mathbf{D}_4[\rho_x, \kappa_6]$	$\mathbf{D}_4[\rho_x, \kappa_6]$	$\mathbf{1}$
e_5	$\mathbf{D}_4[\rho_z, \kappa_1]$	$\mathbf{D}_4[\rho_z, \kappa_1]$	$\mathbf{1}$
e_6	$\mathbf{D}_3[\tau_2, \kappa_1]$	$\mathbf{D}_3[\tau_2, \kappa_1]$	$\mathbf{1}$
e_7	$\mathbf{D}_3[\tau_4, \kappa_5]$	$\mathbf{D}_3[\tau_4, \kappa_5]$	$\mathbf{1}$
e_8	$\mathbf{D}_3[\tau_3, \kappa_3]$	$\mathbf{D}_3[\tau_3, \kappa_3]$	$\mathbf{1}$
e_{11}	$\mathbf{D}_2[\rho_x^2, \kappa_6]$	$\mathbf{D}_2[\rho_x^2, \kappa_6]$	$\mathbf{1}$
e_{12}	$\mathbf{D}_2[\rho_x^2, \kappa_6]$	$\mathbf{D}_2[\rho_x^2, \kappa_6]$	$\mathbf{1}$
e_{13}	$\mathbf{D}_2[\rho_y^2, \kappa_5]$	$\mathbf{D}_2[\rho_y^2, \kappa_5]$	$\mathbf{1}$
e_{14}	$\mathbf{D}_2[\rho_y^2, \kappa_5]$	$\mathbf{D}_2[\rho_y^2, \kappa_5]$	$\mathbf{1}$
e_{15}	$\mathbf{D}_2[\rho_z^2, \kappa_1]$	$\mathbf{D}_2[\rho_z^2, \kappa_1]$	$\mathbf{1}$
e_{16}	$\mathbf{D}_2[\rho_z^2, \kappa_1]$	$\mathbf{D}_2[\rho_z^2, \kappa_1]$	$\mathbf{1}$
c_1	$\mathbf{Z}_4[\rho_x]$	$\mathbf{D}_4[\rho_x, \kappa_6]$	$\mathbf{Z}_2$
c_3	$\mathbf{Z}_4[\rho_y]$	$\mathbf{D}_4[\rho_y, \kappa_5]$	$\mathbf{Z}_2$
c_5	$\mathbf{Z}_3[\tau_1]$	$\mathbf{D}_3[\tau_3, \kappa_3]$	$\mathbf{Z}_2$
c_7	$\mathbf{Z}_2[\kappa_1]$	$\mathbf{D}_2[\rho_z^2, \kappa_1]$	$\mathbf{Z}_2$
c_9	$\mathbf{Z}_2[\kappa_2]$	$\mathbf{D}_2[\rho_z^2, \kappa_1]$	$\mathbf{Z}_2$
c_{10}	$\mathbf{Z}_2[\kappa_2]$	$\mathbf{D}_2[\rho_z^2, \kappa_1]$	$\mathbf{Z}_2$
c_{13}	$\mathbf{Z}_3[\tau_2]$	$\mathbf{D}_3[\tau_2, \kappa_1]$	$\mathbf{Z}_2$
c_{17}	$\mathbf{Z}_3[\tau_4]$	$\mathbf{D}_3[\tau_4, \kappa_5]$	$\mathbf{Z}_2$
c_{21}	$\mathbf{Z}_3[\tau_3]$	$\mathbf{D}_3[\tau_3, \kappa_3]$	$\mathbf{Z}_2$
c_{23}	$\mathbf{Z}_2[\rho_x^2]$	$\mathbf{D}_4[\rho_x, \kappa_6]$	$\mathbf{D}_2$
c_{25}	$\mathbf{Z}_2[\rho_y^2]$	$\mathbf{D}_4[\rho_y, \kappa_5]$	$\mathbf{D}_2$
c_{33}	$\mathbf{Z}_4[\rho_z]$	$\mathbf{D}_4[\rho_z, \kappa_1]$	$\mathbf{Z}_2$
c_{37}	$\mathbf{Z}_2[\kappa_1]$	$\mathbf{D}_2[\rho_z^2, \kappa_1]$	$\mathbf{Z}_2$
c_{38}	$\mathbf{Z}_2[\rho_z^2]$	$\mathbf{D}_4[\rho_z, \kappa_1]$	$\mathbf{D}_2$
c_{39}	$\mathbf{Z}_2[\rho_y^2]$	$\mathbf{D}_2[\rho_y^2, \kappa_3]$	$\mathbf{Z}_2$
c_{40}	$\mathbf{Z}_2[\kappa_3]$	$\mathbf{D}_2[\rho_y^2, \kappa_3]$	$\mathbf{Z}_2$
c_{41}	$\mathbf{Z}_2[\kappa_4]$	$\mathbf{D}_2[\rho_x^2, \kappa_6]$	$\mathbf{Z}_2$
c_{42}	$\mathbf{Z}_2[\kappa_4]$	$\mathbf{D}_2[\rho_x^2, \kappa_6]$	$\mathbf{Z}_2$
c_{43}	$\mathbf{Z}_2[\kappa_5]$	$\mathbf{D}_2[\rho_y^2, \kappa_3]$	$\mathbf{Z}_2$
c_{44}	$\mathbf{Z}_2[\kappa_5]$	$\mathbf{D}_2[\rho_y^2, \kappa_3]$	$\mathbf{Z}_2$
c_{45}	$\mathbf{Z}_2[\kappa_6]$	$\mathbf{D}_2[\rho_x^2, \kappa_6]$	$\mathbf{Z}_2$
c_{46}	$\mathbf{Z}_2[\kappa_6]$	$\mathbf{D}_2[\rho_x^2, \kappa_6]$	$\mathbf{Z}_2$

Table 9.8: Knots relative to orbit representatives of $C \in \mathscr{C}_{\mathbb{O}}$ for the BCC lattice.

Element of $\mathscr{C}_{\mathbb{O}}$	Knots
c_1	e_1, e_4
c_5	e_1, e_2
c_7	e_1, e_4
c_{10}	e_4, e_2
c_{23}	e_4, e_{11}

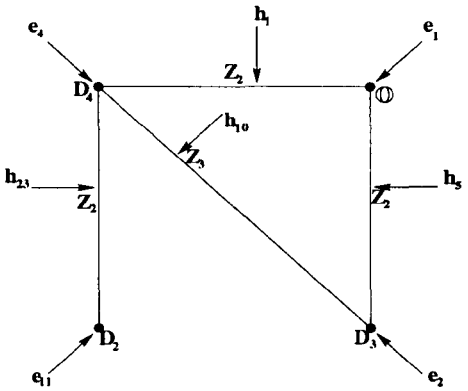

Figure 9.1: The projected skeleton $\mathbb{X}_{\mathbb{O}}^{p}$. Here $h_1 = \{(\theta,0,0)|\theta \in (0,\pi)\}$, $h_5 = \{(0,0,\theta)|\theta \in (0,\pi)\}$, $h_7 = \{(\theta,\theta,0)|\theta \in (0,\pi)\}$, $h_{10} = \{(\theta,-\theta,\pi)|\theta \in (0,\pi)\}$, and $h_{23} = \{(\theta,\pi,0)|\theta \in (0,\pi)\}$.

All knots must be equilibria, and since each (orbit representative) C, that satisfies $S(C) \cong \mathbf{Z}_2$ contains two equilibria, these equilibria are the knots. The (orbit representative) c_{23} is different; c_{23} contains four equilibria e_3, e_5, e_{11}, and e_{12}, which project into two orbit representatives e_4 and e_{11}. The group $S(c_{23})$ acts as rotation by π on c_{23}, mapping the equilibrium e_3 to e_5, and e_{11} to e_{12}. There are also two reflections; one fixes the line between e_3 and e_5, the other the line between e_{11} and e_{12}. These equilibria are the knots relative to c_{23}. This is the first example we have of a connection where $S(C) \cong \mathbf{D}_2$. We summarise this information in Table 9.8.

Projected Skeleton

The action of $\mathbb{O}$ on $\mathscr{C}_{\mathbb{O}}$ shows that there are five orbit representatives for the elements of $\mathscr{C}_{\mathbb{O}}$ that are homeomorphic to $\mathbf{S}^1$. These are c_1, c_5, c_7, c_{10}, and c_{23}. The orbit representatives for the equilibria are e_1, e_2, e_4, and e_{11}. Each C projects into the orbit space as a line joining the two knots. More precisely, we have the following relations: c_1 connects e_1 to e_4, c_5 connects e_1 to e_2, c_7 connects e_1 to e_4, c_{10} connects e_2 to e_4, and c_{23} connects e_4 to e_{11}. Figure 9.1 illustrates the projected skeleton. From the projected skeleton we may deduce that there exist at most 32 qualitatively different $\mathbb{O}$-equivariant flows on $\mathbb{X}_{\mathbb{O}}$.

Remark 9.12
The projected skeleton has a structure that is more general than that of a heteroclinic network as introduced by Kirk and Silber [55]. It is still possible for there to exist heteroclinic cycles on the projected skeleton, but the presence of the connection h_{23} implies that a heteroclinic network cannot exist.

We shall not investigate this problem any further. There are two reasons for this omission. Firstly, the invariant theory is complex, making the equivariant vector field complex, leading to long and tedious calculations related to the flow formulas. Secondly, our application for forced

symmetry breaking on the BCC lattice in Part IV requires knowledge only of forced symmetry breaking to the group $\mathbf{D}_3[\tau_3, \kappa_3]$.

9.2.3 Forced Symmetry Breaking to $\mathbf{D}_4[\rho_x, \kappa_6]$

In this subsection we consider the behaviour of the group orbit X_0 when symmetry breaking terms with $\mathbf{D}_4[\rho_x, \kappa_6]$ symmetry are added to (9.3). Since the manifold X_0 is normally hyperbolic, it persists to give a new invariant manifold X_ε. The action of $\mathbf{D}_4[\rho_x, \kappa_6]$ on $\mathbb{C}^6$ is in Table 9.9.

Table 9.9: Action of $\mathbf{D}_4[\rho_x, \kappa_6]$ on $\mathbb{C}^6$ for the BCC lattice.

Element of $\mathbb{O}$	Action on $\mathbb{C}^6$
ρ_x	$(z_4, z_1, z_2, z_3, \overline{z_6}, z_5)$
ρ_x^2	$(z_3, z_4, z_1, z_2, \overline{z_5}, \overline{z_6})$
ρ_x^3	$(z_2, z_3, z_4, z_1, z_6, \overline{z_5})$
ρ_y^2	$(\overline{z_3}, \overline{z_2}, \overline{z_1}, \overline{z_4}, \overline{z_6}, \overline{z_5})$
ρ_z^2	$(\overline{z_1}, \overline{z_4}, \overline{z_3}, \overline{z_2}, z_6, z_5)$
κ_4	$(\overline{z_4}, \overline{z_3}, \overline{z_2}, \overline{z_1}, z_5, \overline{z_6})$
κ_6	$(\overline{z_2}, \overline{z_1}, \overline{z_4}, \overline{z_3}, \overline{z_5}, z_6)$

Calculation of the Skeleton

Using the action of $\mathbf{D}_4[\rho_x, \kappa_6]$ in Table 9.9 we may compute the skeleton. The next proposition is crucial.

Proposition 9.13
Let $\mathbf{D}_4[\rho_x, \kappa_6]$ act on X_0 with the action induced from Table 9.9. Then

$$\mathscr{C}_{\mathbf{D}_4[\rho_x,\kappa_6]} = \{e_1, e_3, e_4, e_5, e_{11}, e_{12}, c_1, c_3, c_{23}, c_{25}, c_{33}, c_{38}, c_{41}, c_{42}, c_{45}, c_{46}\}.$$

Proof. This follows from Lemmas 9.5, 9.7, 9.8 and 9.10. □

Symmetry Properties of $\mathbf{D}_4[\rho_x, \kappa_6]$

Here we use the $\mathbf{D}_4[\rho_x, \kappa_6]$ symmetry to study the action induced on the skeleton.

Pointwise and Setwise Isotropy Subgroups The action of $\mathbf{D}_4[\rho_x, \kappa_6]$ on $\mathbb{C}^6$ in Table 9.9 induces a natural action on X_0, as follows:

$$\begin{aligned} \rho_x(\theta_1, \theta_2, \theta_3) &= (\theta_1 - \theta_2, -\theta_2 - \theta_3, 2\theta_2 + \theta_3), \\ \kappa_6(\theta_1, \theta_2, \theta_3) &= (-\theta_1 + \theta_2, \theta_2, 2\theta_2 - \theta_3). \end{aligned}$$

The complete action of $\mathbf{D}_4[\rho_x, \kappa_6]$ on X_0 is in Table 9.10. The action of $\mathbf{D}_4[\rho_x, \kappa_6]$ on X_0 induces an action on $\mathscr{C}_{\mathbf{D}_4[\rho_x,\kappa_6]}$ by permutation. We present this action in Table 9.11.

Proposition 9.14
Let $\mathbf{D}_4[\rho_x, \kappa_6]$ act on $\mathscr{C}_\mathbb{O}$ as in Table 9.11 and on X_0 as in Table 9.10. Then given $C \in \mathscr{C}_{\mathbf{D}_4[\rho_x,\kappa_6]}$, the setwise isotropy $\mathrm{Stab}(C)$, *pointwise isotropy* $\mathrm{stab}(C)$ *and $S(C)$ are in Table 9.12.*

Proof. The proof follows the usual lines. □

Table 9.10: Action of $\mathbf{D}_4[\rho_x, \kappa_6]$ induced on X_0 for the BCC lattice.

Element of $\mathbf{D}_4[\rho_x, \kappa_6]$	Action on X_0
ρ_x	$(\theta_1 - \theta_2, -\theta_2 - \theta_3, 2\theta_2 + \theta_3)$
ρ_x^2	$(\theta_1 + \theta_3, -\theta_2, -\theta_3)$
ρ_x^3	$(\theta_1 + \theta_2 + \theta_3, \theta_2 + \theta_3, -2\theta_2 - \theta_3)$
ρ_y^2	$(-\theta_1, \theta_2 + \theta_3, -\theta_3)$
ρ_z^2	$(-\theta_1 - \theta_3, -\theta_2 - \theta_3, \theta_3)$
κ_4	$(-\theta_1 - \theta_2 - \theta_3, -\theta_2, 2\theta_2 + \theta_3)$
κ_6	$(-\theta_1 + \theta_2, \theta_2, 2\theta_2 - \theta_3)$

Table 9.11: Action of $\mathbf{D}_4[\rho_x, \kappa_6]$ induced on $\mathscr{C}_{\mathbf{D}_4[\rho_x,\kappa_6]}$ for the BCC lattice.

Element of $\mathscr{C}_{\mathbf{D}_4[\rho_x,\kappa_6]}$	Elements of $\mathbb{O}$ acting nontrivially	Action
e_1	None	
e_3	ρ_x, ρ_x^3, κ_4, κ_6,	e_5
e_4	None	
e_5	ρ_x, ρ_x^3, κ_4, κ_6,	e_3
e_{11}	ρ_x, ρ_x^3, ρ_z^2, ρ_y^2	e_{12}
e_{12}	ρ_x, ρ_x^3, ρ_z^2, ρ_y^2	e_{11}
c_1	None	
c_3	ρ_x, ρ_x^3, κ_4, κ_6,	c_{33}
c_{23}	None	
c_{25}	ρ_x, ρ_x^3, κ_4, κ_6,	c_{38}
c_{33}	ρ_x, ρ_x^3, κ_4, κ_6,	c_3
c_{38}	ρ_x, ρ_x^3, κ_4, κ_6,	c_{25}
c_{41}	ρ_x, ρ_x^3, ρ_y^2, ρ_z^2	c_{45}
c_{42}	ρ_x, ρ_x^3, ρ_y^2, ρ_z^2	c_{46}
c_{45}	ρ_x, ρ_x^3, ρ_y^2, ρ_z^2	c_{41}
c_{46}	ρ_x, ρ_x^3, ρ_y^2, ρ_z^2	c_{42}

Table 9.12: Isotropy data for $C \in \mathscr{C}_{\mathbf{D}_4[\rho_x,\kappa_6]}$ for the BCC lattice.

$C \in \mathscr{C}_{\mathbf{D}_4[\rho_x,\kappa_6]}$	stab(C)	Stab(C)	$S(C) = \text{Stab}(C)/\text{stab}(C)$
e_1	$\mathbf{D}_4[\rho_x, \kappa_6]$	$\mathbf{D}_4[\rho_x, \kappa_6]$	$\mathbf{1}$
e_3	$\mathbf{D}_2[\rho_x^2, \rho_y^2]$	$\mathbf{D}_2[\rho_x^2, \rho_y^2]$	$\mathbf{1}$
e_4	$\mathbf{D}_4[\rho_x, \kappa_6]$	$\mathbf{D}_4[\rho_x, \kappa_6]$	$\mathbf{1}$
e_5	$\mathbf{D}_2[\rho_x^2, \rho_y^2]$	$\mathbf{D}_2[\rho_x^2, \rho_y^2]$	$\mathbf{1}$
e_{11}	$\mathbf{D}_2[\rho_x, \kappa_6]$	$\mathbf{D}_2[\rho_x, \kappa_6]$	$\mathbf{1}$
e_{12}	$\mathbf{D}_2[\rho_x, \kappa_6]$	$\mathbf{D}_2[\rho_x, \kappa_6]$	$\mathbf{1}$
c_1	$\mathbf{Z}_4[\rho_x]$	$\mathbf{D}_4[\rho_x, \kappa_6]$	$\mathbf{Z}_2$
c_3	$\mathbf{Z}_2[\rho_y^2]$	$\mathbf{D}_2[\rho_x^2, \rho_y^2]$	$\mathbf{Z}_2$
c_{23}	$\mathbf{Z}_2[\rho_x^2]$	$\mathbf{D}_4[\rho_x, \kappa_6]$	$\mathbf{D}_2$
c_{25}	$\mathbf{Z}_2[\rho_y^2]$	$\mathbf{D}_2[\rho_x^2, \rho_y^2]$	$\mathbf{Z}_2$
c_{33}	$\mathbf{Z}_2[\rho_z^2]$	$\mathbf{D}_2[\rho_x^2, \rho_y^2]$	$\mathbf{Z}_2$
c_{38}	$\mathbf{Z}_2[\rho_z^2]$	$\mathbf{D}_2[\rho_x^2, \rho_y^2]$	$\mathbf{Z}_2$
c_{41}	$\mathbf{Z}_2[\kappa_4]$	$\mathbf{D}_2[\rho_x^2, \kappa_6]$	$\mathbf{Z}_2$
c_{42}	$\mathbf{Z}_2[\kappa_4]$	$\mathbf{D}_2[\rho_x^2, \kappa_6]$	$\mathbf{Z}_2$
c_{45}	$\mathbf{Z}_2[\kappa_6]$	$\mathbf{D}_2[\rho_x^2, \kappa_6]$	$\mathbf{Z}_2$
c_{46}	$\mathbf{Z}_2[\kappa_6]$	$\mathbf{D}_2[\rho_x^2, \kappa_6]$	$\mathbf{Z}_3$

Table 9.13: Knots relative to orbit representatives of $C \in \mathscr{C}_{\mathbf{D}_4[\rho_x,\kappa_6]}$ for the BCC lattice.

Element of $\mathscr{C}_{\mathbf{D}_4[\rho_x,\kappa_6]}$	Knots
c_1	e_1, e_4
c_3	e_1, e_3
c_{23}	e_3, e_{11}
c_{25}	e_3, e_4
c_{41}	e_1, e_4
c_{42}	e_3, e_{11}

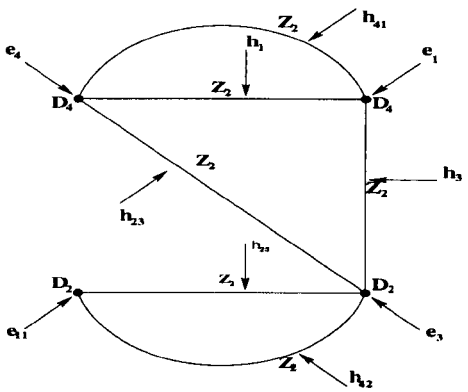

Figure 9.2: The projected skeleton $\mathbb{X}^p_{\mathbf{D}_4[\rho_x,\kappa_6]}$. Here $h_1 = \{(\theta,0,0)|\theta \in [0,\pi)\}$, $h_3 = \{(0,\theta,0)|\theta \in [0,\pi)\}$, $h_5 = \{(0,0,\theta)|\theta \in (0,\pi)\}$, $h_{23} = \{(\theta,\pi,0)|\theta \in (0,\pi)\}$, $h_{41} = \{(\theta,0,-2\theta)|\theta \in (0,\pi)\}$ and $h_{42} = \{(\theta,\pi,\theta-2\pi)|\theta \in (0,\pi)\}$.

These computations show that $S(C) \cong \mathbf{Z}_2$ for all $C \in \mathscr{C}_{\mathbf{D}_4[\rho_x,\kappa_6]}$, except c_{23}, where $S(c_{23}) \cong \mathbf{D}_2$.

Knots Relative to C. The action of $\mathbf{D}_4[\rho_x,\kappa_6]$ on $\mathscr{C}_{\mathbf{D}_4[\rho_x,\kappa_6]}$ in Table 9.11 shows that there are six C's that are not symmetrically related, namely: c_1, c_3, c_{23}, c_{25}, c_{41}, and c_{42}. The representatives of the equilibria which lie on these C's are: e_1, e_3, e_4, and e_{11}. The (orbit representative) connections c_1, c_3, c_{25}, c_{41}, and c_{42} all satisfy $S(C) \cong \mathbf{Z}_2$. So we expect two knots on these connections, and these knots are given by the equilibria on C. The connection c_{23} is different; here $S(C) \cong \mathbf{D}_2$, which acts as reflections about the line joining the equilibria e_3 and e_5, and the line joining e_{11} and e_{12}, together with a rotation by π around the connection. In this case all the equilibria on c_{23} are knots, but there are only two orbit representatives e_3 and e_{11}. We summarise this information in Table 9.13.

Projected Skeleton

The action of $\mathbf{D}_4[\rho_x,\kappa_6]$ on $\mathscr{C}_{\mathbf{D}_4[\rho_x,\kappa_6]}$ shows that there are six orbit representatives for the elements of $\mathscr{C}_{\mathbf{D}_4[\rho_x,\kappa_6]}$ that are homeomorphic to $\mathbf{S}^1$. These are: c_1, c_3, c_{23}, c_{25}, c_{41}, and c_{42}. The orbit representatives for the equilibria are: e_1, e_3, e_4, and e_{11}. We have seen that each C has two or four knots; these give axes of reflection symmetry. Thus each C projects into the orbit space as a line joining the orbit representatives of the knots. More precisely, we have the following relations: c_1 connects e_1 to e_2, c_3 connects e_1 to e_3, c_{23} connects e_3 to e_{11}, c_{25} connects e_3 to e_4, c_{41} connects e_1 to e_4, and c_{42} connects e_{11} to e_3. Figure 9.2 illustrates the projected skeleton. From the projected skeleton we deduce that there exists at most 64 qualitatively different $\mathbf{D}_4[\rho_x,\kappa_6]$-equivariant flows on $\mathbb{X}_{\mathbf{D}_4[\rho_x,\kappa_6]}$. We shall not consider this case any further, for the same reason as in the $\mathbb{O}$ case.

9.2.4 Forced Symmetry Breaking to $\mathbb{T}$

In this subsection we study the behaviour of the group orbit X_0 when symmetry breaking terms with $\mathbb{T}$ symmetry are added to the vector field (9.4). The normal hyperbolicity of X_0 guarantees, by the Equivariant Persistence Theorem, the existence of a manifold X_ε diffeomorphic to X_0 and invariant under the new dynamics. The action of $\mathbb{T}$ on $\mathbb{C}^6$ is in Table 9.14.

Table 9.14: Action of $\mathbb{T}$ on $\mathbb{C}^6$ for the BCC lattice.

Element of $\mathbb{T}$	Action on $\mathbb{C}^6$
τ_1	$(z_2, z_5, \overline{z_4}, z_6, z_1, \overline{z_3})$
τ_1^2	$(z_5, z_1, \overline{z_6}, \overline{z_3}, z_2, z_4)$
τ_2	$(\overline{z_2}, \overline{z_6}, z_4, \overline{z_5}, \overline{z_3}, z_1)$
τ_2^2	$(z_6, \overline{z_1}, \overline{z_5}, z_3, \overline{z_4}, \overline{z_2})$
τ_3	$(z_4, \overline{z_5}, \overline{z_2}, \overline{z_6}, z_3, \overline{z_1})$
τ_3^2	$(\overline{z_6}, \overline{z_3}, z_5, z_1, \overline{z_2}, \overline{z_4})$
τ_4	$(\overline{z_5}, z_3, z_6, \overline{z_1}, z_4, z_2)$
τ_4^2	$(\overline{z_4}, z_6, z_2, z_5, \overline{z_1}, z_3)$
ρ_x^2	$(z_3, z_4, z_1, z_2, \overline{z_5}, \overline{z_6})$
ρ_y^2	$(\overline{z_3}, \overline{z_2}, \overline{z_1}, \overline{z_4}, \overline{z_6}, \overline{z_5})$
ρ_z^2	$(\overline{z_1}, \overline{z_4}, \overline{z_3}, \overline{z_2}, z_6, z_5)$

Calculation of the Skeleton

Here we calculate the skeleton of X_0 under the action of $\mathbb{T}$.

Proposition 9.15
Let $\mathbb{T}$ act on X_0 with the action induced from Table 9.14. Then

$$\mathscr{C}_\mathbb{T} = \{e_1, e_3, e_4, e_5, c_1, c_3, c_5, c_{13}, c_{17}, c_{21}, c_{23}, c_{25}, c_{33}, c_{38}\}.$$

Proof. The proof follows from Lemmas 9.4, 9.8, 9.9, and 9.10. □

We can now use this information to form the skeleton

$$\mathbb{X}_\mathbb{T} = \bigcup_{C \in \mathscr{C}_\mathbb{T}} C \subset \mathbf{T}^3 \cong X_0.$$

Symmetry Properties of $\mathbb{X}_\mathbb{T}$

Pointwise and Setwise Isotropy Subgroups. The action of $\mathbb{T}$ on $\mathbb{C}^6$ in Table 9.14 induces a natural action on X_0, as follows:

$$\begin{aligned} \tau_1(\theta_1, \theta_2, \theta_3) &= (-\theta_2, \theta_1 - \theta_2, 2\theta_2 + \theta_3), \\ \tau_2(\theta_1, \theta_2, \theta_3) &= (\theta_1 - \theta_2, \theta_1 + \theta_3, -2\theta_1 - \theta_3). \end{aligned}$$

The complete action of $\mathbb{T}$ on X_0 is in Table 9.15. The action of $\mathbb{T}$ on X_0 induces an action of $\mathbb{T}$ on the set $\mathscr{C}_\mathbb{T}$ by permutation. We present this action in Table 9.16.

Proposition 9.16
Let $\mathbb{T}$ act on $\mathscr{C}_\mathbb{T}$ as in Table 9.16 and on X_0 as in Table 9.15. Then given $C \in \mathscr{C}_\mathbb{T}$, the setwise isotropy Stab(C), *pointwise isotropy* stab(C) *and $S(C)$ are given in Table 9.17.*

Proof. The proof follows the standard lines. □

Table 9.15: Action of $\mathbb{T}$ induced on X_0 for the BCC lattice.

Element of $\mathbb{T}$	Action on X_0
τ_1	$(-\theta_2, \theta_1 - \theta_2, 2\theta_2 + \theta_3)$
τ_1^2	$(\theta_2 - \theta_1, -\theta_1, 2\theta_1 + \theta_3)$
τ_2	$(\theta_1 - \theta_2, \theta_1 + \theta_3, -2\theta_1 - \theta_3)$
τ_2^2	$(-\theta_2 - \theta_3, -\theta_1 - \theta_2 - \theta_3, 2\theta_2 + \theta_3)$
τ_3	$(\theta_2, \theta_1 + \theta_2 + \theta_3, -2\theta_2 - \theta_3)$
τ_3^2	$(\theta_1 + \theta_2 + \theta_3, \theta_1, -2\theta_1 - \theta_3)$
τ_4	$(-\theta_1 - \theta_2 - \theta_3, -\theta_1 - \theta_3, 2\theta_1 + \theta_3)$
τ_4^2	$(\theta_2 + \theta_3, -\theta_1 + \theta_2, -2\theta_2 - \theta_3)$
ρ_x^2	$(\theta_1 + \theta_3, -\theta_2, -\theta_3)$
ρ_y^2	$(-\theta_1, \theta_2 + \theta_3, -\theta_3)$
ρ_z^2	$(-\theta_1 - \theta_3, -\theta_2 - \theta_3, \theta_3)$

Table 9.16: Action of $\mathbb{T}$ induced on $\mathscr{C}_{\mathbb{T}}$ for the BCC lattice.

Element of $\mathscr{C}_{\mathbb{T}}$	Elements of $\mathbb{T}$ acting nontrivially	Action
e_1	None	
e_3	$\tau_1, \tau_2^2, \tau_3, \tau_4^2$	e_5
	$\tau_1^2, \tau_2, \tau_3^2, \tau_4$	e_4
e_4	$\tau_1^2, \tau_2, \tau_3^2, \tau_4$	e_5
	$\tau_1, \tau_2^2, \tau_3, \tau_4^2$	e_3
e_5	$\tau_1^2, \tau_2, \tau_3^2, \tau_4$	e_3
	$\tau_1, \tau_2^2, \tau_3, \tau_4^2$	e_4
c_1	$\tau_1^2, \tau_2, \tau_3^2, \tau_4$	c_{33}
	$\tau_1, \tau_2^2, \tau_3, \tau_4^2$	c_3
c_3	$\tau_1, \tau_2^2, \tau_3, \tau_4^2$	c_{33}
	$\tau_1^2, \tau_2, \tau_3^2, \tau_4$	c_1
c_5	ρ_y^2, τ_2, τ_3	c_{17}
	$\rho_x^2, \tau_3^2, \tau_4^2$	c_{13}
	$\rho_z^2, \tau_2^2, \tau_4$	c_{21}
c_{13}	$\rho_y^2, \tau_1^2, \tau_4^2$	c_{21}
	ρ_x^2, τ_3, τ_4	c_5
	$\rho_z^2, \tau_1, \tau_3^2$	c_{17}
c_{17}	$\rho_z^2, \tau_1^2, \tau_3$	c_{13}
	ρ_x^2, τ_1, τ_2	c_{21}
	$\rho_y^2, \tau_2^2, \tau_3^2$	c_5
c_{21}	$\rho_z^2, \tau_2, \tau_4^2$	c_5
	$\rho_x^2, \tau_1^2, \tau_2^2$	c_{17}
	ρ_y^2, τ_1, τ_4	c_{13}
c_{23}	$\tau_1^2, \tau_2, \tau_3^2, \tau_4$	c_{38}
	$\tau_1, \tau_2^2, \tau_3, \tau_4^2$	c_{25}
c_{25}	$\tau_1, \tau_2^2, \tau_3, \tau_4^2$	c_{38}
	$\tau_1^2, \tau_2, \tau_3^2, \tau_4$	c_{23}
c_{33}	$\tau_1^2, \tau_2, \tau_3^2, \tau_4$	c_3
	$\tau_1, \tau_2^2, \tau_3, \tau_4^2$	c_1
c_{38}	$\tau_1^2, \tau_2, \tau_3^2, \tau_4$	c_{25}
	$\tau_1, \tau_2^2, \tau_3, \tau_4^2$	c_{23}

Table 9.17: Isotropy data for $C \in \mathscr{C}_{\mathbb{T}}$ for the BCC lattice.

$C \in \mathscr{C}_{\mathbb{T}}$	stab(C)	Stab(C)	$S(C) = \text{Stab}(C)/\text{stab}(C)$
e_1	$\mathbb{T}$	$\mathbb{T}$	$\mathbf{1}$
e_3	$\mathbf{D}_2[\rho_x^2, \rho_y^2]$	$\mathbf{D}_2[\rho_x^2, \rho_y^2]$	$\mathbf{1}$
e_4	$\mathbf{D}_2[\rho_x^2, \rho_y^2]$	$\mathbf{D}_2[\rho_x^2, \rho_y^2]$	$\mathbf{1}$
e_5	$\mathbf{D}_2[\rho_x^2, \rho_y^2]$	$\mathbf{D}_2[\rho_x^2, \rho_y^2]$	$\mathbf{1}$
c_1	$\mathbf{Z}_2[\rho_x^2]$	$\mathbf{D}_2[\rho_x^2, \rho_y^2]$	$\mathbf{Z}_2$
c_3	$\mathbf{Z}_2[\rho_y^2]$	$\mathbf{D}_2[\rho_x^2, \rho_y^2]$	$\mathbf{Z}_2$
c_5	$\mathbf{Z}_3[\tau_1]$	$\mathbf{Z}_3[\tau_1]$	$\mathbf{1}$
c_{13}	$\mathbf{Z}_3[\tau_2]$	$\mathbf{Z}_3[\tau_2]$	$\mathbf{1}$
c_{17}	$\mathbf{Z}_3[\tau_4]$	$\mathbf{Z}_3[\tau_4]$	$\mathbf{1}$
c_{21}	$\mathbf{Z}_3[\tau_3]$	$\mathbf{Z}_3[\tau_3]$	$\mathbf{1}$
c_{23}	$\mathbf{Z}_2[\rho_x^2]$	$\mathbf{D}_2[\rho_x^2, \rho_y^2]$	$\mathbf{Z}_2$
c_{25}	$\mathbf{Z}_2[\rho_y^2]$	$\mathbf{D}_2[\rho_x^2, \rho_y^2]$	$\mathbf{Z}_2$
c_{33}	$\mathbf{Z}_2[\rho_z^2]$	$\mathbf{D}_2[\rho_x^2, \rho_y^2]$	$\mathbf{Z}_2$
c_{38}	$\mathbf{Z}_2[\rho_z^2]$	$\mathbf{D}_2[\rho_x^2, \rho_y^2]$	$\mathbf{Z}_2$

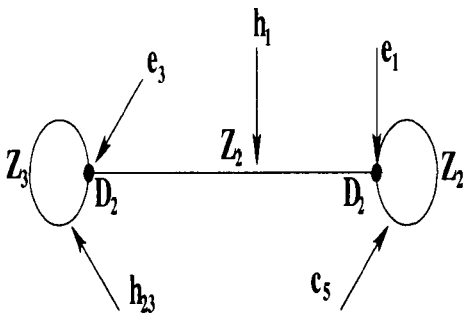

Figure 9.3: The projected skeleton $\mathbb{X}_{\mathbb{T}}^p$. Here $h_1 = \{(\theta, 0, 0) | \theta \in (0, \pi)\}$, $c_5 = \{(0, 0, \theta) | \theta \in (0, 2\pi)\}$ and, $h_{23} = \{(\theta, \pi, 0) | \theta \in = (0, \pi)\}$.

Knots Relative to C. The action of $\mathbb{T}$ on $\mathscr{C}_{\mathbb{T}}$ in Table 9.16 shows that there are three C's that are not symmetrically related, namely: $c_1 = \{(\theta, 0, 0) | \theta \in [0, 2\pi)\}$, $c_5 = \{(0, 0, \theta) | \theta \in [0, 2\pi)\}$, and $c_{23} = \{(\theta, \pi, 0) | \theta \in [0, 2\pi)\}$. The representatives of the equilibria that lie on these C's are e_1 and e_3. The connections c_1 has two knots given by the equilibria e_1 and e_3. The connection c_{23} has two knots given by e_3 and e_5, but e_5 lies in the same orbit as e_3. The connection c_5 has no knots.

Projected Skeleton

The action of $\mathbb{T}$ on $\mathscr{C}_{\mathbb{T}}$ shows that there are three orbit representatives for the elements of $\mathscr{C}_{\mathbb{T}}$ that are homeomorphic to $\mathbf{S}^1$. These are c_1, c_5 and c_{23}. The orbit representatives for the equilibria are e_1 and e_3. We have seen that c_1 and c_{23} have two knots; this implies that there is an axis of reflection symmetry. So each such C projects into the orbit space as a line joining the two knots. More precisely, we have the following relations: c_1 connects e_1 to e_3, c_5 connects e_1 to e_1 and c_{23} connects e_3 to e_3. Figure 9.3 illustrates the projected skeleton. From the projected skeleton we deduce that there exist at most $2^3 = 8$ qualitatively different $\mathbb{T}$-equivariant flows on $\mathbb{X}_{\mathbb{T}}$.

9.2.5 Forced Symmetry Breaking to $\mathbf{D}_3[\tau_3, \kappa_3]$

In this subsection we study the behaviour of the group orbit X_0 when symmetry breaking terms with $\mathbf{D}_3[\tau_3, \kappa_3]$ symmetry are added to the vector field (9.4). This group is of particular interest for our intended application in Part IV. We have also chosen a slightly different $\mathbf{D}_3$ subgroup; again this choice is motivated by our intended application in Part IV. The normal hyperbolicity of X_0 guarantees, by the Equivariant Persistence Theorem, the existence of a manifold X_ε diffeomorphic to X_0 and invariant under the new dynamics. The action of the group $\mathbf{D}_3[\tau_3, \kappa_3]$ on $\mathbb{C}^6$ is in Table 9.18.

Table 9.18: Action of the elements of $\mathbf{D}_3[\tau_3, \kappa_3]$ on $\mathbb{C}^6$ for the BCC lattice.

Element of $\mathbf{D}_3[\tau_3, \kappa_3]$	Action on $\mathbb{C}^6$
τ_3	$(z_4, \overline{z_5}, \overline{z_2}, \overline{z_6}, z_3, \overline{z_1})$
τ_3^2	$(\overline{z_6}, \overline{z_3}, z_5, z_1, \overline{z_2}, \overline{z_4})$
κ_2	$(\overline{z_1}, \overline{z_5}, z_3, z_6, \overline{z_2}, z_4)$
κ_3	$(z_6, z_2, z_5, \overline{z_4}, z_3, z_1)$
κ_4	$(\overline{z_4}, \overline{z_3}, \overline{z_2}, \overline{z_1}, z_5, \overline{z_6})$

Calculation of the Skeleton

Here we calculate the skeleton of X_0 under the action of $\mathbf{D}_3[\tau_3, \kappa_3]$.

Proposition 9.17
Let $\mathbf{D}_3[\tau_3, \kappa_3]$ act on X_0 with the action induced from Table 9.18. Then

$$\mathscr{C}_{\mathbf{D}_3[\tau_3,\kappa_3]} = \{e_1, e_8, c_9, c_{10}, c_{21}, c_{39}, c_{40}, c_{41}, c_{42}\}.$$

Proof. The proof follows from Lemmas 9.4, 9.9 and 9.8. □

We can now use this information to form the skeleton

$$\mathbb{X}_{\mathbf{D}_3[\tau_3,\kappa_3]} = \bigcup_{C \in \mathscr{C}_{\mathbf{D}_3[\tau_3,\kappa_3]}} C \subset \mathbf{T}^3 \cong X_0.$$

Symmetry Properties of $\mathbb{X}_{\mathbf{D}_3[\tau_3,\kappa_3]}$

The action of $\mathbf{D}_3[\tau_3, \kappa_3]$ on $\mathbb{C}^6$ in Table 9.18 induces a natural action on X_0 as follows:

$$\begin{aligned} \tau_1(\theta_1, \theta_2, \theta_3) &= (-\theta_2, \theta_1 - \theta_2, 2\theta_2 + \theta_3), \\ \kappa_5(\theta_1, \theta_2, \theta_3) &= (\theta_1, \theta_1 - \theta_2, -2\theta_1 - \theta_3). \end{aligned}$$

The complete action of $\mathbf{D}_3[\tau_3, \kappa_3]$ on X_0 is in Table 9.19. The action of $\mathbf{D}_3[\tau_3, \kappa_3]$ on X_0 induces an action of $\mathbf{D}_3[\tau_3, \kappa_3]$ on the set $\mathscr{C}_{\mathbf{D}_3[\tau_3,\kappa_3]}$ by permutation. We present this action in Table 9.20.

Proposition 9.18
Let $\mathbf{D}_3[\tau_3, \kappa_3]$ act on $\mathscr{C}_{\mathbf{D}_3[\tau_3,\kappa_3]}$ as in Table 9.20 and on X_0 as in Table 9.19. Then given $C \in \mathscr{C}_{\mathbf{D}_3[\tau_3,\kappa_3]}$, the setwise isotropy $\mathrm{Stab}(C)$, pointwise isotropy $\mathrm{stab}(C)$ and $S(C)$ are given in Table 9.21.

Proof. The proof follows the standard lines. □

These computations show that $S(c_{21}) \cong \mathbf{Z}_2$ and $S(C)$ is trivial otherwise, so there is an axis of symmetry on c_{21}. This axis is given by two knots, clearly these are e_1 and e_8.

Table 9.19: Action of $\mathbf{D}_3[\tau_3, \kappa_3]$ induced on X_0 for the BCC lattice.

Element of $\mathbf{D}_3[\tau_3, \kappa_3]$	Action on X_0
τ_3	$(\theta_2, \theta_1 + \theta_2 + \theta_3, -2\theta_2 - \theta_3)$
τ_3^2	$(\theta_1 + \theta_2 + \theta_3, \theta_1, -2\theta_1 - \theta_3)$
κ_2	$(-\theta_2, -\theta_1, -\theta_3)$
κ_3	$(-\theta_1, -(\theta_1 + \theta_2 + \theta_3), 2\theta_1 + \theta_3)$
κ_4	$(-(\theta_1 + \theta_2 + \theta_3), -\theta_2, 2\theta_2 + \theta_3)$

Table 9.20: Action of $\mathbf{D}_3[\tau_3, \kappa_3]$ induced on $\mathscr{C}_{\mathbf{D}_3[\tau_3,\kappa_3]}$ for the BCC lattice.

Element of $\mathscr{C}_{\mathbf{D}_3[\tau_3,\kappa_3]}$	Elements of $\mathbf{D}_3[\tau_3, \kappa_3]$ acting nontrivially	Action
e_1	None	
e_8	None	
c_9	κ_4, τ_3^2,	c_{39}
	κ_3, τ_3	c_{41}
c_{10}	κ_4, τ_3^2,	c_{40}
	κ_3, τ_3	c_{42}
c_{21}	None	
c_{39}	κ_4, τ_3,	c_9
	κ_2, τ_3^2	c_{41}
c_{40}	κ_4, τ_3,	c_{10}
	κ_2, τ_3^2	c_{38}
c_{41}	κ_3, τ_3^2	c_9
	κ_2, τ_3	c_{39}
c_{42}	κ_3, τ_3^2	c_{10}
	κ_2, τ_3	c_{40}

Table 9.21: Isotropy data for $C \in \mathscr{C}_{\mathbf{D}_3[\tau_3,\kappa_3]}$ for the BCC lattice.

$C \in \mathscr{C}_{\mathbf{D}_3[\tau_3,\kappa_3]}$	stab(C)	Stab(C)	$S(C) = \text{Stab}(C)/\text{stab}(C)$
e_1	$\mathbf{D}_3[\tau_3, \kappa_3]$	$\mathbf{D}_3[\tau_3, \kappa_3]$	$\mathbf{1}$
e_8	$\mathbf{D}_3[\tau_3, \kappa_3]$	$\mathbf{D}_3[\tau_3, \kappa_3]$	$\mathbf{1}$
c_9	$\mathbf{Z}_2[\kappa_2]$	$\mathbf{Z}_2[\kappa_2]$	$\mathbf{1}$
c_{10}	$\mathbf{Z}_2[\kappa_2]$	$\mathbf{Z}_2[\kappa_2]$	$\mathbf{1}$
c_{21}	$\mathbf{Z}_3[\tau_3]$	$\mathbf{D}_3[\tau_3, \kappa_3]$	$\mathbf{Z}_2$
c_{39}	$\mathbf{Z}_2[\kappa_3]$	$\mathbf{Z}_2[\kappa_3]$	$\mathbf{1}$
c_{40}	$\mathbf{Z}_2[\kappa_3]$	$\mathbf{Z}_2[\kappa_3]$	$\mathbf{1}$
c_{41}	$\mathbf{Z}_2[\kappa_4]$	$\mathbf{Z}_2[\kappa_4]$	$\mathbf{1}$
c_{42}	$\mathbf{Z}_2[\kappa_4]$	$\mathbf{Z}_2[\kappa_5]$	$\mathbf{1}$

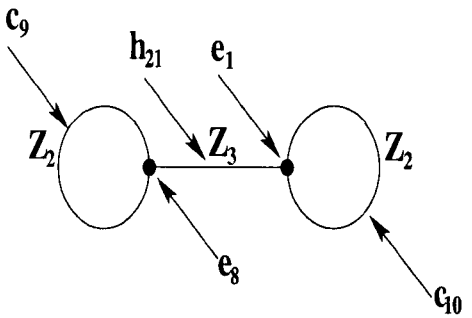

Figure 9.4: The projected skeleton $\mathbb{X}^p_{\mathbf{D}_3[\tau_3,\kappa_3]}$. Here $c_9 = \{(\theta,-\theta,0)|\theta \in [0,2\pi)\}$, $c_{10} = \{(\theta,-\theta,\pi)|\theta \in [0,2\pi)\}$, and $h_{21} = \{(\theta,\theta,-\theta)|\theta \in (0,\pi)\}$.

Projected Skeleton

The action of $\mathbf{D}_3[\tau_3,\kappa_3]$ on $\mathscr{C}_{\mathbf{D}_3[\tau_3,\kappa_3]}$ shows that there are three orbit representatives for the elements of $\mathscr{C}_{\mathbf{D}_3[\tau_3,\kappa_3]}$ that are homeomorphic to $\mathbf{S}^1$. These are c_9, c_{10}, and c_{21}. The orbit representatives for the equilibria are e_1 and e_8. The connection c_{21} has two knots, implying that there is an axis of reflection symmetry. So c_{21} projects into the orbit space as a line joining the two knots. More precisely, we have the following relations. The element c_{21} connects e_1 to e_8, c_9 connects e_1 to itself and c_{10} connects e_8 itself. Figure 9.4 illustrates the projected skeleton. From the projected skeleton we may deduce the following there exists at most $2^3 = 8$ qualitatively different $\mathbf{D}_3[\tau_3,\kappa_3]$-equivariant flows on $\mathbb{X}_{\mathbf{D}_3[\tau_3,\kappa_3]}$.

9.2.6 Forced Symmetry Breaking to $\mathbf{D}_2[\rho_x^2,\kappa_6]$

In this subsection we study the behaviour of the group orbit X_0 when symmetry breaking terms with $\mathbf{D}_2[\rho_x^2,\kappa_6]$ symmetry are added to the vector field (9.4). The normal hyperbolicity of X_0 guarantees, by the Equivariant Persistence Theorem, the existence of a manifold X_ε diffeomorphic to X_0 and invariant under the new dynamics. The action of the group $\mathbf{D}_2[\rho_x^2,\kappa_6]$ on $\mathbb{C}^6$ is in Table 9.22.

Table 9.22: Action of the elements of $\mathbf{D}_2[\rho_x^2,\kappa_6]$ on $\mathbb{C}^6$ for the BCC lattice.

Element of $\mathbf{D}_2[\rho_x^2,\kappa_6]$	Action on $\mathbb{C}^6$
ρ_x^2	$(z_3,z_4,z_1,z_2,\overline{z_5},\overline{z_6})$
κ_4	$(\overline{z_4},\overline{z_3},\overline{z_2},\overline{z_1},z_5,\overline{z_6})$
κ_6	$(\overline{z_2},\overline{z_1},\overline{z_4},\overline{z_3},\overline{z_5},z_6)$

Calculation of the Skeleton

Here we calculate the skeleton of X_0 under the action of $\mathbf{D}_2[\rho_x^2,\kappa_6]$.

Proposition 9.19
Let $\mathbf{D}_2[\rho_x^2,\kappa_6]$ act on X_0 with the action induced from Table 9.22. Then

$$\mathscr{C}_{\mathbf{D}_2[\rho_x^2,\kappa_6]} = \{e_1,e_4,e_{11},e_{12},c_1,c_{23},c_{41},c_{42},c_{45},c_{46}\}.$$

Proof. The proof follows from Lemmas 9.8 and 9.10. □

Table 9.23: Action of $\mathbf{D}_2[\rho_x^2, \kappa_6]$ induced on X_0 for the BCC lattice.

Element of $\mathbf{D}_2[\rho_x^2, \kappa_6]$	Action on X_0
ρ_x^2	$(\theta_1 + \theta_3, -\theta_2, -\theta_3)$
κ_4	$(-\theta_1 - \theta_2 - \theta_3, -\theta_2, 2\theta_2 + \theta_3)$
κ_6	$(-\theta_1 + \theta_2, \theta_2, 2\theta_2 - \theta_3)$

Table 9.24: Isotropy data for $C \in \mathscr{C}_{\mathbf{D}_2[\rho_x^2, \kappa_6]}$ for the BCC lattice.

$C \in \mathscr{C}_{\mathbf{D}_2[\rho_x^2, \kappa_6]}$	stab(C)	Stab(C)	$S(C)$ = Stab(C)/stab(C)
e_1	$\mathbf{D}_2[\rho_x^2, \kappa_6]$	$\mathbf{D}_2[\rho_x^2, \kappa_6]$	$\mathbf{1}$
e_4	$\mathbf{D}_2[\rho_x^2, \kappa_6]$	$\mathbf{D}_2[\rho_x^2, \kappa_6]$	$\mathbf{1}$
e_7	$\mathbf{D}_2[\rho_x^2, \kappa_6]$	$\mathbf{D}_2[\rho_x^2, \kappa_6]$	$\mathbf{1}$
e_8	$\mathbf{D}_2[\rho_x^2, \kappa_6]$	$\mathbf{D}_2[\rho_x^2, \kappa_6]$	$\mathbf{1}$
c_1	$\mathbf{Z}_2[\rho_x^2]$	$\mathbf{D}_2[\rho_x^2, \kappa_6^2]$	$\mathbf{Z}_2$
c_{23}	$\mathbf{Z}_2[\rho_x^2]$	$\mathbf{D}_2[\rho_x^2, \kappa_6^2]$	$\mathbf{Z}_2$
c_{41}	$\mathbf{Z}_2[\kappa_4]$	$\mathbf{D}_2[\rho_x^2, \kappa_6^2]$	$\mathbf{Z}_2$
c_{42}	$\mathbf{Z}_2[\kappa_4]$	$\mathbf{D}_2[\rho_x^2, \kappa_6]$	$\mathbf{Z}_2$
c_{45}	$\mathbf{Z}_2[\kappa_6]$	$\mathbf{D}_2[\rho_x^2, \kappa_6]$	$\mathbf{Z}_2$
c_{46}	$\mathbf{Z}_2[\kappa_6]$	$\mathbf{D}_2[\rho_x^2, \kappa_6]$	$\mathbf{Z}_2$

We can now use this information to form the skeleton

$$\mathbb{X}_{\mathbf{D}_2[\rho_x^2, \kappa_6]} = \bigcup_{C \in \mathscr{C}_{\mathbf{D}_2[\rho_x^2, \kappa_6]}} C \subset \mathbf{T}^3 \cong X_0.$$

Symmetry Properties of $\mathbb{X}_{\mathbf{D}_2[\rho_x^2, \kappa_6]}$

Here we study the $\mathbf{D}_2[\rho_x^2, \kappa_6]$ action induced on the skeleton. The action of $\mathbf{D}_2[\rho_x^2, \kappa_6]$ on $\mathbb{C}^6$ in Table 9.22 induces a natural action on X_0 as follows:

$$\begin{aligned} \rho_x^2(\theta_1, \theta_2, \theta_3) &= (\theta_1 + \theta_3, -\theta_2, -\theta_3), \\ \kappa_6(\theta_1, \theta_2, \theta_3) &= (-\theta_1 + \theta_2, \theta_2, 2\theta_2 - \theta_3). \end{aligned}$$

The complete action of $\mathbf{D}_2[\rho_x^2, \kappa_6]$ on X_0 is in Table 9.23. The action of $\mathbf{D}_2[\rho_x^2, \kappa_6]$ on X_0 induces an action of $\mathbf{D}_2[\rho_x^2, \kappa_6]$ on $\mathscr{C}_{\mathbf{D}_2[\rho_x^2, \kappa_6]}$ by permutation of its elements and is trivial.

Proposition 9.20
Let $\mathbf{D}_2[\rho_x^2, \kappa_6]$ act on $\mathscr{C}_{\mathbf{D}_2[\rho_x^2, \kappa_6]}$ with the induced trivial action and on X_0 as in Table 9.23. Then given $C \in \mathscr{C}_{\mathbf{D}_2[\rho_x^2, \kappa_6]}$, the setwise isotropy Stab(C), *pointwise isotropy* stab(C) *and $S(C)$ are given in Table 9.24.*

Proof. The proof follows the standard lines. □

Knots Relative to C. There are eight different $C \in \mathscr{C}_{\mathbf{D}_2[\rho_x^2, \kappa_6]}$ homeomorphic to $\mathbf{S}^1$, and the $\mathbf{D}_2[\rho_x^2, \kappa_6^2]$ symmetry does not give any simplifications. Since all the knots must be equilibria, Table 9.25 is immediate.

Projected Skeleton

The action of $\mathbf{D}_2[\rho_x^2, \kappa_6]$ on $\mathscr{C}_{\mathbf{D}_2[\rho_x^2, \kappa_6]}$ shows that there are six orbit representatives for the elements of $\mathscr{C}_{\mathbf{D}_2[\rho_x^2, \kappa_6]}$ that are homeomorphic to $\mathbf{S}^1$. These are: c_1, c_{23}, c_{41}, c_{42}, c_{45}, and c_{46}. The orbit representatives for the equilibria are: e_1, e_4, e_{11}, and e_{12}. Each C has two

Table 9.25: Knots relative to orbit representatives of $C \in \mathscr{C}_{\mathbf{D}_2[\rho_x^2,\kappa_6^2]}$ for the BCC lattice.

Element of $\mathscr{C}_{\mathbf{D}_2[\rho_x^2,\kappa_6^2]}$	Knots
c_1	e_1, e_4
c_{23}	e_{11}, e_{12}
c_{41}	e_1, e_4
c_{42}	e_{11}, e_{12}
c_{45}	e_1, e_4
c_{46}	e_{11}, e_{12}

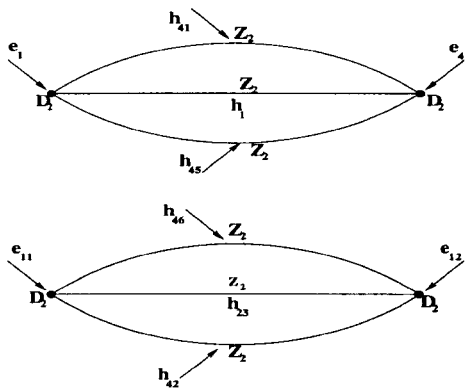

Figure 9.5: The projected skeleton $\mathbb{X}^p_{\mathbf{D}_2[\rho_x^2,\kappa_6]}$. Here $h_1 = \{(\theta,0,0)|\theta \in (0,\pi)\}$, $h_{23} = \{(\theta,\pi,0)|\theta \in (0,\pi)\}$, $h_{41} = \{(\theta,0,-2\pi)|\theta \in (0,\pi)\}$, $h_{42} = \{(\theta,\pi,\pi-2\theta)|\theta \in (0,\pi)\}$, $h_{45} = \{(\theta,2\theta,-2\theta)|\theta \in (0,\pi)\}$ and $h_{46} = \{(\theta,2\theta,\pi-2\theta)|\theta \in (0,2\pi)\}$.

knots; this implies that there is an axis of reflection symmetry. So each C projects into the orbit space as a line joining the two knots. More precisely, we have the following relations: c_1 connects e_1 to e_4, c_{23} connects e_{11} to e_{12}, c_{41} connects e_1 to e_4, c_{42} connects e_{11} to e_{12}, c_{45} connects e_1 to e_4, and c_{46} connects e_{11} to e_{12}. Figure 9.5 illustrates the projected skeleton. From the projected skeleton we may deduce there exists at most $2^6 = 64$ qualitatively different $\mathbf{D}_2[\rho_x^2,\kappa_6]$-equivariant flows on $\mathbb{X}_{\mathbf{D}_2[\rho_x^2,\kappa_6]}$.

9.2.7 Forced Symmetry Breaking to $\mathbf{D}_2[\rho_x^2,\rho_y^2]$

In this subsection we study the behaviour of the group orbit X_0 when symmetry breaking terms with $\mathbf{D}_2[\rho_x^2,\rho_y^2]$ symmetry are added to the vector field (9.4). The normal hyperbolicity of X_0 guarantees, by the Equivariant Persistence Theorem, the existence of a manifold X_ε diffeomorphic to X_0 and invariant under the new dynamics. The action of $\mathbf{D}_2[\rho_x^2,\rho_y^2]$ on $\mathbb{C}^6$ is given in Table 9.26.

Table 9.26: Action of $\mathbf{D}_2[\rho_x^2,\rho_y^2]$ on $\mathbb{C}^6$ for the BCC lattice.

Element of $\mathbf{D}_2[\rho_x^2,\rho_y^2]$	Action on $\mathbb{C}^6$
ρ_x^2	$(z_3,z_4,z_1,z_2,\overline{z_5},\overline{z_6})$
ρ_y^2	$(\overline{z_3},\overline{z_2},\overline{z_1},\overline{z_4},\overline{z_6},\overline{z_5})$
ρ_z^2	$(\overline{z_1},\overline{z_4},\overline{z_3},\overline{z_2},z_6,z_5)$

Calculation of the Skeleton

Here we calculate the skeleton of X_0 under the action of $\mathbf{D}_2[\rho_x^2, \rho_y^2]$.

Proposition 9.21
Let $\mathbf{D}_2[\rho_x^2, \rho_y^2]$ act on X_0 with the action induced from Table 9.26. Then

$$\mathscr{C}_{\mathbf{D}_2[\rho_x^2,\rho_y^2]} = \{e_1, e_3, e_4, e_5, c_1, c_3, c_{23}, c_{25}, c_{33}, c_{38}\}.$$

Proof. The proof follows from Lemmas 9.8 and 9.10. □

We can now use this information to form the skeleton

$$\mathbb{X}_{\mathbf{D}_2[\rho_x^2,\rho_y^2]} = \bigcup_{C \in \mathscr{C}_{\mathbf{D}_2[\rho_x^2,\rho_y^2]}} C \subset \mathbf{T}^3 \cong X_0.$$

Symmetry Properties of $\mathbb{X}_{\mathbf{D}_2[\rho_x^2,\rho_y^2]}$

Here we study the $\mathbf{D}_2[\rho_x^2, \rho_y^2]$ action induced on the skeleton. The action of $\mathbf{D}_2[\rho_x^2, \rho_y^2]$ on $\mathbb{C}^6$ in Table 9.26 induces a natural action on X_0, as follows:

$$\begin{aligned} \rho_x^2(\theta_1, \theta_2, \theta_3) &= (\theta_1 + \theta_3, -\theta_2, -\theta_3), \\ \rho_y^2(\theta_1, \theta_2, \theta_3) &= (-\theta_1, \theta_2 + \theta_3, -\theta_3). \end{aligned}$$

The complete action of $\mathbf{D}_2[\rho_x^2, \rho_y^2]$ on X_0 is given in Table 9.27. The action of $\mathbf{D}_2[\rho_x^2, \rho_y^2]$ on X_0 induces an action of $\mathbf{D}_2[\rho_x^2, \rho_y^2]$ on $\mathscr{C}_{\mathbf{D}_2[\rho_x^2,\rho_y^2]}$ by permutation, this action is trivial.

Proposition 9.22
Let $\mathbf{D}_2[\rho_x^2, \rho_y^2]$ act with the induced trivial action on $\mathscr{C}_{\mathbf{D}_2[\rho_x^2,\rho_y^2]}$ and on X_0 as in Table 9.27. Then given $C \in \mathscr{C}_{\mathbf{D}_2[\rho_x^2,\rho_y^2]}$, the setwise isotropy $\mathrm{Stab}(C)$, pointwise isotropy $\mathrm{stab}(C)$ and $S(C)$ are given in Table 9.7.

Proof. The proof follows from the standard calculations. □

Table 9.27: Action of $\mathbf{D}_2[\rho_x^2, \rho_y^2]$ induced on X_0 for the BCC lattice.

Element of $\mathbf{D}_2[\rho_x^2, \rho_y^2]$	Action on X_0
ρ_x^2	$(\theta_1 + \theta_3, -\theta_2, -\theta_3)$
ρ_y^2	$(-\theta_1, \theta_2 + \theta_3, -\theta_3)$
ρ_z^2	$(-\theta_1 - \theta_3, -\theta_2 - \theta_3, \theta_3)$

Knots Relative to C. For each $C \in \mathscr{C}_{\mathbf{D}_2[\rho_x^2,\rho_y^2]}$ $S(C) \cong \mathbf{Z}_2$, so the two equilibria that are contained on C are the knots. This information is given in Table 9.29.

Projected Skeleton

The action of $\mathbf{D}_2[\rho_x^2, \rho_y^2]$ on $\mathscr{C}_{\mathbf{D}_2[\rho_x^2,\rho_y^2]}$ shows that there are six orbit representatives for the elements of $\mathscr{C}_{\mathbf{D}_2[\rho_x^2,\rho_y^2]}$ that are homeomorphic to $\mathbf{S}^1$; that is, the symmetry does not simplify our calculations in this respect. However, each C has two knots; this implies that there is an axis of reflection symmetry. So each C projects into the orbit space as a line joining the two knots. More precisely, each $C \in \mathscr{C}_{\mathbf{D}_2[\rho_x^2,\rho_y^2]}$ joins the two knots given in Table 9.29. Figure 9.1 illustrates the projected skeleton. From the projected skeleton we deduce that there exist at most $2^6 = 64$ qualitatively different $\mathbf{D}_2[\rho_x^2, \rho_y^2]$-equivariant flows on $\mathbb{X}_{\mathbf{D}_2[\rho_x^2,\rho_y^2]}$. The projected skeleton can be arranged to support a variety of different flows, including heteroclinic networks.

Table 9.28: Isotropy data for $C \in \mathscr{C}_{\mathbf{D}_2[\rho_x^2,\rho_y^2]}$ for the BCC lattice.

$C \in \mathscr{C}_{\mathbf{D}_2[\rho_x^2,\rho_y^2]}$	stab(C)	Stab(C)	$S(C)$ = Stab(C)/stab(C)
e_1	$\mathbf{D}_2[\rho_x^2, \rho_y^2]$	$\mathbf{D}_2[\rho_x^2, \rho_y^2]$	$\mathbf{1}$
e_3	$\mathbf{D}_2[\rho_x^2, \rho_y^2]$	$\mathbf{D}_2[\rho_x^2, \rho_y^2]$	$\mathbf{1}$
e_4	$\mathbf{D}_2[\rho_x^2, \rho_y^2]$	$\mathbf{D}_2[\rho_x^2, \rho_y^2]$	$\mathbf{1}$
e_5	$\mathbf{D}_2[\rho_x^2, \rho_y^2]$	$\mathbf{D}_2[\rho_x^2, \rho_y^2]$	$\mathbf{1}$
c_1	$\mathbf{Z}_2[\rho_x^2]$	$\mathbf{D}_2[\rho_x^2, \rho_y^2]$	$\mathbf{Z}_2$
c_3	$\mathbf{Z}_2[\rho_y^2]$	$\mathbf{D}_2[\rho_x^2, \rho_y^2]$	$\mathbf{Z}_2$
c_{23}	$\mathbf{Z}_2[\rho_x^2]$	$\mathbf{D}_2[\rho_x^2, \rho_y^2]$	$\mathbf{Z}_2$
c_{25}	$\mathbf{Z}_2[\rho_y^2]$	$\mathbf{D}_2[\rho_x^2, \rho_y^2]$	$\mathbf{Z}_2$
c_{33}	$\mathbf{Z}_2[\rho_z^2]$	$\mathbf{D}_2[\rho_x^2, \rho_y^2]$	$\mathbf{Z}_2$
c_{38}	$\mathbf{Z}_2[\rho_z^2]$	$\mathbf{D}_2[\rho_x^2, \rho_y^2]$	$\mathbf{Z}_2$

Table 9.29: Knots relative to orbit representatives of $C \in \mathscr{C}_{\mathbf{D}_2[\rho_x^2,\rho_y^2]}$ for the BCC lattice.

Element of $\mathscr{C}_{\mathbf{D}_2[\rho_x^2,\rho_y^2]}$	Knots
c_1	e_1, e_4
c_3	e_1, e_3
c_{23}	e_3, e_5
c_{25}	e_4, e_5
c_{33}	e_1, e_5
c_{38}	e_4, e_3

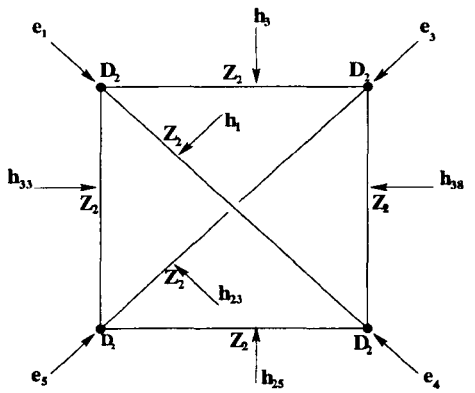

Figure 9.6: The projected skeleton $\mathbb{X}^p_{\mathbf{D}_2[\rho_x^2,\rho_y^2]}$. Here $h_1 = \{(\theta,0,0)|\theta \in (0,\pi)\}$, $h_{23} = \{(\theta,\pi,0)|\theta \in (0,\pi)\}$, $h_{25} = \{(\pi,\theta,0)|\theta \in (0,\pi)\}$, $h_{33} = \{(\theta,\theta,-2\theta)|\theta \in (0,\pi)\}$ and $h_{38} = \{(\theta+\pi,\theta,-2\theta)|\theta \in (0,\pi)\}$.

9.2.8 Example

In this subsection we present an example to illustrate how the structure of the planform with $\mathbb{O}\oplus\mathbf{Z}_2^c$ symmetry is altered when forced symmetry breaking terms are taken into account. The example we consider is forced symmetry breaking to $\mathbf{D}_3[\tau_3,\kappa_3]$. This example is chosen since it has direct relevance to the application we shall consider in Part IV.

Breaking the original Γ symmetry of the system to $\mathbf{D}_3[\tau_3,\kappa_3]$ symmetry corresponds to a perturbation of the BCC lattice in three mutually perpendicular direction with respect to the body diagonal of the cube, see Figure 9.7.

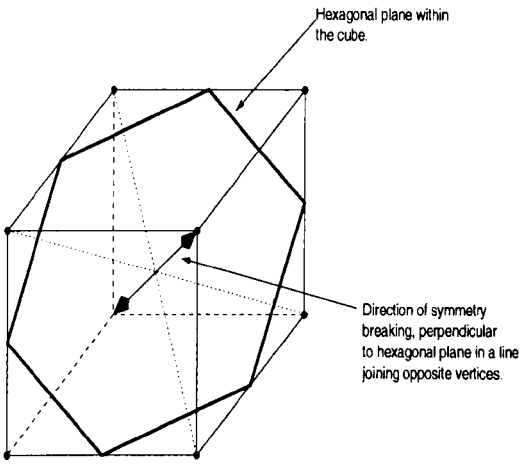

Figure 9.7: Perturbation of the cube along the body diagonal.

Our renderings of the three-dimensional planforms follow identical lines to those for the SC and FCC lattices. We consider the pattern in the body hexagonal plane of the cube. To make the symmetry breaking easier to perform, we introduce a new coordinate system. In which the body hexagon of the cube is parallel to the Z-axis. The coordinates used are from Gomes [39]. Define

$$A = \begin{pmatrix} \frac{1}{\sqrt{2}} & -\frac{1}{\sqrt{2}} & 0 \\ \frac{1}{\sqrt{6}} & \frac{1}{\sqrt{6}} & \frac{2}{\sqrt{6}} \\ \frac{1}{\sqrt{3}} & \frac{1}{\sqrt{3}} & -\frac{1}{\sqrt{3}} \end{pmatrix}. \tag{9.5}$$

This orthogonal change of coordinates $(x, y, z) \mapsto (X, Y, Z)$ changes the dual lattice vectors, and we denote the new vectors by $\mathbf{M}_j$. The resulting eigenfunction is

$$\mathbf{u}(\mathbf{x}) = \sum_{j=1}^{6} z_j \exp\left(i\mathbf{M}_j \cdot (\mathbf{X})\right). \tag{9.6}$$

In all cases we consider $z_j = 1$ for all j, which corresponds to the equilibrium e_1. Figure 9.8 (a) presents a rendering of (9.6); in this unperturbed case we see the black-eye patterns as found by Gomes [39]. This figure shows the BCC pattern in (X, Y, Z) coordinates restricted to the region $-1/4\sqrt{6} \leq Z \leq 1/4\sqrt{6}$; this region is called a "monolayer" in [39]. The pattern has then been integrated over the depth of the region to give the resulting pattern. We now consider what happens when symmetry-breaking terms are present. In the new coordinate system we define $\Psi(X, Y, Z) = ((1+\varepsilon)^{-1}X, (1+\varepsilon)^{-1}Y, Z + \varepsilon Z^{0.5})$. The choice of the Z perturbation is to reflect the experimentally relevant chemical gradient along the body diagonal of the cube, and we shall discuss this in more depth in Part IV. The eigenfunction is now

$$\mathbf{u}(\mathbf{x}) = \sum_{j=1}^{6} z_j \exp\left(i\mathbf{M}_j \cdot (\Psi^{-1}(\mathbf{X}))\right). \tag{9.7}$$

Figure 9.8 (b) presents a rendering of (9.7). It is important to realise that we have plotted the perturbed planform as if the points representing the eigenfunction are contained in X_0, which is not true. We now consider a brief example where the planform is plotted using the information contained on the perturbed skeleton. A more detailed discussion will follow in Part IV. Consider the equilibrium e_1; on X_ε this corresponds to a point of the form $e_1 + \varepsilon\hat{\mathbf{z}}$. Writing $\hat{\mathbf{z}}$ in polar coordinates, the j^{th} component is $r_j e^{i\phi_j}$, where $r_j \in \mathbb{R}^+$ and $\phi_j \in [0, 2\pi)$.

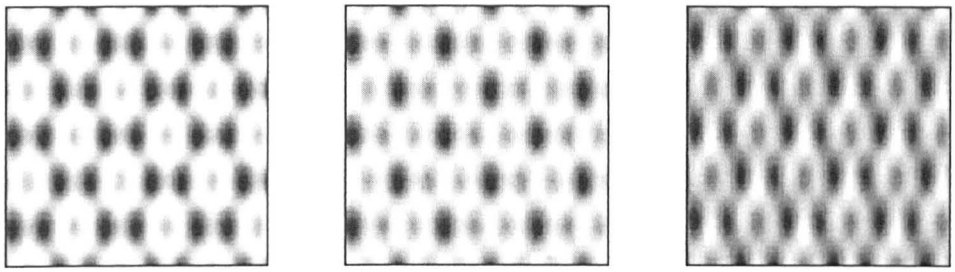

(a) (b) (c)

Figure 9.8: Three density plots of the BCC axial solution with $\mathbb{O} \oplus \mathbf{Z}_2^c$ in a hexagonal cross section of the cube. (a) Planform when no forced symmetry breaking is present ($\varepsilon = 0$). (b) Planform when symmetry-breaking terms are present. (c) Planform when we consider the equilibria as a point on X_ε.

The eigenfunction is now

$$\mathbf{u}(\mathbf{x}) = \sum_{j=1}^{6} r_j e^{\mathrm{i}\phi_j} \exp(\mathrm{i}\mathbf{K}_j \cdot (\Psi^{-1}(\mathbf{x})).$$

To realise $\mathbf{u}(\mathbf{x})$ in physical space we must compute its real part; this is

$$\mathbf{u}(\mathbf{x}) = \sum_{j=1}^{6} r_j \left(\cos\phi_j \cos(\mathbf{K}_j \cdot \Psi^{-1}(\mathbf{x})) - \sin\phi_j \sin(\mathbf{K}_j \cdot \Psi^{-1}(\mathbf{x}))\right). \tag{9.8}$$

For any chosen equilibrium the values of r_j and ϕ_j are fixed (provided ε is fixed). We assume that e_1 is close to e_1^ε; so ε is small. Figure 9.8 (c) presents an example of the eigenfunction (9.8) under the same conditions as those used to plot Figure 9.8 (b), with the only change being to plot e_1^ε rather then e_1. Even with this apparently simple change, the structure of the planform is alter drastically; in particular, we see more of the previous black-eye structure, together with the "ghosts" of stripes. Perhaps the most important observation is the movement of the "eye" away from the centre of the pattern. These issues will be investigated further in the light of experimental results in Part IV.

9.3 High Dimensional Representations

In this section we consider the higher dimensional representations of the group Γ. These representations are much more complex than the previous twelve-dimensional case. However, for a certain class of solutions, the high dimensional problem may be identified with the twelve-dimensional problem, and the results concerning the skeleton, symmetry properties and the projected skeleton are identical. Beyond these special solutions we do not consider these representations further. In particular, by an argument identical to Remark 7.24, those solutions with symmetry isomorphic to $\mathbb{O} \oplus \mathbf{Z}_2^c$ can be studied using the twelve-dimensional results.

9.3.1 Existence of Translation Free Axial Solutions

In this subsection we discuss the results of Dionne [19] concerning the existence of translation free axial solutions for the high dimensional representations of Γ. We recall that there are

Table 9.30: Translation free axial subgroups of Γ. Superscripts distinguish groups with different generators. The groups $\widetilde{\mathbf{D}}_4^a \oplus \mathbf{Z}_2^c$ and $\widetilde{\mathbf{D}}_4^b \oplus \mathbf{Z}_2^c$ occur only in the twenty-four-dimensional type 1 representation when certain defining conditions on the representation are satisfied [19].

Dimension	Axial Subgroup Σ
24 Type 1 (case 1)	$\mathbb{O} \oplus \mathbf{Z}_2^c$
	$\widetilde{\mathbb{O}} \oplus \mathbf{Z}_2^c$
24 Type 1 (case 2)	$\mathbb{O} \oplus \mathbf{Z}_2^c$
	$\widetilde{\mathbb{O}}$
	$\widetilde{\mathbb{T}} \oplus \mathbf{Z}_2^c$
	$\widetilde{\mathbf{D}}_4^a \oplus \mathbf{Z}_2^c$
	$\widetilde{\mathbf{D}}_4^b \oplus \mathbf{Z}_2^c$
24 Type 2	$\mathbb{O} \oplus \mathbf{Z}_2^c$
	$\widetilde{\mathbb{O}}^a \oplus \mathbf{Z}_2^c$
	$\mathbb{O}^a$
48	$\mathbb{O} \oplus \mathbf{Z}_2^c$
	$\widetilde{\mathbb{O}} \oplus \mathbf{Z}_2^c$

two twenty-four-dimensional representations, and one forty-eight-dimensional representation. Dionne [19] proves the existence of 13 translation free axial solutions, given in Table 9.30.

The construction of general equivariant mappings for the high dimensional representations is a task of incredible complexity, and one that we do not address. We content ourselves with the following classification theorem for those solutions in Table 9.30 with symmetry isomorphic to $\mathbb{O} \oplus \mathbf{Z}_2^c$.

Theorem 9.23
Let $\Gamma = \mathbb{O} \oplus \mathbf{Z}_2^c + \mathbf{T}^3$, $\Sigma \cong \mathbb{O} \oplus \mathbf{Z}_2^c$. Let Δ be one of the group (or isomorphic to) $\mathbb{O}$, $\mathbf{D}_4[\rho_x, \kappa_6]$, $\mathbb{T}$, $\mathbf{D}_3[\tau_3, \kappa_3]$, $\mathbf{D}_2[\rho_x^2, \kappa_6]$, $\mathbf{D}_2[\rho_x^2, \rho_y^2]$. Let Γ act on $\mathbb{C}^s$, where $s = 6$, 12 or 24 depending on the representation. Let $\mathbf{f} \in \vec{\mathcal{E}}_\Gamma$ be a Γ-equivariant bifurcation problem. Let $\mathbf{g} \in \vec{\mathcal{E}}_\Delta$ be a Δ-equivariant vector field that satisfies $\mathbf{g}(\mathbf{0}) = \mathbf{0}$. Then there exist branches of steady-state solutions to $\mathbf{f}(\mathbf{0}, \lambda) = \mathbf{0}$ bifurcating from the origin with isotropy Σ. The group orbit of these solutions is diffeomorphic to a standard 3-torus. Consider the perturbed system $\mathbf{F}(\mathbf{z}, \lambda, \varepsilon) = \mathbf{f}(\mathbf{z}, \lambda) + \varepsilon \mathbf{g}(\mathbf{z})$, where ε is real and small. Then for sufficiently small ε, X_0 persists to give a new $\mathbf{F}$-invariant manifold X_ε, which is Δ-equivariantly diffeomorphic to X_0. The behaviour of the vector field on X_0 is characterised by:

1. *When $\Delta \cong \mathbb{O}$ there are four (group orbits of) equilibria e_1, e_2, e_4, and e_{11}, together with five (group orbits of) heteroclinic connections h_1, h_5, h_7, h_{10}, and h_{23}. Figure 9.1 shows the arrangement of the equilibria and connections.*

2. *When $\Delta \cong \mathbf{D}_4[\rho_x, \kappa_6]$ there are four (group orbits of) equilibria e_1, e_3, e_4, and e_{11}, together with six (group orbits of) heteroclinic connections h_1, h_3, h_5, h_{23}, h_{41}, and h_{42}. Figure 9.2 shows the arrangement of the equilibria and connections.*

3. *When $\Delta \cong \mathbb{T}$ there are two (group orbits of) equilibria e_1 and e_3, together with three (group orbits of) heteroclinic connections h_1, c_5, and h_{23}. Figure 9.3 shows the arrangement of the equilibria and connections.*

4. *When $\Delta \cong \mathbf{D}_3[\tau_3, \kappa_3]$ there are two equilibria e_1 and e_8, together with three (group orbits of) heteroclinic connections c_9, c_{10} and h_{21}. Figure 9.4 shows the arrangement of these equilibria and connections. There exist perturbation which give two heteroclinic cycles, the first between the equilibria e_1 and the second e_2.*

5. *When* $\Delta \cong \mathbf{D}_2[\rho_x^2, \kappa_6]$ *there are four equilibria* e_1, e_4, e_{11} ,*and* e_{12}, *together with six (group orbits of) heteroclinic connections* h_1, h_{23}, h_{41}, h_{42}, h_{45}, *and* h_{46}. *Figure 9.5 shows the arrangement of these equilibria and connections.*

6. *When* $\Delta \cong \mathbf{D}_2[\rho_x^2, \rho_y^2]$ *there are four equilibria* e_1, e_3, e_4, *and* e_5, *together with five (group orbits of) heteroclinic connections* h_1, h_{23}, h_{25}, h_{33}, *and* h_{38}. *Figure 9.6 the arrangement of these equilibria and connections.*

This classification theorem is as far as we can go: because of the complexities of the invariant theory we cannot make any further general statements.

9.3.2 Examples

In this subsection we present examples to illustrate how the structure of the planforms with $\mathbb{O} \oplus \mathbf{Z}_2^c$ symmetry are altered when forced symmetry breaking terms are taken into account. These planforms are considered purely to keep the examples as simple as possible: there is no reason for not considering other planforms with symmetry isomorphic to $\mathbb{O} \oplus \mathbf{Z}_2^c$. We consider forced symmetry breaking to $\mathbf{D}_3[\tau_3, \kappa_3]$. This is chosen since it has direct relevance to the application we shall consider in Part IV. We follow the same ideas as those used in the twelve-dimensional case. Breaking the original Γ symmetry of the system to $\mathbf{D}_3[\tau_3, \kappa_3]$ symmetry corresponds to a perturbation of the BCC lattice in three mutually perpendicular direction with respect to the body diagonal of the cube, see Figure 9.7.

We use the new coordinate system (X, Y, Z) as used in the twelve-dimensional representation. The eigenfunction is

$$\mathbf{u}(\mathbf{x}) = \sum_{j=1}^{s} z_j \exp\left(i\mathbf{M}_j \cdot (\mathbf{X})\right), \tag{9.9}$$

where $s = 12$ or 24 and $\mathbf{M}_j$ are the dual lattice vectors. In all cases we consider $z_j = 1$ for all j, which corresponds to the equilibrium e_1. If we consider the perturbation $\Psi(X, Y, Z) = ((1+\varepsilon)^{-1}X, (1+\varepsilon)^{-1}Y, Z + \varepsilon Z^{0.5})$, as we did for the twelve-dimensional representation, then the eigenfunction is

$$\mathbf{u}(\mathbf{x}) = \sum_{j=1}^{s} z_j \exp\left(i\mathbf{M}_j \cdot (\Psi^{-1}(\mathbf{X}))\right). \tag{9.10}$$

To complete the analysis, we must consider what happens to the planform when we plot the perturbed equilibrium e_1^ε. The eigenfunction in this case is

$$\mathbf{u}(\mathbf{x}) = \sum_{j=1}^{s} r_j \left(\cos\phi_j \cos(\mathbf{K}_j \cdot \Psi^{-1}(\mathbf{x})) - \sin\phi_j \sin(\mathbf{K}_j \cdot \Psi^{-1}(\mathbf{x}))\right), \tag{9.11}$$

where $s = 12$ or 24.

We consider examples of the behaviour of the eigenfunctions (9.9), (9.10) and (9.11) for each of the high dimensional representations of Γ.

Examples of Planforms in Twenty-four-Dimensional Type 1 Representation

Figure 9.9 (a) present a rendering of the function (9.9); in this unperturbed case, we see a highly elaborate and complex pattern. Figures 9.9 (b) and (c) show how this planform is affected by symmetry breaking terms with $\mathbf{D}_3[\tau_3, \kappa_3]$ symmetry. In (b) we plot the eigenfunction (9.10), and in (c) the function (9.11).

Examples of Planforms in Twenty-four-Dimensional Type 2 Representation

Figure 9.10 (a) presents a rendering of the function (9.9); in this unperturbed case, we see a highly elaborate and complex pattern. Figures 9.10 (b) and (c) show how this planform is affected by symmetry breaking terms with $\mathbf{D}_3[\tau_3, \kappa_3]$ symmetry. In (b) we plot the eigenfunction (9.10), and in (c) the function (9.11).

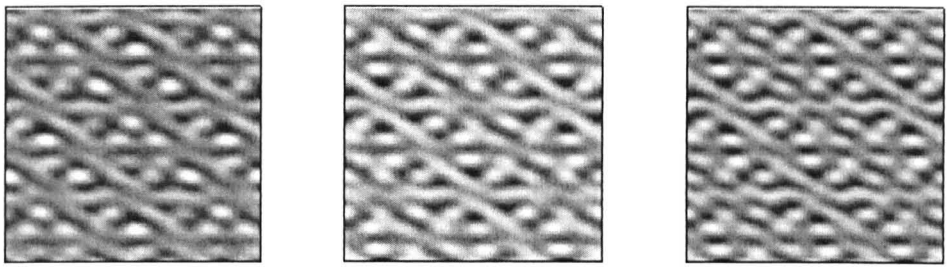

(a) (b) (c)

Figure 9.9: Three density plots of the BCC axial solution with $\mathbb{O} \oplus \mathbf{Z}_2^c$ symmetry in a hexagonal cross section of the cube. (a) Planform when no forced symmetry breaking is present ($\varepsilon = 0$). (b) Planform when symmetry-breaking terms are present. (c) Experimentally relevant plot showing (in an *ad hoc* manner) the solution as it would be seen in physical space.

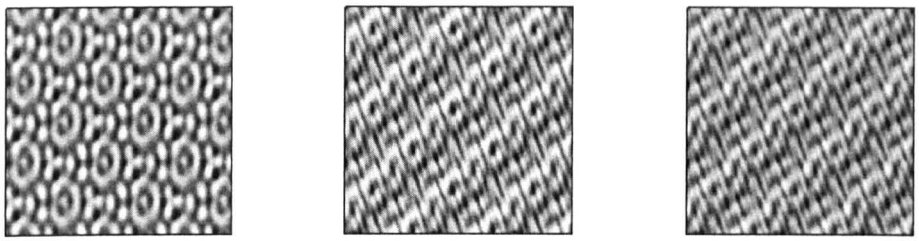

(a) (b) (c)

Figure 9.10: Three density plots of the BCC axial solution with $\mathbb{O} \oplus \mathbf{Z}_2^c$ in a hexagonal cross section of the cube. (a) Planform when no forced symmetry breaking is present ($\varepsilon = 0$). (b) Planform when symmetry-breaking terms are present. (c) Experimentally relevant plot showing (in an *ad hoc* manner) the solutions as it would be seen in physical space.

Examples of Planforms in Forty-eight-Dimensional Representation

Figure 9.11 (a) presents a rendering of the function (9.9), in this unperturbed case, we see a highly elaborate and complex pattern. Figures 9.11 (b) and (c) show how this planform is affected by symmetry breaking terms with $\mathbf{D}_3[\tau_3, \kappa_3]$ symmetry. In (b) we plot the eigenfunction (9.10), and in (c) the function (9.11).

9.4 Conclusion

We have seen that the BCC, like the FCC and SC lattices before, is capable of supporting dynamics much richer than those supported by any two-dimensional lattice. In particular, heteroclinic cycles and networks are possible. In this chapter we have again not considered the class II and III subgroups of $\mathbb{O} \oplus \mathbf{Z}_2^c$, the reasons being identical to those given for the FCC and SC lattice. The Class III subgroups do not seem to have an obvious application, and the

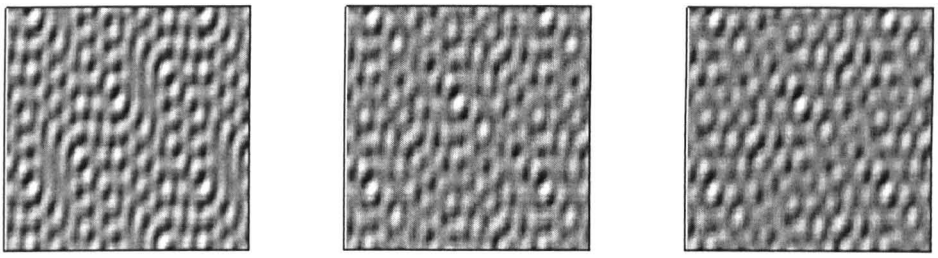

(a) (b) (c)

Figure 9.11: Three density plots of the BCC axial solution with $\mathbb{O} \oplus \mathbf{Z}_2^c$ in a hexagonal cross section of the cube. (a) Planform when no forced symmetry breaking is present ($\varepsilon = 0$). (b) Planform when symmetry-breaking terms are present. (c) Experimentally relevant plot showing (in an *ad hoc* manner) the solutions as it would be seen in physical space.

Class II subgroups are essentially the same as the class I subgroups.

The main result of the chapter is Theorem 9.23. This theorem gives a partial classification of the behaviour that we may expect from a solution with symmetry (isomorphic to) $\mathbb{O} \oplus \mathbf{Z}_2^c$ of a Γ-equivariant bifurcation problem when symmetry breaking effects are taken into account. Our results concerning breaking the symmetry to $\mathbf{D}_3[\tau_3, \kappa_3]$ have direct applications to the black-eye instability, and we pursue these ideas in Part IV.

Part IV

Pattern Formation and Turing Instabilities

Chapter 10

Pattern Formation and Turing Instabilities

In this chapter we address some of the results of Part III, (and to a less extent those of Part II) in an experimental context. Whilst we cannot use the findings of Part III to produce specific testable predictions, we can nonetheless provide an indication of the applicability of the theory.

10.1 Pattern Formation

We have already seen that general equivariant bifurcation theory is an indispensable tool for the study of pattern forming phenomena. Here we present examples to illustrate possible applications of the theory and the results of Parts II and III. This list is by no means exhaustive and provides only an illustration, see Callahan [7] for a more comprehensive list.

Turing Patterns

The seminal paper of Alan Turing [82] published in 1952, (see also Murray [70]) proposed a "simple" model for the "complex" process of morphogenesis—the method by which a zygote acquires form and becomes an embryo [70]. In this model, diffusion, rather than homogenising the system, counterintuitively is essential in the pattern forming process. Murray [70] has produced much work along these lines, but the idea is still controversial. A key issue, as yet unresolved, is the identification of morphogens—chemicals that set-up a "prepattern" that subsequently, through the reaction-diffusion mechanism, leads to pattern formation. Debate still rages about the existence of morphogens; although certain chemicals are essential for development, they are not necessarily morphogens. In the 1970's retinoic acid was put forward as a candidate, but this issue is still open and experiments are still being performed to assess this proposal [64].

Turing Instabilities

Turing instabilities are closely related to the ideas underlying Turing patterns but are not specific to morphogenesis. Here we consider a uniform stable solution of a system of PDEs. These PDEs model a system of reactants[1] which can acts as activators and inhibitors for each other. If the uniform state becomes unstable upon the introduction of diffusion, producing a pattern, then this instability is called a Turing instability. The first experimental evidence for Turing instabilities was found only 12 years ago, which considering that the mechanism was proposed in

[1] Here "reactants" is used in a general way, and does not necessarily mean chemicals, just species which react or interact.

1952, is relatively recent [10]. Further to these experiments Ouyang and Swinney [73] produced stripes, hexagons, stripy hexagons, and a transition from stripes to hexagons. The patterns found usually reflect those predicted for the standard representations of the hexagonal lattice. However, further investigations revealed the occurrence of honeycombs [72] and a puzzling new structure called black-eyes [46] which are not expected to occur on the hexagonal lattice (or any other two-dimensional lattice). The paper of Gunaratne [46] proposed that the pattern is produced by a nonlinear superposition of two different hexagonal modes. However, Gomes [39] has shown that black-eyes can be produced using a three-dimensional model. We shall discuss, in detail, the issues raised here in Section 10.2.

Hallucination Patterns

An interesting example is the primary visual cortex (V1) [33]. It has been shown that the pattern of neuronal connections in V1 leads to an action of the Euclidean group on $\mathbb{R}^2 \times \mathbf{S}^1$, and both scalar and pseudoscalar bifurcation may occur. Furthermore, it is argued that the geometric patterns seen in visual hallucinations may be the result of symmetry-breaking bifurcations in V1 [4, 24]. The V1 layer is divided into many small areas about 1mm in diameter called hypercolumns, and each cell in the hypercolumns receives signals from one small area in the retina [52, 53, 51]. The coupling of the hypercolumns leads to a Euclidean group action on $\mathbb{R}^2 \times \mathbf{S}^1$. In the Wilson-Cowan model [88] hypercolumns are assume infinitesimal and modelled by circles, with each point of the circle corresponding to a boundary orientation; this gives the physical space of V1 as $\mathbb{R}^2 \times \mathbf{S}^1$, and the action of the Euclidean group is dictated by the coupling. Furthermore, since both scalar and pseudoscalar bifurcations can occur, the situation is more complex than that found in reaction-diffusion systems.

Faraday Instabilities

If a layer of liquid with free upper surface is subjected to a vertical oscillation, pattern-forming instabilities can occur when the amplitude of the vertical forcing exceeds a critical value [23]. The patterns which arise are standing waves, and often have the periodicity of the square lattice, but quasiperiodic patterns have also been observed. More interesting, (from our point of view,) is the occurrence of patterns with a good resemblance to those found for the high dimensional representations of the square and hexagonal lattices, see Zhang and Viñals [91] and Edwards and Fauve [23]. The patterns are not disrupted by the presence of sidewalls, except for a small healing zone; this is demonstrated by Edwards and Fauve [23], where the experiments are performed in a number of different containers, including an outline of France.

Nonlinear Optical Systems

Lasers have been found to exhibit fields with spatial structures [80]. The underlying reason for pattern formation in these systems is the small Fresnel number[2]. Recent research has seen a great deal of progress in the understanding of laser and other nonlinear optical systems [15, 78, 80, 83]. Many different phenomena now have modelling equations, and the formation of spatial patterns predicted by these models has, in some cases, been observed experimentally [80].

Nonlinear optical systems are of particular interest to us since Staliunas [78] illustrates how the dynamics of certain photorefractive oscillations, called degenerate optical parametric oscillators (DOPOs), may be described by the three-dimensional Swift–Hohenberg equation. Using numerical integration with suitable parameter values (detuning in [78]), he shows that stable three-dimensional structures exist, in addition to the more usual stripe and hexagonal patterns. Further to this work, Staliunas and J.Sánchez-Morcillo [79] have shown that patterns in DOPOs can form via a Turing mechanism as discussed above. The same authors also state that other systems may form patterns via a Turing mechanism. Staliunas [78] points out that

[2]The Fresnel number is the optical analogue of the aspect ratio in other pattern forming systems [80].

other optical systems may support three-dimensional patterns, since the only requirement for these structures to exist is that the nonlinearity acts rapidly [78].

There are ranges of different and interesting patterns that have been observed in nonlinear optical systems. Vorontsov and Samson [85] have shown the existence of black-eye patterns, whereas D'Alessandro and Firth [15] have numerically shown the existence of honeycomb structures.

Polyacrylamide–Methylene Blue–Oxygen Reaction

The Polyacrylamide–Methylene Blue-Oxygen (PA–MBO) reaction shows pattern formation to hexagons, stripes and zigzag structures [81], much like other pattern forming systems. However, it is unclear whether the underlying mechanism is Turing-like or Rayleigh–Bénard in nature. Currently, Kurin-Csörgei *et al.* [59] and Orbán *et al.* [71] have concluded that the mechanism is Rayleigh–Bénard in nature. However, this conclusion has been question in Steinbock *et al.* [81], where the lack of dependence of the pattern wavelength on the thickness of the system found by Orbán *et al.* [71] raises Turing instabilities again. In addition to the usual stripes, hexagons and zigzags, Steinbock *et al.* [81] report the formation of black-eyes (called white-eye by Steinbock, due to their white, rather than black central "eye") and a honeycomb structure.

Here we have illustrated some of the systems where our results could be applicable, there are many more including: bacterial colony growth, vibrating granular layers, and block co-polymer melts [7]. Block co-polymer melts are an interesting example; they can form three-dimensional structures, in particular double diamonds, as found on the FCC lattice. Microemulsions have also been shown to exhibit three-dimensional structure, see Góźdź and Hołst [43].

The systems above were chosen since they provide examples where black-eyes have been found, or areas where extensions of our theory would prove useful. We shall explore the CIMA, PA–MBO reaction, and nonlinear optical systems in subsequent sections.

10.2 Turing Instabilities in the CIMA reaction

In this section we discuss the (possible) experimental relevance for our results from Part III. Our exposition focuses on our findings for forced symmetry breaking on the BCC lattice; these results give some illumination to current theories put forward to explain the formation of black-eye patterns in the CIMA reaction.

10.2.1 Introduction

Traditionally, pattern forming systems in thin domains, such as Rayleigh–Bénard convection [36], are formulated as purely two-dimensional problems. Whilst such models have produced good agreement between theory and experiment, there now exist both numerical [17, 86] and experimental [10, 46, 78, 81, 85] evidence for highly developed structures which are unexpected in two-dimensional systems.

As discussed in Section 10.1, the formation of spatial structures in reaction-diffusion systems (Turing instabilities) was first reported by Castets *et al.* [10] working with the chlorite-iodide-malonic acid (CIMA) reaction in an open thin strip gel reactor. This work was extended by Ouyang and Swinney [73] who performed a number of experiments on the same reaction, although their experimental set-up was different. In the experiments of Ouyang and Swinney [73], the gel was contained between two continuously fed well-stirred reactors. The authors found a number of different patterns: stripes, hexagons, and zigzags. The most surprising result was the occurrence of black-eyes—a pattern not predicted by standard equivariant bifurcation theory in two dimensions, and not previously reported. A model of Gunaratne *et al.* [46] assumes that the patterns are basically two-dimensional and can produce stripes and hexagons, but not black-eyes. Fourier analysis performed by the authors showed that black-eyes are the superposition of two hexagonal arrays of spots with wavelengths in the ratio $\sqrt{3}$. The authors

proposed that black-eyes are generated by nonlinear interactions of the hexagonal modes which are observed at onset.

There are two problems with this theory. The harmonics were not detected until well beyond onset, whilst one would expect from standard analysis for the amplitude of these harmonics to grow continuously beyond the primary instabilities [39]. Secondly, if black-eyes were the result of a nonlinear interaction of the basic modes, one would expect the "eyes" of the black-eye pattern to be centralised. Indeed, if the eyes are caused by harmonics of the primary modes, then they should be totally constrained by the positioning of the principal modes [38], but this is not supported by experimental evidence, see Figure 1 of Gomes [39]. The authors of [46] discuss the lack of harmonics and suggest that the sensitivity of their experiments was insufficient to resolve the harmonics, or that the secondary modes are not "slaved" to the primary modes [39, 46]. These discrepancies lead Gomes [39] to develop a three-dimensional model for the black-eye instability. This model naturally produces, stripes, hexagons and black-eyes as linear modes.

The three-dimensional model of Gomes proposes that black-eyes are a slice of the BCC planform seen in projection. It has been shown in three dimensions that the BCC structure is the most stable [86]. Numerical simulations of the Brusselator model of Turing instability by De Wit *et al.* [17] shows that BCC structures are possible. The work of Callahan and Knobloch [9] provides a detailed study of pattern selection in three-dimensional Turing systems. Further, many authors have shown that *hidden symmetries* are important in Euclidean invariant systems . These symmetries, which do not leave the domain invariant, nevertheless play an essential role in pattern formation and selection processes, introducing additional structure and restrictions on the bifurcation problem [42, 41, 40]. Thus it may be mathematically correct, and physically important, to consider the influence of three-dimensional symmetries on the CIMA reaction (and other pattern forming systems). As pointed out by Gomes, Winfree [89] has shown that certain wave patterns observed in thin domains are most appropriately interpreted as three-dimensional structures in projection.

When Gomes [39] originally proposed the three-dimensional model, the CIMA reaction was the only reaction that exhibited black-eye patterns. This lead to the following puzzle: if the black-eyes are really two-dimensional, then the CIMA system is, from a symmetry point of view, in the same class as (say) Rayleigh–Bénard convection (or any other two-dimensional system). So why do systems (such as) Rayleigh–Bénard convection *not* exhibit black-eyes? Recent experiments have shown the existence of black-eyes in nonlinear optical systems [85] and the PA–MBO reaction [81]. Although at first glance the appearance of black-eyes in other systems would appear to answer the question above, it does not. As discussed in the introduction, the formation of three-dimensional structures in (some) nonlinear optical systems and the PA–MBO reaction arises via a Turing instability[3]—the same as in the CIMA reaction. So, the question above is still valid: why does no other purely two-dimensional system exhibit black-eyes? Another question can now be posed: if black-eye have been found only in systems where three-dimensional structures or Turing instabilities occur, then why must black-eyes be two-dimensional?

The analysis of Gomes [39] originally suggested studying bifurcation problems with approximate BCC symmetry. This scenario has been discussed in Part III; we shall apply our results to make some qualitative comments on the models of Gomes [39] and Gunaratne [46] and comparison with experiments. The remainder of this section is organised as follows. In Subsection 10.2.2 we discuss the experimental set-up, showing how the chemical gradient naturally gives rise to forced symmetry breaking and how this enters the Gomes model. In Subsection 10.2.3 we make use of the results of Part III concerning symmetry breaking on the BCC lattice, applying these to the Gomes model of black-eyes. We finish in Subsection 10.2.4 with a discussion of our results, and compare them with experimental findings.

[3]Although this is still a point under debate, the weight of evidence at the moment favours the Turing mechanism.

10.2.2 Experimental Apparatus

We begin by recalling the orthogonal coordinates introduced by Gomes [39] and defined by (9.5), which we denoted by (X, Y, Z). These coordinates are convenient for discussion of the experimental apparatus. The experiments of Ouyang and Swinney [46, 73, 92] were performed in a circular layer of gel with diameter 25mm in the (X, Y) plane and a thickness of 1mm in the Z plane. The gel was sandwiched between sheets of porous glass 0.4mm thick, the diffusion of which is five times lower than the gel. The reactant were fed through the planes $Z = 0$, 1 giving a chemical gradient in the Z direction. The patterns were visualised in the X, Y directions. See Figure 10.1 for a diagram of the experimental apparatus.

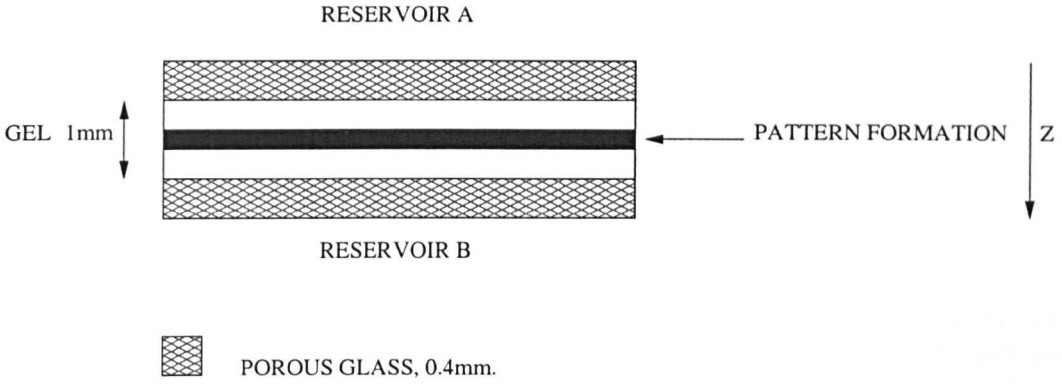

Figure 10.1: The experimental apparatus of Ouyang and Swinney.

The black-eye pattern emerges well beyond the primary instability; which consists of an hexagonal array of spots. The fully developed black-eye patterns is shown in Figure 10.2, this figure is taken from Gunaratne *et al.* [46]. The ratio of the two wavelength is $\sqrt{3}$. The bifucation from hexagons to black-eyes is non-hysteretic, upon a further increase in the bifurcation parameter a hysteric bifurcation from black-eyes to stripes is observed. The patterns form in a layer much thinner than the gel layer, and Gunaratne *et al.* [46] used this feature to support their hypothesis that the patterns are two-dimensional, and that black-eyes are a spatial harmonic generated by a nonlinear interaction of the basic modes responsible for the two-dimensional hexagonal pattern.

The Gomes Model

Consider the BCC planform as predicted by Theorem 9.1. Gomes [39] shows that black-eyes can be observed in the section $z = x + y$. However, we make an immediate change of coordinates to the (X, Y, Z) system. In these coordinates the sections $Z = N/2\sqrt{6}$, where N is an integer, consist of hexagonal lattices. To compare the model with experimental results, the BCC planform must be integrated in the Z direction over the depth of two consecutive sections. In Figure 10.3 we present a rendering of the BCC planform integrated over a depth of $1/2\sqrt{6}$.

The Gomes model is an idealisation of the true experimental situation. As Gomes discusses, an understanding should be developed of how the chemical gradient influences the pattern formation process. In the context of Part III the chemical gradient in the Z direction corresponds to breaking the original $\Gamma = \mathbb{O} \oplus \mathbf{Z}_2^c \dotplus \mathbf{T}^3$ symmetry to the subgroup $\mathbf{D}_3[\tau_3, \kappa_3]$. In the (X, Y, Z) coordinates the group $\mathbf{D}_3[\tau_3, \kappa_3]$ corresponds to the two-dimensional symmetry of the X, Y plane. Thus mathematically the chemical gradient can be studied via the techniques introduced to study forced symmetry breaking of Γ to $\mathbf{D}_3[\tau_3, \kappa_3]$.

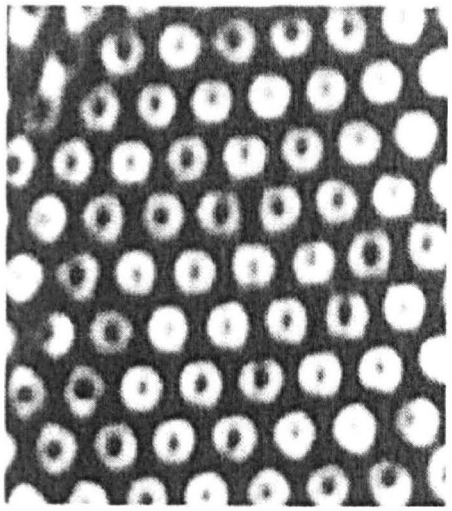

Figure 10.2: The black-eye patterns as produced by Ouyang and Swinney. The region illustrated is 1.6mm × 1.6mm. The wavelength of the white spots is 0.15mm and that of the black spots is 0.086mm.

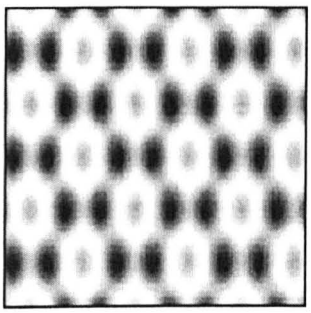

Figure 10.3: Black-eyes produced by integrating the BCC planform over the depth $Z = 1/2\sqrt{6}$ of a monolayer.

10.2.3 Bifurcation with Approximate BCC Symmetry

In this subsection we discuss the effect of breaking the Γ symmetry present in the Gomes model of the black-eye instability, so only $\mathbf{D}_3[\tau_3, \kappa_3]$ symmetry remains. The results of Part III concerning forced symmetry breaking on the BCC lattice show that when the symmetry is broken in this way, two equilibria persist and there exist two (possible) heteroclinic cycles, see Figure 9.4. The equilibria, when realised as points on the unperturbed skeleton, have the form $e_1 = (x, x, x, x, x, x)$ and $e_8 = (-x, x, x, -x, x, -x)$. However, these points are not a good representation of the equilibria in physical space. To give a more precise idea how the planforms would look in physical space, we use the equilibria on the perturbed skeleton corresponding to e_1 and e_8. Indeed, we have the equilibria $e_1^\varepsilon = e_1 + \varepsilon\hat{\mathbf{z}}_1$ and $e_8^\varepsilon = e_8 + \varepsilon\hat{\mathbf{z}}_8$, where $\hat{\mathbf{z}}_1$ and $\hat{\mathbf{z}}_8$ are vectors in $\mathbb{C}^6$. The next problem is to give a "good" representation of the points $\hat{\mathbf{z}}_1$ and $\hat{\mathbf{z}}_8$. This is difficult; their determination requires knowledge of the unknown diffeomorphism Θ_ε

defined by Theorem 2.3. However, it is not unreasonable to assume that e_1^ε and e_8^ε are close to e_1 and e_8, that is that ε is small. We write (say) $\hat{\mathbf{z}}_1 = (r_1 e^{i\phi_1}, \ldots, r_6 e^{i\phi_6})$, where $r_j \in \mathbb{R}^+$ and $\phi \in [0, 2\pi)$.

To model the chemical gradient we introduce the following perturbation function $\Psi(\mathbf{X}) = ((1+\varepsilon)^{-1}X, (1+\varepsilon)^{-1}Y, Z + \varepsilon Z^{0.5})$. There is no experimental evidence that this is a good or representative function to use, but even if not, it illustrates how symmetry breaking influences the patterns observed in experiments. The eigenfunction is

$$\mathbf{u}(\mathbf{x}) = \sum_{j=1}^{6} r_j \left(\cos\phi_j \cos(\mathbf{K}_j \cdot \Psi^{-1}(\mathbf{x})) - \sin\phi_j \sin(\mathbf{K}_j \cdot \Psi^{-1}(\mathbf{x}))\right). \tag{10.1}$$

Figure 10.4 presents examples that illustrate how the planform corresponding to the equilibrium e_1 is changed under the perturbation discussed above; the numbers r_j and ϕ_j were chosen at random. In particular, these figures illustrate how forced symmetry breaking reduces the dependency of the black-eye pattern on the depth of integration. In the unperturbed model very specific layers are selected, otherwise the black-eye pattern is not observed.

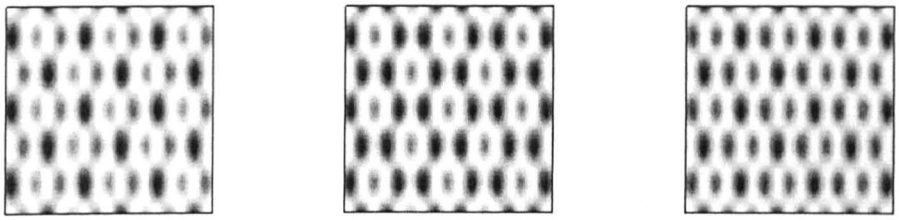

(a) One Layer (b) Two Layers (c) Three Layers

Figure 10.4: Black-eyes corresponding to the equilibria e_1 formed by integrating the function in (10.1) over three different depths. In each case a layer is the region $[1/2N\sqrt{6}, 1/2(N+1)\sqrt{6}]$ in the Z direction, where N is an integer. (a) Integrate over one layer. (b) Integrate over two layers. (c) Integrate over three layers. The figures used for the r_j's and ϕ_j's were $r_1 = 0.254$, $r_2 = 0.265$, $r_3 = -0.278$, $r_4 = -0.276$, $r_5 = 0.298$, $r_6 = -0.265$, $\phi_1 = 0.232$, $\phi_2 = -0.265$, $\phi_3 = 0.2876$, $\phi_4 = 0.2231$, $\phi_5 = -0.2341$, $\phi_6 = 0.2954$.

Next we consider the behaviour near the equilibrium e_8. Figure 10.5 illustrates the appearance of this planform under the forced symmetry breaking discussed above. The values of r_j and ϕ_j are the same as those used to generate Figure 10.4.

The equilibria are only part of the overall behaviour; to illustrate some of the patterns that can be produced along the heteroclinic cycle c_9, we present some examples. These are contained in Figure 10.6. These perturbations are interesting since the "eye" of the pattern can move slightly off centre and we see patterns where black-eyes and stripes are superimposed. Along the connection c_{10} we expect similar types of behaviour, but we do not give examples. It is possible to consider how different perturbation functions influence the patterns, but we shall not consider this issue.

10.2.4 Discussion

The original paper of Gomes [39] established a mathematical correspondence between the BCC and black-eye patterns. Of course, improving this mathematical link to a statement pertaining to what actually happens in experiments is difficult. Here we discuss the implications of

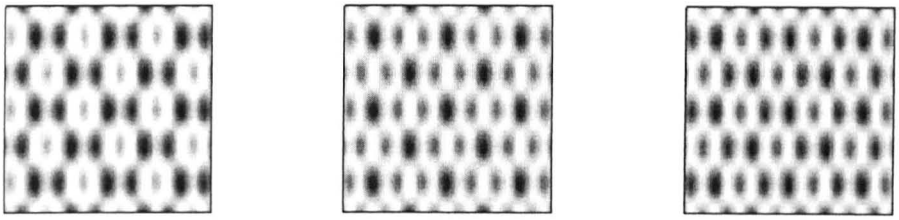

(a) One Layer (b) Two Layers (c) Three Layers

Figure 10.5: Black-eyes corresponding to the equilibria e_8 formed by integrating the function in (10.1) over three different depths, in each case a layer is the region $[1/2N\sqrt{6}, 1/2(N+1)\sqrt{6}]$ in the Z direction, where N is an integer. (a) Integrate over one layer. (b) Integrate over two layers. (c) Integrate over three layers. The values used for the r_j's and ϕ_j's were $r_1 = 0.254$, $r_2 = 0.265$, $r_3 = -0.278$, $r_4 = -0.276$, $r_5 = 0.298$, $r_6 = -0.265$, $\phi_1 = 0.232$, $\phi_2 = -0.265$, $\phi_3 = 0.2876$, $\phi_4 = 0.2231$, $\phi_5 = -0.2341$, $\phi_6 = 0.2954$.

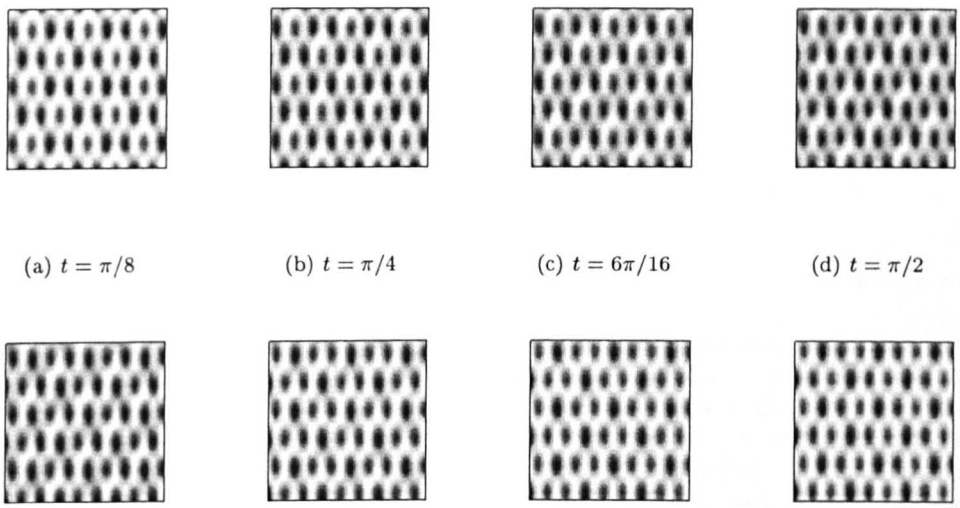

(a) $t = \pi/8$ (b) $t = \pi/4$ (c) $t = 6\pi/16$ (d) $t = \pi/2$

(e) $t = 10\pi/16$ (f) $t = 12\pi/4$ (g) $t = 14\pi/16$ (h) $t = \pi$

Figure 10.6: Patterns found along the heteroclinic cycle c_9, formed by integrating the function in (10.1) over two layers. The values used for the r_j's and ϕ_j's were $r_1 = 0.254$, $r_2 = 0.265$, $r_3 = -0.278$, $r_4 = -0.276$, $r_5 = 0.298$, $r_6 = -0.265$, $\phi_1 = 0.232$, $\phi_2 = -0.265$, $\phi_3 = 0.2876$, $\phi_4 = 0.2231$, $\phi_5 = -0.2341$, $\phi_6 = 0.2954$. The interval between each picture is $\pi/8$.

the results of Subsection 10.2.3 to this ongoing problem, which has seen much recent development including additional experimental studies [92] and theoretical work [90]. In particular, both these studies claim the black-eye pattern is two-dimensional. We believe that our results emphasise that the three-dimensional model still offers viable explanation for black-eyes. However, our discussion is by no means as comprehensive as possible, and cannot be without more

experimental evidence; we mean only to provide an illustration of some of the ideas.

The issue of black-eyes and an appropriate model have presented many problems in recent years; the only model of black-eyes was, for a time, that of Gomes. To determine the dimensionality of the black-eye pattern Zhou *et al.* [92] performed a series of experiments designed to settle this difficulty. Their experimental set-up was very similar to that used previously by Ouyang and Swinney [73, 46], although modifications were performed on the reactor. Previously the reacting medium was sandwiched between two porous glass discs; now the gel consisted of two thin discs, one of polyvinyl alcohol (PVA) gel and the other polyacrylamide gel [92]. We illustrate this new experimental apparatus in Figure 10.7. The polyacrylamide gel had no indicator present, and no Turing patterns can appear in this layer. However, as a result of the experimental set-up, Turing patterns can appear in the PVA gel layer. Experiments were conducted on PVA gels of varying thickness: 0.144, 0.10 and 0.09mm, but the overall thickness of the PVA and polyacrylamide gel was kept constant at 1mm. The experimental results led Zhou

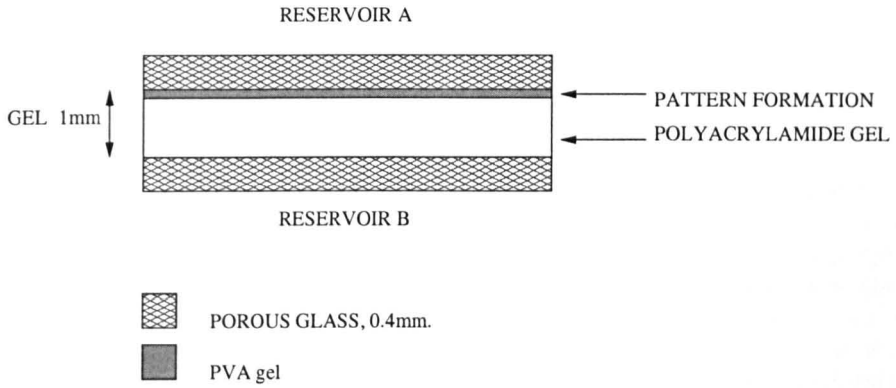

Figure 10.7: The experimental apparatus of Zhou and co-workers.

et al. [92] to argue that the Gomes model of black-eyes is not appropriate. We discuss some of their arguments in the light of the results of Subsection 10.2.3.

Their first objection concerns the specific region of the BCC planform that must be viewed in order for black-eyes to be seen. That is, the occurrence of black-eyes in the Gomes model is highly sensitive to the thickness and the number of lattice layers over which the integration is performed. Indeed, Zhou and co-authors state their experiments have two or three layers present and even more in the original experiments of Ouyang and Swinney [73]. Using this argument they deduce that black-eyes could not be observed in experiments, *even if BCC patterns are present.* However, as we have seen in Subsection 10.2.3, when the chemical gradient (which is still present in the experiments of Zhou and co-workers,) is taken into account, the symmetry-breaking effects reduce the dependency of the black-eye patterns on the integration depth. The example considered used a random choice of perturbation in the Z direction which may (and probably does) not give a good representation of the chemical gradient. Even with this caveat, the example does serve to illustrate how forced symmetry breaking can reduce (or at least alter) the critical dependence in the original Gomes model on the depth of integration.

A second objection of Zhou *et al.* [92] concerns the wavelength of the Turing patterns. Traditional pattern formation theory predicts that a dispersion relation determines the wavelength of a Turing pattern, which is independent of the dimensionality of the system. The experiments performed by the authors give black-eyes a wavelength of 0.22mm which is not compatible with all other observed patterns and previous experiements [92]. They argue that since the black-eye pattern is a slice of the BCC pattern, the BCC structure must have a wavelength of approximately 0.11 mm, implying hexagons and strips should have the same wavelength—a situation not in agreement with experiments. There is a solution to this problem; if we are supposing that the black-eyes are a three-dimensional phenomenon occurring on a slice of the BCC structure,

then we must expect all other patterns to occur on this slice also. Indeed, we can produce stripes, hexagons and black-eyes on the slice of the BCC planform, see Figure 10.8. Under these conditions the wavelength argument is weakened.

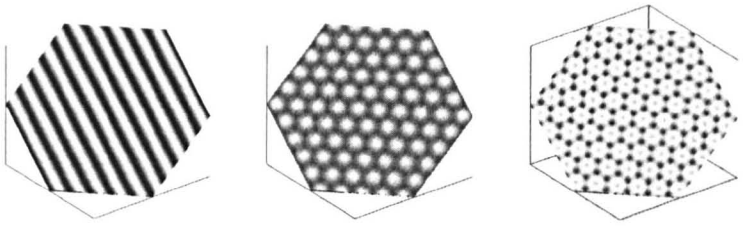

(a) Stripes (b) Hexagons (c) Black-eyes

Figure 10.8: The occurrence of (a) stripes (b) hexagons and (c) black-eyes on the slice of the BCC planform.

The discussion above illustrates how forced symmetry breaking, when applied to the Gomes model of black-eye pattern formation, leads to more realistic model. In particular, we believe that the arguments of Zhou *et al.* [92] cannot be used to conclude that black-eyes are two-dimensional. To clarify some of these issues, a greater understanding of how the chemical gradient manifests itself as a symmetry-breaking effect must be undertaken. An interesting further point also supports the three-dimensional model. Previous experiments of Ouyang *et al.* [72] show the existence of a honeycomb structure. Furthermore, it was shown this structure is three-dimensional. Interestingly, the same figure (Figure 2 of Ouyang *et al.* [72]) that shows the honeycomb structure also shows (at the bottom) what appear to be black-eyes. We are not aware if any discrepancies have been found with the conclusions of this paper. If not, then this would offer experimental evidence that the three-dimensional model is a realistic alternative to the current two-dimensional theory.

Where does this leave the theoretical model of Yang *et al.* [90]? The point that cannot be argued is the production of black-eyes. However, there are some points worth discussing. The model of Yang and co-workers is constructed so that there are two interacting Turing modes. This is achieved by a linear coupling of two systems, each possessing a single Turing mode. To give a physical interpretation of this model, the authors describe the following situation. Suppose there are two thin layers of gel that meet at an interface, with each layer containing the same set of reactants with the same kinetics. The two layers have different diffusion rates due to physical and chemical conditions. In the context of experiments of Yang *et al.* [92] described above, this would require either one of the Turing modes to lie within the non-pattern forming polyacrylamide gel layer or for the PVA gel to be considered as two separate pieces of gel, but both these situations are difficult to justify. In fact, the physical interpretation is really saying that three-dimensional factors must be taken into account since the two modes lie in different gel layers. This does not necessarily mean three-dimensional in the sense of the Gomes model, where three-dimensional structures form and the patterns we see in experiments are projections, rather two-dimensional patterns superimposed. It would seem that these two interpretations are really one in the same, so the Yang model is the Gomes model in a different light. The advantages of the Gomes explanation lie in its genericity and lack of strange physical constraints on the system. Furthermore, Yang and co-workers show their model produces "white-eye" patterns, which have a white center surrounded by a black ring and then a white ring. It is claimed that these are the white-eye structures seen by Steinbock *et al.* [81], but this is not true: the white-eyes found by Steinbock and co-workers are black-eyes but with the colours inverted.

Here we reach a critical problem. The establishment of a mathematical correspondence between a model and experiments is normally straightforward. However, we have the subtle

problem of disentangling what happens in the experiments and the models. To help with progress in this direction, a detailed study of the Brusselator and Lengyel–Epstein PDEs should be undertaken which, in conjunction with the results of Part III, could be used to produce experimentally testable predictions. Such a study should help to resolve some of the modelling issues.

10.3 Nonlinear Optical Systems

In this section we discuss applications of the material in Part III to nonlinear optical systems. We have seen in the introduction that nonlinear optical systems, like the CIMA reaction, can produce black-eye patterns. It is this correlation between the two otherwise disparate systems that leads to our interest.

10.3.1 Introduction

Pattern formation in nonlinear optical systems is of considerable importance. There is a large number of different nonlinear optical systems; of which we mention three: degenerate optical parametric oscillators (DOPOs) [78], the Kerr-slice feedback mirror system [15] and the liquid-crystal light-value (LCLV) system [85]. There are many more [78]; the number of patterns exhibited is striking and increasing. Staliunas [78] performed a numerical analysis on the modelling equations of DOPOs showing the existence of stable three-dimensional structures. Staliunas and J.Sánchez-Morcillo [79] demonstrate that patterns in DOPOs can form via a Turing mechanism; that is, activator-inhibitor. The authors also state that such a mechanism is not particular to DOPOs, and could generalise to other nonlinear optical systems.

Degenerate Optical Parametric Oscillators

Staliunas [78] shows that the spatial temporal dynamics of DOPOs are governed by the three-dimensional Swift–Hohenberg equation. Numerical integration shows the existence of three-dimensional structures, of which some are Turing in nature. In particular, it is shown that stripes exist, and also a three-dimensional structure generated by four coplanar wave vectors. This three-dimensional structure has a resemblance to Figure 6.3 for the BCCI planform, although obviously they are not the same. A stability analysis shows that the three-dimensional structure can be stable. The occurrence of three-dimensional structures in optical systems is, in itself, interesting, and shows certain elements that are also found in reaction-diffusion systems.

Recently, Staliunas and J.Sánchez-Morcillo [79] have shown that DOPOs can form patterns via a Turing mechanism. As they point out, pattern formation in nonlinear optical systems commonly occurs due to off-resonance excitation mechanisms; a mismatch between excitation and resonance frequencies leads to patterns. Examples of such systems are lasers, injected nonlinear resonators, photorefractive oscillators and DOPOs. The Turing mechanism in optical systems had not been explored prior to the work of Staliunas and J.Sánchez-Morcillo. The reason underlying this omission is the ratio of the diffraction of the interacting fields; this is normally fixed, and not considered (diffraction plays the same role in optical systems as diffusion in reaction-diffusion systems). The authors show if the diffraction coefficients take independent values, their ratio enters as a parameter of the system, allowing the role of diffraction to be explored. Turing patterns arise from the interplay between diffractions of interacting fields; this mechanism is of activator-inhibitor type, as described originally by Turing. The authors conclude that DOPOs are not the only optical system that could exhibit patterns via this mechanism. The work of Staliunas and J.Sánchez-Morcillo considers only two-dimensional systems and reports the formation of hexagons. Rather tentatively, we can couple this work with that of Staliunas concerning three-dimensional structures in DOPOs, and see the possibility of DOPOs forming three-dimensional structures via a Turing mechanism. We emphasise that this is an idealised extrapolation. We hope that further work in the area will clarify the issue.

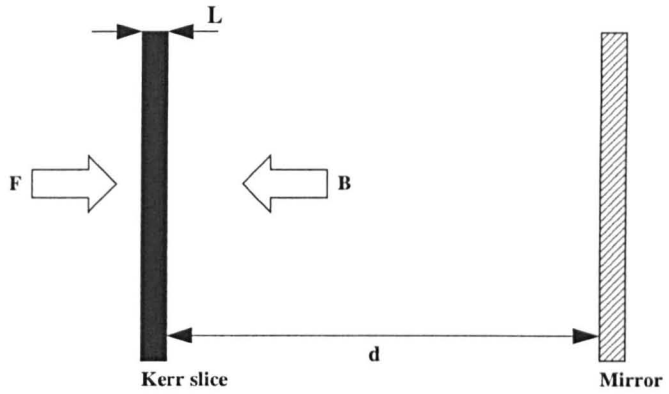

Figure 10.9: Kerr-slice feedback mirror experimental apparatus of D'Alessandro and Firth. The Kerr material is of thickness L. The mirror is at a distance of d from the Kerr material. F denotes the forward field, and B the backward field.

Kerr-Slice Feedback Mirror System

The Kerr-slice feedback mirror system is a very simple nonlinear optical system, which has been shown to exhibit patterns. We consider the experimental set-up of D'Alessandro and Firth [15], see Figure 10.9. Here a thin slice of Kerr material[4] is illuminated from one side. The mirror creates a feedback loop that causes the total field in the slice to be the sum of the forward (F in the figure) and backward (B in the figure) fields. Numerical investigations of this system, by D'Alessandro and Firth, have shown the existence of hexagonal structures. These can have the form of standard hexagons—like those predicted by standard equivariant bifurcation theory—or hexagons with a developed inner structure, as well as a honeycomb structure. More recently, Vorontsov and Karpov [84] and Degtiarev and Vorontsov [18] have shown the existence of highly developed decagon structures in numerical simulations of the system. We shall return to these patterns shortly in our discussion of the LCLV system.

Liquid-Crystal Light-Value System

The liquid-crystal light-value (LCLV) phase modulator with diffractive feedback was studied by Vorontsov and Samson [85]. This system, like the previous optical systems we have discussed, also exhibits hexagonal types of patterns. The system considered by Vorontsov and Samson differs from previous studies, in that a Fourier spatial filter is present in the feedback loop, see Figure 10.10. The controlling parameter is the voltage V applied to each liquid crystal element. The resulting pattern can be seen on the photoconductor in Figure 10.10. Variation of the voltage V leads to the formation of hexagons and, importantly, black-eyes. Optical noise caused by inhomogeneities in the sensitivity of the LCLV's photosensitive layer and in the input beam phases and intensity distributions causes irregularity of the observed patterns. To overcome this problem, an amplitude mask was placed into the feedback loop; this regulated the patterns. In particular, black-eyes occurred as regular hexagonal arrays, the same as those seen by Ouyang and Swinney in the CIMA reaction. The analysis of Vorontsov and Samson suggests a common origin in both systems for black-eyes. The authors base their analysis, like Gunaratne [46], on interacting hexagonal modes. Their numerical analysis reveals the occurrence of hexagons, black-eyes, dodecagons and a decagon structure with tenfold symmetry. The dodecagon pattern has been reported previously by Degtiarev and Vorontsov [18] and Vorontsov and Karpov [84].

[4]Certain materials become doubly refracting when placed in strong electric fields. This phenomenon which is limited to regions of very high electric fields or for only certain materials at low electric fields, is not a first order electric effect. This effect is called (generally) the Kerr Electro-Optic effect. The rotation and reorientation of the molecular lattice of the medium, called the Kerr medium, cause this nonlinear effect [76].

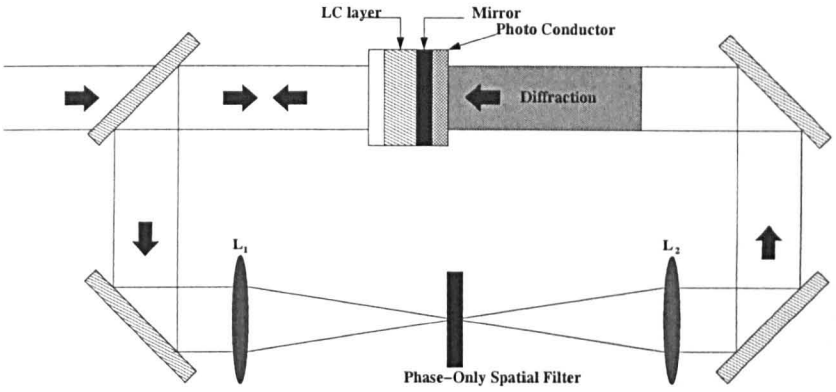

Figure 10.10: The liquid-crystal light-valve experimental apparatus of Vorontsov and Samson.

However, the decagon structure is new, and since it exhibits tenfold symmetry is not supported by a lattice. Such quasiperiodic states have been examined previously, see Shechtman *et al.* [77].

10.3.2 Discussion

We have seen that nonlinear optical systems are capable of exhibiting diverse and highly developed pattern forming behaviour. We wish to place these systems, as we did with the CIMA reaction before, in a possible three-dimensional context, and to suggest applications for the theory developed in Part III.

The occurrence of black-eyes in the LCLV system is explained by Vorontsov and Samson as a spatial harmonic of the primary hexagonal modes—exactly the explanation offer by Gunaratne *et al.* [46] for black-eyes in the CIMA reaction. The Gomes model offers an alternative explanation. Coupling this model with the work in Part III, an interesting new model emerges. The mathematical correspondence between the Gomes model and black-eyes is easy to see. A more delicate question is whether there is agreement on the physical level; does the Gomes model represent what happens in the LCLV system? We address some of the issues arising from this question.

It has been shown that considering only the symmetries of the domain of a system can lead to only partial agreement between experiments and models. Often symmetries that do not leave the domain invariant are essential in the pattern selection process [13, 42, 41, 40]. This suggests that a three-dimensional extension of nonlinear optical systems may benefit our understanding. In light of the results of Staliunas [78], it is not unexpected that the appropriate first order modelling hypothesis for (certain and perhaps most) nonlinear optical systems should include three-dimensional symmetries. The extension to a three-dimensional system has a critical influence on the pattern selection process, and we would expect the preferred planforms to change. In particular, a detailed mathematical analysis is required to assess what structures are the "most stable" for three-dimensional nonlinear optical systems. The investigation by Staliunas [78] on DOPOs is the first step in this direction, but should be extended to encompass a larger class of nonlinear optical systems, including LCLV's. The presence of three-dimensional symmetries yields the Gomes explanation for the formation of black-eyes. When combined with the results of Part III, which we have already partially illustrated in Subsection 10.2.3, then we can start to explain some of the more detailed behaviour of the black-eyes in the LCLV system, like the off centre "eyes". The occurrence of patterns in DOPOs via a Turing mechanism should also be placed in the more general context; at present, the theory only is formulated for two-dimensional DOPOs. In light of such investigations it is hoped that a less tenuous link between the CIMA and LCLV's black-eyes can be established. At present we have the following similarities between reaction-diffusion and the DOPO nonlinear optical system. Firstly, both reaction-diffusion systems and DOPOs have been shown to support

three-dimensional structures. Perhaps this can be extended to other nonlinear optical systems. Secondly, both systems can form patterns via a Turing mechanism. Again it is hoped that further investigation will increase this correspondence to a larger class of nonlinear optical systems.

The occurrence of honeycombs in both the CIMA and Kerr-slice feedback system provides another common link between nonlinear optical systems and the CIMA reaction. Honeycombs were found by Ouyang *et al.* [72] when investigating the dimensionality of certain patterns in the CIMA reaction. The honeycombs were found to be three-dimensional. The common occurrence of honeycombs in both these systems suggests a common origin, and leads to the suggestion that the Kerr-slice feedback system produces honeycombs via a three-dimensional pattern formation process. In light of this, it is important to investigate the Gomes model to assess whether honeycomb structures are possible within its theoretical set-up.

Finally, the occurrence of dodecagons and decagons in a nonlinear optical system appears, to date, to be a unique feature. By this we mean that the CIMA reaction has not exhibited such patterns. Figure 10.11 presents the pattern produced when the Gomes model is applied, not to the fundamental representation of the BCC lattice, but to the twenty-four-dimensional type 2 representation. This figure shows a dodecagon structure very similar to that found by

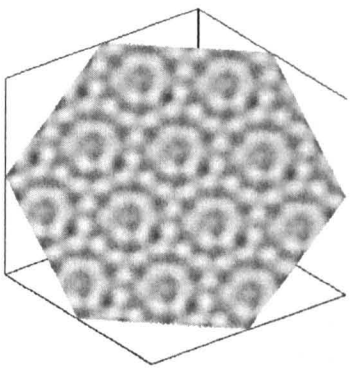

Figure 10.11: BCC pattern produced using the twenty-four-dimensional type 2 representation. The section is given by $z = x + y$, on which we see the dodecagons.

Vorontsov and Samson in their simulations of the LCLV system. This shows that the Gomes model is compatible with their results. However, the occurrence of decagons cannot be explained by standard lattice theory. The work of Shechtman [77] and Komarova [56] have shown how, under appropriate conditions, quasiperiodic states can result in two and three dimensions. We do not pursue this problem further.

10.4 Polyacrylamide-Methylene Blue-Oxygen Reaction

Here we examine the Polyacrylamide-Methylene Blue-Oxygen (PA–MBO) reaction. In this reaction Turing type patterns have been observed, in particular black-eyes. Again we examine possible application for the theory of Part III.

10.4.1 Introduction

The PA–MBO reaction shows patterns such as hexagons, stripes and zigzags, and the recent work of Steinbock *et al.* [81] has revealed further structures including black-eyes and honeycombs. Such patterns have been found in nonlinear optical systems and the CIMA reaction. Currently, there exists debate as to the nature of the pattern forming process, although recent evidence makes a tentative case for a Turing mechanism [81].

The reaction occurs via oscillatory properties of the Methylene Blue-Sulphide-Oxygen (MBO) system. Here MBO catalyses the oxidation of HS^- by O_2. The monomer Methylene Blue has two stable forms: the blue MB^+ and the colourless reduced form MBH. The blue colour allows the observation of patterns.

10.4.2 Experimental Apparatus and Results

The complete details of the experimental set-up can be found in Steinbock *et al.* [81]; we summarise the important points. A petri dish is used to contain the PA–MBO reacting medium. Oxygen is supplied from the air and the light intensity is kept constant since the reaction is photosensitive. The system is otherwise closed, so all patterns are transient.

Unlike the CIMA reaction, patterns emerge in the PA–MBO reaction after approximately 10 minutes, with a wavelength of 2–3mm. The patterns can have hexagonal, chevron, black-eye and honeycomb structures. Transition between these patterns is on the order of minutes, rather than the hours encountered for the CIMA reaction. The occurrence of black-eyes in the PA–MBO reaction is explained by the authors as a spatial harmonic of the hexagonal pattern (the same as the explanation of Gunaratne *et al.* [46] for the CIMA reaction). However, an additional honeycomb structure occurs 20–40 minutes after black-eyes. The transition from black-eyes to honeycomb occurs via a front propagating across the reactants. This front can originate from the boundary of the system, or sometimes from regions with penta-hepta defects and grain boundaries [81]. The two-dimensional Fourier spectra of the honeycombs contains wave vectors $\mathbf{K}_j$, $2\mathbf{K}_j$, $3\mathbf{K}_j$ where $j = 1, 2, 3$ and other wave vectors of lower amplitude, the $\mathbf{K}_j$'s are the wave vectors on the hexagonal lattice. The phases of the $n\mathbf{K}_j$ alternate between 0 and π. The authors conclude that the honeycomb pattern is the superposition of three hexagonal patterns with identical orientations.

10.4.3 Discussion

The PA–MBO reaction is capable of producing all the patterns seen in the CIMA reaction and certain nonlinear optical systems. The common occurrence of black-eyes and honeycomb structure in all these systems is an important characteristic. Since honeycombs have been shown by Ouyang *et al.* [72] to be three-dimensional, we believe the dimensionality of the PA–MBO reaction deserves further investigation. This may provide important experimental and theoretic data leading to a more complete understanding of the honeycomb and black-eye patterns in all three reactions: CIMA, nonlinear optical systems and the PA–MBO.

An important experimental and theoretical issue which requires resolution is the mechanism underlying pattern formation in the PA–MBO reaction. Is it Turing, or Rayleigh–Bénard in nature? If it can be shown conclusively that patterns form via a Turing mechanism, then this result is very important, since all three systems: CIMA, nonlinear optical and PA–MBO will then have been shown to exhibit similar complex patterns (i.e. black-eyes and honeycombs) via a common Turing mechanism.

10.5 General Discussion and Conclusion

The CIMA reaction can exhibit highly developed and complex patterns not typically expected from a two-dimensional model. Certain nonlinear optical systems and the PA–MBO reaction are also capable of producing complex patterns such as black-eyes and honeycomb structures. The honeycomb structures found in the CIMA reaction occur as a three-dimensional pattern [72]. It is likely that there is a common origin for the honeycomb pattern in all three systems; this suggests that the dimensionality of nonlinear optical systems and the PA–MBO reaction should be investigated further. Importantly, the PA–MBO exhibits a transition from black-eyes to honeycombs. If there were a common three-dimensional explanation for honeycombs, then it would be strange for the dimensionality of the system to change from two to three . By this we

mean that black-eyes are usually assumed to occur as a two-dimensional spatial harmonic of the hexagonal patterns. If the honeycomb structure in the PA–MBO reaction is three-dimensional, as in the CIMA reaction, the transition from black-eyes to honeycombs would require a change in dimensionality of the system, an occurrence which is difficult to explain.

The systems considered share several important characteristics. Firstly, they all exhibit black-eyes and honeycomb structures, suggesting a common origin for these patterns in all three systems. The CIMA reaction produces patterns via a Turing mechanism. There are suggestion that (some) nonlinear optical systems and the PA–MBO reaction, also form patterns via a Turing mechanism. This provides an important, but at present, tentative link between the mechanisms involved in all three systems. Finally, the occurrence of honeycombs as a three-dimensional pattern in the CIMA reaction and the (possible) common origin of patterns in each system suggests that a three-dimensional approach may be more appropriate. At present these features are not much more than circumstantial, but we believe that clarification of the above points is vital to a proper understanding of the pattern forming process.

In the systems considered above, the mathematical correspondence between the Gomes model of black-eyes and those found experimentally is easy to see. However, a more delicate question is whether this model has any physical correspondence to what happens in either the CIMA reaction, nonlinear optical systems, or the PA–MBO reaction. To make progress in this direction, further investigations of the Gomes model must be undertaken. We make suggestions in this area. Ideally a full reduction of the Brusselator and Lengyel–Epstein models should be performed, producing concrete predictions about the influence of forced symmetry breaking in the Gomes model. A preferable situation is the prediction of behaviour seen in experiments, but not expected from the usual two-dimensional models. The development of three-dimensional models for the LCLV and Kerr-slice feedback nonlinear optical systems is important and should follow previous work of Staliunas [78] for DOPOs. From these models we could again perform reductions to make predictions concerning the behaviour of these systems.

The fundamental problem is whether the patterns seen in the CIMA and PA–MBO reactions, together with those in nonlinear optical systems, are three-dimensional. If so, then the Gomes model represents the most natural way to explain the common occurrence of black-eyes and the other highly developed patterns in these systems. Another related and interesting problem is: are these systems related by a common Turing mechanism? Questions such as these cannot be answered at present, but further studies should answer these issues.

Chapter 11

Concluding Remarks

In this final chapter we summarise the main results and their implications, and give suggestions for further research.

11.1 Summary of Results

We have provided a partial classification for the behaviour of spatially periodic solutions to Euclidean equivariant differential equations. In particular, we have shown the existence of heteroclinic cycles, and more generally heteroclinic networks.

The results for the BCC lattice were applied to Gomes's model of the black-eye Turing instability. This investigation has shown that previous arguments that the Gomes model is not appropriate are not as convincing when symmetry breaking effects are considered. This leaves plenty of room for further work in this direction. We have seen that the PA–MBO reaction, the LCLV, Kerr-slice and DOPO nonlinear optical systems can exhibit highly developed patterns, and we have suggested that a reformulation of standard two-dimensional models into the three-dimensional framework of the Gomes model should provide extra insight into the pattern forming process.

11.2 Future Work

During the compilation of this work, many ideas were not pursued or omitted, and further avenues of research were suggested. We list some of these topics.

- Numerical investigation of the bifurcation diagrams associated with the perturbed problems, in particular the BCC problem. These are important if we are to understand how the sequence and branching behaviour is changed by perturbations.
- Further experimental and mathematical investigations should be undertaken to determine the nature of the chemical gradient present in the experimental apparatus of Ouyang and associates.
- Application of this work to non-scalar Euclidean invariant systems, for example hallucinations.
- Performing the Liapunov-Schmidt reduction to determine reduced equations and so experimentally testable predictions.
- Investigation of the PA–MBO and nonlinear optical systems to understand the nature of the black-eyes (and the other patterns) found in these systems.
- Investigation of the attractive properties of the networks found on many of the projected skeletons.

Appendix A

A.1 The Symmetry Package

In our work on the forced symmetry breaking of two-dimensional planforms we required information about certain equivariant vector fields. The problem of finding the most general equivariant vector field with respect to a given group is difficult for all but the simplest groups and representations. Here we summarise the Symmetry [28] package available for the symbolic manipulation program Maple [66]. The Symmetry packages offers a number of commands, which allow us to use a computer to determine invariants and equivariants. We saw in Chapter 1 that Poincaré series provide generating functions for the numbers of invariants and equivariants of a chosen degree. The general procedure for computing invariants and equivariants is as follows:

1. The representation of the group (which we denote by Δ) is on $\mathbb{C}^N$ for a suitable $N \in \mathbb{N}$. We choose coordinates $(z_1, z_2, \ldots, z_N, \overline{z_1}, \ldots, \overline{z_N}) = (z_1, \ldots, z_{2N})$ for $\mathbb{C}^N$. This gives $\mathbb{C}^N$ the structure of a real vector space. The action of the group with respect to this basis is then permutation of the coordinates. Thus each element of Δ can be realised as a $2N \times 2N$ permutation matrix.

2. We must encode this matrix action of Δ for use by Maple. This is achieved using the Symmetry command
$$\texttt{mkfinitegroup}(A_1, \ldots, A_M),$$
where $A_1, \ldots A_M$ are the matrices for the generators of the group Δ. The result is a table containing each element of Δ.

3. From here there is a simple list of commands to achieve our aims. To compute the Poincaré series for the invariants we use
$$\texttt{molien}(\texttt{op}(\Delta), t)$$
and for the equivariants
$$\texttt{equimolien}(\texttt{op}(\Delta), \texttt{op}(\Delta), t).$$

4. A generating set of primary invariants can be computed with
$$\texttt{primaries}(\texttt{op}(\Delta), [z1, \ldots, zN]).$$
A generating set of equivariants over the primary invariants is found with
$$\texttt{equis}(\texttt{op}(\Delta), \texttt{op}(\Delta), [z1, \ldots, zN], p),$$
where p is an optional argument which, if given, returns a complete set of generating equivariants up to degree p. Finally, a generating set of secondary invariants can be found using
$$\texttt{CMbasis}(\texttt{op}(\Delta), [z1, \ldots, zN], p),$$
where p is again optional and denotes the upper limit on the degree of the secondary invariants.

We must be cautious when interpreting our results, which are in the $(z_1, \ldots, z_{2N})$ coordinate system. This must be converted back into the more usual $(z_1, \ldots, z_N, \overline{z_1}, \ldots, \overline{z_N})$ system.

All computations reported in this thesis were run on a standard Sun Ultra 5 workstation with 128MB of main memory and one Ultra Sparc II processor, or a Sun Ultra Enterprise 450 with 2GB of main memory and four Ultra Sparc II processors.

A.2 Invariants for Subgroups of $\mathbf{D}_4$

In this section we present the results from Maple that were produced during the computations of the invariants and equivariants. All computations were produced using Symmetry [28].

A.2.1 Four-Dimensional Representation

Here we investigate the invariants and equivariants for subgroups of $\mathbf{D}_4$ in the four-dimensional representation of Γ_s.

Invariants and Equivariants for $\mathbf{D}_4$

We start by choosing coordinates $(z_1, z_2, \overline{z_1}, \overline{z_2}) = (z_1, z_2, z_3, z_4)$ on $\mathbb{C}^2$. With respect to these coordinates the generators ρ and κ of $\mathbf{D}_4$ acts as matrices with real entries.

$$\rho := \begin{bmatrix} 0 & 0 & 1 & 0 \\ 0 & 1 & 0 & 0 \\ 1 & 0 & 0 & 0 \\ 0 & 0 & 0 & 1 \end{bmatrix},$$
$$\kappa := \begin{bmatrix} 0 & 1 & 0 & 0 \\ 1 & 0 & 0 & 0 \\ 0 & 0 & 0 & 1 \\ 0 & 0 & 1 & 0 \end{bmatrix}. \tag{A.1}$$

We now define the group $\mathbf{D}_4$ for use by Maple.

$$\begin{aligned} D4 := \ & \texttt{mkfinitegroup}(\_\texttt{A} = \texttt{array}(1..4, 1..4, [[0,0,1,0],[0,1,0,0],[1,0,0,0], \\ & [0,0,0,1]]), \_\texttt{B} = \texttt{array}(1..4, 1..4, [[0,1,0,0], \\ & [1,0,0,0],[0,0,0,1],[0,0,1,0]])). \end{aligned} \tag{A.2}$$

From this we compute the Poincaré series for the invariants,

$$M := \texttt{molien}(\texttt{op}(D4), t),$$

which is

$$M = 1 + t + 3t^2 + 4t^3 + 8t^4 + 10t^5 + 16t^6 + O(t^7).$$

Similarly, we compute the Poincaré series for the equivariants:

$$ME := \texttt{equimolien}(\texttt{op}(D4), \texttt{op}(D4), t),$$

getting

$$ME = 1 + 3t + 7t^2 + 13t^3 + 22t^4 + 34t^5 + 50t^6 + O(t^7).$$

This verifies Lemmas 4.10 and 4.12. Finally, we compute a set of primary invariants and a generating set of equivariants. This is achieved by the command

$$\texttt{equis}(D4, D4, [z1, z2, z3, z4]),$$

leading to the result

$$\begin{aligned}[primary\_invs &= [z4 + z2 + z3 + z1, z4^2 + z2^2 + z3^2 + z1^2, z3\,z4 + z4\,z1 + z3\,z2 + z2\,z1,\\ &\quad z4^4 + z2^4 + z3^4 + z1^4],\\ equivariants &= [[1,1,1,1],[z1,z2,z3,z4],[z4 + z2, z1 + z3, z4 + z2, z1 + z3],\\ &\quad [z1^2, z2^2, z3^2, z4^2],[z2^2 + z4^2, z1^2 + z3^2, z2^2 + z4^2, z1^2 + z3^2],\\ &\quad [z1^3, z2^3, z3^3, z4^3],[z2^3 + z4^3, z1^3 + z3^3, z2^3 + z4^3, z1^3 + z3^3],\\ &\quad [z1^4, z2^4, z3^4, z4^4]]]\end{aligned}$$

Invariants and Equivariants for $\mathbf{D}_2[\rho^2, \kappa]$

We start by choosing coordinates $(z_1, z_2, \overline{z_1}, \overline{z_2}) = (z_1, z_2, z_3, z_4)$ on $\mathbb{C}^2$. With respect to these coordinates the generators ρ^2 and κ of $\mathbf{D}_2[\rho^2, \kappa]$ acts as matrices with real entries. We find

$$\rho^2 := \begin{bmatrix} 0 & 0 & 1 & 0 \\ 0 & 0 & 0 & 1 \\ 1 & 0 & 0 & 0 \\ 0 & 1 & 0 & 0 \end{bmatrix},$$

with κ as before. We now define the group $\mathbf{D}_2[\rho^2, \kappa]$ for use by Maple.

$$\begin{aligned}D2A &:= \texttt{mkfinitegroup(\_A = array(1..4, 1..4, [[0,0,1,0],[0,0,0,1],[1,0,0,0],}\\ &\quad \texttt{[0,1,0,0]]), \_B = array(1..4, 1..4, [[0,1,0,0],}\\ &\quad \texttt{[1,0,0,0],[0,0,0,1],[0,0,1,0]])).}\end{aligned}$$

From this we compute the Poincaré series for the invariants,

$$M := \texttt{molien(op(}D2A\texttt{)},t),$$

which is

$$M = 1 + t + 4t^2 + 5t^3 11t^4 + 14t^5 + 24t^6 + O(t^7).$$

Similarly, we compute the Poincaré series for the equivariants using

$$ME := \texttt{equimolien(op(}D2A\texttt{),op(}D2A\texttt{)},t),$$

to get

$$ME = 1 + 4t + 10t^2 + 20t^3 + 35t^4 + 56t^5 + 84t^6 + O(t^7).$$

This verifies Lemmas 4.26 and 4.28. Finally, we compute a set of primary invariants and a generating set of equivariants. This is achieved using

$$\texttt{equis(}D2A, D2A, [z1, z2, z3, z4]\texttt{)},$$

with the result

$$\begin{aligned}[primary\_invs &= [z4 + z3 + z2 + z1, z4^2 + z3^2 + z2^2 + z1^2, z3\,z4 + z2\,z1, z4\,z2 + z3\,z1],\\ equivariants &= [[1,1,1,1],[z1,z2,z3,z4],[z2,z1,z4,z3],[z3,z4,z1,z2],[z1^2, z2^2, z3^2, z4^2],\\ &\quad [z2^2, z1^2, z4^2, z3^2],[z3^2, z4^2, z1^2, z2^2],[z1^3, z2^3, z3^3, z4^3]]]\end{aligned}$$

A.3 Invariants for Subgroups of $\mathbf{D}_6$

In this section we describe the procedure required to construct the Poincaré series, invariants and equivariants for the subgroup $\mathbf{D}_3[\rho^2, \kappa\rho]$ of $\mathbf{D}_6$. We shall consider only the six-dimensional representation of $\Gamma_h = \mathbf{D}_6 \dot{+} \mathbf{T}^2$. The twelve-dimensional representation is too complex, even for modern computers.

A.3.1 Invariants and Equivariants for $\mathbf{D}_3[\rho^2, \kappa\rho]$

Here we construct the Poincaré series for the invariants and equivariants of $\mathbf{D}_3[\rho^2, \kappa\rho]$. Using this information, we compute a generating set of primary invariants and equivariants.

We start by choosing coordinates $(z_1, z_2, z_3, \overline{z_1}, \overline{z_2}, \overline{z_3}) = (z_1, z_2, z_3, z_4, z_5, z_6)$ on $\mathbb{C}^3$. With respect to these coordinates, the generators ρ^2 and κ of $\mathbf{D}_3[\rho^2, \kappa\rho]$ acts as matrices with real entries.

$$\rho^2 := \begin{bmatrix} 0 & 0 & 1 & 0 & 0 & 0 \\ 1 & 0 & 0 & 0 & 0 & 0 \\ 0 & 1 & 0 & 0 & 0 & 0 \\ 0 & 0 & 0 & 0 & 0 & 1 \\ 0 & 0 & 0 & 1 & 0 & 0 \\ 0 & 0 & 0 & 0 & 1 & 0 \end{bmatrix},$$

$$\kappa\rho := \begin{bmatrix} 0 & 0 & 0 & 0 & 1 & 0 \\ 0 & 0 & 0 & 1 & 0 & 0 \\ 0 & 0 & 0 & 0 & 0 & 1 \\ 0 & 1 & 0 & 0 & 0 & 0 \\ 1 & 0 & 0 & 0 & 0 & 0 \\ 0 & 0 & 1 & 0 & 0 & 0 \end{bmatrix}.$$

We now define the group $\mathbf{D}_3[\rho^2, \kappa\rho]$ for use by Maple.

$$D3B := \texttt{mkfinitegroup(\_A = array(1..6, 1..6, [[0,0,1,0,0,0],[1,0,0,0,0,0],[0,1,0,0,0,0],[0,0,0,0,0,1],[0,0,0,1,0,0],[0,0,0,0,1,0]]), \_B = array(1..6, 1..6, [[0,0,0,0,1,0],[0,0,0,1,0,0],[0,0,0,0,0,1],[0,1,0,0,0,0],[1,0,0,0,0,0],[0,0,1,0,0,0]]))}.$$

From this we compute the Poincaré series for the invariants,

$$M := \texttt{molien(op(}D3B\texttt{)},t),$$

which is given

$$M = 1 + t + 5t^2 + 10t^3 + 24t^4 + 42t^5 + 83t^6 + O(t^7).$$

Similarly, we compute the Poincaré series for the equivariants using

$$ME := \texttt{equimolien(op(}D3B\texttt{),op(}D3B\texttt{)},t),$$

to get

$$ME = 1 + 6t + 21t^2 + 56t^3 + 126t^4 + 252t^5 + O(t^6).$$

This verifies Lemmas 5.18 and 5.20. Finally, we compute a set of primary invariants and a generating set of equivariants up to quadratic order. This is achieved using

$$\texttt{equis(}D3B, D3B, [z1, z2, z3, z4, z5, z6], 2),$$

with the result

$$
\begin{aligned}
[\mathit{primary\_invs} &= [z4 + z6 + z2 + z5 + z3 + z1, z4^2 + z6^2 + z2^2 + z5^2 + z3^2 + z1^2,\\
&\quad z4\ z6 + z6\ z5 + z3\ z2 + z4\ z5 + z1\ z3 + z1\ z2, z5\ z2 + z6\ z3 + z1\ z4,\\
&\quad z4^3 + z6^3 + z2^3 + z5^3 + z3^3 + z1^3,\\
&\quad z4^2 z6 + z5\ z6^2 + z2^2 z3 + z4\ z5^2 + z1\ z3^2 + z1^2 z2],\\
\mathit{equivariants} &= [[1, 1, 1, 1, 1, 1], [z1, z2, z3, z4, z5, z6], [z3, z1, z2, z5, z6, z4],\\
&\quad [z2, z3, z1, z6, z4, z5], [z4, z5, z6, z1, z2, z3], [z5, z6, z4, z3, z1, z2],\\
&\quad [z1^2, z2^2, z3^2, z4^2, z5^2, z6^2], [z3^2, z1^2, z2^2, z5^2, z6^2, z4^2],\\
&\quad [z2^2, z3^2, z1^2, z6^2, z4^2, z5^2], [z4^2, z5^2, z6^2, z1^2, z2^2, z3^2],\\
&\quad [z5^2, z6^2, z4^2, z3^2, z1^2, z2^2], [z1\ z2, z3\ z2, z1\ z3, z4\ z6, z4\ z5, z6\ z5],\\
&\quad [z1\ z3, z1\ z2, z3\ z2, z4\ z5, z6\ z5, z4\ z6], [z4\ z6, z4\ z5, z6\ z5, z1\ z2, z3\ z2, z1\ z3],\\
&\quad [z4\ z5, z6\ z5, z4\ z6, z1\ z3, z1\ z2, z3\ z2], [z1\ z4, z5\ z2, z6\ z3, z1\ z4, z5\ z2, z6\ z3],\\
&\quad [z6\ z3, z1\ z4, z5\ z2, z5\ z2, z6\ z3, z1\ z4], [z1\ z5, z6\ z2, z4\ z3, z4\ z3, z1\ z5, z6\ z2]]]
\end{aligned}
$$

Recalling the coordinate system $(z_1, z_2, z_3, \overline{z_1}, \overline{z_2}, \overline{z_3}) = (z_1, z_2, z_3, z_4, z_5, z_6)$ we have verified Lemmas 5.19 and 5.21.

This completes the computation of the invariants and equivariants.

Appendix B

In this appendix we address the computation of the subgroups of $\mathbb{O}$, the orientation preserving symmetries of the cube and $\mathbb{O} \oplus \mathbf{Z}_2^c$, the full symmetry of the cube. This result seems to be in the folklore category. Some work has been done related to this problem, but is concerned only with the conjugacy classes [35]. Despite extensive searching we were unable to find a reference which contained explicit information about all subgroups.

B.1 Notation and Preliminaries

We begin by choosing coordinates (x, y, z) for $\mathbb{R}^3$. To define the notation used for the various elements of $\mathbb{O}$ we begin with a (standard) cube centred at the origin with its faces oriented so they are perpendicular to the coordinate axis, see Figure B.1.

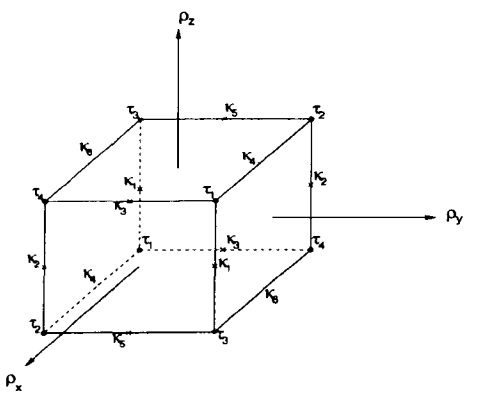

Figure B.1: A standard cube centred at the origin. The elements ρ_x, ρ_y and ρ_z represent rotations by $\pi/2$ anticlockwise about the x, y and z axis, respectively.

The group $\mathbb{O}$ is generated by the elements ρ_x and ρ_y, rotations about the x and y axis anticlockwise by $\pi/2$, respectively. The group $\mathbb{O}$ has the following disjoint union decomposition, see Lemma 6.2, page 105 of Golubitsky *et al.* [35].

$$\mathbb{O} = \dot{\bigcup}^{6} \mathbf{Z}_2 \dot{\bigcup}^{4} \mathbf{Z}_3 \dot{\bigcup}^{3} \mathbf{Z}_4. \tag{B.1}$$

We use this decomposition to explain our notation. The three groups isomorphic to $\mathbf{Z}_4$ in (B.1) represent rotations about the x, y and z axis by $\pi/2$ anticlockwise, respectively, see Figure B.1. We label these elements ρ_x, ρ_y, and ρ_z, respectively. The four groups isomorphic to $\mathbf{Z}_3$ represent rotations about the four opposite vertices of the cube connected through the origin, and we label these elements τ_1, τ_2, τ_3, and τ_4. Finally, the six groups isomorphic to $\mathbf{Z}_2$ represent rotations by π about the midpoints of opposite edges of the cube; these elements we label κ_1, κ_2, κ_3, κ_4, κ_5, and κ_6.

Using this notation we can write down the action of the elements of the group $\mathbb{O}$ on the coordinates (x, y, z). The action is given in Table B.1. In each case the action can be calculate by observing how the coordinate axes are moved under each of these elements.

Table B.1: The action of $\mathbb{O}$ on $\mathbb{R}^3$.

Element	Action	Element	Action
ρ_x	$(x,-z,y)$	τ_2^2	$(-z,-x,y)$
ρ_x^2	$(x,-y,-z)$	τ_3	$(-z,x,-y)$
ρ_x^3	$(x,z,-y)$	τ_3^2	$(y,-z,-x)$
ρ_y	$(z,y,-x)$	τ_4	$(-y,-z,x)$
ρ_y^2	$(-x,y,-z)$	τ_4^2	$(z,-x,-y)$
ρ_y^3	$(-z,y,x)$	κ_1	$(y,x,-z)$
ρ_z	$(-y,x,z)$	κ_2	$(-y,-x,-z)$
ρ_z^2	$(-x,-y,z)$	κ_3	$(z,-y,x)$
ρ_z^3	$(y,-x,z)$	κ_4	$(-x,z,y)$
τ_1	(z,x,y)	κ_5	$(-z,-y,-x)$
τ_1^2	(y,z,x)	κ_6	$(-x,-z,-y)$
τ_2	$(-y,z,-x)$		

B.2 Proof of the Main Result

Having introduced our notation, we now prove the following lemma.

Lemma B.1
There are 30 subgroups of $\mathbb{O}$. They are:

$\mathbb{O}$, $\mathbb{T}$, $\mathbf{D}_4[\rho_x,\kappa_6]$, $\mathbf{D}_4[\rho_y,\kappa_5]$, $\mathbf{D}_4[\rho_z,\kappa_1]$, $\mathbf{D}_3[\tau_1,\kappa_5]$,
$\mathbf{D}_3[\tau_4,\kappa_5]$, $\mathbf{D}_3[\tau_3,\kappa_3]$, $\mathbf{D}_3[\tau_2,\kappa_1]$, $\mathbf{Z}_4[\rho_x]$, $\mathbf{Z}_4[\rho_y]$, $\mathbf{Z}_4[\rho_z]$,
$\mathbf{D}_2[\rho_x^2,\kappa_4]$, $\mathbf{D}_2[\rho_y^2,\kappa_5]$, $\mathbf{D}_2[\rho_z^2,\kappa_1]$, $\mathbf{D}_2[\rho_x^2,\rho_y^2]$, $\mathbf{Z}_3[\tau_1]$, $\mathbf{Z}_3[\tau_2]$,
$\mathbf{Z}_3[\tau_3]$, $\mathbf{Z}_3[\tau_4]$, $\mathbf{Z}_2[\rho_x^2]$, $\mathbf{Z}_2[\rho_y^2]$, $\mathbf{Z}_2[\rho_z^2]$, $\mathbf{Z}_2[\kappa_1]$,
$\mathbf{Z}_2[\kappa_2]$, $\mathbf{Z}_2[\kappa_3]$, $\mathbf{Z}_2[\kappa_4]$, $\mathbf{Z}_2[\kappa_5]$, $\mathbf{Z}_2[\kappa_6]$,

and the trivial subgroup.

Proof. The proof we give is direct since this elaborates the relationships between the elements of $\mathbb{O}$. Other proofs could be quicker, but would not show the relations between the elements, which we require.

Ihrig and Golubitsky [54] and Golubitsky *et al.* [35], Section 6(d) p. 106, give the conjugacy classes of subgroups of $\mathbb{O}$, see Figure B.2. These conjugacy classes are $\mathbb{O}$, $\mathbb{T}$, $\mathbf{D}_4$, $\mathbf{D}_3$, $\mathbf{D}_2$, $\mathbf{Z}_4$, $\mathbf{Z}_3$, $\mathbf{Z}_2$, and the trivial subgroup.

To complete the proof it is just a matter of determining two things: how many groups are contained in each conjugacy class, and the form of each of these groups.

By Lagrange's theorem, any subgroup of $\mathbb{O}$ must have order 24, 12, 8, 6, 4, 3, 2 or 1. The cases 24 and 1 are just the whole group and the trivial group. The subgroup of order 12 is the subgroup $\mathbb{T}$; the elements of $\mathbb{T}$ are

$$\mathbb{T} = \{\rho_x^2, \rho_y^2, \rho_z^2, \tau_1, \tau_1^2, \tau_2, \tau_2^2, \tau_3, \tau_3^2, \tau_4, \tau_4^2\}.$$

$\mathbb{T}$ is well-known to be normal since it has index 2. So only one conjugate.

Next we consider the groups of order eight. The only conjugacy classes of subgroups of $\mathbb{O}$ with eight elements are those isomorphic to $\mathbf{D}_4$, the dihedral group of order eight. Any group

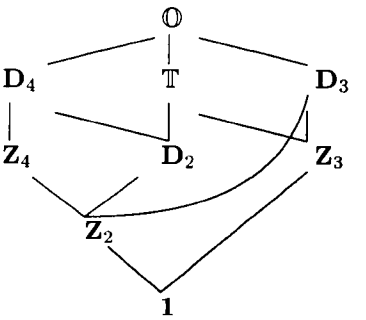

Figure B.2: Containment relations for conjugacy classes of subgroups of $\mathbb{O}$.

isomorphic to $\mathbf{D}_4$ must contain two generators ρ and κ. The element ρ has order four and κ order two. The only elements of $\mathbb{O}$ of order four are ρ_x, ρ_y and ρ_z. And the only elements of order two which are not ρ_x^2, ρ_y^2 and ρ_z^2 are the elements κ_i, where $i = 1, \ldots, 6$. It is now a matter of determining for each of ρ_x, ρ_y and ρ_z which elements of order two generate a group isomorphic to $\mathbf{D}_4$. This is a rather long-winded task, but it does give every element of all the subgroups isomorphic to $\mathbf{D}_4$.

Let us begin with the groups isomorphic to $\mathbf{D}_4$ which have ρ_x as the order four generating element. Now the only order two elements that can be generators are κ_4 and κ_6. The reason is that these elements are the only order two elements that do not permute the x axis with either the y or the z axis. Now we observe that $\kappa_4\rho_x^2 = \kappa_6$, so we need consider only the order two element κ_4 (say). Next we see that $\kappa_4\rho_x = \rho_y^2$ and $\kappa_4\rho_x^3 = \rho_z^2$. So we find that the only group isomorphic to $\mathbf{D}_4$ with ρ_x as the order four generator is $\mathbf{D}_4[\rho_x, \kappa_6]$, which when written out in full has the following elements.

$$\mathbf{D}_4[\rho_x, \kappa_6] = \{\mathrm{id}, \rho_x, \rho_x^2, \rho_x^3, \kappa_4, \rho_y^2, \kappa_6, \rho_z^2\}.$$

We can use similar reasoning to determine the other $\mathbf{D}_4$ subgroups. For the subgroup containing ρ_y the order two elements are either κ_5 or κ_3, so we consider only κ_5. This subgroup contains the elements ρ_x^2 and ρ_z^2, since $\kappa_5\rho_y = \rho_x^2$ and $\kappa_5\rho_y^3 = \rho_z^2$. Therefore the group is

$$\mathbf{D}_4[\rho_y, \kappa_5] = \{\mathrm{id}, \rho_y, \rho_y^2, \rho_y^3, \kappa_5, \rho_x^2, \kappa_3, \rho_z^2\}.$$

Finally we come to the $\mathbf{D}_4$ group with ρ_z as the order four generator. Now we need consider only the order two elements κ_1 and κ_2, but since $\kappa_1\rho_z^2 = \kappa_2$ we consider only κ_1 and next we observe that $\kappa_1\rho_z = \rho_x^2$ and $\kappa_1\rho_z^3 = \rho_y^2$. So we have

$$\mathbf{D}_4[\rho_z, \kappa_1] = \{\mathrm{id}, \rho_z, \rho_z^2, \rho_z^3, \kappa_1, \rho_x^2, \kappa_2, \rho_y^2\}.$$

This completes the computation of all subgroups of $\mathbb{O}$ isomorphic to $\mathbf{D}_4$.

Next we must consider the subgroups of order six. Using the conjugacy classes of subgroups we know that the only subgroup of order six in $\mathbb{O}$ is conjugate to $\mathbf{D}_3$. The process we adopt is similar to that used for the subgroups conjugate to $\mathbf{D}_4$. Any group conjugate to $\mathbf{D}_3$ is generated by two elements τ and κ, where τ has order three and κ has order two. The only elements of $\mathbb{O}$ of order three are τ_i where $i = 1, \ldots, 4$. The order two elements cannot be ρ_x^2, ρ_y^2 or ρ_z^2 because, for example, $\rho_x^2\tau_1 = \tau_4$ and we lose closure of the group; this holds in general. So the order two elements we consider are κ_j where $j = 1, \ldots, 6$. We must now select each τ_1 and determine those elements κ_j which respect closure of the group. Consider the element τ_1, we find that $\tau_1\kappa_1 = \rho_y^3$, $\tau_1\kappa_3 = \rho_x^3$, $\tau_1\kappa_4 = \rho_z^3$ so these elements do not respect closure of the group since the result is always an element of order four. This leaves the elements κ_2, κ_5 and κ_6. Now we find

that $\tau_1\kappa_5 = \kappa_6$ and $\tau_1^2\kappa_5 = \kappa_2$. Therefore our group is $\mathbf{D}_3[\tau_1, \kappa_5]$, which when written out in full gives

$$\mathbf{D}_3[\tau_1, \kappa_5] = \{\mathrm{id}, \tau_1, \tau_1^2, \kappa_5, \kappa_6, \kappa_2\}.$$

The computation of the other subgroups conjugate to $\mathbf{D}_3$ is similar. We find the subgroups:

$$\begin{aligned}
\mathbf{D}_3[\tau_2, \kappa_1] &= \{\mathrm{id}, \tau_2, \tau_2^2, \kappa_1, \kappa_3, \kappa_6\}, \\
\mathbf{D}_3[\tau_3, \kappa_3] &= \{\mathrm{id}, \tau_3, \tau_3^2, \kappa_3, \kappa_2, \kappa_4\}, \\
\mathbf{D}_3[\tau_4, \kappa_5] &= \{\mathrm{id}, \tau_4, \tau_4^2, \kappa_1, \kappa_4, \kappa_5\}.
\end{aligned}$$

This completes the computations of the subgroups conjugate to $\mathbf{D}_3$.

Now we consider the subgroups conjugate to $\mathbf{Z}_4$. This is straightforward since the only elements of order four in $\mathbb{O}$ are ρ_x, ρ_y and ρ_z. This gives the subgroups $\mathbf{Z}_4[\rho_x]$, $\mathbf{Z}_4[\rho_y]$ and $\mathbf{Z}_4[\rho_z]$.

Next we consider the groups conjugate to $\mathbf{D}_2$. Using the containment relations for the conjugacy classes of subgroups we know that the $\mathbf{D}_2$ subgroups are contained in $\mathbf{D}_4$ and $\mathbb{T}$. Any group conjugate to $\mathbf{D}_2$ is generated by two elements of order two. Let us consider those $\mathbf{D}_2$ subgroups which are contained in $\mathbf{D}_4[\rho_x, \kappa_6]$. There are two such subgroups. The first is

$$\mathbf{D}_2[\rho_x^2, \kappa_6] = \{\mathrm{id}, \rho_x^2, \kappa_6, \kappa_4\}.$$

The other $\mathbf{D}_2$ subgroup is

$$\mathbf{D}_2[\rho_x^2, \rho_y^2] = \{\mathrm{id}, \rho_x^2, \rho_y^2, \rho_z^2\}.$$

This is the only $\mathbf{D}_2$ subgroup which is contained in $\mathbb{T}$.

Next we consider the subgroup $\mathbf{D}_4[\rho_y, \kappa_5]$. There are again two $\mathbf{D}_2$ subgroups. The first we have seen already; it is $\mathbf{D}_2[\rho_x^2, \rho_y^2]$. The second is

$$\mathbf{D}_2[\rho_y^2, \kappa_5] = \{\mathrm{id}, \rho_y^2, \kappa_5, \kappa_3\}.$$

Finally we consider the $\mathbf{D}_2$ subgroups of $\mathbf{D}_4[\rho_z, \kappa_1]$. We find again the subgroup $\mathbf{D}_2[\rho_x^2, \rho_y^2]$ and in addition the subgroup

$$\mathbf{D}_2[\rho_z^2, \kappa_1] = \{\mathrm{id}, \rho_z^2, \kappa_1, \kappa_2\}.$$

This completes the computation of the subgroups of $\mathbb{O}$ that are conjugate to $\mathbf{D}_2$.

Now we consider the subgroups conjugate to $\mathbf{Z}_3$. Since the only elements of $\mathbb{O}$ of order three are τ_j, where $j = 1, \ldots, 4$, the $\mathbf{Z}_3$ subgroups are $\mathbf{Z}_3[\tau_j]$ where $j = 1, \ldots, 4$. Each of these subgroups is contained in some conjugate of $\mathbf{D}_3$, and all are contained in $\mathbb{T}$.

We now come to the final case: the subgroups conjugate to $\mathbf{Z}_2$. These groups are generated by the elements of $\mathbb{O}$ of order two. The containment relations make their identification easy. We have six subgroups of the form $\mathbf{Z}_2[\kappa_j]$ where $j = 1, \ldots, 6$ and we have $\mathbf{Z}_2[\rho_x^2]$, $\mathbf{Z}_2[\rho_y^2]$ and $\mathbf{Z}_2[\rho_z^2]$. By use of the containment relations we have now found all the subgroups of $\mathbb{O}$. □

B.3 Subgroups of $\mathbb{O} \oplus \mathbf{Z}_2^c$

In this section we consider the subgroups of $\mathbb{O} \oplus \mathbf{Z}_2^c$, where $\mathbf{Z}_2^c$ acts on $\mathbb{R}^3$ as $\mathbf{x} \mapsto -\mathbf{x}$ and is generated by the element $-I$. The work on this section is based on Golubitsky *et al.* [35], Chapter XIII, Section 9 p. 119 (see also Golubitsky and Ihrig [54]).

The subgroups of $\mathbb{O} \oplus \mathbf{Z}_2^c$ fall into three classes:

I Subgroups of $\mathbb{O}$,

II Subgroups containing $-I$,

III Subgroups not in $\mathbb{O}$ and not containing $-I$.

These are referred to in the literature as Class I, II and III subgroups. In Section B.2 we fully determined the class I subgroups. The Class II subgroups have the form $H \oplus \mathbf{Z}_2^c$ and so again the material in Section B.2 fully determines the Class II subgroups. The Class III subgroups are different and require additional treatment. It is important to note that each class III subgroup is isomorphic to some subgroup H of $\mathbb{O}$ but not conjugate to it.

For our applications the Class II subgroups are essentially the same as the Class I subgroups, whilst we cannot find any applications for the Class III subgroups and so these are not discussed further. This completes our discussion of the subgroups of $\mathbb{O} \oplus \mathbf{Z}_2^c$.

Appendix C

In this appendix we present the Matlab files used to create the pictures of the hexagonal slices of the cube. These files are adaptations of those originally used by Gomes [37] to create the pictures in Gomes [39].

Below are the three Matlab programs, cube.m, eigen3d.m and slicebox.m, used to create the unperturbed and perturbed pictures. The programs below would generate the planforms associated with the SC lattice. The wave vectors are given by the u_j's and these must be changed for the particular representation of the group.

cube.m

```
set(0,'DefaultFigurePaperType','A4')
bdwidth = 5;
topbdwidth = 60;
bottombdwidth = 50;
set(0,'Units','pixels');
scnsize = get(0,'ScreenSize');
%set(gcf,'Position',[14 0.5 (3/5)*21.0 (3/5)*29.7]);
pos1 = [scnsize(3)-bdwidth-(scnsize(4)-(topbdwidth+bottombdwidth))*(210/297),...
         bottombdwidth,...
         (scnsize(4)-(topbdwidth+bottombdwidth))*(210/297),...
         scnsize(4)-(topbdwidth+bottombdwidth)];

figure(1);
clf
set(gcf,'Position',pos1)

% blackeye C=1
% hexagon  C=0

N=10;
C=1;
X=-1:.015:1;
Y=-1:.015:1;
Z=-1:.015:1;
[x,y,z]=meshgrid(X,Y,Z);

map=gray;
colormap(map);

m=[N N*C N*0];

%
```

```
%Depending on the lattice and the dimension of the representation
%there can be between
%3 and 24 u's. Each u is a wave vector.
%


[u1,u2,u3]=eigen3d(m,x,y,z,C,N);

axes('position',[.275 .5 .37 .275]);

%The V term is dependent on the particular situation
%so there can be between 3 and 24 u's.


V=u1+u2+u3;
xslice=[-1];
yslice=[-1];
zslice=[0.995];
figure(2);
h=slice(x,y,z,-V,xslice,yslice,zslice);

axes('position',[.275 .2 .37 .275]);
xslice=[1];
yslice=[1];
zslice=[-1];
figure(2);
h=slice(x,y,z,-V,xslice,yslice,zslice);
figure(1);
axis([-1 1 -1 1 -1 1]);
slicebox(h);
[u,v]=meshgrid(-1:.01:1);
w=u+v;
slice(x,y,z,-V,u,v,w);
axis([-1 1 -1 1 -1 1]);
set(gca,'xtick',[],'ytick',[],'ztick',[]);
text(-0.1,-1.2,-1.2,'x','FontSize',12);
text(-1.2,-0.1,-1.2,'y','FontSize',12);
text(-1.2,1.2,0,'z','FontSize',12);

shading flat;
```

eigen3d.m

```
%The number of u's must be altered depending on the
%situation.
%

function [u1,u2,u3]=eigen3d(m,x,y,z,C,N)
z=z+(1-C/2)/N;

%Here we can set the epsilon term

e=0.5;
```

```
%And here was can defined the perturbation functions.

x=(1+e)*x;
y=(1+e)*y;
z=(1+e)*z;

%Here the u's are defined, the numbering being equal to the number of wave vectors.

u1=cos(N*x*pi);
u2=cos(N*y*pi);
u3=cos(N*z*pi);
```

slicebox.m

```
function hout=slicebox(h);
set(gca,'nextplot','add')
view(3)
for i=1:length(h)
    x=get(h(i),'xdata');
    y=get(h(i),'ydata');
    z=get(h(i),'zdata');
    [m,n]=size(x);
    x1=[x(1,1:n),x(1:m,n)',x(m,n:-1:1),x(m:-1:1,1)'];
    y1=[y(1,1:n),y(1:m,n)',y(m,n:-1:1),y(m:-1:1,1)'];
    z1=[z(1,1:n),z(1:m,n)',z(m,n:-1:1),z(m:-1:1,1)'];
    hout(i)=plot3(x1,y1,z1);
end
```

Bibliography

[1] M. A. Armstrong. *Groups and symmetry*. Undergraduate Texts in Mathematics. Springer-Verlag, New York, 1988.

[2] P. Ashwin and M. Field. Heteroclinic networks in coupled cell systems. *Arch. Ration. Mech. Anal.*, 148(2):107–143, 1999.

[3] I. Bosch Vivancos, P. Chossat, and I. Melbourne. New planforms in systems of partial differential equations with Euclidean symmetry. *Arch. Rational Mech. Anal.*, 131(3):199–224, 1995.

[4] P. C. Bresloff, J. D. Cowan, M. Golubitsky, P. J. Thomas, and M. C. Wienar. Geometric visual hallucinations, euclidean symmetry, and the functional architecture of striate cortex. *Phil. Trans. Roy. Soc. London Ser. B*, submitted.

[5] F. H. Busse and K. E. Heikes. Convection in a rotating layer: a simple case of turbulence. *Science*, 208:173–175, 1980.

[6] E. Buzano and M. Golubitsky. Bifurcation on the hexagonal lattice and the planar Bénard problem. *Philos. Trans. Roy. Soc. London Ser. A*, 308(1505):617–667, 1983.

[7] T. K. Callahan. Pattern formation. URL: `http://www.math.lsa.umich.edu/~timcall/patterns/`.

[8] T. K. Callahan and E. Knobloch. Symmetry-breaking bifurcations on cubic lattices. *Nonlinearity*, 10(5):1179–1216, 1997.

[9] T. K. Callahan and E. Knobloch. Pattern formation in three-dimensional reaction-diffusion systems. *Phys. D*, 132(3):339–362, 1999.

[10] V. Castets, E. Dulos, J. Boissonade, and P. De Kepper. Experimental evidence of a sustained standing turing-type nonequilibrium chemical pattern. *Phys. Rev. Lett.*, 64:2953–2956, 1990.

[11] P. Chossat. Forced reflectional symmetry breaking of an O(2)-symmetric homoclinic cycle. *Nonlinearity*, 6(5):723–731, 1993.

[12] P. Chossat and R. Lauterbach. *Methods in equivariant bifurcations and dynamical systems*, volume 15 of *Advanced Series in Nonlinear Dynamics*. World Scientific Publishing Co. Inc., River Edge, NJ, 2000.

[13] J. D. Crawford. $D_4 \dot{+} T^2$ mode interactions and hidden rotational symmetry. *Nonlinearity*, 7(3):697–739, 1994.

[14] J. D. Crawford and E. Knobloch. On degenerate Hopf bifurcation with broken O(2) symmetry. *Nonlinearity*, 1(4):617–652, 1988.

[15] G. D'Alessandro and W. J. Firth. Hexagonal spatial patterns for a kerr slice with a feedback mirror. *Phys. Rev. A*, 46:537–548, 1992.

[16] G. Dangelmayr and E. Knobloch. Hopf bifurcation with broken circular symmetry. *Nonlinearity*, 4(2):399–427, 1991.

[17] A. De Wit, G. Dewel, P. Borckmans, and D. Walgraef. Three-dimensional dissipative structures. *Phys. D*, 61:289–296, 1992.

[18] E. V. Degtiarev and M. A. Vorontsov. Dodecagonal patterns in a kerr-slice/feedback-mirror type optical system. *J. Mod. Opt.*, 43:93–98, 1996.

[19] B. Dionne. Planforms in three dimensions. *Z. Angew. Math. Phys.*, 44(4):673–694, 1993.

[20] B. Dionne and M. Golubitsky. Planforms in two and three dimensions. *Z. Angew. Math. Phys.*, 43(1):36–62, 1992.

[21] B. Dionne, M. Silber, and A. C. Skeldon. Stability results for steady, spatially periodic planforms. *Nonlinearity*, 10(2):321–353, 1997.

[22] G. L. dos Reis. Structural stability of equivariant vector fields on two-manifolds. *Trans. Amer. Math. Soc.*, 283(2):633–643, 1984.

[23] W. S. Edwards and S. Fauve. Patterns and quasi-patterns in the faraday experiment. *J. Fluid Mech.*, 278:123–148, 1994.

[24] G. B. Ermentrout and J. D. Cowan. A mathematical theory of visual hallucination patterns. *Biol. Cybernetics*, 34:137–150, 1979.

[25] M. J. Field. Equivariant dynamical systems. *Trans. Amer. Math. Soc.*, 259(1):185–205, 1980.

[26] J.-É. Furter, A. M. Sitta, and I. Stewart. Singularity theory and equivariant bifurcation problems with parameter symmetry. *Math. Proc. Cambridge Philos. Soc.*, 120(3):547–578, 1996.

[27] J.-É. Furter, A. M. Sitta, and I. Stewart. Algebraic path formulation for equivariant bifurcation problems. *Math. Proc. Cambridge Philos. Soc.*, 124(2):275–304, 1998.

[28] K. Gaterman. Symmetry. URL. `http://www.zib.de/gatermann/symmetry.html`.

[29] M. Golubitsky and V. Guillemin. *Stable mappings and their singularities*. Springer-Verlag, New York, 1973. Graduate Texts in Mathematics, Vol. 14.

[30] M. Golubitsky and D. Schaeffer. A discussion of symmetry and symmetry breaking. In *Singularities, Part 1 (Arcata, Calif., 1981)*, volume 40 of *Proc. Sympos. Pure Math.*, pages 499–515. Amer. Math. Soc., Providence, RI, 1983.

[31] M. Golubitsky and D. G. Schaeffer. *Singularities and groups in bifurcation theory. Vol. I*, volume 51 of *Applied Mathematical Sciences*. Springer-Verlag, New York, 1985.

[32] M. Golubitsky and I. Stewart. Symmetry and stability in Taylor-Couette flow. *SIAM J. Math. Anal.*, 17(2):249–288, 1986.

[33] M. Golubitsky and I. Stewart. *The symmetry perspective*, volume 200 of *Progress in Mathematics*. Birkhäuser Verlag, Basel, 2002. From equilibrium to chaos in phase space and physical space.

[34] M. Golubitsky, I. Stewart, and B. Dionne. Coupled cells: wreath products and direct products. In *Dynamics, bifurcation and symmetry (Cargèse, 1993)*, volume 437 of *NATO Adv. Sci. Inst. Ser. C Math. Phys. Sci.*, pages 127–138. Kluwer Acad. Publ., Dordrecht, 1994.

[35] M. Golubitsky, I. Stewart, and D. G. Schaeffer. *Singularities and groups in bifurcation theory. Vol. II*, volume 69 of *Applied Mathematical Sciences*. Springer-Verlag, New York, 1988.

[36] M. Golubitsky, J. W. Swift, and E. Knobloch. Symmetries and pattern selection in Rayleigh-Bénard convection. *Phys. D*, 10(3):249–276, 1984.

[37] M. G. M. Gomes. Private communication. Matlab files used to produce the figures seen in Gomes [39].

[38] M. G. M. Gomes. Private communication.

[39] M. G. M. Gomes. Black-eye patterns: a representation of three-dimensional symmetries in thin domains. *Phys. Rev. E (3)*, 60(4, part A):3741–3747, 1999.

[40] M. G. M. Gomes, I. S. Labouriau, and E. M. Pinho. Spatial hidden symmetries in pattern formation. In *Pattern formation in continuous and coupled systems (Minneapolis, MN, 1998)*, volume 115 of *IMA Vol. Math. Appl.*, pages 83–99. Springer, New York, 1999.

[41] M. G. M. Gomes and I. Stewart. Symmetry of generic bifurcations in cubic domains. *Internat. J. Bifur. Chaos Appl. Sci. Engrg.*, 7(1):147–171, 1997.

[42] M. G. M. Gomes and I. N. Stewart. Steady PDEs on generalized rectangles: a change of genericity in mode interactions. *Nonlinearity*, 7(1):253–272, 1994.

[43] Wojciech T. Góźdź and Robert Hołst. Triply periodic surfaces and multiply continuous structures from the landau model of microemulsions. *Phy. Rev. E*, 54:5012–5027, 1996.

[44] J. Guckenheimer and P. Holmes. Structurally stable heteroclinic cycles. *Math. Proc. Cambridge Philos. Soc.*, 103(1):189–192, 1988.

[45] J. Guckenheimer and P. Holmes. *Nonlinear oscillations, dynamical systems, and bifurcations of vector fields*, volume 42 of *Applied Mathematical Sciences*. Springer-Verlag, New York, 1990. Revised and corrected reprint of the 1983 original.

[46] G. H. Gunaratne, Q. Ouyang, and H. L. Swinney. Pattern formation in the presence of symmetries. *Phys. Rev. E (3)*, 50(4):2802–2820, 1994.

[47] F. Guyard and R. Lauterbach. Forced symmetry breaking perturbations for periodic solutions. *Nonlinearity*, 10(1):291–310, 1997.

[48] P. Hirschberg and E. Knobloch. Complex dynamics in the Hopf bifurcation with broken translation symmetry. *Phys. D*, 90(1-2):56–78, 1996.

[49] M. W. Hirsh, C. C. Pugh, and M. Shub. *Invariant Manifolds*, volume 583 of *Lecture Notes is Mathematics*. Springer-Verlag, New York, 1977.

[50] C. Hou and M. Golubitsky. An example of symmetry breaking to heteroclinic cycles. *J. Differential Equations*, 133(1):30–48, 1997.

[51] D. H. Hubel and T. N. Wiesel. Ordered arrangement of orientation columns in monkeys lacking visual experience. *J. Comp. Neurol.*, 158:307–318, 1974.

[52] D. H. Hubel and T. N. Wiesel. Sequence regularity and geometry of orientation columns in the monkey striate cortex. *J. Comp. Neurol.*, 158:267–294, 1974.

[53] D. H. Hubel and T. N. Wiesel. Uniformity of monkey striate cortex: a parallel relationship between field size, scatter, and magnification factor. *J. Comp. Neurol.*, 158:295–306, 1974.

[54] E. Ihrig and M. Golubitsky. Pattern selection with O(3) symmetry. *Phys. D*, 13(1-2):1–33, 1984.

[55] V. Kirk and M. Silber. A competition between heteroclinic cycles. *Nonlinearity*, 7(6):1605–1621, 1994.

[56] N. L. Komarova, B. A. Malomed, J. V. Moloney, and A. C. Newell. Resonant quasiperiodic patterns in a three-dimensional lasing medium. *Phys. Rev. A*, 56:803–812, 1997.

[57] M. Krupa and I. Melbourne. Asymptotic stability of heteroclinic cycles in systems with symmetry II. Preprint.

[58] M. Krupa and I. Melbourne. Asymptotic stability of heteroclinic cycles in systems with symmetry. *Ergodic Theory Dynam. Systems*, 15(1):121–147, 1995.

[59] K. Kurin-Csörgei, M. Orbán, A. M. Zhabotinsky, and I. R. Epstein. On the nature of patterns arising during polymerization of acrlamide in the presence of methylene blue-sulfide-oxygen oscillation reaction. *Chem. Rev. Lett.*, 295:70–74, 1998.

[60] A. S. Landsberg and E. Knobloch. Oscillatory bifurcation with broken translation symmetry. *Phys. Rev. E (3)*, 53(4, part A):3579–3600, 1996.

[61] R. Lauterbach. Symmetry breaking in dynamical systems. In *Nonlinear dynamical systems and chaos (Groningen, 1995)*, volume 19 of *Progr. Nonlinear Differential Equations Appl.*, pages 121–143. Birkhäuser, Basel, 1996.

[62] R. Lauterbach, S. Maier-Paape, and E. Reissner. A systematic study of heteroclinic cycles in dynamical systems with broken symmetries. *Proc. Roy. Soc. Edinburgh Sect. A*, 126(4):885–909, 1996.

[63] R. Lauterbach and M. Roberts. Heteroclinic cycles in dynamical systems with broken spherical symmetry. *J. Differential Equations*, 100(1):22–48, 1992.

[64] D. Lohnes, M. Mark, C. Mendelsohn, P. Dollé, A. Dierich, P. Gorry, A. Gansmuller, and P. Chambon. Function of the retinoic acid receptors (rars) during development: I craniofacial and skeletal abnormalities in rar double mutants. *Development*, 120:2723–2748, 1994.

[65] S. Maier-Paape and R. Lauterbach. Heteroclinic cycles for reaction diffusion systems by forced symmetry-breaking. *Trans. Amer. Math. Soc.*, 352(7):2937–2991, 2000.

[66] Maple. Waterloo Maple Inc., 1998. Version 7.

[67] Matlab. The MathWorks Inc., 1999. Version 6.5 Release 12.

[68] I. Melbourne. An example of a nonasymptotically stable attractor. *Nonlinearity*, 4(3):835–844, 1991.

[69] I. Melbourne. Steady-state bifurcation with Euclidean symmetry. *Trans. Amer. Math. Soc.*, 351(4):1575–1603, 1999.

[70] J. D. Murray. *Mathematical biology*, volume 19 of *Biomathematics*. Springer-Verlag, Berlin, second edition, 1993.

[71] M. Orbán, K. Kurin-Csörgei, A. M. Zhabotinsky, and I. R. Epstein. Pattern formation during polymerization of acrylamide in the presence of sulfide ions. *J. Phys. Chem.*, 103:36–40, 1999.

[72] Q. Ouyang, Z. Noszticzius, and H. L. Swinney. Spatial bistability of two-dimensional turing patterns in a reaction-diffusion system. *J. Phys. Chem.*, 96:6773–6776, 1992.

[73] Q. Ouyang and H. L. Swinney. Transition from a uniform state to hexagonal and striped turing patterns. *Nature*, 352:610–612, 1991.

[74] M. J. Parker. *Steady-State Symmetry-Breaking on the Body Centred Tetragonal Lattice with Applications.* M.Sc. Thesis, University of Warwick, 2000.

[75] D. H. Sattinger. *Group-theoretic methods in bifurcation theory*, volume 762 of *Lecture Notes in Mathematics.* Springer, Berlin, 1979. With an appendix entitled "How to find the symmetry group of a differential equation" by Peter Olver.

[76] J. Shakya and M. L. Nakarmi. Nonlinear electro-optica effect and kerr shutter. URL. `http://www-personal.ksu.edu/~jagat/ed2_final_report.pdf`, 2001.

[77] D. Shechtman, I. Blech, D. Gratias, and J. W. Cahn. Metallic phase with long-range orientation order and no translational symmetry. *Phys. Rev. Lett.*, 53:1951–1953, 1984.

[78] K. Staliunas. Three-dimensional turing structures and spatial solitons in optical parametric oscillators. *Phys. Rev. Lett.*, 81:81–84, 1998.

[79] K. Staliunas and V. J.Sánchez-Morcillo. Turing patterns in nonlinear optics. *Opt. Commun.*, 177:389–395, 2000.

[80] K. Staliunas, G. Slekys, and C. O. Weiss. Nonlinear pattern formation in active optical systems: shocks, domains of tilted waves, and cross-roll patterns. *Phys. Rev. Lett.*, 79:2658–2661, 1997.

[81] O. Steinbock, E. Kasper, and S.C. Müller. Complex pattern formation in the polyacrylamide–methylene blue–oxygen reaction. *J. Phys. Chem. A*, 103:3442–3446, 1999.

[82] A. M. Turing. The chemical basis for morphogenesis. *Phil. Trans. R. Soc. London B*, 327:37–72, 1952.

[83] M. A. Vorontsov and W. J. Firth. Pattern formation and competition in nonlinear optical systems with two-dimensional feedback. *Phys. Rev. A*, 49:2891–2906, 1994.

[84] M. A. Vorontsov and A. Yu. Karpov. Pattern formation due to interballoon spatial mode coupling. *J. Opt. Soc. Am. B*, 14:34–50, 1997.

[85] M. A. Vorontsov and B. A. Samson. Nonlinear dynamics in an optical system with controlled two-dimensional feedback: Black-eye patterns and related phenomena. *Phys. Rev. A*, 57:3040–3049, 1998.

[86] D. Walgraef, G. Dewel, and P. Borckmans. Nonequilibrium phase transitions and chemical instabilities. *Adv. Chem. Phys.*, 49:311–355, 1982.

[87] S. Wiggins. *Introduction to applied nonlinear dynamical systems and chaos*, volume 2 of *Texts in Applied Mathematics.* Springer-Verlag, New York, 1990.

[88] H. R. Wilson and J. D. Cowan. Excitatory and inhibitory interactions in localized populations of model neurons. *J. Biophys.*, 12:1–24, 1972.

[89] A. T. Winfree. *The geometry of biological time.* Springer Study Edition. Springer-Verlag, Berlin, 1990. Corrected reprint of the 1980 original.

[90] L. Yang, M. Dolnik, A. M. Zhabotinsky, and I. R. Epstein. Spatial resonances and superposition patterns in a reaction-diffusion model with interacting turing modes. *Phys. Rev. Lett.*, 88:208303–1, 2002.

[91] W. Zhang and J. Winñals. Square patterns and quasi-patterns in weakly damped faraday waves. *Phys. Rev. E*, 53:4283–4286, 1996.

[92] C. Zhou, H. Guo, and Q. Ouyang. Experimental study of the dimensionality of black-eye patterns. *Phys. Rev. E*, 65:0366118, 2002.